## DOCTOR OF PHILOSOPHY

# The impact of cannabis on brain health




**Saba Ishrat**

St Cross College
Department of Psychiatry
University of Oxford

**Supervised by**

Dr Anya Topiwala and Prof. Klaus P. Ebmeier

First submission: 03/10/2025; Final submission: 12/12/2025
This thesis is submitted to the Medicine Sciences Division, University of Oxford in partial fulfilment of the requirements for the degree of Doctor of Philosophy

## Declaration

I declare that this thesis is entirely my own work and is the result of my own research, which I have undertaken independently. Where contributions from others have been made, these have been appropriately acknowledged within the text.

**S. Ishrat**

## Abstract

Cannabis is the most widely used illicit drug worldwide, and its use is increasing rapidly among older adults. While adolescent and young adult use has been associated with differences in brain and cognitive outcomes, much less is known about its long-term impact on brain health in later life. This thesis draws on multimodal data from the UK Biobank, one of the largest population cohorts, to provide a comprehensive investigation of cannabis and brain health in mid- to late adulthood. Across chapters, structural and functional neuroimaging, cognitive testing, and genetic epidemiology were integrated to examine whether lifetime cannabis use is associated with brain structure, functional connectivity, cognition, or dementia risk, and whether these associations are likely to be causal.

In analyses of nearly 16,000 participants with brain imaging, cannabis users demonstrated associations with white matter microstructure, particularly in the corpus callosum, anterior corona radiata, and cingulum. These patterns, characterised by lower fractional anisotropy and intracellular volume fraction and higher mean diffusivity, suggest reduced white matter integrity, consistent with prior findings in younger cohorts. In contrast, no hippocampal differences were observed, suggesting that grey matter associations may diminish with age or abstinence, while white matter remains more sensitive to earlier exposure. Functional analyses revealed associations with resting-state connectivity across default mode, central executive, and salience networks, as well as heightened task-related activation during emotional face processing, suggesting reorganisation of network activity. In cognitive analyses of around 79,000 participants, lifetime cannabis users performed better on cross-sectional tests of working memory and reasoning, yet no differences were observed in longitudinal trajectories of decline. These apparent advantages are more plausibly explained by sociodemographic selection, such as higher educational attainment among users, than by neurocognitive benefits of cannabis.

To strengthen causal inference, bidirectional two-sample Mendelian randomization (MR) was applied using the largest available genome-wide association study (GWAS) of cannabis use, dependence, brain imaging-derived phenotypes, cognition, and dementia. Across all domains, no significant genetic associations was identified. While MR analyses are constrained by power and assumptions that cannot be fully verified, these null genetic findings contrast with observational results, suggesting that apparent associations are more likely to reflect confounding, sample characteristics, or methodological artefacts rather than direct neurobiological effects.

Taken together, this thesis provides one of the most comprehensive investigations to date of cannabis use and brain health in later life. The findings suggest that while cannabis use is associated observationally with subtle differences in brain structure, functional networks, and cross-sectional cognition, these associations do not persist longitudinally and are not supported by genetic evidence. Cannabis use therefore appears unlikely to exert a major causal effect on brain structure, cognition, or dementia risk in ageing populations.

## Acknowledgements

I would like to express my deepest gratitude to my supervisors, Dr Anya Topiwala and Professor Klaus P. Ebmeier, for their invaluable guidance, support, and encouragement throughout this project. Their expertise, guidance, and mentorship have been instrumental in shaping both this thesis and my development as a researcher. I am especially grateful for their immense patience and unyielding support, and for all they have taught me as a scientist and as a person. Their high standards and thoughtful feedback challenged me to grow, while their encouragement and kindness helped me navigate the inevitable difficulties of research. Their generosity with their time and ideas has been remarkable, and I am deeply grateful for the countless hours they invested in guiding me. Their mentorship has not only shaped this thesis but also inspired the direction of my future research career.

This doctoral research was generously funded by the Society for the Study of Addiction (SSA). I am profoundly grateful for their support, without which this PhD would not have been possible. In particular, I would like to thank Rob Calder, CEO, for his encouragement and support of early-career researchers, as well as Martin Wheeler, retired CEO, and Graham Hunt, Executive Officer, whose dedication to advancing addiction research has had a lasting impact.

I gratefully acknowledge the use of UK Biobank data, as well as the publicly available GWAS summary statistics that underpinned the genetic analyses presented here. These invaluable resources made this research feasible.

I am indebted to my college, St Cross, and in particular to the staff and fellows who created such a welcoming and supportive environment. Serving as Junior Dean, with responsibilities for student welfare and college life, was one of the most rewarding aspects of my time in Oxford, and I am deeply grateful to the St Cross community for their trust and friendship.

I have also learned a great deal from all my colleagues and friends in the lab and department, whose advice, feedback and camaraderie have enriched this project in countless ways. Thank you for the discussions and encouragement that have shaped my thinking and brightened my days. Working alongside such talented and generous people has been a privilege, and their friendship has made this journey even more rewarding.

To my friends in Oxford, especially Vrinda, Priyanshu, Athanasios, Tymek, Jisoo, Moumili, Srinandini, Sofia, Chamu, Vidushi, Indrajeet, Faseel, Afra and Huishu—thank you for your warmth, humour, and unwavering companionship. You have truly been like family to me during these years, and your support has been invaluable both inside and outside the academic sphere. To all the other friends I made in Oxford and at St Cross, thank you for enriching this journey in countless ways. From late-night deadline rants to last-minute celebrations, you made these years not only survivable but genuinely joyful. I will cherish the endless debates, the impromptu coffee breaks, the formal dinners and balls, and above all the laughter that carried me through even the greyest Oxford days.

To my friends from back home—Annie, Deepika, Habiba—thank you for sharing this journey and for sending your warm wishes across the miles; they reached me when I needed them most. I am also especially grateful to my friend Bryan, whose encouragement and kindness have been a constant source of strength, always reminding me of the bigger picture when I lost sight of it, and for his generous support throughout this journey.

I am profoundly grateful to my family, who have been the foundation of everything I have achieved. To my mum, whose dream of Oxford became my own, and whose belief in me never wavered—I carry your pride with me in every step of this journey. To my dad, thank you for your love, guidance, and steady encouragement, even from afar. To my brother, Rashid, whose steadfast support made this journey possible: thank you for encouraging my studies abroad, for always offering practical help and kindness, and for reminding me that I was capable of more than I believed. To my sister, Shaista, thank you for your constant encouragement and for always being there with words of support when I needed them most. To my nephew, Khabib, whose calls always made me smile and momentarily forget the stresses of research, thank you for those moments of lightness. To my niece, Maryam, who was born during the writing of this thesis, you have been a bright reminder of joy, hope, and the future that lies ahead. To my family—you are the heart of all that I have achieved, and I truly could not have done this without you.

Finally, I would like to thank all those who believed in me and supported me through the challenges of doctoral study. This thesis is dedicated to you all, near and far—*'ad quattuor cardines mundi*', to the four corners of the world.

## Publications associated with this DPhil

1. **Ishrat S,** Levey DF, Gelernter J, Ebmeier K, Topiwala A. Association between cannabis use and brain structure and function: an observational and Mendelian randomisation study. BMJ Ment Health. 2024 Oct 30;27(1):e301065. doi: 10.1136/bmjment-2024-301065. PMID: 39477366; PMCID: PMC11529520

**Manuscript under peer review:**

Title: Cannabis use, cognitive function, and dementia risk in older adults: Observational and genetic analyses
**Submitted for publication (under peer review).**

## Other publications

2. Stevering, C., Lequin, M., Szczepaniak, K., Sadowski, K., **Ishrat, S**., De Luca, A., Leemans, A., Otte, W., Kwiatkowski, D. J., Curatolo, P., Weschke, B., Riney, K., Feucht, M., Krsek, P., Nabbout, R., Jansen, A., Wojdan, K., Sijko, K., Glowacka-Walas, J., Borkowska, J., … Jansen, F. (2025). Vigabatrin-associated brain magnetic resonance imaging abnormalities and clinical symptoms in infants with tuberous sclerosis complex. Epilepsia, 66(2), 356–368. https://doi.org/10.1111/epi.18190

# Table of Contents

**Declaration** ..... 2
**Abstract** ..... 3
**Acknowledgements** ..... 4
**Publications associated with this DPhil** ..... 6
**Table of Contents** ..... 7
**List of Tables** ..... 10
**List of Figures** ..... 12
**Abbreviations** ..... 14
***Chapter 1: Introduction*** ..... ***16***
**1.1 Background** ..... 16
**1.2 Aims and Objectives** ..... 17
**1.3 Novel contribution** ..... 19
**1.4 Scope and limitations** ..... 20
**1.5 Thesis outline** ..... 21
***Chapter 2: Literature Review*** ..... ***23***
**2.1 Overview and prevalence of cannabis use** ..... 23
**2.2 Types and forms of cannabis** ..... 26
**2.3 The endocannabinoid system** ..... 27
**2.4 Clinical phenotypes and comorbidity** ..... 29
**2.5 Effect of cannabis on brain: insights from animal studies** ..... 31
**2.6 Effects of cannabis on brain structure** ..... 34
**2.7 Effects of cannabis on brain function** ..... 38
**2.8 Effects of cannabis on cognitive performance** ..... 42
**2.9 Current knowledge about cannabis and dementia risk** ..... 46
**2.10 Sex-dependent effects of cannabis use on brain health** ..... 48
**2.11 Limitations and gaps in the existing literature** ..... 50
***Chapter 3: Methods*** ..... ***53***
**3.1 Study sample and data source** ..... 53
**3.2 Cannabis use data** ..... 54
**3.3 Imaging data** ..... 55
**3.4 Cognitive test data** ..... 58
**3.5 Confounding variables** ..... 59
**3.6 Genetic instruments for Mendelian randomisation** ..... 60

**3.7 Statistical analysis** ..... **64**
**3.7.1 Software** ..... 64
***3.7.2 Observational analyses*** ..... 64
***3.7.3 Genetic analyses*** ..... 65
***Chapter 4: Associations between cannabis use and brain structure*** ..... ***68***
**4.1 Introduction** ..... **68**
**4.2 Methods** ..... **68**
**4.2.1 Study sample** ..... 68
**4.2.2 Cannabis use data** ..... 69
**4.2.3 MRI acquisition and data processing** ..... 69
**4.2.4 Outcomes** ..... 70
**4.2.5 Confounds** ..... 70
**4.2.6 Genetic variants** ..... 70
**4.2.7 Statistical analyses** ..... 72
**4.3 Results** ..... **73**
**4.3.1 Demographics** ..... 73
**4.3.2 Results from observational analysis** ..... 76
**4.3.3 Sensitivity Analyses** ..... 80
**4.3.4 Results from Mendelian randomization analysis** ..... 83
**4.4 Discussion** ..... **87**
***Chapter 5: Association between cannabis use and brain function*** ..... ***90***
**5.1 Introduction** ..... **90**
**5.2 Methods** ..... **90**
**5.2.1 Study sample** ..... 90
**5.2.2 Cannabis use data** ..... 91
**5.2.3 MRI acquisition and data processing** ..... 91
**5.2.4 Confounds** ..... 91
**5.2.5 Genetic variants** ..... 91
**5.2.6 Statistical analyses** ..... 92
**5.3 Results** ..... **93**
**5.3.1 Demographics** ..... 93
**5.3.2 Observational analyses** ..... 94
**5.3.3 Sensitivity analyses** ..... 99
**5.3.4 Results from Mendelian randomization analysis** ..... 103
**5.4 Discussion** ..... **105**
***Chapter 6: Association between cannabis use, cognitive function and dementia risk*** ..... ***108***
**6.1 Introduction** ..... **108**
**6.2 Methods** ..... **109**
**6.2.1 Study sample** ..... 109
**6.2.2 Cannabis use data** ..... 109
**6.2.3 Cognitive test data** ..... 110
**6.2.4 Confounds** ..... 110
**6.2.5 Genetic variants** ..... 111
**6.2.6 Statistical analyses** ..... 113
**6.3 Results** ..... **114**
**6.3.1 Demographics** ..... 114
**6.3.2 Results from observational analysis** ..... 115
**6.3.3 Sensitivity Analyses** ..... 118

**6.3.4 Results from Mendelian randomization analysis** ..... 120
**6.4 Discussion** ..... **126**
***Chapter 7: Discussion*** ..... ***129***
**7.1 Summary of key findings** ..... **129**
**7.2 Interpretation in the context of existing literature** ..... **131**
**7.3 Integration of observational and Mendelian randomization results** ..... **138**
**7.4 Strengths and limitations of the study** ..... **143**
**7.5 Implications for clinical practice and public health policy** ..... **145**
**7.6 Ethical considerations** ..... **147**
**7.7 Future research directions** ..... **148**
**7.8 Final thoughts and concluding remarks** ..... **149**
***References*** ..... ***151***
***Appendices*** ..... ***178***
**Appendix 1: Individual image-derived structure phenotypes in UK Biobank (n= 2,128)** ..... **178**
**Appendix 2: Individual image-derived functional phenotypes in UK Biobank (n= 1,793)** ..... **229**
**Appendix 3: Brain imaging confounds in UK Biobank (n = 613)** ..... **299**
**Appendix 4: GWAS data on cannabis use disorder used from Million Veteran Program** ..... **314**
**Appendix 5a: ICD-9 codes used in the definition of Million Veteran Program (MVP) cases** **314**
**Appendix 5b: ICD-10 codes used in the definition of Million Veteran Program (MVP) cases** ..... **315**
**Appendix 6: Demographic characteristics (missing vs non missing cannabis data)** ..... **316**
**Appendix 7: Associations between cannabis use and brain structure (Model 1: core covariates)** ..... **316**
**Appendix 8: Associations between cannabis use and brain structure (Model 2: core covariates + alcohol + smoking)** ..... **317**
**Appendix 9: Associations between cannabis use and brain function (Model 1: core covariates)** ..... **317**
**Appendix 10: Associations between cannabis use and brain function (Model 2: core covariates + alcohol + smoking)** ..... **318**
**Appendix 11: Associations between cannabis use and cognitive function (Model 1-5)** ..... **318**

## List of Tables

Table 1: Cognitive tests in UK Biobank included in the final analysis ..... 59
Table 2: Outcome-specific instrument availability and strength ..... 63
Table 3: MR power (α=0.05, 80% power) ..... 64
Table 4: SNPs identified in GWAS associated with cannabis use ..... 71
Table 5: SNPs identified in GWAS associated with brain structure ..... 72
Table 6: Demographic characteristics ..... 74
Table 7: Demographic characteristics (male and female) ..... 74
Table 8: Association between cannabis use and hippocampus volume ..... 76
Table 9: Summary of the association between cannabis use and brain structure ..... 78
Table 10: Associations between cannabis use and individual image-derived phenotypes ..... 78
Table 11: Associations between cannabis use and brain structure surviving Bonferroni correction ..... 79
Table 12: Association between duration of cannabis abstinence and brain structure ..... 80
Table 13: Association between high frequency cannabis use (compared to low frequency) and brain structure ..... 81
Table 14: Associations between cannabis use and brain structure in males surviving False Discovery Rate ..... 81
Table 15: Associations between cannabis use and brain measures in females surviving False Discovery Rate ..... 82
Table 16: Two-sample linear MR estimates assessing evidence for the causal effect of cannabis use on brain structure ..... 84
Table 17: Two-sample linear Reverse MR assessing evidence estimates for the causal effect of brain structure on cannabis use ..... 86
Table 18: SNPs identified in GWAS associated with brain function ..... 92
Table 19: Associations between cannabis use and individual image-derived phenotypes ..... 96
Table 20: Summary of the associations between cannabis use and brain functional connectivity ..... 97
Table 21: Resting-state functional connectivity associations with cannabis use and brain function, including edge ID, brain regions, and networks (main analysis) ..... 98
Table 22: Association between duration of cannabis abstinence and brain function ..... 99
Table 23: Association between high frequency cannabis use (compared to low frequency) and brain function ..... 100
Table 24: Associations between cannabis use and brain function in males surviving False Discovery Rate ..... 101
Table 25: Resting-state functional connectivity associations with cannabis use and brain function in males, including edge ID, brain regions, and networks (sensitivity analysis) ... 102
Table 26: Associations between cannabis use and brain function in females surviving False Discovery Rate ..... 102
Table 27: Resting-state functional connectivity associations with cannabis use and brain function in females, including edge ID, brain regions, and networks (sensitivity analysis) 102
Table 28: Two-sample linear MR estimates assessing evidence for the causal effect of Cannabis use disorder/ Lifetime Cannabis use on brain function ..... 104
Table 29: Two-sample linear reverse MR estimates assessing evidence for the causal effect of brain function on Cannabis use disorder ..... 105
Table 30: Genome-wide significant SNPs associated with cannabis use for cognitive function and dementia association ..... 112

Table 31: Genome-wide significant SNPs associated with Fluid intelligence test ..... 113
Table 32: Genome-wide significant SNPs for all-cause dementia in Million Veteran Program (MVP) ..... 113
Table 33: Demographic characteristics ..... 114
Table 34: Longitudinal trends in cognitive test performance in UK Biobank participants (main effect of time) ..... 116
Table 35: Longitudinal change in cognitive functioning according to cannabis use in UK Biobank cannabis × time interaction effects ..... 118
Table 36: Interaction between cannabis use and sex in relation to cross-sectional cognitive performance in UK Biobank ..... 118
Table 37: Association between high frequency cannabis use (compared to low frequency) and cross-sectional cognitive performance in UK Biobank ..... 119
Table 38: Two-sample linear MR estimates assessing evidence for the causal effect of cannabis use on cognitive functioning ..... 121
Table 39: Two-sample linear Reverse MR estimates assessing evidence for the causal effect of fluid intelligence test on cannabis use disorder ..... 123
Table 40: Two-sample linear MR estimates assessing evidence for the causal effect of cannabis use on all-cause dementia ..... 124
Table 41: Two-sample linear Reverse MR estimates assessing evidence for the causal effect of all-cause dementia on cannabis use disorder ..... 125

## List of Figures

Figure 1: Global and regional past-year prevalence of cannabis use among people aged 15–16 years, and among the general population aged 15–64 years, 2017 ..... 24
Figure 2: Cannabis use, by region and subregions, 2018 ..... 25
Figure 3: Trends in past-year cannabis use in selected Western and Central European countries, 2004–2018 ..... 26
Figure 4: Distribution of cannabinoid receptors (CB1 and CB2) in human brain and peripheral organs ..... 28
Figure 5: CB1 receptor activity: effects of endocannabinoids (Arachidonic acid and 2-arachidonylglycerol) and Δ9-THC on neurotransmitter release at the synapse ..... 29
Figure 6: Overview of UK Biobank data collection timepoints used in this thesis ..... 53
Figure 7: Flow chart of the participants from the UK Biobank included in the observational analysis ..... 54
Figure 8: Flow chart of the genome wide association studies included in the genetic analysis ..... 61
Figure 9: Two-sample Mendelian Randomisation study design ..... 66
Figure 10: Flow chart of the participants from the UK Biobank included in the final analysis ..... 69
Figure 11: Source genome-wide association studies used in Mendelian randomization analysis ..... 71
Figure 12: Distribution of lifetime frequency of cannabis use in UK biobank used in the analysis ..... 75
Figure 13: A) Age when last took cannabis and B) Duration of years without cannabis ..... 76
Figure 14: Associations between cannabis use and brain structure ..... 77
Figure 15: White matter regions significantly associated with cannabis use ..... 79
Figure 16: Genetic associations between cannabis use and brain structure ..... 83
Figure 17: Two-sample linear MR plot assessing evidence for the causal effect of Cannabis use disorder (CanUD)/Lifetime Cannabis use (CanLU) on brain structure ..... 86
Figure 18: Source genome-wide association studies used in Mendelian randomization analysis ..... 92
Figure 19: Associations between cannabis use and brain function ..... 95
Figure 20: Resting state functional connectivity significantly associated with cannabis use 97
Figure 21: Genetic associations between cannabis use and brain function ..... 103
Figure 22: Two-sample linear MR plot assessing evidence for the causal effect of Cannabis use disorder/ Lifetime Cannabis use on brain function ..... 105
Figure 23: Flow chart of the participants from the UK Biobank included in the final analysis ..... 109
Figure 24: Cognitive tests in UK Biobank included in the final analysis ..... 110
Figure 25: Source genome-wide association studies used in Mendelian randomization analysis ..... 111
Figure 26: Associations between cannabis use and cross-sectional cognitive functioning in UK Biobank ..... 115
Figure 27: Associations between cannabis use and longitudinal change in cognitive functioning in UK Biobank ..... 117
Figure 28: Association between cannabis use and sex in relation to cross-sectional fluid intelligence in UK Biobank ..... 119

Figure 29: Associations between cannabis use frequency and cross-sectional cognitive performance in UK Biobank..... 120
Figure 30: Genetic associations between cannabis use, cognitive tests and dementia..... 121
Figure 31: Two-sample linear MR plot assessing evidence for the causal effect of Cannabis use disorder/ Lifetime Cannabis use on Cognitive tests..... 123
Figure 32: Reverse two-sample linear MR plot assessing evidence for the causal effect of Fluid intelligence test on Cannabis use disorder..... 124
Figure 33: Two-sample linear MR plot assessing evidence for the causal effect of Cannabis use disorder/ Lifetime Cannabis use on All-Cause Dementia..... 125
Figure 34: Reverse two-sample linear MR plot assessing evidence for the causal effect of All-cause Dementia on Cannabis use disorder..... 126
Figure 35: Observational vs Genetic Findings..... 139

## Abbreviations

| Abbreviations | Definition |
|---|---|
| **THC** | Delta-9-tetrahydrocannabinol |
| **CBD** | Cannabidiol |
| **CB1** | Cannabinoid receptors 1 |
| **DMN** | Default mode network |
| **fMRI** | Functional magnetic resonance imaging |
| **MR** | Mendelian randomization |
| **GWAS** | Genome-wide association study |
| **IDPs** | Imaging-derived phenotypes |
| **MRI** | Magnetic resonance imaging |
| **CUD** | Cannabis use disorder |
| **CB2** | Cannabinoid receptors 2 |
| **DSM** | Diagnostic and Statistical Manual of Mental Disorders |
| **ICD** | International Classification of Diseases |
| **GABA** | Gamma-aminobutyric |
| **FA** | Fractional anisotropy |
| **WM** | White matter |
| **GM** | Grey matter |
| **MD** | Mean diffusivity |
| **CEN** | Central executive network |
| **rsFC** | Resting-state functional connectivity |
| **CUDIT** | Cannabis use disorders identification test |
| **NHS** | National health service |
| **EHR** | Electronic health record |
| **dMRI** | Diffusion magnetic resonance imaging |
| **SWI** | Susceptibility-weighted imaging |
| **tfMRI** | Task functional magnetic resonance imaging |
| **rsfMRI** | Resting-state functional magnetic resonance imaging |
| **DTI** | Diffusion tensor imaging |
| **L1** | Axial diffusivity |
| **L2, L3** | Radial diffusivity |
| **MO** | Mode of anisotropy |
| **ICVF** | Intracellular volume fraction |
| **OD** | Orientation dispersion |
| **ISOVF** | Isotropic volume fraction |
| **TBSS** | Tract-based spatial statistics |
| **ICA** | Independent component analysis |
| **BP** | Blood pressure |
| **BMI** | Body mass index |
| **SNPs** | Single nucleotide polymorphisms |

| | |
|---|---|
| **CanUD** | Cannabis use disorder |
| **MVP** | Million Veteran Program |
| **CanLU** | Lifetime cannabis use |
| **FDR** | False discovery rate |
| **IVW** | Inverse-variance weighted |
| **A1** | Effect allele |
| **A2** | Other allele |
| **SE** | Standard error |
| **SD** | Standard deviation |
| **LCI** | Lower confidence interval |
| **UCI** | Upper confidence interval |
| **BOLD** | Blood oxygenation level dependent |
| **PC** | Partial correlation |
| **PHQ** | Patient Health Questionnaire |
| **GAD** | Generalised Anxiety Disorder |

# Chapter 1: Introduction

## 1.1 Background

Cannabis, also referred to as marijuana, is currently the most widely cultivated and consumed illicit substance worldwide [1]. It is derived from the Cannabis sativa and cannabis indica plant species and contains over 500 chemical constituents, among which approximately 104 are classified as cannabinoids. The most prominent cannabinoids are delta-9-tetrahydrocannabinol (THC), the primary psychoactive compound, and cannabidiol (CBD), which lacks intoxicating effects but is being investigated for therapeutic properties [2]. These compounds interact with the body's endocannabinoid system, a neuromodulatory network responsible for regulating various physiological and cognitive processes, including mood, memory, appetite, and pain sensation. THC primarily targets cannabinoid receptors 1 (CB1), which are densely located in brain regions involved in cognition, emotion, and reward processing, such as the prefrontal cortex, hippocampus, amygdala, and basal ganglia [3–6].

Over the past two decades, there has been a significant global increase in cannabis use, largely driven by legal reforms and shifting social attitudes [7, 8]. According to the 2024 World Drug Report, an estimated 228 million people aged 15 to 64, approximately 4.4% of the global population, reported using cannabis [1]. Countries such as Uruguay, Canada, Germany, and Thailand, along with numerous U.S. states, have legalized cannabis either for medical or recreational purposes [7, 9–12]. These policy changes have been accompanied by broader shifts in public perception, with cannabis increasingly viewed as a less harmful alternative to other substances [7, 8]. However, legal access has also coincided with the production of higher-potency cannabis products, particularly those with elevated THC concentrations, raising new concerns about dose-dependent health risks and potential long-term effects [13, 14].

Historically, cannabis use has been most prevalent among adolescents and young adults, with initiation typically occurring in late adolescence [15]. Cannabis is often associated with youth culture, and globally, individuals aged 18–25 consistently report the highest usage rates. Nevertheless, recent data show an emerging trend of increasing cannabis use among middle-aged and older adults [16]. This shift is influenced by a combination of cannabis legalization, increased medical availability, reduced stigma, and changing public health narratives. Older adults increasingly report using cannabis for conditions such as chronic pain, insomnia, or anxiety, ailments that are common in aging populations [17, 18].

While much of the existing research has focused on the effects of cannabis in younger populations, far less is known about its impact on brain health and cognitive function in older individuals. This gap is particularly important given that cognitive decline is a central concern in aging. There is overlap in the brain regions most affected by aging, such as the hippocampus and prefrontal cortex, and those rich in CB1 receptors and therefore most affected by THC [19–

22]. Neuroimaging studies in younger population as well as animal studies have shown that cannabis exposure is associated with brain structure, including differences in grey matter (GM) volume and white matter (WM) microstructure and with functional connectivity such as default mode network (DMN) [23–27]. These findings have been especially pronounced in regions supporting memory, attention, and executive functioning [23, 27].

Animal research has demonstrated that THC can induce both neurochemical and morphological changes in brain regions critical for cognitive processing [28, 29]. While some studies have suggested neuroprotective effects under controlled conditions [30, 31], most indicate that repeated exposure may impair working memory and learning [32, 33]. Similar concerns are also observed in human studies. Neuropsychological assessments of adolescent and adult cannabis users frequently report impairments in verbal memory, processing speed, attention, and decision-making. These effects can persist beyond the period of acute intoxication and may accumulate with prolonged daily or near-daily use [34–36].

The relationship between cannabis use and long-term cognitive decline as well as dementia remains poorly understood. While some studies suggest that cannabis use may exacerbate age-related changes in brain structure, function and cognitive performance [35, 37, 38], others report no adverse effects [39–41]. Methodological inconsistencies, including differences in cannabis dosage, age of initiation, duration of use, and neuroimaging techniques, have contributed to mixed findings. Additionally, older users are underrepresented in most datasets, making it difficult to assess whether cannabis poses distinct risks or effects in later life compared to earlier stages of adulthood.

As cannabis becomes increasingly integrated into both medical and recreational usage [16, 42], the need for a comprehensive understanding of its potential effects on cognitive aging has become more urgent. Aging populations are particularly susceptible to age-related changes in the brain [43, 44], and any factor that may interact with or accelerate cognitive decline warrants close examination. In this context, cannabis use in older adults represents a growing public health consideration, particularly in light of the limited empirical data available to inform clinical or policy guidance.

## 1.2 Aims and Objectives

This study aims to investigate the impact of cannabis use on brain health in later life using a multi-method approach that integrates structural and functional neuroimaging, cognitive testing, and genetic epidemiology. While cannabis is increasingly used by older adults [16, 42], the long-term effects of such use on the aging brain remain poorly understood. Most existing studies have concentrated on adolescents and young adults, leaving a substantial knowledge gap regarding how cannabis may influence brain health in older populations.

Prior neuroimaging studies have identified potential associations between cannabis use and differences in brain structure, including reduced GM volume in key regions such as the hippocampus and amygdala [45, 46]. Functional magnetic resonance imaging (fMRI) studies have reported associations with resting-state connectivity, particularly within the DMN, which is implicated in memory and self-referential thought [47]. These neural changes are believed to underlie cognitive difficulties frequently observed in long-term cannabis users, particularly in domains such as memory, attention, and executive function [48, 49]. However, findings across studies have been inconsistent [23, 34, 50], and few have included older adults in their samples.

To address this gap, the present study will evaluate whether lifetime cannabis use is associated with brain structural and functional connectivity in older adults and whether such use is linked to measurable cognitive decline. Importantly, the study goes beyond conventional observational analysis by incorporating Mendelian randomization (MR), a genetic epidemiological approach that uses inherited genetic variants as instrumental variables to infer causality between modifiable exposures and health outcomes. MR helps overcome key limitations of traditional observational studies, including residual confounding and reverse causation, which are especially problematic in cannabis research due to the complexity of behavioural, social, and genetic factors [51].

The UK Biobank data provides an ideal cohort for this research. It includes a large, demographically diverse sample of older adults with well-characterized data on lifestyle behaviours, neuroimaging, cognitive function, and genetic profiles [52–55]. Leveraging this dataset enhances the study's statistical power and generalizability, and allows for integrated analysis of cannabis exposure, brain metrics, and cognition in the same individuals, an approach rarely applied in cannabis research. In addition, publicly available genome-wide association study (GWAS) summary statistics will be used [56–60] to support MR analyses, in order to investigate potential causal relationships between lifetime cannabis use and neurocognitive outcomes.

Together, these methods offer a comprehensive framework to examine both the epidemiological and genetic links between cannabis use and brain health in aging. By bridging neuroimaging, cognitive science, and genetic epidemiology, this research has the potential to generate novel insights that inform clinical guidance, public health policy, and future studies on substance use and cognitive aging.

**Specific Aims**

The primary objectives of this study are to investigate the relationship between lifetime cannabis use and brain health in later life through a combination of observational and genetic approaches. The specific aims are as follows:

1. To assess both observational and genetic associations between lifetime cannabis use and brain structure in older adults.

2. To evaluate observational and genetic associations between lifetime cannabis use and functional brain connectivity.
3. To assess both observational and genetic associations between lifetime cannabis use and cognitive function in later life.
4. To examine the potential causal relationship between cannabis use and the risk of developing dementia.

**Hypotheses**

Based on the aims outlined above, the study will test the following hypotheses:

1. Lifetime cannabis use is associated with structural brain differences in older adults, most notably reduced hippocampal volume.
2. Lifetime cannabis use is associated with reduced functional brain connectivity, particularly within the DMN.
3. Lifetime cannabis use is linked to a greater risk of cognitive decline, including impairments in working memory and slower reaction time.
4. Lifetime cannabis use is causally associated with an increased risk of developing dementia.

Prior studies, conducted mainly in younger populations, have reported associations between cannabis use and differences in brain structure, functional connectivity, and cognitive outcomes [23]. These hypotheses reflect prior evidence that cannabis use impacts brain regions and networks implicated in memory and cognitive control, particularly the hippocampus and the DMN [24, 45–47, 61, 62]. The DMN, in particular, plays a central role in self-referential processing, memory, and attention [63], and prior work has shown altered DMN connectivity in both adolescent and adult users [47, 61, 62]. The hippocampus and DMN are central to age-related cognitive decline and dementia risk [38, 64, 65], providing a strong rationale for the study's focus on structural, functional, and clinical outcomes.

## 1.3 Novel contribution

This study addresses several critical gaps in the existing literature on cannabis use and brain health. While the majority of prior research has concentrated on adolescents and young adults, this study focuses specifically on middle-aged and older adults, a demographic that remains significantly underrepresented despite rising rates of cannabis use. By leveraging large-scale datasets from the UK Biobank, the study overcomes key limitations of earlier work, including small sample sizes, restricted age ranges, and limited external validity.

A central contribution of this research is the integration of both observational and genetic methodologies to examine associations between lifetime cannabis use and a broad range of neurobiological and cognitive outcomes. Specifically, the study explores the relationships

between cannabis use and brain structure, task-based and resting-state functional connectivity, cognitive performance, and dementia risk. To assess potential causality, both forward and reverse MR were applied across all outcome domains. To the best of current knowledge, this is the largest study to date examining cannabis use in relation to neuroimaging and cognitive outcomes in older adults, and the first to implement MR in this context, including dementia risk.

In the neuroimaging domain, the analysis spans more than 3,900 imaging-derived phenotypes (IDPs), greatly extending the scope of prior studies that have typically focused on specific brain regions or networks [53, 54]. Associations were examined across structural metrices such as GM and WM, and functional metrics, including within and between network-level connectivity. To ensure analytical robustness, stringent multiple testing corrections were applied, and a range of sensitivity analyses, such as dose-response modelling, abstinence duration, and sex-stratified comparisons, were conducted.

In the cognitive domain, the study offers novel insights by assessing performance across multiple cognitive tests [55], including working memory, attention, processing speed, executive function, reasoning, and episodic memory. Both cross-sectional and longitudinal analyses were conducted to examine baseline differences and changes in performance over time, offering a more comprehensive view of the relationship between lifetime cannabis use and cognitive decline. Dementia risk, a key concern in aging populations, was also evaluated using large-scale genetic data.

Crucially, bidirectional MR was applied across all outcome areas, enabling the investigation of both forward and reverse pathways. This approach strengthens causal inference by helping to disentangle true causal effects from residual confounding and reverse causation, issues that are particularly challenging in behavioural epidemiology.

By integrating large-scale observational data with robust genetic inference in well-characterized aging cohorts, this study offers one of the most comprehensive and methodologically rigorous evaluations to date of how cannabis use may influence brain health and cognitive aging. The findings provide a valuable evidence base to inform future public health policy, clinical decision-making, and research on substance use and neurodegenerative risk in later life.

### 1.4 Scope and limitations

This thesis investigates how cannabis use relates to brain structure, functional connectivity, cognitive performance, and dementia risk in later life. It employs a multimodal, integrative framework that combines large-scale observational data with genetic causal inference through bidirectional MR. The study focuses specifically on middle-aged and older adults, a population

underrepresented in cannabis research despite rising usage rates, and draws on one of the largest available datasets, the UK Biobank.

The scope of the research is shaped by both the strengths and limitations of the data and methodologies applied. Cannabis use was self-reported as lifetime exposure, and neuroimaging outcomes were derived from cross-sectional structural and functional magnetic resonance imaging (MRI) scans. Cognitive performance was assessed through both cross-sectional and longitudinal measures, covering multiple domains including memory, attention, and executive function. This design enables a broad, systems-level exploration of potential cannabis-related effects on brain health and cognitive aging.

Nevertheless, several limitations define the interpretive boundaries of this work. While the UK Biobank cohort is large and population-based, it is not fully representative of the general population. Participants are generally healthier, better educated, and less likely to engage in high-risk behaviours, and cannabis use disorder (CUD) are underrepresented. As such, findings may be more generalisable to light or moderate users than to those with problematic or clinical levels of use.

Moreover, the cannabis exposure data lack granularity in several key areas. Variables such as age of initiation, cumulative duration of use, product potency, and cannabinoid composition (e.g., THC-to-CBD ratio) were not available. These limitations constrain the ability to comprehensively characterise patterns of use or to evaluate differential effects associated with specific types or compositions of cannabis. Additionally, the classification of high-frequency users in this study likely encompasses a heterogeneous group due to the broad nature of the variable, limiting the ability to disentangle cannabis-related effects by dose or frequency.

Although MR is used to strengthen causal inference, it is not immune to assumptions and constraints. MR estimates reflect lifelong genetic liability to cannabis use, which may not align perfectly with actual usage patterns. Furthermore, MR assumes no unmeasured pleiotropy or confounding between instruments and outcomes, assumptions that cannot be fully tested.

These methodological and data-related constraints are not unique to this study but reflect broader challenges in epidemiological cannabis research. A more detailed discussion of these limitations and their implications is provided in **Chapter 7, Section 7.4**.

## 1.5 Thesis outline

This thesis is organised into seven chapters, each addressing a distinct component of the research. The structure follows a logical progression from conceptual framing and literature context through methodological implementation, analytical findings, and broader interpretation.

- Chapter 1 introduces the study by outlining the background, aims and objectives, novel contributions, and scope and limitations. It presents the rationale for examining the associations between lifetime cannabis use and brain structure, brain function, cognitive outcomes, and dementia risk in later life.

- Chapter 2 provides a comprehensive review of the relevant literature. Topics covered include global trends in cannabis use, cannabinoid pharmacology, and the biological mechanisms of the endocannabinoid system. The chapter also synthesises prior research on the effects of cannabis on brain structure, functional connectivity, cognitive performance, and dementia risk, and identifies key gaps in the existing literature.

- Chapter 3 outlines the methodological framework of the study. It details the sample and data sources, with a focus on the UK Biobank data, and describes the measures of cannabis use, brain imaging, cognitive function, and confounding variables. The chapter also explains the selection of genetic instruments and the statistical approaches used for both observational and MR analyses.

- Chapter 4 presents findings on the association between cannabis use and brain structure, including both GM and WM outcomes. Results from observational and genetic analyses are reported, beginning with a hypothesis-driven investigation of the association between lifetime cannabis use and GM volume of the hippocampus. This is followed by an exploratory, whole-brain analysis examining associations across all IDPs.

- Chapter 5 investigates the relationship between cannabis use and functional brain connectivity, focusing on both task-based and resting-state networks. The chapter presents results from observational analyses and MR, providing insight into potential cannabis-related associations in functional brain network organisation.

- Chapter 6 examines associations between cannabis use, cognitive performance, and dementia risk. It integrates cross-sectional and longitudinal cognitive data to assess domains including working memory, attention, processing speed, executive function, reasoning, and episodic memory and applies MR to explore potential causal relationships with cognitive performance and dementia risk.

- Chapter 7 synthesises findings across domains and methods, integrating results from both observational and genetic analyses. It discusses public health and clinical implications, addresses the study's limitations, considers ethical issues related to cannabis research in older adults, and outlines directions for future research. The thesis concludes with reflections on the broader significance of the findings.

# Chapter 2: Literature Review

## 2.1 Overview and prevalence of cannabis use

Cannabis is currently the most widely cultivated and consumed illicit drug worldwide, followed by opioids and amphetamines. According to the World Drug Report as of 2024, an estimated 228 million people, accounting for 4.4% of the global population aged 15-64, reported the use of cannabis [1]. The prevalence of cannabis use has increased significantly over the past decade, most prominently in regions that have legalized it for medical or recreational purposes [66]. The trend towards legalization or decriminalization has been accompanied by changes in societal perceptions and policy reforms in different parts of the world [7, 8].

In 2013, Uruguay was the first country in the world to fully legalise recreational cannabis, followed by Canada in 2018 [9]. While Mexico has proposed cannabis legalization, which is currently under review, other countries such as Colombia, Argentina, Peru, Ecuador and Chile have legalised medical cannabis and are considering legal changes [10]. In the United States, most states have legalized medical cannabis, and a growing number have decriminalized or legalized recreational use [7]. In 2024, Germany partially legalized recreational cannabis for adults over 18 years, which is expected to influence policy shifts in other European countries [11]. In Asia, Thailand became the first country in the region to legalize medical cannabis in 2018 and to decriminalize low-THC cannabis products by removing them from the list of narcotic drugs [12].

The legalisation trend has also been accompanied by an increase in the potency of the cannabis-based products, particularly in the concentration of delta-9-THC, the primary psychoactive chemical component in cannabis [13, 14]. Substance with a higher potency is associated with increased frequency of use and thereby a higher risk of leading to addiction [14]. Cannabis is associated with youth culture, as the age of initiation in general is lower compared to other drugs [15]. Globally, drug use among individuals aged 18–25 is higher compared to any other age group, where cannabis remains the most commonly used drug among adolescents. Among students aged 15–16, the global past-year prevalence of cannabis use was estimated at 4.7% in 2018, where the rate among the general population aged 15-64 was 3.9%. **Figure 1** shows the global and regional past-year prevalence of cannabis use among individuals aged 15–16 compared to the general population aged 15-64 [16].

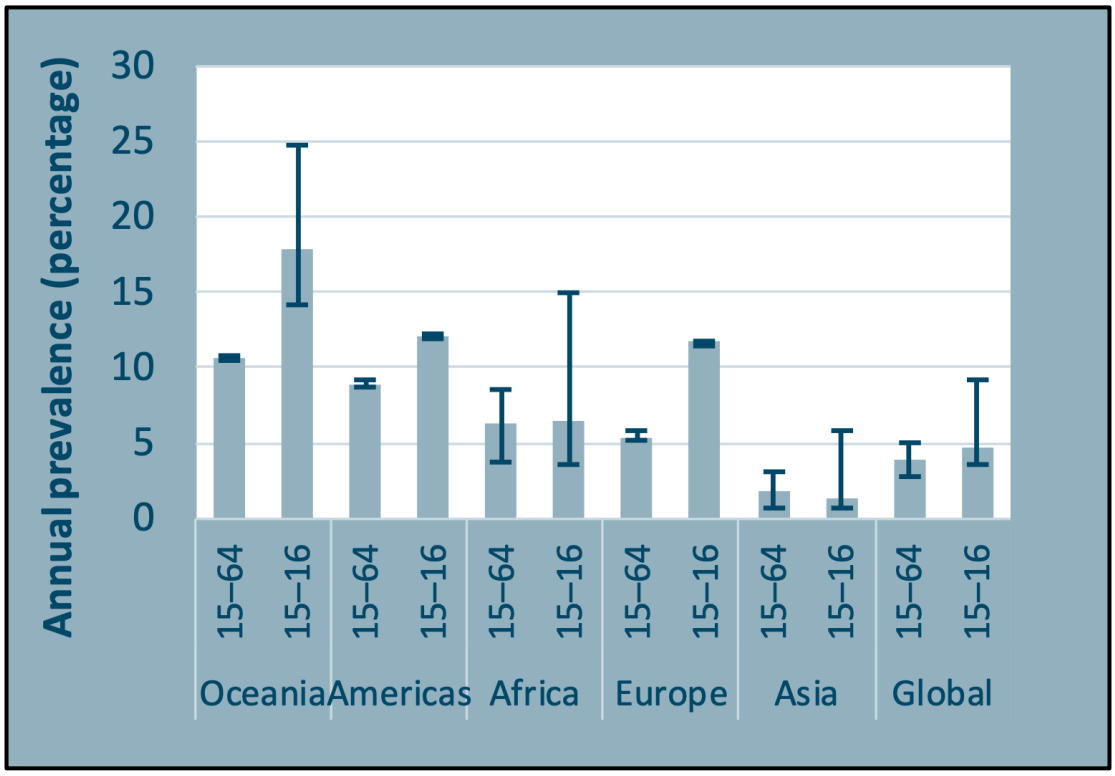



*Figure 1: Global and regional past-year prevalence of cannabis use among people aged 15–16 years, and among the general population aged 15–64 years, 2017*

Note: The estimate of the annual prevalence of cannabis use among those aged 15-16 is based on school surveys in most countries and may not be representative of all individuals in this age group. Source: United Nations Office on Drugs and Crime (UNODC) World Drug Report, 2020 [16].

The prevalence of cannabis use also varies across different regions and subregions. In 2018, North America reported the highest annual prevalence rates at 14.6%, followed by Australia and New Zealand at 10.6%, and West and Central Africa at 9.3%. However, some regions in Asia and the Middle East reported significantly lower usage rates. **Figure 2** shows the cannabis use prevalence in 2018 by regions and subregions [16].

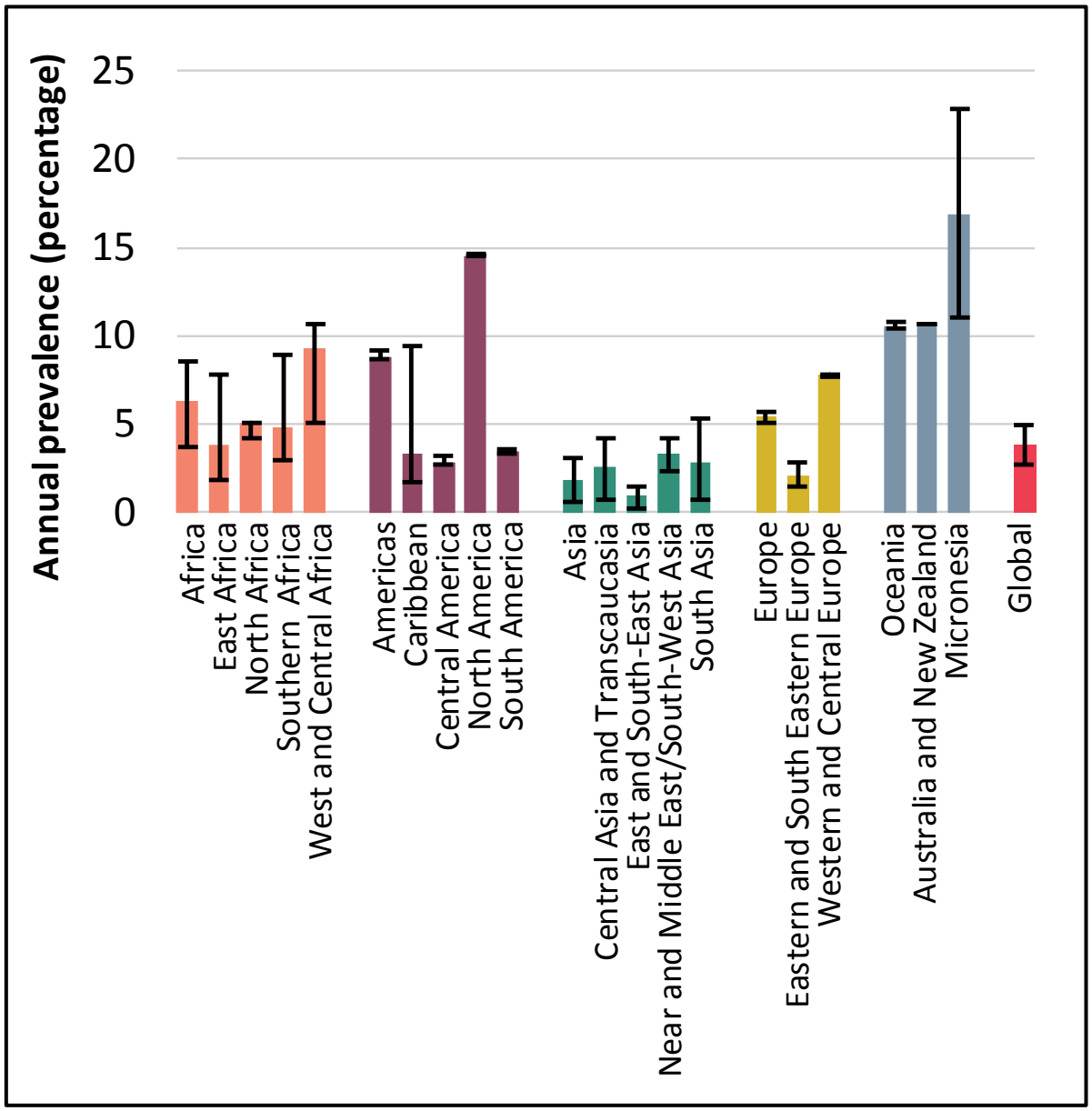



*Figure 2: Cannabis use, by region and subregions, 2018*

Source: United Nations Office on Drugs and Crime (UNODC) World Drug Report, 2020 [16].

In Western and Central Europe, cannabis use among individuals aged 15–64 has fluctuated modestly between 6% and 7% over the past decade. **Figure 3** illustrates trends in cannabis use across selected countries between 2004 and 2018. Germany and Norway have maintained relatively stable and moderate prevalence levels (~4–5%), while Sweden and Portugal report consistently low rates (~2–3%). In contrast, Spain and Italy exhibit the highest usage, with Italy peaking sharply around 2008–2010 (up to ~15%) and Spain consistently reporting high levels (~10–12%) throughout the period. The Netherlands also displays a consistently high prevalence (~7–9%) with minor fluctuations. The United Kingdom (England and Wales) shows a gradual increase from approximately 6% to nearly 8%, indicating a steady upward trend in use [16]. However, actual prevalence estimates of cannabis use in the UK may differ from those

generated by the Crime Survey for England and Wales, which may underestimate true levels of use. Self-reported rates from an online panel survey were notably higher, with 51.3% reporting lifetime use and 11.9% reporting past-year use (age range 18–64 years), compared to Crime Survey for England and Wales estimates of 37.2% lifetime and 5.8% past-year use (age range 18–59 years) [67]. Obtaining more accurate estimates of cannabis use is essential for informing evidence-based policy decisions and for the effective planning and allocation of health services aimed at addressing cannabis-related risks. It should be noted that **Figure 3** shows trends in selected Western and Central European countries between 2004 and 2018 and therefore does not capture more recent increases.

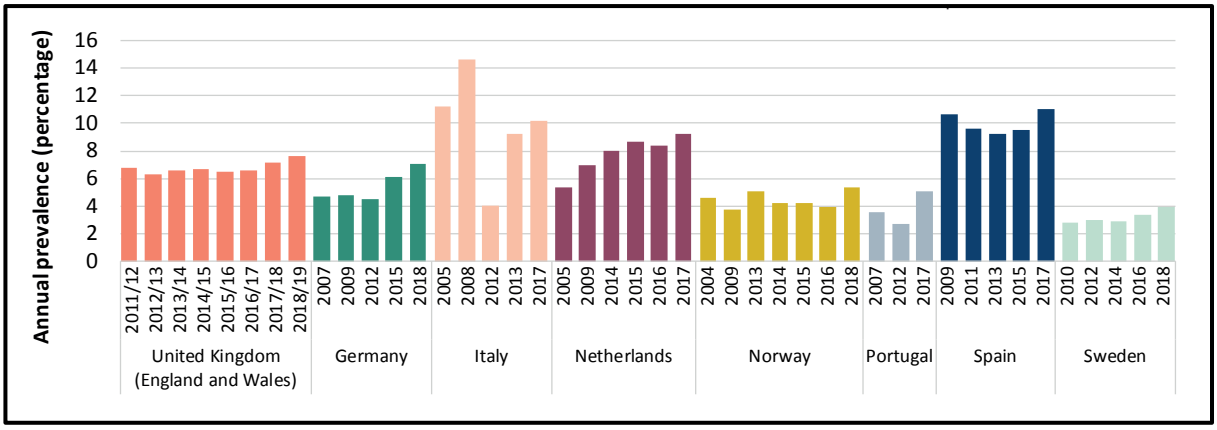



*Figure 3: Trends in past-year cannabis use in selected Western and Central European countries, 2004–2018*

Source: United Nations Office on Drugs and Crime (UNODC) World Drug Report, 2020 [16].

To summarise, cannabis use prevalence has increased significantly across age groups as well as globally. The rising trends in cannabis use, particularly among mid-to-old age adults, a demographic which is significantly underrepresented in the literature, need to be addressed both in terms of research and public health initiatives.

## 2.2 Types and forms of cannabis

Cannabis, also known as marijuana, is a natural product derived primarily from the cannabis sativa plant. It contains over 500 chemical compounds, of which around 104 are cannabinoids [68]. The two most well-studied and active cannabinoids are THC and CBD [2]. THC is the primary psychoactive component of cannabis and is well known for inducing the feeling of being “high” or a sense of euphoria [69].

The content and potency of THC have varied significantly across different sources and preparation methods [70, 71]. In the past 20 years, advanced cultivation and plant-breeding techniques have significantly increased THC concentration in cannabis-based products.

Compared to an average concentration of 10mg of THC in a cannabis cigarette in the 1960s, modern cannabis products may contain anywhere between 150-300mg of THC [70]. This tremendous increase in THC concentration raises concerns of the potential short- and long-term health effects [72].

In recent years, the diversity of cannabis products available for recreational and medicinal use has expanded significantly. Beyond traditional plant material, users now commonly consume concentrated oils, edibles, and vaporized extracts. Some of these products, such as "dabs" or high-potency THC oils, can contain THC concentrations exceeding 70–90%, far beyond the levels present in natural cannabis flowers [70–73]. The increased availability of these high-potency products raises concerns about their potential to overstimulate the endocannabinoid system, particularly CB1 receptors, which may increase the risk of adverse cognitive and psychiatric outcomes [74]. This trend also complicates comparisons across studies, as the form and potency of cannabis used can drastically influence both pharmacokinetics and neurobiological impact [73].

Additionally, recent attention has turned to lesser-known forms of THC, such as delta-8-THC, a structural analogue of delta-9-THC with lower potency but similar receptor binding properties. Although delta-8-THC occurs naturally in small amounts, it is now commonly synthesized from hemp-derived CBD and marketed as a legal alternative in some jurisdictions [75]. Like synthetic cannabinoids (e.g., "Spice," "K2"), which fully activate CB1 receptors with greater potency than natural THC, these emerging compounds have unclear safety profiles. Their rise in popularity underscores the need for further research into how variations in cannabinoid structure, potency, and delivery method influence endocannabinoid signaling and, consequently, brain health [76].

Cannabinoids are found in different parts of the cannabis plant, including the stalks, leaves, flowers, and seeds. Female cannabis plants produce raisins, which are particularly rich in THC [70, 77]. The active component in marijuana, i.e. THC, which contributes to its desirable effect, was not well known until researchers observed the calming and sedative response after injecting THC into aggressive rhesus monkeys. This led to the discovery of the specific receptors in the brain that bind with THC, and hence were named cannabinoid receptors [68, 70, 78]. Cannabis can be consumed in multiple forms, including smoking, vaporization, and ingestion. The route of administration of cannabis can affect the onset, intensity and duration of its effects [73].

### 2.3 The endocannabinoid system

A key pathway through which cannabis exerts its effects is the endocannabinoid system, a complex signalling network in the human body with which THC interacts to produce its effects. The endocannabinoid system is composed of cannabinoid receptors, primarily CB1 and CB2 (cannabinoid receptors 2), endogenous ligands, and metabolic enzymes [74, 79]. The main

target of THC is the cannabinoid CB1 receptors, which are highly abundant in the central nervous system and the brain, particularly in regions associated with cognition, emotion, and reward, including the prefrontal cortex, amygdala, hippocampus, hypothalamus, and forebrain (**Figure 4**) [3–6]. CB2 receptors are mainly found in the peripheral tissues, especially within the immune system, including spleen, immune cells, and gastrointestinal tract [3, 6].

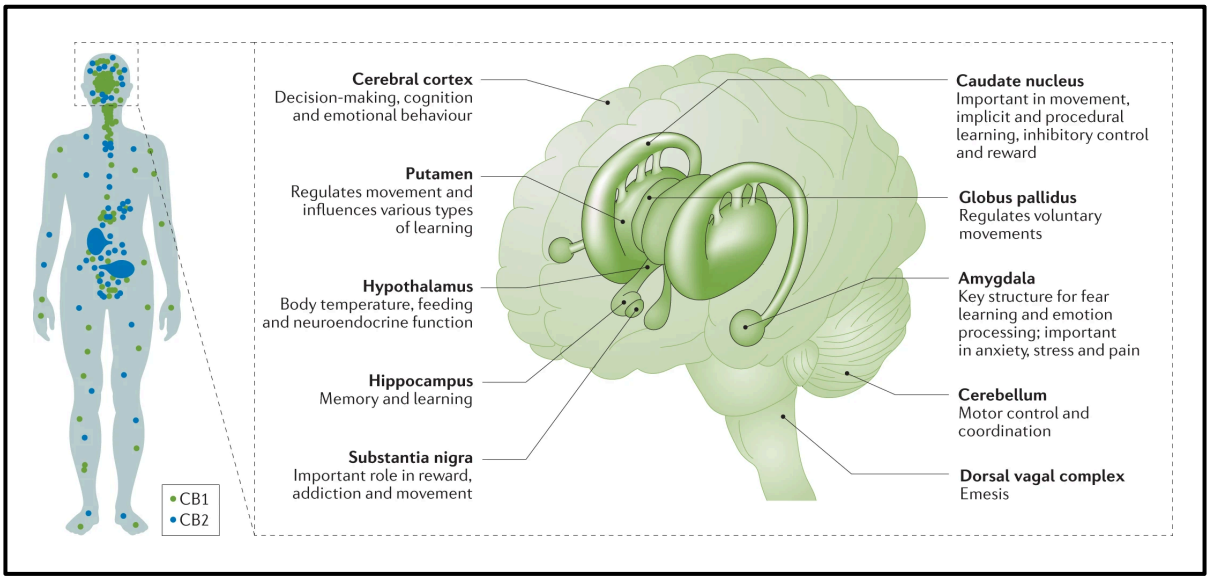



*Figure 4: Distribution of cannabinoid receptors (CB1 and CB2) in human brain and peripheral organs*

Sources: Adapted from Connor et al., 2021[5]. Part **a** is adapted from ref. [80], CC BY 4.0 (). Part **b**, image courtesy of the Canadian Consortium for the Investigation of Cannabinoids [81].

The endocannabinoid system uses endogenous cannabinoids (endocannabinoids) such as arachidonic acid and 2-arachidonylglycerol [82, 83], which bind to CB1 and CB2 receptors to maintain various physiological processes such as memory, mood, stress response, pain perception, and appetite [84]. THC acts as a partial agonist by binding to CB1 receptors and mimicking the action of these endogenous ligands. This, in turn, disrupts the normal functioning of the brain due to the changes in neurotransmitter release and synaptic signaling [85]. This is believed to increase the release of dopamine, glutamate and acetylcholine in certain brain regions, possibly by inhibiting the release of an inhibitory neurotransmitter like GABA onto dopamine, glutamate or acetylcholine-releasing neurons (**Figure 5**) [86, 87]. Understanding the endocannabinoid system and the evolving potency of cannabis is crucial for assessing the impacts of cannabis use on brain structure, function, and cognition, especially in vulnerable populations such as older adults.

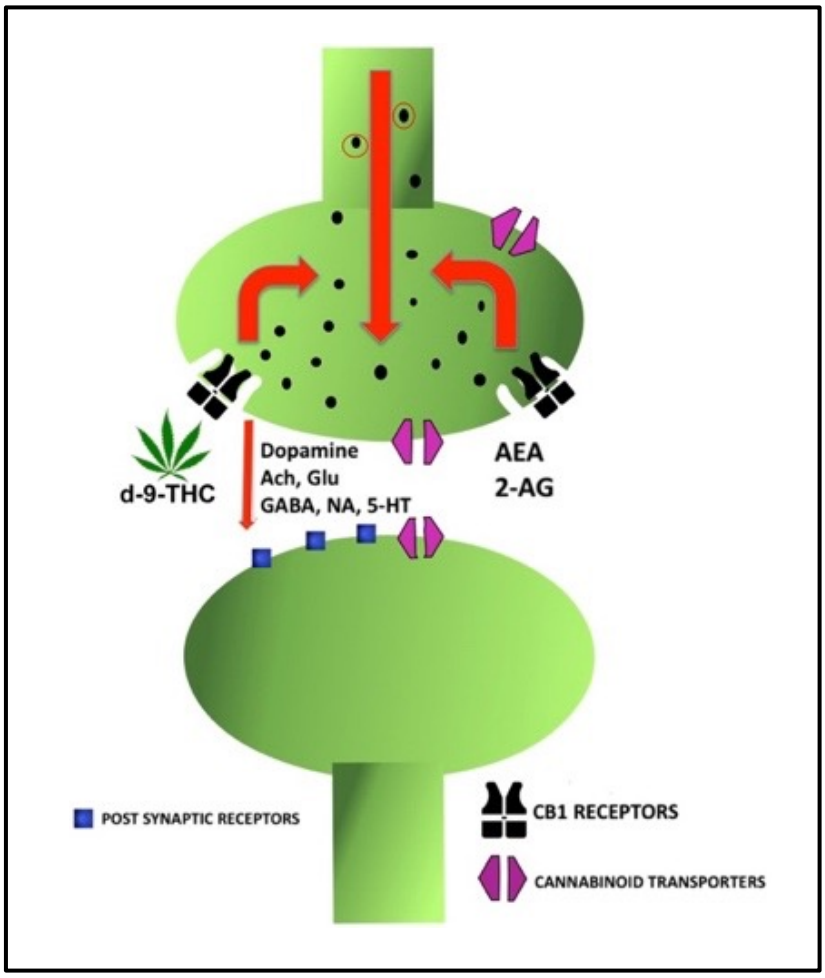



*Figure 5: CB1 receptor activity: effects of endocannabinoids (Arachidonic acid and 2-arachidonylglycerol) and Δ9-THC on neurotransmitter release at the synapse*

Sources: Adapted from Atakan et al., 2011 [87].

## 2.4 Clinical phenotypes and comorbidity

Cannabis use is studied both in terms of clinical diagnoses (e.g., cannabis use disorder) and non-clinical measures of exposure (e.g., ever-use or frequency). The Diagnostic and Statistical Manual of Mental Disorders, Fifth Edition (DSM-5) defines CUD by the presence of at least two out of eleven criteria within a 12-month period, reflecting impaired control, social impairment, risky use, and pharmacological features such as tolerance and withdrawal. Severity is specified as mild (2–3 criteria), moderate (4–5), or severe (≥6) [88]. In parallel, the International Classification of Diseases, Tenth Revision (ICD-10) classifies cannabis-related disorders under F12 (with fourth-character subdivisions such as harmful use, dependence, withdrawal, psychotic disorder, and amnesic syndrome), while ICD-11 classifies them under 6C41 (including harmful pattern of use, dependence, withdrawal, cannabis-induced delirium, and cannabis-induced psychotic disorder), encompassing both substance use and cannabis-

induced mental or behavioural syndromes [89]. Importantly, these diagnostic constructs differ from the non-clinical measures of cannabis exposure often used in epidemiological cohorts, which reflect use but not disorder [90].

*Risk factors and developmental trajectory:* The likelihood of developing CUD is highest in adolescence and early adulthood, with peak onset between ages 18–30. Early initiation is particularly important: those who begin using before age 16 are at substantially increased risk, and weekly or daily use during youth elevates the risk 8–17 fold [91]. Neuroimaging studies suggest that adolescent cannabis use is associated with accelerated cortical thinning, particularly in prefrontal regions, as shown in the IMAGEN cohort [92, 93]. Emerging data from the ABCD study also point toward neuroanatomical differences associated with early cannabis initiation [94], though the evidence of thinning over time in ABCD is still developing. Sex is another key determinant: while males are more likely to be diagnosed with CUD overall, females show faster progression, greater withdrawal severity, and higher comorbidity with mood and anxiety disorders [91].

*Construct validity:* Recent validation work indicates DSM-5 CUD severity levels have construct validity. In adults with problematic substance use, mild and moderate CUD were chiefly associated with cannabis-specific validators (use frequency, craving, perceived problems), whereas severe CUD additionally correlated with psychiatric comorbidity, functional impairment, and greater social impairment, supporting the clinical utility of the three-level severity distinction [90, 95].

*Polysubstance comorbidity:* Cannabis use rarely occurs in isolation. Tobacco and alcohol are the most common co-used substances, both of which may independently affect brain structure, function or cognition [96, 97]. A large-scale imaging study reported that even moderate alcohol intake is associated with widespread reductions in GM volume, altered WM microstructure, and changes in functional connectivity [96]. Similarly, smoking has been linked to lower total and regional GM volumes, particularly in the thalamus, as well as reduced cognitive performance, with some evidence of partial recovery following cessation [97]. Yet, many neuroimaging studies inadequately adjust for these exposures, relying on crude self-report or omitting alcohol- or tobacco-only comparison groups [98]. This methodological gap complicates attribution of brain differences to cannabis specifically.

*Psychiatric comorbidity and psychosis risk:* Elevated rates of mood, anxiety, and psychotic disorders are consistently observed among cannabis users [95]. The association between cannabis and psychosis has been debated for decades. Longitudinal cohort studies show a dose–response pattern whereby more frequent cannabis use predicts higher risk of later psychotic outcomes, and earlier initiation (mid-teens) further elevates risk [99]. Importantly, recent evidence indicates that this relationship persists even after accounting for genetic liability. For example, Austin-Zimmerman et al. (2024) reported that daily use of high-potency cannabis increases psychosis risk independently of polygenic risk for schizophrenia, suggesting additive rather than interactive effects of genetic and environmental risks [100]. This converges with

earlier meta-analyses showing that cannabis use predicts psychotic outcomes even after adjusting for confounders and baseline symptoms [101].

Taken together, these findings highlight the complexity of cannabis phenotyping in research. Diagnostic frameworks such as DSM or ICD capture disorder, whereas population-based cohorts often rely on frequency-based measures of exposure. Moreover, the high prevalence of polysubstance use and psychiatric comorbidity means that cannabis-related brain associations cannot be interpreted in isolation. Careful phenotyping and rigorous adjustment for confounding factors are essential for drawing valid conclusions about cannabis's neurobiological and cognitive effects.

## 2.5 Effect of cannabis on brain: insights from animal studies

The understanding of how THC impacts the brain largely stems from studies on rodents and non-human primates. These models provide a controlled setting to examine THC's effects at cellular, molecular, and systems levels. While findings cannot be generalised directly to humans, they offer important mechanistic insights into the neurobiological processes that may underlie cannabis-related changes in brain structure, function, and cognition. These studies have reported both neurochemical and morphological changes in brain regions with high expression of CB1 receptors following THC exposure [28, 29, 102, 103]. THC has been shown to induce dose-dependent neurotoxicity in cortical neurons and to cause structural differences in hippocampal regions, with prolonged exposure associated with impairments in cognitive performance [104, 105]. Consistent with these findings, CB1 receptors are densely expressed in cortical and hippocampal areas, as demonstrated by Positron Emission Tomography receptor-mapping studies [106]. These findings are derived from a range of experimental techniques, including intracranial microinjection, electrophysiological recordings, and behavioural paradigms such as place conditioning and self-administration, which have allowed for controlled investigation of THC's neurobiological effects.

While most preclinical studies have used injection as the route of cannabinoid administration [34, 107, 108], smoking is the primary method of cannabis use in humans. To explore this, one rat model examined whether acute cannabis smoke exposure affects working memory. In this study, smoke exposure did not impair cognitive performance in male rats, whereas female rats demonstrated improved working memory accuracy compared to their baseline performance. A subsequent experiment, however, found that acute THC administration impaired working memory performance [109]. These findings suggest that variations in dose, timing, and route of administration may influence cognitive outcomes, which warrants further investigation.

Brain regions that have shown structural and functional changes associated with THC include the hippocampus, amygdala, cerebellum, prefrontal cortex, and striatum [104–106, 110, 111]. In studies on male rats, prolonged THC exposure has been associated with morphological changes in the hippocampus, potentially reflecting associations related to learning and memory.

These changes resemble those observed after ischemic or toxic damage [110]. In the prefrontal cortex, exposure to cannabinoid agonists during early and mid-adolescence was reported to result in frequency-dependent disinhibition, i.e., repeated CB1 receptor activation reduces inhibitory signaling in adulthood due to the downregulation of gamma-aminobutyric (GABA) transmission. These associations in the prefrontal cortex may also reduce synaptic plasticity, which is critical for the maturation of neural circuits involved in decision-making and executive functioning [112].

Further studies in rats exposed to THC have reported sex-specific volumetric and microstructural differences in the striatum, globus pallidus, lateral ventricles, thalamus, and septal nuclei. A reduction in the volume of the lateral ventricles and globus pallidus was observed in THC-treated females, along with a decrease in dorsal striatal volume, which was not observed in males. Rats administered THC also showed reduced fractional anisotropy (FA) in several WM tracts, particularly in rostral sections. In adolescent male rats, THC exposure was found to disrupt and delay myelination in the dorsal striatum, as indicated by lower FA values. Additionally, male rats displayed increased metabolism in the cerebellum and olfactory bulb and decreased metabolism in the cingulate cortex. In contrast, female rats exhibited hypermetabolism in a cluster of voxels encompassing the entorhinal and piriform cortices, as well as in the cingulate cortex. These findings indicate that adolescent THC exposure has a profound and lasting impact on brain structure and function in a sex-specific manner [113].

Recent studies have further emphasized the age-dependent effects of THC on brain structure and function. Komorowska-Müller et al. (2023) demonstrated that administration of a low dose of THC (3 mg/kg/day) over 28 days led to increased dendritic spine stability and density in the somatosensory cortex of aged mice, correlating with improved spatial memory performance. In contrast, the same treatment in young mice induced transient spine destabilization and cognitive impairment. These opposing effects were linked to differences in endocannabinoid tone and synaptic plasticity across the lifespan. In aged mice, THC was also associated with reduced H3K9 methylation and upregulation of brain-derived neurotrophic factor, potentially enhancing synaptic structure via TrkB receptor activation. These findings suggest that while low-dose THC may counteract age-related synaptic decline, it can disrupt neural integrity in the developing brain, highlighting the importance of age and neural context in mediating cannabinoid effects [114].

Sex differences have also emerged as a significant factor in cannabinoid neurobiology, with accumulating evidence showing that female animals often exhibit greater neurophysiological sensitivity to THC than males. Farquhar et al. (2018) investigated the effects of repeated THC administration (30 mg/kg, twice daily for one week) on CB1 receptor density and G-protein coupling in several brain regions of male and female rats. While vehicle-treated animals showed minimal sex differences in receptor characteristics, except for enhanced CB1 activation in the hippocampus of females, THC exposure resulted in widespread receptor downregulation and desensitization in both sexes, with significantly greater effects in females across all regions examined, including the hippocampus, cerebellum, prefrontal cortex, and striatum. These results align with human studies reporting faster progression to cannabis tolerance and

dependence in women, suggesting that sex-related neurobiological mechanisms, particularly involving CB1 receptor signaling, may contribute to differential outcomes in repeated or prolonged cannabis exposure [115].

On a cellular level, repeated or prolonged cannabis exposure triggers several neuroadaptive processes that may underlie its cognitive and structural effects [111, 116, 117]. One prominent change observed in animal models is a reduction in cannabinoid receptor signaling capacity: prolonged THC administration leads to CB1 receptor downregulation and desensitization in the brain [115]. Additionally, repeated THC can induce neuroinflammatory responses. Studies have found that THC exposure activates microglia (the brain's immune cells) and promotes pro-inflammatory signaling, which may contribute to neuronal damage and cognitive deficits associated with long-term use [116–119]. There is also evidence that adolescent THC exposure can induce lasting epigenetic modifications in the brain, resulting in reprogramming of gene expression, particularly affecting genes related to synaptic plasticity [111, 117, 119]. These molecular and cellular associations provide a mechanistic basis for the structural changes and functional impairments reported in studies of repeated or prolonged cannabis studies [110, 111, 113].

Overall, the expanded body of animal research reinforces that repeated or prolonged cannabinoid exposure can produce persistent changes in brain structure and function across the lifespan [103, 110, 111, 113]. Long-term THC exposure, especially during critical periods like adolescence or prenatal development, is associated with lasting impairments in learning, memory, and executive functions, accompanied by anatomical changes in regions such as the hippocampus and prefrontal cortex [110–113, 120, 121]. At the same time, certain low-dose or short-term exposures hint at potentially complex or even beneficial effects under specific conditions (as seen in aged animals), emphasizing that dose and timing are crucial determinants of outcomes [114, 122]. Taken together, these findings underscore the complexity of cannabis's impact on the brain. They highlight the need for careful consideration of age, sex, dose, and duration in both preclinical experiments and in translating these results to humans [111, 115, 117]. Importantly, insights from animal models continue to inform current understanding of cannabis-related neurobiological mechanisms and risks, guiding future research and potential clinical interventions in the context of brain health [103, 111, 117].

In addition, there is evidence of developmental toxicity associated with prenatal THC exposure [120, 121, 123]. Animal studies have reported that even low doses of cannabinoid compounds administered during development can result in altered locomotor activity, cognitive impairments, emotional behaviour changes, and increased drug sensitivity later in life. Further evidence indicates that cannabinoids may induce enduring neurobehavioral abnormalities in exposed offspring, with some findings that parallel clinical reports of hyperactivity, cognitive deficits, and emotional disturbances in humans prenatally exposed to cannabis [121].

Most animal studies have reported that prolonged exposure to cannabinoid compounds leads to persistent impairments in learning and memory. However, one study found that a single ultra-low dose of THC reversed age-related cognitive decline in aged mice. In this study, THC-

treated mice showed elimination of cognitive deficits that persisted for at least seven weeks. MRI also revealed increased brain volume and tissue density in several brain regions. Nonetheless, these findings are correlational, and no definitive causal relationship has been established between the structural changes and the observed cognitive improvements [122]. This contrast underscores the complexity of cannabinoid effects on the aging brain and highlights the importance of dose, timing, and duration of exposure in interpreting cognitive outcomes.

Animal studies have been instrumental in localizing specific brain regions associated with cannabis exposure under controlled conditions. This has provided more precise insight into the neurobiological mechanisms associated with cannabis use and may further support the application of these findings in informing both human research and clinical practice. Findings from these models have revealed dose-dependent structural associations, impairments in learning and memory, and sex-specific vulnerabilities, particularly in brain areas such as the hippocampus, prefrontal cortex, and striatum. The use of advanced imaging and behavioural techniques in animals continues to be a critical resource for identifying long-term effects and informing potential therapeutic or preventative strategies. While these findings cannot be taken as direct evidence in humans, they highlight mechanisms and vulnerable brain regions that provide an essential framework for interpreting neuroimaging and cognitive studies.

## 2.6 Effects of cannabis on brain structure

Structural MRI studies in humans have reported associations between cannabis use and differences in both GM volume and WM microstructure, particularly in brain regions enriched with CB1 receptors [24, 36, 46, 124–128]. CB1 receptors are known to be highly expressed in several key structures, including the hippocampus, basal ganglia, cerebellum, and prefrontal cortex [3–6]. They are also found in olfactory regions, caudate putamen, accumbens nucleus, substantia nigra, globus pallidus, periaqueductal GM, dorsal horn of the medulla, cingulate gyrus, neocortex, hypothalamus, amygdala and solitary nucleus [129–131]. These brain regions are implicated in a range of functions including memory, stress responsivity, reward and motivated behaviour, mood regulation, motor coordination, cognition and pain.

The understanding of cannabis-related structural brain changes primarily stems from studies conducted in adolescents and young adults who engage in regular, daily or near-daily recreational cannabis use [124, 132]. Both long-term and recent cannabis use in these populations has been associated with reductions in localized hippocampal GM volumes [24, 45, 46, 133, 134]. These reductions were observed specifically in hippocampal subregions with high CB1 receptor density, and not in areas such as the parietal cortex, which has low CB1 receptor expression [23]. Notably, hippocampal volume reductions associated with adolescent cannabis use have been shown to persist into adulthood, with structural associations lasting several decades even after extended periods of abstinence, suggesting long-term impacts on brain integrity [37].

Although most structural MRI findings relate to regular or long-term cannabis use, experimental studies of acute cannabinoid administration suggest that single-dose exposure primarily induces rapid neurochemical rather than morphological changes. Acute cannabis exposure does not produce detectable changes in brain structure on MRI, and the systematic review by Cupo et al. (2021) [135] emphasizes that structural alterations are documented almost exclusively in the context of chronic or long-term use, not single-dose experimental administration. Nonetheless, acute studies reveal rapid neurochemical effects relevant to structural pathways. Using magnetic resonance spectroscopy, Colizzi et al. (2020) [136] demonstrated that 10mg oral THC acutely increased glutamate+glutamine (Glx) concentrations in the left caudate head, particularly among individuals with lower baseline Glx and greater psychotomimetic response, suggesting acute modulation of excitatory neurotransmission [135]. PET studies also show that acute THC can influence striatal dopamine availability: for instance, Bossong et al. (2009) [137] found reduced [11C]-raclopride binding in the ventral striatum after inhaled THC, consistent with increased dopamine release, although other studies reported null findings [138], reflecting methodological variability [135]. Together, these studies indicate that while acute cannabis does not alter structural morphology, it produces immediate neurochemical shifts within striatal and limbic pathways that underpin longer-term structural and functional vulnerabilities.

Structural neuroimaging studies have reported persistent differences even after extended periods of abstinence. Cross-sectional work in adolescents and young adults abstinent for approximately one month has identified alterations in cortical thickness and regional brain morphology [139–142]. Evidence for recovery of brain structure is limited, as most abstinence research has focused on functional rather than structural outcomes, and the few available studies suggest that some structural differences may outlast acute intoxication and early withdrawal. Heterogeneity in imaging protocols and mixed use of cognitive and MRI-based tasks further complicate interpretation, underscoring the need for longitudinal structural MRI studies extending beyond the first month of cessation.

Associations between cannabis use and amygdala volume have yielded inconsistent and mixed results [46, 125, 143–149]. Some studies report reduced amygdala volumes in cannabis users, for instance, reductions of approximately 7.1% compared to non-users, while others have found no significant differences [46]. One study noted smaller left amygdala volumes in cannabis users aged 22–35 years, although the differences fell within the range of normal anatomical variation and appeared to be largely driven by shared genetic factors [143]. In contrast, other research has reported increased GM density or volumetric reductions in the amygdala, further highlighting variability in the findings [148].

Beyond the hippocampus and amygdala, several other brain regions have been implicated in cannabis-related structural changes. Some studies have reported larger volumes in areas such as the left nucleus accumbens (extending to the subcallosal cortex), hypothalamus, sublenticular extended amygdala, and left amygdala [148]. However, other studies found no significant associations between cannabis use and subcortical structures, including the

putamen, caudate, pallidum, hippocampus, amygdala, nucleus accumbens, and thalamus [150]. Additionally, some studies reported that cannabis users had similar or even larger cerebellar volumes than non-users [24, 125]. Other brain regions rich in CB1 receptors that have shown GM volume reductions among cannabis users include the insula, orbitofrontal cortex, parahippocampal gyrus, medial temporal cortex, and temporal pole [24].

More recent studies and meta-analyses have provided additional insight into these structural effects, particularly among individuals with regular, frequent or daily cannabis use [98, 151]. A recent review has confirmed that regular, frequent, and long-term cannabis use—including use patterns consistent with CUD are indeed associated with brain volume differences in specific regions, most consistently the hippocampus and orbitofrontal cortex, which tend to be smaller in cannabis users than in non-users [5, 98, 132, 152, 153]. Similarly, another recent analysis focusing on individuals with CUD found reductions in subcortical structures including the thalamus, amygdala, nucleus accumbens, and hippocampus [151]. Notably, these structural differences appear to be most pronounced in near-daily or dependent users; studies often find no volumetric differences between non-users and users who consume cannabis less than near daily or without meeting criteria for dependence [150, 154]. This suggests a dose- or dependence-related threshold effect, wherein only frequent or long-term use leads to measurable brain structural associations.

In addition to GM associations, numerous studies have examined associations between cannabis use and WM microstructure [126, 127, 155–160]. These differences have frequently been observed in regions such as the superior longitudinal fasciculus, arcuate fasciculus, corpus callosum, and forceps minor [127, 156, 159–162]. These WM associations are typically measured using diffusion tensor imaging (DTI), with cannabis use often associated with lower FA and higher mean diffusivity (MD), which are indicative of disrupted WM tract integrity. Studies have also found that differences in WM integrity, particularly in the corpus callosum, are associated with the age of onset of cannabis use [162, 163]. Earlier onset has been linked with greater disruption in WM pathways, including impaired axonal connectivity in the splenium of the corpus callosum, the right fimbria of the hippocampus (fornix), and commissural fibers. Radial (L2 and L3) and axial diffusivity (L1) in these tracts has been shown to correlate with the age at which regular cannabis use began, suggesting increased vulnerability of the developing brain to cannabis-related WM associations [163].

Further studies have reported differences in WM microstructure across various frontal, temporal, and parietal tracts, as well as reductions in the inferior longitudinal fasciculus. These associations appear to vary according to the extent and duration of cannabis exposure over time [159, 164]. However, the evidence is inconsistent; other studies have reported no significant group differences in WM integrity [156, 165]. Interestingly, even when overall group differences were absent, early-onset cannabis use was still associated with lower FA and higher radial diffusivity in the inferior longitudinal fasciculus, superior longitudinal fasciculus, forceps major, and forceps minor [156].

Longitudinal studies examining the effects of cannabis use on brain structure are relatively scarce. One five-year follow-up study in adolescents found that higher lifetime cannabis use was associated with bilateral cortical thinning in the prefrontal cortex. Notably, cortical thickness at baseline was not predictive of later cannabis use, suggesting that cannabis exposure maybe associated with structural change. Moreover, cannabis use was found to accelerate age-related cortical thinning in a dose-dependent manner, with greater use over the five-year period associated with increased cortical thinning, primarily in prefrontal regions [166]. However, other longitudinal studies have not consistently replicated these findings [167, 168]. One study reported no association between adolescent cannabis use and GM volume or cortical thickness in adulthood [167], while another reported altered cerebellar development, including a greater increase in thickness in specific cerebellar lobules [168].

The literature on the effects of cannabis use in older adults is especially limited. One study focusing on individuals over the age of 60 who reported regular cannabis use found that these individuals exhibited GM reductions in the frontal pole and precentral cortex [169]. Additionally, in a study of 50 older adults (aged 57–75 years), former cannabis users who began regular cannabis use before age 20, used it ≥20 days/month for at least a year, and had been abstinent for nearly three decades (n = 24) showed reduced GM in hippocampal subregions. Importantly, these differences remained significant after controlling for age, sex, years of education, premorbid intelligence, and cigarette use [37]. These findings suggest that cannabis use during adolescence may have long-lasting structural consequences that persist into later life, potentially impacting brain aging.

Recent work using UK Biobank data has begun to address the limited evidence available in older adults. A large cross-sectional and longitudinal study of nearly 20,000 participants aged 60 years and above reported that lifetime cannabis users had smaller total brain, grey matter, white matter, and cortical grey matter volumes compared with non-users, with stronger associations observed among current users and among those who used cannabis more often, for longer durations, or started at younger ages. In contrast, longitudinal analyses indicated that cannabis use was associated with a slightly slower decline in total brain and cortical grey matter volumes between MRI assessments. These mixed findings highlight the complexity of cannabis–brain associations in ageing populations and provide important sample-specific context for interpreting the structural imaging results presented in this thesis [170].

Importantly, recent studies have begun linking these structural associations to functional outcomes. Cannabis-related brain changes have been correlated with cognitive performance differences, highlighting their potential relevance for brain health. For instance, lower left hippocampal volume in cannabis users was found to mediate poorer working memory performance [171]. Similarly, reduced volume in the left anterior cingulate cortex among young adult users was associated with lower accuracy on an emotion discrimination task [172]. Differences in cortical–subcortical circuits have also been tied to behavioural deficits: thinning of the entorhinal cortex and orbito-frontal cortex in male users correlated with worse verbal learning outcomes [173]. These findings underscore that the structural brain differences

observed in cannabis users are not merely anatomical; they may have real consequences for cognition and behaviour.

However, many of the observed associations between cannabis use and brain structure remain contradictory and inconsistent across studies. These discrepancies may be attributed to several factors, including variability in cannabis use patterns (e.g., severity, frequency, and age of onset), differences in sample characteristics (e.g., sex, comorbid substance use, socioeconomic background), and methodological variation across studies. Notably, co-use of alcohol and tobacco with cannabis is highly prevalent but often under-reported or not controlled for in analyses, despite clear evidence that these substances exert independent and potentially interacting effects on brain health [98]. Differences in MRI scanner hardware, image acquisition protocols, and preprocessing pipelines may introduce variability in structural findings [46, 124, 174, 175]. While current evidence supports a relationship between cannabis use and changes in brain structure, particularly in regions rich in CB1 receptors, heterogeneity in research design and imaging methods continues to pose a significant limitation to drawing definitive conclusions. Larger studies using advanced methodologies are needed to disentangle the direct effects of cannabis from pre-existing vulnerabilities, an essential step toward determining whether cannabis use causally contributes to lasting brain changes.

### 2.7 Effects of cannabis on brain function

Several studies have reported that cannabis use is associated with brain functional connectivity, both in resting-state and task-based fMRI [23, 26, 47, 61, 62, 176–181]. Resting-state studies in frequent or near-daily cannabis users, primarily adolescents and young adults, have consistently reported altered connectivity in networks such as the DMN, central executive network (CEN), salience network, and limbic systems [47, 61, 62, 176, 177]. The DMN is typically active during rest and internally directed thought, including self-referential processing and memory retrieval. The CEN supports goal-directed cognition, working memory, and attentional control. The salience network facilitates the detection of behaviourally relevant stimuli and the dynamic switching between the DMN and CEN. The limbic system, encompassing structures such as the hippocampus and amygdala, plays a central role in emotional processing, motivation, and memory [63]. Increased connectivity within the DMN and insular networks has been observed in near-daily cannabis users [61], while regional differences in connectivity involving the limbic and sensorimotor striatum, DMN, CEN, and salience networks have been found in regular users [47]. These networks are involved in processes such as self-referential thoughts, emotional processing, self-awareness, memory, cognitive control, decision making interoception, and conscious experience, highlighting potential cannabis-related disruptions in higher-order cognitive integration [182–184].

Advances in neuroimaging over the last few years have further detailed how cannabis use affects brain function. A systematic review of resting-state fMRI studies concluded that cannabis users often exhibit atypical connectivity in frontal networks, with about 40% of

studies finding elevated fronto-frontal, fronto-striatal, or fronto-temporal connectivity relative to non-users [185]. Altered cerebellar-cerebral connectivity has also been observed: cannabis users who reported regular (near-daily) use exhibited enhanced coupling between the anterior cerebellum and the posterior cingulate (a central DMN node), alongside reduced connectivity between other cerebellar subregions and the frontal and insular cortices [186].

In addition to these findings in frequent or long-term users, pharmacological neuroimaging studies of acute THC administration indicate that cannabis can rapidly alter brain function in otherwise healthy individuals. Acute cannabis administration consistently produces widespread functional alterations across cortico-limbic, striatal, and default-mode networks. Task-based fMRI studies reviewed by Cupo et al. (2021) [135] show that THC often reduces activation in prefrontal and insular regions during cognitive and inhibitory control tasks—such as decreased inferior frontal gyrus and anterior insula engagement during response inhibition [187, 188], while enhancing activity in limbic regions including the hippocampus and amygdala during emotional and mnemonic processing [135, 189, 190]. Resting-state studies demonstrate similarly pronounced effects: THC reduces connectivity between the nucleus accumbens and frontal–limbic regions [191], disrupts coupling within DMN hubs such as the precuneus [192], and increases connectivity between the dorsomedial prefrontal cortex and dorsal visual stream [135, 192, 193]. Arterial spin labelling further shows increased perfusion in the ACC, frontal cortex, and insula, alongside decreased perfusion in occipital regions following THC [194], highlighting the broad hemodynamic impact of acute intoxication [135]. Collectively, these findings indicate that acute THC produces significant functional disruptions, particularly in networks implicated in salience processing, emotional regulation, and psychosis risk.

Cannabis use has been specifically associated with weaker connectivity within the DMN, particularly between the posterior cingulate cortex and other DMN nodes, especially in adolescents and young adults [61, 177, 195]. Even after prolonged abstinence, associations in the connectivity of the DMN and CEN have been reported [196]. Functional neuroimaging evidence consistently indicates that cannabis-related alterations can persist despite abstinence. Differences in cerebral blood flow have been observed up to seven days after last use compared with controls [197], and fMRI studies of adolescents and young adults abstinent for approximately one month have reported continued differences in task-related activation [198, 199]. Additional studies show persistent abnormalities after two to four weeks of cessation, including altered inhibitory-control responses [200] and disrupted reward-processing activity in dependent users abstinent for around four weeks [201]. These findings align with a recent meta-analysis reporting that alterations within the default mode and central executive networks may persist for up to 25 days post-abstinence [196]. Collectively, the available evidence suggests that functional abnormalities can remain detectable for several weeks after cessation and may reflect enduring neural adaptations rather than residual intoxication alone, highlighting the need for longer-term longitudinal functional imaging studies.

Longer durations of cannabis use have also been linked with weakened connectivity in the DMN and other sensory and executive networks [177]. However, findings remain mixed, with some studies reporting increased connectivity and others reporting reductions, particularly in

regions such as the left posterior cingulate cortex and insula [61, 177]. These inconsistencies may be influenced by variations in age, frequency of use, and methodological differences across studies.

While most functional connectivity studies have focused on younger populations, cannabis-related effects in middle-aged and older adults remain limited. Recent findings suggest that older adult cannabis users (age 60-88) show stronger resting-state functional connectivity (rsFC) between the hippocampus, parahippocampal cortex, and anterior cerebellum compared to non-users—patterns resembling those seen in younger individuals. These results raise the possibility that cannabis use may help preserve age-sensitive neural circuits, though longitudinal research is needed to confirm this. Such connectivity patterns may have implications for cognitive aging and brain health in later life [40].

In addition to resting-state fMRI, task-based fMRI studies have investigated how cannabis use may affect brain activity during cognitive processing. These tasks have included working memory, decision-making, inhibition, reward processing, error monitoring, emotional reactivity, time perception, and cue-reactivity [26, 98, 200, 202–207]. A study on working memory reported cannabis users had increased activation in bilateral temporal regions and the right superior frontal gyrus on an N-back task relative to non-users, along with altered connectivity between frontal and temporal regions [207]. Furthermore, increased cannabis cue-reactivity has been associated with greater activation in brain regions involved in reward, attention, and memory processing, including the bilateral posterior cingulate, cuneus, fusiform, precuneus, inferior temporal and parahippocampal gyri, as well as left thalamus, medial frontal and superior frontal gyri [208].

Altered activation and connectivity during emotional and face processing tasks have been observed in cannabis users compared to controls [205]. During a monetary incentive delay task, weekly cannabis users showed higher feedback-related activity in the inferior parietal cortex and right frontopolar cortex [200], while more severe cannabis use, indexed by Cannabis Use Disorders Identification Test (CUDIT) scores, was linked to reduced activity in the lingual gyrus and putamen during inaccurate trials, and in the anterior cingulate cortex and dorsomedial prefrontal cortex during punished inaccurate trials [209]. Cannabis users, particularly those with higher CUDIT scores, exhibited reduced neural responsiveness to facial stimuli, characterized by altered activation in the left superior-medial prefrontal cortex and anterior cingulate cortex, irrespective of the emotion presented [205].

In addition, novel analytical approaches like dynamic causal modeling have shed light on how cannabis affects the directionality of information flow in cognitive circuits. For example, a study reported that individuals with CUD showed blunted changes in effective connectivity from the dorsolateral prefrontal cortex to the caudate during a working memory task, compared to healthy controls. At the same time, CUD participants had exaggerated connectivity changes in left and right dorsolateral prefrontal cortex during the task. Early-onset CUD was associated with unique connectivity patterns, characterized by greater working memory-related associations in effective connectivity between the left and right dorsolateral prefrontal cortex,

and comparatively smaller changes between the left ventrolateral prefrontal cortex and right dorsolateral prefrontal cortex [210].

Increased engagement of the DMN has been observed during task performance following THC administration, reflected in reduced deactivation of regions such as the posterior cingulate cortex and angular gyrus. This altered neural activity was accompanied by impaired task performance, including more false alarms and fewer detected targets [211]. Cannabis-related associations in central executive function, which are thought to support higher-order cognitive processes such as attentional control, working memory, and executive functioning, have also been observed, particularly in regions including the left perigenual anterior cingulate cortex, left lateral and right dorsolateral prefrontal cortices, bilateral medial frontal and parietal lobules, left superior parietal cortex, and right occipital, insular, and parietal regions, which are key components of the CEN [199, 212, 213]. Consistent with these findings, a meta-analysis of 20 task-based fMRI studies examining the effects of prolonged cannabis use identified distinct patterns of brain activation in adult and adolescent users compared to non-users, with evidence of altered activity in regions linked to the DMN and CEN [196].

Although research on functional brain changes in mid-to-older adults who use cannabis remains limited, a few studies suggest potential cognitive and neuroprotective effects [40, 214]. One study found that adults aged 65+ who regularly use cannabis showed stronger resting-state connectivity between the hippocampus, parahippocampal cortex, and anterior cerebellum, patterns similar to those seen in younger adults [40]. Another study of medical marijuana users (mean age ~50) reported improved cognitive performance, normalized brain activation, and reduced use of opioids after 3 months of treatment [214]. These findings underscore the need for further longitudinal research to better understand cannabis's impact on brain health in aging populations.

Current evidence indicates that cannabis use is associated with functional differences in the brain across both resting-state and task-based conditions [23, 26, 47, 61, 62, 176–181], primarily in the DMN and CEN [47, 61, 62, 176, 177]. These changes are observed in key neural networks involved in a range of cognitive and affective processes, including attentional control, working memory, executive functioning, decision-making, response inhibition, reward processing, error monitoring, emotional reactivity, time perception, and cue-reactivity [26, 98, 199, 200, 202–206, 208, 212, 213]. The direction and magnitude of these associations appear to depend on a range of individual and contextual factors, including the age at which cannabis use is initiated, the frequency, duration, and cumulative severity of use, as well as user-specific characteristics such as dependence status [23, 26, 47, 61, 62, 176–181].

Despite a growing body of research linking cannabis use to changes in functional brain connectivity and activation, findings across the literature remain inconsistent. These inconsistencies likely stem from methodological limitations such as small sample sizes, demographic variability, and heterogeneous cannabis use patterns across studies. Additional sources of variation include differences in participant characteristics (e.g., sex, socioeconomic status), as well as technical inconsistencies in neuroimaging methodology, such as MRI scanner

hardware, image acquisition protocols, and preprocessing pipelines and the types of cognitive or emotional tasks employed [124, 160, 215]. Moving forward, studies employing standardized imaging protocols and more representative samples, particularly those including mid-to-late life populations, will be essential to better characterize the functional effects of cannabis use on the brain and their implications for cognitive aging and long-term mental health outcomes.

## 2.8 Effects of cannabis on cognitive performance

Cannabis use has been associated with cognitive impairments across the lifespan, affecting adolescents, adults, and older individuals [23, 216]. Both acute and chronic use can negatively impact a wide range of cognitive domains, including attention, working memory, executive functioning, verbal learning, processing speed, and decision-making. These impairments have been consistently reported across diverse studies and populations, indicating that the cognitive effects of cannabis use are both widespread and not confined to specific domains [23, 27, 35, 48, 49, 216–222]. Notably, these impairments may persist well beyond the period of acute intoxication, particularly among early-onset or frequent (near-daily) users, underscoring their potential relevance for long-term cognitive health [27, 34, 48, 219].

### *Acute effects*

Acute cannabis intoxication has been shown to produce small to moderate deficits across several cognitive domains [34, 48, 219]. A meta-analysis encompassing over 50 studies and 1,500 healthy individuals reported that the most significantly affected areas were verbal learning and memory, specifically encoding, consolidation, and retrieval, whereas attention and impulsivity were the least affected [49]. Other domains frequently impacted include executive functioning, working memory, processing speed, inhibitory control, and psychomotor performance [34, 35, 221–232]. In contrast, attention and impulsivity were less consistently impaired, especially among young and middle-aged adults [34, 49, 219]. These acute effects may be moderated by factors such as cannabis composition (e.g., THC:CBD ratio), genetic predisposition, and prior cannabis use history. For instance, studies suggest that non-users and recreational users experience greater acute impairments than individuals with frequent near-daily users, possibly due to the development of tolerance [48, 233–236]. Acute administration of high-potency cannabis has been shown to produce dose-dependent impairments in executive function, psychomotor performance, and response inhibition [222, 231, 232]. These effects, evident up to six hours post-use, have been consistently observed in tasks such as the Tower of London, Critical Tracking Task, and Stop Signal Task [231].

Emerging research has also examined the influence of cannabis composition, particularly the ratio of CBD to THC, on cognitive outcomes. Preliminary findings suggest that strains with higher CBD content may attenuate some of the memory and executive impairments typically induced by THC, potentially due to CBD's modulatory effects on CB1 receptors or its

neuroprotective properties. For example, one naturalistic study observed that co-administration of CBD with THC reduced the severity of acute memory deficits compared to THC alone [237].

Supporting these findings, two major reviews provide comprehensive evidence of cannabis's cognitive effects. A meta-analysis by Zhornitsky et al. [49] revealed small-to-moderate impairments across all cognitive domains. Verbal learning, memory, and working memory were the most prominently affected while attention and impulsivity were the least impacted. Meta-regression further revealed that higher male representation in samples was associated with stronger THC-related deficits in processing speed and impulsivity, likely reflecting sex differences in CB1 receptor density. The route of administration also mattered: oral cannabis produced milder deficits in processing speed compared to inhaled or intravenous forms.

In parallel, a 2022 meta-review by Dellazizzo et al. [48] synthesized findings from ten meta-analyses covering over 43,000 individuals to assess the magnitude of cannabis's acute and residual cognitive effects. The review found that acute cannabis intoxication most consistently impaired verbal learning and memory, while executive function, working memory, and decision-making also showed small-to-moderate deficits. Notably, residual cognitive effects, particularly in learning and memory, persisted beyond acute intoxication, though these were typically mild and more pronounced in among individuals with more frequent or daily patterns of cannabis use. The authors concluded that while acute impairments are robust, residual effects tend to be reversible in moderate users, especially with sustained abstinence.

***Residual effects***

Residual cognitive effects of cannabis use have been consistently reported in cross-sectional studies, particularly in domains such as learning and memory, executive functioning, and processing speed, with effect sizes generally in the small-to-moderate range [179, 238–241]. These deficits appear to be short-term and reversible, as studies show significant improvement after 3–30 days of abstinence [179, 238, 241]. However, frequency of use plays a critical role: daily users show mild to moderate impairments, while light users often exhibit no measurable deficits [241]. Residual impairments are typically mild and diminish with sustained abstinence, although in frequent or heavy users—defined in some studies as cannabis dependence or use exceeding 20–30 times per month—deficits, particularly in episodic memory, may persist for several weeks post-cessation [179, 241].

Whether cannabis-related cognitive differences persist following cessation remains debated. Some studies suggest that impairments may diminish after short abstinence periods, indicating a possible contribution of residual intoxication [238], while CB1 receptor downregulation may also reverse with sustained abstinence [242]. Longitudinal behavioural studies directly examining monitored abstinence—Hanson et al. (2010), Schuster et al. (2018), and Roten et al. (2015)—show recovery of verbal learning and memory within one to two weeks and improvements in psychomotor speed after about one month, whereas deficits in sustained and selective attention often persist for several weeks [243–245]. The longitudinal study by Wallace et al. (2020) [246] found significant improvement in sustained attention after two weeks of

toxicology-confirmed abstinence, despite no baseline differences on brief cognitive tests, potentially reflecting additional abstinence before testing. Recovery appears to vary according to age of onset and cumulative exposure, with earlier-onset users showing slower improvement [225, 247]. Overall, behavioural evidence suggests that some cannabis-related cognitive differences may resolve with abstinence—particularly in learning and memory—while attentional deficits may be more persistent.

Residual effects observed across cognitive domains, such as learning, memory, and executive functioning, closely resemble those reported during acute intoxication, indicating continuity in the affected domains [179, 238, 239]. Meta-analyses have also examined potential moderators, including age of cannabis onset, participant age, and duration of use, but found no significant influence of these variables on the extent of residual impairment [179, 238–241]. These findings are primarily drawn from cross-sectional studies that compare cannabis users and non-users on cognitive performance while matching for confounding variables.

Supporting this, Fried et al. [248] conducted a prospective longitudinal study in which participants were cognitively assessed before initiating cannabis use and again in young adulthood. They found that current heavy cannabis users (defined as smoking ≥5 joints per week) showed significantly poorer performance in overall IQ, memory, and processing speed compared to non-users. However, these deficits were not observed in former regular users who had abstained for at least three months, suggesting that some cognitive impairments may be reversible with sustained cessation. This highlights the importance of pre-drug baselines and abstinence duration in understanding cannabis-related cognitive effects.

***Chronic or long-term effects***

Chronic or long-term cannabis use has been most consistently associated with impairments in verbal learning and memory, as demonstrated across numerous studies involving both adolescents and adults [34, 249–254]. These deficits are often dose-dependent and have been linked to frequency, quantity, duration of use, and early age of onset [250, 253, 255, 256]. Regular users, particularly those who began during adolescence, a critical neurodevelopmental window, also show impairments in executive functioning, including planning and inhibition, and in working memory and processing speed [224, 226, 252]. Although several studies report partial or full recovery of cognitive function following abstinence period, others, particularly those focused on adolescents or individuals with more frequent or regular patterns of use, suggest that impairments, especially in executive functioning and memory, may persist [243, 255, 257–259]. These effects appear to be domain-specific and influenced by factors such as age of onset, frequency of use, and cumulative exposure.

Emerging longitudinal research suggests that persistent cannabis use from adolescence into adulthood may contribute to broad and lasting cognitive decline, particularly in memory and executive functions [35, 38]. Meier et al. [35] found that persistent cannabis use from adolescence into adulthood was associated with broad neuropsychological decline, which remained evident even after cessation and was most pronounced among adolescent-onset users.

This study followed participants from childhood to age 38 and demonstrated that persistent users experienced significant declines across multiple cognitive domains, even when controlling for education. In a subsequent follow-up of the same cohort to age 45, Meier et al. [38] reported that long-term cannabis use was associated with an average IQ decline of 5.5 points from childhood, along with deficits in learning and processing speed. These cognitive impairments were specific to long-term cannabis users and could not be explained by other substance use, childhood socioeconomic status, or family history. While users also exhibited smaller hippocampal volumes, this did not fully account for the cognitive decline, raising concern about lasting neurocognitive impacts that may persist into older age.

Some studies have examined how genetic factors might influence the effects of cannabis on the brain. In a longitudinal study, Caspi et al. (2005) reported that a functional polymorphism in the *COMT* gene moderated the impact of adolescent cannabis use on later development of psychotic symptoms. Individuals with the Val/Val genotype were most likely to exhibit psychotic symptoms and develop schizophreniform disorder if they used cannabis during adolescence. Cannabis use had no such adverse effect among individuals with two copies of the Met allele. In a separate study, French et al. (2015) investigated whether the relationship between cannabis use and cortical thickness during adolescence was moderated by a polygenic risk score for schizophrenia. They found that among male adolescents with a high-risk score, cannabis use was associated with greater reductions in cortical thickness. This association was not observed in females or in males with low genetic risk. The authors concluded that cannabis use in early adolescence may moderate the relationship between genetic risk for schizophrenia and brain development in males [260, 261].

Findings from longitudinal studies remain mixed. In contrast to above studies, a large-scale study tracking over 5,000 men from early adulthood to late midlife found no evidence of accelerated cognitive decline associated with cannabis use [41]. Although age-related effects are less well studied, available data suggest that older long-term users may exhibit lasting memory deficits, while other cognitive effects appear less consistent or more reversible with abstinence [255, 259, 262]. Overall, frequent or long-term cannabis use, particularly when use is frequent or early-onset use, may lead to persistent impairments in specific cognitive domains, although the degree and reversibility of these effects remain subjects of ongoing research.

***Summary***

While growing evidence indicate that cannabis intoxication impairs core cognitive functions such as episodic memory, attentional control, and motor inhibition, the long-term cognitive consequences of frequent or long-term cannabis use, and the extent of cognitive recovery after abstinence, remain inconclusive [34, 35, 221–232]. The severity and persistence of cognitive impairment appear to be influenced by several individual-level factors, including age of initiation, biological sex, genetic vulnerability, and the frequency and duration of cannabis exposure [35, 219, 263, 264]. Early-onset cannabis use, particularly during adolescence, is thought to confer greater susceptibility to long-term cognitive decline due to heightened neurodevelopmental sensitivity [35, 263, 265].

While substantial evidence supports the association between cannabis use and cognitive deficits, inconsistencies persist in the literature [34, 35, 221–232]. These discrepancies may reflect heterogeneity in study design, variations in cannabis potency and dosage, user characteristics (e.g., dependence status, co-occurring substance use), and differences in cognitive assessment methods. Although many studies point to negative effects of cannabis on cognition, others report no significant differences between users and non-users. Continued research, especially in older adult populations, is critical to further elucidate the scope, persistence, and clinical relevance of cannabis-related cognitive impairments.

## 2.9 Current knowledge about cannabis and dementia risk

Cannabis use has been associated with a range of cognitive impairments [23, 216]; however, whether it causally contributes to an increased risk of all-cause dementia remains unclear. While numerous studies have shown cannabis to negatively affect cognitive domains such as memory, attention, and executive function, most have been cross-sectional, with limited sample sizes and single-point assessments of cannabis exposure and cognitive outcomes [23, 216, 266]. Brain imaging studies further support these findings, revealing structural and functional changes in the brains of frequent or long-term cannabis users, including reduced hippocampal volume and altered connectivity [23, 38, 45–47, 126, 261]. Long-term, defined as near-daily users over many years, particularly those with CUD, tend to perform worse on neurocognitive assessments [267]. Nonetheless, the extent to which these impairments predict future dementia remains uncertain.

Recent large-scale epidemiological evidence suggests a possible association between severe cannabis use and subsequent dementia diagnosis. A population-based study of over 6 million individuals reported that those who received hospital-based treatment for cannabis use had a significantly higher risk of receiving a dementia diagnosis within 5–10 years compared to matched controls [268]. This association remained significant after adjusting for demographic factors, mental health comorbidities, and chronic health conditions, with an adjusted hazard ratio of 1.72 compared to the general population and 1.23 compared to individuals hospitalized for other reasons. Notably, individuals with cannabis-related acute care encounters had a lower dementia risk than those hospitalized due to alcohol use, highlighting differential risks between substances. The elevated dementia risk was consistent across sexes and robust in sensitivity analyses, suggesting both direct and indirect pathways through which cannabis could influence cognitive decline. Cannabis use may also contribute to dementia risk indirectly by exacerbating established risk factors such as depression, hypertension, head trauma, and social isolation [268]. Nevertheless, it is important to emphasize that these observational and epidemiological associations do not confirm causation; thus, findings should be interpreted cautiously.

Longitudinal evidence from the Dunedin cohort further elucidates possible mechanisms linking cannabis use to dementia risk. Long-term cannabis users exhibited measurable cognitive

deficits in midlife, including significant IQ decline (approximately 5.5 IQ points), reduced processing speed, impaired learning, and informant-reported memory and attention problems. Additionally, these individuals with persistent, long-term cannabis user demonstrated reduced hippocampal volumes. Hippocampal atrophy is one of the most consistent MRI findings in dementia research and is widely recognised as a hallmark biomarker of Alzheimer's disease. The presence of hippocampal volume reductions in long-term cannabis users therefore represents a potentially important intermediate marker linking cannabis exposure to heightened dementia risk. Importantly, these deficits were independent of confounding factors such as tobacco, alcohol, or other drug use, socioeconomic background, and family history. Although hippocampal volume did not statistically mediate cognitive deficits, both reduced cognitive reserve and structural brain changes observed in midlife among long-term cannabis users represent critical intermediate markers potentially contributing to heightened dementia risk later in life. Future research is essential to determine if these midlife impairments ultimately translate into increased dementia incidence as these individuals age [38].

Preclinical research suggests that the endocannabinoid system may play a protective role in the pathophysiology of Alzheimer's disease [269]. Studies have demonstrated that cannabinoids, particularly those targeting CB1 and CB2 receptors, can reduce neuroinflammation, oxidative stress, and excitotoxicity, three key processes implicated in neurodegeneration [270–273]. Cannabinoids have also been shown to modulate glial activation [270, 274], promote neurogenesis [275], and enhance neuronal survival following injury [273]. Additionally, associations in endocannabinoid system signaling have been observed in Alzheimer's disease brains, such as increased CB2 receptor expression near amyloid plaques, suggesting a disease-related adaptive or pathological role of the system [270, 276].

However, these findings are largely derived from preclinical models, and there is currently limited evidence that such neuroprotective effects translate into long-term benefit in humans, particularly in the context of near-daily or daily recreational cannabis use, which differs significantly from therapeutic cannabinoid application [277, 278]. Further research is needed to evaluate the therapeutic viability and safety of cannabinoid-based interventions for Alzheimer's disease. While preliminary clinical trials have explored symptom management, two recent systematic reviews concluded that current evidence is sparse, low in quality, and inconclusive, and that any potential benefits may be too small to be clinically meaningful, underscoring the need for larger and longer-term trials to evaluate the therapeutic viability and safety of cannabinoid-based interventions for Alzheimer's disease [278, 279].

Overall, the literature presents a complex and inconclusive picture. While existing evidence indicates that cannabis use, particularly when frequent or prolonged, may impair cognitive function and potentially increase dementia risk, a causal relationship has not been definitively established. Concurrently, preclinical research points to the possible neuroprotective properties of certain cannabinoids under specific conditions. This contrasting evidence underscores the importance of rigorous, long-term, and clinically focused research to clarify both the therapeutic potential, and the risks associated with cannabinoid exposure, particularly as cannabis use becomes increasingly prevalent among older adults and vulnerable populations.

Future studies incorporating large-scale longitudinal follow-ups, rigorous clinical trials, and genetic methods such as MR will be essential to address these unresolved questions. Given current uncertainties and the growing prevalence of cannabis use among older adults, a prudent public health stance involves minimizing, near-daily or daily, long-term recreational cannabis exposure until its long-term neurological effects become clearer.

## 2.10 Sex-dependent effects of cannabis use on brain health

The broader literature on substance use highlights that sex plays a significant role in shaping patterns of use and associated outcomes [280, 281]. Sex-related factors, such as biological mechanisms, contribute to how substance use differentially affects males and females. Given the widespread use of cannabis for both medical and recreational purposes, understanding these sex-specific effects is crucial for informing public health messaging and interventions. Although still underexplored, sex differences in cannabis use and its effects represent a critical area of research, as men and women differ in their reasons for use, usage patterns, and physiological responses, all of which have implications for their overall health and well-being [281].

Cannabis, like many other substances, tends to be used more frequently by males than females [282]. Epidemiological studies consistently show that men are more likely to initiate cannabis use, use it more heavily, and develop CUD. However, despite lower overall usage rates, females may progress more rapidly from initial use to problematic patterns [283]. Notably, women appear more prone to experiencing certain withdrawal symptoms, such as anxiety, and nausea, compared to men [282]. Evidence from clinical studies examining sex differences in cannabis withdrawal severity support this pattern, indicating that women may experience more intense withdrawal symptoms than men [284, 285]. These findings align with preclinical research showing that female rodents exhibit stronger withdrawal responses than males, including increased cognitive disruption, anxiety-like behaviour, and motor agitation [286, 287]. In terms of therapeutic effects, men are reported to experience greater cannabis-induced analgesia than women, despite comparable subjective experiences [283].

These sex differences are believed to be modulated, at least in part, by hormonal fluctuations. Specifically, oestrogen and progesterone influence endocannabinoid system functioning across the oestrous cycle, with elevated oestrogen states enhancing CB1 receptor signaling and increasing female rodents' sensitivity to THC [288]. As a result, female animals tend to self-administer lower THC doses to achieve similar effects, develop tolerance more rapidly, and show stronger withdrawal profiles. Although direct human evidence is more limited, similar hormonal influences are suspected in mediating sex-specific cannabis responses. Taken together, these findings underscore the importance of considering sex hormones and neuroendocrine status in both clinical and preclinical cannabinoid research [283, 288, 289].

These mechanistic insights also carry practical clinical implications. For instance, the observation that women may experience more intense withdrawal symptoms (anxiety, irritability, etc.) suggests that women may face greater challenges when trying to quit cannabis, potentially benefiting from tailored withdrawal management strategies. Clinical trials for cannabis dependence have indeed noted sex-related differences in treatment outcomes and relapse rates. Women may also respond differently to medications aimed at easing withdrawal or reducing use (for example, there is preliminary evidence that oral THC might differentially affect withdrawal symptoms in men vs women, but sample sizes are small) [283, 288, 289].

Previous research has explored how sex differences influence the impact of cannabis use on brain structure [98, 290, 291]. Findings have shown that in adolescent cannabis users, a higher proportion of females in study samples was associated with increased GM volume in the middle occipital gyrus compared to non-users [290]. Additionally, female adolescent users exhibited greater prefrontal cortex volume than their male counterparts, a difference linked to impaired executive functioning, suggesting that sex may moderate the relationship between cannabis use and prefrontal cortex development [141]. Larger amygdala volumes have also been reported in female adolescent users compared to non-users, a pattern not observed in male users [140]. However, not all studies have found consistent sex-based interactions in relation to cannabis use and brain structure, indicating that these effects may vary depending on study design and sample characteristics [292].

Functional neuroimaging studies have revealed sex-specific patterns in brain responses to cannabis [98, 291, 293–295]. For example, males have shown greater WM-related activity in the superior frontal gyrus [296], while females may be more vulnerable to cannabis-related neurotoxic effects, particularly in the frontal and occipital regions [292]. However, findings in this area remain mixed, as a recent meta-analysis reported inconsistent results [98, 293]. Additional research using a cannabis cue task has found that females exhibit stronger activation in regions such as the striatum, left hippocampus, amygdala, and left lateral orbitofrontal cortex compared to males. These findings suggest that females may engage more cortical regions when processing cannabis-related stimuli. Notably, female users also demonstrated a negative correlation between activity in the left lateral orbitofrontal cortex and subjective craving, an association not observed in males, indicating potential sex differences in how cannabis cues are valued and processed at the neural level [295].

Sex differences in cognitive functioning among cannabis users have also been observed, with evidence suggesting that the neuropsychological impact of cannabis varies between males and females [264, 297, 298]. For example, male cannabis users, but not female users, demonstrated poorer performance on tasks assessing intelligence, psychomotor speed, and both immediate and delayed verbal recall when compared to non-using males. In contrast, female cannabis users outperformed their non-using female counterparts on measures of psychomotor function and immediate verbal recall [264]. One study also reported that greater cannabis use in males was more strongly associated with deficits in sequencing ability and psychomotor speed [297]. Further findings indicate that males may exhibit poorer visual memory, while females may show more difficulties with sustained attention, multitasking, and planning [298]. Despite these

observations, inconsistencies across these studies highlight the need for further research to clarify these patterns.

In summary, the existing literature suggests that cannabis use has sex-dependent effects across various domains, including behavioral patterns, brain structure and function, and cognitive outcomes. Although current findings point to clear differences between males and females, much of the evidence is drawn from adolescent samples and studies with limited sample sizes. As such, there is a pressing need for larger, more comprehensive studies, particularly in adult populations, to determine whether these sex-specific effects persist or change over time. Future research should aim to clarify the neurobiological and psychological mechanisms underlying these differences, ultimately contributing to more targeted and effective approaches to cannabis-related health interventions.

## 2.11 Limitations and gaps in the existing literature

Despite the substantial growth of cannabis research in recent years, significant limitations persist in the literature, particularly regarding its long-term effects on brain structure, function, and cognition in later life. These limitations not only limit the understanding of cannabis-related neurobiological outcomes but also underscore the critical need for more robust and methodologically diverse investigations.

To date, the majority of studies examining the effects of cannabis on brain health have focused on adolescents and young adults [34, 61, 124, 132, 176, 249–254]. This focus is reasonable given the heightened neurodevelopmental vulnerability of these populations; however, it has resulted in a relative neglect of middle-aged and older adults, demographics in which cannabis use is rising, largely due to medical legalization and evolving social norms. As the population of older users grows, understanding the neurocognitive consequences of cannabis in later life has become increasingly urgent, yet remains insufficiently addressed in current research. In contrast, this thesis specifically focuses on mid- to later-life adults, providing much-needed evidence for an understudied and increasingly relevant population.

Additionally, most existing studies have concentrated on individuals with daily or near-daily cannabis use, or those meeting criteria for dependence, providing limited insight into more typical patterns of recreational or moderate use [47, 61, 62, 176, 177]. This overrepresentation of extreme usage profiles constrains the generalizability of findings to broader populations and potentially inflates estimates of harm. Compounding this issue, many studies focus narrowly on select brain regions, particularly the hippocampus [24, 45, 46, 133, 134], while neglecting more comprehensive assessments of whole-brain structure and network-level function. Consequently, the understanding of how cannabis affects large-scale brain health and its role in cognition remains incomplete.

Sample size constraints have also characterized much of the literature. Many studies are based on small or regionally limited cohorts, limiting statistical power and the ability to explore subgroup differences based on age, sex, comorbidities, or genetic factors. Additionally, the reliance on cross-sectional, observational designs makes it difficult to infer directionality or causality. Common issues such as residual confounding, reverse causation, and selection bias further diminish the robustness of conclusions. These design limitations are particularly problematic when attempting to evaluate long-term or delayed outcomes, such as age-related cognitive decline or dementia risk. In contrast, the present study draws on the exceptionally large, well-characterised UK Biobank imaging cohort, which provides sufficient power to detect subtle associations and to conduct stratified analyses by sex and other covariates. By integrating observational analyses with MR, it also addresses questions of causality that cannot be answered by cross-sectional designs alone. The combination of multimodal neuroimaging, cognitive testing, and dementia endpoints further strengthens the approach, enabling a more comprehensive evaluation of cannabis use across multiple domains of brain health.

Another major limitation is the inconsistency and lack of standardization in cognitive assessments across studies. Many studies rely on brief or non-standardized cognitive batteries that limit domain-specific insights and hinder comparability across studies. Similarly, cannabis exposure is often measured through self-report, which is subject to recall bias and limited precision, particularly regarding frequency and duration of use. This complicates the interpretation of dose-response relationships and reduces the accuracy of estimating overall cannabis use across the lifespan.

While neuroimaging studies have offered important insights into the effects of cannabis on the brain, most have followed a hypothesis-driven approach, targeting specific brain regions or networks believed to be affected [24, 46, 133, 146]. This has resulted in a narrow focus, often limited to areas like the hippocampus or prefrontal cortex, rather than exploring the full range of potential brain changes. Few studies have adopted a more exploratory, whole-brain approach that could reveal widespread or unanticipated effects of cannabis exposure. Moreover, most existing studies have examined brain structure, function, or cognition in isolation, often using different cohorts or analytic frameworks. Few have investigated all three within the same large, well-characterized dataset, which limits consistency and comparability across domains. This fragmented approach reduces the ability to draw meaningful conclusions about how cannabis use affects the brain and cognition over time.

Although evidence suggests that genetic factors contribute to individual differences in substance use, brain structure, and cognitive function [98, 153], cannabis research has not employed causal genetic methods, such as MR, to investigate these relationships. This gap is particularly important given the need to clarify whether associations between cannabis use and outcomes such as cognitive impairment or increased dementia risk reflect direct causal effects or are instead driven by shared genetic or environmental influences. To date, no MR studies have examined these associations, and there is a broader lack of large-scale population-based research that combines genetic methods with detailed cognitive phenotyping and neuroimaging

data. Addressing this gap is essential for understanding the long-term consequences of cannabis exposure on brain and cognitive health.

A further limitation in the existing literature is the limited consideration of how the amount and frequency of cannabis use may influence outcomes. Many studies simply compare people who use cannabis with those who do not, without examining variation within users themselves. As a result, these studies often fail to capture whether differences in dose or frequency of use affect cognitive or brain-related outcomes. This gap is particularly relevant for older adults, whose patterns of use may differ substantially from younger populations. The present study addresses this by comparing people who use cannabis more often with those who use it less frequently, allowing a clearer understanding of whether potential effects are limited to heavier use or also emerge at lower levels of exposure.

Few studies have systematically explored how brain or cognitive outcomes differ across varying levels of cannabis use. While some research acknowledges that effects may increase with greater use, most investigations still rely on simple group comparisons and rarely consider how frequent or occasional use might influence results. When frequency is included, studies often use inconsistent definitions and do not examine how differences in use may translate into different outcomes. This has contributed to uncertainty around whether occasional use poses the same level of risk as regular or long-term use. Evidence in older adults remains especially limited. To help address this gap, the current study examines both higher- and lower-frequency use, providing a more detailed picture of how cannabis exposure may relate to cognitive health in mid-to-later life.

Another key limitation is the limited exploration of sex differences in cannabis-related outcomes. Although preclinical and clinical evidence suggests that males and females may differ in their patterns of cannabis use, withdrawal experiences, neurobiological responses, and cognitive outcomes, most human neuroimaging and cognitive studies have been underpowered to test sex-specific effects. Where sex has been examined, findings are often inconsistent, likely due to small sample sizes and heterogeneous methods. This highlights the need for large-scale studies with sufficient statistical power to investigate sex-stratified associations, which the current study addresses.

In summary, the current literature on cannabis and brain health is constrained by a focus on younger populations, small and selective samples, an overrepresentation of individuals with daily, near-daily use or dependent users, and narrow assessments of brain and cognitive outcomes. Most studies examine brain structure, function, or cognition in isolation, often using separate cohorts, limiting cross-domain comparability. Additionally, genetically informed methods such as MR have not yet been applied to investigate the potential causal effects of cannabis use on cognition or dementia risk. There is a pressing need for large, well-powered studies in older adults that incorporate whole-brain imaging, network-level functional analysis, and comprehensive cognitive assessments. Integrating genetic approaches alongside observational methods offers a promising avenue to strengthen causal inference and improve the understanding of how cannabis may influence brain aging and long-term cognitive health.

# Chapter 3: Methods

## 3.1 Study sample and data source

This study included data from the UK Biobank for observational analyses. UK Biobank is a large-scale, longitudinal biomedical database and research resource which provides resources for examining the genetic, environmental and lifestyle factors of a multitude of health conditions in mid to old age adults. The timeline of UK Biobank data collection relevant to this thesis is shown in **Figure 6**.

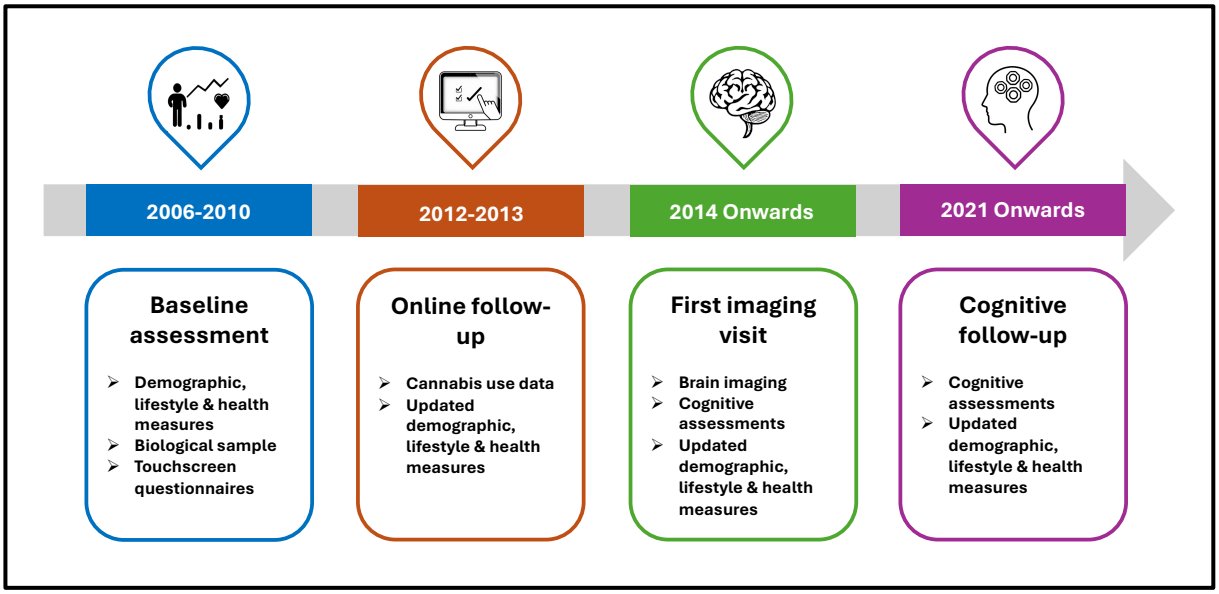



*Figure 6: Overview of UK Biobank data collection timepoints used in this thesis*

Between 2006–2010 UK Biobank recruited more than 500,000 participants aged 40–69 years who were registered with the National Health Service (NHS) in England, Wales or Scotland and living within 25 miles of residence from one of the 22 assessment centers [52]. Approximately 5% of those invited agreed to participate. At the baseline visit, participants completed a 90-minute assessment touch screen questionnaire on various sociodemographic, lifestyle and medical history, completed a range of physical measures and also provided biological samples on blood, urine and saliva. Detailed follow-up data on the health and lifestyle measures of the participants has since been collected. A subset of the UK Biobank cohort was invited to take part in an imaging enhancement study, which aimed to collect multimodal brain imaging data on approximately 100,000 participants [53]. All participants gave written informed consents and had the right to withdraw at any time from the study. UK Biobank has been granted ethical approval by the National Information Governance Board for Health and Social Care and the NHS North-West Multi-Centre Research Ethics Committee. Participants who had complete data on cannabis use, brain measure of structure and function, cognitive performance and relevant covariates were used in the analyzed sample. Description of the participants from the UK Biobank used in this study is in **Figure 7.**

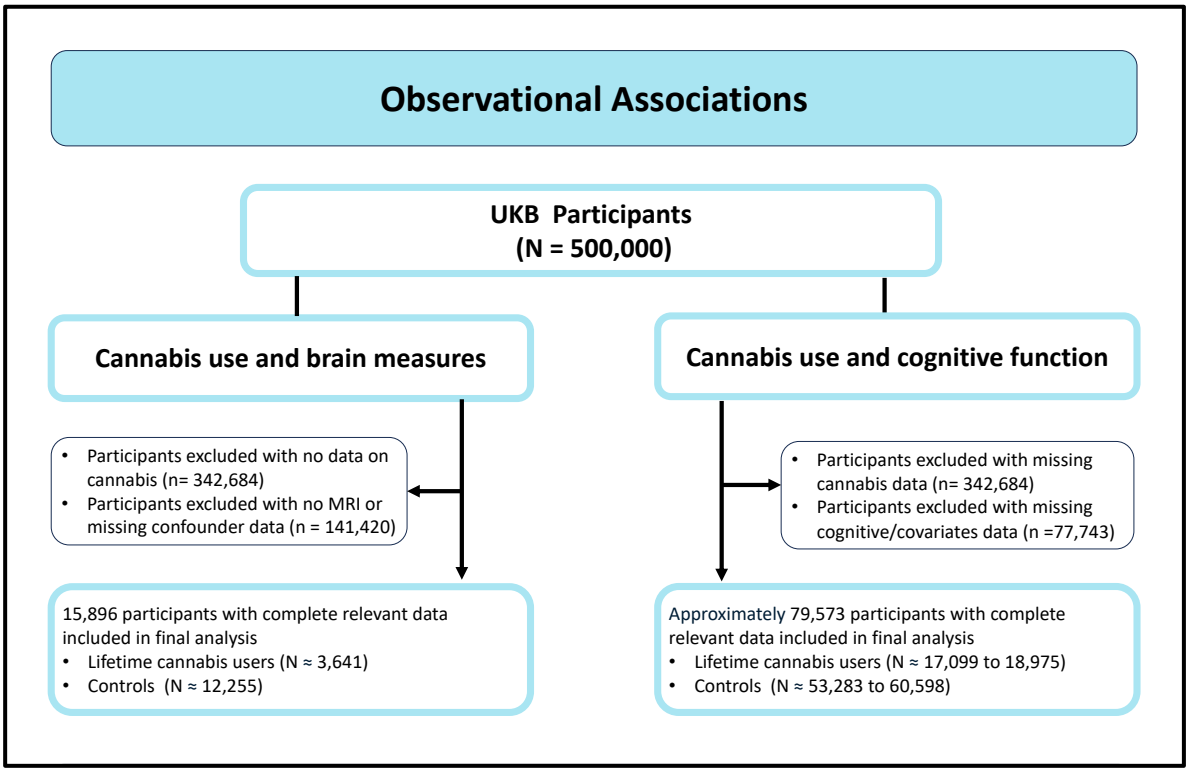



*Figure 7: Flow chart of the participants from the UK Biobank included in the observational analysis*

Abbreviations: MRI, magnetic resonance imaging.

## 3.2 Cannabis use data

Cannabis use was self-reported at the online follow-up during the first repeat assessment visit (**Figure 6**). Participants reported if they had "Ever taken Cannabis". Possible answers were: 'no', 'prefer not to say', 'yes, 1–2 times', 'yes, 3–10 times', 'yes, 11–100 times', and 'yes, more than 100 times'**.** All participants who responded 'yes' were categorized as lifetime cannabis users, and 'no' responders were categorized as controls. Cannabis users were further divided into two subgroups: (a) low-frequency cannabis use (lifetime cannabis use of 1-10 times), and (b) high-frequency cannabis use (lifetime cannabis use of 11-100+ times). This subgroup categorization for cannabis users was introduced in a previous study [299, 300]. Stratifying cannabis users by frequency of use allows for the exploration of potential dose–response relationships. Participants also reported their "Age when cannabis was last taken" and years since the participants last took cannabis were computed by the difference between the age when last cannabis was used and the age when subjects were scanned. This variable was used to assess whether the duration of abstinence from cannabis prior to neuroimaging had any influence on brain structure or functional connectivity. Participants further reported the maximum frequency of cannabis consumed during the lifespan to which they responded: 'every day', 'once a week or more but not every day', 'once a month or more but not every week', 'less than once a month', 'do not know' and 'prefer not to say'. Additionally, only two

participants were identified with CUD in UK Biobank, which was insufficient for conducting an analysis. These were defined using linked secondary care electronic health record (EHR), based on the presence of the ICD-10 code F12.20 (cannabis dependence).

It is important to note that in the wider literature, cannabis exposure is often described using terms such as ‘chronic,’ ‘heavy,’ or ‘recreational’ use. These terms are variably defined, for example by daily or near-daily consumption, cumulative lifetime exposure, or clinical diagnoses of CUD. In the present study, such labels were avoided, and cannabis exposure were instead operationalised strictly according to the frequency and recency measures available in UK Biobank (ever use, lifetime frequency, maximum frequency, and recency of last use). This approach ensures clarity and avoids conflating heterogeneous definitions used in the literature.

### 3.3 Imaging data

The imaging data from the UK Biobank used in this study were from the first imaging visit (2014-2019) (**Figure 6)**. MRI data and sociodemographic measures used in the study were collected during the imaging visit.

The exclusion criteria established by the UK Biobank team for MRI scanning include standard MRI safety/quality criteria, such as exclusions for metal implants, recent surgery, or health conditions directly problematic for MRI scanning, such as hearing problems, breathing issues, or extreme claustrophobia. Additionally, the raw MRI data that had the wrong dimensions, was corrupted, missing, or otherwise unusable were not processed any further [301].

The imaging data were obtained on Siemens Skyra 3T MRI scanners equipped with 32-channel head coils. The UK Biobank team performed image processing, quality control checks, and automated brain tissue volume computations and their IDPs were made available to the researchers. The brain imaging protocol utilized in the UK Biobank includes structural, diffusion, and functional imaging from six distinct modalities: T1-weighted, T2-weighted flair, diffusion magnetic resonance imaging (dMRI), susceptibility-weighted imaging (SWI), task functional magnetic resonance imaging (tfMRI) timeseries, and resting-state functional magnetic resonance imaging (rsfMRI) timeseries data [53].

T1-weighted MPRAGE and T2-weighted FLAIR volumes were obtained at 1×1×1mm (208×256×256 field of view [FOV] matrix) and 1.05×1×1mm (192×256×256 FOV matrix) respectively. Linear and non-linear registration to MNI152 "nonlinear 6th generation" standard-space was conducted using FMRIB's Linear Registration Tool (FLIRT) [302, 303] and FMRIB's Nonlinear Image Registration Tool (FNIRT) [304, 305] respectively. Additionally, brain extraction was performed using the Brain Extraction Tool (BET) [306], followed by defacing and segmentation into tissue types using FMRIB's Automated Segmentation Tool (FAST) [307]. GM was extracted from FAST and the estimation of the GM was performed for a total of 139 regions of interest (ROIs) defined by the HarvardOxford

cortical and subcortical atlases [308] and the Diedrichsen cerebellar atlas [309]. Subcortical volumes were generated by using FMRIB's Integrated Registration and Segmentation Tool (FIRST) [310] and estimation was done using the population priors on shape and intensity variation across subjects. Image segmentation was performed to identify white matter hyperintensities (WMH) using the Brain Intensity AbNormality Classification Algorithm (BIANCA), an automated supervised method implemented in FSL that classifies WMHs based on intensity and spatial features [311]. WMHs are areas of high signal on T2-weighted or FLAIR images, commonly observed in older adults and associated with vascular risk, functional decline, and cognitive impairment [312–314]. Additionally, periventricular WMH (pWMH) and deep WMH (dWMH), were defined based on subsets of total WMH based on their spatial location.

DMRI were obtained at 2×2×2mm (104×104×72 FOV matrix) using a spin-echo echo-planar sequence with two b-values (b = 1000 and 2000 s/mm2). 50 diffusion encoding directions were acquired for each diffusion-weighted shell and the tensor fitting was performed using the b = 1000 s/mm2 shell. The diffusion tensor and the neurite orientation dispersion (OD) and density imaging (NODDI) models were applied to pre-processed data, generating nine microstructural maps.

From the diffusion tensor imaging (DTI) model, the following indices were derived:

- Fractional anisotropy (FA): quantifies the directional dependence of water diffusion, providing a measure of white matter coherence and integrity.
- Mean diffusivity (MD): represents the average magnitude of water diffusion across all directions, reflecting overall tissue density and cellularity.
- Axial diffusivity (L1): corresponds to diffusion along the principal fiber axis, and has been linked to axonal integrity.
- Radial diffusivity (L2, L3): describes diffusion perpendicular to the main fiber axis, often interpreted as being sensitive to myelination.
- Mode of anisotropy (MO): characterises the geometric shape of diffusion (e.g. linear, planar), capturing aspects of fiber configuration.

From the NODDI model, three additional indices were estimated:

- Intracellular volume fraction (ICVF): an index of neurite density, reflecting the fraction of tissue comprised of axons and dendrites.
- Isotropic volume fraction (ISOVF): the proportion of isotropic diffusion signal, typically associated with free water or cerebrospinal fluid.
- Orientation dispersion (OD): quantifies the angular variability of neurite orientations, providing a measure of fiber complexity and fanning.

Tract-Based Spatial Statistics (TBSS) processing was then performed using these DTI-derived maps and TBSS-derived measures were computed by averaging the skeletonized images of

each DTI map within a predefined set of 48 standard-space tract masks defined by the JHU White Matter Atlas (ICBM-DTI-81) [315].

SWI was obtained at 0.8×0.8×3mm (256×288×48 FOV matrix). T2* was used to generate the IDPs. T2* is sensitive to local magnetic field inhomogeneities and provides an indirect index of iron deposition, myelin content, and blood oxygenation. First T1-weighted structural brain scan was used to derive subject-specific masks for 14 subcortical regions that correspond to the left and right of the 7 subcortical structure ROIs. Subsequently, IDPs were calculated based on the median T2* for each of these regions.

TfMRI were obtained at 2.4×2.4×2.4mm (88×88×64 FOV matrix) involving Hariri faces/shapes "emotion" task with either angry or fearful faces. Participants were presented with blocks of trials where they were required to determine which of the two faces displayed at the bottom of the screen correspond to the face shown at the top, or which of the two shapes presented at the bottom match the shape displayed at the top. Preprocessing and modelling of task-induced activation were conducted using FEAT (FMRI Expert Analysis Tool), while time-series statistical analysis utilized FILM with local autocorrelation correction. The three contrasts of interest were: 1 (Shapes), 2 (Faces), and 5 (Faces-Shapes), with the last contrast was with respect to amygdala activation. Group-average activation maps were generated from analysis across all subjects and Regions of Interest (ROIs) were defined. Task fMRI IDPs represent summary measures of activation, including the median and 90th percentile for both the percent signal change and the z-statistic. These measures are computed from regions selected from the group-level activation map [54].

RsfMRI were also obtained as per tfMRI at 2.4×2.4×2.4mm (88×88×64 FOV matrix). On a preprocessed sample of 4162 participants, grouped average independent component analysis (ICA) was carried out using MELODIC [54, 316, 317]. ICA was performed with dimensionality set to 25 and 100, which resulted in 21 and 55 components, respectively, after discarding the noise components. These 21×21 and 55×55 partial correlation matrices were used as measurements of functional connections. The ICA maps were mapped on each participant's rsfMRI timeseries data in order to acquire one representative node timeseries per ICA component for each subject. These network 'nodes' are a measure of within-network functional connectivity. Subject-specific network-matrices ('edges') were also extracted from the node timeseries that provide a measure of functional connectivity between the nodes [318] Each edge corresponds to one pairwise connection between nodes in the partial correlation matrix. Edge numbers (e.g., Edge 21) refer to the index assigned to each unique node–node pair in the UK Biobank rsFC matrices. Anatomical and network labels corresponding to these edge numbers are provided in the results tables in **Chapter 5**.

A total of 3,921 brain measures of structural (n = 2,128) and functional (n = 1,793) connectivity were used in the study as presented in **Appendix 1 and 2** respectively.

### 3.4 Cognitive test data

Cognitive assessment in the UK Biobank was brief and bespoke and was administered as a part of touchscreen questionnaire without any supervision [55]. The primary cognitive assessment in UK Biobank was brief of around 5 minutes but later on more comprehensive measures of cognitive functions were included which examined those cognitive domains which are known to decline with age. In this study, data were used from the online follow-up (**Figure 6)**, where the cognitive functioning was assessed either at one or two timepoints: assessment run 2014 and assessment run 2021 (**Table 1)**. This decision was based on the larger sample size and more complete data available at these follow-up timepoints. Cognitive performance was examined though 5 different tests:

1. Numeric Memory: Numeric memory test was performed only at the first timepoint. This test was designed to estimate attention and working memory. Participants were shown a 2-digit number to remember which then disappeared and after a short time they were asked to enter the number onto the screen. Each time the participants remember the number correctly; it became one digit longer up to a maximum of 12 digits. From this test, the variable analysed was the *Maximum digits remembered correctly (UKB data field 20240).*

2. Fluid intelligence: Fluid intelligence test was performed at both timepoints. This test was incorporated into the touchscreen at the end of the recruitment. This test was designed to estimate 'Fluid intelligence' which is the ability of the individual to solve the problems that require logic and reasoning ability which is independent of acquired knowledge. Participants were presented with 13 question and had 2 minutes to complete as many questions as possible. From this test, the variable analysed was the *Fluid intelligence score (UKB data field 20191).*

3. Trail Making: Trail making test was performed at both timepoints. Participants were presented with sets of digits/letters in circles scattered around the screen and asked to click on them sequentially according to a specific algorithm. This test estimates information on visual search, scanning, processing speed, mental flexibility, and executive functions. From this test, the variable analysed was the *Duration to complete numeric path (trail A and B) (UKB data field 20156 and 20157).*

4. Symbol Digit Substitution: Symbol digit substitution test was performed at both timepoints. Participants were shown one grid linking symbols to single-digit integers and a second grid which contained only the symbols. They were then asked to specify the numbers that was attached to each of the symbols in the second grip while using the first grid as a key. This test estimates information on visual memory. From this test, the variable analysed was the *Number of symbol digit matches made correctly (UKB data field 20159).*

5. Pairs Matching: Pairs matching test was performed at both timepoints. Participants were presented with either 3 or 6 pairs of cards and were asked to memorize the position of as many matching pairs of cards as possible. Cards were turned face down and participants were then tasked to identify as many pairs as possible in the fewest tries. This test was estimated to access episodic visual memory, executive functions and processing speed. From this test, the variable analysed was the *Number of correct matches in round (UKB data field 20131).*

*Table 1: Cognitive tests in UK Biobank included in the final analysis*

| Cognitive tests (Variables Code) | Variables used | Cognitive domains assessed | Participants assessed in 2014 (N) | Participants assessed in 2021 (N) |
|---|---|---|---|---|
| **Numeric Memory (20240)** | Maximum digits remembered correctly | Attention and working memory | 111,001 | 0 |
| **Fluid Intelligence (20191)** | Fluid intelligence score | Verbal and numeric reasoning ability | 123,546 | 180,619 |
| **Trail Making A (20156)** | Duration to complete numeric path | Visual search, scanning, speed of processing, mental flexibility, and executive functions | 103,972 | 175,358 |
| **Trail Making B (20157)** | Duration to complete alphanumeric path | Visual search, scanning, speed of processing, mental flexibility, and executive functions | 103,970 | 152,742 |
| **Symbol Digit Substitution (20159)** | Number of correct matches in round | Visual Memory | 118,400 | 177,210 |
| **Pairs Matching (20131)** | Number of symbol digit matches made correctly | Executive function, processing speed, visual memory | 118,462 | 118,462 |

## 3.5 Confounding variables

In UK Biobank, confounding variables were measured at multiple timepoints, from baseline assessment through to the imaging visit. Several potential confounding variables were adjusted for in this study. Age (in years) was derived either from baseline visit or from the imaging visit depending on the analysis. Sex (male and female) was included as binary covariate. Socioeconomic status was captured using the Townsend deprivation index, a measure of material deprivation derived from participants residential postcodes and national census information, were controlled for. Current employment status was recorded as: in paid employment/self-employed, retired, looking after home and/or family, unable to work because of sickness or disability, unemployed, doing unpaid or voluntary work, full or part-time student or none of the above. Historic job type was categorized according to the Standard Occupational Classification 2000 guidelines. Job types with a sufficient number of participants such as,

managerial and senior officials, professional occupations, associate professional and technical occupations and administrative and technical occupations, were included and dummy coded.

Educational qualifications were recorded as: college or university degree, Advanced level/Advanced Subsidiary levels or equivalent, Ordinary levels/General Certificate of Secondary Educations or equivalent, Certificate of Secondary Educations or equivalent, National Vocational Qualifications or Higher National Diploma or Higher National Certificate or equivalent, other professional qualifications or none of the above. Smoking and alcohol drinking status was reported as: current, previous or never. Alcohol drinking frequency was reported as daily or almost daily, three or four times a week, once or twice a week, one or three times a month, special occasions only, and never. Systolic and diastolic blood pressure (BP) were measured in mmHg and body mass index (BMI) in $kg/m^2$. For a measurement of mental health status, participants were asked if they had 'seen a psychiatrist for nerves, anxiety, tension or depression' and the response was noted as 'yes', or 'no'.

In addition to the core sociodemographic, lifestyle, and health-related covariates described above, further behavioural and psychological variables were incorporated into the extended sensitivity analyses. These included baseline measures of risk-taking, loneliness, and neuroticism, which was standardised (z-score) to align with previous UK Biobank analyses. To capture subclinical symptoms, scores from the Patient Health Questionnaire–9 (PHQ-9)—a measure of depressive symptoms—and the Generalised Anxiety Disorder–2 (GAD-2)—a brief screening tool for anxiety symptoms—were also included where available. Finally, clinically diagnosed depression and anxiety were derived from linked Hospital Episode Statistics using ICD-10 codes for depression and anxiety. These variables were incorporated into a series of nested models to evaluate their potential role as confounders or mediators.

In the imaging data analysis, a set of 613 brain imaging-related confounds were also accounted for as described in Alfaro-Almagro et al (2021) [319] and detailed in **Appendix 3**. These included: assessment centre, intracranial volume, head motion, table position, and scanner acquisition parameters (site, scanner software, protocol, scan ramp, head coil).

In the cognitive data analysis, the time difference between baseline and the first cognitive assessment was included in both cross-sectional and longitudinal analyses, and the time difference between the two cognitive assessments was included as an additional covariate in the longitudinal analysis.

Information regarding which confounders were adjusted for in the observational analyses is provided in the confounds sections of the relevant chapters (**Chapter 4, 5, and 6**).

## 3.6 Genetic instruments for Mendelian randomisation

Genetic variants (single nucleotide polymorphisms, SNPs) were used as instrumental variables in MR. These were identified using the largest available GWAS for two different cannabis

phenotypes [56, 57] (**Figure 8).** In order to fulfil a key MR assumption that genetic variants are robustly associated with the exposure (cannabis), only variants at genome-wide significance ($P<5\times10^{-8}$) were selected. F statistics were calculated as a quantitative measure of instrument strength **(see chapter 4 and 6)**. If matching SNPs were not available in the outcome GWAS, proxy SNPs ($R^2 > 0.9$) were identified from LDlink (https://ldlink.nci.nih.gov/).

Full lists of SNPs used as instruments for each phenotype are presented in **Chapter 4, 5 and 6**. All GWAS used for both exposures and outcomes had already been adjusted for the same core set of confounding factors, including age, sex, and genetic ancestry principal components, as part of their original study designs.

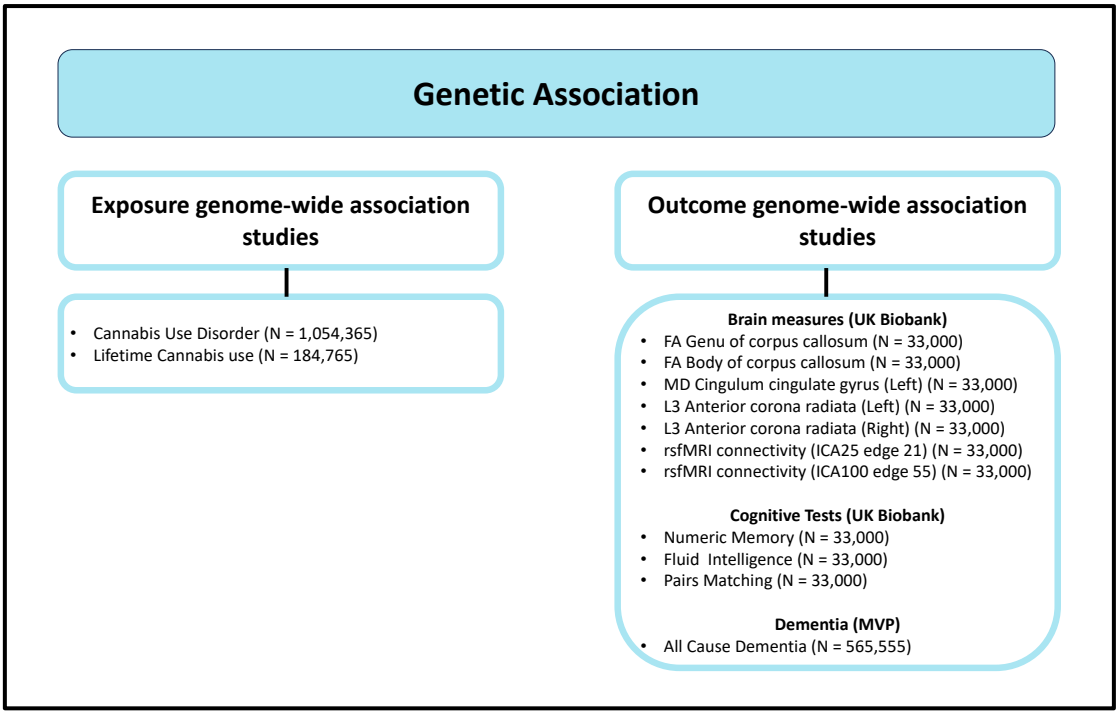



*Figure 8: Flow chart of the genome wide association studies included in the genetic analysis*

Source GWAS references: cannabis use disorder [56]; lifetime cannabis use [57]; brain measures (UK Biobank) [320]; cognitive tests (UK Biobank) [58, 60]; dementia (MVP) [59]. Abbreviations: FA, fractional anisotropy; MD, mean diffusivity; L3, radial diffusivities; rsfMRI, resting-state functional magnetic resonance imaging; ICA independent component analysis; MVP, Million Veteran Program.

For the first cannabis phenotype, GWAS summary statistics for *cannabis use disorder* (CanUD) (N = 886,025) from individuals of European ancestry were used [56]. This consisted of five datasets from PGC, deCODE, Million Veteran Program (MVP), iPSYCH2, MGB and Yale-Penn 3 (**Appendix 4)** with 42,281 cases and 843,744 controls. This GWAS identified 23 genome-wide significant independent SNPs, where the lead signal was found near *CHRNA2* (rs56372821, P = 7.3 × 10-14). Linked and de-identified EHR data were used to identify individuals with International Classification of Diseases (ICD) codes for cannabis dependence or cannabis abuse (**Appendix 5a and 5b)**. Ancestry-specific linkage disequilibrium clumping

was performed using PLINK v2.0 with the respective 1000 Genomes Project phase 3 linkage disequilibrium reference panels. Lead variants were identified using r2=0.001 within 10,000 kb. In the CanUD GWAS, SNP-heritability was estimated at $h^2 \approx 6.7\%$.

The second cannabis phenotype was *lifetime cannabis use* (CanLU) from the International Cannabis Consortium (ICC), 23andMe and UK Biobank (N = 184,765) from individuals of European ancestry [57]. ICC included of 35,297 individuals from 16 cohorts from North America, Europe and Australia (55.5% were females; age ranged from 16 to 87 years, with a mean of 35.7 years) where an average of 42.8% of the individuals reported to have used cannabis during their lifetime. 23andMe included 22,683 individuals (55.3% were females; age ranged from 18 to 94 years, with a mean of 54.0 years) where 43.2% reported to have used cannabis during their lifetime. The third sample from UK Biobank consisted of 126,785 individuals (56.3% were females; age ranged from 39 to 72 years, with a mean of 55.0 years) with 22.3% reported to have used cannabis during their lifetime. Participants reported if they had ever used cannabis during their lifetime and the response was recorded as yes or no. This GWAS identified 8 genome-wide significant independent SNPs on chromosomes 3, 7, 8, 11, 16 and 17. Lead variants were identified using $r^2<0.1$ within 250 kb. The top SNP and two other independent associations were located in *CADM2* on chromosome 3 (rs2875907, $P = 9.38 \times 10^{-17}$; rs1448602, $P = 6.55 \times 10^{-11}$; rs7651996, $P = 2.37 \times 10^{-9}$) and other hits were located in *ZNF704, SDK1, NCAM1, RABEP2 or ATP2A1* and *SMG6*. In the CanLU GWAS, SNP-heritability was estimated at $h^2 \approx 11\%$.

Three outcome variables were used in the genetic analysis, each obtained from previously published GWAS data.

For the first outcome variable, summary statistics for the brain IDPs were obtained from the GWAS performed by the UK Biobank, which included approximately 33,000 participants [320]. Of 23 GWS SNPs for CanUD, 20 were available in the current outcome GWAS and 2 proxy SNPs were identified, resulting in a total of 22 SNPs. All 8 SNPs associated with CanLU were available in the outcome GWAS. For the reverse MR analysis, the brain IDP GWAS identified 1 SNP associated at genome-wide significance ($p < 5 \times 10^{-8}$) with FA of the genu of the corpus callosum, and 2 SNPs associated with rsfMRI connectivity (ICA25 edge 21 and ICA100 edge 55) that matched with SNPs in the CanUD GWAS. Notably, only 1 SNP associated with rsfMRI connectivity (ICA25 edge 21) had a matching SNP in the CanLU GWAS.

The second outcome variable was derived from GWAS summary statistics on cognitive test using UK Biobank data [58] The cognitive tests included in the genetic analysis were numeric memory, fluid intelligence, and pairs matching, based on approximately 33,000 participants. A few matching SNPs were not available in the outcome GWAS, and no proxy SNPs meeting the threshold of $R^2 > 0.9$ were identified. For cognitive tests, 20 SNPs related to CanUD and 8 SNPs related to CanLU were available as outcome variables. For the reverse MR analysis, 3 independent SNPs for fluid intelligence were identified from the available GWAS [60]; however, only 2 SNPs (1 matching and 1 proxy) were used, as these were available in the

CanUD GWAS, while no SNPs or proxies were available in the CanLU GWAS. No SNPs or proxy SNPs were identified for numeric memory or pairs matching.

The third outcome variable was identified from a large GWAS on all-cause dementia [59] consisting of 451,317 participants from European ancestry individuals in the MVP. No proxy SNPs meeting this threshold of $R^2 > 0.9$ were available. For all-cause dementia, 21 SNPs related to CanUD and 7 SNPs related to CanLU were available as outcome variables. Five independent SNPs associated with all-cause dementia were identified from the MVP GWAS; of these, 3 matching SNPs were available in the CanUD GWAS. No proxy SNPs meeting the threshold were available, and no matching SNPs were identified in the CanLU GWAS

***Instrument strength:*** The CanUD instrument comprised genome-wide significant, LD-independent variants; after harmonisation, the canonical set explained ~3% of variance in liability ($R^2 \approx 0.03$) with mean (median) per-SNP F ≈ 35 (33). The CanLU instrument explained ~1.3% ($R^2 \approx 0.01$) with mean (median) per-SNP F ≈ 38 (36). Per-SNP F and global F were computed using the exposure summary file actually used (CanUD EUR N≈161,053; CanLU EUR N=184,765). All instruments exceeded F>10. Instruments were harmonised separately to each outcome; consequently, the number of SNPs (k) varied by outcome, and outcome-specific k and $R^2$ is reported in **Table 2**.

*Table 2: Outcome-specific instrument availability and strength*

| Exposure | Outcome (type) | k (SNPs) | $R^2$ (exposure variance) | Mean F (per-SNP) | Median F (per-SNP) | Global F (from $R^2$) |
|---|---|---|---|---|---|---|
| **CanUD** | Brain IDPs | 22 | 0.03 | 34.44 | 32.38 | 208.60 |
| **CanLU** | Brain IDPs | 8 | 0.01 | 37.90 | 36.10 | 310.00 |
| **CanUD** | Cognition | 20 | 0.03 | 36.17 | 34.51 | 209.50 |
| **CanLU** | Cognition | 8 | 0.01 | 37.90 | 36.10 | 310.00 |
| **CanUD** | Dementia (MVP) | 21 | 0.03 | 36.02 | 33.41 | 212.80 |
| **CanLU** | Dementia (MVP) | 7 | 0.01 | 38.65 | 37.35 | 326.50 |

SNPs = instruments used after outcome-specific harmonisation (proxies $r^2>0.9$ where available). $R^2$ and F-statistics were calculated from the exposure GWAS (see Section 3.6). For dementia, power uses the MVP European-ancestry effective sample (25,473 cases / 425,844 controls). Continuous outcomes are reported in SD units; dementia effects are odds ratios per doubling of exposure liability. Abbreviations: CanUD, cannabis use disorder; CanLU, lifetime cannabis use; IDPs, imaging-derived phenotypes; MVP, Million Veteran Program; k, number of SNP instruments used; $R^2$, variance in exposure explained; F, per-SNP F-statistic; Global F, instrument-level F derived from $R^2$.

***Power calculations:*** Power was estimated using the mRnd online MR power calculator under a two-sample design (two-sided $\alpha = 0.05$, 80% power), combining exposure-side $R^2$ with outcome sample sizes (effective N for case–control). Results are presented in **Table 3**.

*Table 3: MR power (α=0.05, 80% power)*

| Exposure | Outcome (type) | K (SNPs) | Outcome N (cases/controls) | Minimum detectable effect (80% power) |
|---|---|---|---|---|
| **CanUD** | Brain IDPs (continuous) | 22 | ~33,000 | ≥ 0.09 SD |
| **CanLU** | Brain IDPs (continuous) | 8 | ~33,000 | ≥ 0.13 SD |
| **CanUD** | Cognition (continuous) | 20 | ~33,000 | ≥ 0.10 SD |
| **CanLU** | Cognition (continuous) | 8 | ~33,000 | ≥ 0.13 SD |
| **CanUD** | Dementia (binary) | 21 | 451,317 (≈25k/425k) | OR ≥ 1.06 per doubling |
| **CanLU** | Dementia (binary) | 7 | 451,317 (≈25k/425k) | OR ≥ 1.09 per doubling |

SD = standard deviation of the outcome. Power assumes a two-sample MR design, two-sided α = 0.05, and 80% power. For dementia, the effective sample size was N_eff ≈ 96,100 from 25,473 cases and 425,844 controls; effects are reported as odds ratios per doubling of exposure liability. If a specific IDP or cognitive phenotype used a different N, the minimum detectable effect (MDE) scales approximately as 1/√N. Abbreviations: CanUD, cannabis use disorder; CanLU, lifetime cannabis use; IDPs, imaging-derived phenotypes; MVP, Million Veteran Program; SD, standard deviation; OR, odds ratio; N_eff, effective case–control sample size.

## 3.7 Statistical analysis

### 3.7.1 Software

All statistical analysis was performed in R (R version 4.0.0, https://www.r-project.org/) and visualisations were performed in MATLAB (version R2018_a). Several R packages were used to support data handling, modelling, and presentation:

- data.table and dplyr: for efficient data manipulation and wrangling.
- tidyr: to restructure data into tidy formats suitable for analysis.
- psych: to compute descriptive statistics and reliability measures.
- broom: to extract and summarise model outputs into tidy data frames.
- lme4: to fit linear and mixed-effects models [321].
- lmerTest: to obtain significance testing for mixed-effects models [322].
- ggplot2: for graphical visualisation of statistical results [323].
- TwoSampleMR: for conducting MR analyses [324].
- LDlink: for proxy lookup
- mRnd: for conducting power calculation for MR analyses

### *3.7.2 Observational analyses*

A series of independent samples *t*-tests and chi-squared analyses were conducted to compare the sociodemographic characteristics between the cannabis users and controls. Independent samples t-tests were used to compare the means of a continuous variable between the two groups, while chi-squared tests were used to examine the relationship between categorical variables. For cross-sectional analyses, multiple linear regression was performed to determine the association between cannabis use and brain measures or cognitive function, accounting for

confounds. For the longitudinal analysis, linear mixed effect models were used to determine the association between cannabis use and cognitive function over time.

Several sensitivity analyses were conducted while controlling for potential covariates. These were performed for the associations that remained statistically significant after adjusting for multiple comparisons using the false discovery rate (FDR), 5% [325] or Bonferroni test. Amongst cannabis users, sensitivity analyses assessed whether: 1) years of cannabis abstinence, and 2) cannabis dose (low vs. high frequency), modified cannabis-brain associations. In addition, 3) a sex-stratified analysis were performed and 4) associations were examined according to frequencies of cannabis use.

In addition, a further set of nested sensitivity analyses was conducted to assess the robustness of the observational associations to alternative covariate specifications. These models were fitted sequentially, beginning with core sociodemographic and health covariates and then progressively adding smoking and alcohol use, baseline psychological traits (risk-taking, loneliness, and standardised neuroticism), and subclinical depressive and anxiety symptoms (PHQ-9 and GAD-2). A final model incorporated clinically diagnosed depression and anxiety derived from ICD codes in linked Hospital Episode Statistics. This stepwise framework was used to evaluate whether these additional variables altered the direction or magnitude of the associations and to explore their potential role as confounders or mediators in the cannabis–brain and cannabis–cognition relationships. Sample sizes differed across models due to missingness in the extended covariate set, and this was taken into account when interpreting changes in effect magnitude.

The specific statistical approaches for observational analyses varied by chapter, depending on the research question and outcome under investigation. Detailed methods are provided within the relevant chapters (**Chapter 4, 5 and 6**).

### *3.7.3 Genetic analyses*

MR is an analytical framework that uses genetic variants as instrumental variables to investigate potential causal effects of an exposure on an outcome [51]. Because alleles are randomly allocated at conception, MR can strengthen causal inference by reducing bias from confounding and reverse causation that typically affect observational studies.

MR relies on three core assumptions:

1. *Relevance* – the genetic variants (instruments) are robustly associated with the exposure.
2. *Independence* – the instruments are not associated with confounders of the exposure–outcome relationship.
3. *Exclusion restriction* – the instruments affect the outcome only through their influence on the exposure, and not via alternative pathways.

When these assumptions are satisfied, MR provides an unbiased estimate of the causal effect of the exposure on the outcome. A schematic representation of the two-sample MR design used in this study, with the three assumptions labelled, is presented in **Figure 9.**

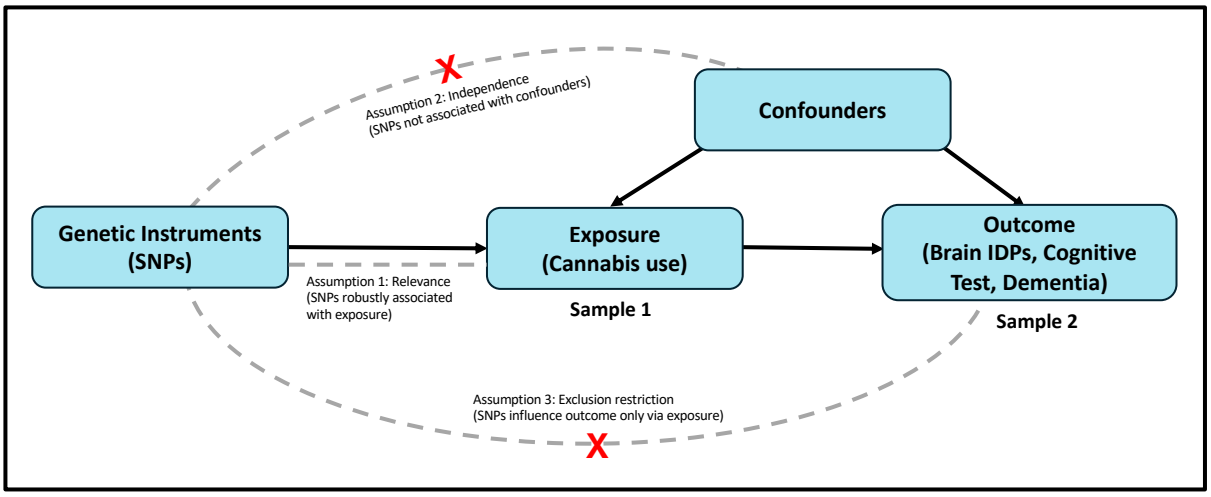



*Figure 9: Two-sample Mendelian Randomisation study design*

Abbreviations: SNPs, single nucleotide polymorphisms; IDPs, imaging derived phenotypes.

Two-sample MR analyses were performed by using the TwoSampleMR in an R package [324]. Genome-wide significant SNPs associated with cannabis use phenotypes, CanUD and CanLU, were used as genetic instruments.

The inverse-variance weighted (IVW) method was applied as the primary analysis, as it provides the most efficient estimate under the assumption that all genetic instruments are valid. To assess robustness and potential violations of MR assumptions, additional approaches were implemented, including MR Egger, weighted median, weighted mode, and simple mode estimators. These complementary methods make different assumptions about the presence and influence of horizontal pleiotropy, and consistency across them increases confidence in causal inference. P-values were adjusted for multiple testing using 5% FDR. The MR-Egger intercept test was used to assess the presence of horizontal pleiotropy, which represents a potential violation of a core MR assumption. Additionally, a reverse MR analysis was conducted in which brain IDPs, cognitive outcomes, and dementia were treated as exposures and cannabis use as the outcome. This was done to test for potential reverse causation, that is, to assess whether variation in brain IDPs, cognitive performance, or dementia risk might predispose individuals to cannabis use, rather than cannabis use influencing these outcomes. SNP effects were harmonised to the exposure effect allele; palindromic SNPs with intermediate EAF were excluded. Binary exposure estimates are reported per doubling of exposure liability.

*Sample overlap*: Exposure and outcome GWAS were drawn from non-overlapping cohorts where possible. Any residual overlap is expected to be minimal; given strong instruments (per-SNP F > 10; global F > 200), material bias is unlikely.

Given the limited number of dementia cases in UK Biobank, observational analyses of cannabis use and dementia were not included in this thesis. Complementary analyses conducted in an independent cohort (MVP) did not show significant associations, and MR was therefore prioritised to strengthen causal inference regarding dementia risk.

#### *3.7.3.1 Robust Methods MR*

For the SNPs significantly associated with cannabis dependence or abuse and lifetime cannabis use, six different MR methods were applied: IVW [326], MR Egger [327], weighted median [328], weighted mode, simple mode [329] and wald ratio. Each method is briefly described below:

- IVW: The IVW method was utilized because the instruments used in the study consisted of multiple SNPs. To ensure valid results, the IVW method requires that all instruments are associated with the exposure variable, but not directly associated with the outcome variable or any confounding factors affecting the relationship between the exposure and outcome [326].
- MR Egger: This method tests for horizontal pleiotropy, which assumes that the pleiotropy effects are independent of the strength of the instrument used [327, 330].
- Weighted median: The estimate obtained from the weighted median gives an estimate of the causal effect when at least half of the genetic variants used are valid instrumental variables [328].
- Weighted mode: This method assumes that the validity of the instruments is based on the largest number of instruments with consistent MR estimates [329].
- Simple mode: This approach uses the mode of the instrumental variable estimate to estimate the causal effect [329].
- Wald ratio: This method is applied when a single SNP is available as an instrument, providing a causal estimate calculated as the ratio of the SNP–outcome to SNP–exposure association [51].

Consistency across these complementary approaches increases confidence in causal inference.

# Chapter 4: Associations between cannabis use and brain structure

## 4.1 Introduction

**The content of this chapter has been published previously:**

*Ishrat S, Levey DF, Gelernter J, Ebmeier K, Topiwala A. Association between cannabis use and brain structure and function: an observational and Mendelian randomisation study. BMJ Ment Health. 2024 Oct 30;27(1):e301065. doi: 10.1136/bmjment-2024-301065. PMID: 39477366; PMCID: PMC11529520*

In this chapter I examine the association between cannabis use and measures of brain structure in a large cohort of older adults in UK Biobank. Past use of cannabis has been linked with multiple aspects of brain structure in adult and adolescent populations [23]. The most consistent brain regions linked to cannabis use are the subcortical regions. Smaller hippocampal GM volume with cannabis use has been observed in individuals with long-term, near-daily use [46] as well as with recent cannabis use [45]. DTI studies have also reported associations with WM microstructure in the corpus callosum inferred by a lower FA and a higher MD [126]. Whether similar brain aspects are affected in mid- to late-life adults are unclear, as only a few studies have included these age groups [165], and the focus has been on heavy or dependent users who appear to show abnormalities in structural connectivity in different brain regions [23, 46]. Further, most studies have limited their analysis to a narrow range of brain regions.

In this study, I employ both hypothesis-driven and exploratory approaches and help the causal interpretation of epidemiological results by using MR [51].

## 4.2 Methods

### 4.2.1 Study sample

The study comprised participants from the UK Biobank [52] listed in **Figure 10**. Out of the initial 157,316 data entries related to cannabis use, 141,420 were excluded due to either lacking MRI data, or missing confounding variables. No other exclusion criteria were applied. Consequently, the final analysis comprised 15,896 participants with complete cases.

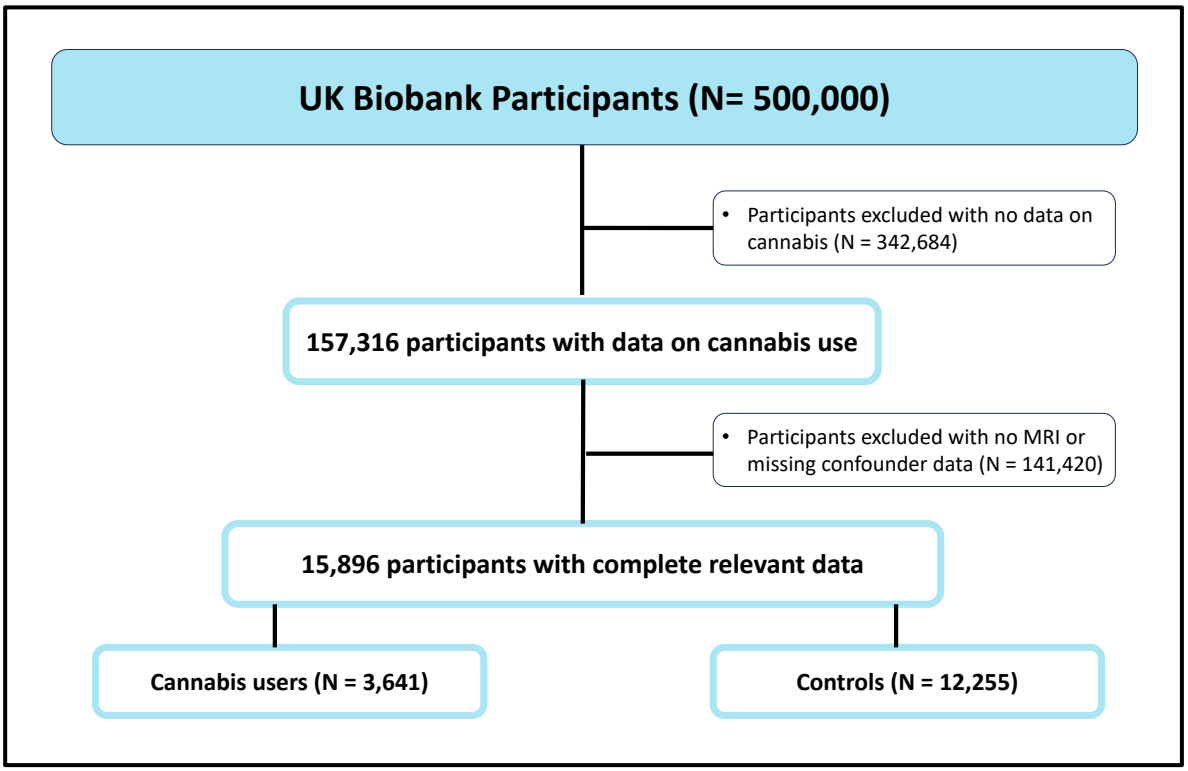



*Figure 10: Flow chart of the participants from the UK Biobank included in the final analysis*

### 4.2.2 Cannabis use data

Cannabis use was self-reported in UK Biobank as described in **Section 3.2**. Participants who reported yes to "Ever taken Cannabis" were classified as lifetime cannabis users and those who responded no were categorised as controls. Cannabis users were further subdivided into low-frequency cannabis use and high-frequency cannabis use. Number of years since cannabis was last used was calculated as the difference between the age when cannabis was last used and the age when subjects were scanned.

### 4.2.3 MRI acquisition and data processing

Full details of the acquisition protocol and processing are given in **Section 3.3** In brief, the structural brain imaging protocol utilized in the UK Biobank includes structural, and diffusion imaging from four distinct modalities: T1-weighted, T2-weighted flair, diffusion MRI (dMRI), and susceptibility-weighted imaging (SWI) [53].

T1-weighted measures estimated GM and cortical measure. T2-weighted flair identified total and periventricular white matter hyperintensities (WMH). DMRI-derived measures of WM

volume and WM microstructure (such as FA, MD, L1, L2, L3 and MO from DTI, and ICVF, ISOVF, OD) from NODDI.

### 4.2.4 Outcomes

In a hypothesis-driven approach, the hippocampus was selected as the primary outcome region, given prior evidence of its sensitivity to cannabis exposure. Previous studies in adolescents and young adults have consistently reported associations with hippocampal volume associated with cannabis use, and cannabinoid CB1 receptors are densely expressed in this region. Accordingly, hippocampal GM volume was selected as the primary outcome measure.

In addition, an exploratory analysis was preformed including the full set of 2,128 brain structural measures derived from UK Biobank imaging (**Appendix 1**).

### 4.2.5 Confounds

Analysis was adjusted for potential confounds self-reported at the time of the MRI scan. These included: age at first scan (in years), sex (male or female), age^2, age^3, and age-by-sex interactions, Townsend deprivation Index, current employment status, highest educational qualifications, smoking and alcohol drinking status, BMI, systolic and diastolic BP, nerves/anxiety/tension/depression status and 613 brain imaging-related confounds [319] (**Appendix 3**). Additional details on the confounding variables are provided in **Section 3.5**.

### 4.2.6 Genetic variants

Genetic variants associated with cannabis use in large GWAS were used as instrumental variables (see **Section 3.6**). GWAS studies included in the genetic analysis are presented in **Figure 11.** Two exposure phenotypes were examined: CanUD and CanLU [56, 57]. Of the 23 genome-wide significant SNPs for CanUD, 20 were available in the UKB brain imaging GWAS of structural brain measures, and 2 proxy SNPs were identified, giving a total of 22 instruments. All 8 CanLU SNPs were available (**Table 4**). The outcome measures were derived from the GWAS summary statistics of structural brain measures in UK Biobank [320]. For reverse MR analyses, the brain structure GWAS identified one genome-wide significant SNP for FA of the genu of the corpus callosum that overlapped with a CanUD variant (**Table 5**).

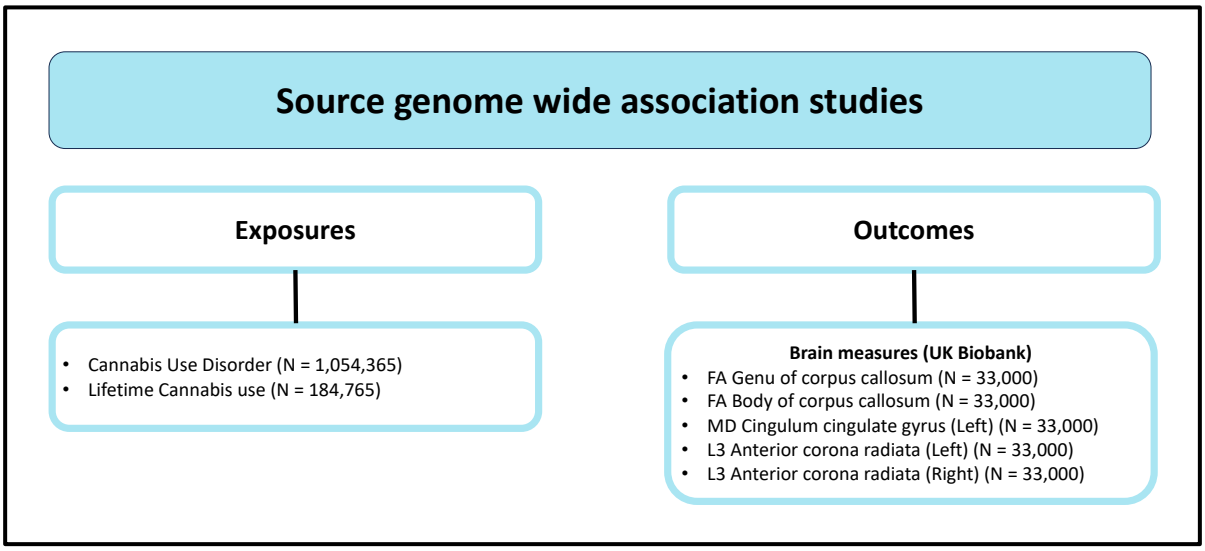



*Figure 11: Source genome-wide association studies used in Mendelian randomization analysis*

Source GWAS references: cannabis use disorder [56]; lifetime cannabis use [57]; brain measures (UK Biobank) [320]. Abbreviations: FA, fractional anisotropy; MD, mean diffusivity; L3, radial diffusivities.

*Table 4: SNPs identified in GWAS associated with cannabis use*

| GWAS | SNP | Chr | BP | A1 | A2 | Beta | SE | *P*-value | *F* stats |
|---|---|---|---|---|---|---|---|---|---|
| **Cannabis use disorder (CanUD) [56]** | rs10835372 | 11 | 28643913 | C | T | 0.05 | 0.01 | 3.03E-08 | 27.28 |
| | rs10986600 | 9 | 127928735 | C | T | 0.06 | 0.01 | 2.17E-10 | 34.67 |
| | rs11711407 | 3 | 50225029 | G | A | 0.05 | 0.01 | 2.95E-08 | 29.06 |
| | rs1526480 | 1 | 91209986 | C | T | -0.05 | 0.01 | 5.91E-10 | 40.25 |
| | rs159365 | 5 | 60500273 | G | A | 0.05 | 0.01 | 3.33E-08 | 29.06 |
| | rs17007864 | 3 | 70876858 | C | T | 0.05 | 0.01 | 1.05E-09 | 30.22 |
| | rs62461183 | 7 | 77716309 | C | T | 0.07 | 0.01 | 5.86E-10 | 43.64 |
| | rs73247642* | 4 | 47114175 | C | T | -0.11 | 0.05 | 1.70E-02 | 6.50 |
| | rs11608109* | 11 | 113303448 | C | G | -0.05 | 0.01 | 1.55E-08 | 29.25 |
| | rs1637570 | 10 | 118619529 | A | G | -0.05 | 0.01 | 4.79E-08 | 27.78 |
| | rs2014920 | 11 | 113466565 | T | G | 0.05 | 0.01 | 8.00E-09 | 31.89 |
| | rs2189010 | 7 | 114119430 | A | G | 0.05 | 0.01 | 1.28E-08 | 29.78 |
| | rs3774800 | 3 | 49334768 | A | G | -0.06 | 0.01 | 1.72E-12 | 40.00 |
| | rs545943750 | 8 | 16059558 | A | AT | -0.68 | 0.12 | 1.45E-08 | 38.94 |
| | rs56070621 | 5 | 30825684 | A | T | 0.05 | 0.01 | 1.15E-08 | 29.25 |
| | rs56372821 | 8 | 27436500 | A | G | -0.09 | 0.01 | 7.27E-14 | 52.64 |
| | rs62051488 | 16 | 72652784 | A | C | -0.07 | 0.01 | 2.98E-08 | 39.33 |
| | rs6690119 | 1 | 73580964 | T | C | 0.05 | 0.01 | 4.99E-08 | 27.28 |
| | rs726610 | 3 | 85551403 | T | C | -0.06 | 0.01 | 4.29E-11 | 35.11 |

| | | | | | | | | | |
|---|---|---|---|---|---|---|---|---|---|
| | rs7519259 | 1 | 66434743 | A | G | 0.05 | 0.01 | 1.83E-09 | 35.00 |
| | rs80030908 | 13 | 55159898 | A | G | 0.17 | 0.03 | 2.13E-08 | 184.27 |
| | rs9344740 | 6 | 88619412 | T | G | -0.06 | 0.01 | 8.34E-10 | 35.11 |
| **Lifetime cannabis use (CanLU) [57]** | rs2875907 | 3 | 85518580 | A | G | 0.07 | 0.01 | 9.38E-17 | 68.89 |
| | rs1448602 | 3 | 85780454 | A | G | -0.06 | 0.01 | 6.55E-11 | 38.44 |
| | rs7651996 | 3 | 85057349 | T | G | 0.05 | 0.01 | 2.37E-09 | 29.06 |
| | rs10085617 | 7 | 3634711 | A | T | 0.05 | 0.01 | 2.93E-08 | 29.06 |
| | rs9773390 | 8 | 81565692 | T | C | -0.17 | 0.03 | 5.66E-09 | 104.22 |
| | rs9919557 | 11 | 112877408 | T | C | -0.06 | 0.01 | 9.94E-11 | 30.11 |
| | rs10499 | 16 | 28915527 | A | G | 0.05 | 0.01 | 1.13E-09 | 31.89 |
| | rs17761723 | 17 | 2107090 | T | C | 0.05 | 0.01 | 3.24E-08 | 27.28 |

Significance threshold was set at $p$<5E-08. *Proxy SNPs. Source GWAS references: cannabis use disorder [56]; lifetime cannabis use [57]. Abbreviations: GWAS, genome-wide association studies; SNP, single nucleotide polymorphism; Chr, Chromosome; BP, location in base pairs; A1, effect allele; A2, other allele; SE, standard error of beta.

*Table 5: SNPs identified in GWAS associated with brain structure*

| GWAS | SNP | Chr | BP | A1 | A2 | Beta | SE | *P*-value |
|---|---|---|---|---|---|---|---|---|
| **Brain measure: FA Genu of Corpus callosum** | rs72776055 | 5 | 85744869 | G | T | 3.33E-10 | 0.08 | 1.44E-9 |

Significance threshold was set at $p$<5E-08. Source GWAS references: brain measures [320]. Abbreviations: GWAS, genome-wide association studies; SNP, single nucleotide polymorphism; Chr, Chromosome; BP, location in base pairs; A1, effect allele; A2, other allele; SE, standard error of beta; FA, fractional anisotropy.

### 4.2.7 Statistical analyses

Independent samples *t*-tests and chi-squared analyses assessed the potential univariate differences in the sociodemographic characteristics between the lifetime cannabis users and controls. Multiple linear regression was performed to determine the relationship between cannabis use and brain structure, accounting for potential covariates. A total of 2,128 brain structures were tested with an adjusted cut-off p-value of 0.05 using Bonferroni correction ($p = 2.23 \times 10^{-5}$). For comparison, p-values in the analyses were also corrected for multiple testing using a 5% FDR.

Before model fitting, the standard assumptions of linear regression were considered. With the large sample size, the central limit theorem supports approximate normality of residuals and stability of parameter estimates. The UK Biobank pipeline also applies a rank-based inverse Gaussian transformation to IDPs. This reduces skewness, limits the impact of outliers, and helps to satisfy the assumptions of parametric modelling [54]. As a result, structural IDP distributions were approximately normal, which minimises concerns about non-normality.

Three sensitivity analyses were conducted among cannabis users, with all models adjusted for the same sociodemographic and lifestyle covariates as in the primary analyses. First, years of

abstinence were modelled as a continuous predictor to test whether duration since last use modified cannabis–brain structure associations. Second, cannabis dose was examined by classifying participants into low- and high-frequency groups, which were entered as a binary predictor in the regression models. Third, to assess sex-specific effects, regression models were repeated separately in males and females. Multiple comparisons were controlled for using a 5% FDR.

To complement the primary analytic strategy for structural imaging outcomes, the nested sensitivity analysis framework outlined in Chapter 3.7.2 was applied to the subset of IDPs that survived FDR correction in the main analysis. Sequential models were fitted to evaluate the robustness of these associations under expanded covariate sets. Model 1 included core demographic and health covariates (age, sex, education, employment, assessment centre, deprivation, BMI, blood pressure, and imaging confounds). Model 2 incorporated smoking and alcohol use; Model 3 further added psychological traits (risk-taking, standardised neuroticism, and loneliness); Model 4 included subclinical mental-health symptoms (PHQ-9 and GAD-2); and Model 5 added clinically diagnosed depression and anxiety derived from HES records (ICD-10). These extended models were used to assess whether the structural associations persisted after accounting for lifestyle, psychological, and mental-health factors, and to determine whether these variables explained additional variance beyond core demographic and physiological covariates.

Finally, two-sample MR analyses were performed to investigate the strength of the evidence that significant observed associations between cannabis use and brain structures were causal. P-values in the MR analyses were additionally adjusted for multiple testing FDR. Additionally, reverse MR analysis was performed. More details on the robust MR methods performed are provided in the **Section 3.7.3.1.**

## 4.3 Results

### 4.3.1 Demographics

There were 3,641 cannabis users and 12,255 control subjects with complete data (**Figure 10**). Individuals with complete as opposed to incomplete cannabis data had a slightly lower proportion of males and a higher proportion were in employment and had college degrees (**Appendix 6).** Only two individuals had cannabis abuse or dependence ICD codes in the linked EHR. Cannabis users were significantly younger than non-users (**Table 6**). While the subjects were well matched for BMI and diastolic BP, the user group had significantly lower systolic BP and were less socially deprived than the control group. There was a slightly higher proportion of males in the user group, a higher proportion of the user group were in employment and had college degrees. A higher proportion of cannabis users than controls drank

alcohol and smoked cigarettes. Additionally, a higher proportion of the user group complained of nerves/anxiety/tension/depression (**Table 6**).

*Table 6: Demographic characteristics*

| **Variables (at time of imaging)** | **Cannabis users (n = 3,641)** | **Controls (n = 12,255)** | **Statistics** | |
|---|---|---|---|---|
| | ***Mean (SD) or % (n)*** | | ***t or $\chi^2$**** | ***p-value*** |
| **Age at 1st scan (years)** | 61.00 (7.07) | 64.49 (7.51) | 24.94 | 2.20E-16 |
| **Sex (male % (n))** | 52.40% (1,908) | 43.96% (5,387) | 80.29* | 2.20E-16 |
| **Townsend deprivation index** | -1.23 (2.99) | -2.24 (2.50) | -20.31 | 2.20E-16 |
| **Employment status (current; % (n))** | 52.89% (1,962) | 34.30% (4,204) | 519.40* | 2.20E-16 |
| **College/university degree (% (n))** | 65.42% (2,382) | 46.37% (5,683) | 477.89* | 2.20E-16 |
| **BMI (kg/m$^2$)** | 26.21 (4.23) | 26.37 (4.36) | 1.97 | 0.05 |
| **Diastolic BP (mmHg)** | 78.54 (10.46) | 78.69 (10.70) | 0.76 | 0.45 |
| **Systolic BP (mmHg)** | 137.36 (19.18) | 141.19 (19.88) | 10.30 | 2.20E-16 |
| **Alcohol use (current; % (n))** | 96.26% (3,505) | 93.43% (11,450) | 93.47* | 2.20E-16 |
| **Smoking (current; % (n))** | 7.39% (269) | 1.93% (337) | 1320.10* | 2.20E-16 |
| **Nerves/anxiety/tension,/ depression status (% (n))** | 11.40% (415) | 7.90% (968) | 42.83* | 5.98E-11 |

Abbreviations: SD, standard deviation; BMI, body mass index; BP, blood pressure.

The demographic characteristics between male versus female is presented in **Table 7.** Broadly similar patterns were observed across sexes: both male and female cannabis users were younger, less socially deprived, and more likely to be in employment or hold a college degree compared with their respective controls. Male and female users also showed higher rates of alcohol use, cigarette smoking, and self-reported nerves/anxiety/tension/depression. BMI and diastolic BP were comparable between groups, while systolic BP was consistently lower in users than controls.

*Table 7: Demographic characteristics (male and female)*

| **Variables (at time of imaging)** | **Male Cannabis users (n = 1,908)** | **Male Controls (n = 5,387)** | **Female Cannabis users (n = 1,733)** | **Female Controls (n = 6,868)** |
|---|---|---|---|---|
| | **Mean (SD) or % (n)** | | **Mean (SD) or % (n)** | |
| **Age at 1st scan (years)** | 61.44 (7.29) | 65.61 (7.52) | 60.52 (6.79) | 63.62 (7.39) |
| **Townsend deprivation index** | -1.33 (2.98) | -2.27 (2.49) | -1.12 (2.99) | -2.21 (2.50) |
| **Employment status (current; % (n))** | 53.93% (1,029) | 32.67% (1,760) | 53.84% (933) | 35.59% (2,444) |
| **College degree (% (n))** | 62.84% (1,199) | 47.24% (2,545) | 68.26% (1,183) | 45.69% (3138) |
| **BMI (kg/m2)** | 26.78 (3.89) | 26.83 (3.82) | 25.57 (4.49) | 26.01 (4.71) |
| **Diastolic BP (mmHg)** | 80.48 (10.03) | 80.62 (10.54) | 76.41 (10.52) | 77.19 (10.59) |
| **Systolic BP (mmHg)** | 140.99 (18.46) | 144.34 (18.45) | 133.36 (19.17) | 138.72 (20.60) |

| | | | | |
|---|---|---|---|---|
| **Alcohol use (current; % (n))** | 96.59% (1,843) | 95.01% (5,118) | 95.90% (1,662) | 92.20% (6,332) |
| **Smoking (current; % (n))** | 8.07% (154) | 2.32% (125) | 6.64% (115) | 1.63% (112) |
| **Nerves/anxiety/tension/ depression status (% (n))** | 10.90% (208) | 7.02% (378) | 11.94% (207) | 8.59% (590) |

Abbreviations: SD, standard deviation; BMI, body mass index; BP, blood pressure.

Participants reported whether they had "ever taken cannabis," with possible responses ranging from "no" to varying lifetime frequencies (1–2, 3–10, 11–100, and more than 100 times). For analysis, cannabis users were grouped into low-frequency use (1–10 times) and high-frequency use (11–100+ times). In this sample, 1,605 participants were classified as high-frequency users and 2,036 as low-frequency users, indicating a greater proportion of low-frequency use (**Figure 12**). Among users, the average age at last use was 32 years (SD = 12.8; median 28, range 2–76), and the average duration without cannabis was 29.3 years (SD = 13.8; median 32, range 0–70). Age at last use showed a slight right skew (**Figure 13 A**), while years without use showed a slight left skew (**Figure 13 B**).

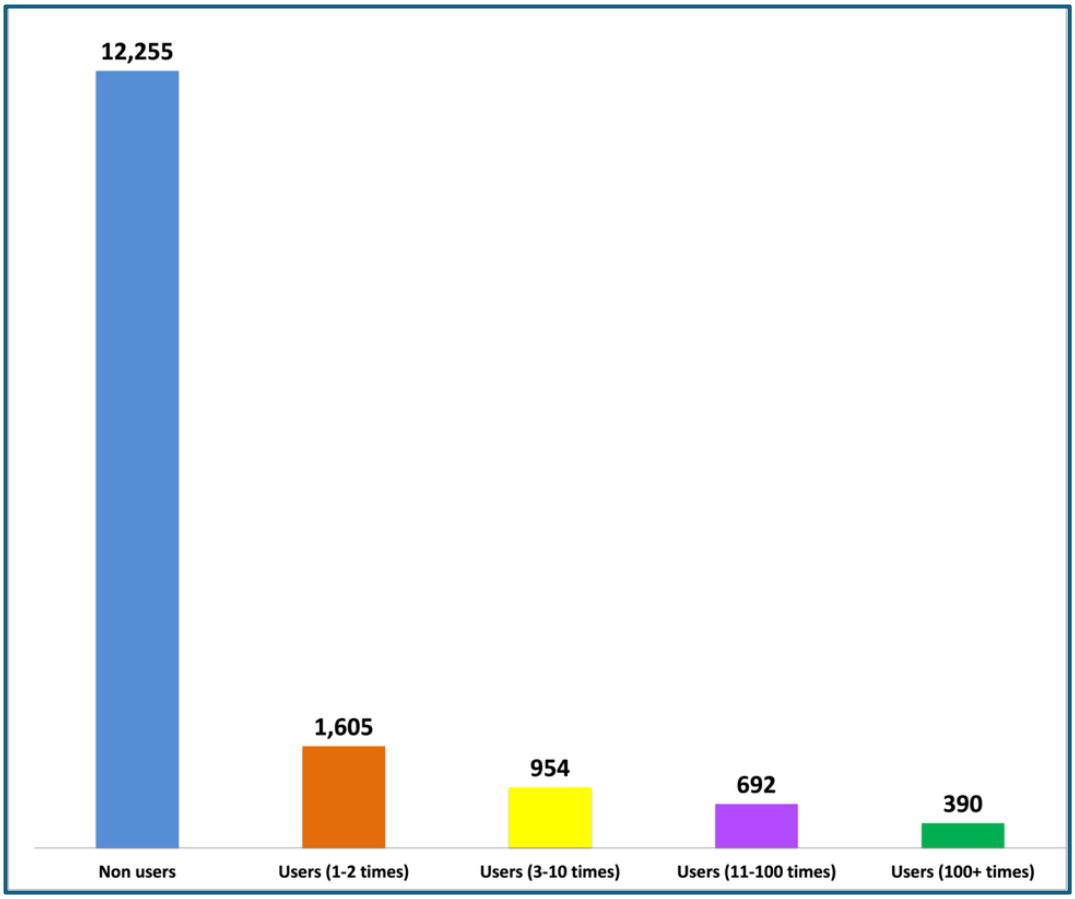



*Figure 12: Distribution of lifetime frequency of cannabis use in UK biobank used in the analysis*

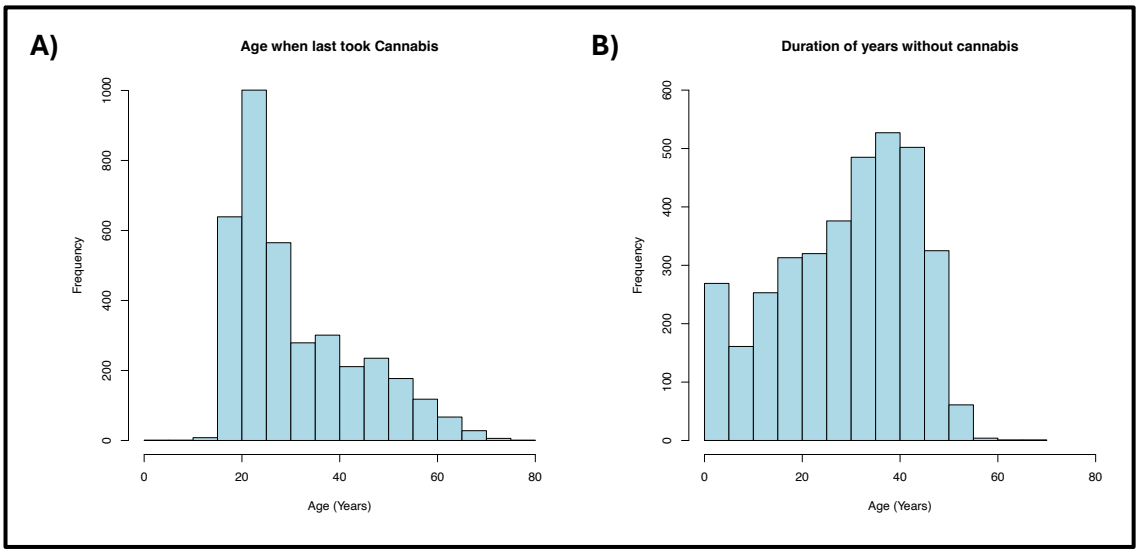



*Figure 13: A) Age when last took cannabis and B) Duration of years without cannabis*

### 4.3.2 Results from observational analysis

In view of previously observed associations with hippocampal volume (derived from FSL-FIRST segmentation), this region was examined as a region of interest in a hypothesis-driven approach. There were no significant associations observed with cannabis use (**Table 8**).

*Table 8: Association between cannabis use and hippocampus volume*

| | Lifetime cannabis use vs. controls | | | |
|---|---|---|---|---|
| | **Beta** | **LCI** | **UCI** | **P-value** |
| **Hippocampus Left** | 0.03 | -0.01 | 0.06 | 0.18 |
| **Hippocampus Right** | 0.01 | -0.03 | 0.05 | 0.61 |

Estimates were generated using multiple linear regression models adjusted for: age, sex, Townsend deprivation index, employment status, educational qualifications, alcohol drinking status, smoking status, body mass index, systolic and diastolic blood pressure, assessment center, nerves/anxiety/tension/depression status and brain imaging confounds including assessment centre, intracranial volume, head motion, table position, and scanner acquisition parameters (site, scanner software, protocol, scan ramp, head coil). Abbreviations: LCI, lower confidence interval; UCI, upper confidence interval.

Out of 2,128 brain structures, cannabis use was significantly associated with 16 brain structures after *FDR* correction (0.05%, p = 0.009) (**Figure 14**, **Table 9**, **Table 10**). The strongest associations were with measures of white matter microstructure. Most significant associations identified in the DTI metrics were found in the genu and body of the corpus callosum, demonstrating lower FA and ICVF, as well as higher MD, and L2 and L3. Furthermore, a higher MD was observed in the left cingulum cingulate gyrus, while increased L2 was detected in the

cingulum bundle, and higher L2 and L3 were observed in the anterior corona radiata (**Figure 15**).

Cannabis use also associated with specific brain structures including a larger volume of the right inferior lateral ventricles, a larger surface area of the frontal pole, greater thickness in the posterior ventral cingulate gyrus, and higher tissue intensity in the right pallidum (**Figure 14**, **Table 9**, **Table 10**).

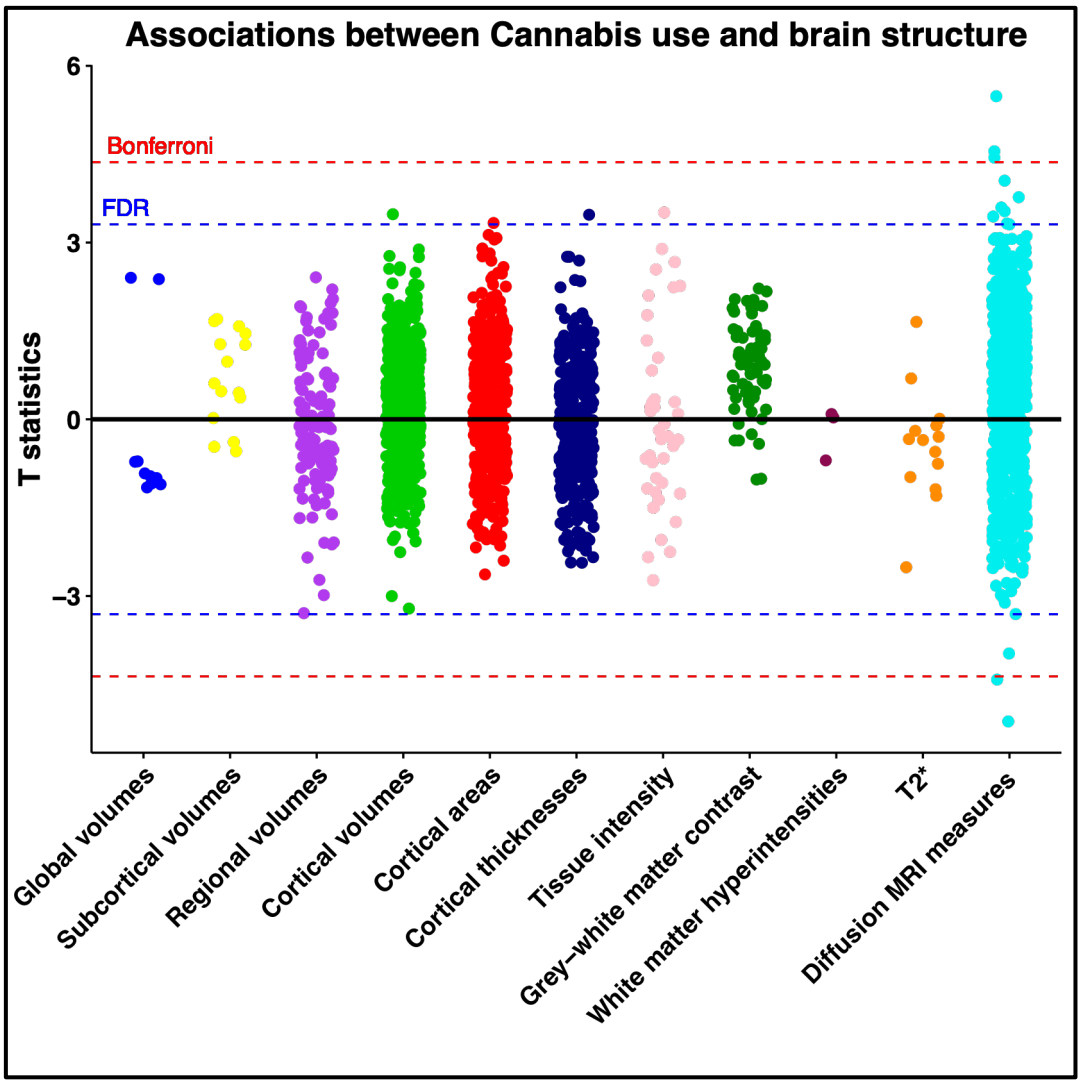



*Figure 14: Associations between cannabis use and brain structure*

Estimates were generated using multiple linear regression models adjusted for: age, sex, Townsend deprivation index, employment status, educational qualifications, alcohol drinking status, smoking status, body mass index, systolic and diastolic blood pressure, assessment center, nerves/anxiety/tension/depression status and brain imaging confounds including assessment centre, intracranial volume, head motion, table position, and scanner acquisition parameters (site, scanner software, protocol, scan ramp, head coil). Red line indicates the Bonferroni threshold (3,921 tests, $p = 1.28 \times 10^{-5}$, T statistics = 4.36) and blue line indicates the False Discovery rate threshold (3,921 tests, $p = 9.38 \times 10^{-4}$, T statistics = 3.31). Abbreviations: MRI, magnetic resonance imaging; FDR, false discovery rate.

*Table 9: Summary of the association between cannabis use and brain structure*

| Brain measures | Regions | | Direction/strength of association with cannabis use |
|---|---|---|---|
| Volume | Right inferior lateral ventricles | | Positive |
| Area | Left frontal pole | | Positive |
| Thickness | Left posterior ventral cingulum gyrus | | Positive |
| Tissue Intensity | Right pallidum | | Positive |
| Diffusion tensor imaging | FA | Genu and body of corpus callosum | Negative |
| | ICVF | Genu of corpus callosum | |
| | MD | Genu of corpus callosum, cingulum cingulate gyrus | Positive |
| | L2 | Genu and body of corpus callosum, and left cingulum cingulate gyrus | |
| | L3 | Genu and body of corpus callosum, genu, and right and left anterior corona radiata | |

Abbreviations: MRI, magnetic resonance imaging; FA, fractional anisotropy; ICVF, intracellular volume fraction; MD, mean diffusivity; L2 and L3, radial diffusivities; BOLD, blood oxygenation level dependent.

*Table 10: Associations between cannabis use and individual image-derived phenotypes*

| Brain measures | Beta | LCI | UCI | P-value |
|---|---|---|---|---|
| **Volume – Inferior lateral ventricle (Right)** | 0.06 | 0.03 | 0.10 | 5.01E-04 |
| **Surface area – Frontal pole (Left)** | 0.06 | 0.03 | 0.10 | 8.63E-04 |
| **Cortical thickness – Posterior ventral cingulate gyrus (Left)** | 0.07 | 0.03 | 0.11 | 5.18E-04 |
| **Tissue intensity – Pallidum (Right)** | 0.07 | 0.03 | 0.11 | 4.50E-04 |
| **FA Genu of corpus callosum** | -0.10 | -0.14 | -0.06 | 2.95E-07 |
| **FA Body of corpus callosum** | -0.08 | -0.12 | -0.04 | 7.05E-05 |
| **MD Genu of corpus callosum** | 0.08 | 0.04 | 0.12 | 8.99E-06 |
| **MD Cingulum, cingulate gyrus (Left)** | 0.06 | 0.03 | 0.10 | 5.78E-04 |
| **L2 Genu of corpus callosum** | 0.09 | 0.05 | 0.12 | 5.43E-06 |
| **L2 Body of corpus callosum** | 0.07 | 0.04 | 0.11 | 1.64E-04 |
| **L3 Genu of corpus callosum** | 0.10 | 0.07 | 0.14 | 4.23E-08 |
| **L3 Body of corpus callosum** | 0.08 | 0.04 | 0.12 | 5.13E-05 |
| **L3 Anterior corona radiata (Right)** | 0.07 | 0.03 | 0.10 | 3.25E-04 |
| **L3 Anterior corona radiata (Left)** | 0.06 | 0.03 | 0.10 | 4.14E-04 |
| **L2 Cingulum (cingulate gyrus, Left)** | 0.06 | 0.03 | 0.10 | 8.94E-04 |
| **ICVF Genu of corpus callosum** | -0.09 | -0.13 | -0.05 | 1.00E-05 |

Estimates represent beta coefficients from multiple linear regression models surviving FDR correction and adjusted for: age, sex, Townsend deprivation index, employment status, educational qualifications, alcohol drinking status, smoking status, body mass index, systolic and diastolic blood pressure, assessment centre, nerves/anxiety/tension/depression status and brain imaging confounds including assessment centre, intracranial volume, head motion, table position, and scanner acquisition parameters (site, scanner software, protocol, scan ramp, head coil). Abbreviations: LCI, lower confidence interval; UCI, upper confidence interval; FA, fractional anisotropy; MD, mean diffusivity; L2 and L3, radial diffusivities; ICVF, intracellular volume fraction.

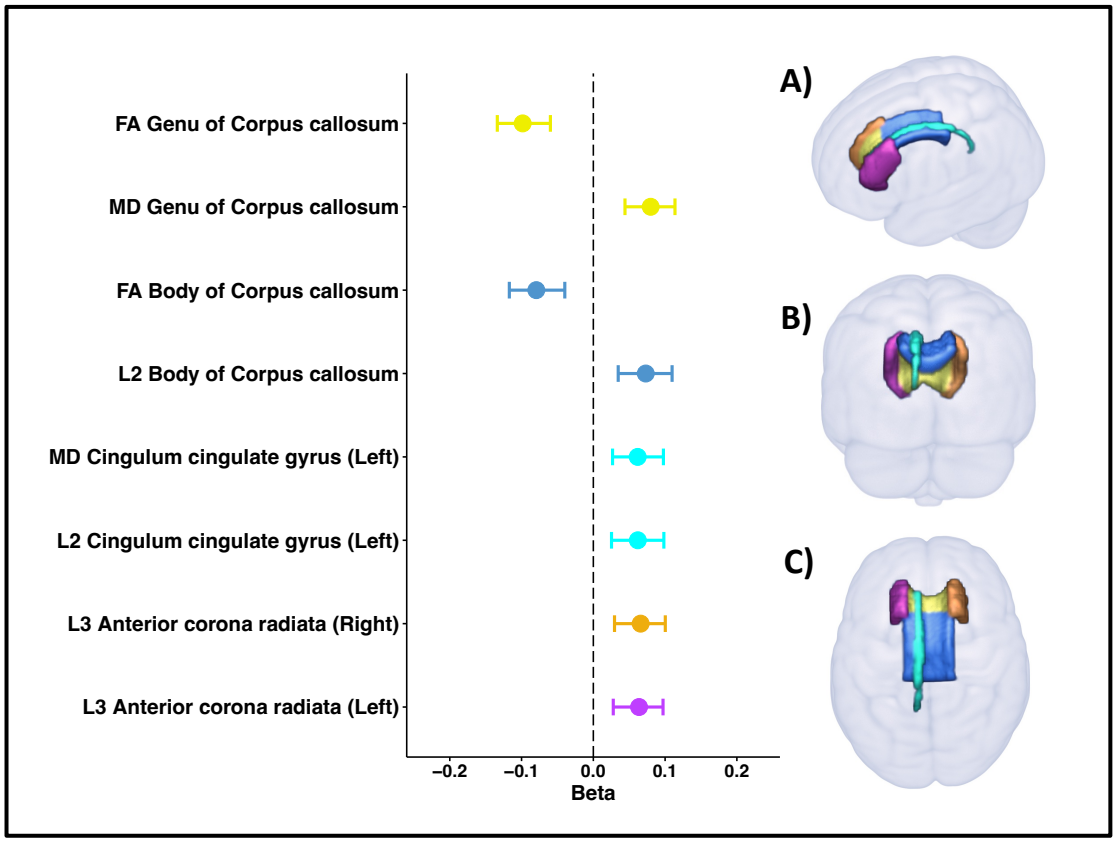



*Figure 15: White matter regions significantly associated with cannabis use*

Structures delineated by the JHU White Matter Atlas (ICBM-DTI-81) are presented in A) sagittal, B) coronal, and C) axial views. Abbreviations: FA, fractional anisotropy; MD, mean diffusivity; L2 and L3, radial diffusivities.

Associations with five brain structures additionally survived the more stringent Bonferroni-corrected threshold ($p = 1.275 \times 10^{-5}$). Cannabis users were characterized by lower FA and ICVF, and higher MD, L2, and L3 in the genu of the corpus callosum **(Table 11)**.

*Table 11: Associations between cannabis use and brain structure surviving Bonferroni correction*

| Brain measures | Beta | LCI | UCI | P-value |
|---|---|---|---|---|
| **FA Genu of corpus callosum** | -0.10 | -0.13 | -0.06 | 2.95E-07 |
| **MD Genu of corpus callosum** | 0.08 | 0.04 | 0.11 | 8.99E-06 |
| **L2 Genu of corpus callosum** | 0.09 | 0.05 | 0.12 | 5.43E-06 |
| **L3 Genu of corpus callosum** | 0.10 | 0.06 | 0.14 | 4.23E-08 |
| **ICVF Genu of corpus callosum** | -0.09 | -0.13 | -0.05 | 1.00E-05 |

Estimates represent beta coefficients from multiple linear regression models adjusted for: age, sex, Townsend deprivation index, employment status, educational qualifications, alcohol drinking status, smoking status, body mass index, systolic and diastolic blood pressure, assessment centre, nerves/anxiety/tension/depression status and brain imaging confounds including assessment centre, intracranial volume, head motion, table position, and scanner acquisition parameters (site, scanner software, protocol, scan ramp, head coil). Abbreviations: LCI, lower

confidence interval; UCI, upper confidence interval; FA, fractional anisotropy; MD, mean diffusivity; L2 and L3, radial diffusivities; ICVF intracellular volume fraction.

Despite these localized associations, the vast majority of brain structures showed no evidence of association with cannabis use. Of the 2,128 IDPs examined, only 16 (0.05%) survived FDR correction, while the remaining measures were non-significant. No associations were identified for global indices of brain volume, subcortical or regional volumes, grey–white matter contrast, white matter hyperintensities, or T2* measures. Likewise, most WM regions did not show robust relationships with cannabis use.

### 4.3.3 Sensitivity Analyses

In the sensitivity analysis, the study assessed whether the duration of abstinence or dose impacted the relationships between cannabis use and brain structures that survived the FDR correction in the main analysis. After correcting for FDR, neither the duration of cannabis abstinence (**Table 12**) nor the frequency of cannabis dosage (as assessed through low and high-frequency use) (**Table 13**) significantly moderated the associations between cannabis use and brain measures.

*Table 12: Association between duration of cannabis abstinence and brain structure*

| Brain measures | Beta | LCI | UCI | P-value |
|---|---|---|---|---|
| **Volume – Inferior lateral ventricle (Right)** | -1.02E-04 | -2.77E-03 | 2.57E-03 | 9.40E-01 |
| **Surface area – Frontal pole (Left)** | 1.83E-04 | -2.77E-03 | 2.57E-03 | 8.86E-01 |
| **Cortical thickness – Posterior ventral cingulate gyrus (Left)** | -3.10E-04 | -2.77E-03 | 2.57E-03 | 8.36E-01 |
| **Tissue intensity – Pallidum (Right)** | -1.27E-04 | -2.77E-03 | 2.57E-03 | 9.33E-01 |
| **FA Genu of corpus callosum** | 1.22E-03 | -2.77E-03 | 2.57E-03 | 3.69E-01 |
| **FA Body of corpus callosum** | 2.25E-03 | -2.77E-03 | 2.57E-03 | 1.12E-01 |
| **MD Genu of corpus callosum** | -1.92E-03 | -2.77E-03 | 2.57E-03 | 1.37E-01 |
| **MD Cingulum, cingulate gyrus (Left)** | -2.01E-03 | -2.77E-03 | 2.57E-03 | 1.14E-01 |
| **L2 Genu of corpus callosum** | -7.22E-04 | -2.77E-03 | 2.57E-03 | 5.92E-01 |
| **L2 Body of corpus callosum** | -2.03E-03 | -2.77E-03 | 2.57E-03 | 1.39E-01 |
| **L3 Genu of corpus callosum** | -2.13E-03 | -2.77E-03 | 2.57E-03 | 1.08E-01 |
| **L3 Body of corpus callosum** | -2.49E-03 | -2.77E-03 | 2.57E-03 | 6.94E-02 |
| **L3 Anterior corona radiata (Right)** | -2.03E-03 | -2.77E-03 | 2.57E-03 | 1.22E-01 |
| **L3 Anterior corona radiata (Left)** | -1.71E-03 | -2.77E-03 | 2.57E-03 | 1.84E-01 |
| **L2 Cingulum (cingulate gyrus, Left)** | -1.21E-03 | -2.77E-03 | 2.57E-03 | 3.61E-01 |
| **ICVF Genu of corpus callosum** | 2.72E-03 | -2.77E-03 | 2.57E-03 | 5.78E-02 |

Estimates represent beta coefficients from multiple linear regression models and adjusted for: age, sex, Townsend deprivation index, employment status, educational qualifications, alcohol drinking status, smoking status, body mass index, systolic and diastolic blood pressure, assessment centre, nerves/anxiety/tension/depression status and

brain imaging confounds including assessment centre, intracranial volume, head motion, table position, and scanner acquisition parameters (site, scanner software, protocol, scan ramp, head coil). Abbreviations: LCI, lower confidence interval; UCI, upper confidence interval; FA, fractional anisotropy; MD, mean diffusivity; L2 and L3, radial diffusivities; ICVF, intracellular volume fraction.

*Table 13: Association between high frequency cannabis use (compared to low frequency) and brain structure*

| Brain measures | Beta | LCI | UCI | P-value |
|---|---|---|---|---|
| **Volume – Inferior lateral ventricle (Right)** | -0.02 | -0.09 | 0.05 | 0.53 |
| **Surface area – Frontal pole (Left)** | -0.02 | -0.09 | 0.05 | 0.55 |
| **Cortical thickness – Posterior ventral cingulate gyrus (Left)** | -0.03 | -0.09 | 0.05 | 0.36 |
| **Tissue intensity – Pallidum (Right)** | 0.04 | -0.09 | 0.05 | 0.32 |
| **FA Genu of corpus callosum** | 0.05 | -0.09 | 0.05 | 0.18 |
| **FA Body of corpus callosum** | 0.03 | -0.09 | 0.05 | 0.41 |
| **MD Genu of corpus callosum** | -0.04 | -0.09 | 0.05 | 0.26 |
| **MD Cingulum, cingulate gyrus (Left)** | -0.02 | -0.09 | 0.05 | 0.47 |
| **L2 Genu of corpus callosum** | -0.05 | -0.09 | 0.05 | 0.18 |
| **L2 Body of corpus callosum** | -0.03 | -0.09 | 0.05 | 0.40 |
| **L3 Genu of corpus callosum** | -0.04 | -0.09 | 0.05 | 0.21 |
| **L3 Body of corpus callosum** | -0.04 | -0.09 | 0.05 | 0.20 |
| **L3 Anterior corona radiata (Right)** | -0.05 | -0.09 | 0.05 | 0.12 |
| **L3 Anterior corona radiata (Left)** | -0.05 | -0.09 | 0.05 | 0.12 |
| **L2 Cingulum (cingulate gyrus, Left)** | -0.08 | -0.09 | 0.05 | 0.02 |
| **ICVF Genu of corpus callosum** | 0.05 | -0.09 | 0.05 | 0.18 |

Estimates represent beta coefficients from multiple linear regression models and adjusted for: age, sex, Townsend deprivation index, employment status, educational qualifications, alcohol drinking status, smoking status, body mass index, systolic and diastolic blood pressure, assessment centre, nerves/anxiety/tension/depression status and brain imaging confounds including assessment centre, intracranial volume, head motion, table position, and scanner acquisition parameters (site, scanner software, protocol, scan ramp, head coil). Abbreviations: LCI, lower confidence interval; UCI, upper confidence interval; FA, fractional anisotropy; MD, mean diffusivity; L2 and L3, radial diffusivities; ICVF, intracellular volume fraction.

There were notable sex differences. After *FDR* correction, while significant associations were observed in one brain structure among males, females exhibited a more widespread effect across 22 brain structures. **(Table 14 and 15).**

*Table 14: Associations between cannabis use and brain structure in males surviving False Discovery Rate*

| Brain measures | Beta | LCI | UCI | P-value |
|---|---|---|---|---|
| **MO Fornix cres + Stria terminalis (Right)** | 0.10 | 0.05 | 0.16 | 3.54E-04 |

Estimates represent beta coefficients from multiple linear regression models adjusted for: age, Townsend deprivation index, employment status, educational qualifications, alcohol drinking status, smoking status, body mass index, systolic and diastolic blood pressure, assessment centre, nerves/anxiety/tension/depression status and

brain imaging confounds including assessment centre, intracranial volume, head motion, table position, and scanner acquisition parameters (site, scanner software, protocol, scan ramp, head coil). Abbreviations: LCI, lower confidence interval; UCI, upper confidence interval; MO, diffusion tensor mode.

*Table 15: Associations between cannabis use and brain measures in females surviving False Discovery Rate*

| Brain measures | Beta | LCI | UCI | P-value |
|---|---|---|---|---|
| **FA Genu of corpus callosum*** | -0.13 | -0.18 | -0.08 | 2.28E-06 |
| **FA Body of corpus callosum** | -0.11 | -0.17 | -0.05 | 1.54E-04 |
| **MD Genu of corpus callosum** | 0.10 | 0.05 | 0.15 | 1.47E-04 |
| **MD Anterior corona radiata (Right)** | 0.09 | 0.04 | 0.14 | 4.21E-04 |
| **L2 Genu of corpus callosum** | 0.12 | 0.06 | 0.17 | 2.25E-05 |
| **L2 Body of corpus callosum** | 0.10 | 0.05 | 0.16 | 2.27E-04 |
| **L3 Genu of corpus callosum*** | 0.13 | 0.08 | 0.18 | 1.63E-06 |
| **L3 Body of corpus callosum** | 0.11 | 0.06 | 0.17 | 6.31E-05 |
| **L3 Anterior limb of internal capsule (Right)** | 0.11 | 0.06 | 0.16 | 3.15E-05 |
| **L3 Anterior corona radiata (Right)** | 0.10 | 0.05 | 0.16 | 9.17E-05 |
| **L3 Anterior corona radiata (Left)** | 0.10 | 0.05 | 0.15 | 1.98E-04 |
| **L3 Superior corona radiata (Right)** | 0.10 | 0.05 | 0.15 | 1.39E-04 |
| **L3 Superior corona radiata (Left)** | 0.09 | 0.04 | 0.14 | 3.80E-04 |
| **MD Inferior fronto-occipital fasciculus (Right)** | 0.10 | 0.05 | 0.15 | 1.49E-04 |
| **MD Posterior thalamic radiation (Right)** | 0.09 | 0.04 | 0.14 | 3.30E-04 |
| **L2 Inferior fronto-occipital fasciculus (Right)** | 0.10 | 0.05 | 0.15 | 3.21E-04 |
| **L2 Inferior longitudinal fasciculus (Left)** | 0.10 | 0.05 | 0.15 | 2.63E-04 |
| **L2 Inferior longitudinal fasciculus (Right)** | 0.10 | 0.04 | 0.15 | 3.95E-04 |
| **L2 Posterior thalamic radiation (Right)** | 0.09 | 0.04 | 0.14 | 4.60E-04 |
| **L3 Inferior fronto-occipital fasciculus (Right)** | 0.11 | 0.05 | 0.16 | 1.03E-04 |
| **L3 Posterior thalamic radiation (Right)** | 0.10 | 0.04 | 0.15 | 4.02E-04 |
| **ICVF Genu of corpus callosum** | -0.11 | -0.17 | -0.05 | 1.57E-04 |

Estimates represent beta coefficients from multiple linear regression models adjusted for: age, Townsend deprivation index, employment status, educational qualifications, alcohol drinking status, smoking status, body mass index, systolic and diastolic blood pressure, assessment centre, nerves/anxiety/tension/depression status and brain imaging confounds including assessment centre, intracranial volume, head motion, table position, and scanner acquisition parameters (site, scanner software, protocol, scan ramp, head coil). *Brain measures after surviving Bonferroni correction Abbreviations: LCI, lower confidence interval; UCI, upper confidence interval; FA, fractional anisotropy; MD, mean diffusivity; L2 and L3, radial diffusivities; ICVF intracellular volume fraction.

Re-estimating the structural associations under the extended covariate framework showed that the 10 IDPs identified in the primary analysis remained FDR-significant in the core model (Model 1; N = 15,896) (**Appendix 7**), with effect sizes and directions closely matching the original results. These associations—including diffusion metrics in the genu and body of the corpus callosum, anterior corona radiata, and selected subcortical and cortical measures—also

remained FDR-significant when smoking and alcohol were added (Model 2) (**Appendix 8**). In contrast, once psychological traits were introduced (Model 3; N = 2,462), no IDPs survived FDR correction, although all effects remained directionally consistent with Models 1–2. Further adjustment for subclinical mental-health symptoms (Model 4; N = 818) and for ICD-10 diagnoses of depression and anxiety (Model 5; N = 2,781) similarly yielded no FDR-significant IDPs. Across all extended structural models, attenuation rather than reversal of estimates was observed, with the loss of significance largely attributable to substantial reductions in sample size in models containing psychological and mental-health variables.

### 4.3.4 Results from Mendelian randomization analysis

A total of 22 SNP instruments were available for CanUD and 8 for CanLU. After correcting for multiple comparisons, there were no significant associations between genetically predicted *CanUD* (IVW beta= 0.01 [95% CI -0.09 to 0.11], p = 0.85) or *CanLU* (IVW beta= -0.05 [95% CI -0.15 to 0.05], p = 0.33), and FA in genu of the corpus callosum. No significant associations were observed with other brain IDPs either. There was no indication of horizontal pleiotropy as determined by the MR-Egger intercept test for any of the outcomes **(Figure 16, Table 16 and Figure 17)**. Reverse MR analysis did not show any significant associations between brain IDPs and *CanUD* or *CanLU* **(Table 17)**.

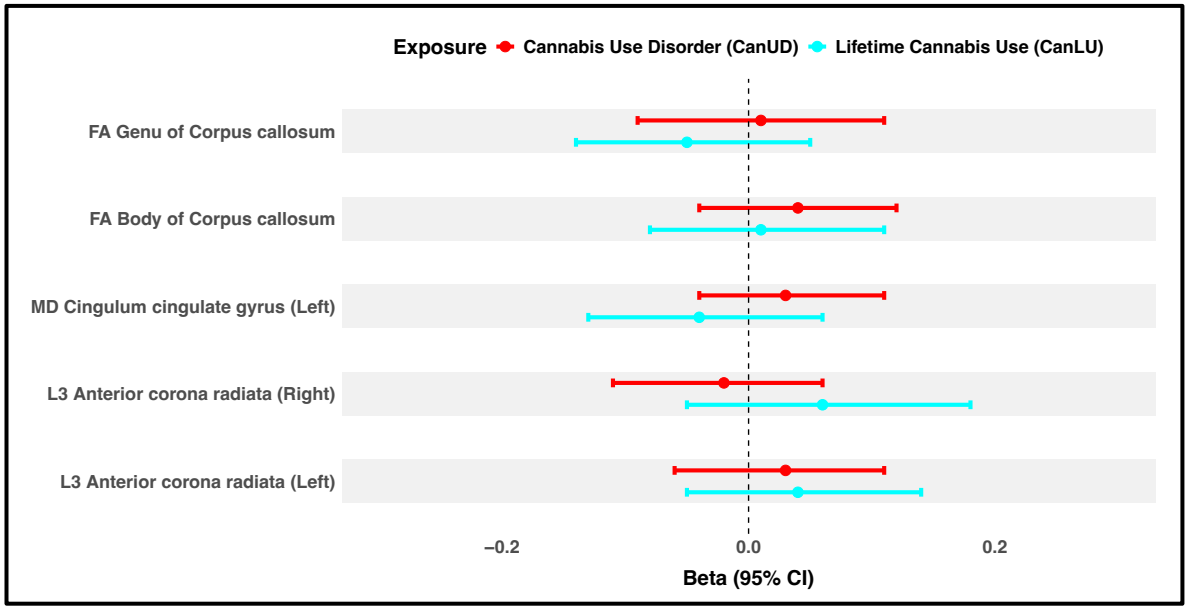



*Figure 16: Genetic associations between cannabis use and brain structure*

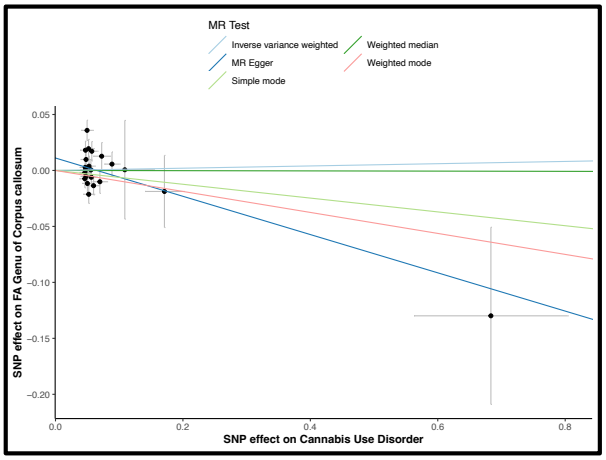
Forest plot displays beta (dots) and 95% confidence intervals (lines) for brain structure in cannabis use disorder (in red) or lifetime cannabis use (in cyan) prevalence. Estimates were generated using two sample inverse-variance weighted method from source genome-wide association studies used to derive genetic associations, with SNPs as instruments detailed in **Figure 11**.

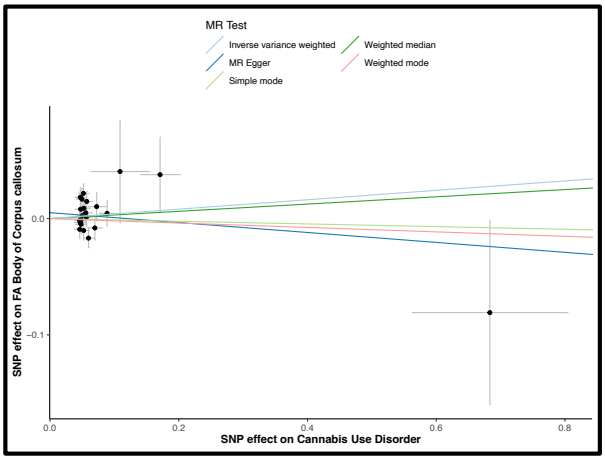
*Table 16: Two-sample linear MR estimates assessing evidence for the causal effect of cannabis use on brain structure*

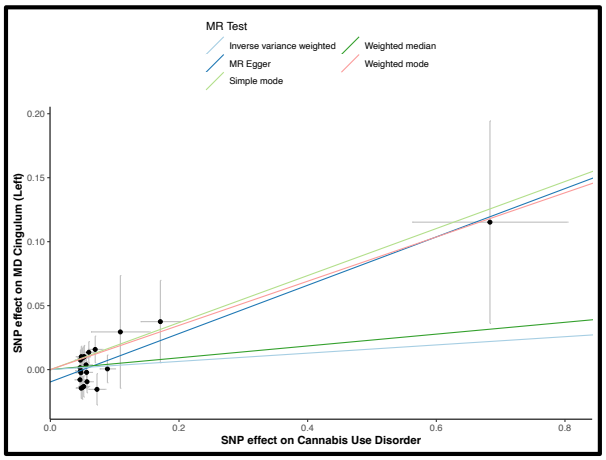
| Brain measures | Cannabis Phenotypes | SNPs (n) | MR Tests | Estimates | LCI | UCI | P-value |
|---|---|---|---|---|---|---|---|
| **FA Genu of Corpus callosum** | CanUD | 22 | MR Egger | -0.17 | -0.47 | 0.13 | 0.28 |
| | | | Weighted mean | 0.00 | -0.11 | 0.11 | 0.99 |
| | | | IVW | 0.01 | -0.09 | 0.11 | 0.85 |
| | | | Simple mode | -0.06 | -0.27 | 0.14 | 0.56 |
| | | | Weighted mode | -0.09 | -0.27 | 0.09 | 0.32 |
| | CanLU | 8 | MR Egger | -0.07 | -0.34 | 0.19 | 0.61 |
| | | | Weighted mean | -0.07 | -0.19 | 0.06 | 0.31 |
| | | | IVW | -0.05 | -0.14 | 0.05 | 0.33 |
| | | | Simple mode | -0.07 | -0.26 | 0.11 | 0.47 |
| | | | Weighted mode | -0.07 | -0.23 | 0.09 | 0.44 |
| **FA Body of Corpus callosum** | CanUD | 22 | MR Egger | -0.04 | -0.29 | 0.20 | 0.74 |
| | | | Weighted mean | 0.03 | -0.07 | 0.13 | 0.54 |
| | | | IVW | 0.04 | -0.04 | 0.12 | 0.33 |
| | | | Simple mode | -0.01 | -0.21 | 0.18 | 0.91 |
| | | | Weighted mode | -0.02 | -0.19 | 0.15 | 0.83 |
| | CanLU | 8 | MR Egger | -0.03 | -0.29 | 0.24 | 0.86 |
| | | | Weighted mean | 0.01 | -0.12 | 0.13 | 0.90 |
| | | | IVW | 0.01 | -0.08 | 0.11 | 0.80 |
| | | | Simple mode | 0.03 | -0.14 | 0.20 | 0.77 |
| | | | Weighted mode | 0.01 | -0.14 | 0.17 | 0.87 |
| **MD Cingulum cingulate gyrus (Left)** | CanUD | 22 | MR Egger | 0.19 | -0.03 | 0.40 | 0.10 |
| | | | Weighted mean | 0.05 | -0.05 | 0.14 | 0.36 |
| | | | IVW | 0.03 | -0.04 | 0.11 | 0.41 |
| | | | Simple mode | 0.18 | -0.02 | 0.39 | 0.09 |
| | | | Weighted mode | 0.17 | 0.00 | 0.34 | 0.06 |
| | CanLU | 8 | MR Egger | 0.18 | -0.08 | 0.45 | 0.22 |
| | | | Weighted mean | -0.05 | -0.18 | 0.08 | 0.47 |
| | | | IVW | -0.04 | -0.13 | 0.06 | 0.45 |
| | | | Simple mode | -0.08 | -0.28 | 0.12 | 0.46 |
| | | | Weighted mode | -0.07 | -0.26 | 0.12 | 0.49 |
| **L3 Anterior corona radiate (Right)** | CanUD | 22 | MR Egger | 0.16 | -0.08 | 0.40 | 0.21 |
| | | | Weighted mean | -0.07 | -0.17 | 0.04 | 0.21 |
| | | | IVW | -0.02 | -0.11 | 0.06 | 0.61 |
| | | | Simple mode | -0.09 | -0.27 | 0.09 | 0.35 |
| | | | Weighted mode | -0.08 | -0.27 | 0.11 | 0.43 |
| | CanLU | 8 | MR Egger | 0.18 | -0.14 | 0.50 | 0.32 |
| | | | Weighted mean | 0.10 | -0.04 | 0.23 | 0.15 |
| | | | IVW | 0.06 | -0.05 | 0.18 | 0.30 |
| | | | Simple mode | 0.18 | -0.07 | 0.42 | 0.21 |
| | | | Weighted mode | 0.16 | -0.04 | 0.37 | 0.16 |
| **L3 Anterior corona radiate (Left)** | CanUD | 22 | MR Egger | 0.17 | -0.07 | 0.41 | 0.18 |
| | | | Weighted mean | 0.00 | -0.10 | 0.10 | 0.99 |
| | | | IVW | 0.03 | -0.06 | 0.11 | 0.56 |
| | | | Simple mode | -0.01 | -0.20 | 0.17 | 0.88 |
| | | | Weighted mode | -0.01 | -0.18 | 0.17 | 0.94 |
| | CanLU | 8 | MR Egger | 0.23 | -0.03 | 0.49 | 0.14 |
| | | | Weighted mean | 0.10 | -0.04 | 0.23 | 0.16 |
| | | | IVW | 0.04 | -0.05 | 0.14 | 0.37 |
| | | | Simple mode | 0.14 | -0.09 | 0.37 | 0.29 |
| | | | Weighted mode | 0.14 | -0.06 | 0.35 | 0.21 |

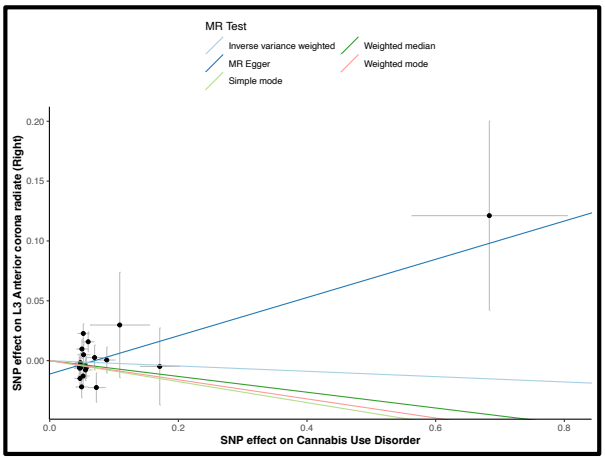
Abbreviations: SNP, single nucleotide polymorphism; LCI, lower confidence interval; UCI, upper confidence

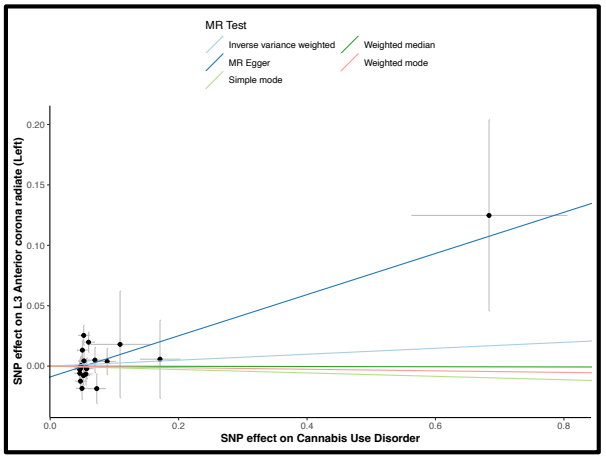
interval; CanUD, cannabis use disorder; CanLU, lifetime cannabis use; MR, mendelian randomisation; IVW, inverse-variance weighted; FA, fractional anisotropy; MD, mean diffusivity; L3, radial diffusivities.

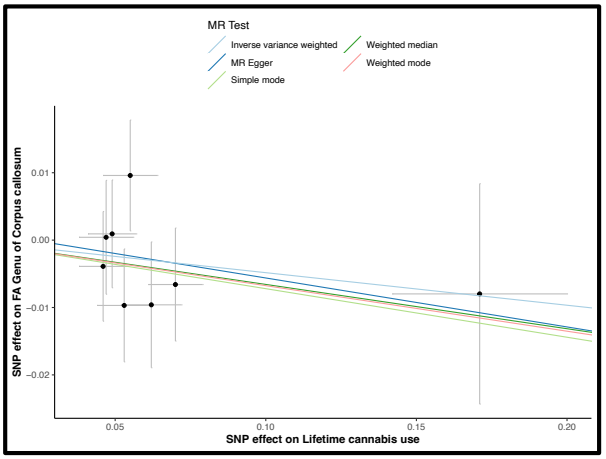


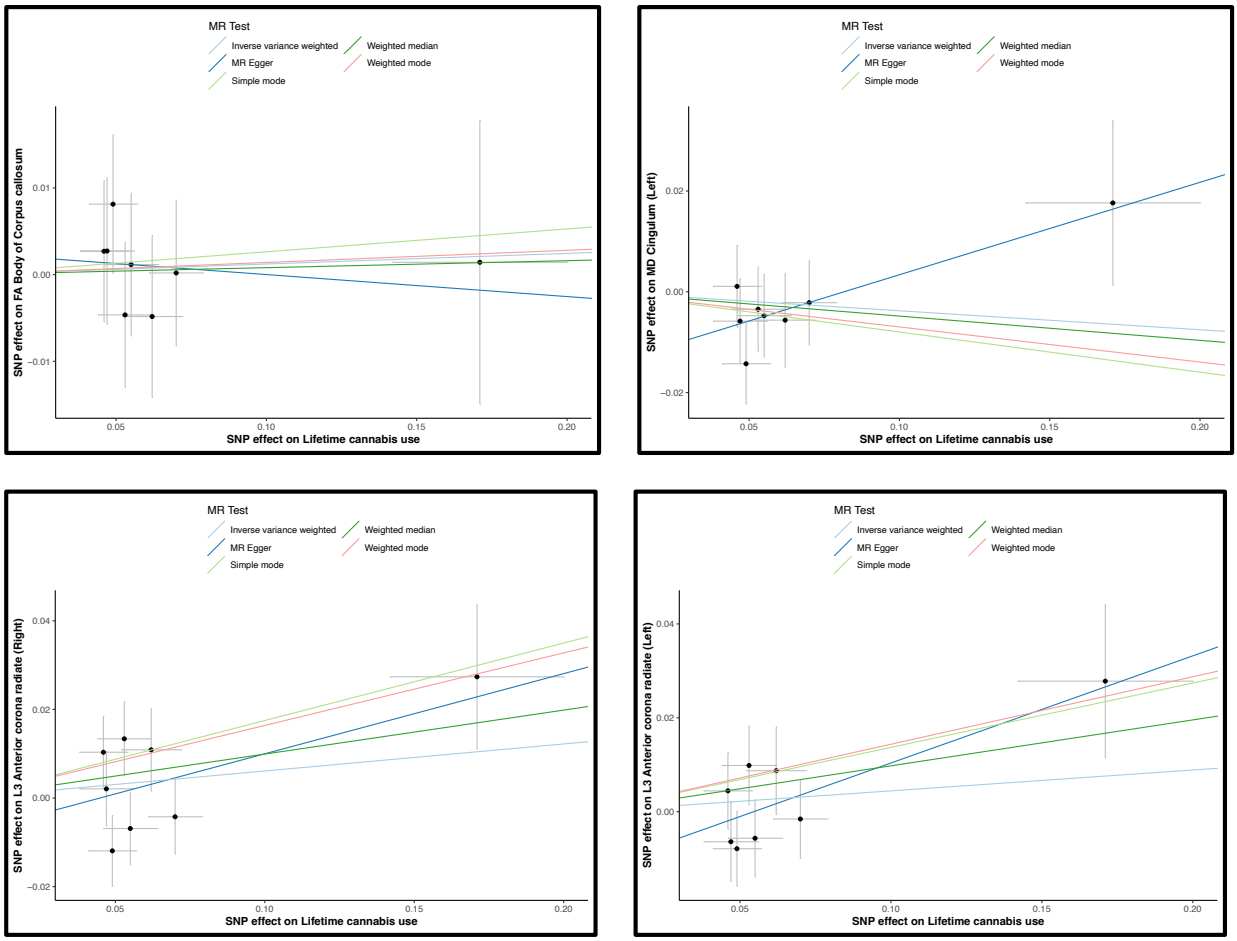



*Figure 17: Two-sample linear MR plot assessing evidence for the causal effect of Cannabis use disorder (CanUD)/Lifetime Cannabis use (CanLU) on brain structure*

*Table 17: Two-sample linear Reverse MR assessing evidence estimates for the causal effect of brain structure on cannabis use*

| Cannabis Phenotypes | Brain Measures | SNPs (n) | MR Test | Estimates | LCI | UCI | P-value |
|---|---|---|---|---|---|---|---|
| **Cannabis use disorder** | FA genu of corpus callosum | 1 | Wald ratio | -283 | -804.36 | 238.36 | 0.92 |
| **Lifetime cannabis use** | FA genu of corpus callosum | 1 | Wald ratio | -1837.93 | -3573.61 | -102.25 | 0.04 |
| | FA genu of corpus callosum | 1 | Wald ratio | 20.27 | -58.68 | 99.22 | 0.62 |

Estimates are from Wald ratio MR method. Abbreviations: SNP, single nucleotide polymorphism; LCI, lower confidence interval; UCI, upper confidence interval.

## 4.4 Discussion

The results indicate that cannabis users had significant differences in brain structure compared to non-users, most notably in measures of WM microstructure in the corpus callosum. However, genetic analyses found no significant effect.

Previously observed associations between cannabis use and GM volume in the hippocampus [45, 46] were not replicated. One possible explanation is the lower level of cannabis exposure in this sample. Another factor may be the differing age range of subjects. Previous studies examined adolescents and young adults, whereas sample in this study comprised middle- to late-life adults. In this older age group, no significant difference in hippocampal volume was observed between cannabis users and controls. This may suggest that age-related reductions in hippocampal volume occur regardless of cannabis use, making it harder to detect group differences. The analysis also included more extensive adjustments for potential confounding variables compared to the earlier studies. It is also possible that the GM recovered over time. Additionally, WM microstructural changes may also be more sensitive to cannabis effects than the GM measures used in this study.

Cannabis users showed lower FA and higher MD in the genu of the corpus callosum compared to non-users. Previous studies of the frequent use of high-potency cannabis by adolescents and young adults have reported disruption in corpus callosum integrity. Taken together, this might suggest that the corpus callosum is particularly sensitive to high THC usage [331]. Cannabis users had lower WM integrity, as measured by higher radial diffusivity (L2 and L3) of the anterior corona radiata and higher mean diffusivity in the left cingulum. Although no associations in these diffusion metrics have been observed in past studies, disrupted microstructural integrity in the cingulum was reported with other diffusion measures showing higher FA of the cingulum [332].

There were also a few other brain structures that showed associations with cannabis use after correcting for multiple comparisons. Cannabis users showed a higher surface area of the left frontal pole and higher tissue intensity in the right pallidum. While the literature has not previously reported any similar associations with these measures, others have reported a higher volume of the pallidum [333], and in contrast a decreased gyrification of the frontal pole [334]. A novel association with left inferior lateral ventricle volume and left posterior ventral cingulum gyrus thickness was also observed.

No significant association was observed between the duration of abstinence from cannabis use prior to the brain scan and structural brain connectivity. Furthermore, no significant differences in structural connectivity were identified between low and high-frequency cannabis users, thus indicating the absence of a dose-response relationship. This may reflect the characteristics of the sample, which comprised healthy volunteers [335] and a few high cannabis users. However, past studies suggest that both frequency and duration of cannabis use may impact brain structure. Specifically, regular cannabis use during adolescence was associated with a higher risk of developing cannabis dependence, and the risk of developing CUD was higher among

those who started early and used frequently during adolescence [336]. Additionally, the prevalence of CUD increases over time since initiation of use, with a steeper increase observed among youth compared to emerging adults, indicating that duration of use may also contribute to changes in brain structure [337]. However, further research is needed to elucidate the specific patterns and mechanisms underlying these effects.

The examination of sex differences with cannabis use showed intriguing insights. The observed differences in brain regions suggest potential variations in how cannabis affects males and females. The more widespread impact seen in females, particularly in WM, may potentially indicate differential vulnerability to cannabis-related neurotoxicity. Further research is warranted to elucidate the underlying mechanisms driving these sex-specific differences and their implications for the long-term effects of cannabis use on brain structure. While the impact of gender on cannabis effects remains unclear, a systematic review revealed mixed results [292]. Among the studies examined (n=11), the majority found no sex-specific interactions, yet a subset (n=8) suggested that females might exhibit increased vulnerability to cannabis-related neurotoxicity. Additionally, studies lacking sex differences often had fewer females, impacting statistical power, and underscoring the need for a more in-depth exploration into the underlying mechanisms driving these sex-specific differences [292].

In the extended sensitivity models, the broader covariate framework indicated that the structural MRI findings were predominantly influenced by reductions in sample size rather than by changes in effect direction. The structural associations remained robust when adjusting for core demographic and lifestyle factors, but became statistically fragile once psychological and mental-health variables were introduced. No IDPs survived FDR correction in these extended models; however, the direction of effects was consistently preserved, suggesting attenuation due to reduced power rather than genuine alterations in the underlying associations. Overall, these patterns underscore the importance of sample size and covariate completeness when interpreting multivariable structural neuroimaging analyses.

MR analyses provided no support for a causal effect of cannabis use or dependence on brain structure, nor a causal effect of brain structure on cannabis use. The disparity between observational and MR findings could result from several mechanisms. First, the observational associations may be confounded by an unmeasured variable, such as family history of psychiatric or substance use disorders, dietary intake or use of certain medications that are said to affect the brain structure such as antidepressants [338, 339]. Second, the MR analyses had less statistical power than the observational analyses to detect small effects. However, despite potential concerns about weak instrument bias in MR studies, the SNPs in this study demonstrated robust instrument strength, evident from the F-statistics. Nevertheless, future larger-scale neuroimaging GWAS will be helpful in distinguishing these two hypotheses. Finally, MR assesses the lifelong impact of cannabis use, while changes in observational studies might be due to factors occurring at different points in an individual's life rather than as the sum of lifelong impact.

Although this is one of the largest observational study of relationships between cannabis use and brain structure to date, and the first MR investigation, there are several limitations that needs to be addressed. First, although the sample size was bigger than that of previous studies, UK Biobank is healthier than the general population [335]. It suffers from selection bias with respect to sociodemographic variables, such as physical, lifestyle and health-related characteristics, as well as a lower prevalence of CUD compared to a population sample. Furthermore, this sample is not suitable for examining CUD due to the limited number of participants with this diagnosis. Second, as the age of cannabis initiation was not recorded, it was not possible to examine life stages that may be critical for cannabis effects. Third, participants are susceptible to recall and reporting bias concerning the amount or frequency of cannabis intake in their lifetime, and their response might be affected by external biases arising from social desirability. Determining historical cannabis use is challenging: Urine drug screens have a limited detection period, typically just a few days, while hair analyses cover a longer period of months that is still limited by hair length. Fourth, the self-report did not include the potency of cannabis consumed, which might differ across the participants and over time. Fifth, despite the effort to account for potential confounds, the presence of unmeasured confounding variables (residual confounding) cannot be excluded. Sixth, the categorization of high-frequency cannabis users is likely to result in a heterogeneous group due to the broad nature of the classification, limiting the ability to investigate the heterogeneity of cannabis effects according to use patterns. Seventh, it was not possible to distinguish between dose-dependent and frequency-dependent effects. Eighth, neuroimaging measures were cross-sectional, and longitudinal relationships cannot be inferred. Finally, MR relies on several assumptions, some of which can be evaluated but not all. In particular, the assumption that there is no unmeasured confounding between genetic variants and outcomes cannot be directly tested in an observational setting.

# Chapter 5: Association between cannabis use and brain function

## 5.1 Introduction

**This content of this chapter has been published previously:**

*Ishrat S, Levey DF, Gelernter J, Ebmeier K, Topiwala A. Association between cannabis use and brain structure and function: an observational and Mendelian randomisation study. BMJ Ment Health. 2024 Oct 30;27(1):e301065. doi: 10.1136/bmjment-2024-301065. PMID: 39477366; PMCID: PMC11529520*

In this chapter the association between cannabis use and brain functional connectivity were examined in a large cohort of adults in UK Biobank. Cannabis use has been associated with changes in the rsFC in the brain [47, 124]. Studies have reported an association between cannabis use and DMN connectivity in both adolescence and young adults who engage in frequent or near-daily use [61, 177]. Among near-daily use cannabis users, increased functional connectivity in the DMN and insular network has been observed [61]. In regular consumers, cannabis use has been associated with regional differences in limbic and sensorimotor striatum, the DMN, executive control network and the salience network resting state connectivity [181]. Connectivity in these regions is implicated in self-referential thoughts, emotional processing, self-awareness, memory, cognitive control, decision making interoception, and conscious experience which might suggest the potential impact of cannabis on higher-order network interactions [182–184]. However, some of the associations have been found to be inconsistent especially in left PCC and the DMN [61, 177]. While only a few studies to date have included older adults [40, 165], larger studies in these age groups are needed to clarify the impact of cannabis use on functional connectivity in later life.

This study employed agnostic approaches to assess the association between cannabis use and brain functional connectivity and triangulated observational findings using MR [51].

## 5.2 Methods

### 5.2.1 Study sample

The study comprised 15,896 participants from the UK Biobank with complete data as described in **Chapter 4** (**Figure 5**). In this study, out of the initial 157,316 data entries related to cannabis use, 141,420 were excluded due to either lacking MRI data, or missing confounding variables.

No other exclusion criteria were applied. This is the same analytic sample as in **Chapter 4 (Section 4.2.1).**

### 5.2.2 Cannabis use data

Cannabis use was self-reported in UK Biobank as described in **Section 3.2** via touchscreen questionnaire. Participants who reported yes to "Ever taken Cannabis" were classified as lifetime cannabis users and those who responded no were categorised as controls. Cannabis users were further subdivided into low-frequency cannabis use and high-frequency cannabis use. Year since last used cannabis was calculated by the difference between the age when last cannabis was used and the age when subjects were scanned. This classification was identical to that used in **Chapter 4**.

### 5.2.3 MRI acquisition and data processing

Full details of the acquisition protocol and processing are given in **Section 3.3**. In brief, the functional brain imaging protocol utilized in the UK Biobank includes task functional MRI timeseries (tfMRI), and resting-state functional MRI timeseries data (rsfMRI) [53].

Task fMRI employed the Hariri faces/shapes "emotion" task which represented summary measures of activation in regions chosen from the group-level activation map. Resting-state fMRI conducted at two distinct dimensionalities (25 and 100), resulting in 21 and 55 signal networks, provided information on measures of both within-network and between-network functional connectivity. A total of 1,793 brain measures of functional connectivity were used as outcomes in the analysis (**Appendix 1**).

### 5.2.4 Confounds

Confounds were self-reported at baseline or at the time of the MRI scan and included: age at first scan (in years), sex (male or female), age^2, age^3, age-by-sex interaction, Townsend deprivation index, current employment status, highest educational qualification, smoking and alcohol drinking status, BMI, systolic and diastolic BP, nerves/ anxiety/tension/depression status and 613 brain imaging-related [319] (**Appendix 3**). These were the same confounds adjusted in **Chapter 4**. Additional details on the confounding variables are provided in Section 3.5.

### 5.2.5 Genetic variants

GWAS studies included in the genetic analysis are presented in **Figure 18.** Genetic variants associated with cannabis use from large GWAS were used as instrumental variables (**see Section 3.6**). Two exposure phenotypes were examined: CanUD and CanLU [56, 57]. Genetic

associations with outcome variables were obtained from summary statistics of a large UKB brain imaging GWAS [320]. For CanUD, 20 matching SNPs were available in the UKB brain imaging GWAS of structural brain measures, with 2 additional proxy SNPs identified, giving a total of 22 instruments. For CanLU 8 SNPs were available. Full details of these SNPs are provided in Table 4 **(see Section 4.2.6)**. For reverse MR analyses, SNPs identified in the brain function GWAS are presented in **Table 18**.

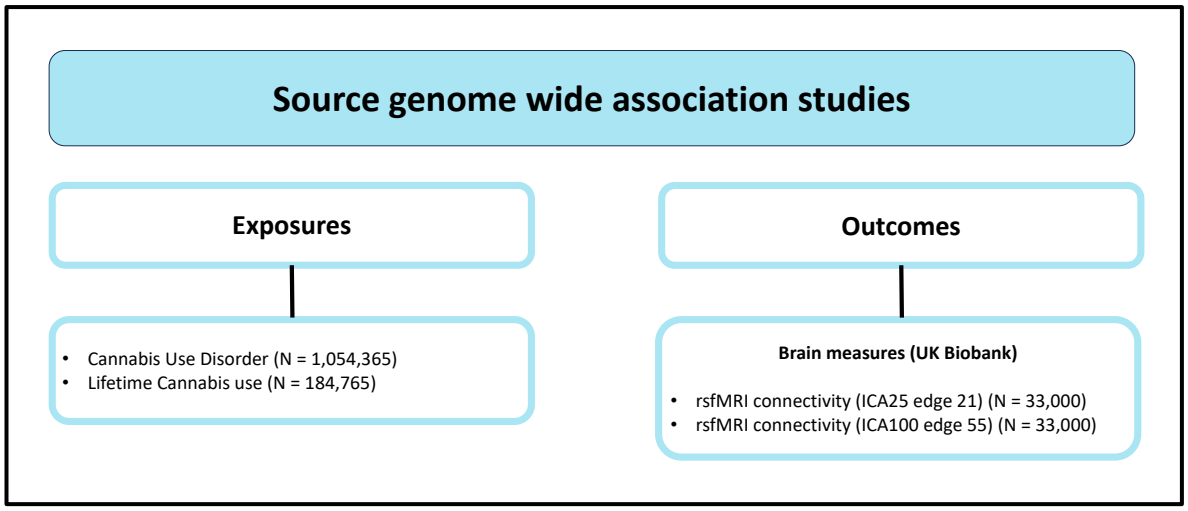



*Figure 18: Source genome-wide association studies used in Mendelian randomization analysis*

Abbreviations: rsfMRI, resting state function magnetic resonance imaging; ICA, independent component analysis. Source GWAS references: cannabis use disorder [56]; lifetime cannabis use [57]; brain measures (UK Biobank) [320].

*Table 18: SNPs identified in GWAS associated with brain function*

| GWAS | SNP | Chr | BP | A1 | A2 | β | SE | *P*-value |
|---|---|---|---|---|---|---|---|---|
| **rsfMRI connectivity (ICA25 edge 21)** | rs559370521 | 5 | 172852051 | T | C | -7.55E-9 | 0.08 | 3.11E-8 |
| | rs7113557 | 11 | 48317492 | C | T | -5.86E-11 | 0.01 | 2.18E-9 |
| **rsfMRI connectivity (ICA100 edge 55)** | rs147270121 | 5 | 153248944 | C | T | -3.43E-9 | 0.05 | 2.48E-8 |
| | rs28649975 | 8 | 92275269 | C | T | -1.21E-9 | 0.01 | 3.12E-8 |

Significance threshold was set at $p$<5E-08. Abbreviations: Abbreviations: GWAS, genome-wide association studies; SNPS, single nucleotide polymorphism; Chr, Chromosome; BP, location in base pairs; A1, effect allele; A2, other allele; SE, standard error of beta.

### 5.2.6 Statistical analyses

Statistical analyses were conducted using the same approach as outlined in **Chapter 4 (see Section 4.2.7)**, adapted here for functional measures. Independent samples *t*-tests and chi-squared analyses assessed the potential univariate differences in the sociodemographic characteristics between the lifetime cannabis users and controls. Multiple linear regression was

performed to determine the relationship between cannabis use and functional brain measures, accounting for confounds. Prior to model fitting, the assumptions of linear regression were considered in the context of the large sample size. By the central limit theorem, residuals can be expected to approximate normality, and parameter estimates remain stable. Functional IDPs released by UK Biobank are already subject to a quantile Gaussian transformation, a rank-based procedure that produces near-Gaussian distributions and reduces the influence of outliers [54]. These steps mean that the assumptions of linear modelling were largely satisfied.

An exploratory approach was employed to examine the association between cannabis use and brain function. A total of 1,793 brain IDPs were tested with an adjusted cut-off p-value of 0.05 using Bonferroni correction ($p = 2.23 \times 10^{-5}$). For comparison, p-values in the analyses were also corrected for multiple testing using a 5% FDR.

The same three sensitivity analyses described in the structural chapter were conducted for the functional outcomes. First, years of abstinence were modelled as a continuous predictor to test whether duration since last use modified cannabis–functional associations. Second, cannabis dose was examined by classifying participants into low- and high-frequency groups, which were entered as a binary predictor in the regression models. Third, sex-specific effects were assessed by repeating the regression models separately in males and females. All models were adjusted for the same sociodemographic and lifestyle covariates as in the primary analyses, and multiple comparisons were controlled for using a 5% FDR.

The nested sensitivity modelling framework described in the structural chapter was applied to functional IDPs. Models sequentially incorporated smoking and alcohol use, psychological traits, subclinical mental-health symptoms, and ICD-10 diagnoses of depression and anxiety. These supplementary models allowed evaluation of whether functional associations detected in the primary analysis were robust to broader covariate adjustment and whether behavioural or mental-health characteristics explained additional variability in functional activation or connectivity patterns.

Finally, two-sample MR analyses were performed to investigate whether significant observed associations between cannabis use and brain function could be causal. P-values in the analyses were additionally adjusted for multiple testing FDR. Additionally, reverse MR analysis was performed. Additional details on robust MR methods performed are provided in **Section 3.7.3.1.**

## 5.3 Results

### 5.3.1 Demographics

The demographic characteristics of participants included in the functional analyses were the same as those described in **Table 6 (see Section 4.3.1)**, as both structural and functional outcomes were derived from the same analytic sample (n = 15,896; 3,641 cannabis users and 12,255 controls). For clarity, the key characteristics are summarised here.

Cannabis users were on average younger than non-users (mean age ~61 vs. 64 years) and included a slightly higher proportion of men. They tended to be less socially deprived, more likely to be in current employment, and more likely to hold a college or university degree compared with controls. Lifestyle differences were also apparent: cannabis users reported higher rates of current alcohol consumption and cigarette smoking, and a greater proportion reported experiencing nerves, anxiety, tension, or depression. In contrast, BMI and diastolic BP did not differ between groups, while systolic BP was modestly lower among users.

Sex-specific comparisons showed similar patterns in both men and women, with cannabis users in each sex being younger, less deprived, and more likely to be employed or hold a degree relative to their same-sex controls. Male and female users also reported higher rates of alcohol and cigarette use and more frequent psychological symptoms. Detailed sex-specific characteristics are provided in **Table 7 (see Section 4.3.1)**.

### 5.3.2 Observational analyses

A wide range of associations with cannabis use were observed across various rsFC analyses, indicating either weaker or stronger connectivity between multiple networks (**Figure 19, Table 19, Table 20)**. These networks predominantly included brain regions associated with the DMN, CEN and salience network. A summary of the resting-state networks significantly associated with cannabis use is described in **Table 20.** A visual representation of these associations is shown in **Figure 20**, where networks are displayed as nodes, with connecting lines indicating significant associations. Results are presented separately for the 21 networks derived from the 25-component group-ICA and the 55 networks derived from the 100-component group-ICA. Additionally, full edge-level associations, including brain regions and networks corresponding to each rsFC edge, are presented in **Table 21**.

Cannabis use was associated with both increased and decreased functional connectivity across several large-scale networks. Stronger connectivity was observed within and between regions of the default mode, central executive, salience, and motor networks. In particular, users showed greater coupling between prefrontal and occipital regions, as well as between angular gyrus, middle temporal gyrus, and superior frontal areas, all of which form part of the default mode and central executive systems.

Conversely, weaker connectivity was observed across a wider set of networks, including the default mode, central executive, salience, motor, visual, subcortical–cerebellar, attention, and limbic networks. Notable reductions were seen in connectivity between inferior and middle

frontal regions with the precuneus and middle occipital cortex, and between the precuneus and supplementary motor and temporal regions, indicating reduced DMN–CEN–salience interactions. Additional weaker connections were observed between motor–visual, motor–attention, and visual–limbic pathways.

In addition to these rsFC findings, cannabis use was also associated with task-related differences in brain function **(Figure 19, Table 19, Table 20)**. During the emotion-processing task (faces versus shapes), cannabis users demonstrated stronger whole-brain BOLD activation compared with controls.

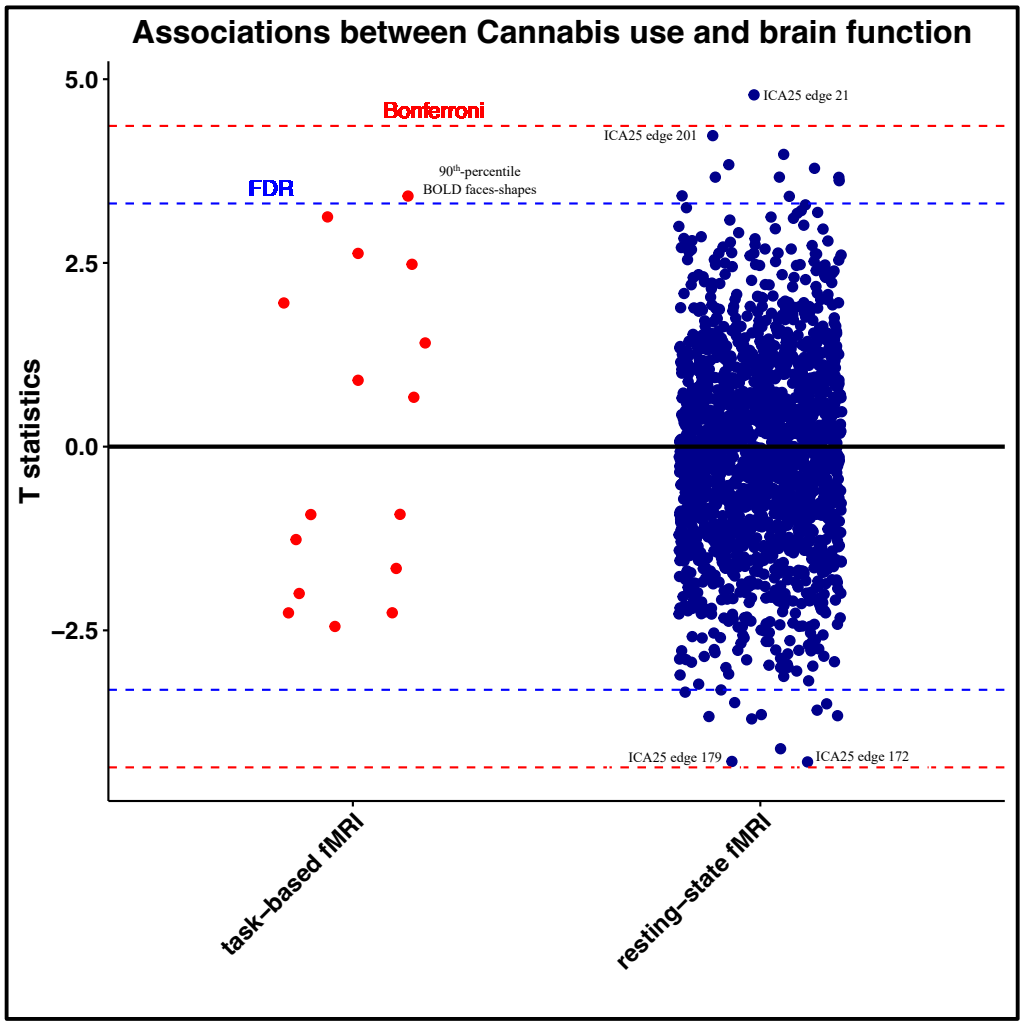



*Figure 19: Associations between cannabis use and brain function*

Estimates were generated using multiple linear regression models adjusted for: age, sex, Townsend deprivation index, employment status, educational qualifications, alcohol drinking status, smoking status, body mass index, systolic and diastolic blood pressure, assessment center, nerves/anxiety/tension/depression status and brain imaging confounds including assessment centre, intracranial volume, head motion, table position, and scanner acquisition parameters (site, scanner software, protocol, scan ramp, head coil). Red line indicates the Bonferroni threshold (3,921 tests, $p = 1.28 \times 10^{-5}$, T statistics = 4.36) and blue line indicates the FDR threshold (3,921 tests, $p = 9.38 \times 10^{-4}$, T statistics = 3.31). Abbreviations: fMRI, functional magnetic resonance imaging; FDR, false discovery rate.

*Table 19: Associations between cannabis use and individual image-derived phenotypes*

| Functional measures | ICA | Edge ID | Estimate | LCI | UCI | P-value |
|---|---|---|---|---|---|---|
| **rsfMRI** | 25 | 21 | 0.10 | 0.06 | 0.14 | 1.71E-06* |
| **rsfMRI** | 25 | 73 | 0.08 | 0.04 | 0.12 | 1.25E-04 |
| **rsfMRI** | 25 | 133 | 0.07 | 0.03 | 0.11 | 2.49E-04 |
| **rsfMRI** | 25 | 172 | -0.09 | -0.13 | -0.05 | 1.80E-05 |
| **rsfMRI** | 25 | 178 | -0.08 | -0.12 | -0.04 | 2.12E-04 |
| **rsfMRI** | 25 | 179 | -0.09 | -0.13 | -0.05 | 1.85E-05 |
| **rsfMRI** | 25 | 191 | 0.08 | 0.04 | 0.12 | 2.97E-04 |
| **rsfMRI** | 100 | 55 | -0.07 | -0.12 | -0.03 | 4.67E-04 |
| **rsfMRI** | 100 | 84 | 0.07 | 0.03 | 0.11 | 6.62E-04 |
| **rsfMRI** | 100 | 132 | 0.08 | 0.04 | 0.12 | 7.02E-05 |
| **rsfMRI** | 100 | 180 | -0.08 | -0.12 | -0.03 | 3.37E-04 |
| **rsfMRI** | 100 | 189 | -0.09 | -0.13 | -0.05 | 3.96E-05 |
| **rsfMRI** | 100 | 201 | 0.09 | 0.05 | 0.13 | 2.33E-05 |
| **rsfMRI** | 100 | 208 | 0.08 | 0.04 | 0.12 | 1.53E-04 |
| **rsfMRI** | 100 | 322 | 0.08 | 0.04 | 0.12 | 2.46E-04 |
| **rsfMRI** | 100 | 336 | -0.08 | -0.12 | -0.04 | 2.67E-04 |
| **rsfMRI** | 100 | 408 | -0.07 | -0.12 | -0.03 | 2.52E-04 |
| **rsfMRI** | 100 | 465 | -0.08 | -0.12 | -0.04 | 2.41E-04 |
| **rsfMRI** | 100 | 606 | -0.07 | -0.11 | -0.03 | 9.33E-04 |
| **rsfMRI** | 100 | 642 | 0.08 | 0.04 | 0.12 | 2.46E-04 |
| **rsfMRI** | 100 | 827 | -0.07 | -0.11 | -0.03 | 8.38E-04 |
| **rsfMRI** | 100 | 957 | -0.07 | -0.12 | -0.03 | 4.97E-04 |
| **rsfMRI** | 100 | 1177 | 0.07 | 0.03 | 0.11 | 6.45E-04 |
| **tfMRI** | 90th-percentile BOLD faces-shapes | | 0.07 | 0.03 | 0.11 | 6.52E-04 |

Estimates represent beta coefficients from multiple linear regression models surviving FDR correction and adjusted for: age, sex, Townsend deprivation index, employment status, educational qualifications, alcohol drinking status, smoking status, body mass index, systolic and diastolic blood pressure, assessment centre, nerves/anxiety/tension/depression status and brain imaging confounds including assessment centre, intracranial volume, head motion, table position, and scanner acquisition parameters (site, scanner software, protocol, scan ramp, head coil). *Associations surviving Bonferroni correction. Edge IDs correspond to pairwise node connections in the UK Biobank resting-state functional connectivity matrices. Abbreviations: ICA, independent component analysis; LCI, lower confidence interval; UCI, upper confidence interval; rsfMRI, resting-state functional magnetic resonance imaging; tfMRI, task-based functional magnetic resonance imaging; BOLD, Blood oxygenation level dependent.

*Table 20: Summary of the associations between cannabis use and brain functional connectivity*

| Brain measures | Tasks/Networks | Direction/strength of association with cannabis use |
|---|---|---|
| Resting state functional MRI | Default mode network, central executive network, salience network, and motor network, | Stronger |
| | Default mode network, central executive network, salience network, motor network, visual network, subcortical-cerebellum network, attention network and limbic network | Weaker |
| Task-based functional MRI | BOLD functional MRI activity to emotional faces-shapes in whole-brain | Stronger |

Abbreviations: MRI – magnetic resonance imaging; BOLD, Blood oxygenation level dependent.

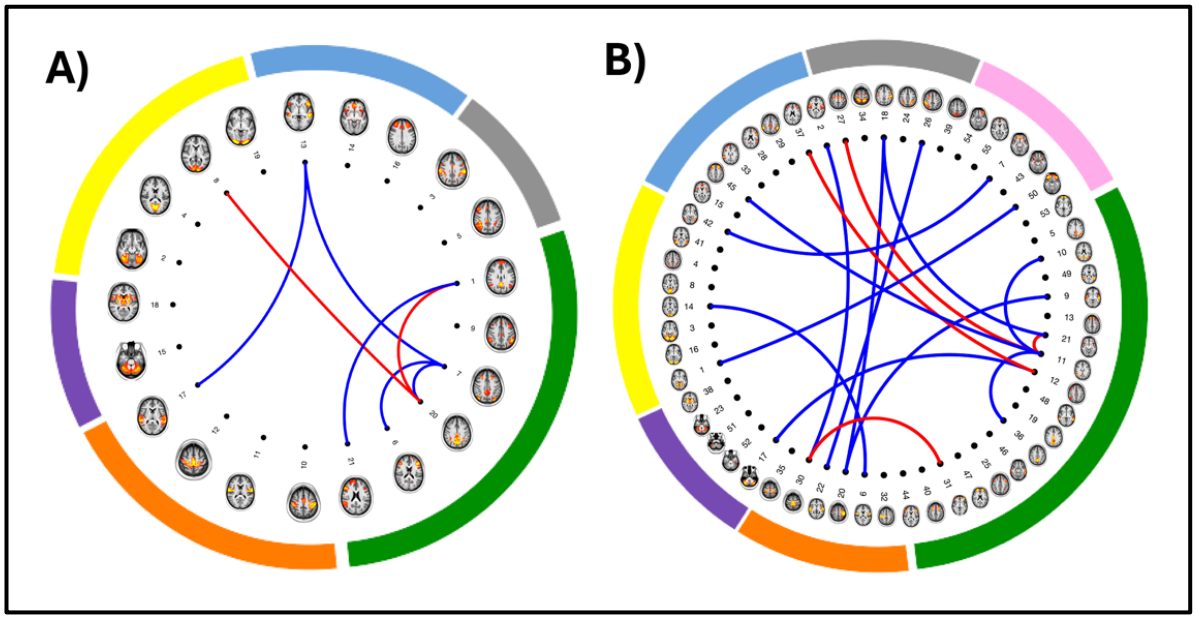



*Figure 20: Resting state functional connectivity significantly associated with cannabis use*

Spatial maps of resting state network nodes (n=21 and n=55) are illustrated in brain images. These were identified as non-noise components from: A) 25-component group-independent component analysis proposed by Miller et al 2016 [53]. Nodes are grouped by networks as follows: default mode/central executive network (green), motor network (orange) subcortical-cerebellum network (purple), visual network (yellow), salience/default mode/central executive network (blue) and attention/default mode/central executive network (grey). B) 100-component group-independent component analysis. Nodes are grouped by networks as follows: default mode/central executive network (green), motor/attention network (orange) subcortical-cerebellum network (purple), visual/attention network (yellow), salience/default mode/central executive network (blue), attention/salience/central executive network (grey) and limbic/default mode network (pink). Connecting lines indicate partial correlations between network nodes significantly associated with cannabis (red lines indicate stronger connectivity and blue lines indicate weaker connectivity).

*Table 21: Resting-state functional connectivity associations with cannabis use and brain function, including edge ID, brain regions, and networks (main analysis)*

| ICA | Edge ID | PC | Beta | Absolute Difference | Location | Network |
|---|---|---|---|---|---|---|
| **25** | 21 | -0.09 | 0.10 | weaker | (Inferior_frontal;Middle_frontal)<=>(Precuneus;Middle_occipital) | (Default_mode;Central_executive)<=>(Default_mode;Central_executive) |
| **25** | 73 | -0.58 | 0.08 | weaker | (Precuneus;Middle_occipital)<=>(Supp_motor_area;Middle_temporal;Inferior_frontal) | (Default_mode;Central_executive)<=>(Default_mode;Salience) |
| **25** | 133 | -0.6 | 0.08 | weaker | (Supp_motor_area;Middle_temporal;Inferior_frontal)<=>(Superior_temporal;Middle_temporal) | (Default_mode;Salience)<=>(Default_mode;Motor) |
| **25** | 172 | -0.1 | -0.09 | stronger | (Cerebellum;Precuneus;Superior_frontal)<=>(Precuneus) | (Default_mode)<=>(Default_mode;Central_executive) |
| **25** | 178 | 1.96 | -0.08 | weaker | (Precuneus;Middle_occipital)<=>(Precuneus) | (Default_mode;Central_executive)<=>(Default_mode;Central_executive) |
| **25** | 179 | -0.45 | -0.8 | stronger | (Lingual;Calcarine;Superior_occipital)<=>(Precuneus) | (Visual)<=>(Default_mode;Central_executive) |
| **25** | 191 | -0.27 | 0.08 | weaker | (Cerebellum;Precuneus;Superior_frontal)<=>(Inferior_frontal;Superior_frontal;Middle_temporal) | (Default_mode)<=>(Default_mode;Central_executive) |
| **100** | 55 | 0.93 | -0.07 | weaker | (Middle_occipital;Precuneus;Calcarine)<=>(Angular;Middle_temporal) | (Default_mode;Central_executive)<=>(Default_mode;Central_executive) |
| **100** | 84 | -0.12 | 0.07 | weaker | (Postcentral;Precentral)<=>(Cuneus;Superior_occipital) | (Motor)<=>(Visual) |
| **100** | 132 | -0.8 | 0.08 | weaker | (Middle_frontal;Cerebellum)<=>(Cerebellum) | (Central_executive;Default_mode)<=>(Subcortical-cerebellum) |
| **100** | 180 | 0.38 | -0.08 | weaker | (Middle_temporal;Temporal_pole)<=>(Postcentral;Precentral) | (Default_mode)<=>(Motor;Attention) |
| **100** | 189 | 1.42 | -0.09 | weaker | (Inferior_parietal;Postcentral)<=>(Postcentral;Precentral) | (Attention;Central_executive;Salience)<=>(Motor;Attention) |
| **100** | 201 | 1.21 | 0.09 | stronger | (Angular;Middle_temporal)<=>(Superior_frontal) | (Default_mode;Central_executive)<=>(Default_mode;Central_executive) |
| **100** | 208 | -0.45 | 0.08 | weaker | (Inferior_parietal;Postcentral)<=>(Superior_frontal) | (Attention;Central_executive;Salience)<=>(Default_mode;Central_executive) |
| **100** | 322 | -0.59 | 0.08 | weaker | (Superior_temporal)<=>(Inferior_parietal;Inferior_frontal;SupraMarginal) | (Default_mode;Motor)<=>(Attention;Central_executive) |
| **100** | 336 | -0.45 | -0.08 | stronger | (Angular;Middle_temporal)<=>(Precentral;Superior_frontal;Supp_motor_area) | (Default_mode;Central_executive)<=>(Attention;Salience;Motor) |
| **100** | 408 | 0.23 | -0.08 | weaker | (Rolandic_operculum;SupraMarginal;Insula)<=>(Paracentral) | (Salience;Motor)<=>(Motor) |
| **100** | 465 | -0.15 | -0.08 | stronger | (Paracentral)<=>(Middel_frontal) | (Motor)<=>(Central_executive) |

| | | | | | | |
|---|---|---|---|---|---|---|
| **100** | 606 | 1.68 | -0.07 | weaker | (Angular;Middle_temporal)<=>(Precuneus) | (Default_mode;Central_executive)<=>(Default_mode;Central_executive) |
| **100** | 642 | 0.6 | 0.08 | stronger | (Middle_frontal;Cerebellum)<=>(Middle_frontal) | (Central_executive;Default_mode)<=>(Central_executive;Salience) |
| **100** | 827 | 0.05 | -0.07 | weaker | (Superior_frontal;Anterior_cingulate)<=>(Inferior_temporal;Inferior_occipital) | (Default_mode;Limbic)<=>(Attention;Visual) |
| **100** | 957 | 0.57 | -0.07 | weaker | (Angular;Middle_temporal)<=>(Superior_frontal;Middle_frontal) | (Default_mode;Central_executive)<=>(Salience;Default_mode) |
| **100** | 1177 | -0.26 | 0.07 | weaker | (Calcarine;Lingual;Cuneus)<=>(Orbital) | (Visual)<=>(Limbic) |

Edge IDs correspond to pairwise node connections in the UK Biobank resting-state functional connectivity matrices. Abbreviations: ICA, independent component analysis; PC, partial correlation.

Associations with one brain IDPs additionally survived the more stringent *Bonferroni-corrected* threshold ($p = 1.275 \times 10^{-5}$) (**Table 19)**. Cannabis users revealed lower functional connectivity between brain regions in the inferior frontal, middle frontal, and precuneus regions, all of which are associated with the DMN and CEN.

### 5.3.3 Sensitivity analyses

The study assessed whether the duration of abstinence or dose impacted the relationships between cannabis use and brain function that survived the FDR correction in the main analysis. Neither the duration of cannabis abstinence (**Table 22**) nor the frequency of cannabis dosage (as assessed through low and high-frequency use) (**Table 23**) significantly moderated the associations between cannabis use and brain function.

*Table 22: Association between duration of cannabis abstinence and brain function*

| Functional measures | ICA | Edge ID | Estimate | LCI | UCI | P-value |
|---|---|---|---|---|---|---|
| **rsfMRI** | 25 | 21 | 8.16E-04 | -2.77E-03 | 2.57E-03 | 5.85E-01 |
| **rsfMRI** | 25 | 73 | -1.91E-03 | -2.77E-03 | 2.57E-03 | 1.86E-01 |
| **rsfMRI** | 25 | 133 | 1.65E-03 | -2.77E-03 | 2.57E-03 | 2.52E-01 |
| **rsfMRI** | 25 | 172 | -1.25E-03 | -2.77E-03 | 2.57E-03 | 3.87E-01 |
| **rsfMRI** | 25 | 178 | -3.45E-03 | -2.77E-03 | 2.57E-03 | 1.94E-02 |
| **rsfMRI** | 25 | 179 | 1.27E-03 | -2.77E-03 | 2.57E-03 | 4.02E-01 |
| **rsfMRI** | 25 | 191 | 1.77E-03 | -2.77E-03 | 2.57E-03 | 2.42E-01 |
| **rsfMRI** | 100 | 55 | 7.47E-04 | -2.77E-03 | 2.57E-03 | 6.20E-01 |
| **rsfMRI** | 100 | 84 | -1.72E-03 | -2.77E-03 | 2.57E-03 | 2.56E-01 |
| **rsfMRI** | 100 | 132 | 4.67E-04 | -2.77E-03 | 2.57E-03 | 7.55E-01 |
| **rsfMRI** | 100 | 180 | -3.46E-03 | -2.77E-03 | 2.57E-03 | 2.13E-02 |

| | | | | | | |
|---|---|---|---|---|---|---|
| **rsfMRI** | 100 | 189 | 2.86E-03 | -2.77E-03 | 2.57E-03 | 5.53E-02 |
| **rsfMRI** | 100 | 201 | -1.91E-03 | -2.77E-03 | 2.57E-03 | 1.96E-01 |
| **rsfMRI** | 100 | 208 | 1.53E-03 | -2.77E-03 | 2.57E-03 | 3.08E-01 |
| **rsfMRI** | 100 | 322 | -4.14E-03 | -2.77E-03 | 2.57E-03 | 5.77E-03 |
| **rsfMRI** | 100 | 336 | -4.12E-04 | -2.77E-03 | 2.57E-03 | 7.83E-01 |
| **rsfMRI** | 100 | 408 | 3.35E-03 | -2.77E-03 | 2.57E-03 | 2.15E-02 |
| **rsfMRI** | 100 | 465 | -2.95E-03 | -2.77E-03 | 2.57E-03 | 5.20E-02 |
| **rsfMRI** | 100 | 606 | -8.29E-04 | -2.77E-03 | 2.57E-03 | 5.77E-01 |
| **rsfMRI** | 100 | 642 | -1.23E-03 | -2.77E-03 | 2.57E-03 | 4.04E-01 |
| **rsfMRI** | 100 | 827 | 4.99E-04 | -2.77E-03 | 2.57E-03 | 7.43E-01 |
| **rsfMRI** | 100 | 957 | -7.73E-04 | -2.77E-03 | 2.57E-03 | 5.97E-01 |
| **rsfMRI** | 100 | 1177 | 9.27E-04 | -2.77E-03 | 2.57E-03 | 5.38E-01 |
| **tfMRI** | 90th-percentile BOLD faces-shapes | | -1.61E-03 | -2.77E-03 | 2.57E-03 | 2.59E-01 |

Estimates represent beta coefficients from multiple linear regression models surviving FDR correction and adjusted for: age, sex, Townsend deprivation index, employment status, educational qualifications, alcohol drinking status, smoking status, body mass index, systolic and diastolic blood pressure, assessment centre, nerves/anxiety/tension/depression status and brain imaging confounds including assessment centre, intracranial volume, head motion, table position, and scanner acquisition parameters (site, scanner software, protocol, scan ramp, head coil). Edge IDs correspond to pairwise node connections in the UK Biobank resting-state functional connectivity matrices. Abbreviations: ICA, independent component analysis; LCI, lower confidence interval; UCI, upper confidence interval; rsfMRI, resting-state functional magnetic resonance imaging; tfMRI, task-based functional magnetic resonance imaging; BOLD, Blood oxygenation level dependent.

*Table 23: Association between high frequency cannabis use (compared to low frequency) and brain function*

| Functional measures | ICA | Edge ID | Estimate | LCI | UCI | P-value |
|---|---|---|---|---|---|---|
| **rsfMRI** | 25 | 21 | -0.05 | -0.09 | 0.05 | 0.18 |
| **rsfMRI** | 25 | 73 | 0.06 | -0.09 | 0.05 | 0.09 |
| **rsfMRI** | 25 | 133 | -0.03 | -0.09 | 0.05 | 0.43 |
| **rsfMRI** | 25 | 172 | -0.01 | -0.09 | 0.05 | 0.81 |
| **rsfMRI** | 25 | 178 | 0.05 | -0.09 | 0.05 | 0.22 |
| **rsfMRI** | 25 | 179 | 0.02 | -0.09 | 0.05 | 0.55 |
| **rsfMRI** | 25 | 191 | 0.00 | -0.09 | 0.05 | 0.90 |
| **rsfMRI** | 100 | 55 | 0.04 | -0.09 | 0.05 | 0.31 |
| **rsfMRI** | 100 | 84 | 0.07 | -0.09 | 0.05 | 0.06 |
| **rsfMRI** | 100 | 132 | -0.04 | -0.09 | 0.05 | 0.25 |
| **rsfMRI** | 100 | 180 | -0.03 | -0.09 | 0.05 | 0.37 |
| **rsfMRI** | 100 | 189 | -0.07 | -0.09 | 0.05 | 0.08 |
| **rsfMRI** | 100 | 201 | 0.05 | -0.09 | 0.05 | 0.18 |
| **rsfMRI** | 100 | 208 | 0.03 | -0.09 | 0.05 | 0.49 |
| **rsfMRI** | 100 | 322 | 0.08 | -0.09 | 0.05 | 0.04 |
| **rsfMRI** | 100 | 336 | -0.04 | -0.09 | 0.05 | 0.32 |

| | | | | | | |
|---|---|---|---|---|---|---|
| **rsfMRI** | 100 | 408 | -0.02 | -0.09 | 0.05 | 0.52 |
| **rsfMRI** | 100 | 465 | 0.07 | -0.09 | 0.05 | 0.06 |
| **rsfMRI** | 100 | 606 | 0.05 | -0.09 | 0.05 | 0.19 |
| **rsfMRI** | 100 | 642 | 0.00 | -0.09 | 0.05 | 0.92 |
| **rsfMRI** | 100 | 827 | 0.02 | -0.09 | 0.05 | 0.65 |
| **rsfMRI** | 100 | 957 | 0.02 | -0.09 | 0.05 | 0.68 |
| **rsfMRI** | 100 | 1177 | -0.01 | -0.09 | 0.05 | 0.75 |
| **tfMRI** | 90th-percentile BOLD faces-shapes | | 0.05 | -0.09 | 0.05 | 0.16 |

Estimates represent beta coefficients from multiple linear regression models surviving FDR correction and adjusted for: age, sex, Townsend deprivation index, employment status, educational qualifications, alcohol drinking status, smoking status, body mass index, systolic and diastolic blood pressure, assessment centre, nerves/anxiety/tension/depression status and brain imaging confounds including assessment centre, intracranial volume, head motion, table position, and scanner acquisition parameters (site, scanner software, protocol, scan ramp, head coil). Edge IDs correspond to pairwise node connections in the UK Biobank resting-state functional connectivity matrices. Abbreviations: ICA, independent component analysis; LCI, lower confidence interval; UCI, upper confidence interval; rsfMRI, resting-state functional magnetic resonance imaging; tfMRI, task-based functional magnetic resonance imaging; BOLD, Blood oxygenation level dependent.

There were notable sex differences. After FDR correction, while significant associations were observed in 5 brain functions among males, while in females 2 brain functions were associated **(Table 24 and 26).** Additionally, full edge-level associations, including brain regions and networks corresponding to each rsFC edge, are presented in **Table 25 and Table 27**.

*Table 24: Associations between cannabis use and brain function in males surviving False Discovery Rate*

| Functional measures | ICA | Edge ID | Beta | LCI | UCI | P-value |
|---|---|---|---|---|---|---|
| **rsfMRI** | 25 | 21 | 0.11 | 0.05 | 0.17 | 2.91E-04 |
| **rsfMRI** | 25 | 133 | 0.11 | 0.05 | 0.17 | 1.27E-04 |
| **rsfMRI** | 25 | 172 | -0.11 | -0.17 | -0.05 | 2.58E-04 |
| **rsfMRI** | 100 | 201 | 0.11 | 0.05 | 0.17 | 2.66E-04 |
| **rsfMRI** | 100 | 957 | -0.11 | -0.17 | -0.05 | 2.17E-04 |

Estimates represent beta coefficients from multiple linear regression models adjusted for: age, Townsend deprivation index, employment status, educational qualifications, alcohol drinking status, smoking status, body mass index, systolic and diastolic blood pressure, assessment centre, nerves/anxiety/tension/depression status and brain imaging confounds including assessment centre, intracranial volume, head motion, table position, and scanner acquisition parameters (site, scanner software, protocol, scan ramp, head coil). Edge IDs correspond to pairwise node connections in the UK Biobank resting-state functional connectivity matrices. Abbreviations: ICA, independent component analysis; LCI, lower confidence interval; UCI, upper confidence interval; rsfMRI, resting-state functional magnetic resonance imaging.

*Table 25: Resting-state functional connectivity associations with cannabis use and brain function in males, including edge ID, brain regions, and networks (sensitivity analysis)*

| ICA | Edge ID | PC | Beta | Absolute Difference | Location | Network |
|---|---|---|---|---|---|---|
| **25** | 21 | -0.09 | 0.11 | weaker | (Inferior_frontal;Middle_frontal)<=>(Precuneus;Middle_occipital) | (Default_mode;Central_executive)<=>(Default_mode;Central_executive) |
| **25** | 133 | -0.6 | 0.11 | weaker | (Supp_motor_area;Middle_temporal;Inferior_frontal)<=>(Superior_temporal;Middle_temporal) | (Default_mode;Salience)<=>(Default_mode;Motor) |
| **25** | 172 | -0.1 | -0.11 | stronger | (Cerebellum;Precuneus;Superior_frontal)<=>(Precuneus) | (Default_mode)<=>(Default_mode;Central_executive) |
| **100** | 201 | 1.21 | 0.11 | stronger | (Angular;Middle_temporal)<=>(Superior_frontal) | (Default_mode;Central_executive)<=>(Default_mode;Central_executive) |
| **100** | 957 | 0.57 | -0.11 | weaker | (Angular;Middle_temporal)<=>(Superior_frontal;Middle_frontal) | (Default_mode;Central_executive)<=>(Salience;Default_mode) |

Edge IDs correspond to pairwise node connections in the UK Biobank resting-state functional connectivity matrices. Abbreviations: ICA, independent component analysis; PC, partial correlation.

*Table 26: Associations between cannabis use and brain function in females surviving False Discovery Rate*

| Functional measures | ICA | Edge ID | Beta | LCI | UCI | P-value |
|---|---|---|---|---|---|---|
| **rsfMRI** | 100 | 694 | 0.11 | 0.05 | 0.17 | 4.25E-04 |
| **rsfMRI** | 100 | 1010 | -0.11 | -0.17 | -0.05 | 2.22E-04 |

Estimates represent beta coefficients from multiple linear regression models adjusted for: age, Townsend deprivation index, employment status, educational qualifications, alcohol drinking status, smoking status, body mass index, systolic and diastolic blood pressure, assessment centre, nerves/anxiety/tension/depression status and brain imaging confounds including assessment centre, intracranial volume, head motion, table position, and scanner acquisition parameters (site, scanner software, protocol, scan ramp, head coil). Edge IDs correspond to pairwise node connections in the UK Biobank resting-state functional connectivity matrices. Abbreviations: ICA, independent component analysis; LCI, lower confidence interval; UCI, upper confidence interval; rsfMRI, resting-state functional magnetic resonance imaging.

*Table 27: Resting-state functional connectivity associations with cannabis use and brain function in females, including edge ID, brain regions, and networks (sensitivity analysis)*

| ICA | Edge ID | PC | Beta | Absolute Difference | Location | Network |
|---|---|---|---|---|---|---|
| **100** | 694 | 0.49 | 0.11 | stronger | (Supp_motor_area;Inferior_frontal)<=>(Putamen;Caudate) | (Salience;Default_mode)<=>(Subcortical-cerebellum) |
| **100** | 1010 | -0.07 | -0.11 | stronger | (Postcentral;Precentral)<=>(Inferior_temporal;Middle_temporal) | (Motor;Attention)<=>(Central_executive;Default_mode) |

Edge IDs correspond to pairwise node connections in the UK Biobank resting-state functional connectivity matrices. Abbreviations: ICA, independent component analysis; PC, partial correlation.

For the functional MRI outcomes, the extended modelling framework demonstrated a similar pattern of sensitivity to covariate expansion. For the faces–shapes task contrast, re-estimation within the restricted IDP set showed that the primary association did not survive FDR correction in either the core model or the model including smoking and alcohol. In resting-state connectivity 3 brain functions remained FDR-significant in Models 1 and 2 (N = 15,896) (**Appendix 9 and 10**), with highly similar effect directions and magnitudes to those observed in the primary analysis. However, once psychological traits were introduced (Model 3; N = 2,462) no IDPs survived FDR correction, although all effects remained directionally consistent with Models 1–2. Further adjustment for subclinical mental-health symptoms (Model 4; N = 818) and for ICD-10 diagnoses of depression and anxiety (Model 5; N = 2,781) similarly yielded no FDR-significant IDPs. As with the structural analyses, no model produced evidence of effect reversal, indicating that the disappearance of significant findings is best explained by reduced sample size and diminished statistical power rather than by genuine changes in the underlying associations.

### 5.3.4 Results from Mendelian randomization analysis

A total of 22 SNP instruments were available for CanUD and 8 for CanLU. After correcting for multiple comparisons, there were no significant associations between genetically predicted *CanUD* (IVW beta= 0.01 [95% CI -0.09 to 0.11], p = 0.85) or *CanLU* (IVW beta= -0.05 [95% CI -0.15 to 0.05], p = 0.33), respectively, and FA in genu of the corpus callosum. No significant associations were observed with other brain IDPs, either. There was no indication of horizontal pleiotropy as determined by the MR-Egger intercept test for any of the outcomes **(Figure 21, Table 28 and Figure 22)**. Reverse MR analysis did not show any significant associations between brain IDPs and *CanUD* or *CanLU* (**Table 29**).

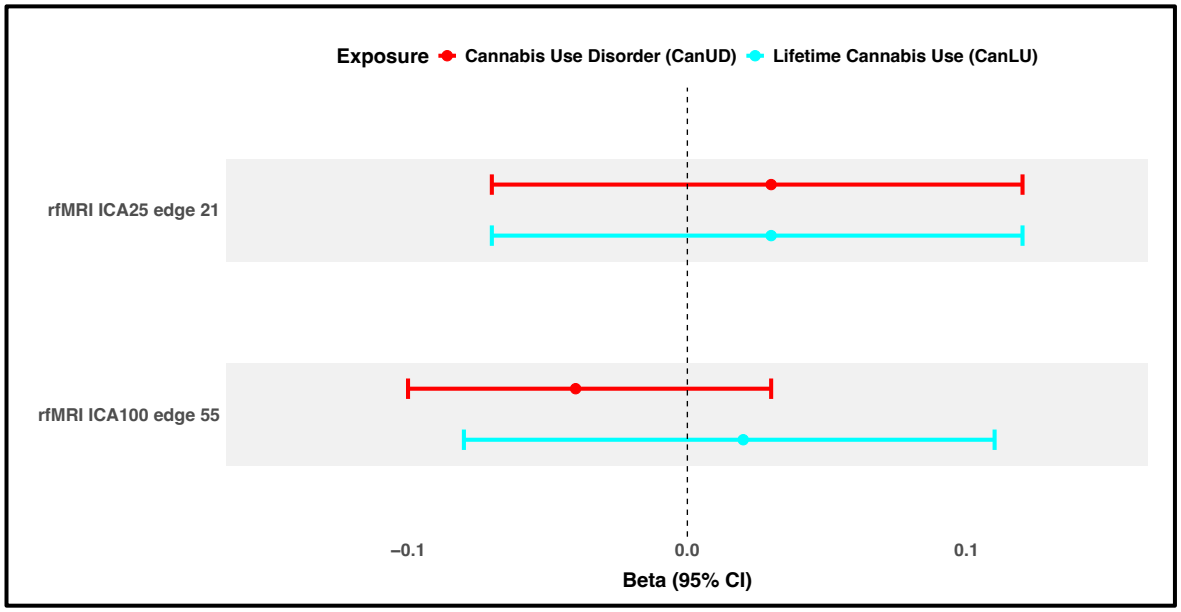


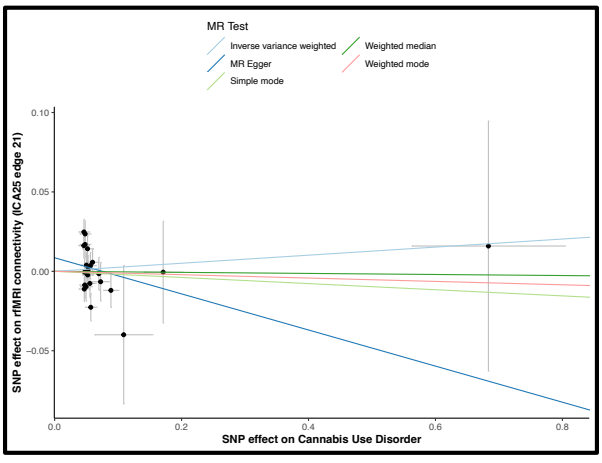

*Figure 21: Genetic associations between cannabis use and brain function*

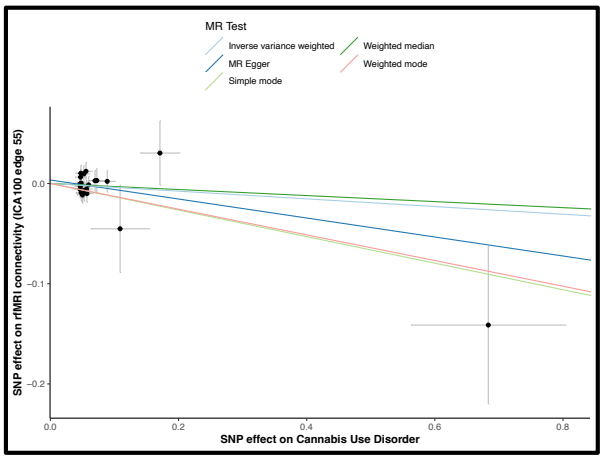
Forest plot displays beta (dots) and 95% confidence intervals (lines) for brain function in cannabis use disorder (in red) or lifetime cannabis use (in cyan) prevalence. Estimates were generated using two sample inverse-variance weighted method from source genome-wide association studies used to derive genetic associations, with SNPs as instruments detailed in **Figure 18.** Edge IDs correspond to pairwise node connections in the UK Biobank resting-state functional connectivity matrices.

*Table 28: Two-sample linear MR estimates assessing evidence for the causal effect of Cannabis use disorder/ Lifetime Cannabis use on brain function*

| Brain IDPs | Cannabis Phenotypes | SNPs (n) | MR Tests | Estimates | LCI | UCI | *P*-value |
|---|---|---|---|---|---|---|---|
| **rsfMRI connectivity (ICA25 edge 21)** | CanUD | 22 | MR Egger | -0.11 | -0.40 | 0.17 | 0.44 |
| | | | Weighted mean | 0.00 | -0.10 | 0.10 | 0.95 |
| | | | IVW | 0.03 | -0.07 | 0.12 | 0.61 |
| | | | Simple mode | -0.02 | -0.20 | 0.17 | 0.84 |
| | | | Weighted mode | -0.01 | -0.16 | 0.14 | 0.89 |
| | CanLU | 8 | MR Egger | 0.10 | -0.16 | 0.36 | 0.48 |
| | | | Weighted mean | 0.04 | -0.08 | 0.17 | 0.50 |
| | | | IVW | 0.03 | -0.07 | 0.12 | 0.61 |
| | | | Simple mode | 0.05 | -0.13 | 0.22 | 0.62 |
| | | | Weighted mode | 0.05 | -0.10 | 0.19 | 0.57 |
| **rsfMRI connectivity (ICA100 edge 55)** | CanUD | 22 | MR Egger | -0.10 | -0.29 | 0.10 | 0.35 |
| | | | Weighted mean | -0.03 | -0.12 | 0.06 | 0.53 |
| | | | IVW | -0.04 | -0.10 | 0.03 | 0.26 |
| | | | Simple mode | -0.13 | -0.32 | 0.05 | 0.17 |
| | | | Weighted mode | -0.13 | -0.31 | 0.05 | 0.17 |
| | CanLU | 8 | MR Egger | 0.05 | -0.21 | 0.32 | 0.70 |
| | | | Weighted mean | 0.01 | -0.12 | 0.13 | 0.91 |
| | | | IVW | 0.02 | -0.08 | 0.11 | 0.76 |
| | | | Simple mode | -0.05 | -0.24 | 0.13 | 0.58 |
| | | | Weighted mode | -0.06 | -0.23 | 0.12 | 0.54 |

Edge IDs correspond to pairwise node connections in the UK Biobank resting-state functional connectivity matrices. Abbreviations: IDP, imaging-derived phenotype; SNP, single nucleotide polymorphism; LCI, lower confidence interval; UCI, upper confidence interval; rsfMRI, resting-state functional magnetic resonance imaging; ICA, independent component analysis; IVW, inverse-variance weighted.



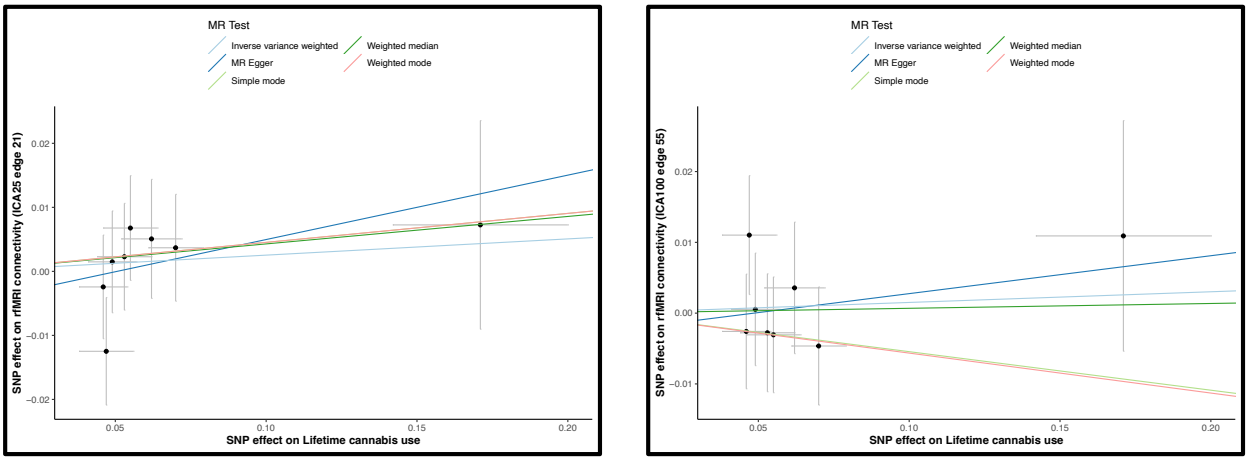



*Figure 22: Two-sample linear MR plot assessing evidence for the causal effect of Cannabis use disorder/ Lifetime Cannabis use on brain function*

Edge IDs correspond to pairwise node connections in the UK Biobank resting-state functional connectivity matrices.

*Table 29: Two-sample linear reverse MR estimates assessing evidence for the causal effect of brain function on Cannabis use disorder*

| Cannabis Phenotypes | Brain Measures | SNPs (n) | MR Test | Estimates | LCI | UCI | P-value |
|---|---|---|---|---|---|---|---|
| **Cannabis use disorder** | rsfMRI connectivity (ICA25 edge 21) | 2 | IVW | -99 | -1499.56 | - 476.44 | 0.71 |
| | rsfMRI connectivity (ICA100 edge 55) | 2 | IVW | -77 | -2640.76 | 1106.78 | 0.42 |

Edge IDs correspond to pairwise node connections in the UK Biobank resting-state functional connectivity matrices. Abbreviations: SNP, single nucleotide polymorphism; LCI, lower confidence interval; UCI, upper confidence interval; rsfMRI, resting-state functional magnetic resonance imaging; IVW, inverse-variance weighted.

## 5.4 Discussion

Cannabis users had significant differences in brain functional connectivity where a weaker rsFC was observed in multiple brain regions underlying the DMN and CEN. Genetic analyses found no support for causal relationships underlying these observed associations.

The most robust association, surviving Bonferroni correction, was reduced connectivity between inferior/middle frontal and precuneus regions, implicating disrupted integration between the DMN and CEN. Other associations included both increases and decreases in connectivity across DMN, salience, motor, and sensory networks, highlighting widespread but heterogeneous effects.

Cannabis use was significantly associated with rsFC mainly in the brain regions underlying default mode, central executive and salience networks. The brain regions underlying these networks were primarily located in the frontal lobe, temporal lobe, occipital cortex, supplementary motor area, precuneus, and cerebellum. These regions are characterized by a high density of CB1, and have also been implicated in younger cannabis users [176, 195]. Interestingly, the precuneus, is also among the first cortical regions to show pathology in Alzheimer's disease [340, 341], although this was not examine directly in the present study. Higher functional connectivity between prefrontal cortex and occipital cortex was reported in young adult near-daily cannabis users compared to controls [176]. Altered patterns of functional connectivity between cerebellum to cerebral cortex that might have an impact on behaviour and cognition have been reported previously [186]. Additionally, increased functional connectivity was reported in regions underlying orbito-frontal cortex with precuneus and cerebellar regions, which may indicate an impairment in decision-making capacity and an increase in impulsive behaviour [40]. These findings, however, suggest a complex pattern of higher or lower functional connectivity between these regions with cannabis use.

Similar to the findings on cannabis-brain structure associations in **Chapter 4**, no influence of the duration of abstinence from cannabis use prior to the brain scan was observed on functional brain connectivity. No significant differences were observed in functional connectivity among low and high-frequency cannabis users. This may reflect the characteristics of the sample, which comprised healthy volunteers [335] and included relatively few individuals with frequent or near-daily cannabis use.

In the extended sensitivity models, the broader covariate framework indicated that the functional MRI findings were largely influenced by reductions in sample size rather than by changes in effect direction. Task-based activation did not retain statistical significance even in the early models; however, estimates remained directionally consistent with the primary analysis. Resting-state findings were more robust, with several edges remaining significant in the core and lifestyle-adjusted models before attenuating once psychological or mental-health variables were included. As observed in the structural analyses, the loss of significant associations in the extended models likely reflects diminished statistical power rather than substantive changes in the underlying relationship, with no evidence of effect reversal across the full modelling framework.

In addition to resting-state associations, cannabis users in this study demonstrated stronger whole-brain BOLD activation during the emotion-processing task (faces versus shapes). This aligns with prior task-based fMRI studies showing cannabis-related associations in emotional reactivity and face processing, including reduced neural responsiveness in the anterior cingulate cortex and prefrontal regions [205]. More broadly, task-based studies have reported altered activity in networks supporting working memory, decision-making, inhibition, reward processing, error monitoring, emotional reactivity, time perception, and cue-reactivity [26, 98, 200, 202–207]. Meta-analytic evidence also supports consistent involvement of DMN and CEN regions across multiple task paradigms [196]. The present finding of enhanced responsivity to socio-emotional stimuli adds to this body of evidence, suggesting that cannabis

use may impact not only resting-state connectivity but also dynamic recruitment of cognitive and affective networks during task engagement.

MR analyses did not support a causal effect of cannabis use or dependence on brain function, nor the reverse. Discrepancies with observational findings may reflect residual confounding, limited statistical power to detect small effects, or differences between the lifelong impact captured by MR and the life-stage specific effects reflected in observational data. Although instrument strength was robust, larger neuroimaging GWAS will be important to clarify these relationships.

Similar to the analyses of brain structure in **Chapter 4**, the investigation of cannabis use in relation to brain function is subject to a number of important limitations. Most critically, the same methodological issues apply across both domains: UK Biobank participants are generally healthier and less representative of the wider population [335], which limits generalisability. They also show lower prevalence of CUD than would be expected in population-based samples, making this dataset less suitable for examining clinical levels of cannabis involvement. Cannabis use was self-reported and therefore vulnerable to recall and reporting biases, and important details such as age of initiation, potency, and dose–frequency distinctions were not available. These factors limit the precision with which cannabis exposure can be characterised and may obscure dose- or pattern-specific associations. Additionally, limited case numbers prevented robust investigation of CUD, and high-frequency users likely constitute a heterogeneous group.

Residual confounding cannot be fully excluded, despite adjustment for multiple covariates. Factors such as family history of psychiatric or substance use disorders, dietary intake, or use of medications known to influence brain function (e.g. antidepressants) were not considered in the analysis [338, 342, 343], and may contribute to the observed associations.

Neuroimaging measures were cross-sectional, restricting causal inference. Although MR was applied to address causality, it too has limitations. MR relies on several assumptions, including that the genetic instruments are strongly associated with the exposure, not related to confounders, and influence the outcome only through the exposure. While horizontal pleiotropy was tested for where possible, these assumptions cannot be fully validated. In particular, the assumption that genetic instruments are not associated with unmeasured confounders cannot be directly tested in an observational framework. Moreover, MR captures the lifelong liability to cannabis use, while observational findings may reflect effects operating at specific life stages or cumulative exposures over shorter periods.

Taken together, these limitations mirror those outlined in relation to brain structure and must be considered when interpreting the present findings. Future work in larger, more diverse cohorts with repeated imaging, richer exposure measures, and biological validation of cannabis use will be essential to clarify whether cannabis exerts enduring causal effects on brain function.

# Chapter 6: Association between cannabis use, cognitive function and dementia risk

**The content of this chapter has been submitted for publication and is currently under peer review:**

*Title: Cannabis use, cognitive function, and dementia risk in older adults: Observational and genetic analyses*

***Submitted for publication (under peer review)***

## 6.1 Introduction

In this chapter I examine the association between cannabis use, cognitive function and dementia risk. Cannabis use has been associated with cognitive deficits across the lifespan [218], particularly in the domains of learning and memory, attentional control, and motor inhibition [27]. Acute intoxication has been shown to produce small to moderate impairments in executive function, verbal learning, memory, processing speed, and attention in both adolescents and adults [48, 49]. However, findings from longitudinal studies on cannabis and cognitive functioning have been inconsistent [41, 344, 345]. Some report persistent deficits, particularly in verbal memory and recall [344, 345], while others find no evidence of accelerated or age-related cognitive decline [41, 266]. Despite the growing prevalence of cannabis use among middle-aged and older adults, this population remains understudied, particularly with respect to later-life cognitive ageing and dementia risk. Given that midlife cognitive impairments—especially memory [38]—are recognised risk factors or early symptoms of dementia [346], long-term cannabis use may plausibly influence dementia risk trajectories. While memory impairments have been reported in this age group [38, 39, 266], effects on attention and executive function are less clear [223, 262, 347]. Biologically, repeated or long-term THC activation of CB1 receptors in hippocampal and prefrontal circuits may attenuate long-term synaptic strengthening and memory encoding, and has been linked to smaller hippocampal volumes [38, 45–47]. Cannabis use may also exacerbate dementia risk indirectly via sleep disruption, depression, and vascular factors [268], plausibly shifting dementia trajectories. Overall, the potential effect of cannabis on neurodegenerative disease, including dementia, remains largely unexplored.

To address these knowledge gaps, I conducted the largest observational analysis and the first MR study, a genetic approach that helps minimize confounding and reverse causality [51].

## 6.2 Methods

### 6.2.1 Study sample

The study comprised participants from approximately 15,000 to 18,000 lifetime cannabis users and 48,000 to 56,000 controls in UK Biobank [52] as shown in **Figure 23**. Participants were excluded due to either lacking cognitive data or missing confounding variables. No other exclusion criteria were applied.

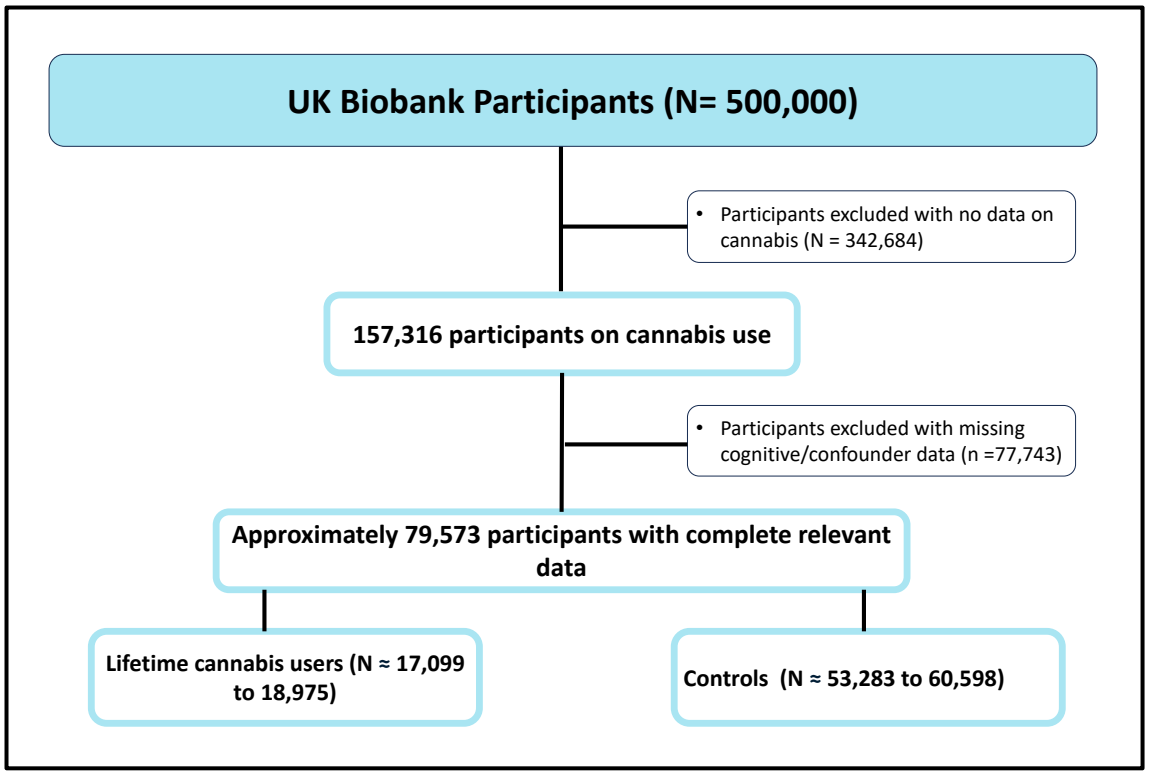



*Figure 23: Flow chart of the participants from the UK Biobank included in the final analysis*

### 6.2.2 Cannabis use data

Self-reported cannabis use data in UK Biobank were available via touchscreen questionnaire as described in **Section 3.2**. All participants who responded yes to "Ever taken Cannabis" were categorized as lifetime cannabis users and those who responded no were categorized as controls. Cannabis users were further divided into low frequency, and high frequency users. Additionally, UK Biobank participants also reported the maximum frequency of cannabis consumed during the lifespan.

### 6.2.3 Cognitive test data

Cognitive assessments were conducted in UKB at baseline, through online follow-up assessments and during imaging visits as part of a touchscreen questionnaire [55]. For this study, data from the online follow-up assessments conducted in 2014 and 2021 were used. This decision was based on the larger sample size and more complete data available at these follow-up timepoints. Cognitive performance was examined in 5 different tests: Numeric Memory, Fluid intelligence, Trail making, Symbol digit substitution and Pairs matching test (**Figure 24**).

The raw cognitive scores for all tests were converted into z-scores to allow comparison between differing tests. This standardized score ensures that the data is on a common scale with a mean of 0 and a standard deviation of 1. More information regarding the cognitive tests, the variable use and what these tests measure is in **Section 3.4.**

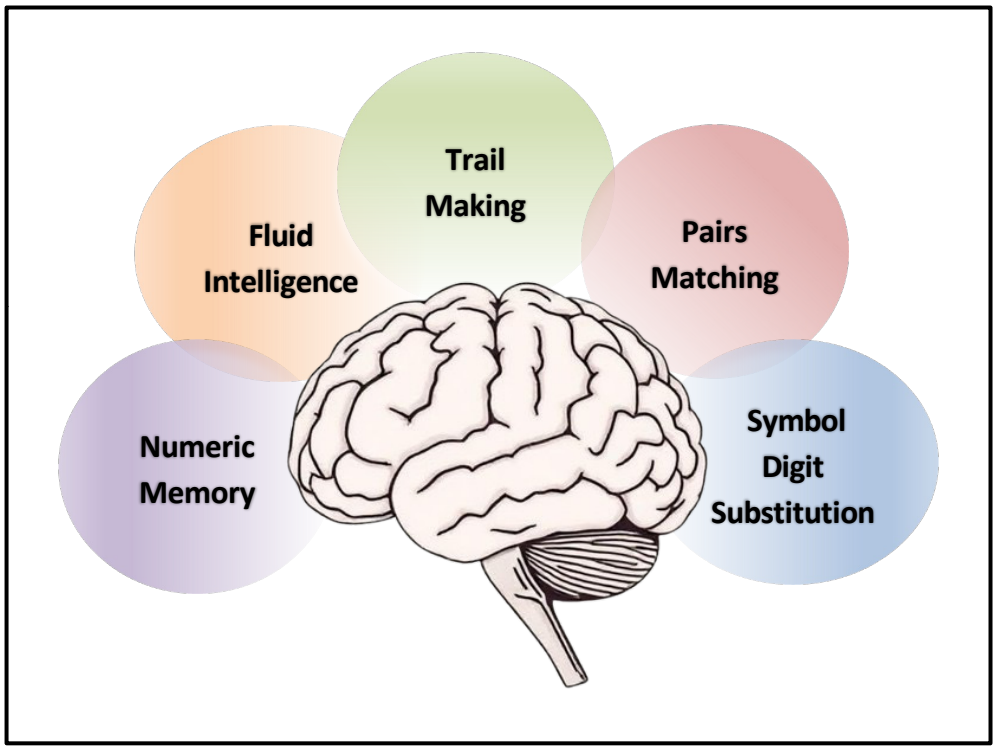



*Figure 24: Cognitive tests in UK Biobank included in the final analysis*

### 6.2.4 Confounds

Based on published literature [344, 345], I identified and adjusted for potential confounds, which were self-reported at baseline. Sociodemographic factors were reported at the baseline visit, including: age, household income, deprivation, educational qualifications, job type, alcohol intake, smoking, BMI, systolic and diastolic BP, and assessment centre. The time difference between baseline and the first cognitive assessment was included in both cross-

sectional and longitudinal analyses, and the time difference between the two cognitive assessments was included as an additional covariate in the longitudinal analysis. Additional details on the confounding variables are provided in **Section 3.5**.

### 6.2.5 Genetic variants

GWAS studies included in the genetic analysis are presented in **Figure 25.** Summary genome-wide data were examined based on two different cannabis phenotypes. For the exposure variable, GWAS summary statistics for *CanUD and CanLU* were used [56, 57], while the outcome variables comprised summary statistics for each of the cognitive tests from UK Biobank GWAS [58]. These cognitive tests included numeric memory, fluid intelligence, and pairs matching. Genetic associations with dementia outcomes were identified from a large GWAS on all-cause dementia [59]. SNPs reaching genome-wide significance ($p < 5\times10^{-8}$) were used as instruments and pruned for LD (PLINK; 1000 Genomes). When an exposure SNP was unavailable in an outcome GWAS, high-LD proxies ($r^2 > 0.90$) were sought using LDlink. In total 20 CanUD SNPs and 8 CanLU SNPs were matched to cognitive test GWAS while 21 CanUD SNPs and 8 CanLU SNPs were matched to all-cause dementia GWAS (**Table 30**). For the reverse MR, 2 SNPs associated with fluid intelligence (**Table 31**) and 3 SNPs associated with all-cause dementia (**Table 32**) were matched to CanUD and CanLU. Additional details on genetic variant selection are provided in **Section 3.6.**

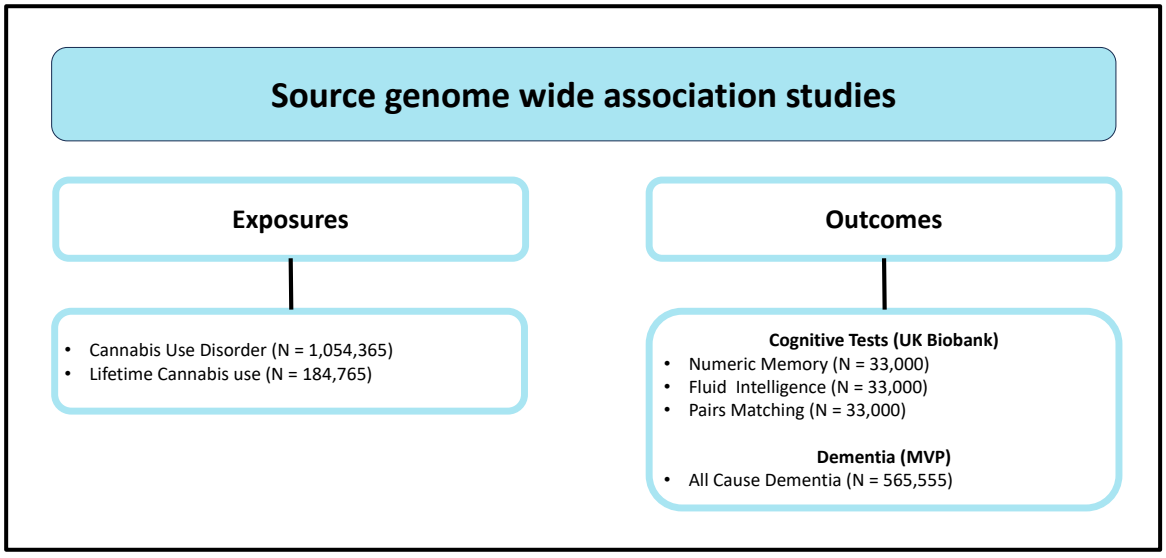



*Figure 25: Source genome-wide association studies used in Mendelian randomization analysis*

Source GWAS references: cannabis use disorder [56]; lifetime cannabis use [57]; cognitive tests (UK Biobank) [58]; dementia (MVP) [59]. Abbreviations: MVP, Million Veteran Program.

*Table 30: Genome-wide significant SNPs associated with cannabis use for cognitive function and dementia association*

| GWAS | SNP | Chr | BP | A1 | A2 | Beta | SE | *P*-value | *F* stats |
|---|---|---|---|---|---|---|---|---|---|
| **Cannabis use disorder (CanUD) [56]** | rs10835372 | 11 | 28643913 | C | T | 0.05 | 0.01 | 3.03E-08 | 27.28 |
| | rs10986600 | 9 | 127928735 | C | T | 0.06 | 0.01 | 2.17E-10 | 34.67 |
| | rs11711407 | 3 | 50225029 | G | A | 0.05 | 0.01 | 2.95E-08 | 29.06 |
| | rs1526480 | 1 | 91209986 | C | T | -0.05 | 0.01 | 5.91E-10 | 40.25 |
| | rs159365 | 5 | 60500273 | G | A | 0.05 | 0.01 | 3.33E-08 | 29.06 |
| | rs17007864 | 3 | 70876858 | C | T | 0.05 | 0.01 | 1.05E-09 | 30.22 |
| | rs62461183 | 7 | 77716309 | C | T | 0.07 | 0.01 | 5.86E-10 | 43.64 |
| | rs1637570 | 10 | 118619529 | A | G | -0.05 | 0.01 | 4.79E-08 | 27.78 |
| | rs201175241[ab] | 4 | 47126053 | G | GA | 0.43 | 0.08 | 1.77E-08 | 32.11 |
| | rs2014920 | 11 | 113466565 | T | G | 0.05 | 0.01 | 8.00E-09 | 31.89 |
| | rs2189010 | 7 | 114119430 | A | G | 0.05 | 0.01 | 1.28E-08 | 29.78 |
| | rs34554234 | 11 | 113292326 | G | GC | -0.05 | 0.01 | 2.20E-09 | 36.00 |
| | rs3774800 | 3 | 49334768 | A | G | -0.06 | 0.01 | 1.72E-12 | 40.00 |
| | rs545943750[ab] | 8 | 16059558 | A | AT | -0.68 | 0.12 | 1.45E-08 | 38.94 |
| | rs555208511[a] | 14 | 58669659 | A | AAT | -0.06 | 0.01 | 9.04E-09 | 33.64 |
| | rs56070621 | 5 | 30825684 | A | T | 0.05 | 0.01 | 1.15E-08 | 29.25 |
| | rs56372821 | 8 | 27436500 | A | G | -0.09 | 0.01 | 7.27E-14 | 52.64 |
| | rs62051488 | 16 | 72652784 | A | C | -0.07 | 0.01 | 2.98E-08 | 39.33 |
| | rs6690119 | 1 | 73580964 | T | C | 0.05 | 0.01 | 5.00E-08 | 27.28 |
| | rs726610 | 3 | 85551403 | T | C | -0.06 | 0.01 | 4.29E-11 | 35.11 |
| | rs7519259 | 1 | 66434743 | A | G | 0.05 | 0.01 | 1.83E-09 | 35.00 |
| | rs80030908 | 13 | 55159898 | A | G | 0.17 | 0.03 | 2.13E-08 | 184.27 |
| | rs9344740 | 6 | 88619412 | T | G | -0.06 | 0.01 | 8.34E-10 | 35.11 |
| **Lifetime cannabis use (CanLU) [57]** | rs2875907 | 3 | 85518580 | A | G | 0.07 | 0.01 | 9.38E-17 | 68.89 |
| | rs1448602 | 3 | 85780454 | A | G | -0.06 | 0.01 | 6.55E-11 | 38.44 |
| | rs7651996 | 3 | 85057349 | T | G | 0.05 | 0.01 | 2.37E-09 | 29.06 |
| | rs10085617[b] | 7 | 3634711 | A | T | 0.05 | 0.01 | 2.93E-08 | 29.06 |
| | rs9773390 | 8 | 81565692 | T | C | -0.17 | 0.03 | 5.66E-09 | 104.22 |
| | rs9919557 | 11 | 112877408 | T | C | -0.06 | 0.01 | 9.94E-11 | 30.11 |
| | rs10499 | 16 | 28915527 | A | G | 0.05 | 0.01 | 1.13E-09 | 31.89 |
| | rs17761723 | 17 | 2107090 | T | C | 0.05 | 0.01 | 3.24E-08 | 27.28 |

Significance threshold was set at $p<5E-08$. [a]SNP unavailable for cognitive test. [b]SNP unavailable for all-cause dementia. Source GWAS references: cannabis use disorder [56]; lifetime cannabis use [57]. Abbreviations: GWAS, genome-wide association studies; SNP, single nucleotide polymorphism; Chr, Chromosome; BP, location in base pairs; A1, effect allele; A2, other allele; SE, standard error of beta.

*Table 31: Genome-wide significant SNPs associated with Fluid intelligence test*

| GWAS | SNP | Chr | BP | A1 | A2 | Beta | SE | *P*-value |
|---|---|---|---|---|---|---|---|---|
| **Fluid intelligence test** | rs5758589* | 22 | 42518382 | G | A | 0.05 | 0.01 | 4.88E-11 |
| | rs9771228 | 7 | 32322496 | C | T | -0.04 | 0.01 | 4.18E-08 |

*Proxy SNPs. Source GWAS references: fluid intelligence test [60]. Abbreviations: GWAS, genome-wide association studies; SNP, single nucleotide polymorphism; Chr, Chromosome; BP, location in base pairs; A1, effect allele; A2, other allele; SE, standard error of beta.

*Table 32: Genome-wide significant SNPs for all-cause dementia in Million Veteran Program (MVP)*

| GWAS | SNP | Chr | BP | A1 | A2 | Beta | SE | *P*-value |
|---|---|---|---|---|---|---|---|---|
| **All-cause dementia** | rs3851179 | 11 | 85868640 | C | T | 0.03 | 0.01 | 1.70E-10 |
| | rs111371860 | 19 | 45345787 | T | A | -0.06 | 0.02 | 8.60E-11 |
| | rs744373 | 2 | 127894615 | G | A | 0.03 | 0.01 | 5.19E-11 |

Source GWAS references: dementia (MVP) [59]. Abbreviations: GWAS, genome-wide association studies; SNP, single nucleotide polymorphism; Chr, Chromosome; BP, location in base pairs; A1, effect allele; A2, other allele; SE, standard error of beta.

### 6.2.6 Statistical analyses

Independent samples *t*-tests and chi-squared analyses were conducted to assess potential univariate differences in the sociodemographic characteristics among cannabis users and the non-users. Multiple linear regression and linear mixed-effects models were conducted in R to examine cross-sectional and longitudinal associations, respectively, between cannabis use and cognitive function, while adjusting for potential covariates.

To test the robustness of the cannabis–cognition associations, three sensitivity analyses were conducted, with all models adjusted for the same sociodemographic and lifestyle covariates as in the primary analyses. First, cannabis dose was examined by classifying participants into low- and high-frequency groups and entering this binary factor as the main predictor. Second, sex-specific effects were assessed by including an interaction term between cannabis use and sex. Third, associations were examined across multiple frequency categories to test for dose–response relationships. Multiple comparisons were controlled for using a 5% FDR.

To evaluate whether behavioural, psychological, and mental-health factors contributed to the observed cognitive associations, the nested modelling framework was applied to numeric memory and fluid intelligence—the two cognitive tests that were significant in the primary analysis. Model 1 included core demographic and health covariates, with Model 2 adding smoking and alcohol use. Psychological traits (risk-taking, loneliness, and standardised neuroticism) were incorporated in Model 3, followed by subclinical depressive and anxiety

symptom scores (PHQ-9 and GAD-2) in Model 4. A final model (Model 5) added clinically diagnosed depression and anxiety based on ICD-10 codes from linked hospital records. This framework enabled assessment of whether cognitive associations remained robust after accounting for increasingly comprehensive sets of potential confounders or mediators.

Finally, to investigate potential causal associations, bidirectional two-sample MR analyses was performed. To enhance interpretability, MR estimates were scaled to reflect a doubling in prevalence of CanUD or CanLU with cognitive effects reported in standard deviation units and dementia effects as odds ratios [348]. Additionally, a reverse analysis was conducted to test for potential reverse causation. More details on the robust MR methods performed are provided in the **Section 3.7.3.1.**

Due to the limited number of dementia cases in UKB, observational analyses of cannabis use and dementia were not performed here. However, complementary analyses conducted in the MVP cohort found no evidence of an association. MR was therefore the primary approach used to evaluate potential causal links.

## 6.3 Results

### 6.3.1 Demographics

In the UK Biobank, approximately 18,000 cannabis users and 56,000 controls were identified in the cross-sectional analysis (**Figure 23**). Missing values varied between cognitive tests, with cannabis users' data ranging from 17,099 to 18,975 and controls' ranging from 53,283 to 60,598. In the longitudinal analysis, around 15,000 cannabis users and 48,000 controls were assessed, with sample sizes ranging from 13,180 to 15,841 for users and 38,171 to 49,006 for controls depending on the cognitive test. Cannabis users were significantly younger (mean age = 58.14 years, standard deviation (SD) = 7.28) than the controls (mean age = 62.24 years, SD = 7.50), and were less socially deprived. There was a higher proportion of males and of people with college degrees in the user group. A higher proportion of cannabis users drank alcohol daily and were currently smoking. While groups were well matched for BMI and diastolic BP, the control group had a slightly higher mean systolic BP. The demographic characteristics are provided in **Table 33.**

*Table 33: Demographic characteristics*

| **Variables** | **Cannabis users (n = 18,975)** | **Controls (n = 60,598)** | **Statistics** | |
|---|---|---|---|---|
| | Mean (SD) or % (n) | | t or $\chi 2$* | p-value |
| **Age at recruitment (years) *** | 52.88 (7.28) | 56.94 (7.51) | 65.41 | < 2.2E-16 |
| **Age at 1st cognitive assessment**** | 58.14 (7.26) | 62.24 (7.50) | 66.16 | < 2.2E-16 |
| **Sex, male % (n)*** | 49.73% (9,436) | 42.38% (25,682) | 316.11* | < 2.2E-16 |
| **Townsend deprivation index*** | -0.79 (3.10) | -1.98 (2.66) | -51.68 | < 2.2E-16 |

| | | | | |
|---|---|---|---|---|
| **BMI (kg/m$^2$)*** | 26.34 (4.49) | 26.73 (4.53) | 10.39 | < 2.2E-16 |
| **Diastolic BP (mmHg)*** | 81.11 (10.66) | 81.76 (10.45) | 7.46 | 9.009E-14 |
| **Systolic BP (mmHg)*** | 134.65 (18.19) | 139.13 (19.25) | 28.33 | < 2.2E-16 |
| **College degree, % (n)*** | 62.86% (11,928) | 44.10% (26,721) | 2391.30* | < 2.2E-16 |
| **Job, % (n)*** | | | | |
| **Managers and Senior Officials** | 20.86% (3,958) | 17.01% (10,306) | 213.08* | < 2.2E-16 |
| **Professional Occupations** | 32.18% (6,107) | 25.40% (15,394) | 470.86* | < 2.2E-16 |
| **Associate Professional/Technical** | 26.92% (5,108) | 21.33% (12,925) | 361.52* | < 2.2E-16 |
| **Occupations** | 15.85% (3,007) | 17.90% (10,850) | 18.05* | < 2.2E-16 |
| **Administrative and Secretarial Occupations** | | | | |
| **Alcohol intake frequency, % (n)*** | | | | |
| **Daily** | 30.41% (5,771) | 22.43% (13,591) | 500.05* | < 2.2E-16 |
| **3-4 times a week** | 29.10% (5,521) | 25.63% (15,533) | 88.90* | < 2.2E-16 |
| **1-2 times a week** | 22.09% (4,191) | 24.99% (15,141) | 65.87* | 4.812E-16 |
| **1-3 times a month** | 9.17% (1,740) | 11.10% (6,725) | 56.29* | 6.263E-14 |
| **Special occasions** | 5.78% (1,096) | 9.81% (5,946) | 291.33* | < 2.2E-16 |
| **Never** | 3.46% (656) | 6.04% (3,662) | 187.78* | < 2.2E-16 |
| **Smoking % (n)*** | | | | |
| **Current** | 14.41% (2,736) | 4.48% (2,713) | 2237.50* | < 2.2E-16 |
| **Previous** | 53.59% (10,169) | 29.87% (18,101) | 3548.70* | < 2.2E-16 |
| **Never** | 31.99% (6,070) | 65.65% (39,784) | 6704.50* | < 2.2E-16 |

*Measured at baseline. **Measured at 1st cognitive assessment. Abbreviations: SD, standard deviation; BMI, body mass index; BP, blood pressure.

### 6.3.2 Results from observational analysis

Cannabis use was significantly positively associated with cross-sectional performance on two out of six examined measures after FDR correction (0.05%, p = 0.009). Cannabis users performed better on numeric memory (beta = $7.42\times10^{-2}$, [$5.61\times10^{-2}$ to $9.23\times10^{-2}$], p = $9.91\times10^{-16}$) and fluid intelligence (beta = $1.16\times10^{-1}$, [$9.92\times10^{-2}$ to $1.32\times10^{-1}$], p < $2\times10^{-16}$). No significant associations were observed for trail making test A (beta = $-1.70\times10^{-2}$, [$-3.49\times10^{-2}$ to $8.75\times10^{-4}$], p = 0.062), trail making test B (beta = $-1.90\times10^{-2}$, [$-3.60\times10^{-2}$ to $-2.03\times10^{-3}$], p = 0.028), symbol digit substitution (beta = $1.25\times10^{-2}$, [$-3.45\times10^{-3}$ to $2.84\times10^{-2}$], p = 0.125), or pairs matching (beta = $-7.79\times10^{-4}$, [$-1.83\times10^{-2}$ to $1.68\times10^{-2}$], p = 0.931) **(Figure 26).**

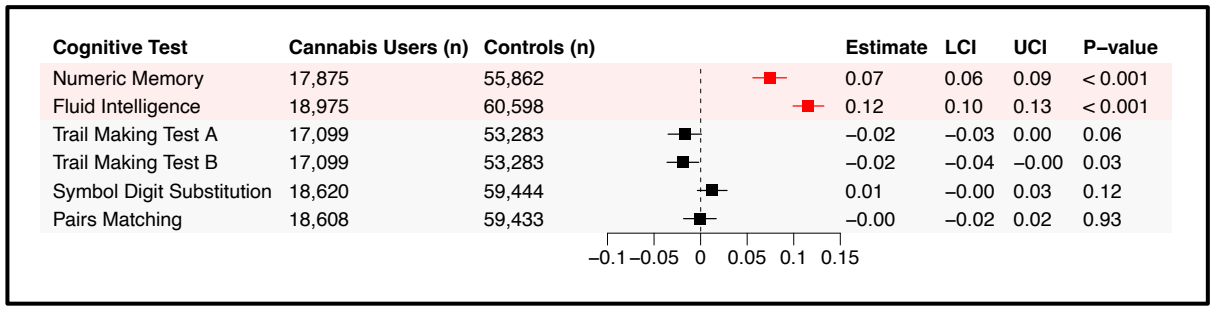



*Figure 26: Associations between cannabis use and cross-sectional cognitive functioning in UK Biobank*

Estimates were generated using multiple linear regression models adjusted for: age at baseline, sex, household income, Townsend deprivation index, educational qualifications, job type, alcohol drinking frequency, smoking status, body mass index, systolic and diastolic blood pressure, assessment centre, and time between baseline and first cognitive assessment. Higher scores reflect better performance for Fluid Intelligence, Symbol Digit Subs and

Symbol Digit Substitution and Pairs Matching. Trail Making Test durations higher values reflecting slower completion times (poorer performance). Abbreviations: LCI, lower confidence interval; UCI, upper confidence interval.

Longitudinal cognitive change was assessed in a subset of UK Biobank participants with repeat testing, with a mean interval of 8.78 years (SD = 3.61; range = 4-14 years) between assessments. Over time, performance improved on fluid intelligence (beta = $9.84\times10^{-3}$, [$8.66\times10^{-3}$, $1.10\times10^{-2}$], $p < 2\times10^{-16}$), trail making test A trail making tests A (beta = $-4.42\times10^{-3}$, [$-5.78\times10^{-3}$, $-3.06\times10^{-3}$], $p = 2.04\times10^{-10}$), and pairs matching (beta = $6.61\times10^{-4}$, [$1.19\times10^{-4}$, $1.20\times10^{-3}$], p = 0.017). Trail making test B performance declined (beta = $2.86\times10^{-3}$, [$1.68\times10^{-3}$, $4.03\times10^{-3}$], $p = 1.82\times10^{-6}$), and symbol digit substitution showed a small, borderline decline (beta = $-1.09\times10^{-3}$, [$-2.23\times10^{-3}$, $4.47\times10^{-5}$], p = 0.060) (**Table 34, Figure 27)**. No significant cannabis × time interaction effects were observed for any cognitive test after FDR correction, including fluid intelligence, which showed cross-sectional associations but no significant longitudinal association (beta = $1.55*10^{-3}$, [$-8.20*10^{-4}$ to $3.93*10^{-3}$], p = 0.20) (**Table 35).**

*Table 34: Longitudinal trends in cognitive test performance in UK Biobank participants (main effect of time)*

| Cognitive Tests | Estimate | LCI | UCI | P-value |
|---|---|---|---|---|
| **Fluid Intelligence** | 9.84E-03 | 8.66E-03 | 1.10E-02 | <2.00E-16 |
| **Trail Making Test A** | −4.42E-03 | −5.78E-03 | −3.06E-03 | 2.04E-10 |
| **Trail Making Test B** | 2.86E-03 | 1.68E-03 | 4.03E-03 | 1.82E-06 |
| **Symbol Digit Substitution** | −1.09E-03 | −2.23E-03 | 4.47E-05 | 5.97E-02 |
| **Pairs Matching** | 6.61E-04 | 1.19E-04 | 1.20E-03 | 1.68E-02 |

Estimates were generated from mixed effects models adjusted for age at baseline, sex, household income, Townsend deprivation index, educational qualifications, job type, alcohol drinking frequency, smoking status, body mass index, systolic and diastolic blood pressure, assessment centre, time between baseline and first cognitive assessment, and time between cognitive assessments. Values represent the estimated change in cognitive function across all participants (main effect of time). Abbreviations: LCI, lower confidence interval; UCI, upper confidence interval.

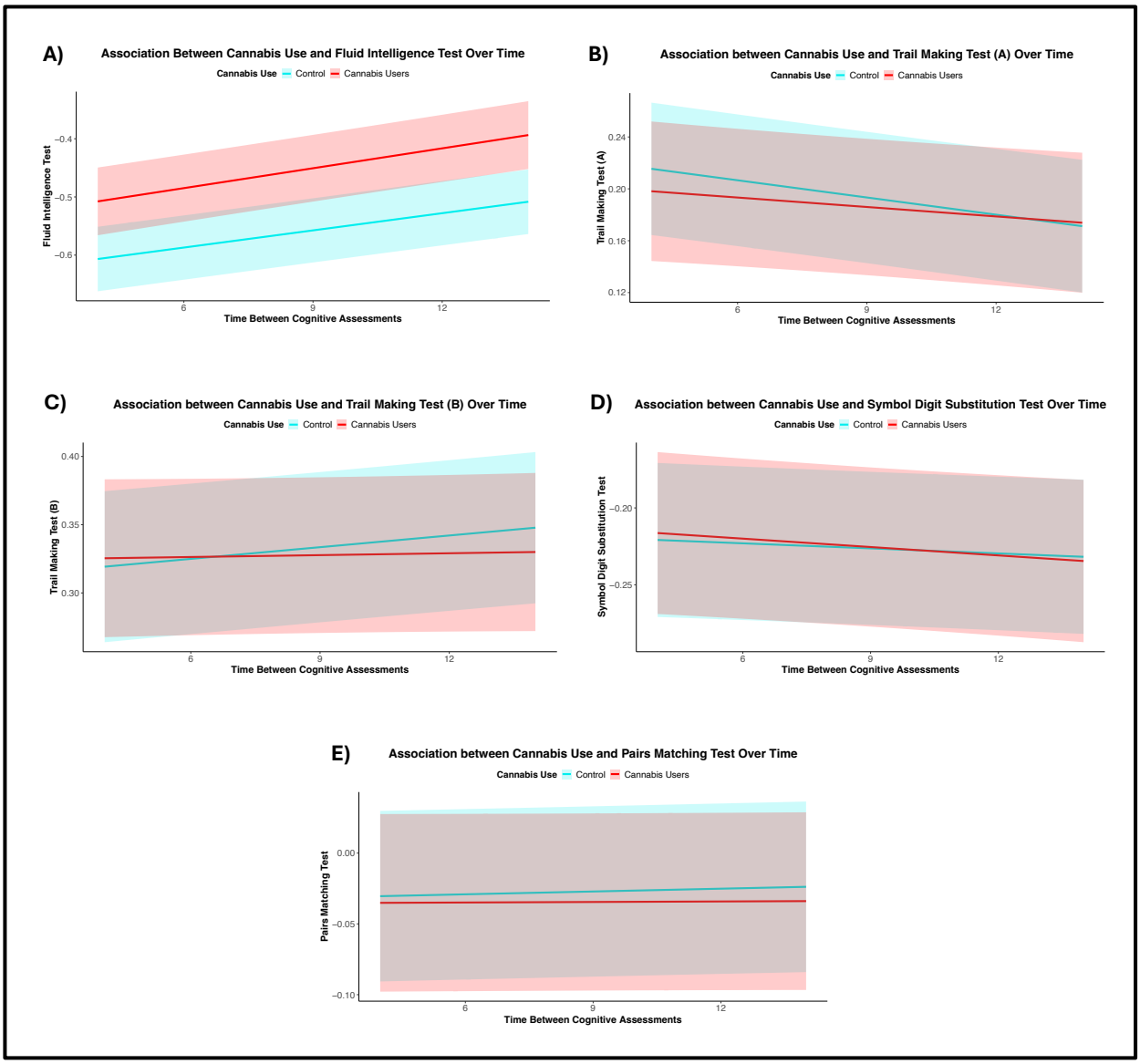



*Figure 27: Associations between cannabis use and longitudinal change in cognitive functioning in UK Biobank*

Plots show the predicted change in cognitive performance over time, according to cannabis use status. The x-axis represents the time difference between cognitive assessments, while the y-axis represents the predicted cognitive tests measures (note different scales for ease of viewing). Red lines represent the expected trajectory for cannabis users, and the blue line for controls, with shaded bands indicating 95% confidence intervals. Predictions were generated from mixed effects models adjusted for age at baseline, sex, household income, Townsend deprivation index, educational qualifications, job type, alcohol drinking frequency, smoking status, body mass index, systolic and diastolic blood pressure, assessment centre, time between baseline and first cognitive assessment and time between cognitive assessments. Scales are different for each test.

*Table 35: Longitudinal change in cognitive functioning according to cannabis use in UK Biobank cannabis × time interaction effects*

| | Lifetime cannabis users vs. controls | | | |
|---|---|---|---|---|
| **Cognitive Tests** | **Estimate** | **LCI** | **UCI** | **P-value** |
| Fluid Intelligence | 1.55E-03 | −8.20E-04 | 3.93E-03 | 1.99E-01 |
| Trail Making Test A | 1.99E-03 | −6.99E-04 | 4.69E-03 | 1.47E-01 |
| Trail Making Test B | −2.40E-03 | −4.69E-03 | −1.05E-04 | 4.04E-02 |
| Symbol Digit Substitution | −7.26E-04 | −3.01E-03 | 1.55E-03 | 5.33E-01 |
| Pairs Matching | −5.39E-04 | −1.63E-03 | 5.56E-04 | 3.35E-01 |

Estimates were generated from mixed effects models adjusted for age at baseline, sex, household income, Townsend deprivation index, educational qualifications, job type, alcohol drinking frequency, smoking status, body mass index, systolic and diastolic blood pressure, assessment centre, time between baseline and first cognitive assessment and time between cognitive assessment. Differences in longitudinal change in cognitive function between cannabis users and controls were assessed using an interaction term between time and cannabis use (yes vs. no). The reference group are non-users. Abbreviations: LCI, lower confidence interval; UCI, upper confidence interval.

### 6.3.3 Sensitivity Analyses

Several sensitivity analyses were performed to test the cross-sectional associations between cannabis use and cognitive performance, for the tests that survived the FDR correction in the main analysis. In the sex-interaction analysis, no significant interaction was observed for numeric memory (beta = -0.02, [-0.05 to 0.01], p = 0.18). However, a significant interaction was found for fluid intelligence (beta = 0.08, [0.05 to 0.11], $p < 0.001$), indicating a stronger positive association in males compared to females (**Table 36, Figure 28).**

*Table 36: Interaction between cannabis use and sex in relation to cross-sectional cognitive performance in UK Biobank*

| **Cognitive Tests** | **Estimate** | **LCI** | **UCI** | **P-value** |
|---|---|---|---|---|
| Numeric Memory | -0.02 | -0.05 | 0.01 | 0.182 |
| Fluid Intelligence | 0.08 | 0.05 | 0.11 | 3.46E-08 |

Estimates represent the interaction effect between lifetime cannabis use (user vs. non-user) and sex on cognitive performance. Estimates were generated using multiple linear regression models adjusted for: age at baseline, household income, Townsend deprivation index, educational qualifications, job type, alcohol drinking frequency, smoking status, body mass index, systolic and diastolic blood pressure, assessment centre, and time between baseline and cognitive assessment. The reference group are non-users. Abbreviations: LCI, lower confidence interval; UCI, upper confidence interval.

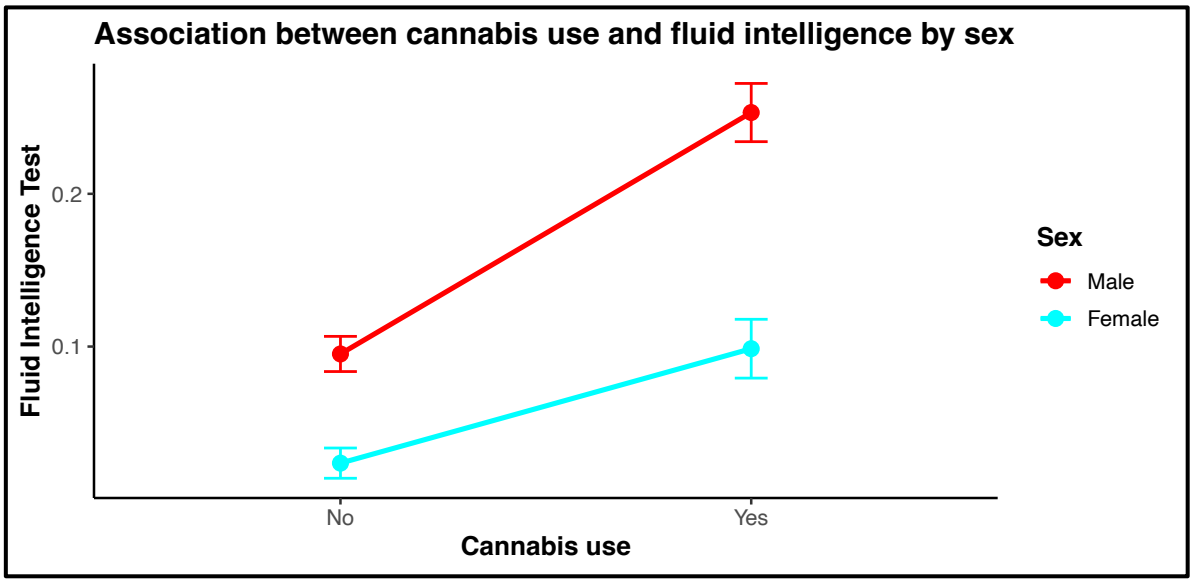



*Figure 28: Association between cannabis use and sex in relation to cross-sectional fluid intelligence in UK Biobank*

Lines show model-adjusted mean fluid-intelligence z-scores (95% CI) by cannabis use (Yes/No), plotted separately for males (red, solid) and females (cyan, dashed). Estimates come from a linear regression including cannabis use, sex, and their interaction, adjusted for age at baseline, household income, Townsend deprivation index, educational qualifications, job type, alcohol drinking frequency, smoking status, body mass index, systolic and diastolic blood pressure, assessment centre, and time between baseline and cognitive assessment. The cannabis × sex interaction was significant indicating a stronger positive association in males.

Cannabis dose effects were assessed comparing low vs high frequency users for the relationships between cannabis use and cognitive performance. No significant differences were found between the groups (**Table 37).**

*Table 37: Association between high frequency cannabis use (compared to low frequency) and cross-sectional cognitive performance in UK Biobank*

| | Low vs. high frequency cannabis users | | | |
|---|---|---|---|---|
| **Cognitive Tests** | **Estimate** | **LCI** | **UCI** | **P-value** |
| Numeric Memory | 2.00E-3 | -0.03 | 0.03 | 0.91 |
| Fluid Intelligence | 2.00E-3 | -0.09 | 0.03 | 0.91 |

Estimates were generated using multiple linear regression models adjusted for: age at baseline, sex, household income, Townsend deprivation index, educational qualifications, job type, alcohol drinking frequency, smoking status, body mass index, systolic and diastolic blood pressure, assessment centre, and time between baseline and first cognitive assessment. Estimates were generated among users only (high n= 6,215; low n= 12,760). Abbreviations: LCI, lower confidence interval; UCI, upper confidence interval.

All frequencies of cannabis use, even less than monthly, were associated with higher cognitive performance compared to non-use, across several tests after FDR correction, with no differential impact of higher frequencies (**Figure 29**).

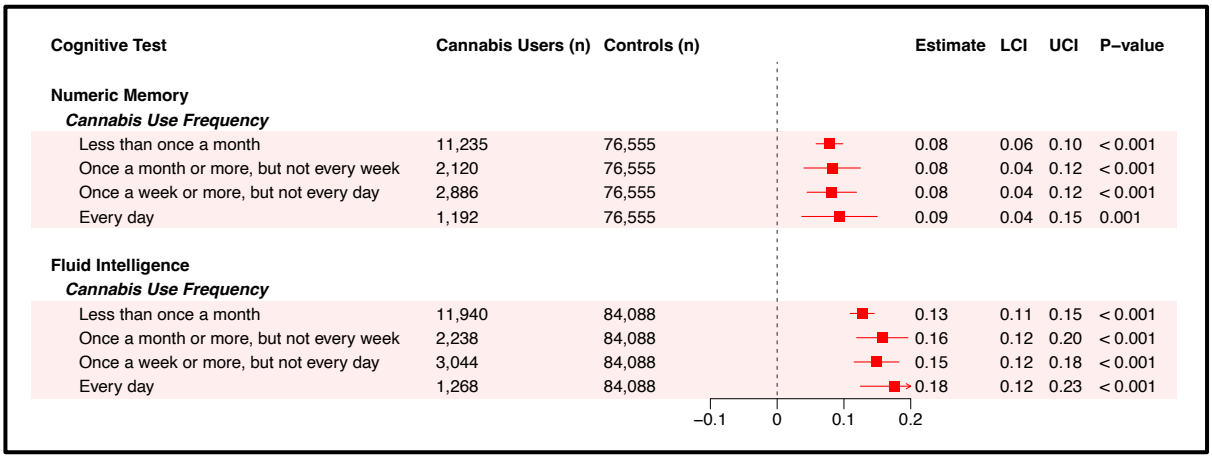



*Figure 29: Associations between cannabis use frequency and cross-sectional cognitive performance in UK Biobank*

Estimates were generated using multiple linear regression models adjusted for: age at baseline, sex, household income, Townsend deprivation index, educational qualifications, job type, alcohol drinking frequency, smoking status, body mass index, systolic and diastolic blood pressure, assessment centre, and time between baseline and first cognitive assessment. The reference group are non-users. Abbreviations: LCI, lower confidence interval; UCI, upper confidence interval.

Across all five sensitivity models, the positive associations between cannabis use and both numeric memory and fluid intelligence remained consistent. The direction of effects was unchanged when adjusting for core covariates (Model 1), adding smoking and alcohol (Model 2), incorporating psychological traits (Model 3), including subclinical depressive and anxiety symptoms (Model 4), or adding ICD-10 diagnoses of depression and anxiety (Model 5). Although effect sizes were slightly larger in the psychological and mental-health models (Models 3 and 4), these models also involved substantially smaller sample sizes. In all models, the associations between cannabis use and cognitive performance remained positive and statistically significant, indicating robustness across the extended covariate framework (**Appendix 11**).

### 6.3.4 Results from Mendelian randomization analysis

In MR analysis using 20 independent SNPs to instrument CanUD, no FDR-significant associations were observed with either numeric memory (IVW beta = $-7.56 \times 10^{-3}$, [-0.06 to 0.05], p = 0.78), fluid intelligence (IVW beta = $4.02 \times 10^{-3}$, [-0.06 to 0.05], p = 0.88, or pairs matching (IVW beta = $-3.59 \times 10^{-3}$, [$8.00 \times 10^{-3}$ to $8.27 \times 10^{-4}$], p = 0.11). No genetic associations were observed either with CanLU and numeric memory (IVW beta = $-3.50 \times 10^{-3}$, [-0.06 to 0.05], p = 0.90), fluid intelligence (IVW beta = -0.06, [-0.14 to 0.02], p = 0.15), or pairs matching (IVW beta = $-2.28 \times 10^{-3}$, [$-9.17 \times 10^{-3}$ to $4.62 \times 10^{-3}$], p = 0.52) (**Figure 30, Table 38** and **Figure 31**). Reverse MR using 2 SNPs to instrument fluid intelligence test did

not show any significant association between fluid intelligence and CanUD for IVW method (**Table 39** and **Figure 32**).

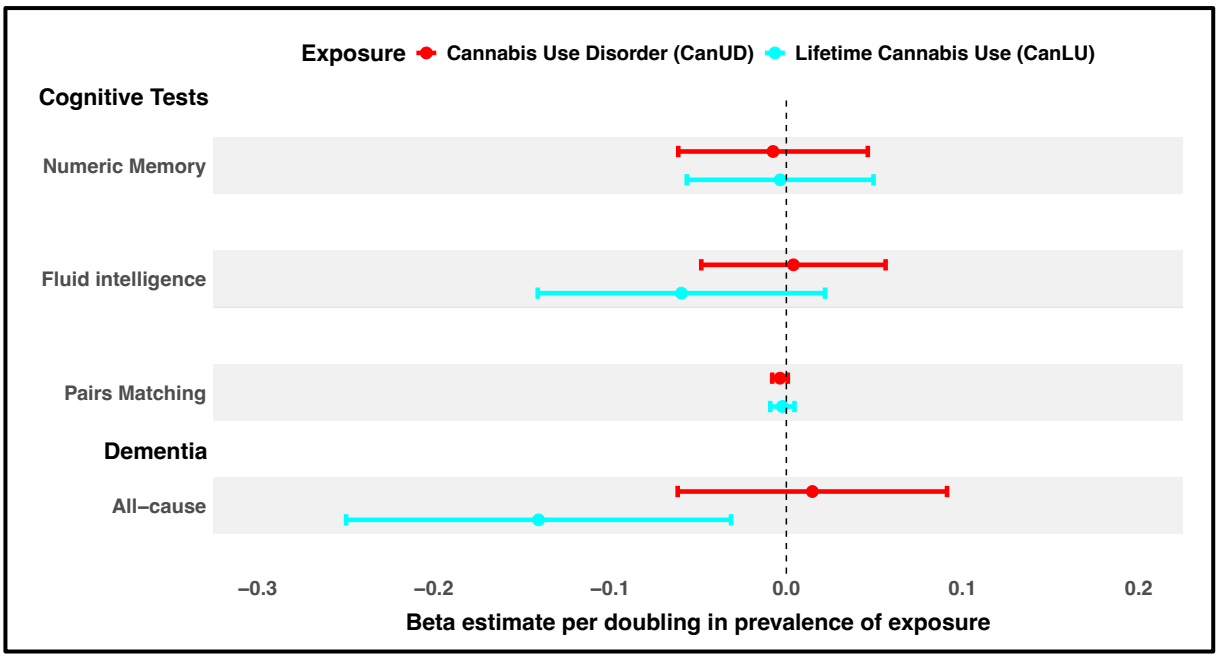



*Figure 30: Genetic associations between cannabis use, cognitive tests and dementia*

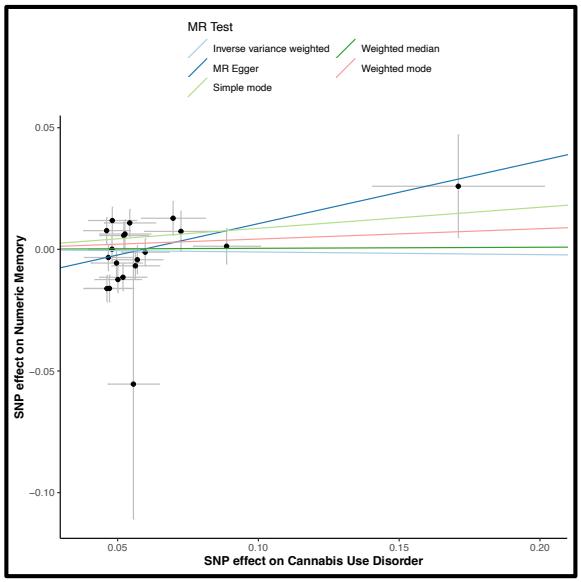
Effect sizes represent SD changes for cognitive outcomes and log odds ratios for dementia per doubling in cannabis use disorder (in red) or lifetime cannabis use (in cyan) prevalence. Estimates were generated using two sample inverse-variance weighted method from source genome-wide association studies used to derive genetic associations [56–60], with SNPs as instruments detailed in Supplementary table 4. All-cause dementia result did not survive FDR correction.

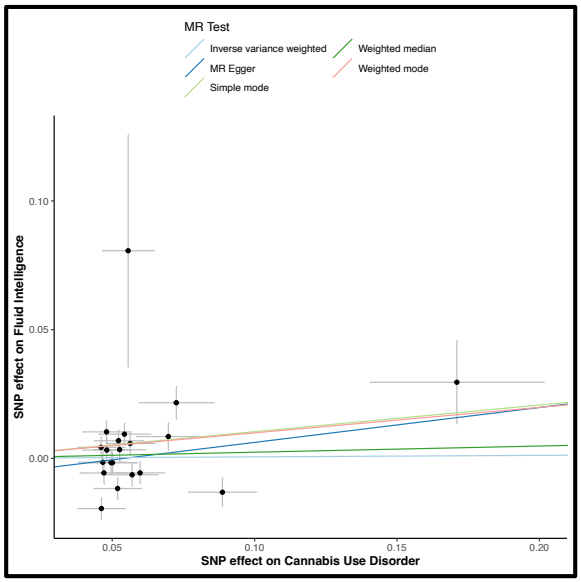
*Table 38: Two-sample linear MR estimates assessing evidence for the causal effect of cannabis use on cognitive functioning*

| Cognitive Tests (Variables) | SNPs | MR Tests | Estimates | LCI | UCI | P-value |
|---|---|---|---|---|---|---|
| **Numeric Memory (Maximum digits remembered correctly)** | 20* | MR Egger | 0.26 | -0.09 | 0.61 | 0.17 |
| | | Weighted mean | 0.00 | -0.07 | 0.08 | 0.91 |
| | | IVW | -0.01 | -0.08 | 0.07 | 0.78 |
| | | Simple mode | 0.09 | -0.06 | 0.24 | 0.29 |
| | | Weighted mode | 0.04 | -0.09 | 0.18 | 0.55 |
| | 8** | MR Egger | 0.01 | -0.21 | 0.23 | 0.96 |
| | | Weighted mean | -0.02 | -0.11 | 0.07 | 0.68 |
| | | IVW | -0.01 | -0.08 | 0.07 | 0.90 |
| | | Simple mode | -0.01 | -0.16 | 0.14 | 0.88 |
| | | Weighted mode | -0.02 | -0.16 | 0.12 | 0.79 |
| **Fluid intelligence test (Fluid intelligence score)** | 20* | MR Egger | 0.14 | -0.22 | 0.49 | 0.47 |
| | | Weighted mean | 0.02 | -0.04 | 0.09 | 0.46 |
| | | IVW | 0.01 | -0.07 | 0.08 | 0.88 |
| | | Simple mode | 0.10 | -0.03 | 0.24 | 0.16 |
| | | Weighted mode | 0.10 | -0.05 | 0.25 | 0.21 |

| | | | | | | |
|---|---|---|---|---|---|---|
| | 8** | MR Egger | 0.05 | -0.27 | 0.37 | 0.76 |
| | | Weighted mean | -0.01 | -0.09 | 0.06 | 0.75 |
| | | IVW | -0.09 | -0.20 | 0.03 | 0.15 |
| | | Simple mode | 0.00 | -0.91 | 0.09 | 0.97 |
| | | Weighted mode | -0.00 | -0.08 | 0.07 | 0.90 |
| **Pairs Matching Test (Number of correct matches in round)** | 20* | MR Egger | 0.00 | -0.03 | 0.34 | 0.76 |
| | | Weighted mean | -0.01 | -0.01 | 0.00 | 0.21 |
| | | IVW | -0.01 | -0.01 | 0.00 | 0.11 |
| | | Simple mode | -0.01 | -0.02 | 0.01 | 0.28 |
| | | Weighted mode | -0.01 | -0.02 | 0.01 | 0.32 |
| | 8** | MR Egger | -0.01 | -0.04 | 0.02 | 0.63 |
| | | Weighted mean | -0.01 | -0.02 | 0.00 | 0.15 |
| | | IVW | -0.00 | -0.01 | 0.01 | 0.52 |
| | | Simple mode | -0.01 | -0.03 | 0.01 | 0.35 |
| | | Weighted mode | -0.01 | -0.02 | 0.01 | 0.24 |

*SNPs associated with *cannabis use disorder*. **SNPs associated *with lifetime cannabis use*. Abbreviations: SNP, single nucleotide polymorphism; SE, standard error; IVW, inverse-variance weighted.



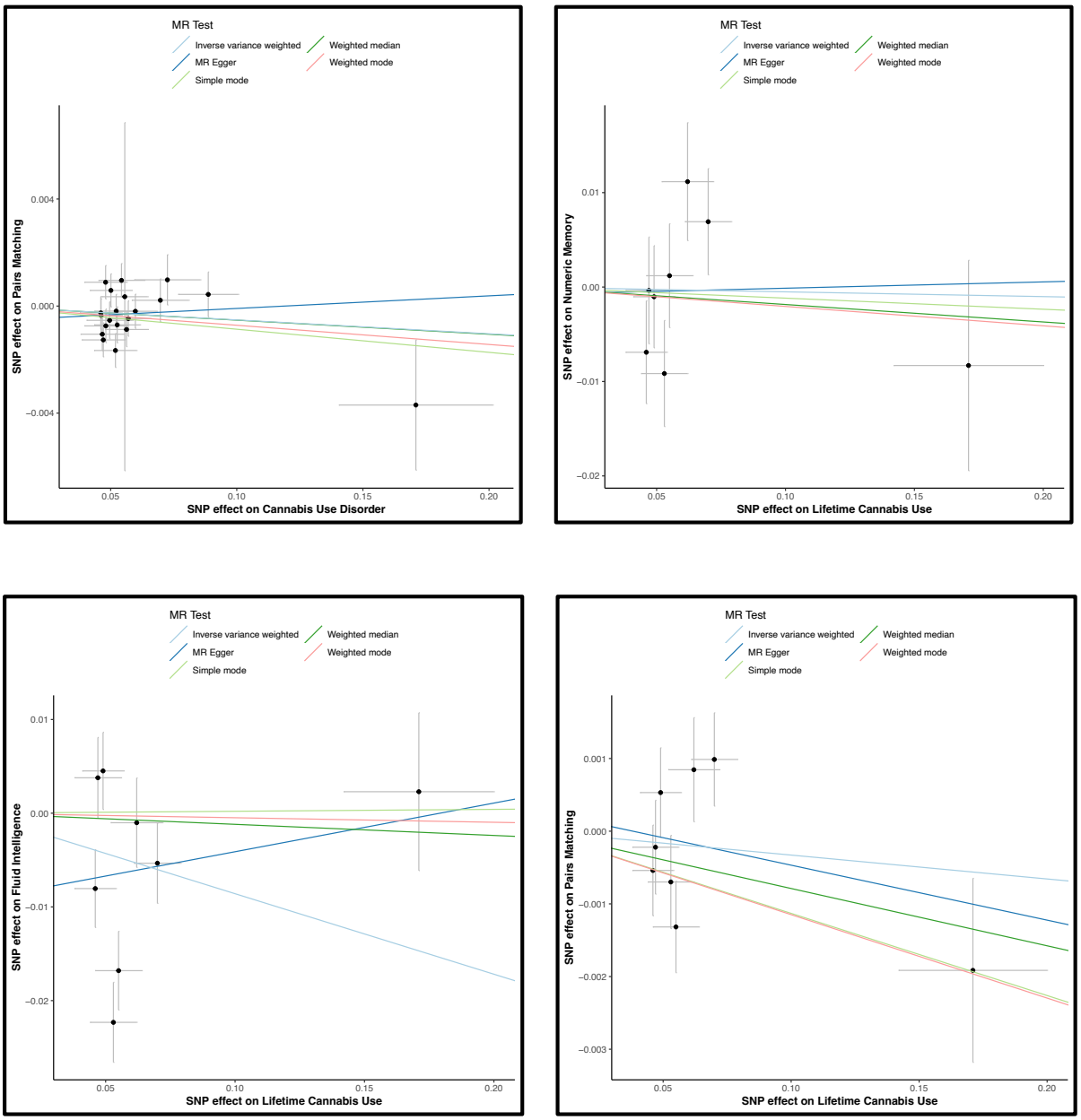



*Figure 31: Two-sample linear MR plot assessing evidence for the causal effect of Cannabis use disorder/ Lifetime Cannabis use on Cognitive tests*

*Table 39: Two-sample linear Reverse MR estimates assessing evidence for the causal effect of fluid intelligence test on cannabis use disorder*

| Cognitive test | SNPs | MR Tests | Estimates | LCI | UCI | P-value |
|---|---|---|---|---|---|---|
| **Fluid Intelligence Test** | 2* | IVW | -0.30 | -0.71 | 0.11 | 0.16 |

*SNPs associated with *cannabis use disorder*. Abbreviations: SNP, single nucleotide polymorphism; SE, standard error; IVW, inverse-variance weighted.

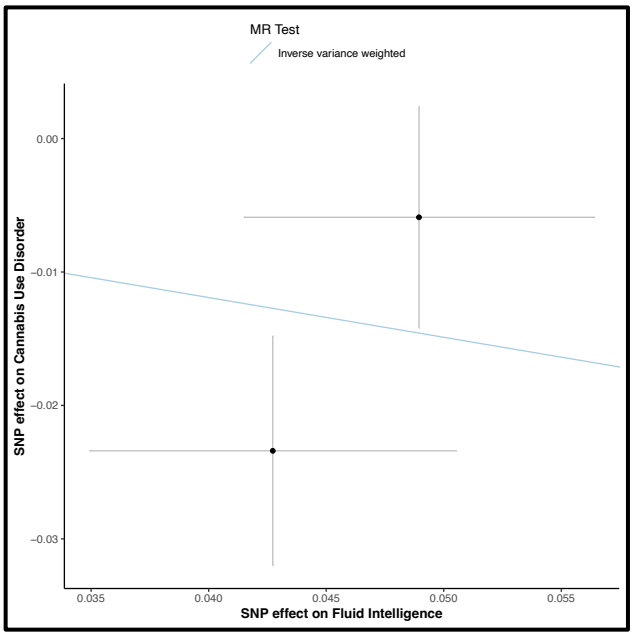



*Figure 32: Reverse two-sample linear MR plot assessing evidence for the causal effect of Fluid intelligence test on Cannabis use disorder*

Additionally, no significant associations between either genetically predicted CanUD (IVW beta = 1.01 [0.94 to 1.10], p = 0.71) or CanLU (IVW beta= 0.87 [0.78 to -0.97], p = 0.01) were observed with all-cause dementia phenotype after FDR correction (**Figure 30, Table 40** and **Figure 33**). Reverse MR did not show any significant association between all-cause dementia and CanUD (**Table 41** and **Figure 34**).

*Table 40: Two-sample linear MR estimates assessing evidence for the causal effect of cannabis use on all-cause dementia*

| Dementia | SNPs | MR Tests | Estimates | LCI | UCI | *P*-value |
|---|---|---|---|---|---|---|
| **All-Cause Dementia** | 21* | MR Egger | -0.18 | -0.72 | 0.37 | 0.53 |
| | | Weighted mean | 0.02 | -0.10 | 0.15 | 0.70 |
| | | IVW | 0.02 | -0.09 | 0.13 | 0.71 |
| | | Simple mode | -0.17 | -0.43 | 0.09 | 0.22 |
| | | Weighted mode | -0.17 | -0.44 | 0.10 | 0.22 |
| | 7** | MR Egger | 0.01 | -0.41 | 0.43 | 0.96 |
| | | Weighted mean | -0.16 | -0.34 | 0.01 | 0.07 |
| | | IVW | -0.20 | -0.36 | 0.05 | 0.01 |
| | | Simple mode | -0.36 | -0.65 | 0.07 | 0.05 |
| | | Weighted mode | -0.15 | -0.36 | 0.06 | 0.21 |

*SNPs associated with *cannabis use disorder*. ** SNPs associated *with lifetime cannabis use*. Abbreviations: SNP, single nucleotide polymorphism; SE, standard error; IVW, inverse-variance weighted.

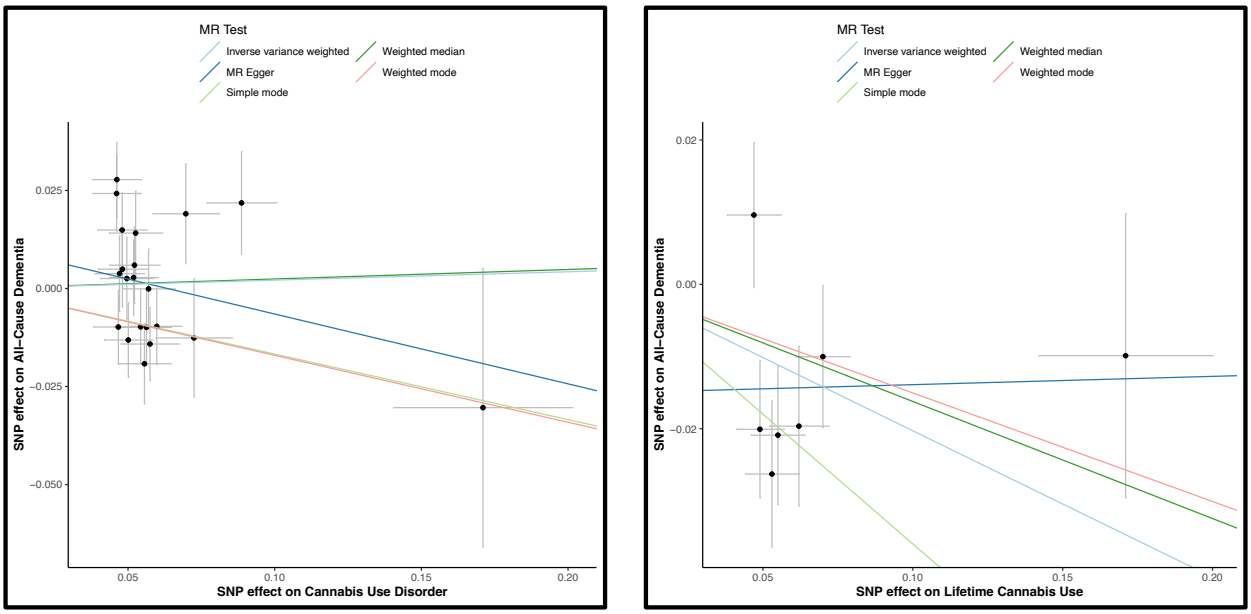



*Figure 33: Two-sample linear MR plot assessing evidence for the causal effect of Cannabis use disorder/ Lifetime Cannabis use on All-Cause Dementia*

*Table 41: Two-sample linear Reverse MR estimates assessing evidence for the causal effect of all-cause dementia on cannabis use disorder*

| Dementia | SNPs | MR Tests | Estimates | LCI | UCI | *P*-value |
|---|---|---|---|---|---|---|
| **All-Cause Dementia** | 3* | MR Egger | 0.23 | -1.25 | 1.72 | 0.81 |
| | | Weighted mean | 0.04 | -0.43 | 0.51 | 0.87 |
| | | IVW | -0.10 | -0.43 | 0.23 | 0.56 |
| | | Simple mode | 0.05 | -0.45 | 0.55 | 0.85 |
| | | Weighted mode | 0.05 | -0.43 | 0.54 | 0.85 |

*SNPs associated with *cannabis use disorder*. Abbreviations: SNP, single nucleotide polymorphism; SE, standard error; IVW, inverse-variance weighted.

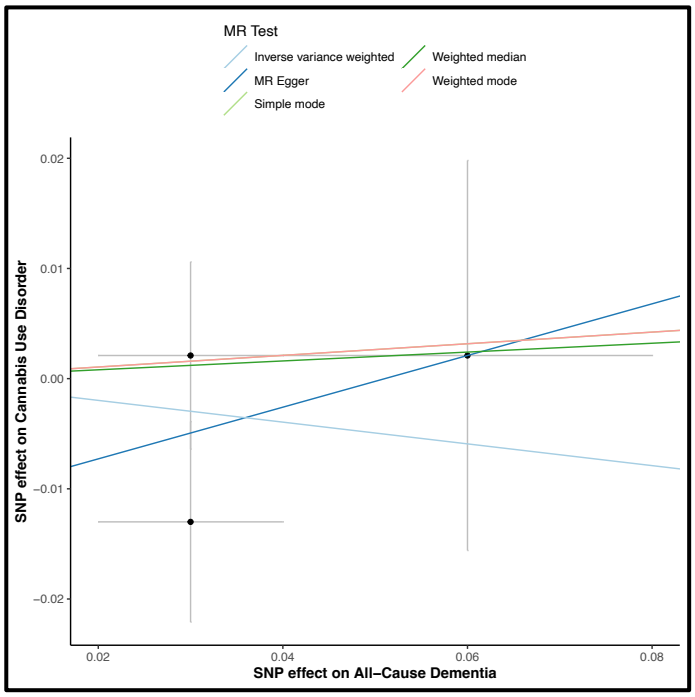



*Figure 34: Reverse two-sample linear MR plot assessing evidence for the causal effect of All-cause Dementia on Cannabis use disorder*

## 6.4 Discussion

Whilst cannabis users demonstrated significantly better cognitive performance in cross-sectional analyses, these findings were not supported by longitudinal data or genetic evidence. Crucially, cannabis use was not associated with an increased risk of dementia in MR analyses.

Lifetime cannabis users demonstrated better performance on a test of numeric memory, which assesses working memory, and on a fluid intelligence test, which measures verbal and numeric reasoning ability. Consistent with the present findings, previous research has also reported that cannabis users scored higher on fluid intelligence tests and genetic analyses have shown that liability to CanLU is positively correlated with higher educational attainment [57]. These observations suggest that the apparent cognitive advantages seen in cannabis users may partly reflect shared genetic or sociodemographic factors, rather than a direct cognitive benefit of cannabis itself. However, these findings contrast with prior research suggesting that THC impairs working memory and reasoning abilities. Acute THC administration has been shown to impair performance on working memory tasks [349–351], where frequent or long-term use has been linked to deficits in immediate recall, verbal reasoning, and verbal working memory [248, 352, 353], though evidence is mixed regarding spatial working memory [250, 354]. These inconsistencies may be attributed to variations in age, timing of exposure, dosage, frequency of use, or sample characteristics, and may also reflect differences between the biology of CanLU, associated with higher educational attainment, and CanUD, associated with lower educational attainment.

In the sex-stratified analysis, no significant interaction was observed for numeric memory, however, a significant interaction emerged for fluid intelligence showing a stronger positive association with cannabis in males than females. While past studies have shown that sex moderates the effects of cannabis on other cognitive domains such as greater vulnerability in visual memory among males and more pronounced impairments in attention and executive functioning among females [264, 298], the present findings indicate that these sex-specific patterns may also extend to reasoning abilities. Further research is needed to clarify the underlying mechanisms, including potential hormonal, neurobiological, and behavioural factors. Hormonal influences may include menstrual cycle effects [355] and cannabis related associations of the hypothalamic–pituitary–ovarian axis [356, 357]. Neurobiological explanations point to sex differences in THC storage in body fat [358, 359] and metabolism [288], as well as markers of neuronal integrity such as N-acetylaspartate [360]. Behavioural factors, including differences in patterns of cannabis use, co-use of substances such as alcohol and tobacco, and high rates of psychiatric comorbidity [361], may also contribute to these sex-specific associations.

Cannabis dose did not significantly influence the relationship between cannabis use and cognitive performance. The absence of a dose-response relationship raises important questions whether confounding factors, such as baseline cognitive abilities, personality traits, or environmental influences, play a more substantial role. It is also important to note that the number of daily, near-daily or dependent cannabis users in UK Biobank was very low, limiting statistical power to detect dose-related effects. As a result, the present findings are more representative of light-to-moderate lifetime use, and may not generalise to patterns of near-daily, long-term, or dependent use where cognitive harms are more consistently reported. Cannabis users across all frequency categories performed better than non-users on numeric memory and fluid intelligence tests. However, the question remains whether cannabis use directly improves cognitive function or whether this relationship is influenced by external factors such as lifestyle, education, or socioeconomic status; or more likely, that more educated individuals are more likely to use cannabis without developing use disorder.

The extended sensitivity analyses conducted under the broader covariate framework demonstrated that the associations between cannabis use and cognitive performance were highly robust. Across all five models, the positive associations with numeric memory and fluid intelligence persisted, with no change in the direction of effects after sequential adjustment for smoking and alcohol use, psychological traits, subclinical depressive and anxiety symptoms, or ICD-10 diagnoses of depression and anxiety. Although modest increases in effect magnitude were observed in models incorporating psychological and mental-health variables, these occurred alongside substantial reductions in sample size. Importantly, in every model examined, the associations between cannabis use and both cognitive measures remained positive and statistically significant. Taken together, these findings indicate that the cognitive results were stable across a wide range of covariate specifications and were not materially altered by the inclusion of lifestyle, psychological, or clinical mental-health factors.

Consistent with these observations reflecting something other than a direct effect of cannabis on cognition, despite the observed associations in the cross-sectional analysis, neither longitudinal analyses nor genetic analyses supported a causal link between cannabis use and cognitive performance. In the longitudinal analysis, counterintuitively, performance on some tests appears to improve over time, which may partly reflect practice effects from repeated testing [362] as well as ceiling effects, where higher-scoring individuals have less room for measurable improvement on the tasks [363]. MR analysis revealed no significant associations between genetically predicted cannabis dependence or lifetime cannabis use and numeric memory, fluid intelligence, or pairs matching test. No significant associations were observed with dementia in MR analyses. However, a recent observational study reported individuals with incident acute care due to cannabis use (a more severe exposure phenotype and, considering the observed medical harm, likely to reflect CanUD rather than CanLU) at an increased risk of developing a new dementia diagnosis compared to individuals with all-cause hospital-based care or the general population. The study did not, however, explore the duration, frequency, or type of cannabis use in detail, which may be relevant in understanding the relationship between cannabis use and dementia [268].

Discrepancies between the observational and MR findings may reflect residual confounding, differences in statistical power, or differences in how exposure is captured (for example, later-life use compared with lifetime liability). In the UK Biobank, cannabis users generally had higher educational attainment and better baseline cognitive performance, raising the possibility that the positive cross-sectional associations observed here are partly explained by socioeconomic background or pre-existing cognitive ability rather than cannabis itself. Cannabis use is also socially patterned: compared to non-users, users are more likely to differ in lifestyle factors such as alcohol and tobacco use, physical activity, and diet, each of which is independently associated with brain and cognitive outcomes [344, 364]. Psychiatric comorbidities add further complexity, as conditions such as depression, anxiety, and psychosis are linked both to cannabis use and to differences in brain cognition [95, 365, 366]. Whilst attempts were made to statistically control for these factors, imperfect measurement means residual confounding could remain. Despite extensive adjustment for these variables, it is unlikely that all sources of bias were fully accounted for, meaning that residual confounding remains a plausible explanation for the observational findings. This underlines the importance of interpreting observational associations with caution, particularly when they do not align with genetic evidence.

# Chapter 7: Discussion

This chapter brings together the central findings of the thesis and places them in the context of existing research. It reflects on how the results contribute to the understanding of the relationship between lifetime cannabis use and brain health in later life. The discussion also highlights the strengths and limitations of the study, the extent to which the findings can inform clinical practice and public health policy, and the broader implications for aging populations. Finally, it highlights areas where further investigation is needed to address gaps and guide future research.

## 7.1 Summary of key findings

In line with the four research questions outlined at the outset of the thesis, this section summarises the main findings across structural brain outcomes, functional brain connectivity, cognitive performance, and dementia risk. Each research question is addressed individually, drawing on both observational and genetic evidence.

***Chapter 4: Is lifetime cannabis use associated with structural brain differences in older adults, particularly in regions such as the hippocampus?***

Significant structural differences were identified between lifetime cannabis users and non-users, with the strongest associations observed in WM microstructure. Of the brain structural phenotypes examined (n = 2128), 16 survived FDR correction. Cannabis users exhibited lower fractional anisotropy and intracellular volume fraction, alongside higher mean and radial diffusivities of the genu and body of the corpus callosum, the anterior corona radiata, and the left cingulum cingulate gyrus compared to non-users. Additional associations with lifetime cannabis use were observed with larger right inferior lateral ventricle volume, greater surface area of the left frontal pole, increased thickness of the posterior ventral cingulate gyrus, and higher tissue intensity in the right pallidum. Associations with five WM measures in the genu of the corpus callosum also withstood the more stringent Bonferroni correction. Sensitivity analyses indicated that neither abstinence duration nor cannabis frequency influenced these associations. However, sex-stratified analysis revealed that females exhibited a more widespread pattern of structural associations than males. In contrast to previous studies [24, 45, 46] in adolescents and young adults, no significant differences in hippocampal GM volume were observed. MR analyses similarly provided no evidence to support a causal effect of cannabis use or dependence on brain structure, nor for an effect of brain structure on cannabis use. Taken together, these findings indicate that a lifetime history of cannabis use in older adults is associated with widespread differences in WM microstructure, however genetic analyses suggest these relationships are unlikely to reflect a direct causal impact of cannabis and may instead be influenced by the limited power of MR analyses.

***Chapter 5: Does lifetime cannabis use relate to differences in functional brain connectivity, especially within the default mode network (DMN)?***

Cannabis use was significantly associated with differences in functional brain connectivity, as assessed using fMRI (n = 1,793), particularly within networks involving the DMN, CEN, and salience network. Across resting-state analyses, 21 associations survived FDR correction, with patterns indicating both stronger and weaker connectivity between frontal, temporal, occipital, precuneus, cerebellar, and motor regions. Lifetime cannabis users also showed greater task-related BOLD activation to emotional faces and shapes. One resting-state association, involving connectivity between inferior and middle frontal regions with the precuneus (DMN and CEN), survived Bonferroni correction. Sensitivity analyses indicated no influence of abstinence duration or cannabis frequency on these associations, and sex-stratified analyses revealed somewhat different patterns, with males showing more associations than females. In contrast to the observational findings, MR analyses provided no evidence for a causal effect of cannabis use or dependence on functional connectivity, nor for an effect of functional connectivity on cannabis use. Taken together, these results suggest that lifetime cannabis use in older adults is linked to altered functional connectivity within large-scale brain networks, although these associations are unlikely to reflect direct causal effects and may instead result from the limited power of MR analysis.

***Chapter 6: Is lifetime cannabis use linked to measurable differences in cognitive performance in later life, including working memory and reaction time?***

Beyond neural measures, associations between cannabis use and cognitive performance were assessed. Lifetime cannabis users demonstrated significantly better cross-sectional performance on tests of numeric memory and fluid intelligence, but not on other domains such as trail making, symbol digit substitution, or pairs matching. These associations were consistent across all frequencies of use, with no evidence of a dose–response effect, although sex-stratified analyses revealed a stronger positive association with fluid intelligence in males. However, longitudinal analyses showed no differences in trajectories of cognitive decline between cannabis users and non-users, and MR analyses provided no evidence for a causal effect of cannabis use or dependence on cognitive performance. Taken together, these findings suggest that while lifetime cannabis users had higher cross-sectional performance in working memory and reasoning ability, these associations likely reflect confounding by sociodemographic or lifestyle factors rather than direct cognitive benefits of cannabis.

***Chapter 6: Is there evidence for a causal relationship between lifetime cannabis use and dependence and the risk of developing dementia?***

Finally, given the importance of long-term outcomes, the study examined whether genetically predicted lifetime cannabis use and dependence is causally related to all-cause dementia using MR. The analyses provided no evidence that either lifetime cannabis use or cannabis use disorder increased the risk of all-cause dementia, and reverse analyses similarly did not support

dementia liability influencing cannabis use. Overall, these findings suggest that lifetime cannabis use is unlikely to have a causal impact on the risk of all-cause dementia, at least within the limits of current GWAS data.

## 7.2 Interpretation in the context of existing literature

### *Brain structure*

In Chapter 4, the study examined whether lifetime cannabis use was associated with structural brain measures in older adults. This question builds directly on the literature reviewed in Chapter 2, where structural MRI studies in adolescents and young adults have consistently reported cannabis-related associations in both GM and WM [24, 46, 124–127, 155]. Prior studies have reported reduced hippocampal volume with cannabis use, particularly among adolescents and young adults [24, 45, 46], with some effects persisting into adulthood even after abstinence [37]. These findings suggest that cannabis use during vulnerable developmental periods may have long-term effects on hippocampal integrity. In addition to the hippocampus, studies have also implicated regions such as the orbitofrontal cortex, amygdala, and cerebellum, although results have often been inconsistent across cohorts and methodologies [24, 46].

Recent UK Biobank research also provides relevant context for interpreting the structural findings in this thesis. Vered et al. (2025) [170] reported that older cannabis users (≥60 years) exhibited smaller total, grey matter, white matter, and cortical grey matter volumes compared with non-users, with stronger associations among current or more frequent users. However, their longitudinal analyses indicated a slightly slower decline in certain volumetric measures among cannabis users over time. These mixed cross-sectional and longitudinal findings highlight the complexity of cannabis–brain associations in ageing, population-based samples and underscore the importance of considering exposure patterns, cohort characteristics, and normative age-related change when evaluating the structural results presented in this thesis.

The results described in this thesis are partly consistent with, yet also differ from, the existing literature. On one hand, I observed differences in WM microstructure between lifetime cannabis users and non-users. Specifically, users exhibited lower FA and higher MD in the genu of the corpus callosum, as well as differences in the anterior corona radiata and cingulum. These results are consistent with past studies suggesting that WM integrity, particularly in interhemispheric and frontal tracts, is sensitive to cannabis exposure. The genu of the corpus callosum, in particular, has been highlighted in adolescent and young adult samples [162, 163] as a vulnerable region, and the results in this study extend this evidence to mid-to-late adulthood, suggesting that associations in this tract may persist across the lifespan.

The genu of the corpus callosum emerged as a consistent region of difference. This finding is in line with earlier studies in adolescents and young adults, which have reported disruption to

corpus callosum integrity with frequent or high-potency cannabis use [159, 160, 162]. The present results extend this evidence to older adults, suggesting that this tract may remain particularly sensitive to cannabis across the life course. As the corpus callosum is a major interhemispheric pathway, associations in this region may have wider implications for integration of cognitive and emotional processing, even if those effects were not directly measurable in this study.

On the other hand, no hippocampal volume differences were observed among cannabis users in this cohort, in contrast to the majority of previous studies [24, 45, 46]. Several factors could explain this discrepancy. First, the sample comprised older adults, in whom hippocampal volume reductions are already common due to normative aging processes and in some cases, neurodegenerative disease. Age- and disease-related atrophy may overshadow group differences related to cannabis. Second, cannabis exposure in this cohort was relatively low compared with studies of adolescent who engage in daily or near-daily use, and it is possible that hippocampal differences only emerge at higher cannabis doses or during vulnerable developmental periods, earlier ages of initiation. Third, some recovery of GM may occur over time, particularly if cannabis use ceases or reduces in midlife. Importantly, while these factors may mask changes in hippocampal GM, WM microstructure may be more sensitive to even low-to-moderate exposure and less affected by normative age-related atrophy, allowing subtle differences to remain detectable. Together, these factors may explain why associations were observed in WM but not in hippocampal GM.

Several associations that have not been consistently reported in the literature were also observed, including differences in the frontal pole, pallidum, and ventricular measures. While some prior studies have noted increased pallidal volume or altered gyrification of the frontal pole, the evidence is limited, and the findings should be interpreted with caution. Overall, the structural findings suggest that while WM associations remain a consistent correlate of cannabis exposure, GM differences may be subtler, more age-dependent, or more reversible than previously assumed.

No influence of abstinence was observed prior to the brain scan on structural connectivity, and no significant differences were identified between low- and high-frequency cannabis users, indicating an absence of a dose–response relationship. This may reflect the characteristics of the sample, which included mainly healthy volunteers and relatively few individuals with daily or near-daily cannabis use. Previous studies, however, suggest that both frequency and duration, particularly when use begins in adolescence, can impact brain structure and increase the risk of developing CUD [336, 337].

Examination of sex differences revealed that females exhibited a broader pattern of white-matter associations, potentially reflecting greater vulnerability to cannabis-related neurotoxicity. While prior evidence is mixed, with some studies reporting no sex interactions and others indicating increased female susceptibility, these findings highlight the need for further research to elucidate the mechanisms and long-term implications of sex-specific effects [292]. This may be partly explained by hormonal influences, as estrogen and progesterone

modulate endocannabinoid signaling, increasing female sensitivity to THC [288]. Females also tend to progress more rapidly from initial use to problematic patterns and experience more intense withdrawal symptoms, which could exacerbate neural impact [284, 285]. These mechanisms provide plausible explanations for the broader white-matter associations observed in females, though further research is needed to clarify how hormonal, developmental, and exposure-related factors interact.

The extended sensitivity modelling further showed that structural associations were robust to adjustments involving core demographic and lifestyle covariates but did not survive in models incorporating psychological traits or mental-health variables. Importantly, no effect reversals were observed; estimates remained directionally consistent with the primary analysis. The loss of statistical significance appears primarily attributable to reduced sample size in these extended models rather than to substantive attenuation of the underlying associations.

Finally, the MR analysis found no support for a causal effect of cannabis use on structural brain outcomes. Notably, there are currently no prior MR studies examining the causal impact of cannabis use on structural brain outcomes, making these findings a novel contribution to the literature. This divergence between observational and genetic evidence raises important questions. One possibility is that observational associations are confounded by unmeasured variables such as psychiatric history, lifestyle, or socioeconomic status. Although these factors were adjusted for where possible, errors in measurement and gaps in the available data mean that residual confounding cannot be fully ruled out, as is typical in all observational studies. Another possibility is that the MR analyses may have been underpowered to detect small causal effects, though larger neuroimaging GWAS in the future may help to resolve this. A further explanation is that MR estimates capture the lifelong liability to cannabis use, whereas observational analyses may detect effects that depend on timing or intensity of exposure. Taken together, these points highlight the difficulty of aligning structural findings across methodologies.

***Brain function***

In Chapter 5, I examined whether lifetime cannabis use was associated with brain functional connectivity. As discussed in Chapter 2, a large body of evidence has demonstrated cannabis-related associations in resting-state networks such as the DMN, CEN and salience network, particularly among adolescents and younger adults [47, 61, 62, 176, 177]. Studies have reported that frequent or long-term cannabis users show increased connectivity within the DMN and insular networks [61], whereas regular users display regional differences in connectivity across the limbic and sensorimotor striatum, DMN, executive control, and salience networks [47]. However, the direction of these effects has been inconsistent, with some studies reporting increased connectivity and others reporting reductions, often depending on the frequency and duration of use, the age of initiation, and the specific analytic approach employed [26, 37, 61, 62, 176–181].

The findings in this study are consistent with this broader literature, where associations in functional connectivity between cannabis users and non-users was observed. The networks most affected, namely, the DMN, CEN, and salience network were the same as those most frequently implicated in prior work [47, 61, 62, 176, 177], and the key regions involved, such as the frontal and temporal lobes, occipital cortex, precuneus, and cerebellum. These results suggest that cannabis exposure, even in older adults, continues to be associated with large-scale network differences. However, the pattern of associations was complex: some connections were weaker in users, while others were stronger. This aligns with the variability reported in the literature and indicates that cannabis is unlikely to exert a uniform effect on neural connectivity. Instead, it may contribute to a reorganisation of network dynamics, with some circuits showing increased connectivity and others reduced.

Importantly, this study found no evidence for a dose–response relationship or abstinence effect in functional connectivity, consistent with the findings for brain structure. This is particularly striking given earlier studies indicating that cannabis-related brain differences are influenced by both frequency of use and time since last use [26, 37, 61, 62, 176–181]. One explanation may be the sample characteristics: there were relatively few individuals with frequent or near-daily cannabis use, which limited the ability to detect dose-related trends. Notably, sex-specific analyses revealed differences in the number of associated networks, with males showing significant associations in five functional networks, whereas females exhibited associations in only two networks, suggesting potential sex-dependent effects of cannabis on functional connectivity.

The extended sensitivity analyses indicated that results were broadly stable in the core and lifestyle-adjusted models, with estimated effects remaining directionally consistent with those reported in the primary analysis. However, no functional associations survived in models that included psychological traits or mental-health variables, a pattern that appears largely attributable to substantial reductions in sample size rather than genuine changes in the associations themselves.

In addition to resting-state associations, cannabis users also showed stronger whole-brain activation during an emotion-processing task. This is consistent with studies reporting altered neural responsivity during socio-emotional and cognitive tasks, implicating anterior cingulate, prefrontal, and limbic regions [196, 205]. Together, these findings suggest that cannabis use may influence both intrinsic network organisation and dynamic recruitment of socio-emotional circuits during task engagement.

In line with structural outcomes, MR analyses provided no support for a causal effect of cannabis use on brain resting-state functional connectivity. This again raises the possibility that observational associations reflect residual confounding or cohort-specific characteristics rather than direct causal effects. Alternatively, cannabis-related changes in functional connectivity may exist but be too subtle to detect with current GWAS-based MR methods. Either way, the differences between approaches point to the need for larger, longitudinal imaging studies that combine genetic data to better understand how cannabis use relates to brain function.

***Cognitive function***

Chapter 6 addressed whether lifetime cannabis use is linked to differences in cognitive outcomes. The literature reviewed in Chapter 2 has consistently highlighted cognitive impairments as one of the most robust consequences of cannabis exposure. Acute THC administration impairs working memory, attention, and executive function, while frequent or long-term use, particularly when initiated in adolescence, has been linked to persistent deficits in learning, processing speed, and reasoning ability [34, 167, 221–232]. Longitudinal evidence suggests that persistent cannabis use can lead to measurable IQ decline across adulthood [248]. Meta-analyses have reinforced these findings, showing small-to-moderate impairments in verbal learning, memory, and executive function, though effects vary depending on frequency of use, dose, and age of onset [48].

In light of this literature, findings in this study present a notable contrast. In cross-sectional analyses, lifetime cannabis users performed significantly better on tasks of numeric memory and fluid intelligence. These results contradict the existing literature, which tends to report deficits rather than advantages [23, 216]. However, these advantages did not persist in longitudinal analyses and were not supported by MR, suggesting that the positive cross-sectional associations observed with cannabis may be confounded by higher educational attainment among users.

The absence of persistent cognitive advantages over time may partly reflect practice effects from repeated testing [362], which generally improve scores across all participants, as well as ceiling effects, where higher-scoring individuals have less room for measurable improvement [363]. Another important factor is that cannabis users in UK Biobank tended to have higher educational attainment, and genetic studies show that liability to lifetime cannabis use is positively correlated with education [57]. More broadly, sociodemographic background, lifestyle, and baseline cognitive ability could all influence both cannabis use and cognitive performance, creating associations that are not truly causal. The lack of a dose–response effect and only minimal evidence for sex differences reinforces this interpretation: if cannabis genuinely improved cognition, clearer and more consistent effects would be expected, especially among heavier users or specific subgroups.

Sensitivity analyses further indicated that cannabis dose did not significantly influence cognitive performance, with no evidence of a dose–response relationship. Cannabis users across all frequency categories performed similarly, and the low prevalence of individuals with frequent, near-daily, or dependent patterns of use in UK Biobank limited the ability to detect dose-related effects. These findings are therefore most representative of light-to-moderate lifetime use and may not generalise to heavier or chronic patterns where cognitive harms are more consistently reported. Only minimal evidence for sex differences was observed, reinforcing the interpretation that cross-sectional associations are likely driven by selection effects rather than a true causal impact of cannabis. While some studies have reported sex-specific effects, such as males showing deficits in intelligence, psychomotor speed, and verbal

recall, and females showing impairments in sustained attention, multitasking, and planning [264, 297, 298], the inconsistencies across these studies are in line with the present finding of limited sex-specific associations in this cohort.

The extended sensitivity analyses, the associations between cannabis use and cognitive performance—numeric memory and fluid intelligence—remained positive and statistically robust. Sequential adjustment for smoking and alcohol, psychological traits, subclinical symptoms, and ICD-10 diagnoses did not alter the direction of effects. Although some models showed slight increases in magnitude, these occurred alongside reductions in sample size, suggesting that the cognitive findings are stable across a wide range of covariate specifications.

Taken together, these findings suggest that cannabis use is unlikely to enhance cognition in later life. Instead, the associations are more plausibly explained by selection effects, whereby more educated and higher-functioning individuals in this cohort were somewhat more likely to report lifetime cannabis use. This highlights the importance of triangulating evidence across multiple methodological approaches, as relying on cross-sectional associations alone could have produced misleading conclusions. These results also raised the question of whether cannabis might influence longer-term clinical outcomes such as dementia, which was examined next.

***Dementia risk***

Finally, Chapter 6 also explored the potential link between cannabis use and dementia risk, a question that remains poorly understood in the literature. As noted in Chapter 2, preclinical research has suggested potential neuroprotective effects of cannabinoids via mechanisms such as anti-inflammatory activity, reduced excitotoxicity, and modulation of glial function [277, 278]. On the other hand, epidemiological studies have raised concerns that cannabis use severe enough to require hospitalisation, may increase dementia risk [268]. These conflicting lines of evidence highlight the uncertainty surrounding this question.

The MR analyses provided no support for a causal effect of lifetime cannabis use or cannabis use disorder on all-cause dementia. This is an important addition to the field, as it represents one of the first applications of genetic causal inference to this question. The absence of evidence for causality contrasts with observational findings of elevated dementia risk among individuals hospitalised for cannabis use [268]. This discrepancy is likely explained by confounding factors; hospitalised individuals may differ in numerous ways that predispose them to dementia, including psychiatric comorbidity, head trauma, cardiovascular risk factors, and socioeconomic disadvantage. The genetic results suggest that cannabis use itself is unlikely to be a direct causal factor in dementia onset.

Nevertheless, these findings should be interpreted with caution. Current GWAS of dementia are still relatively small given the scale of the problem, and much larger datasets will be needed to confidently confirm or reject a null causal effect. It is also possible that cannabis interacts with other risk factors not captured by MR, for example, worsening the impact of hypertension

or depression on dementia risk. That said, these results are reassuring in suggesting that cannabis is unlikely to be an independent driver of dementia in the general population.

***Cross-domain synthesis***

Beyond these domain-specific findings, it is also important to reflect on the disparities observed across structural, functional, cognitive, and dementia outcomes. The results suggest that cannabis-related effects are not uniform across levels of brain organisation. The most consistent observational associations were seen in WM microstructure (Chapter 4) and resting-state connectivity (Chapter 5). By contrast, cognitive performance (Chapter 6) showed apparent cross-sectional advantages that did not hold up over time and in genetic analyses, and dementia outcomes showed no signal of risk in genetic analyses. These differences may reflect the fact that structural, functional, and cognitive associations operate on different timescales and may be differentially sensitive to cannabis exposure, sample characteristics, and potential confounding factors.

For instance, structural changes may build up gradually over years of use, particularly in tracts such as the corpus callosum that develops over a prolonged period. Functional connectivity, on the other hand, may be more dynamic, reflecting temporary disruptions or compensatory adjustments to underlying microstructural changes. In contrast, cognitive outcomes reflect a more distal phenotype shaped not only by brain integrity but also by baseline intelligence, education, and social context. Dementia is an even later-life outcome with multiple causes, where any contribution from cannabis is likely to be small relative to vascular, genetic, or lifestyle risk factors.

Animal studies provide further support for this interpretation. THC exposure has been shown to produce morphological changes in hippocampal subregions and other CB1-dense areas that resemble ischemic or toxic damage [110]. Such mechanistic evidence suggests that structural associations may be a primary substrate of cannabis effects, with downstream consequences for functional networks and, ultimately, behaviour. However, the translation of these findings to humans is complicated by variability in dose, duration, age of exposure, and recovery potential, all of which may shape whether changes are detectable in older adults. Longitudinal multimodal imaging, incorporating structural, functional, and cognitive measures, will therefore be critical to disentangle whether functional associations precede, follow, or compensate for microstructural changes, and how these processes interact over time to influence cognition and dementia risk.

Across domains, there was no evidence of dose–response or abstinence effects. In other words, the differences were not greater among heavier users or reduced with longer abstinence, suggesting that the associations are shaped by more complex or context-dependent factors. It remains possible, however, that heavier or dependent use carries different risks, but this could not be examined here given the small number of such users. This distinction is important, since the UK Biobank cohort is more representative of light or moderate lifetime use, whereas heavier patterns of use are more strongly linked to clinical problems.

A further point that cuts across domains is the possibility of sex-specific effects. In this study, females showed a broader pattern of white-matter associations, while males demonstrated a stronger positive association with fluid intelligence. Similar patterns have been reported in previous studies suggesting that cannabis may affect men and women differently, although the overall evidence remains mixed [98, 140, 264, 290–293, 298]. In many studies, including this one, smaller numbers of female participants and relatively few individuals with frequent or near-daily cannabis use limit the strength of conclusions. Even so, the findings point to sex as a factor worth considering more carefully in future research, rather than assuming uniform effects across groups.

Taken together, the disparities across outcome domains underline the complexity of cannabis-related brain and cognitive effects. Cannabis does not appear to have a single, uniform impact on the brain; instead, the picture is mixed. White-matter changes, particularly in the corpus callosum, were the most consistent finding, while functional connectivity and cognition showed more variable patterns, and dementia showed no causal associations. Overall, the findings point to cannabis influencing some brain systems more than others, and in ways that likely depend on individual factors and patterns of use. The next section takes up this point and considers the extent to which the observational and genetic findings converge and where they do not.

### 7.3 Integration of observational and Mendelian randomization results

While Section 7.2 situated the findings within the wider body of literature, this section brings the focus back to this study's analyses by directly integrating the observational and MR results across the main outcome domains. To aid interpretation, **Figure 23** provides a visual integration of the observational and genetic findings across the four key outcome domains. As shown, observational analyses suggested associations between cannabis use and WM microstructure, functional connectivity, and certain cognitive measures, whereas MR analyses consistently provided no evidence for a causal relationship in any domain, including all-cause dementia. Taken together, **Figure 23** highlights the contrast between associations detected in observational data and the absence of associations in genetic analyses, underscoring the importance of considering residual confounding and methodological differences when interpreting cannabis use and brain health relationships.

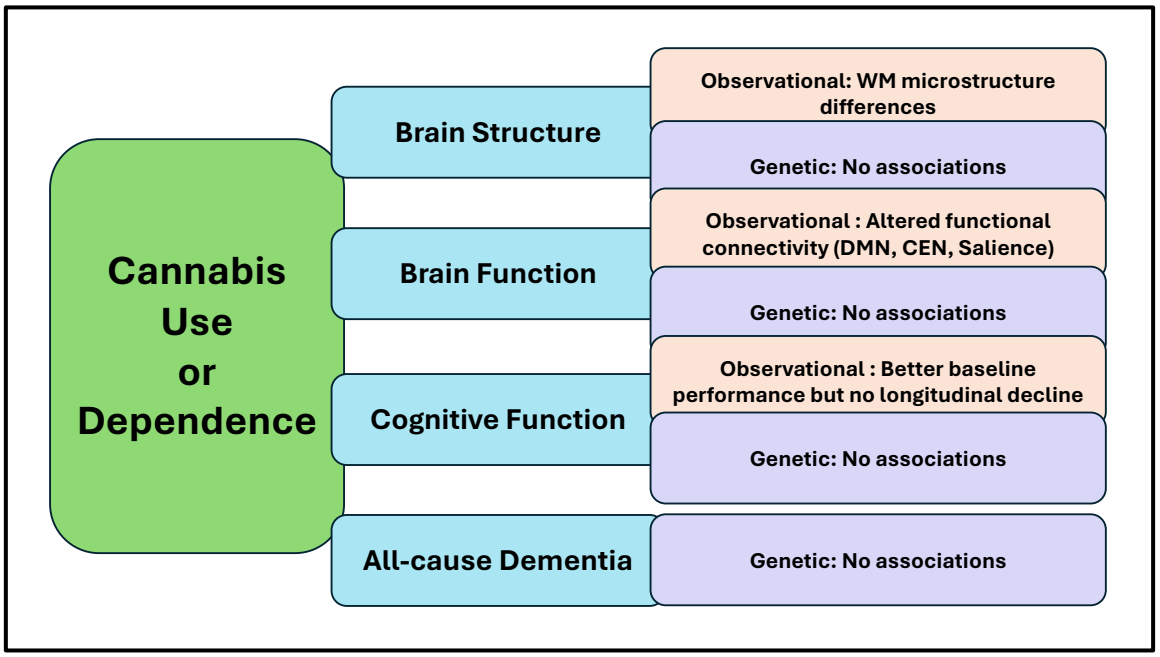



*Figure 35: Observational vs Genetic Findings*

This figure summarises the main findings across brain structure, brain function, cognitive function, and dementia. Observational results (orange) are contrasted with Mendelian randomization results (purple) for each domain, with cannabis use as the central exposure. Abbreviations: WM, white matter; DMN, default mode network; CEN, central executive network.

In Chapter 4, I investigated the association between lifetime cannabis use and structural brain outcomes. The observational analyses suggested that cannabis users displayed widespread associations in WM microstructure compared to non-users, with the strongest and most consistent effects in the genu of the corpus callosum. Cannabis users showed reduced FA and increased MD in this region, a pattern consistent with prior studies in adolescents and young adults where frequent or near-daily cannabis use was linked to reduced corpus callosum integrity. The corpus callosum develops over a prolonged period and plays a central role in interhemispheric communication, making it particularly vulnerable to disruption during development and across the life course. Previous research has also implicated WM pathways in mediating cognitive control and interhemispheric communication, suggesting that cannabis-related associations in this region could have wider functional implications. Beyond the corpus callosum, associations were identified in the anterior corona radiata and cingulum, tracts that have also been highlighted in studies of younger cohorts. Together, these findings support the possibility that WM pathways with high CB1 receptor density and prolonged developmental trajectories may be particularly sensitive to cannabis exposure.

Interestingly, the study did not replicate the widely cited reduction in hippocampal volume observed in adolescent and young adult cannabis users. This discrepancy may reflect differences in age, as the cohort consisted of mid- to late-life adults in whom age-related hippocampal atrophy is already prominent. It is possible that such age-related decline masks more subtle cannabis-related effects or that GM associations observed in younger samples partially recover with abstinence or reduced use over time. Another explanation is

methodological: the analyses adjusted for a broad set of sociodemographic and health covariates, potentially reducing residual confounding relative to earlier studies. A small number of novel associations were also observed, including larger frontal pole surface area and higher tissue intensity in the pallidum, although these findings were less consistent with prior literature and should be interpreted cautiously.

When examined using MR analysis, however, no evidence was found to support a causal role of cannabis use on measures of brain structure. Neither genetic liability to either lifetime cannabis use or cannabis use disorder was associated with structural brain measures. This divergence between observational and genetic findings raises important questions for interpretation. One possibility is that the associations observed in observational data are explained by residual confounding, such as shared sociodemographic or educational factors, psychiatric comorbidity, or other health-related factors that may differ between cannabis users and non-users. Another possibility is methodological: while the observational analyses benefited from a very large imaging sample, current neuroimaging GWAS remain underpowered, limiting the ability of MR to detect small effects. Moreover, MR captures the influence of genetic liability to lifelong cannabis use, which may not fully reflect the impact of cannabis exposure during critical developmental windows such as adolescence. Thus, the discrepancy between observational and genetic results does not necessarily rule out an effect of cannabis on brain structure but suggests that any such effect is likely to be subtle, context-dependent, and difficult to disentangle from confounding influences at present.

In Chapter 5, I examined whether lifetime cannabis use was associated with differences in functional brain connectivity, with a particular emphasis on resting-state networks. The observational analyses revealed significant associations between cannabis use and connectivity across several large-scale networks, including the DMN, CEN, and the salience network. These networks are rich in CB1 receptors and play critical roles in higher-order cognitive processes such as self-referential thought, working memory, attentional control, and emotion regulation. Cannabis users showed altered patterns of connectivity involving frontal, temporal, occipital, precuneus, and cerebellar regions, findings that closely align with prior reports from adolescent and young adult cohorts. For example, increased connectivity between prefrontal and occipital regions has previously been reported in adults with more than 10 years of daily or near-daily cannabis use [176], and these results suggest that these differences persist into later life. At the same time, reduction in connectivity within DMN regions was observed, suggesting that cannabis does not exert uniformly positive or negative effects, but may instead be linked to a more complex reorganisation of brain network activity. It is also noteworthy that the precuneus, where cannabis-related differences in connectivity were observed, is among the earliest cortical regions to show Alzheimer's-related pathology [340, 341]. Although MR analyses in this study focused on all-cause dementia rather than Alzheimer's disease specifically, the convergence of cannabis-related differences in this region with sites of early neurodegeneration highlights a potential avenue for future investigation.

Importantly, no evidence of dose–response or abstinence effects was found. That is, the degree of cannabis use and the duration of abstinence prior to MRI scanning did not significantly

influence functional connectivity. This pattern mirrors the findings from Chapter 4 on structural outcomes and raises the question of whether the observed associations reflect cannabis exposure itself, or instead broader lifestyle and demographic factors that differentiate users from non-users. It is also possible that functional connectivity measures are influenced by cumulative exposures across the lifespan in ways that are not easily captured by self-reported cannabis use patterns, particularly in an older population with highly variable life histories.

In contrast, MR analyses provided no evidence that genetic liability to either lifetime cannabis use or cannabis use disorder causally influenced functional connectivity. Across the DMN, CEN, and salience networks, no genetic associations were observed despite the relatively strong observational effects. Several factors may explain this discrepancy. First, functional connectivity is a relatively noisy phenotype with high within-individual variability, and GWAS of resting-state metrics are still at an early stage, with sample sizes far smaller than those available for behavioural or clinical traits, limiting the power to detect small causal effects. Second, as with brain structure, MR captures lifelong liability to cannabis use rather than exposure at specific developmental windows such as adolescence or early adulthood, when the brain may be especially sensitive to cannabinoids. Finally, residual confounding in observational analyses remains a possibility, as cannabis use is associated with social and demographic factors such as education, socioeconomic status, and comorbid substance use, all factors that can independently influence functional brain networks.

A particularly important source of residual confounding is comorbid substance use. As highlighted in Chapter 2, cannabis use rarely occurs in isolation, with alcohol and tobacco being the most common co-used substances [98]. Both independently affect brain structure, connectivity, and cognition, and prior neuroimaging studies often fail to fully account for their impact [98]. In this study, smoking and alcohol status and frequency were adjusted for, but residual effects cannot be excluded, particularly given the limitations of self-report and the absence of detailed lifetime exposure data. Furthermore, other illicit drugs, which frequently overlap with cannabis use, were not considered in this study. This polysubstance overlap complicates attribution of observed associations specifically to cannabis, and it remains possible that at least part of the functional differences observed here reflect the broader impact of combined substance use rather than cannabis alone.

Taken together, the results of Chapter 5 parallel those of Chapter 4: although observational analyses pointed to associations between cannabis use and functional brain connectivity, MR provided no evidence for causality. This highlights the value of triangulating methods and suggests that the observed associations may be better explained by shared vulnerabilities or confounding, rather than direct effects of cannabis on large-scale neural networks.

In Chapter 6, I examined whether lifetime cannabis use is linked to differences in cognitive performance and whether it contributes to dementia risk. Observational analyses showed that lifetime users performed better than non-users on some tasks, particularly numeric memory (working memory) and fluid intelligence (reasoning ability). These results align with previous findings of positive correlations between cannabis use and educational attainment, as well as

reports of higher cognitive test scores among users. However, these apparent advantages did not hold up in longitudinal analyses. Over time, cannabis users did not show better cognitive trajectories than non-users, and some differences diminished, likely reflecting practice or learning effects. Taken together, the cross-sectional findings are most likely explained by sociodemographic confounding, such as higher baseline cognitive ability or education among users, rather than a genuine neurocognitive benefit of cannabis.

MR analyses supported this interpretation, showing no evidence that genetic liability to either lifetime cannabis use or cannabis use disorder causally influenced performance on cognitive tasks, including numeric memory, fluid intelligence, or pairs matching. This is notable given the ongoing debate over whether cannabis impairs or enhances cognition in the long term. The null MR findings suggest that, at least in population-based samples, cannabis use does not directly affect cognitive functioning, and that the associations observed in cross-sectional analyses are more likely explained by selection effects or residual confounding.

Finally, I examined whether cannabis use might influence the risk of dementia, an outcome of major public health importance in the context of an aging population. Using MR, I tested the relationship between genetic liability to cannabis use and all-cause dementia. The analyses provided no evidence of an effect: neither liability to lifetime cannabis use nor cannabis use disorder was associated with increased dementia risk. This contrasts with an observational study reporting higher dementia incidence, but that typically involve clinical or hospital-based samples with more severe exposure and comorbidities, making it less comparable to the UK Biobank cohort. Overall, these results suggest that cannabis use, as captured by lifetime use in generally healthy populations, is unlikely to be a causal risk factor for dementia.

The findings of Chapter 6 extend the broader pattern observed across this thesis: associations detected in cross-sectional observational analyses rarely persisted in longitudinal models and were not supported by genetic evidence. This consistency across outcomes strengthens the interpretation that apparent links between cannabis use and cognition are more likely to reflect shared background characteristics, such as baseline cognitive ability, socioeconomic status, or education, rather than true neurobiological effects of cannabis. Although cannabis use may have harms in other contexts, particularly among dependent users or younger, more vulnerable groups, the present analyses provide no evidence that it exerts a lasting causal influence on cognitive performance in later life.

In sum, Chapters 4–6 point to a consistent picture. Observational analyses revealed associations between cannabis use and brain or cognitive outcomes, but these were not supported by genetic analysis. This underlines the importance of using multiple methods and of being cautious when interpreting observational findings on their own. Overall, the evidence suggests that in mid- to late-life populations, cannabis use is unlikely to pose a significant risk for structural brain changes, cognitive decline, or dementia.

## 7.4 Strengths and limitations of the study

This study has several key strengths that help advance the evidence base on cannabis use and brain health. First, it represents the largest observational investigation to date of cannabis use in relation to brain structure and function, drawing on exceptionally large and well-characterised cohort (UK Biobank), offering both great statistical power and access to a wide range of outcome measures. Second, it is the first study to apply MR to brain imaging measures of cannabis use, enabling novel insights into causality. Third, by integrating observational and genetic approaches, the analyses were able to triangulate evidence and address questions of causality that cannot be resolved by any single method. Fourth, the focus on mid- to late-life populations fill an important gap in the literature, as this age group has been largely overlooked despite rising cannabis use among older adults. Finally, the use of multimodal outcomes—including structural and functional neuroimaging, cognitive performance, and dementia endpoints, provided a comprehensive and integrated perspective on cannabis-related brain health across domains.

Despite these strengths, several methodological and data-related limitations need to be acknowledged, as they affect both the interpretation and generalisability of the findings and point to areas for improvement in future research. The key limitations are outlined below:

### *Sample Representativeness and Generalisability*

The UK Biobank cohort is not fully representative of the general population. Participants tend to be healthier, wealthier [335], and more health-conscious than average, with only around 5% of those invited choosing to participate, and the imaging subset being even healthier than the wider cohort. They also show lower rates of substance use disorders, including CUD. For example, only two participants were identified with cannabis dependence through linked EHR data (ICD-10 code F12.20, Hospital Episode Statistics), which was insufficient for conducting any analyses. This “healthy volunteer” bias limits the extent to which the findings can be generalised to individuals with more severe cannabis-related problems. In addition, the cohort is predominantly of White European ancestry and relatively advantaged socioeconomic background, which further restricts generalisability across more diverse ethnic and socioeconomic groups. Patterns of cannabis use, as well as associated health risks, may differ substantially in these populations.

While subtle MRI differences are unlikely to influence study participation, cognitive impairment or dementia may reduce the likelihood of participation due to difficulties with consent, completing assessments, or meeting safety requirements, potentially leading to conservative estimates of associations with cognition or dementia. Furthermore, the low overall cannabis exposure in the cohort, as well as low prevalence of diagnosed CUD prevented subgroup analyses of this population.

### *Exposure Measurement Limitations*

A key limitation of this study is the reliance on self-reported lifetime cannabis use. Such measures are vulnerable to recall bias, misclassification, and reporting error, particularly given the historical stigma surrounding cannabis. Participants may underreport or misstate their use due to social desirability or memory lapses. In addition, the dataset lacks information on potency, formulation (e.g., THC/CBD ratio), and method of administration, as well as age of initiation or changes in use across the life course. These gaps restrict the ability to conduct detailed analyses of use patterns and may mask important dose–response effects or sensitive periods of vulnerability.

### *Confounding and Causal Inference Constraints*

Although this study included extensive covariate adjustment and applied MR to assess causality, residual confounding remains a concern. Important factors such as psychiatric history, family background, and medication use were not consistently available or controlled for. While MR reduces bias from reverse causation and some unmeasured confounding, it rests on core assumptions: that genetic instruments are independent of confounders and influence outcomes only through the exposure of interest. Although sensitivity tests (e.g., MR-Egger intercept) were performed, these assumptions cannot be fully verified, especially for complex traits such as cognition or dementia.

For the observational analyses, an additional limitation is comorbid substance use. As highlighted in Chapter 2, cannabis use rarely occurs in isolation, with alcohol and tobacco being the most common co-used substances [98]. Both exert independent effects on brain structure, connectivity, and cognition, complicating attribution of observed differences to cannabis specifically. Although smoking and alcohol status and frequency were adjusted for in this study, lifetime exposure, dose, and other drug use were not comprehensively captured. Residual polysubstance effects therefore remain possible, representing an important limitation in isolating cannabis-specific associations.

### *Classification of Cannabis Use*

The categorisation of cannabis use, particularly high-frequency use, may introduce heterogeneity. Individuals with very different consumption patterns or potencies may be grouped together due to the broad classifications available. This reduces the precision of exposure–response models. The inability to distinguish between dose-dependent and frequency-dependent effects likely dilutes associations and obscures subgroup-specific findings. Furthermore, the relatively small number of heavy or dependent cannabis users in the cohort restricted the ability to examine dose–response relationships or to draw robust conclusions about CUD specifically.

### *Neuroimaging and Cross-Sectional Design*

All neuroimaging measures in this study were cross-sectional, limiting the ability to establish temporal order or causality beyond what can be inferred from genetic analyses. While associations between cannabis use and structural or functional brain differences are informative, they cannot determine whether cannabis use precedes, follows, or co-develops with these associations. Although longitudinal imaging data are becoming available in UK Biobank, this study did not use them as the number of participants with repeated scans is currently insufficient for adequately powered analyses. Longitudinal imaging data will be necessary to map trajectories of brain change over time. Cognitive outcomes in UK Biobank were limited to brief, bespoke tests administered without supervision, which, despite showing moderate-to-high concurrent validity and short-term reliability, may not fully capture all domains of cognitive function [55]. Finally, outcome measures such as dementia were partly derived from linked health records, which may under-detect milder or subclinical cases, leading to conservative estimates of cannabis-related associations.

### *Limitations of MR*

Although MR helps address issues of confounding and reverse causation, it has its own limitations. Current imaging GWAS remain underpowered, reducing the ability to detect small effects. In addition, MR estimates lifelong liability to cannabis use, which may not reflect the impact of use during specific developmental windows, such as adolescence. Observational findings may therefore capture effects that MR, given current data, cannot yet detect. Finally, MR relies on several assumptions, some of which cannot be directly tested, and violation of these assumptions could bias causal estimates.

### *Conclusion*

In conclusion, this study makes a substantial contribution by leveraging large-scale, multimodal, and methodologically diverse datasets to address important, underexplored questions about cannabis use and brain health. At the same time, the limitations outlined above should be carefully considered when interpreting the findings. Together, these strengths and limitations highlight priorities for future research, including improving exposure measurement, adopting longitudinal designs, and extending analyses to more representative and clinically diverse populations.

## 7.5 Implications for clinical practice and public health policy

The findings of this thesis carry several implications for clinical practice and public health policy, especially at a time when cannabis use is becoming more socially accepted and legally available. Observational analyses suggested associations between cannabis use and brain

structure, functional connectivity, and cognitive performance. However, genetic analyses provided no evidence of causality in any domain, including all-cause dementia. This divergence has important implications for how results should be interpreted.

From a clinical standpoint, the results caution against making strong causal claims when assessing patients with a history of cannabis use. Differences in WM microstructure or functional connectivity may be detectable among users, but genetic evidence suggests these are unlikely to reflect direct neurotoxic effects of cannabis. Instead, they may arise from shared vulnerabilities, lifestyle factors, or unmeasured confounding. Clinicians should therefore avoid attributing brain or cognitive abnormalities solely to cannabis exposure and instead adopt a broader perspective that considers sociodemographic background, psychiatric comorbidity, and other health behaviours. At the same time, clinicians should remain mindful of the risks associated with CUD, which was underrepresented in the UK Biobank sample but has been consistently linked to adverse outcomes in prior research.

At a public health level, the findings help to address ongoing concerns. In particular, the absence of evidence for a causal link between cannabis use and dementia suggests that cannabis is unlikely to make a meaningful contribution to dementia risk in the general population. This is a relevant point as cannabis use grows among older people, often for medical reasons. Prevention efforts should continue to prioritise discouraging early initiation and heavy, high-potency use, particularly during adolescence when the brain is most vulnerable. However, the findings from this study suggest that moderate use in later life may not pose the same level of risk that has often been assumed.

For policymakers, these findings underline the importance of clear, balanced, and evidence-based communication. With cannabis laws changing rapidly, the challenge lies in protecting vulnerable groups without overstating risks for everyone. Overstating the neurocognitive risks of cannabis could undermine public trust in scientific and governmental messaging, while underestimating risks could encourage patterns of use that are genuinely harmful in subsets of the population. The integration of observational and genetic evidence presented in this thesis suggests that cannabis-related harms should be described as conditional and context-dependent, with greatest concern for heavy, chronic, or early-onset use. Public health strategies may therefore be most effective if they distinguish between light or moderate users, dependent users, and adolescents or young adults.

Finally, these results highlight the need for continued monitoring. The cannabis landscape is evolving quickly, with high-THC strains, synthetic cannabinoids, and CBD-rich products now widely available. Their neurobiological effects are unlikely to be uniform. Clinical guidelines and public health policy will need to remain adaptable, ensuring that risks and potential therapeutic opportunities are addressed with both scientific accuracy and social responsibility.

### 7.6 Ethical considerations

Ethical issues are central to the interpretation and dissemination of research on cannabis and brain health. Cannabis remains a stigmatised substance in many societies, and research findings can be misinterpreted or misused in ways that reinforce stigma and disadvantage. A key ethical responsibility, therefore, is careful and balanced communication. While this thesis found no evidence of causal effects of cannabis on brain integrity, cognition, or dementia, this does not imply that cannabis use is entirely without risk. Overly simplistic messages, whether of reassurance or alarm, risk misleading both the public and policymakers. It is ethically essential to present findings with appropriate nuance, emphasising the contexts in which risks are likely to be greater such as early initiation, severe or dependent pattern of use, or comorbid psychiatric conditions.

A second ethical consideration relates to equity. Cannabis use is not evenly distributed across populations, nor are the risks associated with it. Individuals from disadvantaged socioeconomic backgrounds may experience higher rates of CUD, differential access to treatment, and disproportionate consequences of legal sanctions. Public health policies informed by cannabis research must therefore aim to reduce, rather than exacerbate these social inequalities. There is a danger that if cannabis is framed exclusively as a public health problem, punitive approaches may be reinforced, disproportionately affecting vulnerable communities. On the other hand, if cannabis is promoted solely as harmless or therapeutic, individuals at risk of harm may be left unsupported. Striking a balance between these narratives is therefore an ethical necessity.

Medical cannabis presents further ethical challenges. As cannabinoids continue to be investigated for therapeutic potential in conditions ranging from chronic pain to epilepsy and neurodegenerative disease, there is a risk of confusing recreational use with medical application. The findings of this thesis, focused on recreational and lifetime use in population cohorts, should not be extrapolated to medical settings where formulations, dosages, and routes of administration differ significantly. Researchers and clinicians have an ethical responsibility to distinguish between these contexts in both communication and practice, ensuring that medical cannabis research is not held back by stigma, nor that recreational cannabis use is inappropriately medicalised.

Finally, the use of large-scale data raises its own ethical considerations, particularly in relation to informed consent, data linkage, and privacy. While UK Biobank is an invaluable resource, its use also requires vigilance to ensure that participants trust is maintained and that findings are not misapplied in ways that could harm the very populations that contributed data. Strong ethical governance, transparency, and sensitivity in interpretation are therefore essential for sustaining both the legitimacy and the societal value of this research.

## 7.7 Future research directions

The findings of this thesis point clearly to several priorities for future research.

***1. Improving measurement of cannabis exposure.***

A central limitation of current epidemiological studies is the reliance on self-reported lifetime use, which does not capture the heterogeneity of cannabis exposure. Future research should employ more detailed phenotyping, including frequency, potency, THC/CBD composition, age of initiation, method of administration, and cumulative duration of use. Biomarkers of exposure, such as hair, blood, or urine assays, could supplement self-report and provide more objective measures. Such improvements would allow for dose–response modelling and help identify critical developmental periods of vulnerability.

***2. Larger and more diverse imaging genetics studies.***

The MR analyses in this thesis were constrained by modest size of current imaging GWAS. As larger datasets become available, MR will have the statistical power necessary to detect subtle effects and test more nuanced hypotheses. Importantly, future work should not only aim for larger samples but also for more representative cohorts with broader age ranges and demographic diversity. Many existing datasets—including the UK Biobank—are enriched for healthier, more educated, and less socioeconomically deprived individuals, which may limit generalisability. Cohorts that better reflect the general population, including younger and midlife adults, would enhance external validity and help determine whether the associations observed in this thesis replicate across different population structures.

***3. Longitudinal multimodal designs.***

Cross-sectional imaging provides only a snapshot of brain structure and function. Longitudinal neuroimaging, ideally combined with repeated cognitive assessments and clinical outcomes, will be essential for mapping trajectories of brain change. Such designs can reveal whether cannabis use accelerates age-related decline, contributes to brain reserve, or interacts with genetic or environmental risk factors for dementia. Importantly, findings suggest that structural and functional associations may not always align, potentially reflecting changes on different timescales. Longitudinal, multimodal approaches are therefore critical to determine whether functional associations emerge earlier as markers of risk or compensation, or whether they follow structural disruption, clarifying the temporal and mechanistic interplay between brain systems.

***4. Focus on older adults and high-risk groups.***

While most research to date has centred on adolescents and young adults, cannabis use is becoming increasingly common in midlife and older adulthood. Older adults may be more

susceptible to interactions between cannabis and age-related neurobiological processes, medications, or comorbidities. In parallel, individuals with CUD, largely underrepresented in population cohorts, remain a critical group for investigation, given the more consistent evidence of harm in this population.

***5. Sex differences and individual variability.***

Preliminary evidence, including findings from this thesis, suggests potential sex-specific effects of cannabis on brain and cognition, but these remain underexplored. Future studies should be adequately powered to detect sex interactions and investigate biological and hormonal mechanisms. Beyond sex, genetic predispositions, psychiatric vulnerabilities, and lifestyle factors likely moderate cannabis effects, underscoring the need to study individual variability rather than treating cannabis use as a single, uniform exposure.

***6. Triangulation of methods.***

Future progress will depend on the triangulation of evidence from multiple methods, including observational epidemiology, MR, polygenic risk analyses, randomised controlled trials of cannabinoid therapies, and preclinical models. Only by drawing on this range of methods can causal inference be strengthened and findings translated into clinical and policy contexts.

***7. Validation in independent and representative cohorts, including improved cognitive assessment.***

A key next step is to validate the associations reported in this thesis in independent cohorts that are more representative of the general population, including those with younger age distributions and a broader range of sociodemographic characteristics. This would clarify whether the patterns observed in UK Biobank generalise beyond a healthier, self-selected volunteer cohort. Additionally, the cognitive measures available in UKB are relatively brief and may not capture domain-specific deficits. Future studies should use more sensitive and comprehensive cognitive batteries, and replication across cohorts with richer neuropsychological testing would help strengthen the validity and interpretation of cognitive findings. Such efforts would directly build on the work presented here and help determine the robustness and generalisability of the observed associations.

## 7.8 Final thoughts and concluding remarks

This thesis provides one of the most comprehensive investigations to date of the relationship between cannabis use, and brain health in mid-to-late-life adults. By integrating large-scale observational analyses with genetic causal inference, it helps to bring clarity to a field that has long been characterised by inconsistent findings and methodological difficulties.

Looking across structural neuroimaging, functional connectivity, cognitive performance, and dementia risk, the results reveal a consistent pattern. Observational analyses suggested associations between cannabis use and a wide range of outcomes, including differences in WM integrity, differences in resting-state network connectivity, and higher baseline cognitive performance. Yet none of these associations were replicated in genetic analyses when tested with MR. These results suggest that many of the previously reported harms or benefits of cannabis on the brain and cognition may instead reflect confounding by sociodemographic, educational, or lifestyle factors, rather than direct neurobiological consequences of cannabis exposure.

The implications of this are twofold. On the one hand, the results challenge the assumptions that cannabis is a major driver of dementia or age-related cognitive decline. On the other hand, they underscore the importance of methodological triangulation, demonstrating how combining observational and genetic approaches can move the field closer to causal inference. The results also highlight the limitations of current research tools and the need for better measurement, larger and more diverse genetic resources, and longitudinal multimodal designs.

At the same time, the findings should not be overinterpreted as evidence that cannabis is risk-free. The analyses in this thesis focused specifically on brain structure, cognition, and dementia, and does not address other health outcomes. Heavy, dependent, or early-onset use may still carry risks, and these were not fully captured in the cohorts analysed. Furthermore, the rapid evolution of cannabis products, including high-potency strains and synthetic cannabinoids, poses challenges for generalisation. The message that emerges is therefore one of balance: cannabis use is neither as dangerous to brain health as some earlier accounts have suggested, nor as harmless as some contemporary discourse implies.

In conclusion, this thesis contributes to a timely and critical piece of evidence to ongoing debates about cannabis and brain health. It demonstrates the value of integrating observational and genetic epidemiology, while also underscoring both the opportunities and limitations of current research. As cannabis use continues to rise among older adults, and as medical and recreational policies evolve worldwide, the importance of rigorous, balanced, and ethically responsible research has never been greater.

## References


[1] United Nations Office on Drugs and Crime. (2024, June). UNODC World Drug Report 2024: Harms of world drug problem continue to mount amid expansions in drug use and markets [Press release]. United Nations., https://www.unodc.org/unodc/en/press/releases/2024/June/unodc-world-drug-report-2024_-harms-of-world-drug-problem-continue-to-mount-amid-expansions-in-drug-use-and-markets.html.

[2] Boggs DL, Peckham A, Boggs AA, et al. Delta-9-tetrahydrocannabinol and cannabidiol: Separating the chemicals from the "weed," a pharmacodynamic discussion. Ment Health Clin 2016; 6: 277–284.

[3] Munro S, Thomas KL, Abu-Shaar M. Molecular characterization of a peripheral receptor for cannabinoids. Nature 1993; 365: 61–65.

[4] Mackie K. Distribution of Cannabinoid Receptors in the Central and Peripheral Nervous System. In: Pertwee RG (ed) Cannabinoids. Berlin/Heidelberg: Springer-Verlag, pp. 299–325.

[5] Connor JP, Stjepanović D, Le Foll B, et al. Cannabis use and cannabis use disorder. Nat Rev Dis Primer 2021; 7: 16.

[6] Zou S, Kumar U. Cannabinoid Receptors and the Endocannabinoid System: Signaling and Function in the Central Nervous System. Int J Mol Sci 2018; 19: 833.

[7] United nations office on drugs and crime & division for treaty affairs. World drug report 2022: Booklet 3. S.l.: United Nations, 2022.

[8] Hall W, Weier M. Assessing the public health impacts of legalizing recreational cannabis use in the USA. Clin Pharmacol Ther 2015; 97: 607–615.

[9] Hammond D, Goodman S, Wadsworth E, et al. Evaluating the impacts of cannabis legalization: The International Cannabis Policy Study. Int J Drug Policy 2020; 77: 102698.

[10] Page RL, Allen LA, Kloner RA, et al. Medical Marijuana, Recreational Cannabis, and Cardiovascular Health: A Scientific Statement From the American Heart Association. Circulation; 142. Epub ahead of print 8 September 2020. DOI: 10.1161/cir.0000000000000883.

[11] Manthey J, Rehm J, Verthein U. Germany's cannabis act: a catalyst for European drug policy reform? Lancet Reg Health - Eur 2024; 42: 100929.

[12] Kalayasiri R, Boonthae S. Trends of cannabis use and related harms before and after legalization for recreational purpose in a developing country in Asia. BMC Public Health; 23. Epub ahead of print 19 May 2023. DOI: 10.1186/s12889-023-15883-6.

[13] Matheson J, Le Foll B. Cannabis Legalization and Acute Harm From High Potency Cannabis Products: A Narrative Review and Recommendations for Public Health. Front Psychiatry; 11. Epub ahead of print 23 September 2020. DOI: 10.3389/fpsyt.2020.591979.

[14] Hoch E, Volkow ND, Friemel CM, et al. Cannabis, cannabinoids and health: a review of evidence on risks and medical benefits. Eur Arch Psychiatry Clin Neurosci 2025; 275: 281–292.

[15] World Health Organization. (n.d.). Cannabis. World Health Organization., https://www.who.int/teams/mental-health-and-substance-use/alcohol-drugs-and-addictive-behaviours/drugs-psychoactive/cannabis (2025, accessed 18 July 2025).

[16] United nations office on drugs and labor. World drug report 2020: Booklet 2. S.l.: United Nations, 2021.

[17] Yang KH, Kaufmann CN, Nafsu R, et al. Cannabis: An Emerging Treatment for Common Symptoms in Older Adults. J Am Geriatr Soc 2021; 69: 91–97.

[18] Baumbusch J, Sloan Yip I. Older adults experiences of using recreational cannabis for medicinal purposes following legalization. Int J Drug Policy 2022; 108: 103812.

[19] Gunning-Dixon FM, Brickman AM, Cheng JC, et al. Aging of cerebral white matter: a review of MRI findings. Int J Geriatr Psychiatry 2009; 24: 109–117.

[20] Fjell AM, Westlye LT, Amlien I, et al. High Consistency of Regional Cortical Thinning in Aging across Multiple Samples. Cereb Cortex 2009; 19: 2001–2012.

[21] Fjell AM, McEvoy L, Holland D, et al. What is normal in normal aging? Effects of aging, amyloid and Alzheimer's disease on the cerebral cortex and the hippocampus. Prog Neurobiol 2014; 117: 20–40.

[22] Yoo HB, DiMuzio J, Filbey FM. Interaction of Cannabis Use and Aging: From Molecule to Mind. J Dual Diagn 2020; 16: 140–176.

[23] Burggren AC, Shirazi A, Ginder N, et al. Cannabis effects on brain structure, function, and cognition: considerations for medical uses of cannabis and its derivatives. Am J Drug Alcohol Abuse 2019; 45: 563–579.

[24] Battistella G, Fornari E, Annoni J-M, et al. Long-Term Effects of Cannabis on Brain Structure. Neuropsychopharmacology 2014; 39: 2041–2048.

[25] Lichenstein SD, Manco N, Cope LM, et al. Systematic review of structural and functional neuroimaging studies of cannabis use in adolescence and emerging adulthood: evidence from 90 studies and 9441 participants. Neuropsychopharmacology 2022; 47: 1000–1028.

[26] Sehl H, Terrett G, Greenwood L-M, et al. Patterns of brain function associated with cannabis cue-reactivity in regular cannabis users: a systematic review of fMRI studies. Psychopharmacology (Berl) 2021; 238: 2709–2728.

[27] Kroon E, Kuhns L, Cousijn J. The short-term and long-term effects of cannabis on cognition: recent advances in the field. Curr Opin Psychol 2021; 38: 49–55.

[28] Scallet AC, Uemura E, Andrews A, et al. Morphometric studies of the rat hippocampus following chronic delta-9-tetrahydrocannabinol (THC). Brain Res 1987; 436: 193–198.

[29] Landfield PW, Cadwallader LB, Vinsant S. Quantitative changes in hippocampal structure following long-term exposure to Δ9-tetrahydrocannabinol: possible mediation by glucocorticoid systems. Brain Res 1988; 443: 47–62.

[30] Fishbein-Kaminietsky M, Gafni M, Sarne Y. Ultralow doses of cannabinoid drugs protect the mouse brain from inflammation-induced cognitive damage. J Neurosci Res 2014; 92: 1669–1677.

[31] Assaf F, Fishbein M, Gafni M, et al. Pre- and post-conditioning treatment with an ultra-low dose of Δ9-tetrahydrocannabinol (THC) protects against pentylenetetrazole (PTZ)-induced cognitive damage. Behav Brain Res 2011; 220: 194–201.

[32] Quinn HR, Matsumoto I, Callaghan PD, et al. Adolescent Rats Find Repeated Δ9-THC Less Aversive Than Adult Rats but Display Greater Residual Cognitive Deficits and Changes in Hippocampal Protein Expression Following Exposure. Neuropsychopharmacology 2008; 33: 1113–1126.

[33] Nava F, Carta G, Colombo G, et al. Effects of chronic Δ9-tetrahydrocannabinol treatment on hippocampal extracellular acetylcholine concentration and alternation performance in the T-maze. Neuropharmacology 2001; 41: 392–399.

[34] Broyd SJ, Van Hell HH, Beale C, et al. Acute and Chronic Effects of Cannabinoids on Human Cognition—A Systematic Review. Biol Psychiatry 2016; 79: 557–567.

[35] Meier MH, Caspi A, Ambler A, et al. Persistent cannabis users show neuropsychological decline from childhood to midlife. Proc Natl Acad Sci; 109. Epub ahead of print 2 October 2012. DOI: 10.1073/pnas.1206820109.

[36] Brumback T, Castro N, Jacobus J, et al. Effects of Marijuana Use on Brain Structure and Function. In: International Review of Neurobiology. Elsevier, pp. 33–65.

[37] Burggren AC, Siddarth P, Mahmood Z, et al. Subregional Hippocampal Thickness Abnormalities in Older Adults with a History of Heavy Cannabis Use. Cannabis Cannabinoid Res 2018; 3: 242–251.

[38] Meier MH, Caspi A, R. Knodt A, et al. Long-Term Cannabis Use and Cognitive Reserves and Hippocampal Volume in Midlife. Am J Psychiatry 2022; 179: 362–374.

[39] Thayer RE, YorkWilliams SL, Hutchison KE, et al. Preliminary results from a pilot study examining brain structure in older adult cannabis users and nonusers. Psychiatry Res Neuroimaging 2019; 285: 58–63.

[40] Watson KK, Bryan AD, Thayer RE, et al. Cannabis Use and Resting State Functional Connectivity in the Aging Brain. Front Aging Neurosci 2022; 14: 804890.

[41] Høeg KM, Frodegaard RL, Grønkjær M, et al. Cannabis Use and Age-Related Changes in Cognitive Function From Early Adulthood to Late Midlife in 5162 Danish Men. Brain Behav 2024; 14: e70136.

[42] Han BH, Sherman S, Mauro PM, et al. Demographic trends among older cannabis users in the United States, 2006-13: Cannabis use among older adults. Addiction 2017; 112: 516–525.

[43] Grady C. The cognitive neuroscience of ageing. Nat Rev Neurosci 2012; 13: 491–505.

[44] Hou Y, Dan X, Babbar M, et al. Ageing as a risk factor for neurodegenerative disease. Nat Rev Neurol 2019; 15: 565–581.

[45] Owens MM, Sweet LH, MacKillop J. Recent cannabis use is associated with smaller hippocampus volume: High-resolution segmentation of structural subfields in a large non-clinical sample. Addict Biol 2021; 26: e12874.

[46] Yücel M, Solowij N, Respondek C, et al. Regional Brain Abnormalities Associated With Long-term Heavy Cannabis Use. Arch Gen Psychiatry 2008; 65: 694.

[47] Thijssen S, Rashid B, Gopal S, et al. Regular cannabis and alcohol use is associated with resting-state time course power spectra in incarcerated adolescents. Drug Alcohol Depend 2017; 178: 492–500.

[48] Dellazizzo L, Potvin S, Giguère S, et al. Evidence on the acute and residual neurocognitive effects of cannabis use in adolescents and adults: a systematic meta-review of meta-analyses. Addiction 2022; 117: 1857–1870.

[49] Zhornitsky S, Pelletier J, Assaf R, et al. Acute effects of partial CB1 receptor agonists on cognition – A meta-analysis of human studies. Prog Neuropsychopharmacol Biol Psychiatry 2021; 104: 110063.

[50] Block RI, O'Leary DS, Ehrhardt JC, et al. Effects of frequent marijuana use on brain tissue volume and composition: NeuroReport 2000; 11: 491–496.

[51] Lawlor DA, Harbord RM, Sterne JAC, et al. Mendelian randomization: Using genes as instruments for making causal inferences in epidemiology. Stat Med 2008; 27: 1133–1163.

[52] Allen N, Sudlow C, Downey P, et al. UK Biobank: Current status and what it means for epidemiology. Health Policy Technol 2012; 1: 123–126.

[53] Miller KL, Alfaro-Almagro F, Bangerter NK, et al. Multimodal population brain imaging in the UK Biobank prospective epidemiological study. Nat Neurosci 2016; 19: 1523–1536.

[54] Alfaro-Almagro F, Jenkinson M, Bangerter NK, et al. Image processing and Quality Control for the first 10,000 brain imaging datasets from UK Biobank. NeuroImage 2018; 166: 400–424.

[55] Fawns-Ritchie C, Deary IJ. Reliability and validity of the UK Biobank cognitive tests. PLOS ONE 2020; 15: e0231627.

[56] Levey DF, Galimberti M, Deak JD, et al. Multi-ancestry genome-wide association study of cannabis use disorder yields insight into disease biology and public health implications. Nat Genet 2023; 55: 2094–2103.

[57] the 23andMe Research Team, The Substance Use Disorders Working Group of the Psychiatric Genomics Consortium, International Cannabis Consortium, et al. GWAS of lifetime cannabis use reveals new risk loci, genetic overlap with psychiatric traits, and a causal effect of schizophrenia liability. Nat Neurosci 2018; 21: 1161–1170.

[58] (n.d.). Neale Lab. UK Biobank GWAS, http://www.nealelab.is/uk-biobank/ (2018).

[59] Topiwala A, Levey D, Zhou H, et al. Alcohol use and risk of dementia in diverse populations: evidence from cohort, case–control and Mendelian randomisation approaches. BMJ Evid Based Med. Epub ahead of print September 2025. DOI: 10.1136/bmjebm-2025-113913.

[60] Davies G, Marioni RE, Liewald DC, et al. Genome-wide association study of cognitive functions and educational attainment in UK Biobank (N=112 151). Mol Psychiatry 2016; 21: 758–767.

[61] Pujol J, Blanco-Hinojo L, Batalla A, et al. Functional connectivity alterations in brain networks relevant to self-awareness in chronic cannabis users. J Psychiatr Res 2014; 51: 68–78.

[62] Sweigert J, Pagulayan K, Greco G, et al. A multimodal investigation of cerebellar integrity associated with high-risk cannabis use. Addict Biol 2020; 25: e12839.

[63] Dragomir A, Omurtag A. Brain's Networks and Their Functional Significance in Cognition. In: Thakor NV (ed) Handbook of Neuroengineering. Singapore: Springer Nature Singapore, pp. 2703–2732.

[64] Bettio LEB, Rajendran L, Gil-Mohapel J. The effects of aging in the hippocampus and cognitive decline. Neurosci Biobehav Rev 2017; 79: 66–86.

[65] Ereira S, Waters S, Razi A, et al. Early detection of dementia with default-mode network effective connectivity. Nat Ment Health 2024; 2: 787–800.

[66] Shao H, Du H, Gan Q, et al. Trends of the Global Burden of Disease Attributable to Cannabis Use Disorder in 204 Countries and Territories, 1990–2019: Results from the Disease Burden Study 2019. Int J Ment Health Addict 2024; 22: 2485–2507.

[67] Cunningham JA, Dai P. Assessing the Prevalence of Cannabis Use Through a Survey About Criminal Activity Versus One About Alcohol, Tobacco, and Other Drugs. Subst Use Misuse 2024; 59: 1110–1114.

[68] Pertwee R (ed). Handbook of Cannabis. Oxford University Press. Epub ahead of print 21 August 2014. DOI: 10.1093/acprof:oso/9780199662685.001.0001.

[69] Drennan ML, Karoly HC, Bryan AD, et al. Acute objective and subjective intoxication effects of legal-market high potency THC-dominant versus CBD-dominant cannabis concentrates. Sci Rep; 11. Epub ahead of print 5 November 2021. DOI: 10.1038/s41598-021-01128-2.

[70] Ashton CH. Pharmacology and effects of cannabis: A brief review. Br J Psychiatry 2001; 178: 101–106.

[71] ElSohly MA, Mehmedic Z, Foster S, et al. Changes in Cannabis Potency Over the Last 2 Decades (1995–2014): Analysis of Current Data in the United States. Biol Psychiatry 2016; 79: 613–619.

[72] Stuyt E. The Problem with the Current High Potency THC Marijuana from the Perspective of an Addiction Psychiatrist. Mo Med 2018; 115: 482–486.

[73] Streck JM, Hughes JR, Klemperer EM, et al. Modes of cannabis use: A secondary analysis of an intensive longitudinal natural history study. Addict Behav 2019; 98: 106033.

[74] Lafaye G, Karila L, Blecha L, et al. Cannabis, cannabinoids, and health. Dialogues Clin Neurosci 2017; 19: 309–316.

[75] Leas EC. The Hemp Loophole: A Need to Clarify the Legality of Delta-8-THC and Other Hemp-Derived Tetrahydrocannabinol Compounds. Am J Public Health 2021; 111: 1927–1931.

[76] Tait RJ, Caldicott D, Mountain D, et al. A systematic review of adverse events arising from the use of synthetic cannabinoids and their associated treatment. Clin Toxicol 2016; 54: 1–13.

[77] Abuse NI on D. Cannabis (Marijuana) | National Institute on Drug Abuse (NIDA), https://nida.nih.gov/research-topics/cannabis-marijuana (2024, accessed 18 July 2025).

[78] Gaoni Y, Mechoulam R. Isolation, Structure, and Partial Synthesis of an Active Constituent of Hashish. J Am Chem Soc 1964; 86: 1646–1647.

[79] Eggan SM, Lewis DA. Immunocytochemical Distribution of the Cannabinoid CB1 Receptor in the Primate Neocortex: A Regional and Laminar Analysis. Cereb Cortex 2006; 17: 175–191.

[80] Salami SA, Martinelli F, Giovino A, et al. It Is Our Turn to Get Cannabis High: Put Cannabinoids in Food and Health Baskets. Molecules 2020; 25: 4036.

[81] Weiss SRB, Howlett KD, Baler RD. Building smart cannabis policy from the science up. Int J Drug Policy 2017; 42: 39–49.

[82] Devane WA, Hanuš L, Breuer A, et al. Isolation and Structure of a Brain Constituent That Binds to the Cannabinoid Receptor. Science 1992; 258: 1946–1949.

[83] Mechoulam R, Ben-Shabat S, Hanus L, et al. Identification of an endogenous 2-monoglyceride, present in canine gut, that binds to cannabinoid receptors. Biochem Pharmacol 1995; 50: 83–90.

[84] Howlett AC, Barth F, Bonner TI, et al. International Union of Pharmacology. XXVII. Classification of Cannabinoid Receptors. Pharmacol Rev 2002; 54: 161–202.

[85] Pertwee RG. The diverse $CB_1$ and $CB_2$ receptor pharmacology of three plant cannabinoids: $\Delta^9$ -tetrahydrocannabinol, cannabidiol and $\Delta^9$ -tetrahydrocannabivarin. Br J Pharmacol 2008; 153: 199–215.

[86] Bhattacharyya S, Crippa J, Martin-Santos R, et al. Imaging the Neural Effects of Cannabinoids: Current Status and Future Opportunities for Psychopharmacology. Curr Pharm Des 2009; 15: 2603–2614.

[87] Atakan Z. Cannabis, a complex plant: different compounds and different effects on individuals. Ther Adv Psychopharmacol 2012; 2: 241–254.

[88] Patel J, Marwaha R. Cannabis Use Disorder. In: StatPearls. Treasure Island (FL): StatPearls Publishing, http://www.ncbi.nlm.nih.gov/books/NBK538131/ (2025, accessed 21 September 2025).

[89] World Health Organization. Geneva, https://icd.who.int (2019).

[90] Fink DS, Shmulewitz D, Mannes ZL, et al. Construct validity of DSM-5 cannabis use disorder diagnosis and severity levels in adults with problematic substance use. J Psychiatr Res 2022; 155: 387–394.

[91] Hinckley JD, Ferland J-MN, Hurd YL. The Developmental Trajectory to Cannabis Use Disorder. Am J Psychiatry 2024; 181: 353–358.

[92] Owens MM, Albaugh MD, Allgaier N, et al. Bayesian causal network modeling suggests adolescent cannabis use accelerates prefrontal cortical thinning. Transl Psychiatry 2022; 12: 188.

[93] Albaugh MD, Owens MM, Juliano A, et al. Differential associations of adolescent versus young adult cannabis initiation with longitudinal brain change and behavior. Mol Psychiatry 2023; 28: 5173–5182.

[94] Miller AP, Baranger DAA, Paul SE, et al. Neuroanatomical Variability and Substance Use Initiation in Late Childhood and Early Adolescence. JAMA Netw Open 2024; 7: e2452027.

[95] Hasin D, Walsh C. Cannabis Use, Cannabis Use Disorder, and Comorbid Psychiatric Illness: A Narrative Review. J Clin Med 2020; 10: 15.

[96] Topiwala A, Ebmeier KP, Maullin-Sapey T, et al. Alcohol consumption and MRI markers of brain structure and function: Cohort study of 25,378 UK Biobank participants. NeuroImage Clin 2022; 35: 103066.

[97] Linli Z, Rolls ET, Zhao W, et al. Smoking is associated with lower brain volume and cognitive differences: A large population analysis based on the UK Biobank. Prog Neuropsychopharmacol Biol Psychiatry 2023; 123: 110698.

[98] Colyer-Patel K, Romein C, Kuhns L, et al. Recent Evidence on the Relation Between Cannabis Use, Brain Structure, and Function: Highlights and Challenges. Curr Addict Rep 2024; 11: 371–383.

[99] Hall W, Degenhardt L. Cannabis use and the risk of developing a psychotic disorder. World Psychiatry 2008; 7: 68–71.

[100] Austin-Zimmerman I, Spinazzola E, Quattrone D, et al. The impact of schizophrenia genetic load and heavy cannabis use on the risk of psychotic disorder in the EU-GEI case-control and UK Biobank studies. Psychol Med 2024; 54: 4160–4172.

[101] Moore TH, Zammit S, Lingford-Hughes A, et al. Cannabis use and risk of psychotic or affective mental health outcomes: a systematic review. The Lancet 2007; 370: 319–328.

[102] Heath RG, Fitzjarrell AT, Fontana CJ, et al. Cannabis sativa: effects on brain function and ultrastructure in rhesus monkeys. Biol Psychiatry 1980; 15: 657–690.

[103] Colizzi M, McGuire P, Pertwee RG, et al. Effect of cannabis on glutamate signalling in the brain: A systematic review of human and animal evidence. Neurosci Biobehav Rev 2016; 64: 359–381.

[104] Downer E, Boland B, Fogarty M, et al. Δ9-Tetrahydrocannabinol induces the apoptotic pathway in cultured cortical neurones via activation of the CB1 receptor: Neuroreport 2001; 12: 3973–3978.

[105] Lawston J, Borella A, Robinson JK, et al. Changes in hippocampal morphology following chronic treatment with the synthetic cannabinoid WIN 55,212-2. Brain Res 2000; 877: 407–410.

[106] Burns HD, Van Laere K, Sanabria-Bohórquez S, et al. [$^{18}$ F]MK-9470, a positron emission tomography (PET) tracer for in vivo human PET brain imaging of the cannabinoid-1 receptor. Proc Natl Acad Sci 2007; 104: 9800–9805.

[107] S. V, R. H, B. M, et al. Differential effects of Δ 9 -THC on spatial reference and working memory in mice. Psychopharmacology (Berl) 2001; 157: 142–150.

[108] Fadda P, Robinson L, Fratta W, et al. Differential effects of THC- or CBD-rich cannabis extracts on working memory in rats. Neuropharmacology 2004; 47: 1170–1179.

[109] Blaes SL, Orsini CA, Holik HM, et al. Enhancing effects of acute exposure to cannabis smoke on working memory performance. Neurobiol Learn Mem 2019; 157: 151–162.

[110] Renard J, Vitalis T, Rame M, et al. Chronic cannabinoid exposure during adolescence leads to long-term structural and functional changes in the prefrontal cortex. Eur Neuropsychopharmacol 2016; 26: 55–64.

[111] Rubino T, Parolaro D. The Impact of Exposure to Cannabinoids in Adolescence: Insights From Animal Models. Biol Psychiatry 2016; 79: 578–585.

[112] Cass DK, Flores-Barrera E, Thomases DR, et al. CB1 cannabinoid receptor stimulation during adolescence impairs the maturation of GABA function in the adult rat prefrontal cortex. Mol Psychiatry 2014; 19: 536–543.

[113] Orihuel J, Capellán R, Casquero-Veiga M, et al. The long-term effects of adolescent Δ9-tetrahydrocannabinol on brain structure and function assessed through neuroimaging techniques in male and female rats. Eur Neuropsychopharmacol 2023; 74: 47–63.

[114] Komorowska-Müller JA, Gellner A-K, Ravichandran KA, et al. Chronic low-dose Δ9-tetrahydrocannabinol (THC) treatment stabilizes dendritic spines in 18-month-old mice. Sci Rep 2023; 13: 1390.

[115] Farquhar CE, Breivogel CS, Gamage TF, et al. Sex, THC, and hormones: Effects on density and sensitivity of CB1 cannabinoid receptors in rats. Drug Alcohol Depend 2019; 194: 20–27.

[116] Melis M, Frau R, Kalivas PW, et al. New vistas on cannabis use disorder. Neuropharmacology 2017; 124: 62–72.

[117] Testai FD, Gorelick PB, Aparicio HJ, et al. Use of Marijuana: Effect on Brain Health: A Scientific Statement From the American Heart Association. Stroke; 53. Epub ahead of print April 2022. DOI: 10.1161/STR.0000000000000396.

[118] Cutando L, Busquets-Garcia A, Puighermanal E, et al. Microglial activation underlies cerebellar deficits produced by repeated cannabis exposure. J Clin Invest 2013; 123: 2816–2831.

[119] Kolb B, Li Y, Robinson T, et al. THC alters alters morphology of neurons in medial prefrontal cortex, orbital prefrontal cortex, and nucleus accumbens and alters the ability of later experience to promote structural plasticity. Synapse 2018; 72: e22020.

[120] Mereu G, Fà M, Ferraro L, et al. Prenatal exposure to a cannabinoid agonist produces memory deficits linked to dysfunction in hippocampal long-term potentiation and glutamate release. Proc Natl Acad Sci 2003; 100: 4915–4920.

[121] Campolongo P, Trezza V, Ratano P, et al. Developmental consequences of perinatal cannabis exposure: behavioral and neuroendocrine effects in adult rodents. Psychopharmacology (Berl) 2011; 214: 5–15.

[122] Sarne Y, Toledano R, Rachmany L, et al. Reversal of age-related cognitive impairments in mice by an extremely low dose of tetrahydrocannabinol. Neurobiol Aging 2018; 61: 177–186.

[123] Trezza V, Campolongo P, Manduca A, et al. Altering endocannabinoid neurotransmission at critical developmental ages: impact on rodent emotionality and cognitive performance. Front Behav Neurosci; 6. Epub ahead of print 2012. DOI: 10.3389/fnbeh.2012.00002.

[124] Batalla A, Bhattacharyya S, Yücel M, et al. Structural and Functional Imaging Studies in Chronic Cannabis Users: A Systematic Review of Adolescent and Adult Findings. PLoS ONE 2013; 8: e55821.

[125] Cousijn J, Wiers RW, Ridderinkhof KR, et al. Grey matter alterations associated with cannabis use: Results of a VBM study in heavy cannabis users and healthy controls. NeuroImage 2012; 59: 3845–3851.

[126] Arnone D, Barrick TR, Chengappa S, et al. Corpus callosum damage in heavy marijuana use: Preliminary evidence from diffusion tensor tractography and tract-based spatial statistics. NeuroImage 2008; 41: 1067–1074.

[127] Jakabek D, Yücel M, Lorenzetti V, et al. An MRI study of white matter tract integrity in regular cannabis users: effects of cannabis use and age. Psychopharmacology (Berl) 2016; 233: 3627–3637.

[128] Maleki S, Hendrikse J, Richardson K, et al. White matter alterations associated with chronic cannabis use disorder: a structural network and fixel-based analysis. Transl Psychiatry 2024; 14: 429.

[129] Tsou K, Brown S, Sañudo-Peña MC, et al. Immunohistochemical distribution of cannabinoid CB1 receptors in the rat central nervous system. Neuroscience 1998; 83: 393–411.

[130] Svizenska I, Dubovy P, Sulcova A. Cannabinoid receptors 1 and 2 (CB1 and CB2), their distribution, ligands and functional involvement in nervous system structures — A short review. Pharmacol Biochem Behav 2008; 90: 501–511.

[131] Hu SS-J, Mackie K. Distribution of the Endocannabinoid System in the Central Nervous System. In: Pertwee RG (ed) Endocannabinoids. Cham: Springer International Publishing, pp. 59–93.

[132] Lorenzetti V, Chye Y, Silva P, et al. Does regular cannabis use affect neuroanatomy? An updated systematic review and meta-analysis of structural neuroimaging studies. Eur Arch Psychiatry Clin Neurosci 2019; 269: 59–71.

[133] Wang Y, Zuo C, Wang W, et al. Reduction in hippocampal volumes subsequent to heavy cannabis use: a 3-year longitudinal study. Psychiatry Res 2021; 295: 113588.

[134] Rocchetti M, Crescini A, Borgwardt S, et al. Is cannabis neurotoxic for the healthy brain? A meta-analytical review of structural brain alterations in non-psychotic users. Psychiatry Clin Neurosci 2013; 67: 483–492.

[135] Cupo L, Plitman E, Guma E, et al. A systematic review of neuroimaging and acute cannabis exposure in age-of-risk for psychosis. Transl Psychiatry 2021; 11: 217.

[136] Colizzi M, Weltens N, McGuire P, et al. Delta-9-tetrahydrocannabinol increases striatal glutamate levels in healthy individuals: implications for psychosis. Mol Psychiatry 2020; 25: 3231–3240.

[137] Bossong MG, van Berckel BNM, Boellaard R, et al. Delta 9-tetrahydrocannabinol induces dopamine release in the human striatum. Neuropsychopharmacol Off Publ Am Coll Neuropsychopharmacol 2009; 34: 759–766.

[138] Stokes PRA, Mehta MA, Curran HV, et al. Can recreational doses of THC produce significant dopamine release in the human striatum? NeuroImage 2009; 48: 186–190.

[139] Jacobus J, Squeglia LM, Sorg SF, et al. Cortical thickness and neurocognition in adolescent marijuana and alcohol users following 28 days of monitored abstinence. J Stud Alcohol Drugs 2014; 75: 729–743.

[140] McQueeny T, Padula CB, Price J, et al. Gender effects on amygdala morphometry in adolescent marijuana users. Behav Brain Res 2011; 224: 128–134.

[141] Medina KL, McQueeny T, Nagel BJ, et al. IMAGING STUDY: Prefrontal cortex morphometry in abstinent adolescent marijuana users: subtle gender effects. Addict Biol 2009; 14: 457–468.

[142] Medina KL, Nagel BJ, Tapert SF. Abnormal cerebellar morphometry in abstinent adolescent marijuana users. Psychiatry Res 2010; 182: 152–159.

[143] Pagliaccio D, Barch DM, Bogdan R, et al. Shared Predisposition in the Association Between Cannabis Use and Subcortical Brain Structure. JAMA Psychiatry 2015; 72: 994.

[144] Lorenzetti V, Lubman DI, Whittle S, et al. Structural MRI Findings in Long-Term Cannabis Users: What Do We Know? Subst Use Misuse 2010; 45: 1787–1808.

[145] Weiland BJ, Thayer RE, Depue BE, et al. Daily Marijuana Use Is Not Associated with Brain Morphometric Measures in Adolescents or Adults. J Neurosci 2015; 35: 1505–1512.

[146] Schacht JP, Hutchison KE, Filbey FM. Associations between Cannabinoid Receptor-1 (CNR1) Variation and Hippocampus and Amygdala Volumes in Heavy Cannabis Users. Neuropsychopharmacology 2012; 37: 2368–2376.

[147] Ashtari M, Avants B, Cyckowski L, et al. Medial temporal structures and memory functions in adolescents with heavy cannabis use. J Psychiatr Res 2011; 45: 1055–1066.

[148] Gilman JM, Kuster JK, Lee S, et al. Cannabis Use Is Quantitatively Associated with Nucleus Accumbens and Amygdala Abnormalities in Young Adult Recreational Users. J Neurosci 2014; 34: 5529–5538.

[149] Koenders L, Cousijn J, Vingerhoets WAM, et al. Grey Matter Changes Associated with Heavy Cannabis Use: A Longitudinal sMRI Study. PLOS ONE 2016; 11: e0152482.

[150] Gillespie NA, Neale MC, Bates TC, et al. Testing associations between cannabis use and subcortical volumes in two large population-based samples. Addiction 2018; 113: 1661–1672.

[151] Navarri X, Afzali MH, Lavoie J, et al. How do substance use disorders compare to other psychiatric conditions on structural brain abnormalities? A cross-disorder meta-analytic comparison using the ENIGMA consortium findings. Hum Brain Mapp 2022; 43: 399–413.

[152] Kroon E, Kuhns L, Hoch E, et al. Heavy cannabis use, dependence and the brain: a clinical perspective. Addiction 2020; 115: 559–572.

[153] Nader DA, Sanchez ZM. Effects of regular cannabis use on neurocognition, brain structure, and function: a systematic review of findings in adults. Am J Drug Alcohol Abuse 2018; 44: 4–18.

[154] Scott JC, Rosen AFG, Moore TM, et al. Cannabis use in youth is associated with limited alterations in brain structure. Neuropsychopharmacology 2019; 44: 1362–1369.

[155] Filbey FM, Aslan S, Calhoun VD, et al. Long-term effects of marijuana use on the brain. Proc Natl Acad Sci 2014; 111: 16913–16918.

[156] Orr JM, Paschall CJ, Banich MT. Recreational marijuana use impacts white matter integrity and subcortical (but not cortical) morphometry. NeuroImage Clin 2016; 12: 47–56.

[157] Jacobus J, McQueeny T, Bava S, et al. White matter integrity in adolescents with histories of marijuana use and binge drinking. Neurotoxicol Teratol 2009; 31: 349–355.

[158] Bava S, Jacobus J, Thayer RE, et al. Longitudinal Changes in White Matter Integrity Among Adolescent Substance Users. Alcohol Clin Exp Res; 37. Epub ahead of print January 2013. DOI: 10.1111/j.1530-0277.2012.01920.x.

[159] Becker MP, Collins PF, Lim KO, et al. Longitudinal changes in white matter microstructure after heavy cannabis use. Dev Cogn Neurosci 2015; 16: 23–35.

[160] Robinson EA, Gleeson J, Arun AH, et al. Measuring white matter microstructure in 1,457 cannabis users and 1,441 controls: A systematic review of diffusion-weighted MRI studies. Front Neuroimaging 2023; 2: 1129587.

[161] Shollenbarger SG, Price J, Wieser J, et al. Poorer frontolimbic white matter integrity is associated with chronic cannabis use, FAAH genotype, and increased depressive and apathy symptoms in adolescents and young adults. NeuroImage Clin 2015; 8: 117–125.

[162] Gruber SA, Dahlgren MK, Sagar KA, et al. Worth the wait: effects of age of onset of marijuana use on white matter and impulsivity. Psychopharmacology (Berl) 2014; 231: 1455–1465.

[163] Zalesky A, Solowij N, Yucel M, et al. Effect of long-term cannabis use on axonal fibre connectivity. Brain 2012; 135: 2245–2255.

[164] Manza P, Yuan K, Shokri-Kojori E, et al. Brain structural changes in cannabis dependence: association with MAGL. Mol Psychiatry 2020; 25: 3256–3266.

[165] Koenis MMG, Durnez J, Rodrigue AL, et al. Associations of cannabis use disorder with cognition, brain structure, and brain function in AFRICAN AMERICANS. Hum Brain Mapp 2021; 42: 1727–1741.

[166] Albaugh MD, Ottino-Gonzalez J, Sidwell A, et al. Association of Cannabis Use During Adolescence With Neurodevelopment. JAMA Psychiatry 2021; 78: 1031.

[167] Meier MH, Schriber RA, Beardslee J, et al. Associations between adolescent cannabis use frequency and adult brain structure: A prospective study of boys followed to adulthood. Drug Alcohol Depend 2019; 202: 191–199.

[168] Wang Y, Zuo C, Xu Q, et al. Cerebellar thickness changes associated with heavy cannabis use: A 3-year longitudinal study. Addict Biol 2021; 26: e12931.

[169] Thayer RE. Marijuana use in an aging population: Global brain structure and cognitive function. Dissertation/Thesis, University of Colorado at Boulder, https://www.proquest.com/openview/d0f4efa0af259813c00422972532e961/1?pq-origsite=gscholar&cbl=18750 (2018).

[170] Vered S, Sznitman S, Weinstein G. The association between cannabis use and neuroimaging measures in older adults: Findings from the UK Biobank. Alzheimers Dement 2024; 20: e090279.

[171] Paul S, Bhattacharyya S. Cannabis use-related working memory deficit mediated by lower left hippocampal volume. Addict Biol 2021; 26: e12984.

[172] Maple KE, Thomas AM, Kangiser MM, et al. Anterior cingulate volume reductions in abstinent adolescent and young adult cannabis users: Association with affective processing deficits. Psychiatry Res Neuroimaging 2019; 288: 51–59.

[173] Wittemann M, Brielmaier J, Rubly M, et al. Cognition and Cortical Thickness in Heavy Cannabis Users. Eur Addict Res 2021; 27: 115–122.

[174] Butterworth P, Slade T, Degenhardt L. Factors associated with the timing and onset of cannabis use and cannabis use disorder: Results from the 2007 A ustralian N ational S urvey of M ental H ealth and W ell- B eing. Drug Alcohol Rev 2014; 33: 555–564.

[175] Chen C-Y, O'Brien MS, Anthony JC. Who becomes cannabis dependent soon after onset of use? Epidemiological evidence from the United States: 2000–2001. Drug Alcohol Depend 2005; 79: 11–22.

[176] Harding IH, Solowij N, Harrison BJ, et al. Functional Connectivity in Brain Networks Underlying Cognitive Control in Chronic Cannabis Users. Neuropsychopharmacology 2012; 37: 1923–1933.

[177] Ritchay MM, Huggins AA, Wallace AL, et al. Resting state functional connectivity in the default mode network: Relationships between cannabis use, gender, and cognition in adolescents and young adults. NeuroImage Clin 2021; 30: 102664.

[178] Gowin JL, Ellingson JM, Karoly HC, et al. Brain Function Outcomes of Recent and Lifetime Cannabis Use. JAMA Netw Open 2025; 8: e2457069.

[179] Scott JC, Slomiak ST, Jones JD, et al. Association of Cannabis With Cognitive Functioning in Adolescents and Young Adults: A Systematic Review and Meta-analysis. JAMA Psychiatry 2018; 75: 585.

[180] Figueiredo PR, Tolomeo S, Steele JD, et al. Neurocognitive consequences of chronic cannabis use: a systematic review and meta-analysis. Neurosci Biobehav Rev 2020; 108: 358–369.

[181] Ertl N, Lawn W, Mokrysz C, et al. Associations between regular cannabis use and brain resting-state functional connectivity in adolescents and adults. J Psychopharmacol (Oxf) 2023; 37: 904–919.

[182] Raichle ME. The Brain's Default Mode Network. Annu Rev Neurosci 2015; 38: 433–447.

[183] Vincent JL, Kahn I, Snyder AZ, et al. Evidence for a Frontoparietal Control System Revealed by Intrinsic Functional Connectivity. J Neurophysiol 2008; 100: 3328–3342.

[184] Seeley WW, Menon V, Schatzberg AF, et al. Dissociable Intrinsic Connectivity Networks for Salience Processing and Executive Control. J Neurosci 2007; 27: 2349–2356.

[185] Thomson H, Labuschagne I, Greenwood L-M, et al. Is resting-state functional connectivity altered in regular cannabis users? A systematic review of the literature. Psychopharmacology (Berl) 2022; 239: 1191–1209.

[186] Schnakenberg Martin AM, Kim D-J, Newman SD, et al. Altered cerebellar-cortical resting-state functional connectivity in cannabis users. J Psychopharmacol (Oxf) 2021; 35: 823–832.

[187] Atakan Z, Bhattacharyya S, Allen P, et al. Cannabis affects people differently: inter-subject variation in the psychotogenic effects of Δ9-tetrahydrocannabinol: a functional magnetic resonance imaging study with healthy volunteers. Psychol Med 2013; 43: 1255–1267.

[188] Bhattacharyya S, Iyegbe C, Atakan Z, et al. Protein kinase B (AKT1) genotype mediates sensitivity to cannabis-induced impairments in psychomotor control. Psychol Med 2014; 44: 3315–3328.

[189] Bhattacharyya S, Morrison PD, Fusar-Poli P, et al. Opposite effects of delta-9-tetrahydrocannabinol and cannabidiol on human brain function and psychopathology. Neuropsychopharmacol Off Publ Am Coll Neuropsychopharmacol 2010; 35: 764–774.

[190] Phan KL, Angstadt M, Golden J, et al. Cannabinoid modulation of amygdala reactivity to social signals of threat in humans. J Neurosci Off J Soc Neurosci 2008; 28: 2313–2319.

[191] Ramaekers JG, van Wel JH, Spronk D, et al. Cannabis and cocaine decrease cognitive impulse control and functional corticostriatal connectivity in drug users with low activity DBH genotypes. Brain Imaging Behav 2016; 10: 1254–1263.

[192] Rzepa E, Tudge L, McCabe C. The CB1 Neutral Antagonist Tetrahydrocannabivarin Reduces Default Mode Network and Increases Executive Control Network Resting State Functional Connectivity in Healthy Volunteers. Int J Neuropsychopharmacol 2015; 19: pyv092.

[193] Klumpers LE, Cole DM, Khalili-Mahani N, et al. Manipulating brain connectivity with $\delta^9$-tetrahydrocannabinol: a pharmacological resting state FMRI study. NeuroImage 2012; 63: 1701–1711.

[194] van Hell HH, Bossong MG, Jager G, et al. Evidence for involvement of the insula in the psychotropic effects of THC in humans: a double-blind, randomized pharmacological MRI study. Int J Neuropsychopharmacol 2011; 14: 1377–1388.

[195] Lopez-Larson MP, Rogowska J, Yurgelun-Todd D. Aberrant orbitofrontal connectivity in marijuana smoking adolescents. Dev Cogn Neurosci 2015; 16: 54–62.

[196] Blest-Hopley G, Giampietro V, Bhattacharyya S. Regular cannabis use is associated with altered activation of central executive and default mode networks even after prolonged abstinence in adolescent users: Results from a complementary meta-analysis. Neurosci Biobehav Rev 2019; 96: 45–55.

[197] Sneider JT, Pope HG, Silveri MM, et al. Differences in regional blood volume during a 28-day period of abstinence in chronic cannabis smokers. Eur Neuropsychopharmacol J Eur Coll Neuropsychopharmacol 2008; 18: 612–619.

[198] Padula CB, Schweinsburg AD, Tapert SF. Spatial working memory performance and fMRI activation interaction in abstinent adolescent marijuana users. Psychol Addict Behav J Soc Psychol Addict Behav 2007; 21: 478–487.

[199] Tapert SF, Schweinsburg AD, Drummond SPA, et al. Functional MRI of inhibitory processing in abstinent adolescent marijuana users. Psychopharmacology (Berl) 2007; 194: 173–183.

[200] Skumlien M, Mokrysz C, Freeman TP, et al. Neural responses to reward anticipation and feedback in adult and adolescent cannabis users and controls. Neuropsychopharmacology 2022; 47: 1976–1983.

[201] Zimmermann K, Kendrick KM, Scheele D, et al. Altered striatal reward processing in abstinent dependent cannabis users: Social context matters. Eur Neuropsychopharmacol 2019; 29: 356–364.

[202] Hammond C, Allick A, Park G, et al. A Meta-Analysis of fMRI Studies of Youth Cannabis Use: Alterations in Executive Control, Social Cognition/Emotion Processing, and Reward Processing in Cannabis Using Youth. Brain Sci 2022; 12: 1281.

[203] Kroon E, Kuhns L, Cousijn J. Context dependent differences in working memory related brain activity in heavy cannabis users. Psychopharmacology (Berl) 2022; 239: 1373–1385.

[204] Raymond DR, Paneto A, Yoder KK, et al. Does Chronic Cannabis Use Impact Risky Decision-Making: An Examination of fMRI Activation and Effective Connectivity? Front Psychiatry 2020; 11: 599256.

[205] Leiker EK, Meffert H, Thornton LC, et al. Alcohol use disorder and cannabis use disorder symptomatology in adolescents are differentially related to dysfunction in

brain regions supporting face processing. Psychiatry Res Neuroimaging 2019; 292: 62–71.

[206] Manza P, Shokri-Kojori E, Volkow ND. Reduced Segregation Between Cognitive and Emotional Processes in Cannabis Dependence. Cereb Cortex 2020; 30: 628–639.

[207] Hatchard T, Byron-Alhassan A, Mioduszewski O, et al. Working Overtime: Altered Functional Connectivity in Working Memory Following Regular Cannabis Use in Young Adults. Int J Ment Health Addict 2021; 19: 1314–1329.

[208] Karoly HC, Schacht JP, Meredith LR, et al. Investigating a novel fMRI cannabis cue reactivity task in youth. Addict Behav 2019; 89: 20–28.

[209] Aloi J, Meffert H, White SF, et al. Differential dysfunctions related to alcohol and cannabis use disorder symptoms in reward and error-processing neuro-circuitries in adolescents. Dev Cogn Neurosci 2019; 36: 100618.

[210] Ma L, Steinberg JL, Bjork JM, et al. Fronto-striatal effective connectivity of working memory in adults with cannabis use disorder. Psychiatry Res Neuroimaging 2018; 278: 21–34.

[211] Bossong MG, Jansma JM, Van Hell HH, et al. Default Mode Network in the Effects of Δ9-Tetrahydrocannabinol (THC) on Human Executive Function. PLoS ONE 2013; 8: e70074.

[212] Eldreth DA, Matochik JA, Cadet JL, et al. Abnormal brain activity in prefrontal brain regions in abstinent marijuana users. NeuroImage 2004; 23: 914–920.

[213] Jager G, Kahn RS, Van Den Brink W, et al. Long-term effects of frequent cannabis use on working memory and attention: an fMRI study. Psychopharmacology (Berl) 2006; 185: 358–368.

[214] Gruber SA, Sagar KA, Dahlgren MK, et al. The Grass Might Be Greener: Medical Marijuana Patients Exhibit Altered Brain Activity and Improved Executive Function after 3 Months of Treatment. Front Pharmacol 2018; 8: 983.

[215] Germani E, Fromont E, Maurel P, et al. HCP Multi-Pipeline: a derived dataset to investigate analytical variability in fMRI. Sci Data 2025; 12: 940.

[216] Solowij N, Pesa N. [Cognitive abnormalities and cannabis use]. Rev Bras Psiquiatr Sao Paulo Braz 1999 2010; 32 Suppl 1: S31-40.

[217] Solowij N, Battisti R. The Chronic Effects of Cannabis on Memory in Humans: A Review. Curr Drug Abuse Rev 2008; 1: 81–98.

[218] Meier MH, Olive MF, Jenks OA, et al. Cannabis Use and Cognitive Functioning Across the Lifespan. Curr Addict Rep 2024; 11: 384–395.

[219] Bourque J, Potvin S. Cannabis and Cognitive Functioning: From Acute to Residual Effects, From Randomized Controlled Trials to Prospective Designs. Front Psychiatry 2021; 12: 596601.

[220] Lichtman AH, Varvel SA, Martin BR. Endocannabinoids in cognition and dependence. Prostaglandins Leukot Essent Fat Acids PLEFA 2002; 66: 269–285.

[221] Scott EP, Brennan E, Benitez A. A Systematic Review of the Neurocognitive Effects of Cannabis Use in Older Adults. Curr Addict Rep 2019; 6: 443–455.

[222] Crean RD, Crane NA, Mason BJ. An Evidence-Based Review of Acute and Long-Term Effects of Cannabis Use on Executive Cognitive Functions. J Addict Med 2011; 5: 1–8.

[223] Pope HG, Gruber AJ, Hudson JI, et al. Early-onset cannabis use and cognitive deficits: what is the nature of the association? Drug Alcohol Depend 2003; 69: 303–310.

[224] Gruber SA, Sagar KA, Dahlgren MK, et al. Age of onset of marijuana use and executive function. Psychol Addict Behav 2012; 26: 496–506.

[225] Ehrenreich H, Kunert HJ, Moeller MR, et al. Specific attentional dysfunction in adults following early start of cannabis use. Psychopharmacology (Berl) 1999; 142: 295–301.

[226] Fontes MA, Bolla KI, Cunha PJ, et al. Cannabis use before age 15 and subsequent executive functioning. Br J Psychiatry 2011; 198: 442–447.

[227] Walia A, Scott M, Berg E. Does marijuana usage have impacts on motor and executive functioning? Evid-Based Pract 2021; 24: 31–32.

[228] Wade NE, Courtney KE, Wallace AL, et al. Investigating sex differences and age of onset in emotion regulation, executive functioning, and cannabis use in adolescents and young adults. J Cannabis Res 2024; 6: 20.

[229] Yoon JH, San Miguel GG, Vincent JN, et al. Assessing attentional bias and inhibitory control in cannabis use disorder using an eye-tracking paradigm with personalized stimuli. Exp Clin Psychopharmacol 2019; 27: 578–587.

[230] Morie KP, Potenza MN. A Mini-Review of Relationships Between Cannabis Use and Neural Foundations of Reward Processing, Inhibitory Control and Working Memory. Front Psychiatry 2021; 12: 657371.

[231] Ramaekers JG, Kauert G, Van Ruitenbeek P, et al. High-Potency Marijuana Impairs Executive Function and Inhibitory Motor Control. Neuropsychopharmacology 2006; 31: 2296–2303.

[232] Morin J-FG, Afzali MH, Bourque J, et al. A Population-Based Analysis of the Relationship Between Substance Use and Adolescent Cognitive Development. Am J Psychiatry 2019; 176: 98–106.

[233] Englund A, Atakan Z, Kralj A, et al. The effect of five day dosing with THCV on THC-induced cognitive, psychological and physiological effects in healthy male human volunteers: A placebo-controlled, double-blind, crossover pilot trial. J Psychopharmacol (Oxf) 2016; 30: 140–151.

[234] Dougherty DM, Mathias CW, Dawes MA, et al. Impulsivity, attention, memory, and decision-making among adolescent marijuana users. Psychopharmacology (Berl) 2013; 226: 307–319.

[235] Desrosiers NA, Ramaekers JG, Chauchard E, et al. Smoked Cannabis' Psychomotor and Neurocognitive Effects in Occasional and Frequent Smokers. J Anal Toxicol 2015; 39: 251–261.

[236] Boggs DL, Cortes-Briones JA, Surti T, et al. The dose-dependent psychomotor effects of intravenous delta-9-tetrahydrocannabinol ($\Delta^9$ -THC) in humans. J Psychopharmacol (Oxf) 2018; 32: 1308–1318.

[237] Englund A, Morrison PD, Nottage J, et al. Cannabidiol inhibits THC-elicited paranoid symptoms and hippocampal-dependent memory impairment. J Psychopharmacol (Oxf) 2013; 27: 19–27.

[238] Schreiner AM, Dunn ME. Residual effects of cannabis use on neurocognitive performance after prolonged abstinence: A meta-analysis. Exp Clin Psychopharmacol 2012; 20: 420–429.

[239] Lovell ME, Akhurst J, Padgett C, et al. Cognitive outcomes associated with long-term, regular, recreational cannabis use in adults: A meta-analysis. Exp Clin Psychopharmacol 2020; 28: 471–494.

[240] Grant I, Gonzalez R, Carey CL, et al. Non-acute (residual) neurocognitive effects of cannabis use: A meta-analytic study. J Int Neuropsychol Soc 2003; 9: 679–689.

[241] Schoeler T, Kambeitz J, Behlke I, et al. The effects of cannabis on memory function in users with and without a psychotic disorder: findings from a combined meta-analysis. Psychol Med 2016; 46: 177–188.

[242] Hirvonen J, Goodwin RS, Li C-T, et al. Reversible and regionally selective downregulation of brain cannabinoid CB1 receptors in chronic daily cannabis smokers. Mol Psychiatry 2012; 17: 642–649.

[243] Hanson KL, Winward JL, Schweinsburg AD, et al. Longitudinal study of cognition among adolescent marijuana users over three weeks of abstinence. Addict Behav 2010; 35: 970–976.

[244] Schuster RM, Gilman J, Schoenfeld D, et al. One Month of Cannabis Abstinence in Adolescents and Young Adults Is Associated With Improved Memory. J Clin Psychiatry 2018; 79: 17m11977.

[245] Roten A, Baker NL, Gray KM. Cognitive performance in a placebo-controlled pharmacotherapy trial for youth with marijuana dependence. Addict Behav 2015; 45: 119–123.

[246] Wallace AL, Wade NE, Lisdahl KM. Impact of 2 Weeks of Monitored Abstinence on Cognition in Adolescent and Young Adult Cannabis Users. J Int Neuropsychol Soc JINS 2020; 26: 776–784.

[247] Solowij N, Michie PT, Fox AM. Differential impairments of selective attention due to frequency and duration of cannabis use. Biol Psychiatry 1995; 37: 731–739.

[248] Fried P, Watkinson B, Gray R. Neurocognitive consequences of marihuana—a comparison with pre-drug performance. Neurotoxicol Teratol 2005; 27: 231–239.

[249] Morgan CJA, Schafer G, Freeman TP, et al. Impact of cannabidiol on the acute memory and psychotomimetic effects of smoked cannabis: naturalistic study. Br J Psychiatry 2010; 197: 285–290.

[250] Becker MP, Collins PF, Luciana M. Neurocognition in college-aged daily marijuana users. J Clin Exp Neuropsychol 2014; 36: 379–398.

[251] Cuttler C, McLaughlin RJ, Graf P. Mechanisms Underlying the Link between Cannabis Use and Prospective Memory. PLoS ONE 2012; 7: e36820.

[252] Harvey MA, Sellman JD, Porter RJ, et al. The relationship between non-acute adolescent cannabis use and cognition. Drug Alcohol Rev 2007; 26: 309–319.

[253] Solowij N, Jones KA, Rozman ME, et al. Verbal learning and memory in adolescent cannabis users, alcohol users and non-users. Psychopharmacology (Berl) 2011; 216: 131–144.

[254] Gonzalez R, Schuster RM, Mermelstein RJ, et al. Performance of young adult cannabis users on neurocognitive measures of impulsive behavior and their relationship to symptoms of cannabis use disorders. J Clin Exp Neuropsychol 2012; 34: 962–976.

[255] Thames AD, Arbid N, Sayegh P. Cannabis use and neurocognitive functioning in a non-clinical sample of users. Addict Behav 2014; 39: 994–999.

[256] Wagner D, Becker B, Gouzoulis-Mayfrank E, et al. Interactions between specific parameters of cannabis use and verbal memory. Prog Neuropsychopharmacol Biol Psychiatry 2010; 34: 871–876.

[257] Hanson KL, Thayer RE, Tapert SF. Adolescent marijuana users have elevated risk-taking on the balloon analog risk task. J Psychopharmacol (Oxf) 2014; 28: 1080–1087.

[258] Medina KL, Hanson KL, Schweinsburg AD, et al. Neuropsychological functioning in adolescent marijuana users: Subtle deficits detectable after a month of abstinence. J Int Neuropsychol Soc 2007; 13: 807–820.

[259] Tait RJ, Mackinnon A, Christensen H. Cannabis use and cognitive function: 8-year trajectory in a young adult cohort. Addiction 2011; 106: 2195–2203.

[260] Caspi A, Moffitt TE, Cannon M, et al. Moderation of the Effect of Adolescent-Onset Cannabis Use on Adult Psychosis by a Functional Polymorphism in the Catechol-O-Methyltransferase Gene: Longitudinal Evidence of a Gene X Environment Interaction. Biol Psychiatry 2005; 57: 1117–1127.

[261] French L, Gray C, Leonard G, et al. Early Cannabis Use, Polygenic Risk Score for Schizophrenia and Brain Maturation in Adolescence. JAMA Psychiatry 2015; 72: 1002.

[262] Lyons MJ, Bar JL, Panizzon MS, et al. Neuropsychological consequences of regular marijuana use: a twin study. Psychol Med 2004; 34: 1239–1250.

[263] Gorey C, Kuhns L, Smaragdi E, et al. Age-related differences in the impact of cannabis use on the brain and cognition: a systematic review. Eur Arch Psychiatry Clin Neurosci 2019; 269: 37–58.

[264] Schnakenberg Martin AM, D'Souza DC, Newman SD, et al. Differential Cognitive Performance in Females and Males with Regular Cannabis Use. J Int Neuropsychol Soc 2021; 27: 570–580.

[265] Jacobus J, Tapert SF. Effects of cannabis on the adolescent brain. Curr Pharm Des 2014; 20: 2186–2193.

[266] Stypulkowski K, Thayer RE. Long-Term Recreational Cannabis Use Is Associated With Lower Executive Function and Processing Speed in a Pilot Sample of Older Adults. J Geriatr Psychiatry Neurol 2022; 35: 740–746.

[267] Solowij N. Cognitive Functioning of Long-term Heavy Cannabis Users Seeking Treatment. JAMA 2002; 287: 1123.

[268] Myran DT, Pugliese M, Harrison LD, et al. Risk of Dementia in Individuals With Emergency Department Visits or Hospitalizations Due to Cannabis. JAMA Neurol 2025; 82: 570.

[269] Aso E, Ferrer I. Cannabinoids for treatment of Alzheimerâ€™s disease: moving toward the clinic. Front Pharmacol; 5. Epub ahead of print 5 March 2014. DOI: 10.3389/fphar.2014.00037.

[270] Ramírez BG, Blázquez C, Del Pulgar TG, et al. Prevention of Alzheimer's Disease Pathology by Cannabinoids: Neuroprotection Mediated by Blockade of Microglial Activation. J Neurosci 2005; 25: 1904–1913.

[271] Esposito G, De Filippis D, Steardo L, et al. CB1 receptor selective activation inhibits β-amyloid-induced iNOS protein expression in C6 cells and subsequently blunts tau protein hyperphosphorylation in co-cultured neurons. Neurosci Lett 2006; 404: 342–346.

[272] Hampson AJ, Grimaldi M, Axelrod J, et al. Cannabidiol and $(-)\Delta^9$ -tetrahydrocannabinol are neuroprotective antioxidants. Proc Natl Acad Sci 1998; 95: 8268–8273.

[273] Marsicano G, Goodenough S, Monory K, et al. CB1 Cannabinoid Receptors and On-Demand Defense Against Excitotoxicity. Science 2003; 302: 84–88.

[274] Martín-Moreno AM, Brera B, Spuch C, et al. Prolonged oral cannabinoid administration prevents neuroinflammation, lowers β-amyloid levels and improves cognitive performance in Tg APP 2576 mice. J Neuroinflammation 2012; 9: 8.

[275] Esposito G, Scuderi C, Valenza M, et al. Cannabidiol Reduces Aβ-Induced Neuroinflammation and Promotes Hippocampal Neurogenesis through PPARγ Involvement. PLoS ONE 2011; 6: e28668.

[276] Solas M, Francis PT, Franco R, et al. CB2 receptor and amyloid pathology in frontal cortex of Alzheimer's disease patients. Neurobiol Aging 2013; 34: 805–808.

[277] Volicer L, Stelly M, Morris J, et al. Effects of dronabinol on anorexia and disturbed behavior in patients with Alzheimer's disease. Int J Geriatr Psychiatry 1997; 12: 913–919.

[278] Krishnan S, Cairns R, Howard R. Cannabinoids for the treatment of dementia. Cochrane Database Syst Rev. Epub ahead of print 15 April 2009. DOI: 10.1002/14651858.CD007204.pub2.

[279] Bosnjak Kuharic D, Markovic D, Brkovic T, et al. Cannabinoids for the treatment of dementia. Cochrane Database Syst Rev; 2021. Epub ahead of print 17 September 2021. DOI: 10.1002/14651858.CD012820.pub2.

[280] Schmidt et al. New terrain: Tools to integrate trauma and gender informed responses into substance use practice and policy. Vancouver, BC, Canada: Centre of Excellence for Women's Health, https://cewh.ca/wp-content/uploads/2022/01/NewTerrain_FinalOnlinePDF.pdf (2018).

[281] Greaves L, Hemsing N. Sex and Gender Interactions on the Use and Impact of Recreational Cannabis. Int J Environ Res Public Health 2020; 17: 509.

[282] Cuttler C, Mischley LK, Sexton M. Sex Differences in Cannabis Use and Effects: A Cross-Sectional Survey of Cannabis Users. Cannabis Cannabinoid Res 2016; 1: 166–175.

[283] Cooper ZD, Craft RM. Sex-Dependent Effects of Cannabis and Cannabinoids: A Translational Perspective. Neuropsychopharmacology 2018; 43: 34–51.

[284] Copersino ML, Boyd SJ, Tashkin DP, et al. Sociodemographic Characteristics of Cannabis Smokers and the Experience of Cannabis Withdrawal. Am J Drug Alcohol Abuse 2010; 36: 311–319.

[285] Herrmann ES, Weerts EM, Vandrey R. Sex differences in cannabis withdrawal symptoms among treatment-seeking cannabis users. Exp Clin Psychopharmacol 2015; 23: 415–421.

[286] Weed PF, Filipeanu CM, Ketchum MJ, et al. Chronic Δ9-Tetrahydrocannabinol during Adolescence Differentially Modulates Striatal CB1 Receptor Expression and the Acute and Chronic Effects on Learning in Adult Rats. J Pharmacol Exp Ther 2016; 356: 20–31.

[287] Harte-Hargrove LC, Dow-Edwards DL. Withdrawal from THC during adolescence: Sex differences in locomotor activity and anxiety. Behav Brain Res 2012; 231: 48–59.

[288] Fattore L, Fratta W. How important are sex differences in cannabinoid action? Br J Pharmacol 2010; 160: 544–548.

[289] Craft RM, Marusich JA, Wiley JL. Sex differences in cannabinoid pharmacology: A reflection of differences in the endocannabinoid system? Life Sci 2013; 92: 476–481.

[290] Allick A, Park G, Kim K, et al. Age- and Sex-Related Cortical Gray Matter Volume Differences in Adolescent Cannabis Users: A Systematic Review and Meta-Analysis of Voxel-Based Morphometry Studies. Front Psychiatry 2021; 12: 745193.

[291] Ketcherside A, Baine J, Filbey F. Sex Effects of Marijuana on Brain Structure and Function. Curr Addict Rep 2016; 3: 323–331.

[292] Francis AM, Bissonnette JN, MacNeil SE, et al. Interaction of sex and cannabis in adult in vivo brain imaging studies: A systematic review. Brain Neurosci Adv 2022; 6: 23982128211073431.

[293] Cousijn J, Toenders YJ, Kaag AM, et al. The role of sex in the association between cannabis use disorder and resting-state functional connectivity. Neuropsychopharmacology 2025; 50: 991–999.

[294] Prashad S, Hammonds RP, Wiese AL, et al. Sex-related differences in subjective, but not neural, cue-elicited craving response in heavy cannabis users. Drug Alcohol Depend 2020; 209: 107931.

[295] Wetherill RR, Jagannathan K, Hager N, et al. Sex differences in associations between cannabis craving and neural responses to cannabis cues: Implications for treatment. Exp Clin Psychopharmacol 2015; 23: 238–246.

[296] Kroon E, Kuhns LN, Kaag AM, et al. The role of sex in the association between cannabis use and working memory-related brain activity. J Neurosci Res 2022; 100: 1347–1358.

[297] Lisdahl KM, Price JS. Increased Marijuana Use and Gender Predict Poorer Cognitive Functioning in Adolescents and Emerging Adults. J Int Neuropsychol Soc 2012; 18: 678–688.

[298] Savulich G, Rychik N, Lamberth E, et al. Sex Differences in Neuropsychological Functioning are Domain-Specific in Adolescent and Young Adult Regular Cannabis Users. J Int Neuropsychol Soc 2021; 27: 592–606.

[299] Hodgson K, Coleman JRI, Hagenaars SP, et al. Cannabis use, depression and self-harm: phenotypic and genetic relationships. Addiction 2020; 115: 482–492.

[300] Ishrat S, Levey DF, Gelernter J, et al. Association between cannabis use and brain structure and function: an observational and Mendelian randomisation study. BMJ Ment Health 2024; 27: e301065.

[301] Jenkinson M, Beckmann CF, Behrens TEJ, et al. FSL. NeuroImage 2012; 62: 782–790.

[302] Jenkinson M, Smith S. A global optimisation method for robust affine registration of brain images. Med Image Anal 2001; 5: 143–156.

[303] Jenkinson M, Bannister P, Brady M, et al. Improved Optimization for the Robust and Accurate Linear Registration and Motion Correction of Brain Images. NeuroImage 2002; 17: 825–841.

[304] Andersson JLR, Jenkinson M, Smith S. Non-linear registration, aka spatial normalisation, https://www.fmrib.ox.ac.uk/datasets/techrep/ (2010).

[305] Smith SM, Jenkinson M, Woolrich MW, et al. Advances in functional and structural MR image analysis and implementation as FSL. NeuroImage 2004; 23: S208–S219.

[306] Jenkinson, M.; Pechaud, M.; Smith, S. BET2: MR-based estimation of brain, skull and scalp surfaces. 2005.

[307] Zhang Y, Brady M, Smith S. Segmentation of brain MR images through a hidden Markov random field model and the expectation-maximization algorithm. IEEE Trans Med Imaging 2001; 20: 45–57.

[308] Desikan RS, Ségonne F, Fischl B, et al. An automated labeling system for subdividing the human cerebral cortex on MRI scans into gyral based regions of interest. NeuroImage 2006; 31: 968–980.

[309] Diedrichsen J, Balsters JH, Flavell J, et al. A probabilistic MR atlas of the human cerebellum. NeuroImage 2009; 46: 39–46.

[310] Patenaude B, Smith SM, Kennedy DN, et al. A Bayesian model of shape and appearance for subcortical brain segmentation. NeuroImage 2011; 56: 907–922.

[311] Griffanti L, Zamboni G, Khan A, et al. BIANCA (Brain Intensity AbNormality Classification Algorithm): A new tool for automated segmentation of white matter hyperintensities. NeuroImage 2016; 141: 191–205.

[312] Wardlaw JM, Smith EE, Biessels GJ, et al. Neuroimaging standards for research into small vessel disease and its contribution to ageing and neurodegeneration. Lancet Neurol 2013; 12: 822–838.

[313] De Groot JC, De Leeuw F-E, Oudkerk M, et al. Cerebral white matter lesions and subjective cognitive dysfunction: The Rotterdam Scan Study. Neurology 2001; 56: 1539–1545.

[314] Debette S, Markus HS. The clinical importance of white matter hyperintensities on brain magnetic resonance imaging: systematic review and meta-analysis. BMJ 2010; 341: c3666–c3666.

[315] Mori et al. MRI Atlas of Human White Matter. AJNR Am J Neuroradiol., https://pmc.ncbi.nlm.nih.gov/articles/PMC8133945/ (2006).

[316] Beckmann CF, Smith SM. Probabilistic Independent Component Analysis for Functional Magnetic Resonance Imaging. IEEE Trans Med Imaging 2004; 23: 137–152.

[317] Beckmann CF, DeLuca M, Devlin JT, et al. Investigations into resting-state connectivity using independent component analysis. Philos Trans R Soc B Biol Sci 2005; 360: 1001–1013.

[318] Smith SM, Vidaurre D, Beckmann CF, et al. Functional connectomics from resting-state fMRI. Trends Cogn Sci 2013; 17: 666–682.

[319] Alfaro-Almagro F, McCarthy P, Afyouni S, et al. Confound modelling in UK Biobank brain imaging. NeuroImage 2021; 224: 117002.

[320] Smith SM, Douaud G, Chen W, et al. An expanded set of genome-wide association studies of brain imaging phenotypes in UK Biobank. Nat Neurosci 2021; 24: 737–745.

[321] Bates D, Mächler M, Bolker B, et al. Fitting Linear Mixed-Effects Models Using **lme4**. J Stat Softw; 67. Epub ahead of print 2015. DOI: 10.18637/jss.v067.i01.

[322] Kuznetsova A, Brockhoff PB, Christensen RHB. **lmerTest** Package: Tests in Linear Mixed Effects Models. J Stat Softw; 82. Epub ahead of print 2017. DOI: 10.18637/jss.v082.i13.

[323] Wickham H. ggplot2: Elegant Graphics for Data Analysis. New York, NY: Springer New York. Epub ahead of print 2009. DOI: 10.1007/978-0-387-98141-3.

[324] Hemani G, Zheng J, Elsworth B, et al. The MR-Base platform supports systematic causal inference across the human phenome. eLife 2018; 7: e34408.

[325] Benjamini Y, Hochberg Y. Controlling the False Discovery Rate: A Practical and Powerful Approach to Multiple Testing. J R Stat Soc Ser B Stat Methodol 1995; 57: 289–300.

[326] Burgess S, Butterworth A, Thompson SG. Mendelian Randomization Analysis With Multiple Genetic Variants Using Summarized Data. Genet Epidemiol 2013; 37: 658–665.

[327] Bowden J, Davey Smith G, Burgess S. Mendelian randomization with invalid instruments: effect estimation and bias detection through Egger regression. Int J Epidemiol 2015; 44: 512–525.

[328] Bowden J, Davey Smith G, Haycock PC, et al. Consistent Estimation in Mendelian Randomization with Some Invalid Instruments Using a Weighted Median Estimator. Genet Epidemiol 2016; 40: 304–314.

[329] Hartwig FP, Davey Smith G, Bowden J. Robust inference in summary data Mendelian randomization via the zero modal pleiotropy assumption. Int J Epidemiol 2017; 46: 1985–1998.

[330] Burgess S, Thompson SG. Interpreting findings from Mendelian randomization using the MR-Egger method. Eur J Epidemiol 2017; 32: 377–389.

[331] Rigucci S, Marques TR, Di Forti M, et al. Effect of high-potency cannabis on corpus callosum microstructure. Psychol Med 2016; 46: 841–854.

[332] Lichenstein SD, Shaw DS, Forbes EE. Cannabis, connectivity, and coming of age: Associations between cannabis use and anterior cingulate cortex connectivity during the transition to adulthood. Front Hum Neurosci 2022; 16: 951204.

[333] Moreno-Alcázar A, Gonzalvo B, Canales-Rodríguez EJ, et al. Larger Gray Matter Volume in the Basal Ganglia of Heavy Cannabis Users Detected by Voxel-Based Morphometry and Subcortical Volumetric Analysis. Front Psychiatry 2018; 9: 175.

[334] Shollenbarger SG, Price J, Wieser J, et al. Impact of cannabis use on prefrontal and parietal cortex gyrification and surface area in adolescents and emerging adults. Dev Cogn Neurosci 2015; 16: 46–53.

[335] Fry A, Littlejohns TJ, Sudlow C, et al. Comparison of Sociodemographic and Health-Related Characteristics of UK Biobank Participants With Those of the General Population. Am J Epidemiol 2017; 186: 1026–1034.

[336] Leung J, Chan GCK, Hides L, et al. What is the prevalence and risk of cannabis use disorders among people who use cannabis? a systematic review and meta-analysis. Addict Behav 2020; 109: 106479.

[337] Han B, Compton WM, Blanco C, et al. Time since first cannabis use and 12-month prevalence of cannabis use disorder among youth and emerging adults in the United States. Addiction 2019; 114: 698–707.

[338] Zhang R, Zhang B, Shen C, et al. Associations of dietary patterns with brain health from behavioral, neuroimaging, biochemical and genetic analyses. Nat Ment Health 2024; 2: 535–552.

[339] Arnone D, McKie S, Elliott R, et al. State-dependent changes in hippocampal grey matter in depression. Mol Psychiatry 2013; 18: 1265–1272.

[340] Miners JS, Palmer JC, Love S. Pathophysiology of Hypoperfusion of the Precuneus in Early A lzheimer's Disease. Brain Pathol 2016; 26: 533–541.

[341] Guennewig B, Lim J, Marshall L, et al. Defining early changes in Alzheimer's disease from RNA sequencing of brain regions differentially affected by pathology. Sci Rep 2021; 11: 4865.

[342] Glahn DC, Winkler AM, Kochunov P, et al. Genetic control over the resting brain. Proc Natl Acad Sci 2010; 107: 1223–1228.

[343] Posner J, Hellerstein DJ, Gat I, et al. Antidepressants normalize the default mode network in patients with dysthymia. JAMA Psychiatry 2013; 70: 373–382.

[344] Auer R, Vittinghoff E, Yaffe K, et al. Association Between Lifetime Marijuana Use and Cognitive Function in Middle Age: The Coronary Artery Risk Development in Young Adults (CARDIA) Study. JAMA Intern Med 2016; 176: 352.

[345] McKetin R, Parasu P, Cherbuin N, et al. A longitudinal examination of the relationship between cannabis use and cognitive function in mid-life adults. Drug Alcohol Depend 2016; 169: 134–140.

[346] Knopman DS, Gottesman RF, Sharrett AR, et al. Midlife vascular risk factors and midlife cognitive status in relation to prevalence of mild cognitive impairment and dementia in later life: The Atherosclerosis Risk in Communities Study. Alzheimers Dement 2018; 14: 1406–1415.

[347] Pope HG, Gruber AJ, Hudson JI, et al. Neuropsychological performance in long-term cannabis users. Arch Gen Psychiatry 2001; 58: 909–915.

[348] Burgess S, Labrecque JA. Mendelian randomization with a binary exposure variable: interpretation and presentation of causal estimates. Eur J Epidemiol 2018; 33: 947–952.

[349] Hunault CC, Mensinga TT, Böcker KBE, et al. Cognitive and psychomotor effects in males after smoking a combination of tobacco and cannabis containing up to 69 mg delta-9-tetrahydrocannabinol (THC). Psychopharmacology (Berl) 2009; 204: 85–94.

[350] D'Souza DC, Perry E, MacDougall L, et al. The Psychotomimetic Effects of Intravenous Delta-9-Tetrahydrocannabinol in Healthy Individuals: Implications for Psychosis. Neuropsychopharmacology 2004; 29: 1558–1572.

[351] Morrison PD, Zois V, McKeown DA, et al. The acute effects of synthetic intravenous $\Delta^9$ -tetrahydrocannabinol on psychosis, mood and cognitive functioning. Psychol Med 2009; 39: 1607–1616.

[352] Wadsworth EJK, Moss SC, Simpson SA, et al. Cannabis use, cognitive performance and mood in a sample of workers. J Psychopharmacol (Oxf) 2006; 20: 14–23.

[353] Herzig DA, Nutt DJ, Mohr C. Alcohol and Relatively Pure Cannabis Use, but Not Schizotypy, are Associated with Cognitive Attenuations. Front Psychiatry; 5. Epub ahead of print 29 September 2014. DOI: 10.3389/fpsyt.2014.00133.

[354] Grant JE, Chamberlain SR, Schreiber L, et al. Neuropsychological deficits associated with cannabis use in young adults. Drug Alcohol Depend 2012; 121: 159–162.

[355] Souza EGV, Ramos MG, Hara C, et al. Neuropsychological performance and menstrual cycle: a literature review. Trends Psychiatry Psychother 2012; 34: 5–12.

[356] Brents LK. Marijuana, the Endocannabinoid System and the Female Reproductive System. Yale J Biol Med 2016; 89: 175–191.

[357] Gorzalka BB, Dang SS. Minireview: Endocannabinoids and Gonadal Hormones: Bidirectional Interactions in Physiology and Behavior. Endocrinology 2012; 153: 1016–1024.

[358] Huestis MA. Human cannabinoid pharmacokinetics. Chem Biodivers 2007; 4: 1770–1804.

[359] Davis C, Fattore L. Gender Differences in Cannabis Addiction and Dependence. In: Campolongo P, Fattore L (eds) Cannabinoid Modulation of Emotion, Memory, and Motivation. New York, NY: Springer New York, pp. 283–325.

[360] Newman SD, Cheng H, Schnakenberg Martin A, et al. An Investigation of Neurochemical Changes in Chronic Cannabis Users. Front Hum Neurosci 2019; 13: 318.

[361] Agosti V, Nunes E, Levin F. Rates of Psychiatric Comorbidity Among U.S. Residents with Lifetime Cannabis Dependence. Am J Drug Alcohol Abuse 2002; 28: 643–652.

[362] Rabbitt P, Diggle P, Holland F, et al. Practice and drop-out effects during a 17-year longitudinal study of cognitive aging. J Gerontol B Psychol Sci Soc Sci 2004; 59: P84-97.

[363] Uttl B. Measurement of Individual Differences: Lessons From Memory Assessment in Research and Clinical Practice. Psychol Sci 2005; 16: 460–467.

[364] Gibson LP, Skrzynski CJ, Giordano GR, et al. A daily diary investigation of cannabis use and its diet and exercise correlates. Front Psychol 2023; 14: 1217144.

[365] Lowe DJE, Sasiadek JD, Coles AS, et al. Cannabis and mental illness: a review. Eur Arch Psychiatry Clin Neurosci 2019; 269: 107–120.

[366] McTeague LM, Huemer J, Carreon DM, et al. Identification of Common Neural Circuit Disruptions in Cognitive Control Across Psychiatric Disorders. Am J Psychiatry 2017; 174: 676–685.

# Appendices

## Appendix 1: Individual image-derived structure phenotypes in UK Biobank (n= 2,128)

| | |
|---|---|
| 1) | IDP_T1_SIENAX_peripheral_grey_normalised_volume |
| 2) | IDP_T1_SIENAX_peripheral_grey_unnormalised_volume |
| 3) | IDP_T1_SIENAX_CSF_normalised_volume |
| 4) | IDP_T1_SIENAX_CSF_unnormalised_volume |
| 5) | IDP_T1_SIENAX_grey_normalised_volume |
| 6) | IDP_T1_SIENAX_grey_unnormalised_volume |
| 7) | IDP_T1_SIENAX_white_normalised_volume |
| 8) | IDP_T1_SIENAX_white_unnormalised_volume |
| 9) | IDP_T1_SIENAX_brain-normalised_volume |
| 10) | IDP_T1_SIENAX_brain-unnormalised_volume |
| 11) | IDP_T1_FIRST_left_thalamus_volume |
| 12) | IDP_T1_FIRST_right_thalamus_volume |
| 13) | IDP_T1_FIRST_left_caudate_volume |
| 14) | IDP_T1_FIRST_right_caudate_volume |
| 15) | IDP_T1_FIRST_left_putamen_volume |
| 16) | IDP_T1_FIRST_right_putamen_volume |
| 17) | IDP_T1_FIRST_left_pallidum_volume |
| 18) | IDP_T1_FIRST_right_pallidum_volume |
| 19) | IDP_T1_FIRST_left_hippocampus_volume |
| 20) | IDP_T1_FIRST_right_hippocampus_volume |
| 21) | IDP_T1_FIRST_left_amygdala_volume |
| 22) | IDP_T1_FIRST_right_amygdala_volume |
| 23) | IDP_T1_FIRST_left_accumbens_volume |
| 24) | IDP_T1_FIRST_right_accumbens_volume |
| 25) | IDP_T1_FIRST_brain_stem+4th_ventricle_volume |
| 26) | IDP_T1_FAST_ROIs_L_frontal_pole |
| 27) | IDP_T1_FAST_ROIs_R_frontal_pole |
| 28) | IDP_T1_FAST_ROIs_L_insular_cortex |
| 29) | IDP_T1_FAST_ROIs_R_insular_cortex |
| 30) | IDP_T1_FAST_ROIs_L_sup_front_gyrus |
| 31) | IDP_T1_FAST_ROIs_R_sup_front_gyrus |
| 32) | IDP_T1_FAST_ROIs_L_mid_front_gyrus |
| 33) | IDP_T1_FAST_ROIs_R_mid_front_gyrus |
| 34) | IDP_T1_FAST_ROIs_L_inf_front_gyrus_parstri |
| 35) | IDP_T1_FAST_ROIs_R_inf_front_gyrus_parstri |
| 36) | IDP_T1_FAST_ROIs_L_inf_front_gyrus_parsop |

| | |
|---|---|
| 37) | IDP_T1_FAST_ROIs_R_inf_front_gyrus_parsop |
| 38) | IDP_T1_FAST_ROIs_L_precentral_gyrus |
| 39) | IDP_T1_FAST_ROIs_R_precentral_gyrus |
| 40) | IDP_T1_FAST_ROIs_L_temporal_pole |
| 41) | IDP_T1_FAST_ROIs_R_temporal_pole |
| 42) | IDP_T1_FAST_ROIs_L_sup_temporal_gyrus_ant |
| 43) | IDP_T1_FAST_ROIs_R_sup_temporal_gyrus_ant |
| 44) | IDP_T1_FAST_ROIs_L_sup_temporal_gyrus_post |
| 45) | IDP_T1_FAST_ROIs_R_sup_temporal_gyrus_post |
| 46) | IDP_T1_FAST_ROIs_L_mid_temporal_gyrus_ant |
| 47) | IDP_T1_FAST_ROIs_R_mid_temporal_gyrus_ant |
| 48) | IDP_T1_FAST_ROIs_L_mid_temporal_gyrus_post |
| 49) | IDP_T1_FAST_ROIs_R_mid_temporal_gyrus_post |
| 50) | IDP_T1_FAST_ROIs_L_mid_temporal_gyrus_temporo-occipital |
| 51) | IDP_T1_FAST_ROIs_R_mid_temporal_gyrus_temporo-occipital |
| 52) | IDP_T1_FAST_ROIs_L_inf_temporal_gyrus_ant |
| 53) | IDP_T1_FAST_ROIs_R_inf_temporal_gyrus_ant |
| 54) | IDP_T1_FAST_ROIs_L_inf_temporal_gyrus_post |
| 55) | IDP_T1_FAST_ROIs_R_inf_temporal_gyrus_post |
| 56) | IDP_T1_FAST_ROIs_L_inf_temporal_gyrus_temporo-occipital |
| 57) | IDP_T1_FAST_ROIs_R_inf_temporal_gyrus_temporo-occipital |
| 58) | IDP_T1_FAST_ROIs_L_postcent_gyrus |
| 59) | IDP_T1_FAST_ROIs_R_postcent_gyrus |
| 60) | IDP_T1_FAST_ROIs_L_sup_parietal_lobule |
| 61) | IDP_T1_FAST_ROIs_R_sup_parietal_lobule |
| 62) | IDP_T1_FAST_ROIs_L_supramarg_gyrus_ant |
| 63) | IDP_T1_FAST_ROIs_R_supramarg_gyrus_ant |
| 64) | IDP_T1_FAST_ROIs_L_supramarg_gyrus_post |
| 65) | IDP_T1_FAST_ROIs_R_supramarg_gyrus_post |
| 66) | IDP_T1_FAST_ROIs_L_angular_gyrus |
| 67) | IDP_T1_FAST_ROIs_R_angular_gyrus |
| 68) | IDP_T1_FAST_ROIs_L_lateral-occipital_cortex_sup |
| 69) | IDP_T1_FAST_ROIs_R_lateral-occipital_cortex_sup |
| 70) | IDP_T1_FAST_ROIs_L_lateral-occipital_cortex_inf |
| 71) | IDP_T1_FAST_ROIs_R_lateral-occipital_cortex_inf |
| 72) | IDP_T1_FAST_ROIs_L_intracalcarine_cortex |
| 73) | IDP_T1_FAST_ROIs_R_intracalcarine_cortex |
| 74) | IDP_T1_FAST_ROIs_L_front_med_cortex |
| 75) | IDP_T1_FAST_ROIs_R_front_med_cortex |
| 76) | IDP_T1_FAST_ROIs_L_juxtapositional_lobule_cortex |
| 77) | IDP_T1_FAST_ROIs_R_juxtapositional_lobule_cortex |
| 78) | IDP_T1_FAST_ROIs_L_subcallosal_cortex |

| | |
|---|---|
| 79) | IDP_T1_FAST_ROIs_R_subcallosal_cortex |
| 80) | IDP_T1_FAST_ROIs_L_paracing_gyrus |
| 81) | IDP_T1_FAST_ROIs_R_paracing_gyrus |
| 82) | IDP_T1_FAST_ROIs_L_cing_gyrus_ant |
| 83) | IDP_T1_FAST_ROIs_R_cing_gyrus_ant |
| 84) | IDP_T1_FAST_ROIs_L_cing_gyrus_post |
| 85) | IDP_T1_FAST_ROIs_R_cing_gyrus_post |
| 86) | IDP_T1_FAST_ROIs_L_precun_cortex |
| 87) | IDP_T1_FAST_ROIs_R_precun_cortex |
| 88) | IDP_T1_FAST_ROIs_L_cuneal_cortex |
| 89) | IDP_T1_FAST_ROIs_R_cuneal_cortex |
| 90) | IDP_T1_FAST_ROIs_L_front_orb_cortex |
| 91) | IDP_T1_FAST_ROIs_R_front_orb_cortex |
| 92) | IDP_T1_FAST_ROIs_L_parahipp_gyrus_ant |
| 93) | IDP_T1_FAST_ROIs_R_parahipp_gyrus_ant |
| 94) | IDP_T1_FAST_ROIs_L_parahipp_gyrus_post |
| 95) | IDP_T1_FAST_ROIs_R_parahipp_gyrus_post |
| 96) | IDP_T1_FAST_ROIs_L_lingual_gyrus |
| 97) | IDP_T1_FAST_ROIs_R_lingual_gyrus |
| 98) | IDP_T1_FAST_ROIs_L_temporo_fusiform_cortex_ant |
| 99) | IDP_T1_FAST_ROIs_R_temporo_fusiform_cortex_ant |
| 100) | IDP_T1_FAST_ROIs_L_temporo_fusiform_cortex_post |
| 101) | IDP_T1_FAST_ROIs_R_temporo_fusiform_cortex_post |
| 102) | IDP_T1_FAST_ROIs_L_temporo_occipital_fusiform_cortex |
| 103) | IDP_T1_FAST_ROIs_R_temporo_occipital_fusiform_cortex |
| 104) | IDP_T1_FAST_ROIs_L_occipital_fusiform_gyrus |
| 105) | IDP_T1_FAST_ROIs_R_occipital_fusiform_gyrus |
| 106) | IDP_T1_FAST_ROIs_L_front_opercular_cortex |
| 107) | IDP_T1_FAST_ROIs_R_front_opercular_cortex |
| 108) | IDP_T1_FAST_ROIs_L_cent_opercular_cortex |
| 109) | IDP_T1_FAST_ROIs_R_cent_opercular_cortex |
| 110) | IDP_T1_FAST_ROIs_L_parietal_opercular_cortex |
| 111) | IDP_T1_FAST_ROIs_R_parietal_opercular_cortex |
| 112) | IDP_T1_FAST_ROIs_L_planum_polare |
| 113) | IDP_T1_FAST_ROIs_R_planum_polare |
| 114) | IDP_T1_FAST_ROIs_L_heschl_gyrus |
| 115) | IDP_T1_FAST_ROIs_R_heschl_gyrus |
| 116) | IDP_T1_FAST_ROIs_L_planum_temporale |
| 117) | IDP_T1_FAST_ROIs_R_planum_temporale |
| 118) | IDP_T1_FAST_ROIs_L_supracalc_cortex |
| 119) | IDP_T1_FAST_ROIs_R_supracalc_cortex |
| 120) | IDP_T1_FAST_ROIs_L_occipital_pole |

| | |
|---|---|
| 121) | IDP_T1_FAST_ROIs_R_occipital_pole |
| 122) | IDP_T1_FAST_ROIs_L_thalamus |
| 123) | IDP_T1_FAST_ROIs_R_thalamus |
| 124) | IDP_T1_FAST_ROIs_L_caudate |
| 125) | IDP_T1_FAST_ROIs_R_caudate |
| 126) | IDP_T1_FAST_ROIs_L_putamen |
| 127) | IDP_T1_FAST_ROIs_R_putamen |
| 128) | IDP_T1_FAST_ROIs_L_pallidum |
| 129) | IDP_T1_FAST_ROIs_R_pallidum |
| 130) | IDP_T1_FAST_ROIs_L_hippocampus |
| 131) | IDP_T1_FAST_ROIs_R_hippocampus |
| 132) | IDP_T1_FAST_ROIs_L_amygdala |
| 133) | IDP_T1_FAST_ROIs_R_amygdala |
| 134) | IDP_T1_FAST_ROIs_L_ventral_striatum |
| 135) | IDP_T1_FAST_ROIs_R_ventral_striatum |
| 136) | IDP_T1_FAST_ROIs_brain_stem |
| 137) | IDP_T1_FAST_ROIs_L_cerebellum_I-IV |
| 138) | IDP_T1_FAST_ROIs_R_cerebellum_I-IV |
| 139) | IDP_T1_FAST_ROIs_L_cerebellum_V |
| 140) | IDP_T1_FAST_ROIs_R_cerebellum_V |
| 141) | IDP_T1_FAST_ROIs_L_cerebellum_VI |
| 142) | IDP_T1_FAST_ROIs_V_cerebellum_VI |
| 143) | IDP_T1_FAST_ROIs_R_cerebellum_VI |
| 144) | IDP_T1_FAST_ROIs_L_cerebellum_crus_I |
| 145) | IDP_T1_FAST_ROIs_V_cerebellum_crus_I |
| 146) | IDP_T1_FAST_ROIs_R_cerebellum_crus_I |
| 147) | IDP_T1_FAST_ROIs_L_cerebellum_crus_II |
| 148) | IDP_T1_FAST_ROIs_V_cerebellum_crus_II |
| 149) | IDP_T1_FAST_ROIs_R_cerebellum_crus_II |
| 150) | IDP_T1_FAST_ROIs_L_cerebellum_VIIb |
| 151) | IDP_T1_FAST_ROIs_V_cerebellum_VIIb |
| 152) | IDP_T1_FAST_ROIs_R_cerebellum_VIIb |
| 153) | IDP_T1_FAST_ROIs_L_cerebellum_VIIIa |
| 154) | IDP_T1_FAST_ROIs_V_cerebellum_VIIIa |
| 155) | IDP_T1_FAST_ROIs_R_cerebellum_VIIIa |
| 156) | IDP_T1_FAST_ROIs_L_cerebellum_VIIIb |
| 157) | IDP_T1_FAST_ROIs_V_cerebellum_VIIIb |
| 158) | IDP_T1_FAST_ROIs_R_cerebellum_VIIIb |
| 159) | IDP_T1_FAST_ROIs_L_cerebellum_IX |
| 160) | IDP_T1_FAST_ROIs_V_cerebellum_IX |
| 161) | IDP_T1_FAST_ROIs_R_cerebellum_IX |
| 162) | IDP_T1_FAST_ROIs_L_cerebellum_X |

| | |
|---|---|
| 163) | IDP_T1_FAST_ROIs_V_cerebellum_X |
| 164) | IDP_T1_FAST_ROIs_R_cerebellum_X |
| 165) | aseg_global_volume_BrainSeg |
| 166) | aseg_global_volume_BrainSegNotVent |
| 167) | aseg_global_volume_BrainSegNotVentSurf |
| 168) | aseg_global_volume_SubCortGray |
| 169) | aseg_global_volume_TotalGray |
| 170) | aseg_global_volume_SupraTentorial |
| 171) | aseg_global_volume_SupraTentorialNotVent |
| 172) | aseg_global_volume_EstimatedTotalIntraCranial |
| 173) | aseg_global_volume_VentricleChoroid |
| 174) | aseg_global_volume_3rd-Ventricle |
| 175) | aseg_global_volume_4th-Ventricle |
| 176) | aseg_global_volume_5th-Ventricle |
| 177) | aseg_global_volume_Brain-Stem |
| 178) | aseg_global_volume_CSF |
| 179) | aseg_global_volume_WM-hypointensities |
| 180) | aseg_global_volume_non-WM-hypointensities |
| 181) | aseg_global_volume_Optic-Chiasm |
| 182) | aseg_global_volume_CC-Posterior |
| 183) | aseg_global_volume_CC-Mid-Posterior |
| 184) | aseg_global_volume_CC-Central |
| 185) | aseg_global_volume_CC-Mid-Anterior |
| 186) | aseg_global_volume_CC-Anterior |
| 187) | aseg_global_volume-ratio_BrainSegVol-to-eTIV |
| 188) | aseg_global_volume-ratio_MaskVol-to-eTIV |
| 189) | aseg_lh_volume_Cortex |
| 190) | aseg_lh_volume_CerebralWhiteMatter |
| 191) | aseg_lh_volume_Lateral-Ventricle |
| 192) | aseg_lh_volume_Inf-Lat-Vent |
| 193) | aseg_lh_volume_Cerebellum-White-Matter |
| 194) | aseg_lh_volume_Cerebellum-Cortex |
| 195) | aseg_lh_volume_Thalamus-Proper |
| 196) | aseg_lh_volume_Caudate |
| 197) | aseg_lh_volume_Putamen |
| 198) | aseg_lh_volume_Pallidum |
| 199) | aseg_lh_volume_Hippocampus |
| 200) | aseg_lh_volume_Amygdala |
| 201) | aseg_lh_volume_Accumbens-area |
| 202) | aseg_lh_volume_VentralDC |
| 203) | aseg_lh_volume_vessel |
| 204) | aseg_lh_volume_choroid-plexus |

| | |
|---|---|
| 205) | aseg_lh_number_HolesBeforeFixing |
| 206) | aseg_rh_volume_Cortex |
| 207) | aseg_rh_volume_CerebralWhiteMatter |
| 208) | aseg_rh_volume_Lateral-Ventricle |
| 209) | aseg_rh_volume_Inf-Lat-Vent |
| 210) | aseg_rh_volume_Cerebellum-White-Matter |
| 211) | aseg_rh_volume_Cerebellum-Cortex |
| 212) | aseg_rh_volume_Thalamus-Proper |
| 213) | aseg_rh_volume_Caudate |
| 214) | aseg_rh_volume_Putamen |
| 215) | aseg_rh_volume_Pallidum |
| 216) | aseg_rh_volume_Hippocampus |
| 217) | aseg_rh_volume_Amygdala |
| 218) | aseg_rh_volume_Accumbens-area |
| 219) | aseg_rh_volume_VentralDC |
| 220) | aseg_rh_volume_vessel |
| 221) | aseg_rh_volume_choroid-plexus |
| 222) | aseg_rh_number_HolesBeforeFixing |
| 223) | AmygNuclei_lh_volume_Lateral-nucleus |
| 224) | AmygNuclei_lh_volume_Basal-nucleus |
| 225) | AmygNuclei_lh_volume_Accessory-Basal-nucleus |
| 226) | AmygNuclei_lh_volume_Anterior-amygdaloid-area-AAA |
| 227) | AmygNuclei_lh_volume_Central-nucleus |
| 228) | AmygNuclei_lh_volume_Medial-nucleus |
| 229) | AmygNuclei_lh_volume_Cortical-nucleus |
| 230) | AmygNuclei_lh_volume_Corticoamygdaloid-transitio |
| 231) | AmygNuclei_lh_volume_Paralaminar-nucleus |
| 232) | AmygNuclei_lh_volume_Whole-amygdala |
| 233) | AmygNuclei_rh_volume_Lateral-nucleus |
| 234) | AmygNuclei_rh_volume_Basal-nucleus |
| 235) | AmygNuclei_rh_volume_Accessory-Basal-nucleus |
| 236) | AmygNuclei_rh_volume_Anterior-amygdaloid-area-AAA |
| 237) | AmygNuclei_rh_volume_Central-nucleus |
| 238) | AmygNuclei_rh_volume_Medial-nucleus |
| 239) | AmygNuclei_rh_volume_Cortical-nucleus |
| 240) | AmygNuclei_rh_volume_Corticoamygdaloid-transitio |
| 241) | AmygNuclei_rh_volume_Paralaminar-nucleus |
| 242) | AmygNuclei_rh_volume_Whole-amygdala |
| 243) | HippSubfield_lh_volume_Hippocampal-tail |
| 244) | HippSubfield_lh_volume_subiculum-body |
| 245) | HippSubfield_lh_volume_CA1-body |
| 246) | HippSubfield_lh_volume_subiculum-head |

| | |
|---|---|
| 247) | HippSubfield_lh_volume_hippocampal-fissure |
| 248) | HippSubfield_lh_volume_presubiculum-head |
| 249) | HippSubfield_lh_volume_CA1-head |
| 250) | HippSubfield_lh_volume_presubiculum-body |
| 251) | HippSubfield_lh_volume_parasubiculum |
| 252) | HippSubfield_lh_volume_molecular-layer-HP-head |
| 253) | HippSubfield_lh_volume_molecular-layer-HP-body |
| 254) | HippSubfield_lh_volume_GC-ML-DG-head |
| 255) | HippSubfield_lh_volume_CA3-body |
| 256) | HippSubfield_lh_volume_GC-ML-DG-body |
| 257) | HippSubfield_lh_volume_CA4-head |
| 258) | HippSubfield_lh_volume_CA4-body |
| 259) | HippSubfield_lh_volume_fimbria |
| 260) | HippSubfield_lh_volume_CA3-head |
| 261) | HippSubfield_lh_volume_HATA |
| 262) | HippSubfield_lh_volume_Whole-hippocampal-body |
| 263) | HippSubfield_lh_volume_Whole-hippocampal-head |
| 264) | HippSubfield_lh_volume_Whole-hippocampus |
| 265) | HippSubfield_rh_volume_Hippocampal-tail |
| 266) | HippSubfield_rh_volume_subiculum-body |
| 267) | HippSubfield_rh_volume_CA1-body |
| 268) | HippSubfield_rh_volume_subiculum-head |
| 269) | HippSubfield_rh_volume_hippocampal-fissure |
| 270) | HippSubfield_rh_volume_presubiculum-head |
| 271) | HippSubfield_rh_volume_CA1-head |
| 272) | HippSubfield_rh_volume_presubiculum-body |
| 273) | HippSubfield_rh_volume_parasubiculum |
| 274) | HippSubfield_rh_volume_molecular-layer-HP-head |
| 275) | HippSubfield_rh_volume_molecular-layer-HP-body |
| 276) | HippSubfield_rh_volume_GC-ML-DG-head |
| 277) | HippSubfield_rh_volume_CA3-body |
| 278) | HippSubfield_rh_volume_GC-ML-DG-body |
| 279) | HippSubfield_rh_volume_CA4-head |
| 280) | HippSubfield_rh_volume_CA4-body |
| 281) | HippSubfield_rh_volume_fimbria |
| 282) | HippSubfield_rh_volume_CA3-head |
| 283) | HippSubfield_rh_volume_HATA |
| 284) | HippSubfield_rh_volume_Whole-hippocampal-body |
| 285) | HippSubfield_rh_volume_Whole-hippocampal-head |
| 286) | HippSubfield_rh_volume_Whole-hippocampus |
| 287) | ThalamNuclei_lh_volume_MGN |
| 288) | ThalamNuclei_lh_volume_LGN |

| | |
|---|---|
| 289) | ThalamNuclei_lh_volume_PuI |
| 290) | ThalamNuclei_lh_volume_PuM |
| 291) | ThalamNuclei_lh_volume_L-Sg |
| 292) | ThalamNuclei_lh_volume_VPL |
| 293) | ThalamNuclei_lh_volume_CM |
| 294) | ThalamNuclei_lh_volume_VLa |
| 295) | ThalamNuclei_lh_volume_PuA |
| 296) | ThalamNuclei_lh_volume_MDm |
| 297) | ThalamNuclei_lh_volume_Pf |
| 298) | ThalamNuclei_lh_volume_VAmc |
| 299) | ThalamNuclei_lh_volume_MDl |
| 300) | ThalamNuclei_lh_volume_CeM |
| 301) | ThalamNuclei_lh_volume_VA |
| 302) | ThalamNuclei_lh_volume_MV(Re) |
| 303) | ThalamNuclei_lh_volume_VM |
| 304) | ThalamNuclei_lh_volume_CL |
| 305) | ThalamNuclei_lh_volume_PuL |
| 306) | ThalamNuclei_lh_volume_Pt |
| 307) | ThalamNuclei_lh_volume_AV |
| 308) | ThalamNuclei_lh_volume_Pc |
| 309) | ThalamNuclei_lh_volume_VLp |
| 310) | ThalamNuclei_lh_volume_LP |
| 311) | ThalamNuclei_rh_volume_LGN |
| 312) | ThalamNuclei_rh_volume_MGN |
| 313) | ThalamNuclei_rh_volume_PuI |
| 314) | ThalamNuclei_rh_volume_PuM |
| 315) | ThalamNuclei_rh_volume_L-Sg |
| 316) | ThalamNuclei_rh_volume_VPL |
| 317) | ThalamNuclei_rh_volume_CM |
| 318) | ThalamNuclei_rh_volume_VLa |
| 319) | ThalamNuclei_rh_volume_PuA |
| 320) | ThalamNuclei_rh_volume_MDm |
| 321) | ThalamNuclei_rh_volume_Pf |
| 322) | ThalamNuclei_rh_volume_VAmc |
| 323) | ThalamNuclei_rh_volume_MDl |
| 324) | ThalamNuclei_rh_volume_VA |
| 325) | ThalamNuclei_rh_volume_MV(Re) |
| 326) | ThalamNuclei_rh_volume_CeM |
| 327) | ThalamNuclei_rh_volume_VM |
| 328) | ThalamNuclei_rh_volume_PuL |
| 329) | ThalamNuclei_rh_volume_CL |
| 330) | ThalamNuclei_rh_volume_VLp |

| | |
|---|---|
| 331) | ThalamNuclei_rh_volume_Pc |
| 332) | ThalamNuclei_rh_volume_Pt |
| 333) | ThalamNuclei_rh_volume_AV |
| 334) | ThalamNuclei_rh_volume_LP |
| 335) | ThalamNuclei_lh_volume_LD |
| 336) | ThalamNuclei_rh_volume_LD |
| 337) | ThalamNuclei_lh_volume_Whole-thalamus |
| 338) | ThalamNuclei_rh_volume_Whole-thalamus |
| 339) | Brainstem_global_volume_Medulla |
| 340) | Brainstem_global_volume_Pons |
| 341) | Brainstem_global_volume_SCP |
| 342) | Brainstem_global_volume_Midbrain |
| 343) | Brainstem_global_volume_Whole-brainstem |
| 344) | aparc-Desikan_lh_volume_bankssts |
| 345) | aparc-Desikan_lh_volume_caudalanteriorcingulate |
| 346) | aparc-Desikan_lh_volume_caudalmiddlefrontal |
| 347) | aparc-Desikan_lh_volume_cuneus |
| 348) | aparc-Desikan_lh_volume_entorhinal |
| 349) | aparc-Desikan_lh_volume_fusiform |
| 350) | aparc-Desikan_lh_volume_inferiorparietal |
| 351) | aparc-Desikan_lh_volume_inferiortemporal |
| 352) | aparc-Desikan_lh_volume_isthmuscingulate |
| 353) | aparc-Desikan_lh_volume_lateraloccipital |
| 354) | aparc-Desikan_lh_volume_lateralorbitofrontal |
| 355) | aparc-Desikan_lh_volume_lingual |
| 356) | aparc-Desikan_lh_volume_medialorbitofrontal |
| 357) | aparc-Desikan_lh_volume_middletemporal |
| 358) | aparc-Desikan_lh_volume_parahippocampal |
| 359) | aparc-Desikan_lh_volume_paracentral |
| 360) | aparc-Desikan_lh_volume_parsopercularis |
| 361) | aparc-Desikan_lh_volume_parsorbitalis |
| 362) | aparc-Desikan_lh_volume_parstriangularis |
| 363) | aparc-Desikan_lh_volume_pericalcarine |
| 364) | aparc-Desikan_lh_volume_postcentral |
| 365) | aparc-Desikan_lh_volume_posteriorcingulate |
| 366) | aparc-Desikan_lh_volume_precentral |
| 367) | aparc-Desikan_lh_volume_precuneus |
| 368) | aparc-Desikan_lh_volume_rostralanteriorcingulate |
| 369) | aparc-Desikan_lh_volume_rostralmiddlefrontal |
| 370) | aparc-Desikan_lh_volume_superiorfrontal |
| 371) | aparc-Desikan_lh_volume_superiorparietal |
| 372) | aparc-Desikan_lh_volume_superiortemporal |

| | |
|---|---|
| 373) | aparc-Desikan_lh_volume_supramarginal |
| 374) | aparc-Desikan_lh_volume_frontalpole |
| 375) | aparc-Desikan_lh_volume_transversetemporal |
| 376) | aparc-Desikan_lh_volume_insula |
| 377) | aparc-Desikan_rh_volume_bankssts |
| 378) | aparc-Desikan_rh_volume_caudalanteriorcingulate |
| 379) | aparc-Desikan_rh_volume_caudalmiddlefrontal |
| 380) | aparc-Desikan_rh_volume_cuneus |
| 381) | aparc-Desikan_rh_volume_entorhinal |
| 382) | aparc-Desikan_rh_volume_fusiform |
| 383) | aparc-Desikan_rh_volume_inferiorparietal |
| 384) | aparc-Desikan_rh_volume_inferiortemporal |
| 385) | aparc-Desikan_rh_volume_isthmuscingulate |
| 386) | aparc-Desikan_rh_volume_lateraloccipital |
| 387) | aparc-Desikan_rh_volume_lateralorbitofrontal |
| 388) | aparc-Desikan_rh_volume_lingual |
| 389) | aparc-Desikan_rh_volume_medialorbitofrontal |
| 390) | aparc-Desikan_rh_volume_middletemporal |
| 391) | aparc-Desikan_rh_volume_parahippocampal |
| 392) | aparc-Desikan_rh_volume_paracentral |
| 393) | aparc-Desikan_rh_volume_parsopercularis |
| 394) | aparc-Desikan_rh_volume_parsorbitalis |
| 395) | aparc-Desikan_rh_volume_parstriangularis |
| 396) | aparc-Desikan_rh_volume_pericalcarine |
| 397) | aparc-Desikan_rh_volume_postcentral |
| 398) | aparc-Desikan_rh_volume_posteriorcingulate |
| 399) | aparc-Desikan_rh_volume_precentral |
| 400) | aparc-Desikan_rh_volume_precuneus |
| 401) | aparc-Desikan_rh_volume_rostralanteriorcingulate |
| 402) | aparc-Desikan_rh_volume_rostralmiddlefrontal |
| 403) | aparc-Desikan_rh_volume_superiorfrontal |
| 404) | aparc-Desikan_rh_volume_superiorparietal |
| 405) | aparc-Desikan_rh_volume_superiortemporal |
| 406) | aparc-Desikan_rh_volume_supramarginal |
| 407) | aparc-Desikan_rh_volume_frontalpole |
| 408) | aparc-Desikan_rh_volume_transversetemporal |
| 409) | aparc-Desikan_rh_volume_insula |
| 410) | BA-exvivo_lh_volume_BA1 |
| 411) | BA-exvivo_lh_volume_BA2 |
| 412) | BA-exvivo_lh_volume_BA3a |
| 413) | BA-exvivo_lh_volume_BA3b |
| 414) | BA-exvivo_lh_volume_BA4a |

| | |
|---|---|
| 415) | BA-exvivo_lh_volume_BA4p |
| 416) | BA-exvivo_lh_volume_BA6 |
| 417) | BA-exvivo_lh_volume_BA44 |
| 418) | BA-exvivo_lh_volume_BA45 |
| 419) | BA-exvivo_lh_volume_V1 |
| 420) | BA-exvivo_lh_volume_V2 |
| 421) | BA-exvivo_lh_volume_MT |
| 422) | BA-exvivo_lh_volume_perirhinal |
| 423) | BA-exvivo_lh_volume_entorhinal |
| 424) | BA-exvivo_rh_volume_BA1 |
| 425) | BA-exvivo_rh_volume_BA2 |
| 426) | BA-exvivo_rh_volume_BA3a |
| 427) | BA-exvivo_rh_volume_BA3b |
| 428) | BA-exvivo_rh_volume_BA4a |
| 429) | BA-exvivo_rh_volume_BA4p |
| 430) | BA-exvivo_rh_volume_BA6 |
| 431) | BA-exvivo_rh_volume_BA44 |
| 432) | BA-exvivo_rh_volume_BA45 |
| 433) | BA-exvivo_rh_volume_V1 |
| 434) | BA-exvivo_rh_volume_V2 |
| 435) | BA-exvivo_rh_volume_MT |
| 436) | BA-exvivo_rh_volume_perirhinal |
| 437) | BA-exvivo_rh_volume_entorhinal |
| 438) | aparc-DKTatlas_lh_volume_caudalanteriorcingulate |
| 439) | aparc-DKTatlas_lh_volume_caudalmiddlefrontal |
| 440) | aparc-DKTatlas_lh_volume_cuneus |
| 441) | aparc-DKTatlas_lh_volume_entorhinal |
| 442) | aparc-DKTatlas_lh_volume_fusiform |
| 443) | aparc-DKTatlas_lh_volume_inferiorparietal |
| 444) | aparc-DKTatlas_lh_volume_inferiortemporal |
| 445) | aparc-DKTatlas_lh_volume_isthmuscingulate |
| 446) | aparc-DKTatlas_lh_volume_lateraloccipital |
| 447) | aparc-DKTatlas_lh_volume_lateralorbitofrontal |
| 448) | aparc-DKTatlas_lh_volume_lingual |
| 449) | aparc-DKTatlas_lh_volume_medialorbitofrontal |
| 450) | aparc-DKTatlas_lh_volume_middletemporal |
| 451) | aparc-DKTatlas_lh_volume_parahippocampal |
| 452) | aparc-DKTatlas_lh_volume_paracentral |
| 453) | aparc-DKTatlas_lh_volume_parsopercularis |
| 454) | aparc-DKTatlas_lh_volume_parsorbitalis |
| 455) | aparc-DKTatlas_lh_volume_parstriangularis |
| 456) | aparc-DKTatlas_lh_volume_pericalcarine |

| | |
|---|---|
| 457) | aparc-DKTatlas_lh_volume_postcentral |
| 458) | aparc-DKTatlas_lh_volume_posteriorcingulate |
| 459) | aparc-DKTatlas_lh_volume_precentral |
| 460) | aparc-DKTatlas_lh_volume_precuneus |
| 461) | aparc-DKTatlas_lh_volume_rostralanteriorcingulate |
| 462) | aparc-DKTatlas_lh_volume_rostralmiddlefrontal |
| 463) | aparc-DKTatlas_lh_volume_superiorfrontal |
| 464) | aparc-DKTatlas_lh_volume_superiorparietal |
| 465) | aparc-DKTatlas_lh_volume_superiortemporal |
| 466) | aparc-DKTatlas_lh_volume_supramarginal |
| 467) | aparc-DKTatlas_lh_volume_transversetemporal |
| 468) | aparc-DKTatlas_lh_volume_insula |
| 469) | aparc-DKTatlas_rh_volume_caudalanteriorcingulate |
| 470) | aparc-DKTatlas_rh_volume_caudalmiddlefrontal |
| 471) | aparc-DKTatlas_rh_volume_cuneus |
| 472) | aparc-DKTatlas_rh_volume_entorhinal |
| 473) | aparc-DKTatlas_rh_volume_fusiform |
| 474) | aparc-DKTatlas_rh_volume_inferiorparietal |
| 475) | aparc-DKTatlas_rh_volume_inferiortemporal |
| 476) | aparc-DKTatlas_rh_volume_isthmuscingulate |
| 477) | aparc-DKTatlas_rh_volume_lateraloccipital |
| 478) | aparc-DKTatlas_rh_volume_lateralorbitofrontal |
| 479) | aparc-DKTatlas_rh_volume_lingual |
| 480) | aparc-DKTatlas_rh_volume_medialorbitofrontal |
| 481) | aparc-DKTatlas_rh_volume_middletemporal |
| 482) | aparc-DKTatlas_rh_volume_parahippocampal |
| 483) | aparc-DKTatlas_rh_volume_paracentral |
| 484) | aparc-DKTatlas_rh_volume_parsopercularis |
| 485) | aparc-DKTatlas_rh_volume_parsorbitalis |
| 486) | aparc-DKTatlas_rh_volume_parstriangularis |
| 487) | aparc-DKTatlas_rh_volume_pericalcarine |
| 488) | aparc-DKTatlas_rh_volume_postcentral |
| 489) | aparc-DKTatlas_rh_volume_posteriorcingulate |
| 490) | aparc-DKTatlas_rh_volume_precentral |
| 491) | aparc-DKTatlas_rh_volume_precuneus |
| 492) | aparc-DKTatlas_rh_volume_rostralanteriorcingulate |
| 493) | aparc-DKTatlas_rh_volume_rostralmiddlefrontal |
| 494) | aparc-DKTatlas_rh_volume_superiorfrontal |
| 495) | aparc-DKTatlas_rh_volume_superiorparietal |
| 496) | aparc-DKTatlas_rh_volume_superiortemporal |
| 497) | aparc-DKTatlas_rh_volume_supramarginal |
| 498) | aparc-DKTatlas_rh_volume_transversetemporal |

| | |
|---|---|
| 499) | aparc-DKTatlas_rh_volume_insula |
| 500) | aparc-a2009s_lh_volume_G+S-frontomargin |
| 501) | aparc-a2009s_lh_volume_G+S-occipital-inf |
| 502) | aparc-a2009s_lh_volume_G+S-paracentral |
| 503) | aparc-a2009s_lh_volume_G+S-subcentral |
| 504) | aparc-a2009s_lh_volume_G+S-transv-frontopol |
| 505) | aparc-a2009s_lh_volume_G+S-cingul-Ant |
| 506) | aparc-a2009s_lh_volume_G+S-cingul-Mid-Ant |
| 507) | aparc-a2009s_lh_volume_G+S-cingul-Mid-Post |
| 508) | aparc-a2009s_lh_volume_G-cingul-Post-dorsal |
| 509) | aparc-a2009s_lh_volume_G-cingul-Post-ventral |
| 510) | aparc-a2009s_lh_volume_G-cuneus |
| 511) | aparc-a2009s_lh_volume_G-front-inf-Opercular |
| 512) | aparc-a2009s_lh_volume_G-front-inf-Orbital |
| 513) | aparc-a2009s_lh_volume_G-front-inf-Triangul |
| 514) | aparc-a2009s_lh_volume_G-front-middle |
| 515) | aparc-a2009s_lh_volume_G-front-sup |
| 516) | aparc-a2009s_lh_volume_G-Ins-lg+S-cent-ins |
| 517) | aparc-a2009s_lh_volume_G-insular-short |
| 518) | aparc-a2009s_lh_volume_G-occipital-middle |
| 519) | aparc-a2009s_lh_volume_G-occipital-sup |
| 520) | aparc-a2009s_lh_volume_G-oc-temp-lat-fusifor |
| 521) | aparc-a2009s_lh_volume_G-oc-temp-med-Lingual |
| 522) | aparc-a2009s_lh_volume_G-oc-temp-med-Parahip |
| 523) | aparc-a2009s_lh_volume_G-orbital |
| 524) | aparc-a2009s_lh_volume_G-pariet-inf-Angular |
| 525) | aparc-a2009s_lh_volume_G-pariet-inf-Supramar |
| 526) | aparc-a2009s_lh_volume_G-parietal-sup |
| 527) | aparc-a2009s_lh_volume_G-postcentral |
| 528) | aparc-a2009s_lh_volume_G-precentral |
| 529) | aparc-a2009s_lh_volume_G-precuneus |
| 530) | aparc-a2009s_lh_volume_G-rectus |
| 531) | aparc-a2009s_lh_volume_G-subcallosal |
| 532) | aparc-a2009s_lh_volume_G-temp-sup-G-T-transv |
| 533) | aparc-a2009s_lh_volume_G-temp-sup-Lateral |
| 534) | aparc-a2009s_lh_volume_G-temp-sup-Plan-polar |
| 535) | aparc-a2009s_lh_volume_G-temp-sup-Plan-tempo |
| 536) | aparc-a2009s_lh_volume_G-temporal-inf |
| 537) | aparc-a2009s_lh_volume_G-temporal-middle |
| 538) | aparc-a2009s_lh_volume_Lat-Fis-ant-Horizont |
| 539) | aparc-a2009s_lh_volume_Lat-Fis-ant-Vertical |
| 540) | aparc-a2009s_lh_volume_Lat-Fis-post |

| | |
|---|---|
| 541) | aparc-a2009s_lh_volume_Pole-occipital |
| 542) | aparc-a2009s_lh_volume_Pole-temporal |
| 543) | aparc-a2009s_lh_volume_S-calcarine |
| 544) | aparc-a2009s_lh_volume_S-central |
| 545) | aparc-a2009s_lh_volume_S-cingul-Marginalis |
| 546) | aparc-a2009s_lh_volume_S-circular-insula-ant |
| 547) | aparc-a2009s_lh_volume_S-circular-insula-inf |
| 548) | aparc-a2009s_lh_volume_S-circular-insula-sup |
| 549) | aparc-a2009s_lh_volume_S-collat-transv-ant |
| 550) | aparc-a2009s_lh_volume_S-collat-transv-post |
| 551) | aparc-a2009s_lh_volume_S-front-inf |
| 552) | aparc-a2009s_lh_volume_S-front-middle |
| 553) | aparc-a2009s_lh_volume_S-front-sup |
| 554) | aparc-a2009s_lh_volume_S-interm-prim-Jensen |
| 555) | aparc-a2009s_lh_volume_S-intrapariet+P-trans |
| 556) | aparc-a2009s_lh_volume_S-oc-middle+Lunatus |
| 557) | aparc-a2009s_lh_volume_S-oc-sup+transversal |
| 558) | aparc-a2009s_lh_volume_S-occipital-ant |
| 559) | aparc-a2009s_lh_volume_S-oc-temp-lat |
| 560) | aparc-a2009s_lh_volume_S-oc-temp-med+Lingual |
| 561) | aparc-a2009s_lh_volume_S-orbital-lateral |
| 562) | aparc-a2009s_lh_volume_S-orbital-med-olfact |
| 563) | aparc-a2009s_lh_volume_S-orbital-H-Shaped |
| 564) | aparc-a2009s_lh_volume_S-parieto-occipital |
| 565) | aparc-a2009s_lh_volume_S-pericallosal |
| 566) | aparc-a2009s_lh_volume_S-postcentral |
| 567) | aparc-a2009s_lh_volume_S-precentral-inf-part |
| 568) | aparc-a2009s_lh_volume_S-precentral-sup-part |
| 569) | aparc-a2009s_lh_volume_S-suborbital |
| 570) | aparc-a2009s_lh_volume_S-subparietal |
| 571) | aparc-a2009s_lh_volume_S-temporal-inf |
| 572) | aparc-a2009s_lh_volume_S-temporal-sup |
| 573) | aparc-a2009s_lh_volume_S-temporal-transverse |
| 574) | aparc-a2009s_rh_volume_G+S-frontomargin |
| 575) | aparc-a2009s_rh_volume_G+S-occipital-inf |
| 576) | aparc-a2009s_rh_volume_G+S-paracentral |
| 577) | aparc-a2009s_rh_volume_G+S-subcentral |
| 578) | aparc-a2009s_rh_volume_G+S-transv-frontopol |
| 579) | aparc-a2009s_rh_volume_G+S-cingul-Ant |
| 580) | aparc-a2009s_rh_volume_G+S-cingul-Mid-Ant |
| 581) | aparc-a2009s_rh_volume_G+S-cingul-Mid-Post |
| 582) | aparc-a2009s_rh_volume_G-cingul-Post-dorsal |

| | |
|---|---|
| 583) | aparc-a2009s_rh_volume_G-cingul-Post-ventral |
| 584) | aparc-a2009s_rh_volume_G-cuneus |
| 585) | aparc-a2009s_rh_volume_G-front-inf-Opercular |
| 586) | aparc-a2009s_rh_volume_G-front-inf-Orbital |
| 587) | aparc-a2009s_rh_volume_G-front-inf-Triangul |
| 588) | aparc-a2009s_rh_volume_G-front-middle |
| 589) | aparc-a2009s_rh_volume_G-front-sup |
| 590) | aparc-a2009s_rh_volume_G-Ins-lg+S-cent-ins |
| 591) | aparc-a2009s_rh_volume_G-insular-short |
| 592) | aparc-a2009s_rh_volume_G-occipital-middle |
| 593) | aparc-a2009s_rh_volume_G-occipital-sup |
| 594) | aparc-a2009s_rh_volume_G-oc-temp-lat-fusifor |
| 595) | aparc-a2009s_rh_volume_G-oc-temp-med-Lingual |
| 596) | aparc-a2009s_rh_volume_G-oc-temp-med-Parahip |
| 597) | aparc-a2009s_rh_volume_G-orbital |
| 598) | aparc-a2009s_rh_volume_G-pariet-inf-Angular |
| 599) | aparc-a2009s_rh_volume_G-pariet-inf-Supramar |
| 600) | aparc-a2009s_rh_volume_G-parietal-sup |
| 601) | aparc-a2009s_rh_volume_G-postcentral |
| 602) | aparc-a2009s_rh_volume_G-precentral |
| 603) | aparc-a2009s_rh_volume_G-precuneus |
| 604) | aparc-a2009s_rh_volume_G-rectus |
| 605) | aparc-a2009s_rh_volume_G-subcallosal |
| 606) | aparc-a2009s_rh_volume_G-temp-sup-G-T-transv |
| 607) | aparc-a2009s_rh_volume_G-temp-sup-Lateral |
| 608) | aparc-a2009s_rh_volume_G-temp-sup-Plan-polar |
| 609) | aparc-a2009s_rh_volume_G-temp-sup-Plan-tempo |
| 610) | aparc-a2009s_rh_volume_G-temporal-inf |
| 611) | aparc-a2009s_rh_volume_G-temporal-middle |
| 612) | aparc-a2009s_rh_volume_Lat-Fis-ant-Horizont |
| 613) | aparc-a2009s_rh_volume_Lat-Fis-ant-Vertical |
| 614) | aparc-a2009s_rh_volume_Lat-Fis-post |
| 615) | aparc-a2009s_rh_volume_Pole-occipital |
| 616) | aparc-a2009s_rh_volume_Pole-temporal |
| 617) | aparc-a2009s_rh_volume_S-calcarine |
| 618) | aparc-a2009s_rh_volume_S-central |
| 619) | aparc-a2009s_rh_volume_S-cingul-Marginalis |
| 620) | aparc-a2009s_rh_volume_S-circular-insula-ant |
| 621) | aparc-a2009s_rh_volume_S-circular-insula-inf |
| 622) | aparc-a2009s_rh_volume_S-circular-insula-sup |
| 623) | aparc-a2009s_rh_volume_S-collat-transv-ant |
| 624) | aparc-a2009s_rh_volume_S-collat-transv-post |

| | |
|---|---|
| 625) | aparc-a2009s_rh_volume_S-front-inf |
| 626) | aparc-a2009s_rh_volume_S-front-middle |
| 627) | aparc-a2009s_rh_volume_S-front-sup |
| 628) | aparc-a2009s_rh_volume_S-interm-prim-Jensen |
| 629) | aparc-a2009s_rh_volume_S-intrapariet+P-trans |
| 630) | aparc-a2009s_rh_volume_S-oc-middle+Lunatus |
| 631) | aparc-a2009s_rh_volume_S-oc-sup+transversal |
| 632) | aparc-a2009s_rh_volume_S-occipital-ant |
| 633) | aparc-a2009s_rh_volume_S-oc-temp-lat |
| 634) | aparc-a2009s_rh_volume_S-oc-temp-med+Lingual |
| 635) | aparc-a2009s_rh_volume_S-orbital-lateral |
| 636) | aparc-a2009s_rh_volume_S-orbital-med-olfact |
| 637) | aparc-a2009s_rh_volume_S-orbital-H-Shaped |
| 638) | aparc-a2009s_rh_volume_S-parieto-occipital |
| 639) | aparc-a2009s_rh_volume_S-pericallosal |
| 640) | aparc-a2009s_rh_volume_S-postcentral |
| 641) | aparc-a2009s_rh_volume_S-precentral-inf-part |
| 642) | aparc-a2009s_rh_volume_S-precentral-sup-part |
| 643) | aparc-a2009s_rh_volume_S-suborbital |
| 644) | aparc-a2009s_rh_volume_S-subparietal |
| 645) | aparc-a2009s_rh_volume_S-temporal-inf |
| 646) | aparc-a2009s_rh_volume_S-temporal-sup |
| 647) | aparc-a2009s_rh_volume_S-temporal-transverse |
| 648) | aparc-Desikan_lh_area_TotalSurface |
| 649) | aparc-Desikan_lh_area_bankssts |
| 650) | aparc-Desikan_lh_area_caudalanteriorcingulate |
| 651) | aparc-Desikan_lh_area_caudalmiddlefrontal |
| 652) | aparc-Desikan_lh_area_cuneus |
| 653) | aparc-Desikan_lh_area_entorhinal |
| 654) | aparc-Desikan_lh_area_fusiform |
| 655) | aparc-Desikan_lh_area_inferiorparietal |
| 656) | aparc-Desikan_lh_area_inferiortemporal |
| 657) | aparc-Desikan_lh_area_isthmuscingulate |
| 658) | aparc-Desikan_lh_area_lateraloccipital |
| 659) | aparc-Desikan_lh_area_lateralorbitofrontal |
| 660) | aparc-Desikan_lh_area_lingual |
| 661) | aparc-Desikan_lh_area_medialorbitofrontal |
| 662) | aparc-Desikan_lh_area_middletemporal |
| 663) | aparc-Desikan_lh_area_parahippocampal |
| 664) | aparc-Desikan_lh_area_paracentral |
| 665) | aparc-Desikan_lh_area_parsopercularis |
| 666) | aparc-Desikan_lh_area_parsorbitalis |

| | |
|---|---|
| 667) | aparc-Desikan_lh_area_parstriangularis |
| 668) | aparc-Desikan_lh_area_pericalcarine |
| 669) | aparc-Desikan_lh_area_postcentral |
| 670) | aparc-Desikan_lh_area_posteriorcingulate |
| 671) | aparc-Desikan_lh_area_precentral |
| 672) | aparc-Desikan_lh_area_precuneus |
| 673) | aparc-Desikan_lh_area_rostralanteriorcingulate |
| 674) | aparc-Desikan_lh_area_rostralmiddlefrontal |
| 675) | aparc-Desikan_lh_area_superiorfrontal |
| 676) | aparc-Desikan_lh_area_superiorparietal |
| 677) | aparc-Desikan_lh_area_superiortemporal |
| 678) | aparc-Desikan_lh_area_supramarginal |
| 679) | aparc-Desikan_lh_area_frontalpole |
| 680) | aparc-Desikan_lh_area_transversetemporal |
| 681) | aparc-Desikan_lh_area_insula |
| 682) | aparc-Desikan_rh_area_TotalSurface |
| 683) | aparc-Desikan_rh_area_bankssts |
| 684) | aparc-Desikan_rh_area_caudalanteriorcingulate |
| 685) | aparc-Desikan_rh_area_caudalmiddlefrontal |
| 686) | aparc-Desikan_rh_area_cuneus |
| 687) | aparc-Desikan_rh_area_entorhinal |
| 688) | aparc-Desikan_rh_area_fusiform |
| 689) | aparc-Desikan_rh_area_inferiorparietal |
| 690) | aparc-Desikan_rh_area_inferiortemporal |
| 691) | aparc-Desikan_rh_area_isthmuscingulate |
| 692) | aparc-Desikan_rh_area_lateraloccipital |
| 693) | aparc-Desikan_rh_area_lateralorbitofrontal |
| 694) | aparc-Desikan_rh_area_lingual |
| 695) | aparc-Desikan_rh_area_medialorbitofrontal |
| 696) | aparc-Desikan_rh_area_middletemporal |
| 697) | aparc-Desikan_rh_area_parahippocampal |
| 698) | aparc-Desikan_rh_area_paracentral |
| 699) | aparc-Desikan_rh_area_parsopercularis |
| 700) | aparc-Desikan_rh_area_parsorbitalis |
| 701) | aparc-Desikan_rh_area_parstriangularis |
| 702) | aparc-Desikan_rh_area_pericalcarine |
| 703) | aparc-Desikan_rh_area_postcentral |
| 704) | aparc-Desikan_rh_area_posteriorcingulate |
| 705) | aparc-Desikan_rh_area_precentral |
| 706) | aparc-Desikan_rh_area_precuneus |
| 707) | aparc-Desikan_rh_area_rostralanteriorcingulate |
| 708) | aparc-Desikan_rh_area_rostralmiddlefrontal |

| | |
|---|---|
| 709) | aparc-Desikan_rh_area_superiorfrontal |
| 710) | aparc-Desikan_rh_area_superiorparietal |
| 711) | aparc-Desikan_rh_area_superiortemporal |
| 712) | aparc-Desikan_rh_area_supramarginal |
| 713) | aparc-Desikan_rh_area_frontalpole |
| 714) | aparc-Desikan_rh_area_transversetemporal |
| 715) | aparc-Desikan_rh_area_insula |
| 716) | aparc-pial_lh_area_TotalSurface |
| 717) | aparc-pial_lh_area_bankssts |
| 718) | aparc-pial_lh_area_caudalanteriorcingulate |
| 719) | aparc-pial_lh_area_caudalmiddlefrontal |
| 720) | aparc-pial_lh_area_cuneus |
| 721) | aparc-pial_lh_area_entorhinal |
| 722) | aparc-pial_lh_area_fusiform |
| 723) | aparc-pial_lh_area_inferiorparietal |
| 724) | aparc-pial_lh_area_inferiortemporal |
| 725) | aparc-pial_lh_area_isthmuscingulate |
| 726) | aparc-pial_lh_area_lateraloccipital |
| 727) | aparc-pial_lh_area_lateralorbitofrontal |
| 728) | aparc-pial_lh_area_lingual |
| 729) | aparc-pial_lh_area_medialorbitofrontal |
| 730) | aparc-pial_lh_area_middletemporal |
| 731) | aparc-pial_lh_area_parahippocampal |
| 732) | aparc-pial_lh_area_paracentral |
| 733) | aparc-pial_lh_area_parsopercularis |
| 734) | aparc-pial_lh_area_parsorbitalis |
| 735) | aparc-pial_lh_area_parstriangularis |
| 736) | aparc-pial_lh_area_pericalcarine |
| 737) | aparc-pial_lh_area_postcentral |
| 738) | aparc-pial_lh_area_posteriorcingulate |
| 739) | aparc-pial_lh_area_precentral |
| 740) | aparc-pial_lh_area_precuneus |
| 741) | aparc-pial_lh_area_rostralanteriorcingulate |
| 742) | aparc-pial_lh_area_rostralmiddlefrontal |
| 743) | aparc-pial_lh_area_superiorfrontal |
| 744) | aparc-pial_lh_area_superiorparietal |
| 745) | aparc-pial_lh_area_superiortemporal |
| 746) | aparc-pial_lh_area_supramarginal |
| 747) | aparc-pial_lh_area_frontalpole |
| 748) | aparc-pial_lh_area_transversetemporal |
| 749) | aparc-pial_rh_area_TotalSurface |
| 750) | aparc-pial_rh_area_bankssts |

| | |
|---|---|
| 751) | aparc-pial_rh_area_caudalanteriorcingulate |
| 752) | aparc-pial_rh_area_caudalmiddlefrontal |
| 753) | aparc-pial_rh_area_cuneus |
| 754) | aparc-pial_rh_area_entorhinal |
| 755) | aparc-pial_rh_area_fusiform |
| 756) | aparc-pial_rh_area_inferiorparietal |
| 757) | aparc-pial_rh_area_inferiortemporal |
| 758) | aparc-pial_rh_area_isthmuscingulate |
| 759) | aparc-pial_rh_area_lateraloccipital |
| 760) | aparc-pial_rh_area_lateralorbitofrontal |
| 761) | aparc-pial_rh_area_lingual |
| 762) | aparc-pial_rh_area_medialorbitofrontal |
| 763) | aparc-pial_rh_area_middletemporal |
| 764) | aparc-pial_rh_area_parahippocampal |
| 765) | aparc-pial_rh_area_paracentral |
| 766) | aparc-pial_rh_area_parsopercularis |
| 767) | aparc-pial_rh_area_parsorbitalis |
| 768) | aparc-pial_rh_area_parstriangularis |
| 769) | aparc-pial_rh_area_pericalcarine |
| 770) | aparc-pial_rh_area_postcentral |
| 771) | aparc-pial_rh_area_posteriorcingulate |
| 772) | aparc-pial_rh_area_precentral |
| 773) | aparc-pial_rh_area_precuneus |
| 774) | aparc-pial_rh_area_rostralanteriorcingulate |
| 775) | aparc-pial_rh_area_rostralmiddlefrontal |
| 776) | aparc-pial_rh_area_superiorfrontal |
| 777) | aparc-pial_rh_area_superiorparietal |
| 778) | aparc-pial_rh_area_superiortemporal |
| 779) | aparc-pial_rh_area_supramarginal |
| 780) | aparc-pial_rh_area_frontalpole |
| 781) | aparc-pial_rh_area_transversetemporal |
| 782) | BA-exvivo_lh_area_BA1 |
| 783) | BA-exvivo_lh_area_BA2 |
| 784) | BA-exvivo_lh_area_BA3a |
| 785) | BA-exvivo_lh_area_BA3b |
| 786) | BA-exvivo_lh_area_BA4a |
| 787) | BA-exvivo_lh_area_BA4p |
| 788) | BA-exvivo_lh_area_BA6 |
| 789) | BA-exvivo_lh_area_BA44 |
| 790) | BA-exvivo_lh_area_BA45 |
| 791) | BA-exvivo_lh_area_V1 |
| 792) | BA-exvivo_lh_area_V2 |

| | |
|---|---|
| 793) | BA-exvivo_lh_area_MT |
| 794) | BA-exvivo_lh_area_perirhinal |
| 795) | BA-exvivo_lh_area_entorhinal |
| 796) | BA-exvivo_rh_area_BA1 |
| 797) | BA-exvivo_rh_area_BA2 |
| 798) | BA-exvivo_rh_area_BA3a |
| 799) | BA-exvivo_rh_area_BA3b |
| 800) | BA-exvivo_rh_area_BA4a |
| 801) | BA-exvivo_rh_area_BA4p |
| 802) | BA-exvivo_rh_area_BA6 |
| 803) | BA-exvivo_rh_area_BA44 |
| 804) | BA-exvivo_rh_area_BA45 |
| 805) | BA-exvivo_rh_area_V1 |
| 806) | BA-exvivo_rh_area_V2 |
| 807) | BA-exvivo_rh_area_MT |
| 808) | BA-exvivo_rh_area_perirhinal |
| 809) | BA-exvivo_rh_area_entorhinal |
| 810) | aparc-DKTatlas_lh_area_caudalanteriorcingulate |
| 811) | aparc-DKTatlas_lh_area_caudalmiddlefrontal |
| 812) | aparc-DKTatlas_lh_area_cuneus |
| 813) | aparc-DKTatlas_lh_area_entorhinal |
| 814) | aparc-DKTatlas_lh_area_fusiform |
| 815) | aparc-DKTatlas_lh_area_inferiorparietal |
| 816) | aparc-DKTatlas_lh_area_inferiortemporal |
| 817) | aparc-DKTatlas_lh_area_isthmuscingulate |
| 818) | aparc-DKTatlas_lh_area_lateraloccipital |
| 819) | aparc-DKTatlas_lh_area_lateralorbitofrontal |
| 820) | aparc-DKTatlas_lh_area_lingual |
| 821) | aparc-DKTatlas_lh_area_medialorbitofrontal |
| 822) | aparc-DKTatlas_lh_area_middletemporal |
| 823) | aparc-DKTatlas_lh_area_parahippocampal |
| 824) | aparc-DKTatlas_lh_area_paracentral |
| 825) | aparc-DKTatlas_lh_area_parsopercularis |
| 826) | aparc-DKTatlas_lh_area_parsorbitalis |
| 827) | aparc-DKTatlas_lh_area_parstriangularis |
| 828) | aparc-DKTatlas_lh_area_pericalcarine |
| 829) | aparc-DKTatlas_lh_area_postcentral |
| 830) | aparc-DKTatlas_lh_area_posteriorcingulate |
| 831) | aparc-DKTatlas_lh_area_precentral |
| 832) | aparc-DKTatlas_lh_area_precuneus |
| 833) | aparc-DKTatlas_lh_area_rostralanteriorcingulate |
| 834) | aparc-DKTatlas_lh_area_rostralmiddlefrontal |

| | |
|---|---|
| 835) | aparc-DKTatlas_lh_area_superiorfrontal |
| 836) | aparc-DKTatlas_lh_area_superiorparietal |
| 837) | aparc-DKTatlas_lh_area_superiortemporal |
| 838) | aparc-DKTatlas_lh_area_supramarginal |
| 839) | aparc-DKTatlas_lh_area_transversetemporal |
| 840) | aparc-DKTatlas_lh_area_insula |
| 841) | aparc-DKTatlas_rh_area_caudalanteriorcingulate |
| 842) | aparc-DKTatlas_rh_area_caudalmiddlefrontal |
| 843) | aparc-DKTatlas_rh_area_cuneus |
| 844) | aparc-DKTatlas_rh_area_entorhinal |
| 845) | aparc-DKTatlas_rh_area_fusiform |
| 846) | aparc-DKTatlas_rh_area_inferiorparietal |
| 847) | aparc-DKTatlas_rh_area_inferiortemporal |
| 848) | aparc-DKTatlas_rh_area_isthmuscingulate |
| 849) | aparc-DKTatlas_rh_area_lateraloccipital |
| 850) | aparc-DKTatlas_rh_area_lateralorbitofrontal |
| 851) | aparc-DKTatlas_rh_area_lingual |
| 852) | aparc-DKTatlas_rh_area_medialorbitofrontal |
| 853) | aparc-DKTatlas_rh_area_middletemporal |
| 854) | aparc-DKTatlas_rh_area_parahippocampal |
| 855) | aparc-DKTatlas_rh_area_paracentral |
| 856) | aparc-DKTatlas_rh_area_parsopercularis |
| 857) | aparc-DKTatlas_rh_area_parsorbitalis |
| 858) | aparc-DKTatlas_rh_area_parstriangularis |
| 859) | aparc-DKTatlas_rh_area_pericalcarine |
| 860) | aparc-DKTatlas_rh_area_postcentral |
| 861) | aparc-DKTatlas_rh_area_posteriorcingulate |
| 862) | aparc-DKTatlas_rh_area_precentral |
| 863) | aparc-DKTatlas_rh_area_precuneus |
| 864) | aparc-DKTatlas_rh_area_rostralanteriorcingulate |
| 865) | aparc-DKTatlas_rh_area_rostralmiddlefrontal |
| 866) | aparc-DKTatlas_rh_area_superiorfrontal |
| 867) | aparc-DKTatlas_rh_area_superiorparietal |
| 868) | aparc-DKTatlas_rh_area_superiortemporal |
| 869) | aparc-DKTatlas_rh_area_supramarginal |
| 870) | aparc-DKTatlas_rh_area_transversetemporal |
| 871) | aparc-DKTatlas_rh_area_insula |
| 872) | aparc-a2009s_lh_area_G+S-frontomargin |
| 873) | aparc-a2009s_lh_area_G+S-occipital-inf |
| 874) | aparc-a2009s_lh_area_G+S-paracentral |
| 875) | aparc-a2009s_lh_area_G+S-subcentral |
| 876) | aparc-a2009s_lh_area_G+S-transv-frontopol |

| | |
|---|---|
| 877) | aparc-a2009s_lh_area_G+S-cingul-Ant |
| 878) | aparc-a2009s_lh_area_G+S-cingul-Mid-Ant |
| 879) | aparc-a2009s_lh_area_G+S-cingul-Mid-Post |
| 880) | aparc-a2009s_lh_area_G-cingul-Post-dorsal |
| 881) | aparc-a2009s_lh_area_G-cingul-Post-ventral |
| 882) | aparc-a2009s_lh_area_G-cuneus |
| 883) | aparc-a2009s_lh_area_G-front-inf-Opercular |
| 884) | aparc-a2009s_lh_area_G-front-inf-Orbital |
| 885) | aparc-a2009s_lh_area_G-front-inf-Triangul |
| 886) | aparc-a2009s_lh_area_G-front-middle |
| 887) | aparc-a2009s_lh_area_G-front-sup |
| 888) | aparc-a2009s_lh_area_G-Ins-lg+S-cent-ins |
| 889) | aparc-a2009s_lh_area_G-insular-short |
| 890) | aparc-a2009s_lh_area_G-occipital-middle |
| 891) | aparc-a2009s_lh_area_G-occipital-sup |
| 892) | aparc-a2009s_lh_area_G-oc-temp-lat-fusifor |
| 893) | aparc-a2009s_lh_area_G-oc-temp-med-Lingual |
| 894) | aparc-a2009s_lh_area_G-oc-temp-med-Parahip |
| 895) | aparc-a2009s_lh_area_G-orbital |
| 896) | aparc-a2009s_lh_area_G-pariet-inf-Angular |
| 897) | aparc-a2009s_lh_area_G-pariet-inf-Supramar |
| 898) | aparc-a2009s_lh_area_G-parietal-sup |
| 899) | aparc-a2009s_lh_area_G-postcentral |
| 900) | aparc-a2009s_lh_area_G-precentral |
| 901) | aparc-a2009s_lh_area_G-precuneus |
| 902) | aparc-a2009s_lh_area_G-rectus |
| 903) | aparc-a2009s_lh_area_G-subcallosal |
| 904) | aparc-a2009s_lh_area_G-temp-sup-G-T-transv |
| 905) | aparc-a2009s_lh_area_G-temp-sup-Lateral |
| 906) | aparc-a2009s_lh_area_G-temp-sup-Plan-polar |
| 907) | aparc-a2009s_lh_area_G-temp-sup-Plan-tempo |
| 908) | aparc-a2009s_lh_area_G-temporal-inf |
| 909) | aparc-a2009s_lh_area_G-temporal-middle |
| 910) | aparc-a2009s_lh_area_Lat-Fis-ant-Horizont |
| 911) | aparc-a2009s_lh_area_Lat-Fis-ant-Vertical |
| 912) | aparc-a2009s_lh_area_Lat-Fis-post |
| 913) | aparc-a2009s_lh_area_Pole-occipital |
| 914) | aparc-a2009s_lh_area_Pole-temporal |
| 915) | aparc-a2009s_lh_area_S-calcarine |
| 916) | aparc-a2009s_lh_area_S-central |
| 917) | aparc-a2009s_lh_area_S-cingul-Marginalis |
| 918) | aparc-a2009s_lh_area_S-circular-insula-ant |

| | |
|---|---|
| 919) | aparc-a2009s_lh_area_S-circular-insula-inf |
| 920) | aparc-a2009s_lh_area_S-circular-insula-sup |
| 921) | aparc-a2009s_lh_area_S-collat-transv-ant |
| 922) | aparc-a2009s_lh_area_S-collat-transv-post |
| 923) | aparc-a2009s_lh_area_S-front-inf |
| 924) | aparc-a2009s_lh_area_S-front-middle |
| 925) | aparc-a2009s_lh_area_S-front-sup |
| 926) | aparc-a2009s_lh_area_S-interm-prim-Jensen |
| 927) | aparc-a2009s_lh_area_S-intrapariet+P-trans |
| 928) | aparc-a2009s_lh_area_S-oc-middle+Lunatus |
| 929) | aparc-a2009s_lh_area_S-oc-sup+transversal |
| 930) | aparc-a2009s_lh_area_S-occipital-ant |
| 931) | aparc-a2009s_lh_area_S-oc-temp-lat |
| 932) | aparc-a2009s_lh_area_S-oc-temp-med+Lingual |
| 933) | aparc-a2009s_lh_area_S-orbital-lateral |
| 934) | aparc-a2009s_lh_area_S-orbital-med-olfact |
| 935) | aparc-a2009s_lh_area_S-orbital-H-Shaped |
| 936) | aparc-a2009s_lh_area_S-parieto-occipital |
| 937) | aparc-a2009s_lh_area_S-pericallosal |
| 938) | aparc-a2009s_lh_area_S-postcentral |
| 939) | aparc-a2009s_lh_area_S-precentral-inf-part |
| 940) | aparc-a2009s_lh_area_S-precentral-sup-part |
| 941) | aparc-a2009s_lh_area_S-suborbital |
| 942) | aparc-a2009s_lh_area_S-subparietal |
| 943) | aparc-a2009s_lh_area_S-temporal-inf |
| 944) | aparc-a2009s_lh_area_S-temporal-sup |
| 945) | aparc-a2009s_lh_area_S-temporal-transverse |
| 946) | aparc-a2009s_rh_area_G+S-frontomargin |
| 947) | aparc-a2009s_rh_area_G+S-occipital-inf |
| 948) | aparc-a2009s_rh_area_G+S-paracentral |
| 949) | aparc-a2009s_rh_area_G+S-subcentral |
| 950) | aparc-a2009s_rh_area_G+S-transv-frontopol |
| 951) | aparc-a2009s_rh_area_G+S-cingul-Ant |
| 952) | aparc-a2009s_rh_area_G+S-cingul-Mid-Ant |
| 953) | aparc-a2009s_rh_area_G+S-cingul-Mid-Post |
| 954) | aparc-a2009s_rh_area_G-cingul-Post-dorsal |
| 955) | aparc-a2009s_rh_area_G-cingul-Post-ventral |
| 956) | aparc-a2009s_rh_area_G-cuneus |
| 957) | aparc-a2009s_rh_area_G-front-inf-Opercular |
| 958) | aparc-a2009s_rh_area_G-front-inf-Orbital |
| 959) | aparc-a2009s_rh_area_G-front-inf-Triangul |
| 960) | aparc-a2009s_rh_area_G-front-middle |

| | |
|---|---|
| 961) | aparc-a2009s_rh_area_G-front-sup |
| 962) | aparc-a2009s_rh_area_G-Ins-lg+S-cent-ins |
| 963) | aparc-a2009s_rh_area_G-insular-short |
| 964) | aparc-a2009s_rh_area_G-occipital-middle |
| 965) | aparc-a2009s_rh_area_G-occipital-sup |
| 966) | aparc-a2009s_rh_area_G-oc-temp-lat-fusifor |
| 967) | aparc-a2009s_rh_area_G-oc-temp-med-Lingual |
| 968) | aparc-a2009s_rh_area_G-oc-temp-med-Parahip |
| 969) | aparc-a2009s_rh_area_G-orbital |
| 970) | aparc-a2009s_rh_area_G-pariet-inf-Angular |
| 971) | aparc-a2009s_rh_area_G-pariet-inf-Supramar |
| 972) | aparc-a2009s_rh_area_G-parietal-sup |
| 973) | aparc-a2009s_rh_area_G-postcentral |
| 974) | aparc-a2009s_rh_area_G-precentral |
| 975) | aparc-a2009s_rh_area_G-precuneus |
| 976) | aparc-a2009s_rh_area_G-rectus |
| 977) | aparc-a2009s_rh_area_G-subcallosal |
| 978) | aparc-a2009s_rh_area_G-temp-sup-G-T-transv |
| 979) | aparc-a2009s_rh_area_G-temp-sup-Lateral |
| 980) | aparc-a2009s_rh_area_G-temp-sup-Plan-polar |
| 981) | aparc-a2009s_rh_area_G-temp-sup-Plan-tempo |
| 982) | aparc-a2009s_rh_area_G-temporal-inf |
| 983) | aparc-a2009s_rh_area_G-temporal-middle |
| 984) | aparc-a2009s_rh_area_Lat-Fis-ant-Horizont |
| 985) | aparc-a2009s_rh_area_Lat-Fis-ant-Vertical |
| 986) | aparc-a2009s_rh_area_Lat-Fis-post |
| 987) | aparc-a2009s_rh_area_Pole-occipital |
| 988) | aparc-a2009s_rh_area_Pole-temporal |
| 989) | aparc-a2009s_rh_area_S-calcarine |
| 990) | aparc-a2009s_rh_area_S-central |
| 991) | aparc-a2009s_rh_area_S-cingul-Marginalis |
| 992) | aparc-a2009s_rh_area_S-circular-insula-ant |
| 993) | aparc-a2009s_rh_area_S-circular-insula-inf |
| 994) | aparc-a2009s_rh_area_S-circular-insula-sup |
| 995) | aparc-a2009s_rh_area_S-collat-transv-ant |
| 996) | aparc-a2009s_rh_area_S-collat-transv-post |
| 997) | aparc-a2009s_rh_area_S-front-inf |
| 998) | aparc-a2009s_rh_area_S-front-middle |
| 999) | aparc-a2009s_rh_area_S-front-sup |
| 1000) | aparc-a2009s_rh_area_S-interm-prim-Jensen |
| 1001) | aparc-a2009s_rh_area_S-intrapariet+P-trans |
| 1002) | aparc-a2009s_rh_area_S-oc-middle+Lunatus |

| | |
|---|---|
| 1003) | aparc-a2009s_rh_area_S-oc-sup+transversal |
| 1004) | aparc-a2009s_rh_area_S-occipital-ant |
| 1005) | aparc-a2009s_rh_area_S-oc-temp-lat |
| 1006) | aparc-a2009s_rh_area_S-oc-temp-med+Lingual |
| 1007) | aparc-a2009s_rh_area_S-orbital-lateral |
| 1008) | aparc-a2009s_rh_area_S-orbital-med-olfact |
| 1009) | aparc-a2009s_rh_area_S-orbital-H-Shaped |
| 1010) | aparc-a2009s_rh_area_S-parieto-occipital |
| 1011) | aparc-a2009s_rh_area_S-pericallosal |
| 1012) | aparc-a2009s_rh_area_S-postcentral |
| 1013) | aparc-a2009s_rh_area_S-precentral-inf-part |
| 1014) | aparc-a2009s_rh_area_S-precentral-sup-part |
| 1015) | aparc-a2009s_rh_area_S-suborbital |
| 1016) | aparc-a2009s_rh_area_S-subparietal |
| 1017) | aparc-a2009s_rh_area_S-temporal-inf |
| 1018) | aparc-a2009s_rh_area_S-temporal-sup |
| 1019) | aparc-a2009s_rh_area_S-temporal-transverse |
| 1020) | aparc-Desikan_lh_thickness_GlobalMeanThickness |
| 1021) | aparc-Desikan_lh_thickness_bankssts |
| 1022) | aparc-Desikan_lh_thickness_caudalanteriorcingulate |
| 1023) | aparc-Desikan_lh_thickness_caudalmiddlefrontal |
| 1024) | aparc-Desikan_lh_thickness_cuneus |
| 1025) | aparc-Desikan_lh_thickness_entorhinal |
| 1026) | aparc-Desikan_lh_thickness_fusiform |
| 1027) | aparc-Desikan_lh_thickness_inferiorparietal |
| 1028) | aparc-Desikan_lh_thickness_inferiortemporal |
| 1029) | aparc-Desikan_lh_thickness_isthmuscingulate |
| 1030) | aparc-Desikan_lh_thickness_lateraloccipital |
| 1031) | aparc-Desikan_lh_thickness_lateralorbitofrontal |
| 1032) | aparc-Desikan_lh_thickness_lingual |
| 1033) | aparc-Desikan_lh_thickness_medialorbitofrontal |
| 1034) | aparc-Desikan_lh_thickness_middletemporal |
| 1035) | aparc-Desikan_lh_thickness_parahippocampal |
| 1036) | aparc-Desikan_lh_thickness_paracentral |
| 1037) | aparc-Desikan_lh_thickness_parsopercularis |
| 1038) | aparc-Desikan_lh_thickness_parsorbitalis |
| 1039) | aparc-Desikan_lh_thickness_parstriangularis |
| 1040) | aparc-Desikan_lh_thickness_pericalcarine |
| 1041) | aparc-Desikan_lh_thickness_postcentral |
| 1042) | aparc-Desikan_lh_thickness_posteriorcingulate |
| 1043) | aparc-Desikan_lh_thickness_precentral |
| 1044) | aparc-Desikan_lh_thickness_precuneus |

| | |
|---|---|
| 1045) | aparc-Desikan_lh_thickness_rostralanteriorcingulate |
| 1046) | aparc-Desikan_lh_thickness_rostralmiddlefrontal |
| 1047) | aparc-Desikan_lh_thickness_superiorfrontal |
| 1048) | aparc-Desikan_lh_thickness_superiorparietal |
| 1049) | aparc-Desikan_lh_thickness_superiortemporal |
| 1050) | aparc-Desikan_lh_thickness_supramarginal |
| 1051) | aparc-Desikan_lh_thickness_frontalpole |
| 1052) | aparc-Desikan_lh_thickness_transversetemporal |
| 1053) | aparc-Desikan_lh_thickness_insula |
| 1054) | aparc-Desikan_rh_thickness_GlobalMeanThickness |
| 1055) | aparc-Desikan_rh_thickness_bankssts |
| 1056) | aparc-Desikan_rh_thickness_caudalanteriorcingulate |
| 1057) | aparc-Desikan_rh_thickness_caudalmiddlefrontal |
| 1058) | aparc-Desikan_rh_thickness_cuneus |
| 1059) | aparc-Desikan_rh_thickness_entorhinal |
| 1060) | aparc-Desikan_rh_thickness_fusiform |
| 1061) | aparc-Desikan_rh_thickness_inferiorparietal |
| 1062) | aparc-Desikan_rh_thickness_inferiortemporal |
| 1063) | aparc-Desikan_rh_thickness_isthmuscingulate |
| 1064) | aparc-Desikan_rh_thickness_lateraloccipital |
| 1065) | aparc-Desikan_rh_thickness_lateralorbitofrontal |
| 1066) | aparc-Desikan_rh_thickness_lingual |
| 1067) | aparc-Desikan_rh_thickness_medialorbitofrontal |
| 1068) | aparc-Desikan_rh_thickness_middletemporal |
| 1069) | aparc-Desikan_rh_thickness_parahippocampal |
| 1070) | aparc-Desikan_rh_thickness_paracentral |
| 1071) | aparc-Desikan_rh_thickness_parsopercularis |
| 1072) | aparc-Desikan_rh_thickness_parsorbitalis |
| 1073) | aparc-Desikan_rh_thickness_parstriangularis |
| 1074) | aparc-Desikan_rh_thickness_pericalcarine |
| 1075) | aparc-Desikan_rh_thickness_postcentral |
| 1076) | aparc-Desikan_rh_thickness_posteriorcingulate |
| 1077) | aparc-Desikan_rh_thickness_precentral |
| 1078) | aparc-Desikan_rh_thickness_precuneus |
| 1079) | aparc-Desikan_rh_thickness_rostralanteriorcingulate |
| 1080) | aparc-Desikan_rh_thickness_rostralmiddlefrontal |
| 1081) | aparc-Desikan_rh_thickness_superiorfrontal |
| 1082) | aparc-Desikan_rh_thickness_superiorparietal |
| 1083) | aparc-Desikan_rh_thickness_superiortemporal |
| 1084) | aparc-Desikan_rh_thickness_supramarginal |
| 1085) | aparc-Desikan_rh_thickness_frontalpole |
| 1086) | aparc-Desikan_rh_thickness_transversetemporal |

| | |
|---|---|
| 1087) | aparc-Desikan_rh_thickness_insula |
| 1088) | BA-exvivo_lh_thickness_BA1 |
| 1089) | BA-exvivo_lh_thickness_BA2 |
| 1090) | BA-exvivo_lh_thickness_BA3a |
| 1091) | BA-exvivo_lh_thickness_BA3b |
| 1092) | BA-exvivo_lh_thickness_BA4a |
| 1093) | BA-exvivo_lh_thickness_BA4p |
| 1094) | BA-exvivo_lh_thickness_BA6 |
| 1095) | BA-exvivo_lh_thickness_BA44 |
| 1096) | BA-exvivo_lh_thickness_BA45 |
| 1097) | BA-exvivo_lh_thickness_V1 |
| 1098) | BA-exvivo_lh_thickness_V2 |
| 1099) | BA-exvivo_lh_thickness_MT |
| 1100) | BA-exvivo_lh_thickness_perirhinal |
| 1101) | BA-exvivo_lh_thickness_entorhinal |
| 1102) | BA-exvivo_rh_thickness_BA1 |
| 1103) | BA-exvivo_rh_thickness_BA2 |
| 1104) | BA-exvivo_rh_thickness_BA3a |
| 1105) | BA-exvivo_rh_thickness_BA3b |
| 1106) | BA-exvivo_rh_thickness_BA4a |
| 1107) | BA-exvivo_rh_thickness_BA4p |
| 1108) | BA-exvivo_rh_thickness_BA6 |
| 1109) | BA-exvivo_rh_thickness_BA44 |
| 1110) | BA-exvivo_rh_thickness_BA45 |
| 1111) | BA-exvivo_rh_thickness_V1 |
| 1112) | BA-exvivo_rh_thickness_V2 |
| 1113) | BA-exvivo_rh_thickness_MT |
| 1114) | BA-exvivo_rh_thickness_perirhinal |
| 1115) | BA-exvivo_rh_thickness_entorhinal |
| 1116) | aparc-DKTatlas_lh_thickness_caudalanteriorcingulate |
| 1117) | aparc-DKTatlas_lh_thickness_caudalmiddlefrontal |
| 1118) | aparc-DKTatlas_lh_thickness_cuneus |
| 1119) | aparc-DKTatlas_lh_thickness_entorhinal |
| 1120) | aparc-DKTatlas_lh_thickness_fusiform |
| 1121) | aparc-DKTatlas_lh_thickness_inferiorparietal |
| 1122) | aparc-DKTatlas_lh_thickness_inferiortemporal |
| 1123) | aparc-DKTatlas_lh_thickness_isthmuscingulate |
| 1124) | aparc-DKTatlas_lh_thickness_lateraloccipital |
| 1125) | aparc-DKTatlas_lh_thickness_lateralorbitofrontal |
| 1126) | aparc-DKTatlas_lh_thickness_lingual |
| 1127) | aparc-DKTatlas_lh_thickness_medialorbitofrontal |
| 1128) | aparc-DKTatlas_lh_thickness_middletemporal |

| | |
|---|---|
| 1129) | aparc-DKTatlas_lh_thickness_parahippocampal |
| 1130) | aparc-DKTatlas_lh_thickness_paracentral |
| 1131) | aparc-DKTatlas_lh_thickness_parsopercularis |
| 1132) | aparc-DKTatlas_lh_thickness_parsorbitalis |
| 1133) | aparc-DKTatlas_lh_thickness_parstriangularis |
| 1134) | aparc-DKTatlas_lh_thickness_pericalcarine |
| 1135) | aparc-DKTatlas_lh_thickness_postcentral |
| 1136) | aparc-DKTatlas_lh_thickness_posteriorcingulate |
| 1137) | aparc-DKTatlas_lh_thickness_precentral |
| 1138) | aparc-DKTatlas_lh_thickness_precuneus |
| 1139) | aparc-DKTatlas_lh_thickness_rostralanteriorcingulate |
| 1140) | aparc-DKTatlas_lh_thickness_rostralmiddlefrontal |
| 1141) | aparc-DKTatlas_lh_thickness_superiorfrontal |
| 1142) | aparc-DKTatlas_lh_thickness_superiorparietal |
| 1143) | aparc-DKTatlas_lh_thickness_superiortemporal |
| 1144) | aparc-DKTatlas_lh_thickness_supramarginal |
| 1145) | aparc-DKTatlas_lh_thickness_transversetemporal |
| 1146) | aparc-DKTatlas_lh_thickness_insula |
| 1147) | aparc-DKTatlas_rh_thickness_caudalanteriorcingulate |
| 1148) | aparc-DKTatlas_rh_thickness_caudalmiddlefrontal |
| 1149) | aparc-DKTatlas_rh_thickness_cuneus |
| 1150) | aparc-DKTatlas_rh_thickness_entorhinal |
| 1151) | aparc-DKTatlas_rh_thickness_fusiform |
| 1152) | aparc-DKTatlas_rh_thickness_inferiorparietal |
| 1153) | aparc-DKTatlas_rh_thickness_inferiortemporal |
| 1154) | aparc-DKTatlas_rh_thickness_isthmuscingulate |
| 1155) | aparc-DKTatlas_rh_thickness_lateraloccipital |
| 1156) | aparc-DKTatlas_rh_thickness_lateralorbitofrontal |
| 1157) | aparc-DKTatlas_rh_thickness_lingual |
| 1158) | aparc-DKTatlas_rh_thickness_medialorbitofrontal |
| 1159) | aparc-DKTatlas_rh_thickness_middletemporal |
| 1160) | aparc-DKTatlas_rh_thickness_parahippocampal |
| 1161) | aparc-DKTatlas_rh_thickness_paracentral |
| 1162) | aparc-DKTatlas_rh_thickness_parsopercularis |
| 1163) | aparc-DKTatlas_rh_thickness_parsorbitalis |
| 1164) | aparc-DKTatlas_rh_thickness_parstriangularis |
| 1165) | aparc-DKTatlas_rh_thickness_pericalcarine |
| 1166) | aparc-DKTatlas_rh_thickness_postcentral |
| 1167) | aparc-DKTatlas_rh_thickness_posteriorcingulate |
| 1168) | aparc-DKTatlas_rh_thickness_precentral |
| 1169) | aparc-DKTatlas_rh_thickness_precuneus |
| 1170) | aparc-DKTatlas_rh_thickness_rostralanteriorcingulate |

| | |
|---|---|
| 1171) | aparc-DKTatlas_rh_thickness_rostralmiddlefrontal |
| 1172) | aparc-DKTatlas_rh_thickness_superiorfrontal |
| 1173) | aparc-DKTatlas_rh_thickness_superiorparietal |
| 1174) | aparc-DKTatlas_rh_thickness_superiortemporal |
| 1175) | aparc-DKTatlas_rh_thickness_supramarginal |
| 1176) | aparc-DKTatlas_rh_thickness_transversetemporal |
| 1177) | aparc-DKTatlas_rh_thickness_insula |
| 1178) | aparc-a2009s_lh_thickness_G+S-frontomargin |
| 1179) | aparc-a2009s_lh_thickness_G+S-occipital-inf |
| 1180) | aparc-a2009s_lh_thickness_G+S-paracentral |
| 1181) | aparc-a2009s_lh_thickness_G+S-subcentral |
| 1182) | aparc-a2009s_lh_thickness_G+S-transv-frontopol |
| 1183) | aparc-a2009s_lh_thickness_G+S-cingul-Ant |
| 1184) | aparc-a2009s_lh_thickness_G+S-cingul-Mid-Ant |
| 1185) | aparc-a2009s_lh_thickness_G+S-cingul-Mid-Post |
| 1186) | aparc-a2009s_lh_thickness_G-cingul-Post-dorsal |
| 1187) | aparc-a2009s_lh_thickness_G-cingul-Post-ventral |
| 1188) | aparc-a2009s_lh_thickness_G-cuneus |
| 1189) | aparc-a2009s_lh_thickness_G-front-inf-Opercular |
| 1190) | aparc-a2009s_lh_thickness_G-front-inf-Orbital |
| 1191) | aparc-a2009s_lh_thickness_G-front-inf-Triangul |
| 1192) | aparc-a2009s_lh_thickness_G-front-middle |
| 1193) | aparc-a2009s_lh_thickness_G-front-sup |
| 1194) | aparc-a2009s_lh_thickness_G-Ins-lg+S-cent-ins |
| 1195) | aparc-a2009s_lh_thickness_G-insular-short |
| 1196) | aparc-a2009s_lh_thickness_G-occipital-middle |
| 1197) | aparc-a2009s_lh_thickness_G-occipital-sup |
| 1198) | aparc-a2009s_lh_thickness_G-oc-temp-lat-fusifor |
| 1199) | aparc-a2009s_lh_thickness_G-oc-temp-med-Lingual |
| 1200) | aparc-a2009s_lh_thickness_G-oc-temp-med-Parahip |
| 1201) | aparc-a2009s_lh_thickness_G-orbital |
| 1202) | aparc-a2009s_lh_thickness_G-pariet-inf-Angular |
| 1203) | aparc-a2009s_lh_thickness_G-pariet-inf-Supramar |
| 1204) | aparc-a2009s_lh_thickness_G-parietal-sup |
| 1205) | aparc-a2009s_lh_thickness_G-postcentral |
| 1206) | aparc-a2009s_lh_thickness_G-precentral |
| 1207) | aparc-a2009s_lh_thickness_G-precuneus |
| 1208) | aparc-a2009s_lh_thickness_G-rectus |
| 1209) | aparc-a2009s_lh_thickness_G-subcallosal |
| 1210) | aparc-a2009s_lh_thickness_G-temp-sup-G-T-transv |
| 1211) | aparc-a2009s_lh_thickness_G-temp-sup-Lateral |
| 1212) | aparc-a2009s_lh_thickness_G-temp-sup-Plan-polar |

| | |
|---|---|
| 1213) | aparc-a2009s_lh_thickness_G-temp-sup-Plan-tempo |
| 1214) | aparc-a2009s_lh_thickness_G-temporal-inf |
| 1215) | aparc-a2009s_lh_thickness_G-temporal-middle |
| 1216) | aparc-a2009s_lh_thickness_Lat-Fis-ant-Horizont |
| 1217) | aparc-a2009s_lh_thickness_Lat-Fis-ant-Vertical |
| 1218) | aparc-a2009s_lh_thickness_Lat-Fis-post |
| 1219) | aparc-a2009s_lh_thickness_Pole-occipital |
| 1220) | aparc-a2009s_lh_thickness_Pole-temporal |
| 1221) | aparc-a2009s_lh_thickness_S-calcarine |
| 1222) | aparc-a2009s_lh_thickness_S-central |
| 1223) | aparc-a2009s_lh_thickness_S-cingul-Marginalis |
| 1224) | aparc-a2009s_lh_thickness_S-circular-insula-ant |
| 1225) | aparc-a2009s_lh_thickness_S-circular-insula-inf |
| 1226) | aparc-a2009s_lh_thickness_S-circular-insula-sup |
| 1227) | aparc-a2009s_lh_thickness_S-collat-transv-ant |
| 1228) | aparc-a2009s_lh_thickness_S-collat-transv-post |
| 1229) | aparc-a2009s_lh_thickness_S-front-inf |
| 1230) | aparc-a2009s_lh_thickness_S-front-middle |
| 1231) | aparc-a2009s_lh_thickness_S-front-sup |
| 1232) | aparc-a2009s_lh_thickness_S-interm-prim-Jensen |
| 1233) | aparc-a2009s_lh_thickness_S-intrapariet+P-trans |
| 1234) | aparc-a2009s_lh_thickness_S-oc-middle+Lunatus |
| 1235) | aparc-a2009s_lh_thickness_S-oc-sup+transversal |
| 1236) | aparc-a2009s_lh_thickness_S-occipital-ant |
| 1237) | aparc-a2009s_lh_thickness_S-oc-temp-lat |
| 1238) | aparc-a2009s_lh_thickness_S-oc-temp-med+Lingual |
| 1239) | aparc-a2009s_lh_thickness_S-orbital-lateral |
| 1240) | aparc-a2009s_lh_thickness_S-orbital-med-olfact |
| 1241) | aparc-a2009s_lh_thickness_S-orbital-H-Shaped |
| 1242) | aparc-a2009s_lh_thickness_S-parieto-occipital |
| 1243) | aparc-a2009s_lh_thickness_S-pericallosal |
| 1244) | aparc-a2009s_lh_thickness_S-postcentral |
| 1245) | aparc-a2009s_lh_thickness_S-precentral-inf-part |
| 1246) | aparc-a2009s_lh_thickness_S-precentral-sup-part |
| 1247) | aparc-a2009s_lh_thickness_S-suborbital |
| 1248) | aparc-a2009s_lh_thickness_S-subparietal |
| 1249) | aparc-a2009s_lh_thickness_S-temporal-inf |
| 1250) | aparc-a2009s_lh_thickness_S-temporal-sup |
| 1251) | aparc-a2009s_lh_thickness_S-temporal-transverse |
| 1252) | aparc-a2009s_rh_thickness_G+S-frontomargin |
| 1253) | aparc-a2009s_rh_thickness_G+S-occipital-inf |
| 1254) | aparc-a2009s_rh_thickness_G+S-paracentral |

| | |
|---|---|
| 1255) | aparc-a2009s_rh_thickness_G+S-subcentral |
| 1256) | aparc-a2009s_rh_thickness_G+S-transv-frontopol |
| 1257) | aparc-a2009s_rh_thickness_G+S-cingul-Ant |
| 1258) | aparc-a2009s_rh_thickness_G+S-cingul-Mid-Ant |
| 1259) | aparc-a2009s_rh_thickness_G+S-cingul-Mid-Post |
| 1260) | aparc-a2009s_rh_thickness_G-cingul-Post-dorsal |
| 1261) | aparc-a2009s_rh_thickness_G-cingul-Post-ventral |
| 1262) | aparc-a2009s_rh_thickness_G-cuneus |
| 1263) | aparc-a2009s_rh_thickness_G-front-inf-Opercular |
| 1264) | aparc-a2009s_rh_thickness_G-front-inf-Orbital |
| 1265) | aparc-a2009s_rh_thickness_G-front-inf-Triangul |
| 1266) | aparc-a2009s_rh_thickness_G-front-middle |
| 1267) | aparc-a2009s_rh_thickness_G-front-sup |
| 1268) | aparc-a2009s_rh_thickness_G-Ins-lg+S-cent-ins |
| 1269) | aparc-a2009s_rh_thickness_G-insular-short |
| 1270) | aparc-a2009s_rh_thickness_G-occipital-middle |
| 1271) | aparc-a2009s_rh_thickness_G-occipital-sup |
| 1272) | aparc-a2009s_rh_thickness_G-oc-temp-lat-fusifor |
| 1273) | aparc-a2009s_rh_thickness_G-oc-temp-med-Lingual |
| 1274) | aparc-a2009s_rh_thickness_G-oc-temp-med-Parahip |
| 1275) | aparc-a2009s_rh_thickness_G-orbital |
| 1276) | aparc-a2009s_rh_thickness_G-pariet-inf-Angular |
| 1277) | aparc-a2009s_rh_thickness_G-pariet-inf-Supramar |
| 1278) | aparc-a2009s_rh_thickness_G-parietal-sup |
| 1279) | aparc-a2009s_rh_thickness_G-postcentral |
| 1280) | aparc-a2009s_rh_thickness_G-precentral |
| 1281) | aparc-a2009s_rh_thickness_G-precuneus |
| 1282) | aparc-a2009s_rh_thickness_G-rectus |
| 1283) | aparc-a2009s_rh_thickness_G-subcallosal |
| 1284) | aparc-a2009s_rh_thickness_G-temp-sup-G-T-transv |
| 1285) | aparc-a2009s_rh_thickness_G-temp-sup-Lateral |
| 1286) | aparc-a2009s_rh_thickness_G-temp-sup-Plan-polar |
| 1287) | aparc-a2009s_rh_thickness_G-temp-sup-Plan-tempo |
| 1288) | aparc-a2009s_rh_thickness_G-temporal-inf |
| 1289) | aparc-a2009s_rh_thickness_G-temporal-middle |
| 1290) | aparc-a2009s_rh_thickness_Lat-Fis-ant-Horizont |
| 1291) | aparc-a2009s_rh_thickness_Lat-Fis-ant-Vertical |
| 1292) | aparc-a2009s_rh_thickness_Lat-Fis-post |
| 1293) | aparc-a2009s_rh_thickness_Pole-occipital |
| 1294) | aparc-a2009s_rh_thickness_Pole-temporal |
| 1295) | aparc-a2009s_rh_thickness_S-calcarine |
| 1296) | aparc-a2009s_rh_thickness_S-central |

| | |
|---|---|
| 1297) | aparc-a2009s_rh_thickness_S-cingul-Marginalis |
| 1298) | aparc-a2009s_rh_thickness_S-circular-insula-ant |
| 1299) | aparc-a2009s_rh_thickness_S-circular-insula-inf |
| 1300) | aparc-a2009s_rh_thickness_S-circular-insula-sup |
| 1301) | aparc-a2009s_rh_thickness_S-collat-transv-ant |
| 1302) | aparc-a2009s_rh_thickness_S-collat-transv-post |
| 1303) | aparc-a2009s_rh_thickness_S-front-inf |
| 1304) | aparc-a2009s_rh_thickness_S-front-middle |
| 1305) | aparc-a2009s_rh_thickness_S-front-sup |
| 1306) | aparc-a2009s_rh_thickness_S-interm-prim-Jensen |
| 1307) | aparc-a2009s_rh_thickness_S-intrapariet+P-trans |
| 1308) | aparc-a2009s_rh_thickness_S-oc-middle+Lunatus |
| 1309) | aparc-a2009s_rh_thickness_S-oc-sup+transversal |
| 1310) | aparc-a2009s_rh_thickness_S-occipital-ant |
| 1311) | aparc-a2009s_rh_thickness_S-oc-temp-lat |
| 1312) | aparc-a2009s_rh_thickness_S-oc-temp-med+Lingual |
| 1313) | aparc-a2009s_rh_thickness_S-orbital-lateral |
| 1314) | aparc-a2009s_rh_thickness_S-orbital-med-olfact |
| 1315) | aparc-a2009s_rh_thickness_S-orbital-H-Shaped |
| 1316) | aparc-a2009s_rh_thickness_S-parieto-occipital |
| 1317) | aparc-a2009s_rh_thickness_S-pericallosal |
| 1318) | aparc-a2009s_rh_thickness_S-postcentral |
| 1319) | aparc-a2009s_rh_thickness_S-precentral-inf-part |
| 1320) | aparc-a2009s_rh_thickness_S-precentral-sup-part |
| 1321) | aparc-a2009s_rh_thickness_S-suborbital |
| 1322) | aparc-a2009s_rh_thickness_S-subparietal |
| 1323) | aparc-a2009s_rh_thickness_S-temporal-inf |
| 1324) | aparc-a2009s_rh_thickness_S-temporal-sup |
| 1325) | aparc-a2009s_rh_thickness_S-temporal-transverse |
| 1326) | aseg_global_intensity_3rd-Ventricle |
| 1327) | aseg_global_intensity_4th-Ventricle |
| 1328) | aseg_global_intensity_5th-Ventricle |
| 1329) | aseg_global_intensity_Brain-Stem |
| 1330) | aseg_global_intensity_CSF |
| 1331) | aseg_global_intensity_WM-hypointensities |
| 1332) | aseg_global_intensity_non-WM-hypointensities |
| 1333) | aseg_global_intensity_Optic-Chiasm |
| 1334) | aseg_global_intensity_CC-Posterior |
| 1335) | aseg_global_intensity_CC-Mid-Posterior |
| 1336) | aseg_global_intensity_CC-Central |
| 1337) | aseg_global_intensity_CC-Mid-Anterior |
| 1338) | aseg_global_intensity_CC-Anterior |

| | |
|---|---|
| 1339) | aseg_lh_intensity_Lateral-Ventricle |
| 1340) | aseg_lh_intensity_Inf-Lat-Vent |
| 1341) | aseg_lh_intensity_Cerebellum-White-Matter |
| 1342) | aseg_lh_intensity_Cerebellum-Cortex |
| 1343) | aseg_lh_intensity_Thalamus-Proper |
| 1344) | aseg_lh_intensity_Caudate |
| 1345) | aseg_lh_intensity_Putamen |
| 1346) | aseg_lh_intensity_Pallidum |
| 1347) | aseg_lh_intensity_Hippocampus |
| 1348) | aseg_lh_intensity_Amygdala |
| 1349) | aseg_lh_intensity_Accumbens-area |
| 1350) | aseg_lh_intensity_VentralDC |
| 1351) | aseg_lh_intensity_vessel |
| 1352) | aseg_lh_intensity_choroid-plexus |
| 1353) | aseg_rh_intensity_Lateral-Ventricle |
| 1354) | aseg_rh_intensity_Inf-Lat-Vent |
| 1355) | aseg_rh_intensity_Cerebellum-White-Matter |
| 1356) | aseg_rh_intensity_Cerebellum-Cortex |
| 1357) | aseg_rh_intensity_Thalamus-Proper |
| 1358) | aseg_rh_intensity_Caudate |
| 1359) | aseg_rh_intensity_Putamen |
| 1360) | aseg_rh_intensity_Pallidum |
| 1361) | aseg_rh_intensity_Hippocampus |
| 1362) | aseg_rh_intensity_Amygdala |
| 1363) | aseg_rh_intensity_Accumbens-area |
| 1364) | aseg_rh_intensity_VentralDC |
| 1365) | aseg_rh_intensity_vessel |
| 1366) | aseg_rh_intensity_choroid-plexus |
| 1367) | wg_lh_intensity-contrast_unknown |
| 1368) | wg_lh_intensity-contrast_bankssts |
| 1369) | wg_lh_intensity-contrast_caudalanteriorcingulate |
| 1370) | wg_lh_intensity-contrast_caudalmiddlefrontal |
| 1371) | wg_lh_intensity-contrast_cuneus |
| 1372) | wg_lh_intensity-contrast_entorhinal |
| 1373) | wg_lh_intensity-contrast_fusiform |
| 1374) | wg_lh_intensity-contrast_inferiorparietal |
| 1375) | wg_lh_intensity-contrast_inferiortemporal |
| 1376) | wg_lh_intensity-contrast_isthmuscingulate |
| 1377) | wg_lh_intensity-contrast_lateraloccipital |
| 1378) | wg_lh_intensity-contrast_lateralorbitofrontal |
| 1379) | wg_lh_intensity-contrast_lingual |
| 1380) | wg_lh_intensity-contrast_medialorbitofrontal |

| | |
|---|---|
| 1381) | wg_lh_intensity-contrast_middletemporal |
| 1382) | wg_lh_intensity-contrast_parahippocampal |
| 1383) | wg_lh_intensity-contrast_paracentral |
| 1384) | wg_lh_intensity-contrast_parsopercularis |
| 1385) | wg_lh_intensity-contrast_parsorbitalis |
| 1386) | wg_lh_intensity-contrast_parstriangularis |
| 1387) | wg_lh_intensity-contrast_pericalcarine |
| 1388) | wg_lh_intensity-contrast_postcentral |
| 1389) | wg_lh_intensity-contrast_posteriorcingulate |
| 1390) | wg_lh_intensity-contrast_precentral |
| 1391) | wg_lh_intensity-contrast_precuneus |
| 1392) | wg_lh_intensity-contrast_rostralanteriorcingulate |
| 1393) | wg_lh_intensity-contrast_rostralmiddlefrontal |
| 1394) | wg_lh_intensity-contrast_superiorfrontal |
| 1395) | wg_lh_intensity-contrast_superiorparietal |
| 1396) | wg_lh_intensity-contrast_superiortemporal |
| 1397) | wg_lh_intensity-contrast_supramarginal |
| 1398) | wg_lh_intensity-contrast_frontalpole |
| 1399) | wg_lh_intensity-contrast_temporalpole |
| 1400) | wg_lh_intensity-contrast_transversetemporal |
| 1401) | wg_lh_intensity-contrast_insula |
| 1402) | wg_rh_intensity-contrast_unknown |
| 1403) | wg_rh_intensity-contrast_bankssts |
| 1404) | wg_rh_intensity-contrast_caudalanteriorcingulate |
| 1405) | wg_rh_intensity-contrast_caudalmiddlefrontal |
| 1406) | wg_rh_intensity-contrast_cuneus |
| 1407) | wg_rh_intensity-contrast_entorhinal |
| 1408) | wg_rh_intensity-contrast_fusiform |
| 1409) | wg_rh_intensity-contrast_inferiorparietal |
| 1410) | wg_rh_intensity-contrast_inferiortemporal |
| 1411) | wg_rh_intensity-contrast_isthmuscingulate |
| 1412) | wg_rh_intensity-contrast_lateraloccipital |
| 1413) | wg_rh_intensity-contrast_lateralorbitofrontal |
| 1414) | wg_rh_intensity-contrast_lingual |
| 1415) | wg_rh_intensity-contrast_medialorbitofrontal |
| 1416) | wg_rh_intensity-contrast_middletemporal |
| 1417) | wg_rh_intensity-contrast_parahippocampal |
| 1418) | wg_rh_intensity-contrast_paracentral |
| 1419) | wg_rh_intensity-contrast_parsopercularis |
| 1420) | wg_rh_intensity-contrast_parsorbitalis |
| 1421) | wg_rh_intensity-contrast_parstriangularis |
| 1422) | wg_rh_intensity-contrast_pericalcarine |

| | |
|---|---|
| 1423) | wg_rh_intensity-contrast_postcentral |
| 1424) | wg_rh_intensity-contrast_posteriorcingulate |
| 1425) | wg_rh_intensity-contrast_precentral |
| 1426) | wg_rh_intensity-contrast_precuneus |
| 1427) | wg_rh_intensity-contrast_rostralanteriorcingulate |
| 1428) | wg_rh_intensity-contrast_rostralmiddlefrontal |
| 1429) | wg_rh_intensity-contrast_superiorfrontal |
| 1430) | wg_rh_intensity-contrast_superiorparietal |
| 1431) | wg_rh_intensity-contrast_superiortemporal |
| 1432) | wg_rh_intensity-contrast_supramarginal |
| 1433) | wg_rh_intensity-contrast_frontalpole |
| 1434) | wg_rh_intensity-contrast_temporalpole |
| 1435) | wg_rh_intensity-contrast_transversetemporal |
| 1436) | wg_rh_intensity-contrast_insula |
| 1437) | IDP_T2_FLAIR_BIANCA_WMH_volume |
| 1438) | IDP_T2_FLAIR_BIANCA_periventWMH_volume |
| 1439) | IDP_T2_FLAIR_BIANCA_deepWMH_volume |
| 1440) | IDP_SWI_T2star_left_thalamus |
| 1441) | IDP_SWI_T2star_right_thalamus |
| 1442) | IDP_SWI_T2star_left_caudate |
| 1443) | IDP_SWI_T2star_right_caudate |
| 1444) | IDP_SWI_T2star_left_putamen |
| 1445) | IDP_SWI_T2star_right_putamen |
| 1446) | IDP_SWI_T2star_left_pallidum |
| 1447) | IDP_SWI_T2star_right_pallidum |
| 1448) | IDP_SWI_T2star_left_hippocampus |
| 1449) | IDP_SWI_T2star_right_hippocampus |
| 1450) | IDP_SWI_T2star_left_amygdala |
| 1451) | IDP_SWI_T2star_right_amygdala |
| 1452) | IDP_SWI_T2star_left_accumbens |
| 1453) | IDP_SWI_T2star_right_accumbens |
| 1454) | IDP_dMRI_TBSS_FA_Middle_cerebellar_peduncle |
| 1455) | IDP_dMRI_TBSS_FA_Pontine_crossing_tract |
| 1456) | IDP_dMRI_TBSS_FA_Genu_of_corpus_callosum |
| 1457) | IDP_dMRI_TBSS_FA_Body_of_corpus_callosum |
| 1458) | IDP_dMRI_TBSS_FA_Splenium_of_corpus_callosum |
| 1459) | IDP_dMRI_TBSS_FA_Fornix |
| 1460) | IDP_dMRI_TBSS_FA_Corticospinal_tract_R |
| 1461) | IDP_dMRI_TBSS_FA_Corticospinal_tract_L |
| 1462) | IDP_dMRI_TBSS_FA_Medial_lemniscus_R |
| 1463) | IDP_dMRI_TBSS_FA_Medial_lemniscus_L |
| 1464) | IDP_dMRI_TBSS_FA_Inferior_cerebellar_peduncle_R |

| | |
|---|---|
| 1465) | IDP_dMRI_TBSS_FA_Inferior_cerebellar_peduncle_L |
| 1466) | IDP_dMRI_TBSS_FA_Superior_cerebellar_peduncle_R |
| 1467) | IDP_dMRI_TBSS_FA_Superior_cerebellar_peduncle_L |
| 1468) | IDP_dMRI_TBSS_FA_Cerebral_peduncle_R |
| 1469) | IDP_dMRI_TBSS_FA_Cerebral_peduncle_L |
| 1470) | IDP_dMRI_TBSS_FA_Anterior_limb_of_internal_capsule_R |
| 1471) | IDP_dMRI_TBSS_FA_Anterior_limb_of_internal_capsule_L |
| 1472) | IDP_dMRI_TBSS_FA_Posterior_limb_of_internal_capsule_R |
| 1473) | IDP_dMRI_TBSS_FA_Posterior_limb_of_internal_capsule_L |
| 1474) | IDP_dMRI_TBSS_FA_Retrolenticular_part_of_internal_capsule_R |
| 1475) | IDP_dMRI_TBSS_FA_Retrolenticular_part_of_internal_capsule_L |
| 1476) | IDP_dMRI_TBSS_FA_Anterior_corona_radiata_R |
| 1477) | IDP_dMRI_TBSS_FA_Anterior_corona_radiata_L |
| 1478) | IDP_dMRI_TBSS_FA_Superior_corona_radiata_R |
| 1479) | IDP_dMRI_TBSS_FA_Superior_corona_radiata_L |
| 1480) | IDP_dMRI_TBSS_FA_Posterior_corona_radiata_R |
| 1481) | IDP_dMRI_TBSS_FA_Posterior_corona_radiata_L |
| 1482) | IDP_dMRI_TBSS_FA_Posterior_thalamic_radiation_R |
| 1483) | IDP_dMRI_TBSS_FA_Posterior_thalamic_radiation_L |
| 1484) | IDP_dMRI_TBSS_FA_Sagittal_stratum_R |
| 1485) | IDP_dMRI_TBSS_FA_Sagittal_stratum_L |
| 1486) | IDP_dMRI_TBSS_FA_External_capsule_R |
| 1487) | IDP_dMRI_TBSS_FA_External_capsule_L |
| 1488) | IDP_dMRI_TBSS_FA_Cingulum_cingulate_gyrus_R |
| 1489) | IDP_dMRI_TBSS_FA_Cingulum_cingulate_gyrus_L |
| 1490) | IDP_dMRI_TBSS_FA_Cingulum_hippocampus_R |
| 1491) | IDP_dMRI_TBSS_FA_Cingulum_hippocampus_L |
| 1492) | IDP_dMRI_TBSS_FA_Fornix_cres+Stria_terminalis_R |
| 1493) | IDP_dMRI_TBSS_FA_Fornix_cres+Stria_terminalis_L |
| 1494) | IDP_dMRI_TBSS_FA_Superior_longitudinal_fasciculus_R |
| 1495) | IDP_dMRI_TBSS_FA_Superior_longitudinal_fasciculus_L |
| 1496) | IDP_dMRI_TBSS_FA_Superior_fronto-occipital_fasciculus_R |
| 1497) | IDP_dMRI_TBSS_FA_Superior_fronto-occipital_fasciculus_L |
| 1498) | IDP_dMRI_TBSS_FA_Uncinate_fasciculus_R |
| 1499) | IDP_dMRI_TBSS_FA_Uncinate_fasciculus_L |
| 1500) | IDP_dMRI_TBSS_FA_Tapetum_R |
| 1501) | IDP_dMRI_TBSS_FA_Tapetum_L |
| 1502) | IDP_dMRI_ProbtrackX_FA_ar_l |
| 1503) | IDP_dMRI_ProbtrackX_FA_ar_r |
| 1504) | IDP_dMRI_ProbtrackX_FA_atr_l |
| 1505) | IDP_dMRI_ProbtrackX_FA_atr_r |
| 1506) | IDP_dMRI_ProbtrackX_FA_cgc_l |

| | |
|---|---|
| 1507) | IDP_dMRI_ProbtrackX_FA_cgc_r |
| 1508) | IDP_dMRI_ProbtrackX_FA_cgh_l |
| 1509) | IDP_dMRI_ProbtrackX_FA_cgh_r |
| 1510) | IDP_dMRI_ProbtrackX_FA_cst_l |
| 1511) | IDP_dMRI_ProbtrackX_FA_cst_r |
| 1512) | IDP_dMRI_ProbtrackX_FA_fma |
| 1513) | IDP_dMRI_ProbtrackX_FA_fmi |
| 1514) | IDP_dMRI_ProbtrackX_FA_ifo_l |
| 1515) | IDP_dMRI_ProbtrackX_FA_ifo_r |
| 1516) | IDP_dMRI_ProbtrackX_FA_ilf_l |
| 1517) | IDP_dMRI_ProbtrackX_FA_ilf_r |
| 1518) | IDP_dMRI_ProbtrackX_FA_mcp |
| 1519) | IDP_dMRI_ProbtrackX_FA_ml_l |
| 1520) | IDP_dMRI_ProbtrackX_FA_ml_r |
| 1521) | IDP_dMRI_ProbtrackX_FA_ptr_l |
| 1522) | IDP_dMRI_ProbtrackX_FA_ptr_r |
| 1523) | IDP_dMRI_ProbtrackX_FA_slf_l |
| 1524) | IDP_dMRI_ProbtrackX_FA_slf_r |
| 1525) | IDP_dMRI_ProbtrackX_FA_str_l |
| 1526) | IDP_dMRI_ProbtrackX_FA_str_r |
| 1527) | IDP_dMRI_ProbtrackX_FA_unc_l |
| 1528) | IDP_dMRI_ProbtrackX_FA_unc_r |
| 1529) | IDP_dMRI_TBSS_MO_Middle_cerebellar_peduncle |
| 1530) | IDP_dMRI_TBSS_MO_Pontine_crossing_tract |
| 1531) | IDP_dMRI_TBSS_MO_Genu_of_corpus_callosum |
| 1532) | IDP_dMRI_TBSS_MO_Body_of_corpus_callosum |
| 1533) | IDP_dMRI_TBSS_MO_Splenium_of_corpus_callosum |
| 1534) | IDP_dMRI_TBSS_MO_Fornix |
| 1535) | IDP_dMRI_TBSS_MO_Corticospinal_tract_R |
| 1536) | IDP_dMRI_TBSS_MO_Corticospinal_tract_L |
| 1537) | IDP_dMRI_TBSS_MO_Medial_lemniscus_R |
| 1538) | IDP_dMRI_TBSS_MO_Medial_lemniscus_L |
| 1539) | IDP_dMRI_TBSS_MO_Inferior_cerebellar_peduncle_R |
| 1540) | IDP_dMRI_TBSS_MO_Inferior_cerebellar_peduncle_L |
| 1541) | IDP_dMRI_TBSS_MO_Superior_cerebellar_peduncle_R |
| 1542) | IDP_dMRI_TBSS_MO_Superior_cerebellar_peduncle_L |
| 1543) | IDP_dMRI_TBSS_MO_Cerebral_peduncle_R |
| 1544) | IDP_dMRI_TBSS_MO_Cerebral_peduncle_L |
| 1545) | IDP_dMRI_TBSS_MO_Anterior_limb_of_internal_capsule_R |
| 1546) | IDP_dMRI_TBSS_MO_Anterior_limb_of_internal_capsule_L |
| 1547) | IDP_dMRI_TBSS_MO_Posterior_limb_of_internal_capsule_R |
| 1548) | IDP_dMRI_TBSS_MO_Posterior_limb_of_internal_capsule_L |

| | |
|---|---|
| 1549) | IDP_dMRI_TBSS_MO_Retrolenticular_part_of_internal_capsule_R |
| 1550) | IDP_dMRI_TBSS_MO_Retrolenticular_part_of_internal_capsule_L |
| 1551) | IDP_dMRI_TBSS_MO_Anterior_corona_radiata_R |
| 1552) | IDP_dMRI_TBSS_MO_Anterior_corona_radiata_L |
| 1553) | IDP_dMRI_TBSS_MO_Superior_corona_radiata_R |
| 1554) | IDP_dMRI_TBSS_MO_Superior_corona_radiata_L |
| 1555) | IDP_dMRI_TBSS_MO_Posterior_corona_radiata_R |
| 1556) | IDP_dMRI_TBSS_MO_Posterior_corona_radiata_L |
| 1557) | IDP_dMRI_TBSS_MO_Posterior_thalamic_radiation_R |
| 1558) | IDP_dMRI_TBSS_MO_Posterior_thalamic_radiation_L |
| 1559) | IDP_dMRI_TBSS_MO_Sagittal_stratum_R |
| 1560) | IDP_dMRI_TBSS_MO_Sagittal_stratum_L |
| 1561) | IDP_dMRI_TBSS_MO_External_capsule_R |
| 1562) | IDP_dMRI_TBSS_MO_External_capsule_L |
| 1563) | IDP_dMRI_TBSS_MO_Cingulum_cingulate_gyrus_R |
| 1564) | IDP_dMRI_TBSS_MO_Cingulum_cingulate_gyrus_L |
| 1565) | IDP_dMRI_TBSS_MO_Cingulum_hippocampus_R |
| 1566) | IDP_dMRI_TBSS_MO_Cingulum_hippocampus_L |
| 1567) | IDP_dMRI_TBSS_MO_Fornix_cres+Stria_terminalis_R |
| 1568) | IDP_dMRI_TBSS_MO_Fornix_cres+Stria_terminalis_L |
| 1569) | IDP_dMRI_TBSS_MO_Superior_longitudinal_fasciculus_R |
| 1570) | IDP_dMRI_TBSS_MO_Superior_longitudinal_fasciculus_L |
| 1571) | IDP_dMRI_TBSS_MO_Superior_fronto-occipital_fasciculus_R |
| 1572) | IDP_dMRI_TBSS_MO_Superior_fronto-occipital_fasciculus_L |
| 1573) | IDP_dMRI_TBSS_MO_Uncinate_fasciculus_R |
| 1574) | IDP_dMRI_TBSS_MO_Uncinate_fasciculus_L |
| 1575) | IDP_dMRI_TBSS_MO_Tapetum_R |
| 1576) | IDP_dMRI_TBSS_MO_Tapetum_L |
| 1577) | IDP_dMRI_ProbtrackX_MO_ar_l |
| 1578) | IDP_dMRI_ProbtrackX_MO_ar_r |
| 1579) | IDP_dMRI_ProbtrackX_MO_atr_l |
| 1580) | IDP_dMRI_ProbtrackX_MO_atr_r |
| 1581) | IDP_dMRI_ProbtrackX_MO_cgc_l |
| 1582) | IDP_dMRI_ProbtrackX_MO_cgc_r |
| 1583) | IDP_dMRI_ProbtrackX_MO_cgh_l |
| 1584) | IDP_dMRI_ProbtrackX_MO_cgh_r |
| 1585) | IDP_dMRI_ProbtrackX_MO_cst_l |
| 1586) | IDP_dMRI_ProbtrackX_MO_cst_r |
| 1587) | IDP_dMRI_ProbtrackX_MO_fma |
| 1588) | IDP_dMRI_ProbtrackX_MO_fmi |
| 1589) | IDP_dMRI_ProbtrackX_MO_ifo_l |
| 1590) | IDP_dMRI_ProbtrackX_MO_ifo_r |

| | |
|---|---|
| 1591) | IDP_dMRI_ProbtrackX_MO_ilf_l |
| 1592) | IDP_dMRI_ProbtrackX_MO_ilf_r |
| 1593) | IDP_dMRI_ProbtrackX_MO_mcp |
| 1594) | IDP_dMRI_ProbtrackX_MO_ml_l |
| 1595) | IDP_dMRI_ProbtrackX_MO_ml_r |
| 1596) | IDP_dMRI_ProbtrackX_MO_ptr_l |
| 1597) | IDP_dMRI_ProbtrackX_MO_ptr_r |
| 1598) | IDP_dMRI_ProbtrackX_MO_slf_l |
| 1599) | IDP_dMRI_ProbtrackX_MO_slf_r |
| 1600) | IDP_dMRI_ProbtrackX_MO_str_l |
| 1601) | IDP_dMRI_ProbtrackX_MO_str_r |
| 1602) | IDP_dMRI_ProbtrackX_MO_unc_l |
| 1603) | IDP_dMRI_ProbtrackX_MO_unc_r |
| 1604) | IDP_dMRI_TBSS_MD_Middle_cerebellar_peduncle |
| 1605) | IDP_dMRI_TBSS_MD_Pontine_crossing_tract |
| 1606) | IDP_dMRI_TBSS_MD_Genu_of_corpus_callosum |
| 1607) | IDP_dMRI_TBSS_MD_Body_of_corpus_callosum |
| 1608) | IDP_dMRI_TBSS_MD_Splenium_of_corpus_callosum |
| 1609) | IDP_dMRI_TBSS_MD_Fornix |
| 1610) | IDP_dMRI_TBSS_MD_Corticospinal_tract_R |
| 1611) | IDP_dMRI_TBSS_MD_Corticospinal_tract_L |
| 1612) | IDP_dMRI_TBSS_MD_Medial_lemniscus_R |
| 1613) | IDP_dMRI_TBSS_MD_Medial_lemniscus_L |
| 1614) | IDP_dMRI_TBSS_MD_Inferior_cerebellar_peduncle_R |
| 1615) | IDP_dMRI_TBSS_MD_Inferior_cerebellar_peduncle_L |
| 1616) | IDP_dMRI_TBSS_MD_Superior_cerebellar_peduncle_R |
| 1617) | IDP_dMRI_TBSS_MD_Superior_cerebellar_peduncle_L |
| 1618) | IDP_dMRI_TBSS_MD_Cerebral_peduncle_R |
| 1619) | IDP_dMRI_TBSS_MD_Cerebral_peduncle_L |
| 1620) | IDP_dMRI_TBSS_MD_Anterior_limb_of_internal_capsule_R |
| 1621) | IDP_dMRI_TBSS_MD_Anterior_limb_of_internal_capsule_L |
| 1622) | IDP_dMRI_TBSS_MD_Posterior_limb_of_internal_capsule_R |
| 1623) | IDP_dMRI_TBSS_MD_Posterior_limb_of_internal_capsule_L |
| 1624) | IDP_dMRI_TBSS_MD_Retrolenticular_part_of_internal_capsule_R |
| 1625) | IDP_dMRI_TBSS_MD_Retrolenticular_part_of_internal_capsule_L |
| 1626) | IDP_dMRI_TBSS_MD_Anterior_corona_radiata_R |
| 1627) | IDP_dMRI_TBSS_MD_Anterior_corona_radiata_L |
| 1628) | IDP_dMRI_TBSS_MD_Superior_corona_radiata_R |
| 1629) | IDP_dMRI_TBSS_MD_Superior_corona_radiata_L |
| 1630) | IDP_dMRI_TBSS_MD_Posterior_corona_radiata_R |
| 1631) | IDP_dMRI_TBSS_MD_Posterior_corona_radiata_L |
| 1632) | IDP_dMRI_TBSS_MD_Posterior_thalamic_radiation_R |

| | |
|---|---|
| 1633) | IDP_dMRI_TBSS_MD_Posterior_thalamic_radiation_L |
| 1634) | IDP_dMRI_TBSS_MD_Sagittal_stratum_R |
| 1635) | IDP_dMRI_TBSS_MD_Sagittal_stratum_L |
| 1636) | IDP_dMRI_TBSS_MD_External_capsule_R |
| 1637) | IDP_dMRI_TBSS_MD_External_capsule_L |
| 1638) | IDP_dMRI_TBSS_MD_Cingulum_cingulate_gyrus_R |
| 1639) | IDP_dMRI_TBSS_MD_Cingulum_cingulate_gyrus_L |
| 1640) | IDP_dMRI_TBSS_MD_Cingulum_hippocampus_R |
| 1641) | IDP_dMRI_TBSS_MD_Cingulum_hippocampus_L |
| 1642) | IDP_dMRI_TBSS_MD_Fornix_cres+Stria_terminalis_R |
| 1643) | IDP_dMRI_TBSS_MD_Fornix_cres+Stria_terminalis_L |
| 1644) | IDP_dMRI_TBSS_MD_Superior_longitudinal_fasciculus_R |
| 1645) | IDP_dMRI_TBSS_MD_Superior_longitudinal_fasciculus_L |
| 1646) | IDP_dMRI_TBSS_MD_Superior_fronto-occipital_fasciculus_R |
| 1647) | IDP_dMRI_TBSS_MD_Superior_fronto-occipital_fasciculus_L |
| 1648) | IDP_dMRI_TBSS_MD_Uncinate_fasciculus_R |
| 1649) | IDP_dMRI_TBSS_MD_Uncinate_fasciculus_L |
| 1650) | IDP_dMRI_TBSS_MD_Tapetum_R |
| 1651) | IDP_dMRI_TBSS_MD_Tapetum_L |
| 1652) | IDP_dMRI_TBSS_L1_Middle_cerebellar_peduncle |
| 1653) | IDP_dMRI_TBSS_L1_Pontine_crossing_tract |
| 1654) | IDP_dMRI_TBSS_L1_Genu_of_corpus_callosum |
| 1655) | IDP_dMRI_TBSS_L1_Body_of_corpus_callosum |
| 1656) | IDP_dMRI_TBSS_L1_Splenium_of_corpus_callosum |
| 1657) | IDP_dMRI_TBSS_L1_Fornix |
| 1658) | IDP_dMRI_TBSS_L1_Corticospinal_tract_R |
| 1659) | IDP_dMRI_TBSS_L1_Corticospinal_tract_L |
| 1660) | IDP_dMRI_TBSS_L1_Medial_lemniscus_R |
| 1661) | IDP_dMRI_TBSS_L1_Medial_lemniscus_L |
| 1662) | IDP_dMRI_TBSS_L1_Inferior_cerebellar_peduncle_R |
| 1663) | IDP_dMRI_TBSS_L1_Inferior_cerebellar_peduncle_L |
| 1664) | IDP_dMRI_TBSS_L1_Superior_cerebellar_peduncle_R |
| 1665) | IDP_dMRI_TBSS_L1_Superior_cerebellar_peduncle_L |
| 1666) | IDP_dMRI_TBSS_L1_Cerebral_peduncle_R |
| 1667) | IDP_dMRI_TBSS_L1_Cerebral_peduncle_L |
| 1668) | IDP_dMRI_TBSS_L1_Anterior_limb_of_internal_capsule_R |
| 1669) | IDP_dMRI_TBSS_L1_Anterior_limb_of_internal_capsule_L |
| 1670) | IDP_dMRI_TBSS_L1_Posterior_limb_of_internal_capsule_R |
| 1671) | IDP_dMRI_TBSS_L1_Posterior_limb_of_internal_capsule_L |
| 1672) | IDP_dMRI_TBSS_L1_Retrolenticular_part_of_internal_capsule_R |
| 1673) | IDP_dMRI_TBSS_L1_Retrolenticular_part_of_internal_capsule_L |
| 1674) | IDP_dMRI_TBSS_L1_Anterior_corona_radiata_R |

| | |
|---|---|
| 1675) | IDP_dMRI_TBSS_L1_Anterior_corona_radiata_L |
| 1676) | IDP_dMRI_TBSS_L1_Superior_corona_radiata_R |
| 1677) | IDP_dMRI_TBSS_L1_Superior_corona_radiata_L |
| 1678) | IDP_dMRI_TBSS_L1_Posterior_corona_radiata_R |
| 1679) | IDP_dMRI_TBSS_L1_Posterior_corona_radiata_L |
| 1680) | IDP_dMRI_TBSS_L1_Posterior_thalamic_radiation_R |
| 1681) | IDP_dMRI_TBSS_L1_Posterior_thalamic_radiation_L |
| 1682) | IDP_dMRI_TBSS_L1_Sagittal_stratum_R |
| 1683) | IDP_dMRI_TBSS_L1_Sagittal_stratum_L |
| 1684) | IDP_dMRI_TBSS_L1_External_capsule_R |
| 1685) | IDP_dMRI_TBSS_L1_External_capsule_L |
| 1686) | IDP_dMRI_TBSS_L1_Cingulum_cingulate_gyrus_R |
| 1687) | IDP_dMRI_TBSS_L1_Cingulum_cingulate_gyrus_L |
| 1688) | IDP_dMRI_TBSS_L1_Cingulum_hippocampus_R |
| 1689) | IDP_dMRI_TBSS_L1_Cingulum_hippocampus_L |
| 1690) | IDP_dMRI_TBSS_L1_Fornix_cres+Stria_terminalis_R |
| 1691) | IDP_dMRI_TBSS_L1_Fornix_cres+Stria_terminalis_L |
| 1692) | IDP_dMRI_TBSS_L1_Superior_longitudinal_fasciculus_R |
| 1693) | IDP_dMRI_TBSS_L1_Superior_longitudinal_fasciculus_L |
| 1694) | IDP_dMRI_TBSS_L1_Superior_fronto-occipital_fasciculus_R |
| 1695) | IDP_dMRI_TBSS_L1_Superior_fronto-occipital_fasciculus_L |
| 1696) | IDP_dMRI_TBSS_L1_Uncinate_fasciculus_R |
| 1697) | IDP_dMRI_TBSS_L1_Uncinate_fasciculus_L |
| 1698) | IDP_dMRI_TBSS_L1_Tapetum_R |
| 1699) | IDP_dMRI_TBSS_L1_Tapetum_L |
| 1700) | IDP_dMRI_TBSS_L2_Middle_cerebellar_peduncle |
| 1701) | IDP_dMRI_TBSS_L2_Pontine_crossing_tract |
| 1702) | IDP_dMRI_TBSS_L2_Genu_of_corpus_callosum |
| 1703) | IDP_dMRI_TBSS_L2_Body_of_corpus_callosum |
| 1704) | IDP_dMRI_TBSS_L2_Splenium_of_corpus_callosum |
| 1705) | IDP_dMRI_TBSS_L2_Fornix |
| 1706) | IDP_dMRI_TBSS_L2_Corticospinal_tract_R |
| 1707) | IDP_dMRI_TBSS_L2_Corticospinal_tract_L |
| 1708) | IDP_dMRI_TBSS_L2_Medial_lemniscus_R |
| 1709) | IDP_dMRI_TBSS_L2_Medial_lemniscus_L |
| 1710) | IDP_dMRI_TBSS_L2_Inferior_cerebellar_peduncle_R |
| 1711) | IDP_dMRI_TBSS_L2_Inferior_cerebellar_peduncle_L |
| 1712) | IDP_dMRI_TBSS_L2_Superior_cerebellar_peduncle_R |
| 1713) | IDP_dMRI_TBSS_L2_Superior_cerebellar_peduncle_L |
| 1714) | IDP_dMRI_TBSS_L2_Cerebral_peduncle_R |
| 1715) | IDP_dMRI_TBSS_L2_Cerebral_peduncle_L |
| 1716) | IDP_dMRI_TBSS_L2_Anterior_limb_of_internal_capsule_R |

| | |
|---|---|
| 1717) | IDP_dMRI_TBSS_L2_Anterior_limb_of_internal_capsule_L |
| 1718) | IDP_dMRI_TBSS_L2_Posterior_limb_of_internal_capsule_R |
| 1719) | IDP_dMRI_TBSS_L2_Posterior_limb_of_internal_capsule_L |
| 1720) | IDP_dMRI_TBSS_L2_Retrolenticular_part_of_internal_capsule_R |
| 1721) | IDP_dMRI_TBSS_L2_Retrolenticular_part_of_internal_capsule_L |
| 1722) | IDP_dMRI_TBSS_L2_Anterior_corona_radiata_R |
| 1723) | IDP_dMRI_TBSS_L2_Anterior_corona_radiata_L |
| 1724) | IDP_dMRI_TBSS_L2_Superior_corona_radiata_R |
| 1725) | IDP_dMRI_TBSS_L2_Superior_corona_radiata_L |
| 1726) | IDP_dMRI_TBSS_L2_Posterior_corona_radiata_R |
| 1727) | IDP_dMRI_TBSS_L2_Posterior_corona_radiata_L |
| 1728) | IDP_dMRI_TBSS_L2_Posterior_thalamic_radiation_R |
| 1729) | IDP_dMRI_TBSS_L2_Posterior_thalamic_radiation_L |
| 1730) | IDP_dMRI_TBSS_L2_Sagittal_stratum_R |
| 1731) | IDP_dMRI_TBSS_L2_Sagittal_stratum_L |
| 1732) | IDP_dMRI_TBSS_L2_External_capsule_R |
| 1733) | IDP_dMRI_TBSS_L2_External_capsule_L |
| 1734) | IDP_dMRI_TBSS_L2_Cingulum_cingulate_gyrus_R |
| 1735) | IDP_dMRI_TBSS_L2_Cingulum_cingulate_gyrus_L |
| 1736) | IDP_dMRI_TBSS_L2_Cingulum_hippocampus_R |
| 1737) | IDP_dMRI_TBSS_L2_Cingulum_hippocampus_L |
| 1738) | IDP_dMRI_TBSS_L2_Fornix_cres+Stria_terminalis_R |
| 1739) | IDP_dMRI_TBSS_L2_Fornix_cres+Stria_terminalis_L |
| 1740) | IDP_dMRI_TBSS_L2_Superior_longitudinal_fasciculus_R |
| 1741) | IDP_dMRI_TBSS_L2_Superior_longitudinal_fasciculus_L |
| 1742) | IDP_dMRI_TBSS_L2_Superior_fronto-occipital_fasciculus_R |
| 1743) | IDP_dMRI_TBSS_L2_Superior_fronto-occipital_fasciculus_L |
| 1744) | IDP_dMRI_TBSS_L2_Uncinate_fasciculus_R |
| 1745) | IDP_dMRI_TBSS_L2_Uncinate_fasciculus_L |
| 1746) | IDP_dMRI_TBSS_L2_Tapetum_R |
| 1747) | IDP_dMRI_TBSS_L2_Tapetum_L |
| 1748) | IDP_dMRI_TBSS_L3_Middle_cerebellar_peduncle |
| 1749) | IDP_dMRI_TBSS_L3_Pontine_crossing_tract |
| 1750) | IDP_dMRI_TBSS_L3_Genu_of_corpus_callosum |
| 1751) | IDP_dMRI_TBSS_L3_Body_of_corpus_callosum |
| 1752) | IDP_dMRI_TBSS_L3_Splenium_of_corpus_callosum |
| 1753) | IDP_dMRI_TBSS_L3_Fornix |
| 1754) | IDP_dMRI_TBSS_L3_Corticospinal_tract_R |
| 1755) | IDP_dMRI_TBSS_L3_Corticospinal_tract_L |
| 1756) | IDP_dMRI_TBSS_L3_Medial_lemniscus_R |
| 1757) | IDP_dMRI_TBSS_L3_Medial_lemniscus_L |
| 1758) | IDP_dMRI_TBSS_L3_Inferior_cerebellar_peduncle_R |

| | |
|---|---|
| 1759) | IDP_dMRI_TBSS_L3_Inferior_cerebellar_peduncle_L |
| 1760) | IDP_dMRI_TBSS_L3_Superior_cerebellar_peduncle_R |
| 1761) | IDP_dMRI_TBSS_L3_Superior_cerebellar_peduncle_L |
| 1762) | IDP_dMRI_TBSS_L3_Cerebral_peduncle_R |
| 1763) | IDP_dMRI_TBSS_L3_Cerebral_peduncle_L |
| 1764) | IDP_dMRI_TBSS_L3_Anterior_limb_of_internal_capsule_R |
| 1765) | IDP_dMRI_TBSS_L3_Anterior_limb_of_internal_capsule_L |
| 1766) | IDP_dMRI_TBSS_L3_Posterior_limb_of_internal_capsule_R |
| 1767) | IDP_dMRI_TBSS_L3_Posterior_limb_of_internal_capsule_L |
| 1768) | IDP_dMRI_TBSS_L3_Retrolenticular_part_of_internal_capsule_R |
| 1769) | IDP_dMRI_TBSS_L3_Retrolenticular_part_of_internal_capsule_L |
| 1770) | IDP_dMRI_TBSS_L3_Anterior_corona_radiata_R |
| 1771) | IDP_dMRI_TBSS_L3_Anterior_corona_radiata_L |
| 1772) | IDP_dMRI_TBSS_L3_Superior_corona_radiata_R |
| 1773) | IDP_dMRI_TBSS_L3_Superior_corona_radiata_L |
| 1774) | IDP_dMRI_TBSS_L3_Posterior_corona_radiata_R |
| 1775) | IDP_dMRI_TBSS_L3_Posterior_corona_radiata_L |
| 1776) | IDP_dMRI_TBSS_L3_Posterior_thalamic_radiation_R |
| 1777) | IDP_dMRI_TBSS_L3_Posterior_thalamic_radiation_L |
| 1778) | IDP_dMRI_TBSS_L3_Sagittal_stratum_R |
| 1779) | IDP_dMRI_TBSS_L3_Sagittal_stratum_L |
| 1780) | IDP_dMRI_TBSS_L3_External_capsule_R |
| 1781) | IDP_dMRI_TBSS_L3_External_capsule_L |
| 1782) | IDP_dMRI_TBSS_L3_Cingulum_cingulate_gyrus_R |
| 1783) | IDP_dMRI_TBSS_L3_Cingulum_cingulate_gyrus_L |
| 1784) | IDP_dMRI_TBSS_L3_Cingulum_hippocampus_R |
| 1785) | IDP_dMRI_TBSS_L3_Cingulum_hippocampus_L |
| 1786) | IDP_dMRI_TBSS_L3_Fornix_cres+Stria_terminalis_R |
| 1787) | IDP_dMRI_TBSS_L3_Fornix_cres+Stria_terminalis_L |
| 1788) | IDP_dMRI_TBSS_L3_Superior_longitudinal_fasciculus_R |
| 1789) | IDP_dMRI_TBSS_L3_Superior_longitudinal_fasciculus_L |
| 1790) | IDP_dMRI_TBSS_L3_Superior_fronto-occipital_fasciculus_R |
| 1791) | IDP_dMRI_TBSS_L3_Superior_fronto-occipital_fasciculus_L |
| 1792) | IDP_dMRI_TBSS_L3_Uncinate_fasciculus_R |
| 1793) | IDP_dMRI_TBSS_L3_Uncinate_fasciculus_L |
| 1794) | IDP_dMRI_TBSS_L3_Tapetum_R |
| 1795) | IDP_dMRI_TBSS_L3_Tapetum_L |
| 1796) | IDP_dMRI_ProbtrackX_MD_ar_l |
| 1797) | IDP_dMRI_ProbtrackX_MD_ar_r |
| 1798) | IDP_dMRI_ProbtrackX_MD_atr_l |
| 1799) | IDP_dMRI_ProbtrackX_MD_atr_r |
| 1800) | IDP_dMRI_ProbtrackX_MD_cgc_l |

| | |
|---|---|
| 1801) | IDP_dMRI_ProbtrackX_MD_cgc_r |
| 1802) | IDP_dMRI_ProbtrackX_MD_cgh_l |
| 1803) | IDP_dMRI_ProbtrackX_MD_cgh_r |
| 1804) | IDP_dMRI_ProbtrackX_MD_cst_l |
| 1805) | IDP_dMRI_ProbtrackX_MD_cst_r |
| 1806) | IDP_dMRI_ProbtrackX_MD_fma |
| 1807) | IDP_dMRI_ProbtrackX_MD_fmi |
| 1808) | IDP_dMRI_ProbtrackX_MD_ifo_l |
| 1809) | IDP_dMRI_ProbtrackX_MD_ifo_r |
| 1810) | IDP_dMRI_ProbtrackX_MD_ilf_l |
| 1811) | IDP_dMRI_ProbtrackX_MD_ilf_r |
| 1812) | IDP_dMRI_ProbtrackX_MD_mcp |
| 1813) | IDP_dMRI_ProbtrackX_MD_ml_l |
| 1814) | IDP_dMRI_ProbtrackX_MD_ml_r |
| 1815) | IDP_dMRI_ProbtrackX_MD_ptr_l |
| 1816) | IDP_dMRI_ProbtrackX_MD_ptr_r |
| 1817) | IDP_dMRI_ProbtrackX_MD_slf_l |
| 1818) | IDP_dMRI_ProbtrackX_MD_slf_r |
| 1819) | IDP_dMRI_ProbtrackX_MD_str_l |
| 1820) | IDP_dMRI_ProbtrackX_MD_str_r |
| 1821) | IDP_dMRI_ProbtrackX_MD_unc_l |
| 1822) | IDP_dMRI_ProbtrackX_MD_unc_r |
| 1823) | IDP_dMRI_ProbtrackX_L1_ar_l |
| 1824) | IDP_dMRI_ProbtrackX_L1_ar_r |
| 1825) | IDP_dMRI_ProbtrackX_L1_atr_l |
| 1826) | IDP_dMRI_ProbtrackX_L1_atr_r |
| 1827) | IDP_dMRI_ProbtrackX_L1_cgc_l |
| 1828) | IDP_dMRI_ProbtrackX_L1_cgc_r |
| 1829) | IDP_dMRI_ProbtrackX_L1_cgh_l |
| 1830) | IDP_dMRI_ProbtrackX_L1_cgh_r |
| 1831) | IDP_dMRI_ProbtrackX_L1_cst_l |
| 1832) | IDP_dMRI_ProbtrackX_L1_cst_r |
| 1833) | IDP_dMRI_ProbtrackX_L1_fma |
| 1834) | IDP_dMRI_ProbtrackX_L1_fmi |
| 1835) | IDP_dMRI_ProbtrackX_L1_ifo_l |
| 1836) | IDP_dMRI_ProbtrackX_L1_ifo_r |
| 1837) | IDP_dMRI_ProbtrackX_L1_ilf_l |
| 1838) | IDP_dMRI_ProbtrackX_L1_ilf_r |
| 1839) | IDP_dMRI_ProbtrackX_L1_mcp |
| 1840) | IDP_dMRI_ProbtrackX_L1_ml_l |
| 1841) | IDP_dMRI_ProbtrackX_L1_ml_r |
| 1842) | IDP_dMRI_ProbtrackX_L1_ptr_l |

| | |
|---|---|
| 1843) | IDP_dMRI_ProbtrackX_L1_ptr_r |
| 1844) | IDP_dMRI_ProbtrackX_L1_slf_l |
| 1845) | IDP_dMRI_ProbtrackX_L1_slf_r |
| 1846) | IDP_dMRI_ProbtrackX_L1_str_l |
| 1847) | IDP_dMRI_ProbtrackX_L1_str_r |
| 1848) | IDP_dMRI_ProbtrackX_L1_unc_l |
| 1849) | IDP_dMRI_ProbtrackX_L1_unc_r |
| 1850) | IDP_dMRI_ProbtrackX_L2_ar_l |
| 1851) | IDP_dMRI_ProbtrackX_L2_ar_r |
| 1852) | IDP_dMRI_ProbtrackX_L2_atr_l |
| 1853) | IDP_dMRI_ProbtrackX_L2_atr_r |
| 1854) | IDP_dMRI_ProbtrackX_L2_cgc_l |
| 1855) | IDP_dMRI_ProbtrackX_L2_cgc_r |
| 1856) | IDP_dMRI_ProbtrackX_L2_cgh_l |
| 1857) | IDP_dMRI_ProbtrackX_L2_cgh_r |
| 1858) | IDP_dMRI_ProbtrackX_L2_cst_l |
| 1859) | IDP_dMRI_ProbtrackX_L2_cst_r |
| 1860) | IDP_dMRI_ProbtrackX_L2_fma |
| 1861) | IDP_dMRI_ProbtrackX_L2_fmi |
| 1862) | IDP_dMRI_ProbtrackX_L2_ifo_l |
| 1863) | IDP_dMRI_ProbtrackX_L2_ifo_r |
| 1864) | IDP_dMRI_ProbtrackX_L2_ilf_l |
| 1865) | IDP_dMRI_ProbtrackX_L2_ilf_r |
| 1866) | IDP_dMRI_ProbtrackX_L2_mcp |
| 1867) | IDP_dMRI_ProbtrackX_L2_ml_l |
| 1868) | IDP_dMRI_ProbtrackX_L2_ml_r |
| 1869) | IDP_dMRI_ProbtrackX_L2_ptr_l |
| 1870) | IDP_dMRI_ProbtrackX_L2_ptr_r |
| 1871) | IDP_dMRI_ProbtrackX_L2_slf_l |
| 1872) | IDP_dMRI_ProbtrackX_L2_slf_r |
| 1873) | IDP_dMRI_ProbtrackX_L2_str_l |
| 1874) | IDP_dMRI_ProbtrackX_L2_str_r |
| 1875) | IDP_dMRI_ProbtrackX_L2_unc_l |
| 1876) | IDP_dMRI_ProbtrackX_L2_unc_r |
| 1877) | IDP_dMRI_ProbtrackX_L3_ar_l |
| 1878) | IDP_dMRI_ProbtrackX_L3_ar_r |
| 1879) | IDP_dMRI_ProbtrackX_L3_atr_l |
| 1880) | IDP_dMRI_ProbtrackX_L3_atr_r |
| 1881) | IDP_dMRI_ProbtrackX_L3_cgc_l |
| 1882) | IDP_dMRI_ProbtrackX_L3_cgc_r |
| 1883) | IDP_dMRI_ProbtrackX_L3_cgh_l |
| 1884) | IDP_dMRI_ProbtrackX_L3_cgh_r |

| | |
|---|---|
| 1885) | IDP_dMRI_ProbtrackX_L3_cst_l |
| 1886) | IDP_dMRI_ProbtrackX_L3_cst_r |
| 1887) | IDP_dMRI_ProbtrackX_L3_fma |
| 1888) | IDP_dMRI_ProbtrackX_L3_fmi |
| 1889) | IDP_dMRI_ProbtrackX_L3_ifo_l |
| 1890) | IDP_dMRI_ProbtrackX_L3_ifo_r |
| 1891) | IDP_dMRI_ProbtrackX_L3_ilf_l |
| 1892) | IDP_dMRI_ProbtrackX_L3_ilf_r |
| 1893) | IDP_dMRI_ProbtrackX_L3_mcp |
| 1894) | IDP_dMRI_ProbtrackX_L3_ml_l |
| 1895) | IDP_dMRI_ProbtrackX_L3_ml_r |
| 1896) | IDP_dMRI_ProbtrackX_L3_ptr_l |
| 1897) | IDP_dMRI_ProbtrackX_L3_ptr_r |
| 1898) | IDP_dMRI_ProbtrackX_L3_slf_l |
| 1899) | IDP_dMRI_ProbtrackX_L3_slf_r |
| 1900) | IDP_dMRI_ProbtrackX_L3_str_l |
| 1901) | IDP_dMRI_ProbtrackX_L3_str_r |
| 1902) | IDP_dMRI_ProbtrackX_L3_unc_l |
| 1903) | IDP_dMRI_ProbtrackX_L3_unc_r |
| 1904) | IDP_dMRI_TBSS_ICVF_Middle_cerebellar_peduncle |
| 1905) | IDP_dMRI_TBSS_ICVF_Pontine_crossing_tract |
| 1906) | IDP_dMRI_TBSS_ICVF_Genu_of_corpus_callosum |
| 1907) | IDP_dMRI_TBSS_ICVF_Body_of_corpus_callosum |
| 1908) | IDP_dMRI_TBSS_ICVF_Splenium_of_corpus_callosum |
| 1909) | IDP_dMRI_TBSS_ICVF_Fornix |
| 1910) | IDP_dMRI_TBSS_ICVF_Corticospinal_tract_R |
| 1911) | IDP_dMRI_TBSS_ICVF_Corticospinal_tract_L |
| 1912) | IDP_dMRI_TBSS_ICVF_Medial_lemniscus_R |
| 1913) | IDP_dMRI_TBSS_ICVF_Medial_lemniscus_L |
| 1914) | IDP_dMRI_TBSS_ICVF_Inferior_cerebellar_peduncle_R |
| 1915) | IDP_dMRI_TBSS_ICVF_Inferior_cerebellar_peduncle_L |
| 1916) | IDP_dMRI_TBSS_ICVF_Superior_cerebellar_peduncle_R |
| 1917) | IDP_dMRI_TBSS_ICVF_Superior_cerebellar_peduncle_L |
| 1918) | IDP_dMRI_TBSS_ICVF_Cerebral_peduncle_R |
| 1919) | IDP_dMRI_TBSS_ICVF_Cerebral_peduncle_L |
| 1920) | IDP_dMRI_TBSS_ICVF_Anterior_limb_of_internal_capsule_R |
| 1921) | IDP_dMRI_TBSS_ICVF_Anterior_limb_of_internal_capsule_L |
| 1922) | IDP_dMRI_TBSS_ICVF_Posterior_limb_of_internal_capsule_R |
| 1923) | IDP_dMRI_TBSS_ICVF_Posterior_limb_of_internal_capsule_L |
| 1924) | IDP_dMRI_TBSS_ICVF_Retrolenticular_part_of_internal_capsule_R |
| 1925) | IDP_dMRI_TBSS_ICVF_Retrolenticular_part_of_internal_capsule_L |
| 1926) | IDP_dMRI_TBSS_ICVF_Anterior_corona_radiata_R |

| | |
|---|---|
| 1927) | IDP_dMRI_TBSS_ICVF_Anterior_corona_radiata_L |
| 1928) | IDP_dMRI_TBSS_ICVF_Superior_corona_radiata_R |
| 1929) | IDP_dMRI_TBSS_ICVF_Superior_corona_radiata_L |
| 1930) | IDP_dMRI_TBSS_ICVF_Posterior_corona_radiata_R |
| 1931) | IDP_dMRI_TBSS_ICVF_Posterior_corona_radiata_L |
| 1932) | IDP_dMRI_TBSS_ICVF_Posterior_thalamic_radiation_R |
| 1933) | IDP_dMRI_TBSS_ICVF_Posterior_thalamic_radiation_L |
| 1934) | IDP_dMRI_TBSS_ICVF_Sagittal_stratum_R |
| 1935) | IDP_dMRI_TBSS_ICVF_Sagittal_stratum_L |
| 1936) | IDP_dMRI_TBSS_ICVF_External_capsule_R |
| 1937) | IDP_dMRI_TBSS_ICVF_External_capsule_L |
| 1938) | IDP_dMRI_TBSS_ICVF_Cingulum_cingulate_gyrus_R |
| 1939) | IDP_dMRI_TBSS_ICVF_Cingulum_cingulate_gyrus_L |
| 1940) | IDP_dMRI_TBSS_ICVF_Cingulum_hippocampus_R |
| 1941) | IDP_dMRI_TBSS_ICVF_Cingulum_hippocampus_L |
| 1942) | IDP_dMRI_TBSS_ICVF_Fornix_cres+Stria_terminalis_R |
| 1943) | IDP_dMRI_TBSS_ICVF_Fornix_cres+Stria_terminalis_L |
| 1944) | IDP_dMRI_TBSS_ICVF_Superior_longitudinal_fasciculus_R |
| 1945) | IDP_dMRI_TBSS_ICVF_Superior_longitudinal_fasciculus_L |
| 1946) | IDP_dMRI_TBSS_ICVF_Superior_fronto-occipital_fasciculus_R |
| 1947) | IDP_dMRI_TBSS_ICVF_Superior_fronto-occipital_fasciculus_L |
| 1948) | IDP_dMRI_TBSS_ICVF_Uncinate_fasciculus_R |
| 1949) | IDP_dMRI_TBSS_ICVF_Uncinate_fasciculus_L |
| 1950) | IDP_dMRI_TBSS_ICVF_Tapetum_R |
| 1951) | IDP_dMRI_TBSS_ICVF_Tapetum_L |
| 1952) | IDP_dMRI_ProbtrackX_ICVF_ar_l |
| 1953) | IDP_dMRI_ProbtrackX_ICVF_ar_r |
| 1954) | IDP_dMRI_ProbtrackX_ICVF_atr_l |
| 1955) | IDP_dMRI_ProbtrackX_ICVF_atr_r |
| 1956) | IDP_dMRI_ProbtrackX_ICVF_cgc_l |
| 1957) | IDP_dMRI_ProbtrackX_ICVF_cgc_r |
| 1958) | IDP_dMRI_ProbtrackX_ICVF_cgh_l |
| 1959) | IDP_dMRI_ProbtrackX_ICVF_cgh_r |
| 1960) | IDP_dMRI_ProbtrackX_ICVF_cst_l |
| 1961) | IDP_dMRI_ProbtrackX_ICVF_cst_r |
| 1962) | IDP_dMRI_ProbtrackX_ICVF_fma |
| 1963) | IDP_dMRI_ProbtrackX_ICVF_fmi |
| 1964) | IDP_dMRI_ProbtrackX_ICVF_ifo_l |
| 1965) | IDP_dMRI_ProbtrackX_ICVF_ifo_r |
| 1966) | IDP_dMRI_ProbtrackX_ICVF_ilf_l |
| 1967) | IDP_dMRI_ProbtrackX_ICVF_ilf_r |
| 1968) | IDP_dMRI_ProbtrackX_ICVF_mcp |

| | |
|---|---|
| 1969) | IDP_dMRI_ProbtrackX_ICVF_ml_l |
| 1970) | IDP_dMRI_ProbtrackX_ICVF_ml_r |
| 1971) | IDP_dMRI_ProbtrackX_ICVF_ptr_l |
| 1972) | IDP_dMRI_ProbtrackX_ICVF_ptr_r |
| 1973) | IDP_dMRI_ProbtrackX_ICVF_slf_l |
| 1974) | IDP_dMRI_ProbtrackX_ICVF_slf_r |
| 1975) | IDP_dMRI_ProbtrackX_ICVF_str_l |
| 1976) | IDP_dMRI_ProbtrackX_ICVF_str_r |
| 1977) | IDP_dMRI_ProbtrackX_ICVF_unc_l |
| 1978) | IDP_dMRI_ProbtrackX_ICVF_unc_r |
| 1979) | IDP_dMRI_TBSS_OD_Middle_cerebellar_peduncle |
| 1980) | IDP_dMRI_TBSS_OD_Pontine_crossing_tract |
| 1981) | IDP_dMRI_TBSS_OD_Genu_of_corpus_callosum |
| 1982) | IDP_dMRI_TBSS_OD_Body_of_corpus_callosum |
| 1983) | IDP_dMRI_TBSS_OD_Splenium_of_corpus_callosum |
| 1984) | IDP_dMRI_TBSS_OD_Fornix |
| 1985) | IDP_dMRI_TBSS_OD_Corticospinal_tract_R |
| 1986) | IDP_dMRI_TBSS_OD_Corticospinal_tract_L |
| 1987) | IDP_dMRI_TBSS_OD_Medial_lemniscus_R |
| 1988) | IDP_dMRI_TBSS_OD_Medial_lemniscus_L |
| 1989) | IDP_dMRI_TBSS_OD_Inferior_cerebellar_peduncle_R |
| 1990) | IDP_dMRI_TBSS_OD_Inferior_cerebellar_peduncle_L |
| 1991) | IDP_dMRI_TBSS_OD_Superior_cerebellar_peduncle_R |
| 1992) | IDP_dMRI_TBSS_OD_Superior_cerebellar_peduncle_L |
| 1993) | IDP_dMRI_TBSS_OD_Cerebral_peduncle_R |
| 1994) | IDP_dMRI_TBSS_OD_Cerebral_peduncle_L |
| 1995) | IDP_dMRI_TBSS_OD_Anterior_limb_of_internal_capsule_R |
| 1996) | IDP_dMRI_TBSS_OD_Anterior_limb_of_internal_capsule_L |
| 1997) | IDP_dMRI_TBSS_OD_Posterior_limb_of_internal_capsule_R |
| 1998) | IDP_dMRI_TBSS_OD_Posterior_limb_of_internal_capsule_L |
| 1999) | IDP_dMRI_TBSS_OD_Retrolenticular_part_of_internal_capsule_R |
| 2000) | IDP_dMRI_TBSS_OD_Retrolenticular_part_of_internal_capsule_L |
| 2001) | IDP_dMRI_TBSS_OD_Anterior_corona_radiata_R |
| 2002) | IDP_dMRI_TBSS_OD_Anterior_corona_radiata_L |
| 2003) | IDP_dMRI_TBSS_OD_Superior_corona_radiata_R |
| 2004) | IDP_dMRI_TBSS_OD_Superior_corona_radiata_L |
| 2005) | IDP_dMRI_TBSS_OD_Posterior_corona_radiata_R |
| 2006) | IDP_dMRI_TBSS_OD_Posterior_corona_radiata_L |
| 2007) | IDP_dMRI_TBSS_OD_Posterior_thalamic_radiation_R |
| 2008) | IDP_dMRI_TBSS_OD_Posterior_thalamic_radiation_L |
| 2009) | IDP_dMRI_TBSS_OD_Sagittal_stratum_R |
| 2010) | IDP_dMRI_TBSS_OD_Sagittal_stratum_L |

| | |
|---|---|
| 2011) | IDP_dMRI_TBSS_OD_External_capsule_R |
| 2012) | IDP_dMRI_TBSS_OD_External_capsule_L |
| 2013) | IDP_dMRI_TBSS_OD_Cingulum_cingulate_gyrus_R |
| 2014) | IDP_dMRI_TBSS_OD_Cingulum_cingulate_gyrus_L |
| 2015) | IDP_dMRI_TBSS_OD_Cingulum_hippocampus_R |
| 2016) | IDP_dMRI_TBSS_OD_Cingulum_hippocampus_L |
| 2017) | IDP_dMRI_TBSS_OD_Fornix_cres+Stria_terminalis_R |
| 2018) | IDP_dMRI_TBSS_OD_Fornix_cres+Stria_terminalis_L |
| 2019) | IDP_dMRI_TBSS_OD_Superior_longitudinal_fasciculus_R |
| 2020) | IDP_dMRI_TBSS_OD_Superior_longitudinal_fasciculus_L |
| 2021) | IDP_dMRI_TBSS_OD_Superior_fronto-occipital_fasciculus_R |
| 2022) | IDP_dMRI_TBSS_OD_Superior_fronto-occipital_fasciculus_L |
| 2023) | IDP_dMRI_TBSS_OD_Uncinate_fasciculus_R |
| 2024) | IDP_dMRI_TBSS_OD_Uncinate_fasciculus_L |
| 2025) | IDP_dMRI_TBSS_OD_Tapetum_R |
| 2026) | IDP_dMRI_TBSS_OD_Tapetum_L |
| 2027) | IDP_dMRI_ProbtrackX_OD_ar_l |
| 2028) | IDP_dMRI_ProbtrackX_OD_ar_r |
| 2029) | IDP_dMRI_ProbtrackX_OD_atr_l |
| 2030) | IDP_dMRI_ProbtrackX_OD_atr_r |
| 2031) | IDP_dMRI_ProbtrackX_OD_cgc_l |
| 2032) | IDP_dMRI_ProbtrackX_OD_cgc_r |
| 2033) | IDP_dMRI_ProbtrackX_OD_cgh_l |
| 2034) | IDP_dMRI_ProbtrackX_OD_cgh_r |
| 2035) | IDP_dMRI_ProbtrackX_OD_cst_l |
| 2036) | IDP_dMRI_ProbtrackX_OD_cst_r |
| 2037) | IDP_dMRI_ProbtrackX_OD_fma |
| 2038) | IDP_dMRI_ProbtrackX_OD_fmi |
| 2039) | IDP_dMRI_ProbtrackX_OD_ifo_l |
| 2040) | IDP_dMRI_ProbtrackX_OD_ifo_r |
| 2041) | IDP_dMRI_ProbtrackX_OD_ilf_l |
| 2042) | IDP_dMRI_ProbtrackX_OD_ilf_r |
| 2043) | IDP_dMRI_ProbtrackX_OD_mcp |
| 2044) | IDP_dMRI_ProbtrackX_OD_ml_l |
| 2045) | IDP_dMRI_ProbtrackX_OD_ml_r |
| 2046) | IDP_dMRI_ProbtrackX_OD_ptr_l |
| 2047) | IDP_dMRI_ProbtrackX_OD_ptr_r |
| 2048) | IDP_dMRI_ProbtrackX_OD_slf_l |
| 2049) | IDP_dMRI_ProbtrackX_OD_slf_r |
| 2050) | IDP_dMRI_ProbtrackX_OD_str_l |
| 2051) | IDP_dMRI_ProbtrackX_OD_str_r |
| 2052) | IDP_dMRI_ProbtrackX_OD_unc_l |

| | |
|---|---|
| 2053) | IDP_dMRI_ProbtrackX_OD_unc_r |
| 2054) | IDP_dMRI_TBSS_ISOVF_Middle_cerebellar_peduncle |
| 2055) | IDP_dMRI_TBSS_ISOVF_Pontine_crossing_tract |
| 2056) | IDP_dMRI_TBSS_ISOVF_Genu_of_corpus_callosum |
| 2057) | IDP_dMRI_TBSS_ISOVF_Body_of_corpus_callosum |
| 2058) | IDP_dMRI_TBSS_ISOVF_Splenium_of_corpus_callosum |
| 2059) | IDP_dMRI_TBSS_ISOVF_Fornix |
| 2060) | IDP_dMRI_TBSS_ISOVF_Corticospinal_tract_R |
| 2061) | IDP_dMRI_TBSS_ISOVF_Corticospinal_tract_L |
| 2062) | IDP_dMRI_TBSS_ISOVF_Medial_lemniscus_R |
| 2063) | IDP_dMRI_TBSS_ISOVF_Medial_lemniscus_L |
| 2064) | IDP_dMRI_TBSS_ISOVF_Inferior_cerebellar_peduncle_R |
| 2065) | IDP_dMRI_TBSS_ISOVF_Inferior_cerebellar_peduncle_L |
| 2066) | IDP_dMRI_TBSS_ISOVF_Superior_cerebellar_peduncle_R |
| 2067) | IDP_dMRI_TBSS_ISOVF_Superior_cerebellar_peduncle_L |
| 2068) | IDP_dMRI_TBSS_ISOVF_Cerebral_peduncle_R |
| 2069) | IDP_dMRI_TBSS_ISOVF_Cerebral_peduncle_L |
| 2070) | IDP_dMRI_TBSS_ISOVF_Anterior_limb_of_internal_capsule_R |
| 2071) | IDP_dMRI_TBSS_ISOVF_Anterior_limb_of_internal_capsule_L |
| 2072) | IDP_dMRI_TBSS_ISOVF_Posterior_limb_of_internal_capsule_R |
| 2073) | IDP_dMRI_TBSS_ISOVF_Posterior_limb_of_internal_capsule_L |
| 2074) | IDP_dMRI_TBSS_ISOVF_Retrolenticular_part_of_internal_capsule_R |
| 2075) | IDP_dMRI_TBSS_ISOVF_Retrolenticular_part_of_internal_capsule_L |
| 2076) | IDP_dMRI_TBSS_ISOVF_Anterior_corona_radiata_R |
| 2077) | IDP_dMRI_TBSS_ISOVF_Anterior_corona_radiata_L |
| 2078) | IDP_dMRI_TBSS_ISOVF_Superior_corona_radiata_R |
| 2079) | IDP_dMRI_TBSS_ISOVF_Superior_corona_radiata_L |
| 2080) | IDP_dMRI_TBSS_ISOVF_Posterior_corona_radiata_R |
| 2081) | IDP_dMRI_TBSS_ISOVF_Posterior_corona_radiata_L |
| 2082) | IDP_dMRI_TBSS_ISOVF_Posterior_thalamic_radiation_R |
| 2083) | IDP_dMRI_TBSS_ISOVF_Posterior_thalamic_radiation_L |
| 2084) | IDP_dMRI_TBSS_ISOVF_Sagittal_stratum_R |
| 2085) | IDP_dMRI_TBSS_ISOVF_Sagittal_stratum_L |
| 2086) | IDP_dMRI_TBSS_ISOVF_External_capsule_R |
| 2087) | IDP_dMRI_TBSS_ISOVF_External_capsule_L |
| 2088) | IDP_dMRI_TBSS_ISOVF_Cingulum_cingulate_gyrus_R |
| 2089) | IDP_dMRI_TBSS_ISOVF_Cingulum_cingulate_gyrus_L |
| 2090) | IDP_dMRI_TBSS_ISOVF_Cingulum_hippocampus_R |
| 2091) | IDP_dMRI_TBSS_ISOVF_Cingulum_hippocampus_L |
| 2092) | IDP_dMRI_TBSS_ISOVF_Fornix_cres+Stria_terminalis_R |
| 2093) | IDP_dMRI_TBSS_ISOVF_Fornix_cres+Stria_terminalis_L |
| 2094) | IDP_dMRI_TBSS_ISOVF_Superior_longitudinal_fasciculus_R |

| | |
|---|---|
| 2095) | IDP_dMRI_TBSS_ISOVF_Superior_longitudinal_fasciculus_L |
| 2096) | IDP_dMRI_TBSS_ISOVF_Superior_fronto-occipital_fasciculus_R |
| 2097) | IDP_dMRI_TBSS_ISOVF_Superior_fronto-occipital_fasciculus_L |
| 2098) | IDP_dMRI_TBSS_ISOVF_Uncinate_fasciculus_R |
| 2099) | IDP_dMRI_TBSS_ISOVF_Uncinate_fasciculus_L |
| 2100) | IDP_dMRI_TBSS_ISOVF_Tapetum_R |
| 2101) | IDP_dMRI_TBSS_ISOVF_Tapetum_L |
| 2102) | IDP_dMRI_ProbtrackX_ISOVF_ar_l |
| 2103) | IDP_dMRI_ProbtrackX_ISOVF_ar_r |
| 2104) | IDP_dMRI_ProbtrackX_ISOVF_atr_l |
| 2105) | IDP_dMRI_ProbtrackX_ISOVF_atr_r |
| 2106) | IDP_dMRI_ProbtrackX_ISOVF_cgc_l |
| 2107) | IDP_dMRI_ProbtrackX_ISOVF_cgc_r |
| 2108) | IDP_dMRI_ProbtrackX_ISOVF_cgh_l |
| 2109) | IDP_dMRI_ProbtrackX_ISOVF_cgh_r |
| 2110) | IDP_dMRI_ProbtrackX_ISOVF_cst_l |
| 2111) | IDP_dMRI_ProbtrackX_ISOVF_cst_r |
| 2112) | IDP_dMRI_ProbtrackX_ISOVF_fma |
| 2113) | IDP_dMRI_ProbtrackX_ISOVF_fmi |
| 2114) | IDP_dMRI_ProbtrackX_ISOVF_ifo_l |
| 2115) | IDP_dMRI_ProbtrackX_ISOVF_ifo_r |
| 2116) | IDP_dMRI_ProbtrackX_ISOVF_ilf_l |
| 2117) | IDP_dMRI_ProbtrackX_ISOVF_ilf_r |
| 2118) | IDP_dMRI_ProbtrackX_ISOVF_mcp |
| 2119) | IDP_dMRI_ProbtrackX_ISOVF_ml_l |
| 2120) | IDP_dMRI_ProbtrackX_ISOVF_ml_r |
| 2121) | IDP_dMRI_ProbtrackX_ISOVF_ptr_l |
| 2122) | IDP_dMRI_ProbtrackX_ISOVF_ptr_r |
| 2123) | IDP_dMRI_ProbtrackX_ISOVF_slf_l |
| 2124) | IDP_dMRI_ProbtrackX_ISOVF_slf_r |
| 2125) | IDP_dMRI_ProbtrackX_ISOVF_str_l |
| 2126) | IDP_dMRI_ProbtrackX_ISOVF_str_r |
| 2127) | IDP_dMRI_ProbtrackX_ISOVF_unc_l |
| 2128) | IDP_dMRI_ProbtrackX_ISOVF_unc_r |

Abbreviations: IDP, Imaging-Derived Phenotype; CSF, Cerebrospinal Fluid; ROIs, Regions of Interest; WM, White Matter; CC, Corpus Callosum; eTIV, Estimated Total Intracranial Volume; BA, Brodmann area; DKTatlas, Desikan–Killiany–Tourville cortical atlas; G+S, Combined gyrus and sulcus; Lat-Fis, Lateral fissure; wg, Within-gyrus measure; rh, Right hemisphere; lh, Left hemisphere; TBSS, Tract-Based Spatial Statistics; FA, Fractional Anisotropy; MO, Mode of Anisotropy; MD, Mean Diffusivity; L1, Axial diffusivity (first eigenvalue); L2 and L3, Radial diffusivity (second and third eigenvalues); ICVF, Intra-Cellular Volume Fraction; dMRI, Diffusion MRI; OD, Orientation Dispersion; ISOVF, Isotropic Volume Fraction; ar, Acoustic radiation; atr, Anterior thalamic radiation; cgc, Cingulum bundle (cingulate gyrus part); cgh, Cingulum bundle (hippocampal part); cst, Corticospinal tract; fma, Forceps major (splenium of corpus callosum); fmi, Forceps minor (genu of corpus

callosum); ifo, Inferior fronto-occipital fasciculus; ilf, Inferior longitudinal fasciculus; mcp, Middle cerebellar peduncle; ml, Medial lemniscus; ptr, Posterior thalamic radiation; slf, Superior longitudinal fasciculus; str, Superior thalamic radiation; unc, Uncinate fasciculus.

## Appendix 2: Individual image-derived functional phenotypes in UK Biobank (n= 1,793)

| N | Task-based functional magnetic resonance imaging | | |
|---|---|---|---|
| 1) | IDP_tfMRI_median_BOLD_shapes | | |
| 2) | IDP_tfMRI_90th-percentile_BOLD_shapes | | |
| 3) | IDP_tfMRI_median_zstat_shapes | | |
| 4) | IDP_tfMRI_90th-percentile_zstat_shapes | | |
| 5) | IDP_tfMRI_median_BOLD_faces | | |
| 6) | IDP_tfMRI_90th-percentile_BOLD_faces | | |
| 7) | IDP_tfMRI_median_zstat_faces | | |
| 8) | IDP_tfMRI_90th-percentile_zstat_faces | | |
| 9) | IDP_tfMRI_median_BOLD_faces-shapes | | |
| 10) | IDP_tfMRI_90th-percentile_BOLD_faces-shapes | | |
| 11) | IDP_tfMRI_median_zstat_faces-shapes | | |
| 12) | IDP_tfMRI_90th-percentile_zstat_faces-shapes | | |
| 13) | IDP_tfMRI_median_BOLD_faces-shapes_amygdala | | |
| 14) | IDP_tfMRI_90th-percentile_BOLD_faces-shapes_amygdala | | |
| 15) | IDP_tfMRI_median_zstat_faces-shapes_amygdala | | |
| 16) | IDP_tfMRI_90th-percentile_zstat_faces-shapes_amygdala | | |
| | **Resting-state functional magnetic resonance imaging** | | |
| | **Node ID** | **Location** | **Network** |
| 17) | rfMRI amplitudes (ICA25 node 1) | Cerebellum;Precuneus;Superior_frontal | Default_mode |
| 18) | rfMRI amplitudes (ICA25 node 2) | Middle_occipital | Visual;Attention |
| 19) | rfMRI amplitudes (ICA25 node 3) | SupraMarginal;Inferior_parietal;Postcentral | Attention;Salience;Central_executive |
| 20) | rfMRI amplitudes (ICA25 node 4) | Calcarine;Lingual;Cuneus | Visual |
| 21) | rfMRI amplitudes (ICA25 node 5) | Inferior_parietal;Cerebellum;Angular | Central_executive;Attention;Default_mode |
| 22) | rfMRI amplitudes (ICA25 node 6) | Inferior_frontal;Middle_frontal | Default_mode;Central_executive |
| 23) | rfMRI amplitudes (ICA25 node 7) | Precuneus;Middle_occipital | Default_mode;Central_executive |
| 24) | rfMRI amplitudes (ICA25 node 8) | Lingual;Calcarine;Superior_occipital | Visual |
| 25) | rfMRI amplitudes (ICA25 node 9) | Inferior_parietal;Angular;Middle_temporal | Default_mode;Central_executive |
| 26) | rfMRI amplitudes (ICA25 node 10) | Postcentral;Precentral | Motor |
| 27) | rfMRI amplitudes (ICA25 node 11) | Postcentral;Precentral | Motor |
| 28) | rfMRI amplitudes (ICA25 node 12) | Paracentral;Postcentral | Motor |

| | | | |
|---|---|---|---|
| 29) | rfMRI amplitudes (ICA25 node 13) | Supp_motor_area;Middle_temporal;Inferior_frontal | Default_mode;Salience |
| 30) | rfMRI amplitudes (ICA25 node 14) | Anterior_cingulate;Superior_frontal | Default_mode;Central_executive;Salience |
| 31) | rfMRI amplitudes (ICA25 node 15) | Cerebellum | Subcortical-cerebellum |
| 32) | rfMRI amplitudes (ICA25 node 16) | Superior_frontal;Middle_frontal | Salience;Central_executive |
| 33) | rfMRI amplitudes (ICA25 node 17) | Superior_temporal;Middle_temporal | Default_mode;Motor |
| 34) | rfMRI amplitudes (ICA25 node 18) | Putamen;Caudate;Supp_motor_area | Subcortical-cerebellum |
| 35) | rfMRI amplitudes (ICA25 node 19) | Inferior_occipital;Middle_occipital | Visual |
| 36) | rfMRI amplitudes (ICA25 node 20) | Precuneus | Default_mode;Central_executive |
| 37) | rfMRI amplitudes (ICA25 node 21) | Inferior_frontal;Superior_frontal;Middle_temporal | Default_mode;Central_executive |
| 38) | rfMRI amplitudes (ICA100 node 1) | Calcarine;Lingual;Cuneus | Visual |
| 39) | rfMRI amplitudes (ICA100 node 2) | Rolandic_operculum;SupraMarginal;Insula | Salience;Motor |
| 40) | rfMRI amplitudes (ICA100 node 3) | Lingual;Fusiform | Visual |
| 41) | rfMRI amplitudes (ICA100 node 4) | Middle_occipital;Superior_occipital | Attention;Visual |
| 42) | rfMRI amplitudes (ICA100 node 5) | Precuneus;Angular;Middle_cingulate | Default_mode;Central_executive |
| 43) | rfMRI amplitudes (ICA100 node 6) | Postcentral;Precentral | Motor |
| 44) | rfMRI amplitudes (ICA100 node 7) | Superior_frontal;Anterior_cingulate | Default_mode;Limbic |
| 45) | rfMRI amplitudes (ICA100 node 8) | Calcarine;Lingual | Visual |
| 46) | rfMRI amplitudes (ICA100 node 9) | Middle_temporal;Temporal_pole | Default_mode |
| 47) | rfMRI amplitudes (ICA100 node 10) | Middle_occipital;Precuneus;Calcarine | Default_mode;Central_executive |
| 48) | rfMRI amplitudes (ICA100 node 11) | Angular;Middle_temporal | Default_mode;Central_executive |
| 49) | rfMRI amplitudes (ICA100 node 12) | Middle_frontal;Cerebellum | Central_executive;Default_mode |
| 50) | rfMRI amplitudes (ICA100 node 13) | Superior_frontal | Default_mode |
| 51) | rfMRI amplitudes (ICA100 node 14) | Cuneus;Superior_occipital | Visual |
| 52) | rfMRI amplitudes (ICA100 node 15) | Insula;Anterior_cingulate | Salience;Default_mode |
| 53) | rfMRI amplitudes (ICA100 node 16) | Inferior_occipital;Middle_occipital | Visual |
| 54) | rfMRI amplitudes (ICA100 node 17) | Cerebellum | Subcortical-cerebellum |
| 55) | rfMRI amplitudes (ICA100 node 18) | Inferior_parietal;Postcentral | Attention;Central_executive;Salience |
| 56) | rfMRI amplitudes (ICA100 node 19) | Precuneus;Cuneus | Default_mode;Central_executive |
| 57) | rfMRI amplitudes (ICA100 node 20) | Postcentral;Precentral | Motor;Attention |

| | | | |
|---|---|---|---|
| 58) | rfMRI amplitudes (ICA100 node 21) | Superior_frontal | Default_mode;Central_executive |
| 59) | rfMRI amplitudes (ICA100 node 22) | Superior_temporal | Default_mode;Motor |
| 60) | rfMRI amplitudes (ICA100 node 23) | Cerebellum | Subcortical-cerebellum |
| 61) | rfMRI amplitudes (ICA100 node 24) | Inferior_parietal;Angular | Central_executive;Attention |
| 62) | rfMRI amplitudes (ICA100 node 25) | Inferior_frontal;Precentral | Central_executive |
| 63) | rfMRI amplitudes (ICA100 node 26) | Inferior_parietal;Inferior_frontal;SupraMarginal | Attention;Central_executive |
| 64) | rfMRI amplitudes (ICA100 node 27) | Precentral;Superior_frontal;Supp_motor_area | Attention;Salience;Motor |
| 65) | rfMRI amplitudes (ICA100 node 28) | Supp_motor_area;Inferior_frontal | Salience;Default_mode |
| 66) | rfMRI amplitudes (ICA100 node 29) | SupraMarginal;Inferior_parietal | Central_executive;Salience |
| 67) | rfMRI amplitudes (ICA100 node 30) | Paracentral | Motor |
| 68) | rfMRI amplitudes (ICA100 node 31) | middle_frontal | Central_executive |
| 69) | rfMRI amplitudes (ICA100 node 32) | Postcentral;Precentral | Motor;Attention |
| 70) | rfMRI amplitudes (ICA100 node 33) | Inferior_frontal;Middle_temporal;Supp_motor_area | Default_mode;Salience |
| 71) | rfMRI amplitudes (ICA100 node 34) | Superior_parietal;Postcentral;Precuneus | Attention |
| 72) | rfMRI amplitudes (ICA100 node 35) | Precentral;Postcentral | Motor |
| 73) | rfMRI amplitudes (ICA100 node 36) | Precuneus | Default_mode;Central_executive |
| 74) | rfMRI amplitudes (ICA100 node 37) | Middle_frontal | Central_executive;Salience |
| 75) | rfMRI amplitudes (ICA100 node 38) | Putamen;Caudate | Subcortical-cerebellum |
| 76) | rfMRI amplitudes (ICA100 node 39) | Precuneus;Superior_parietal | Attention;Central_executive |
| 77) | rfMRI amplitudes (ICA100 node 40) | Superior_frontal;Middle_frontal | Central_executive |
| 78) | rfMRI amplitudes (ICA100 node 41) | Inferior_temporal;Middle_temporal | Attention;Visual |
| 79) | rfMRI amplitudes (ICA100 node 42) | Inferior_temporal;Inferior_occipital | Attention;Visual |
| 80) | rfMRI amplitudes (ICA100 node 43) | Inferior_temporal;Fusiform;Temporal_pole | Limbic;Default_mode |
| 81) | rfMRI amplitudes (ICA100 node 44) | Inferior_frontal | Default_mode;Central_executive |
| 82) | rfMRI amplitudes (ICA100 node 45) | Superior_frontal;Middle_frontal | Salience;Default_mode |
| 83) | rfMRI amplitudes (ICA100 node 46) | Inferior_temporal;Middle_temporal | Central_executive;Default_mode |
| 84) | rfMRI amplitudes (ICA100 node 47) | Superior_frontal;Middle_frontal | Central_executive;Salience;Default_mode |
| 85) | rfMRI amplitudes (ICA100 node 48) | Middle_temporal | Default_mode;Central_executive |
| 86) | rfMRI amplitudes (ICA100 node 49) | Middle_temporal;Angular | Default_mode |

| | | | |
|---|---|---|---|
| 87) | rfMRI amplitudes (ICA100 node 50) | Orbital | Limbic |
| 88) | rfMRI amplitudes (ICA100 node 51) | Cerebellum;Inferior_temporal | Subcortical-cerebellum |
| 89) | rfMRI amplitudes (ICA100 node 52) | Cerebellum;Inferior_temporal | Subcortical-cerebellum |
| 90) | rfMRI amplitudes (ICA100 node 53) | Superior_frontal | Limbic |
| 91) | rfMRI amplitudes (ICA100 node 54) | Orbital;Inferior_temporal | Limbic |
| 92) | rfMRI amplitudes (ICA100 node 55) | Superior_frontal | Limbic;Default_mode |
| | **Edge ID** | **Location** | **Network** |
| 93) | rfMRI connectivity (ICA25 edge 1) | (Cerebellum;Precuneus;Superior_frontal) <=>(Middle_occipital) | (Default_mode)<=>(Visual;Attention) |
| 94) | rfMRI connectivity (ICA25 edge 2) | (Cerebellum;Precuneus;Superior_frontal) <=>(SupraMarginal;Inferior_parietal;Postcentral) | (Default_mode)<=>(Attention;Salience;Central_executive) |
| 95) | rfMRI connectivity (ICA25 edge 3) | (Middle_occipital)<=>(SupraMarginal;Inferior_parietal;Postcentral) | (Visual;Attention)<=>(Attention;Salience;Central_executive) |
| 96) | rfMRI connectivity (ICA25 edge 4) | (Cerebellum;Precuneus;Superior_frontal) <=>(Calcarine;Lingual;Cuneus) | (Default_mode)<=>(Visual) |
| 97) | rfMRI connectivity (ICA25 edge 5) | (Middle_occipital)<=>(Calcarine;Lingual;Cuneus) | (Visual;Attention)<=>(Visual) |
| 98) | rfMRI connectivity (ICA25 edge 6) | (SupraMarginal;Inferior_parietal;Postcentral)<=>(Calcarine;Lingual;Cuneus) | (Attention;Salience;Central_executive)<=>(Visual) |
| 99) | rfMRI connectivity (ICA25 edge 7) | (Cerebellum;Precuneus;Superior_frontal) <=>(Inferior_parietal;Cerebellum;Angular) | (Default_mode)<=>(Central_executive;Attention;Default_mode) |
| 100) | rfMRI connectivity (ICA25 edge 8) | (Middle_occipital)<=>(Inferior_parietal;Cerebellum;Angular) | (Visual;Attention)<=>(Central_executive;Attention;Default_mode) |
| 101) | rfMRI connectivity (ICA25 edge 9) | (SupraMarginal;Inferior_parietal;Postcentral)<=>(Inferior_parietal;Cerebellum;Angular) | (Attention;Salience;Central_executive)<=>(Central_executive;Attention;Default_mode) |
| 102) | rfMRI connectivity (ICA25 edge 10) | (Calcarine;Lingual;Cuneus)<=>(Inferior_parietal;Cerebellum;Angular) | (Visual)<=>(Central_executive;Attention;Default_mode) |
| 103) | rfMRI connectivity (ICA25 edge 11) | (Cerebellum;Precuneus;Superior_frontal) <=>(Inferior_frontal;Middle_frontal) | (Default_mode)<=>(Default_mode;Central_executive) |
| 104) | rfMRI connectivity (ICA25 edge 12) | (Middle_occipital)<=>(Inferior_frontal;Middle_frontal) | (Visual;Attention)<=>(Default_mode;Central_executive) |
| 105) | rfMRI connectivity (ICA25 edge 13) | (SupraMarginal;Inferior_parietal;Postcentral)<=>(Inferior_frontal;Middle_frontal) | (Attention;Salience;Central_executive)<=>(Default_mode;Central_executive) |
| 106) | rfMRI connectivity (ICA25 edge 14) | (Calcarine;Lingual;Cuneus)<=>(Inferior_frontal;Middle_frontal) | (Visual)<=>(Default_mode;Central_executive) |
| 107) | rfMRI connectivity (ICA25 edge 15) | (Inferior_parietal;Cerebellum;Angular)<=>(Inferior_frontal;Middle_frontal) | (Central_executive;Attention;Default_mode)<=>(Default_mode;Central_executive) |
| 108) | rfMRI connectivity (ICA25 edge 16) | (Cerebellum;Precuneus;Superior_frontal) <=>(Precuneus;Middle_occipital) | (Default_mode)<=>(Default_mode;Central_executive) |
| 109) | rfMRI connectivity (ICA25 edge 17) | (Middle_occipital)<=>(Precuneus;Middle_occipital) | (Visual;Attention)<=>(Default_mode;Central_executive) |
| 110) | rfMRI connectivity (ICA25 edge 18) | (SupraMarginal;Inferior_parietal;Postcentral)<=>(Precuneus;Middle_occipital) | (Attention;Salience;Central_executive)<=>(Default_mode;Central_executive) |
| 111) | rfMRI connectivity (ICA25 edge 19) | (Calcarine;Lingual;Cuneus)<=>(Precuneus;Middle_occipital) | (Visual)<=>(Default_mode;Central_executive) |

| | | | |
|---|---|---|---|
| 112) | rfMRI connectivity (ICA25 edge 20) | (Inferior_parietal;Cerebellum;Angular)<=>(Precuneus;Middle_occipital) | (Central_executive;Attention;Default_mode)<=>(Default_mode;Central_executive) |
| 113) | rfMRI connectivity (ICA25 edge 21) | (Inferior_frontal;Middle_frontal)<=>(Precuneus;Middle_occipital) | (Default_mode;Central_executive)<=>(Default_mode;Central_executive) |
| 114) | rfMRI connectivity (ICA25 edge 22) | (Cerebellum;Precuneus;Superior_frontal)<=>(Lingual;Calcarine;Superior_occipital) | (Default_mode)<=>(Visual) |
| 115) | rfMRI connectivity (ICA25 edge 23) | (Middle_occipital)<=>(Lingual;Calcarine;Superior_occipital) | (Visual;Attention)<=>(Visual) |
| 116) | rfMRI connectivity (ICA25 edge 24) | (SupraMarginal;Inferior_parietal;Postcentral)<=>(Lingual;Calcarine;Superior_occipital) | (Attention;Salience;Central_executive)<=>(Visual) |
| 117) | rfMRI connectivity (ICA25 edge 25) | (Calcarine;Lingual;Cuneus)<=>(Lingual;Calcarine;Superior_occipital) | (Visual)<=>(Visual) |
| 118) | rfMRI connectivity (ICA25 edge 26) | (Inferior_parietal;Cerebellum;Angular)<=>(Lingual;Calcarine;Superior_occipital) | (Central_executive;Attention;Default_mode)<=>(Visual) |
| 119) | rfMRI connectivity (ICA25 edge 27) | (Inferior_frontal;Middle_frontal)<=>(Lingual;Calcarine;Superior_occipital) | (Default_mode;Central_executive)<=>(Visual) |
| 120) | rfMRI connectivity (ICA25 edge 28) | (Precuneus;Middle_occipital)<=>(Lingual;Calcarine;Superior_occipital) | (Default_mode;Central_executive)<=>(Visual) |
| 121) | rfMRI connectivity (ICA25 edge 29) | (Cerebellum;Precuneus;Superior_frontal)<=>(Inferior_parietal;Angular;Middle_temporal) | (Default_mode)<=>(Default_mode;Central_executive) |
| 122) | rfMRI connectivity (ICA25 edge 30) | (Middle_occipital)<=>(Inferior_parietal;Angular;Middle_temporal) | (Visual;Attention)<=>(Default_mode;Central_executive) |
| 123) | rfMRI connectivity (ICA25 edge 31) | (SupraMarginal;Inferior_parietal;Postcentral)<=>(Inferior_parietal;Angular;Middle_temporal) | (Attention;Salience;Central_executive)<=>(Default_mode;Central_executive) |
| 124) | rfMRI connectivity (ICA25 edge 32) | (Calcarine;Lingual;Cuneus)<=>(Inferior_parietal;Angular;Middle_temporal) | (Visual)<=>(Default_mode;Central_executive) |
| 125) | rfMRI connectivity (ICA25 edge 33) | (Inferior_parietal;Cerebellum;Angular)<=>(Inferior_parietal;Angular;Middle_temporal) | (Central_executive;Attention;Default_mode)<=>(Default_mode;Central_executive) |
| 126) | rfMRI connectivity (ICA25 edge 34) | (Inferior_frontal;Middle_frontal)<=>(Inferior_parietal;Angular;Middle_temporal) | (Default_mode;Central_executive)<=>(Default_mode;Central_executive) |
| 127) | rfMRI connectivity (ICA25 edge 35) | (Precuneus;Middle_occipital)<=>(Inferior_parietal;Angular;Middle_temporal) | (Default_mode;Central_executive)<=>(Default_mode;Central_executive) |
| 128) | rfMRI connectivity (ICA25 edge 36) | (Lingual;Calcarine;Superior_occipital)<=>(Inferior_parietal;Angular;Middle_temporal) | (Visual)<=>(Default_mode;Central_executive) |
| 129) | rfMRI connectivity (ICA25 edge 37) | (Cerebellum;Precuneus;Superior_frontal)<=>(Postcentral;Precentral) | (Default_mode)<=>(Motor) |
| 130) | rfMRI connectivity (ICA25 edge 38) | (Middle_occipital)<=>(Postcentral;Precentral) | (Visual;Attention)<=>(Motor) |
| 131) | rfMRI connectivity (ICA25 edge 39) | (SupraMarginal;Inferior_parietal;Postcentral)<=>(Postcentral;Precentral) | (Attention;Salience;Central_executive)<=>(Motor) |
| 132) | rfMRI connectivity (ICA25 edge 40) | (Calcarine;Lingual;Cuneus)<=>(Postcentral;Precentral) | (Visual)<=>(Motor) |
| 133) | rfMRI connectivity (ICA25 edge 41) | (Inferior_parietal;Cerebellum;Angular)<=>(Postcentral;Precentral) | (Central_executive;Attention;Default_mode)<=>(Motor) |
| 134) | rfMRI connectivity (ICA25 edge 42) | (Inferior_frontal;Middle_frontal)<=>(Postcentral;Precentral) | (Default_mode;Central_executive)<=>(Motor) |
| 135) | rfMRI connectivity (ICA25 edge 43) | (Precuneus;Middle_occipital)<=>(Postcentral;Precentral) | (Default_mode;Central_executive)<=>(Motor) |

| | | | |
|---|---|---|---|
| 136) | rfMRI connectivity (ICA25 edge 44) | (Lingual;Calcarine;Superior_occipital)<=>(Postcentral;Precentral) | (Visual)<=>(Motor) |
| 137) | rfMRI connectivity (ICA25 edge 45) | (Inferior_parietal;Angular;Middle_temporal)<=>(Postcentral;Precentral) | (Default_mode;Central_executive)<=>(Motor) |
| 138) | rfMRI connectivity (ICA25 edge 46) | (Cerebellum;Precuneus;Superior_frontal)<=>(Postcentral;Precentral) | (Default_mode)<=>(Motor) |
| 139) | rfMRI connectivity (ICA25 edge 47) | (Middle_occipital)<=>(Postcentral;Precentral) | (Visual;Attention)<=>(Motor) |
| 140) | rfMRI connectivity (ICA25 edge 48) | (SupraMarginal;Inferior_parietal;Postcentral)<=>(Postcentral;Precentral) | (Attention;Salience;Central_executive)<=>(Motor) |
| 141) | rfMRI connectivity (ICA25 edge 49) | (Calcarine;Lingual;Cuneus)<=>(Postcentral;Precentral) | (Visual)<=>(Motor) |
| 142) | rfMRI connectivity (ICA25 edge 50) | (Inferior_parietal;Cerebellum;Angular)<=>(Postcentral;Precentral) | (Central_executive;Attention;Default_mode)<=>(Motor) |
| 143) | rfMRI connectivity (ICA25 edge 51) | (Inferior_frontal;Middle_frontal)<=>(Postcentral;Precentral) | (Default_mode;Central_executive)<=>(Motor) |
| 144) | rfMRI connectivity (ICA25 edge 52) | (Precuneus;Middle_occipital)<=>(Postcentral;Precentral) | (Default_mode;Central_executive)<=>(Motor) |
| 145) | rfMRI connectivity (ICA25 edge 53) | (Lingual;Calcarine;Superior_occipital)<=>(Postcentral;Precentral) | (Visual)<=>(Motor) |
| 146) | rfMRI connectivity (ICA25 edge 54) | (Inferior_parietal;Angular;Middle_temporal)<=>(Postcentral;Precentral) | (Default_mode;Central_executive)<=>(Motor) |
| 147) | rfMRI connectivity (ICA25 edge 55) | (Postcentral;Precentral)<=>(Postcentral;Precentral) | (Motor)<=>(Motor) |
| 148) | rfMRI connectivity (ICA25 edge 56) | (Cerebellum;Precuneus;Superior_frontal)<=>(Paracentral;Postcentral) | (Default_mode)<=>(Motor) |
| 149) | rfMRI connectivity (ICA25 edge 57) | (Middle_occipital)<=>(Paracentral;Postcentral) | (Visual;Attention)<=>(Motor) |
| 150) | rfMRI connectivity (ICA25 edge 58) | (SupraMarginal;Inferior_parietal;Postcentral)<=>(Paracentral;Postcentral) | (Attention;Salience;Central_executive)<=>(Motor) |
| 151) | rfMRI connectivity (ICA25 edge 59) | (Calcarine;Lingual;Cuneus)<=>(Paracentral;Postcentral) | (Visual)<=>(Motor) |
| 152) | rfMRI connectivity (ICA25 edge 60) | (Inferior_parietal;Cerebellum;Angular)<=>(Paracentral;Postcentral) | (Central_executive;Attention;Default_mode)<=>(Motor) |
| 153) | rfMRI connectivity (ICA25 edge 61) | (Inferior_frontal;Middle_frontal)<=>(Paracentral;Postcentral) | (Default_mode;Central_executive)<=>(Motor) |
| 154) | rfMRI connectivity (ICA25 edge 62) | (Precuneus;Middle_occipital)<=>(Paracentral;Postcentral) | (Default_mode;Central_executive)<=>(Motor) |
| 155) | rfMRI connectivity (ICA25 edge 63) | (Lingual;Calcarine;Superior_occipital)<=>(Paracentral;Postcentral) | (Visual)<=>(Motor) |
| 156) | rfMRI connectivity (ICA25 edge 64) | (Inferior_parietal;Angular;Middle_temporal)<=>(Paracentral;Postcentral) | (Default_mode;Central_executive)<=>(Motor) |
| 157) | rfMRI connectivity (ICA25 edge 65) | (Postcentral;Precentral)<=>(Paracentral;Postcentral) | (Motor)<=>(Motor) |
| 158) | rfMRI connectivity (ICA25 edge 66) | (Postcentral;Precentral)<=>(Paracentral;Postcentral) | (Motor)<=>(Motor) |
| 159) | rfMRI connectivity (ICA25 edge 67) | (Cerebellum;Precuneus;Superior_frontal)<=>(Supp_motor_area;Middle_temporal;Inferior_frontal) | (Default_mode)<=>(Default_mode;Salience) |
| 160) | rfMRI connectivity (ICA25 edge 68) | (Middle_occipital)<=>(Supp_motor_area;Middle_temporal;Inferior_frontal) | (Visual;Attention)<=>(Default_mode;Salience) |
| 161) | rfMRI connectivity (ICA25 edge 69) | (SupraMarginal;Inferior_parietal;Postcentral)<=>(Supp_motor_area;Middle_temporal;Inferior_frontal) | (Attention;Salience;Central_executive)<=>(Default_mode;Salience) |
| 162) | rfMRI connectivity (ICA25 edge 70) | (Calcarine;Lingual;Cuneus)<=>(Supp_motor_area;Middle_temporal;Inferior_frontal) | (Visual)<=>(Default_mode;Salience) |

| | | | |
|---|---|---|---|
| 163) | rfMRI connectivity (ICA25 edge 71) | (Inferior_parietal;Cerebellum;Angular)<=>(Supp_motor_area;Middle_temporal;Inferior_frontal) | (Central_executive;Attention;Default_mode)<=>(Default_mode;Salience) |
| 164) | rfMRI connectivity (ICA25 edge 72) | (Inferior_frontal;Middle_frontal)<=>(Supp_motor_area;Middle_temporal;Inferior_frontal) | (Default_mode;Central_executive)<=>(Default_mode;Salience) |
| 165) | rfMRI connectivity (ICA25 edge 73) | (Precuneus;Middle_occipital)<=>(Supp_motor_area;Middle_temporal;Inferior_frontal) | (Default_mode;Central_executive)<=>(Default_mode;Salience) |
| 166) | rfMRI connectivity (ICA25 edge 74) | (Lingual;Calcarine;Superior_occipital)<=>(Supp_motor_area;Middle_temporal;Inferior_frontal) | (Visual)<=>(Default_mode;Salience) |
| 167) | rfMRI connectivity (ICA25 edge 75) | (Inferior_parietal;Angular;Middle_temporal)<=>(Supp_motor_area;Middle_temporal;Inferior_frontal) | (Default_mode;Central_executive)<=>(Default_mode;Salience) |
| 168) | rfMRI connectivity (ICA25 edge 76) | (Postcentral;Precentral)<=>(Supp_motor_area;Middle_temporal;Inferior_frontal) | (Motor)<=>(Default_mode;Salience) |
| 169) | rfMRI connectivity (ICA25 edge 77) | (Postcentral;Precentral)<=>(Supp_motor_area;Middle_temporal;Inferior_frontal) | (Motor)<=>(Default_mode;Salience) |
| 170) | rfMRI connectivity (ICA25 edge 78) | (Paracentral;Postcentral)<=>(Supp_motor_area;Middle_temporal;Inferior_frontal) | (Motor)<=>(Default_mode;Salience) |
| 171) | rfMRI connectivity (ICA25 edge 79) | (Cerebellum;Precuneus;Superior_frontal)<=>(Anterior_cingulate;Superior_frontal) | (Default_mode)<=>(Default_mode;Central_executive;Salience) |
| 172) | rfMRI connectivity (ICA25 edge 80) | (Middle_occipital)<=>(Anterior_cingulate;Superior_frontal) | (Visual;Attention)<=>(Default_mode;Central_executive;Salience) |
| 173) | rfMRI connectivity (ICA25 edge 81) | (SupraMarginal;Inferior_parietal;Postcentral)<=>(Anterior_cingulate;Superior_frontal) | (Attention;Salience;Central_executive)<=>(Default_mode;Central_executive;Salience) |
| 174) | rfMRI connectivity (ICA25 edge 82) | (Calcarine;Lingual;Cuneus)<=>(Anterior_cingulate;Superior_frontal) | (Visual)<=>(Default_mode;Central_executive;Salience) |
| 175) | rfMRI connectivity (ICA25 edge 83) | (Inferior_parietal;Cerebellum;Angular)<=>(Anterior_cingulate;Superior_frontal) | (Central_executive;Attention;Default_mode)<=>(Default_mode;Central_executive;Salience) |
| 176) | rfMRI connectivity (ICA25 edge 84) | (Inferior_frontal;Middle_frontal)<=>(Anterior_cingulate;Superior_frontal) | (Default_mode;Central_executive)<=>(Default_mode;Central_executive;Salience) |
| 177) | rfMRI connectivity (ICA25 edge 85) | (Precuneus;Middle_occipital)<=>(Anterior_cingulate;Superior_frontal) | (Default_mode;Central_executive)<=>(Default_mode;Central_executive;Salience) |
| 178) | rfMRI connectivity (ICA25 edge 86) | (Lingual;Calcarine;Superior_occipital)<=>(Anterior_cingulate;Superior_frontal) | (Visual)<=>(Default_mode;Central_executive;Salience) |
| 179) | rfMRI connectivity (ICA25 edge 87) | (Inferior_parietal;Angular;Middle_temporal)<=>(Anterior_cingulate;Superior_frontal) | (Default_mode;Central_executive)<=>(Default_mode;Central_executive;Salience) |
| 180) | rfMRI connectivity (ICA25 edge 88) | (Postcentral;Precentral)<=>(Anterior_cingulate;Superior_frontal) | (Motor)<=>(Default_mode;Central_executive;Salience) |
| 181) | rfMRI connectivity (ICA25 edge 89) | (Postcentral;Precentral)<=>(Anterior_cingulate;Superior_frontal) | (Motor)<=>(Default_mode;Central_executive;Salience) |
| 182) | rfMRI connectivity (ICA25 edge 90) | (Paracentral;Postcentral)<=>(Anterior_cingulate;Superior_frontal) | (Motor)<=>(Default_mode;Central_executive;Salience) |
| 183) | rfMRI connectivity (ICA25 edge 91) | (Supp_motor_area;Middle_temporal;Inferior_frontal)<=>(Anterior_cingulate;Superior_frontal) | (Default_mode;Salience)<=>(Default_mode;Central_executive;Salience) |
| 184) | rfMRI connectivity (ICA25 edge 92) | (Cerebellum;Precuneus;Superior_frontal)<=>(Cerebellum) | (Default_mode)<=>(Subcortical-cerebellum) |
| 185) | rfMRI connectivity (ICA25 edge 93) | (Middle_occipital)<=>(Cerebellum) | (Visual;Attention)<=>(Subcortical-cerebellum) |

| | | | |
|---|---|---|---|
| 186) | rfMRI connectivity (ICA25 edge 94) | (SupraMarginal;Inferior_parietal;Postcentral)<=>(Cerebellum) | (Attention;Salience;Central_executive)<=>(Subcortical-cerebellum) |
| 187) | rfMRI connectivity (ICA25 edge 95) | (Calcarine;Lingual;Cuneus)<=>(Cerebellum) | (Visual)<=>(Subcortical-cerebellum) |
| 188) | rfMRI connectivity (ICA25 edge 96) | (Inferior_parietal;Cerebellum;Angular)<=>(Cerebellum) | (Central_executive;Attention;Default_mode)<=>(Subcortical-cerebellum) |
| 189) | rfMRI connectivity (ICA25 edge 97) | (Inferior_frontal;Middle_frontal)<=>(Cerebellum) | (Default_mode;Central_executive)<=>(Subcortical-cerebellum) |
| 190) | rfMRI connectivity (ICA25 edge 98) | (Precuneus;Middle_occipital)<=>(Cerebellum) | (Default_mode;Central_executive)<=>(Subcortical-cerebellum) |
| 191) | rfMRI connectivity (ICA25 edge 99) | (Lingual;Calcarine;Superior_occipital)<=>(Cerebellum) | (Visual)<=>(Subcortical-cerebellum) |
| 192) | rfMRI connectivity (ICA25 edge 100) | (Inferior_parietal;Angular;Middle_temporal)<=>(Cerebellum) | (Default_mode;Central_executive)<=>(Subcortical-cerebellum) |
| 193) | rfMRI connectivity (ICA25 edge 101) | (Postcentral;Precentral)<=>(Cerebellum) | (Motor)<=>(Subcortical-cerebellum) |
| 194) | rfMRI connectivity (ICA25 edge 102) | (Postcentral;Precentral)<=>(Cerebellum) | (Motor)<=>(Subcortical-cerebellum) |
| 195) | rfMRI connectivity (ICA25 edge 103) | (Paracentral;Postcentral)<=>(Cerebellum) | (Motor)<=>(Subcortical-cerebellum) |
| 196) | rfMRI connectivity (ICA25 edge 104) | (Supp_motor_area;Middle_temporal;Inferior_frontal)<=>(Cerebellum) | (Default_mode;Salience)<=>(Subcortical-cerebellum) |
| 197) | rfMRI connectivity (ICA25 edge 105) | (Anterior_cingulate;Superior_frontal)<=>(Cerebellum) | (Default_mode;Central_executive;Salience)<=>(Subcortical-cerebellum) |
| 198) | rfMRI connectivity (ICA25 edge 106) | (Cerebellum;Precuneus;Superior_frontal)<=>(Superior_frontal;Middle_frontal) | (Default_mode)<=>(Salience;Central_executive) |
| 199) | rfMRI connectivity (ICA25 edge 107) | (Middle_occipital)<=>(Superior_frontal;Middle_frontal) | (Visual;Attention)<=>(Salience;Central_executive) |
| 200) | rfMRI connectivity (ICA25 edge 108) | (SupraMarginal;Inferior_parietal;Postcentral)<=>(Superior_frontal;Middle_frontal) | (Attention;Salience;Central_executive)<=>(Salience;Central_executive) |
| 201) | rfMRI connectivity (ICA25 edge 109) | (Calcarine;Lingual;Cuneus)<=>(Superior_frontal;Middle_frontal) | (Visual)<=>(Salience;Central_executive) |
| 202) | rfMRI connectivity (ICA25 edge 110) | (Inferior_parietal;Cerebellum;Angular)<=>(Superior_frontal;Middle_frontal) | (Central_executive;Attention;Default_mode)<=>(Salience;Central_executive) |
| 203) | rfMRI connectivity (ICA25 edge 111) | (Inferior_frontal;Middle_frontal)<=>(Superior_frontal;Middle_frontal) | (Default_mode;Central_executive)<=>(Salience;Central_executive) |
| 204) | rfMRI connectivity (ICA25 edge 112) | (Precuneus;Middle_occipital)<=>(Superior_frontal;Middle_frontal) | (Default_mode;Central_executive)<=>(Salience;Central_executive) |
| 205) | rfMRI connectivity (ICA25 edge 113) | (Lingual;Calcarine;Superior_occipital)<=>(Superior_frontal;Middle_frontal) | (Visual)<=>(Salience;Central_executive) |
| 206) | rfMRI connectivity (ICA25 edge 114) | (Inferior_parietal;Angular;Middle_temporal)<=>(Superior_frontal;Middle_frontal) | (Default_mode;Central_executive)<=>(Salience;Central_executive) |
| 207) | rfMRI connectivity (ICA25 edge 115) | (Postcentral;Precentral)<=>(Superior_frontal;Middle_frontal) | (Motor)<=>(Salience;Central_executive) |
| 208) | rfMRI connectivity (ICA25 edge 116) | (Postcentral;Precentral)<=>(Superior_frontal;Middle_frontal) | (Motor)<=>(Salience;Central_executive) |
| 209) | rfMRI connectivity (ICA25 edge 117) | (Paracentral;Postcentral)<=>(Superior_frontal;Middle_frontal) | (Motor)<=>(Salience;Central_executive) |

| | | | |
|---|---|---|---|
| 210) | rfMRI connectivity (ICA25 edge 118) | (Supp_motor_area;Middle_temporal;Inferior_frontal)<=>(Superior_frontal;Middle_frontal) | (Default_mode;Salience)<=>(Salience;Central_executive) |
| 211) | rfMRI connectivity (ICA25 edge 119) | (Anterior_cingulate;Superior_frontal)<=>(Superior_frontal;Middle_frontal) | (Default_mode;Central_executive;Salience)<=>(Salience;Central_executive) |
| 212) | rfMRI connectivity (ICA25 edge 120) | (Cerebellum)<=>(Superior_frontal;Middle_frontal) | (Subcortical-cerebellum)<=>(Salience;Central_executive) |
| 213) | rfMRI connectivity (ICA25 edge 121) | (Cerebellum;Precuneus;Superior_frontal)<=>(Superior_temporal;Middle_temporal) | (Default_mode)<=>(Default_mode;Motor) |
| 214) | rfMRI connectivity (ICA25 edge 122) | (Middle_occipital)<=>(Superior_temporal;Middle_temporal) | (Visual;Attention)<=>(Default_mode;Motor) |
| 215) | rfMRI connectivity (ICA25 edge 123) | (SupraMarginal;Inferior_parietal;Postcentral)<=>(Superior_temporal;Middle_temporal) | (Attention;Salience;Central_executive)<=>(Default_mode;Motor) |
| 216) | rfMRI connectivity (ICA25 edge 124) | (Calcarine;Lingual;Cuneus)<=>(Superior_temporal;Middle_temporal) | (Visual)<=>(Default_mode;Motor) |
| 217) | rfMRI connectivity (ICA25 edge 125) | (Inferior_parietal;Cerebellum;Angular)<=>(Superior_temporal;Middle_temporal) | (Central_executive;Attention;Default_mode)<=>(Default_mode;Motor) |
| 218) | rfMRI connectivity (ICA25 edge 126) | (Inferior_frontal;Middle_frontal)<=>(Superior_temporal;Middle_temporal) | (Default_mode;Central_executive)<=>(Default_mode;Motor) |
| 219) | rfMRI connectivity (ICA25 edge 127) | (Precuneus;Middle_occipital)<=>(Superior_temporal;Middle_temporal) | (Default_mode;Central_executive)<=>(Default_mode;Motor) |
| 220) | rfMRI connectivity (ICA25 edge 128) | (Lingual;Calcarine;Superior_occipital)<=>(Superior_temporal;Middle_temporal) | (Visual)<=>(Default_mode;Motor) |
| 221) | rfMRI connectivity (ICA25 edge 129) | (Inferior_parietal;Angular;Middle_temporal)<=>(Superior_temporal;Middle_temporal) | (Default_mode;Central_executive)<=>(Default_mode;Motor) |
| 222) | rfMRI connectivity (ICA25 edge 130) | (Postcentral;Precentral)<=>(Superior_temporal;Middle_temporal) | (Motor)<=>(Default_mode;Motor) |
| 223) | rfMRI connectivity (ICA25 edge 131) | (Postcentral;Precentral)<=>(Superior_temporal;Middle_temporal) | (Motor)<=>(Default_mode;Motor) |
| 224) | rfMRI connectivity (ICA25 edge 132) | (Paracentral;Postcentral)<=>(Superior_temporal;Middle_temporal) | (Motor)<=>(Default_mode;Motor) |
| 225) | rfMRI connectivity (ICA25 edge 133) | (Supp_motor_area;Middle_temporal;Inferior_frontal)<=>(Superior_temporal;Middle_temporal) | (Default_mode;Salience)<=>(Default_mode;Motor) |
| 226) | rfMRI connectivity (ICA25 edge 134) | (Anterior_cingulate;Superior_frontal)<=>(Superior_temporal;Middle_temporal) | (Default_mode;Central_executive;Salience)<=>(Default_mode;Motor) |
| 227) | rfMRI connectivity (ICA25 edge 135) | (Cerebellum)<=>(Superior_temporal;Middle_temporal) | (Subcortical-cerebellum)<=>(Default_mode;Motor) |
| 228) | rfMRI connectivity (ICA25 edge 136) | (Superior_frontal;Middle_frontal)<=>(Superior_temporal;Middle_temporal) | (Salience;Central_executive)<=>(Default_mode;Motor) |
| 229) | rfMRI connectivity (ICA25 edge 137) | (Cerebellum;Precuneus;Superior_frontal)<=>(Putamen;Caudate;Supp_motor_area) | (Default_mode)<=>(Subcortical-cerebellum) |
| 230) | rfMRI connectivity (ICA25 edge 138) | (Middle_occipital)<=>(Putamen;Caudate;Supp_motor_area) | (Visual;Attention)<=>(Subcortical-cerebellum) |
| 231) | rfMRI connectivity (ICA25 edge 139) | (SupraMarginal;Inferior_parietal;Postcentral)<=>(Putamen;Caudate;Supp_motor_area) | (Attention;Salience;Central_executive)<=>(Subcortical-cerebellum) |
| 232) | rfMRI connectivity (ICA25 edge 140) | (Calcarine;Lingual;Cuneus)<=>(Putamen;Caudate;Supp_motor_area) | (Visual)<=>(Subcortical-cerebellum) |

| | | | |
|---|---|---|---|
| 233) | rfMRI connectivity (ICA25 edge 141) | (Inferior_parietal;Cerebellum;Angular)<=>(Putamen;Caudate;Supp_motor_area) | (Central_executive;Attention;Default_mode)<=>(Subcortical-cerebellum) |
| 234) | rfMRI connectivity (ICA25 edge 142) | (Inferior_frontal;Middle_frontal)<=>(Putamen;Caudate;Supp_motor_area) | (Default_mode;Central_executive)<=>(Subcortical-cerebellum) |
| 235) | rfMRI connectivity (ICA25 edge 143) | (Precuneus;Middle_occipital)<=>(Putamen;Caudate;Supp_motor_area) | (Default_mode;Central_executive)<=>(Subcortical-cerebellum) |
| 236) | rfMRI connectivity (ICA25 edge 144) | (Lingual;Calcarine;Superior_occipital)<=>(Putamen;Caudate;Supp_motor_area) | (Visual)<=>(Subcortical-cerebellum) |
| 237) | rfMRI connectivity (ICA25 edge 145) | (Inferior_parietal;Angular;Middle_temporal)<=>(Putamen;Caudate;Supp_motor_area) | (Default_mode;Central_executive)<=>(Subcortical-cerebellum) |
| 238) | rfMRI connectivity (ICA25 edge 146) | (Postcentral;Precentral)<=>(Putamen;Caudate;Supp_motor_area) | (Motor)<=>(Subcortical-cerebellum) |
| 239) | rfMRI connectivity (ICA25 edge 147) | (Postcentral;Precentral)<=>(Putamen;Caudate;Supp_motor_area) | (Motor)<=>(Subcortical-cerebellum) |
| 240) | rfMRI connectivity (ICA25 edge 148) | (Paracentral;Postcentral)<=>(Putamen;Caudate;Supp_motor_area) | (Motor)<=>(Subcortical-cerebellum) |
| 241) | rfMRI connectivity (ICA25 edge 149) | (Supp_motor_area;Middle_temporal;Inferior_frontal)<=>(Putamen;Caudate;Supp_motor_area) | (Default_mode;Salience)<=>(Subcortical-cerebellum) |
| 242) | rfMRI connectivity (ICA25 edge 150) | (Anterior_cingulate;Superior_frontal)<=>(Putamen;Caudate;Supp_motor_area) | (Default_mode;Central_executive;Salience)<=>(Subcortical-cerebellum) |
| 243) | rfMRI connectivity (ICA25 edge 151) | (Cerebellum)<=>(Putamen;Caudate;Supp_motor_area) | (Subcortical-cerebellum)<=>(Subcortical-cerebellum) |
| 244) | rfMRI connectivity (ICA25 edge 152) | (Superior_frontal;Middle_frontal)<=>(Putamen;Caudate;Supp_motor_area) | (Salience;Central_executive)<=>(Subcortical-cerebellum) |
| 245) | rfMRI connectivity (ICA25 edge 153) | (Superior_temporal;Middle_temporal)<=>(Putamen;Caudate;Supp_motor_area) | (Default_mode;Motor)<=>(Subcortical-cerebellum) |
| 246) | rfMRI connectivity (ICA25 edge 154) | (Cerebellum;Precuneus;Superior_frontal)<=>(Inferior_occipital;Middle_occipital) | (Default_mode)<=>(Visual) |
| 247) | rfMRI connectivity (ICA25 edge 155) | (Middle_occipital)<=>(Inferior_occipital;Middle_occipital) | (Visual;Attention)<=>(Visual) |
| 248) | rfMRI connectivity (ICA25 edge 156) | (SupraMarginal;Inferior_parietal;Postcentral)<=>(Inferior_occipital;Middle_occipital) | (Attention;Salience;Central_executive)<=>(Visual) |
| 249) | rfMRI connectivity (ICA25 edge 157) | (Calcarine;Lingual;Cuneus)<=>(Inferior_occipital;Middle_occipital) | (Visual)<=>(Visual) |
| 250) | rfMRI connectivity (ICA25 edge 158) | (Inferior_parietal;Cerebellum;Angular)<=>(Inferior_occipital;Middle_occipital) | (Central_executive;Attention;Default_mode)<=>(Visual) |
| 251) | rfMRI connectivity (ICA25 edge 159) | (Inferior_frontal;Middle_frontal)<=>(Inferior_occipital;Middle_occipital) | (Default_mode;Central_executive)<=>(Visual) |
| 252) | rfMRI connectivity (ICA25 edge 160) | (Precuneus;Middle_occipital)<=>(Inferior_occipital;Middle_occipital) | (Default_mode;Central_executive)<=>(Visual) |
| 253) | rfMRI connectivity (ICA25 edge 161) | (Lingual;Calcarine;Superior_occipital)<=>(Inferior_occipital;Middle_occipital) | (Visual)<=>(Visual) |
| 254) | rfMRI connectivity (ICA25 edge 162) | (Inferior_parietal;Angular;Middle_temporal)<=>(Inferior_occipital;Middle_occipital) | (Default_mode;Central_executive)<=>(Visual) |
| 255) | rfMRI connectivity (ICA25 edge 163) | (Postcentral;Precentral)<=>(Inferior_occipital;Middle_occipital) | (Motor)<=>(Visual) |
| 256) | rfMRI connectivity (ICA25 edge 164) | (Postcentral;Precentral)<=>(Inferior_occipital;Middle_occipital) | (Motor)<=>(Visual) |
| 257) | rfMRI connectivity (ICA25 edge 165) | (Paracentral;Postcentral)<=>(Inferior_occipital;Middle_occipital) | (Motor)<=>(Visual) |

| | | | |
|---|---|---|---|
| 258) | rfMRI connectivity (ICA25 edge 166) | (Supp_motor_area;Middle_temporal;Inferior_frontal)<=>(Inferior_occipital;Middle_occipital) | (Default_mode;Salience)<=>(Visual) |
| 259) | rfMRI connectivity (ICA25 edge 167) | (Anterior_cingulate;Superior_frontal)<=>(Inferior_occipital;Middle_occipital) | (Default_mode;Central_executive;Salience)<=>(Visual) |
| 260) | rfMRI connectivity (ICA25 edge 168) | (Cerebellum)<=>(Inferior_occipital;Middle_occipital) | (Subcortical-cerebellum)<=>(Visual) |
| 261) | rfMRI connectivity (ICA25 edge 169) | (Superior_frontal;Middle_frontal)<=>(Inferior_occipital;Middle_occipital) | (Salience;Central_executive)<=>(Visual) |
| 262) | rfMRI connectivity (ICA25 edge 170) | (Superior_temporal;Middle_temporal)<=>(Inferior_occipital;Middle_occipital) | (Default_mode;Motor)<=>(Visual) |
| 263) | rfMRI connectivity (ICA25 edge 171) | (Putamen;Caudate;Supp_motor_area)<=>(Inferior_occipital;Middle_occipital) | (Subcortical-cerebellum)<=>(Visual) |
| 264) | rfMRI connectivity (ICA25 edge 172) | (Cerebellum;Precuneus;Superior_frontal)<=>(Precuneus) | (Default_mode)<=>(Default_mode;Central_executive) |
| 265) | rfMRI connectivity (ICA25 edge 173) | (Middle_occipital)<=>(Precuneus) | (Visual;Attention)<=>(Default_mode;Central_executive) |
| 266) | rfMRI connectivity (ICA25 edge 174) | (SupraMarginal;Inferior_parietal;Postcentral)<=>(Precuneus) | (Attention;Salience;Central_executive)<=>(Default_mode;Central_executive) |
| 267) | rfMRI connectivity (ICA25 edge 175) | (Calcarine;Lingual;Cuneus)<=>(Precuneus) | (Visual)<=>(Default_mode;Central_executive) |
| 268) | rfMRI connectivity (ICA25 edge 176) | (Inferior_parietal;Cerebellum;Angular)<=>(Precuneus) | (Central_executive;Attention;Default_mode)<=>(Default_mode;Central_executive) |
| 269) | rfMRI connectivity (ICA25 edge 177) | (Inferior_frontal;Middle_frontal)<=>(Precuneus) | (Default_mode;Central_executive)<=>(Default_mode;Central_executive) |
| 270) | rfMRI connectivity (ICA25 edge 178) | (Precuneus;Middle_occipital)<=>(Precuneus) | (Default_mode;Central_executive)<=>(Default_mode;Central_executive) |
| 271) | rfMRI connectivity (ICA25 edge 179) | (Lingual;Calcarine;Superior_occipital)<=>(Precuneus) | (Visual)<=>(Default_mode;Central_executive) |
| 272) | rfMRI connectivity (ICA25 edge 180) | (Inferior_parietal;Angular;Middle_temporal)<=>(Precuneus) | (Default_mode;Central_executive)<=>(Default_mode;Central_executive) |
| 273) | rfMRI connectivity (ICA25 edge 181) | (Postcentral;Precentral)<=>(Precuneus) | (Motor)<=>(Default_mode;Central_executive) |
| 274) | rfMRI connectivity (ICA25 edge 182) | (Postcentral;Precentral)<=>(Precuneus) | (Motor)<=>(Default_mode;Central_executive) |
| 275) | rfMRI connectivity (ICA25 edge 183) | (Paracentral;Postcentral)<=>(Precuneus) | (Motor)<=>(Default_mode;Central_executive) |
| 276) | rfMRI connectivity (ICA25 edge 184) | (Supp_motor_area;Middle_temporal;Inferior_frontal)<=>(Precuneus) | (Default_mode;Salience)<=>(Default_mode;Central_executive) |
| 277) | rfMRI connectivity (ICA25 edge 185) | (Anterior_cingulate;Superior_frontal)<=>(Precuneus) | (Default_mode;Central_executive;Salience)<=>(Default_mode;Central_executive) |
| 278) | rfMRI connectivity (ICA25 edge 186) | (Cerebellum)<=>(Precuneus) | (Subcortical-cerebellum)<=>(Default_mode;Central_executive) |
| 279) | rfMRI connectivity (ICA25 edge 187) | (Superior_frontal;Middle_frontal)<=>(Precuneus) | (Salience;Central_executive)<=>(Default_mode;Central_executive) |
| 280) | rfMRI connectivity (ICA25 edge 188) | (Superior_temporal;Middle_temporal)<=>(Precuneus) | (Default_mode;Motor)<=>(Default_mode;Central_executive) |
| 281) | rfMRI connectivity (ICA25 edge 189) | (Putamen;Caudate;Supp_motor_area)<=>(Precuneus) | (Subcortical-cerebellum)<=>(Default_mode;Central_executive) |

| | | | |
|---|---|---|---|
| 282) | rfMRI connectivity (ICA25 edge 190) | (Inferior_occipital;Middle_occipital)<=>(Precuneus) | (Visual)<=>(Default_mode;Central_executive) |
| 283) | rfMRI connectivity (ICA25 edge 191) | (Cerebellum;Precuneus;Superior_frontal)<=>(Inferior_frontal;Superior_frontal;Middle_temporal) | (Default_mode)<=>(Default_mode;Central_executive) |
| 284) | rfMRI connectivity (ICA25 edge 192) | (Middle_occipital)<=>(Inferior_frontal;Superior_frontal;Middle_temporal) | (Visual;Attention)<=>(Default_mode;Central_executive) |
| 285) | rfMRI connectivity (ICA25 edge 193) | (SupraMarginal;Inferior_parietal;Postcentral)<=>(Inferior_frontal;Superior_frontal;Middle_temporal) | (Attention;Salience;Central_executive)<=>(Default_mode;Central_executive) |
| 286) | rfMRI connectivity (ICA25 edge 194) | (Calcarine;Lingual;Cuneus)<=>(Inferior_frontal;Superior_frontal;Middle_temporal) | (Visual)<=>(Default_mode;Central_executive) |
| 287) | rfMRI connectivity (ICA25 edge 195) | (Inferior_parietal;Cerebellum;Angular)<=>(Inferior_frontal;Superior_frontal;Middle_temporal) | (Central_executive;Attention;Default_mode)<=>(Default_mode;Central_executive) |
| 288) | rfMRI connectivity (ICA25 edge 196) | (Inferior_frontal;Middle_frontal)<=>(Inferior_frontal;Superior_frontal;Middle_temporal) | (Default_mode;Central_executive)<=>(Default_mode;Central_executive) |
| 289) | rfMRI connectivity (ICA25 edge 197) | (Precuneus;Middle_occipital)<=>(Inferior_frontal;Superior_frontal;Middle_temporal) | (Default_mode;Central_executive)<=>(Default_mode;Central_executive) |
| 290) | rfMRI connectivity (ICA25 edge 198) | (Lingual;Calcarine;Superior_occipital)<=>(Inferior_frontal;Superior_frontal;Middle_temporal) | (Visual)<=>(Default_mode;Central_executive) |
| 291) | rfMRI connectivity (ICA25 edge 199) | (Inferior_parietal;Angular;Middle_temporal)<=>(Inferior_frontal;Superior_frontal;Middle_temporal) | (Default_mode;Central_executive)<=>(Default_mode;Central_executive) |
| 292) | rfMRI connectivity (ICA25 edge 200) | (Postcentral;Precentral)<=>(Inferior_frontal;Superior_frontal;Middle_temporal) | (Motor)<=>(Default_mode;Central_executive) |
| 293) | rfMRI connectivity (ICA25 edge 201) | (Postcentral;Precentral)<=>(Inferior_frontal;Superior_frontal;Middle_temporal) | (Motor)<=>(Default_mode;Central_executive) |
| 294) | rfMRI connectivity (ICA25 edge 202) | (Paracentral;Postcentral)<=>(Inferior_frontal;Superior_frontal;Middle_temporal) | (Motor)<=>(Default_mode;Central_executive) |
| 295) | rfMRI connectivity (ICA25 edge 203) | (Supp_motor_area;Middle_temporal;Inferior_frontal)<=>(Inferior_frontal;Superior_frontal;Middle_temporal) | (Default_mode;Salience)<=>(Default_mode;Central_executive) |
| 296) | rfMRI connectivity (ICA25 edge 204) | (Anterior_cingulate;Superior_frontal)<=>(Inferior_frontal;Superior_frontal;Middle_temporal) | (Default_mode;Central_executive;Salience)<=>(Default_mode;Central_executive) |
| 297) | rfMRI connectivity (ICA25 edge 205) | (Cerebellum)<=>(Inferior_frontal;Superior_frontal;Middle_temporal) | (Subcortical-cerebellum)<=>(Default_mode;Central_executive) |
| 298) | rfMRI connectivity (ICA25 edge 206) | (Superior_frontal;Middle_frontal)<=>(Inferior_frontal;Superior_frontal;Middle_temporal) | (Salience;Central_executive)<=>(Default_mode;Central_executive) |
| 299) | rfMRI connectivity (ICA25 edge 207) | (Superior_temporal;Middle_temporal)<=>(Inferior_frontal;Superior_frontal;Middle_temporal) | (Default_mode;Motor)<=>(Default_mode;Central_executive) |
| 300) | rfMRI connectivity (ICA25 edge 208) | (Putamen;Caudate;Supp_motor_area)<=>(Inferior_frontal;Superior_frontal;Middle_temporal) | (Subcortical-cerebellum)<=>(Default_mode;Central_executive) |
| 301) | rfMRI connectivity (ICA25 edge 209) | (Inferior_occipital;Middle_occipital)<=>(Inferior_frontal;Superior_frontal;Middle_temporal) | (Visual)<=>(Default_mode;Central_executive) |
| 302) | rfMRI connectivity (ICA25 edge 210) | (Precuneus)<=>(Inferior_frontal;Superior_frontal;Middle_temporal) | (Default_mode;Central_executive)<=>(Default_mode;Central_executive) |

| | | | |
|---|---|---|---|
| 303) | rfMRI connectivity (ICA100 edge 1) | (Calcarine;Lingual;Cuneus)<=>(Rolandic_operculum;SupraMarginal;Insula) | (Visual)<=>(Salience;Motor) |
| 304) | rfMRI connectivity (ICA100 edge 2) | (Calcarine;Lingual;Cuneus)<=>(Lingual;Fusiform) | (Visual)<=>(Visual) |
| 305) | rfMRI connectivity (ICA100 edge 3) | (Rolandic_operculum;SupraMarginal;Insula)<=>(Lingual;Fusiform) | (Salience;Motor)<=>(Visual) |
| 306) | rfMRI connectivity (ICA100 edge 4) | (Calcarine;Lingual;Cuneus)<=>(Middle_occipital;Superior_occipital) | (Visual)<=>(Attention;Visual) |
| 307) | rfMRI connectivity (ICA100 edge 5) | (Rolandic_operculum;SupraMarginal;Insula)<=>(Middle_occipital;Superior_occipital) | (Salience;Motor)<=>(Attention;Visual) |
| 308) | rfMRI connectivity (ICA100 edge 6) | (Lingual;Fusiform)<=>(Middle_occipital;Superior_occipital) | (Visual)<=>(Attention;Visual) |
| 309) | rfMRI connectivity (ICA100 edge 7) | (Calcarine;Lingual;Cuneus)<=>(Precuneus;Angular;Middle_cingulate) | (Visual)<=>(Default_mode;Central_executive) |
| 310) | rfMRI connectivity (ICA100 edge 8) | (Rolandic_operculum;SupraMarginal;Insula)<=>(Precuneus;Angular;Middle_cingulate) | (Salience;Motor)<=>(Default_mode;Central_executive) |
| 311) | rfMRI connectivity (ICA100 edge 9) | (Lingual;Fusiform)<=>(Precuneus;Angular;Middle_cingulate) | (Visual)<=>(Default_mode;Central_executive) |
| 312) | rfMRI connectivity (ICA100 edge 10) | (Middle_occipital;Superior_occipital)<=>(Precuneus;Angular;Middle_cingulate) | (Attention;Visual)<=>(Default_mode;Central_executive) |
| 313) | rfMRI connectivity (ICA100 edge 11) | (Calcarine;Lingual;Cuneus)<=>(Postcentral;Precentral) | (Visual)<=>(Motor) |
| 314) | rfMRI connectivity (ICA100 edge 12) | (Rolandic_operculum;SupraMarginal;Insula)<=>(Postcentral;Precentral) | (Salience;Motor)<=>(Motor) |
| 315) | rfMRI connectivity (ICA100 edge 13) | (Lingual;Fusiform)<=>(Postcentral;Precentral) | (Visual)<=>(Motor) |
| 316) | rfMRI connectivity (ICA100 edge 14) | (Middle_occipital;Superior_occipital)<=>(Postcentral;Precentral) | (Attention;Visual)<=>(Motor) |
| 317) | rfMRI connectivity (ICA100 edge 15) | (Precuneus;Angular;Middle_cingulate)<=>(Postcentral;Precentral) | (Default_mode;Central_executive)<=>(Motor) |
| 318) | rfMRI connectivity (ICA100 edge 16) | (Calcarine;Lingual;Cuneus)<=>(Superior_frontal;Anterior_cingulate) | (Visual)<=>(Default_mode;Limbic) |
| 319) | rfMRI connectivity (ICA100 edge 17) | (Rolandic_operculum;SupraMarginal;Insula)<=>(Superior_frontal;Anterior_cingulate) | (Salience;Motor)<=>(Default_mode;Limbic) |
| 320) | rfMRI connectivity (ICA100 edge 18) | (Lingual;Fusiform)<=>(Superior_frontal;Anterior_cingulate) | (Visual)<=>(Default_mode;Limbic) |
| 321) | rfMRI connectivity (ICA100 edge 19) | (Middle_occipital;Superior_occipital)<=>(Superior_frontal;Anterior_cingulate) | (Attention;Visual)<=>(Default_mode;Limbic) |
| 322) | rfMRI connectivity (ICA100 edge 20) | (Precuneus;Angular;Middle_cingulate)<=>(Superior_frontal;Anterior_cingulate) | (Default_mode;Central_executive)<=>(Default_mode;Limbic) |
| 323) | rfMRI connectivity (ICA100 edge 21) | (Postcentral;Precentral)<=>(Superior_frontal;Anterior_cingulate) | (Motor)<=>(Default_mode;Limbic) |
| 324) | rfMRI connectivity (ICA100 edge 22) | (Calcarine;Lingual;Cuneus)<=>(Calcarine;Lingual) | (Visual)<=>(Visual) |
| 325) | rfMRI connectivity (ICA100 edge 23) | (Rolandic_operculum;SupraMarginal;Insula)<=>(Calcarine;Lingual) | (Salience;Motor)<=>(Visual) |
| 326) | rfMRI connectivity (ICA100 edge 24) | (Lingual;Fusiform)<=>(Calcarine;Lingual) | (Visual)<=>(Visual) |
| 327) | rfMRI connectivity (ICA100 edge 25) | (Middle_occipital;Superior_occipital)<=>(Calcarine;Lingual) | (Attention;Visual)<=>(Visual) |
| 328) | rfMRI connectivity (ICA100 edge 26) | (Precuneus;Angular;Middle_cingulate)<=>(Calcarine;Lingual) | (Default_mode;Central_executive)<=>(Visual) |
| 329) | rfMRI connectivity (ICA100 edge 27) | (Postcentral;Precentral)<=>(Calcarine;Lingual) | (Motor)<=>(Visual) |
| 330) | rfMRI connectivity (ICA100 edge 28) | (Superior_frontal;Anterior_cingulate)<=>(Calcarine;Lingual) | (Default_mode;Limbic)<=>(Visual) |

| | | | |
|---|---|---|---|
| 331) | rfMRI connectivity (ICA100 edge 29) | (Calcarine;Lingual;Cuneus)<=>(Middle_temporal;Temporal_pole) | (Visual)<=>(Default_mode) |
| 332) | rfMRI connectivity (ICA100 edge 30) | (Rolandic_operculum;SupraMarginal;Insula)<=>(Middle_temporal;Temporal_pole) | (Salience;Motor)<=>(Default_mode) |
| 333) | rfMRI connectivity (ICA100 edge 31) | (Lingual;Fusiform)<=>(Middle_temporal;Temporal_pole) | (Visual)<=>(Default_mode) |
| 334) | rfMRI connectivity (ICA100 edge 32) | (Middle_occipital;Superior_occipital)<=>(Middle_temporal;Temporal_pole) | (Attention;Visual)<=>(Default_mode) |
| 335) | rfMRI connectivity (ICA100 edge 33) | (Precuneus;Angular;Middle_cingulate)<=>(Middle_temporal;Temporal_pole) | (Default_mode;Central_executive)<=>(Default_mode) |
| 336) | rfMRI connectivity (ICA100 edge 34) | (Postcentral;Precentral)<=>(Middle_temporal;Temporal_pole) | (Motor)<=>(Default_mode) |
| 337) | rfMRI connectivity (ICA100 edge 35) | (Superior_frontal;Anterior_cingulate)<=>(Middle_temporal;Temporal_pole) | (Default_mode;Limbic)<=>(Default_mode) |
| 338) | rfMRI connectivity (ICA100 edge 36) | (Calcarine;Lingual)<=>(Middle_temporal;Temporal_pole) | (Visual)<=>(Default_mode) |
| 339) | rfMRI connectivity (ICA100 edge 37) | (Calcarine;Lingual;Cuneus)<=>(Middle_occipital;Precuneus;Calcarine) | (Visual)<=>(Default_mode;Central_executive) |
| 340) | rfMRI connectivity (ICA100 edge 38) | (Rolandic_operculum;SupraMarginal;Insula)<=>(Middle_occipital;Precuneus;Calcarine) | (Salience;Motor)<=>(Default_mode;Central_executive) |
| 341) | rfMRI connectivity (ICA100 edge 39) | (Lingual;Fusiform)<=>(Middle_occipital;Precuneus;Calcarine) | (Visual)<=>(Default_mode;Central_executive) |
| 342) | rfMRI connectivity (ICA100 edge 40) | (Middle_occipital;Superior_occipital)<=>(Middle_occipital;Precuneus;Calcarine) | (Attention;Visual)<=>(Default_mode;Central_executive) |
| 343) | rfMRI connectivity (ICA100 edge 41) | (Precuneus;Angular;Middle_cingulate)<=>(Middle_occipital;Precuneus;Calcarine) | (Default_mode;Central_executive)<=>(Default_mode;Central_executive) |
| 344) | rfMRI connectivity (ICA100 edge 42) | (Postcentral;Precentral)<=>(Middle_occipital;Precuneus;Calcarine) | (Motor)<=>(Default_mode;Central_executive) |
| 345) | rfMRI connectivity (ICA100 edge 43) | (Superior_frontal;Anterior_cingulate)<=>(Middle_occipital;Precuneus;Calcarine) | (Default_mode;Limbic)<=>(Default_mode;Central_executive) |
| 346) | rfMRI connectivity (ICA100 edge 44) | (Calcarine;Lingual)<=>(Middle_occipital;Precuneus;Calcarine) | (Visual)<=>(Default_mode;Central_executive) |
| 347) | rfMRI connectivity (ICA100 edge 45) | (Middle_temporal;Temporal_pole)<=>(Middle_occipital;Precuneus;Calcarine) | (Default_mode)<=>(Default_mode;Central_executive) |
| 348) | rfMRI connectivity (ICA100 edge 46) | (Calcarine;Lingual;Cuneus)<=>(Angular;Middle_temporal) | (Visual)<=>(Default_mode;Central_executive) |
| 349) | rfMRI connectivity (ICA100 edge 47) | (Rolandic_operculum;SupraMarginal;Insula)<=>(Angular;Middle_temporal) | (Salience;Motor)<=>(Default_mode;Central_executive) |
| 350) | rfMRI connectivity (ICA100 edge 48) | (Lingual;Fusiform)<=>(Angular;Middle_temporal) | (Visual)<=>(Default_mode;Central_executive) |
| 351) | rfMRI connectivity (ICA100 edge 49) | (Middle_occipital;Superior_occipital)<=>(Angular;Middle_temporal) | (Attention;Visual)<=>(Default_mode;Central_executive) |
| 352) | rfMRI connectivity (ICA100 edge 50) | (Precuneus;Angular;Middle_cingulate)<=>(Angular;Middle_temporal) | (Default_mode;Central_executive)<=>(Default_mode;Central_executive) |
| 353) | rfMRI connectivity (ICA100 edge 51) | (Postcentral;Precentral)<=>(Angular;Middle_temporal) | (Motor)<=>(Default_mode;Central_executive) |
| 354) | rfMRI connectivity (ICA100 edge 52) | (Superior_frontal;Anterior_cingulate)<=>(Angular;Middle_temporal) | (Default_mode;Limbic)<=>(Default_mode;Central_executive) |
| 355) | rfMRI connectivity (ICA100 edge 53) | (Calcarine;Lingual)<=>(Angular;Middle_temporal) | (Visual)<=>(Default_mode;Central_executive) |
| 356) | rfMRI connectivity (ICA100 edge 54) | (Middle_temporal;Temporal_pole)<=>(Angular;Middle_temporal) | (Default_mode)<=>(Default_mode;Central_executive) |
| 357) | rfMRI connectivity (ICA100 edge 55) | (Middle_occipital;Precuneus;Calcarine)<=>(Angular;Middle_temporal) | (Default_mode;Central_executive)<=>(Default_mode;Central_executive) |

| | | | |
|---|---|---|---|
| 358) | rfMRI connectivity (ICA100 edge 56) | (Calcarine;Lingual;Cuneus)<=>(Middle_frontal;Cerebellum) | (Visual)<=>(Central_executive;Default_mode) |
| 359) | rfMRI connectivity (ICA100 edge 57) | (Rolandic_operculum;SupraMarginal;Insula)<=>(Middle_frontal;Cerebellum) | (Salience;Motor)<=>(Central_executive;Default_mode) |
| 360) | rfMRI connectivity (ICA100 edge 58) | (Lingual;Fusiform)<=>(Middle_frontal;Cerebellum) | (Visual)<=>(Central_executive;Default_mode) |
| 361) | rfMRI connectivity (ICA100 edge 59) | (Middle_occipital;Superior_occipital)<=>(Middle_frontal;Cerebellum) | (Attention;Visual)<=>(Central_executive;Default_mode) |
| 362) | rfMRI connectivity (ICA100 edge 60) | (Precuneus;Angular;Middle_cingulate)<=>(Middle_frontal;Cerebellum) | (Default_mode;Central_executive)<=>(Central_executive;Default_mode) |
| 363) | rfMRI connectivity (ICA100 edge 61) | (Postcentral;Precentral)<=>(Middle_frontal;Cerebellum) | (Motor)<=>(Central_executive;Default_mode) |
| 364) | rfMRI connectivity (ICA100 edge 62) | (Superior_frontal;Anterior_cingulate)<=>(Middle_frontal;Cerebellum) | (Default_mode;Limbic)<=>(Central_executive;Default_mode) |
| 365) | rfMRI connectivity (ICA100 edge 63) | (Calcarine;Lingual)<=>(Middle_frontal;Cerebellum) | (Visual)<=>(Central_executive;Default_mode) |
| 366) | rfMRI connectivity (ICA100 edge 64) | (Middle_temporal;Temporal_pole)<=>(Middle_frontal;Cerebellum) | (Default_mode)<=>(Central_executive;Default_mode) |
| 367) | rfMRI connectivity (ICA100 edge 65) | (Middle_occipital;Precuneus;Calcarine)<=>(Middle_frontal;Cerebellum) | (Default_mode;Central_executive)<=>(Central_executive;Default_mode) |
| 368) | rfMRI connectivity (ICA100 edge 66) | (Angular;Middle_temporal)<=>(Middle_frontal;Cerebellum) | (Default_mode;Central_executive)<=>(Central_executive;Default_mode) |
| 369) | rfMRI connectivity (ICA100 edge 67) | (Calcarine;Lingual;Cuneus)<=>(Superior_frontal) | (Visual)<=>(Default_mode) |
| 370) | rfMRI connectivity (ICA100 edge 68) | (Rolandic_operculum;SupraMarginal;Insula)<=>(Superior_frontal) | (Salience;Motor)<=>(Default_mode) |
| 371) | rfMRI connectivity (ICA100 edge 69) | (Lingual;Fusiform)<=>(Superior_frontal) | (Visual)<=>(Default_mode) |
| 372) | rfMRI connectivity (ICA100 edge 70) | (Middle_occipital;Superior_occipital)<=>(Superior_frontal) | (Attention;Visual)<=>(Default_mode) |
| 373) | rfMRI connectivity (ICA100 edge 71) | (Precuneus;Angular;Middle_cingulate)<=>(Superior_frontal) | (Default_mode;Central_executive)<=>(Default_mode) |
| 374) | rfMRI connectivity (ICA100 edge 72) | (Postcentral;Precentral)<=>(Superior_frontal) | (Motor)<=>(Default_mode) |
| 375) | rfMRI connectivity (ICA100 edge 73) | (Superior_frontal;Anterior_cingulate)<=>(Superior_frontal) | (Default_mode;Limbic)<=>(Default_mode) |
| 376) | rfMRI connectivity (ICA100 edge 74) | (Calcarine;Lingual)<=>(Superior_frontal) | (Visual)<=>(Default_mode) |
| 377) | rfMRI connectivity (ICA100 edge 75) | (Middle_temporal;Temporal_pole)<=>(Superior_frontal) | (Default_mode)<=>(Default_mode) |
| 378) | rfMRI connectivity (ICA100 edge 76) | (Middle_occipital;Precuneus;Calcarine)<=>(Superior_frontal) | (Default_mode;Central_executive)<=>(Default_mode) |
| 379) | rfMRI connectivity (ICA100 edge 77) | (Angular;Middle_temporal)<=>(Superior_frontal) | (Default_mode;Central_executive)<=>(Default_mode) |
| 380) | rfMRI connectivity (ICA100 edge 78) | (Middle_frontal;Cerebellum)<=>(Superior_frontal) | (Central_executive;Default_mode)<=>(Default_mode) |
| 381) | rfMRI connectivity (ICA100 edge 79) | (Calcarine;Lingual;Cuneus)<=>(Cuneus;Superior_occipital) | (Visual)<=>(Visual) |
| 382) | rfMRI connectivity (ICA100 edge 80) | (Rolandic_operculum;SupraMarginal;Insula)<=>(Cuneus;Superior_occipital) | (Salience;Motor)<=>(Visual) |
| 383) | rfMRI connectivity (ICA100 edge 81) | (Lingual;Fusiform)<=>(Cuneus;Superior_occipital) | (Visual)<=>(Visual) |
| 384) | rfMRI connectivity (ICA100 edge 82) | (Middle_occipital;Superior_occipital)<=>(Cuneus;Superior_occipital) | (Attention;Visual)<=>(Visual) |
| 385) | rfMRI connectivity (ICA100 edge 83) | (Precuneus;Angular;Middle_cingulate)<=>(Cuneus;Superior_occipital) | (Default_mode;Central_executive)<=>(Visual) |

| | | | |
|---|---|---|---|
| 386) | rfMRI connectivity (ICA100 edge 84) | (Postcentral;Precentral)<=>(Cuneus;Superior_occipital) | (Motor)<=>(Visual) |
| 387) | rfMRI connectivity (ICA100 edge 85) | (Superior_frontal;Anterior_cingulate)<=>(Cuneus;Superior_occipital) | (Default_mode;Limbic)<=>(Visual) |
| 388) | rfMRI connectivity (ICA100 edge 86) | (Calcarine;Lingual)<=>(Cuneus;Superior_occipital) | (Visual)<=>(Visual) |
| 389) | rfMRI connectivity (ICA100 edge 87) | (Middle_temporal;Temporal_pole)<=>(Cuneus;Superior_occipital) | (Default_mode)<=>(Visual) |
| 390) | rfMRI connectivity (ICA100 edge 88) | (Middle_occipital;Precuneus;Calcarine)<=>(Cuneus;Superior_occipital) | (Default_mode;Central_executive)<=>(Visual) |
| 391) | rfMRI connectivity (ICA100 edge 89) | (Angular;Middle_temporal)<=>(Cuneus;Superior_occipital) | (Default_mode;Central_executive)<=>(Visual) |
| 392) | rfMRI connectivity (ICA100 edge 90) | (Middle_frontal;Cerebellum)<=>(Cuneus;Superior_occipital) | (Central_executive;Default_mode)<=>(Visual) |
| 393) | rfMRI connectivity (ICA100 edge 91) | (Superior_frontal)<=>(Cuneus;Superior_occipital) | (Default_mode)<=>(Visual) |
| 394) | rfMRI connectivity (ICA100 edge 92) | (Calcarine;Lingual;Cuneus)<=>(Insula;Anterior_cingulate) | (Visual)<=>(Salience;Default_mode) |
| 395) | rfMRI connectivity (ICA100 edge 93) | (Rolandic_operculum;SupraMarginal;Insula)<=>(Insula;Anterior_cingulate) | (Salience;Motor)<=>(Salience;Default_mode) |
| 396) | rfMRI connectivity (ICA100 edge 94) | (Lingual;Fusiform)<=>(Insula;Anterior_cingulate) | (Visual)<=>(Salience;Default_mode) |
| 397) | rfMRI connectivity (ICA100 edge 95) | (Middle_occipital;Superior_occipital)<=>(Insula;Anterior_cingulate) | (Attention;Visual)<=>(Salience;Default_mode) |
| 398) | rfMRI connectivity (ICA100 edge 96) | (Precuneus;Angular;Middle_cingulate)<=>(Insula;Anterior_cingulate) | (Default_mode;Central_executive)<=>(Salience;Default_mode) |
| 399) | rfMRI connectivity (ICA100 edge 97) | (Postcentral;Precentral)<=>(Insula;Anterior_cingulate) | (Motor)<=>(Salience;Default_mode) |
| 400) | rfMRI connectivity (ICA100 edge 98) | (Superior_frontal;Anterior_cingulate)<=>(Insula;Anterior_cingulate) | (Default_mode;Limbic)<=>(Salience;Default_mode) |
| 401) | rfMRI connectivity (ICA100 edge 99) | (Calcarine;Lingual)<=>(Insula;Anterior_cingulate) | (Visual)<=>(Salience;Default_mode) |
| 402) | rfMRI connectivity (ICA100 edge 100) | (Middle_temporal;Temporal_pole)<=>(Insula;Anterior_cingulate) | (Default_mode)<=>(Salience;Default_mode) |
| 403) | rfMRI connectivity (ICA100 edge 101) | (Middle_occipital;Precuneus;Calcarine)<=>(Insula;Anterior_cingulate) | (Default_mode;Central_executive)<=>(Salience;Default_mode) |
| 404) | rfMRI connectivity (ICA100 edge 102) | (Angular;Middle_temporal)<=>(Insula;Anterior_cingulate) | (Default_mode;Central_executive)<=>(Salience;Default_mode) |
| 405) | rfMRI connectivity (ICA100 edge 103) | (Middle_frontal;Cerebellum)<=>(Insula;Anterior_cingulate) | (Central_executive;Default_mode)<=>(Salience;Default_mode) |
| 406) | rfMRI connectivity (ICA100 edge 104) | (Superior_frontal)<=>(Insula;Anterior_cingulate) | (Default_mode)<=>(Salience;Default_mode) |
| 407) | rfMRI connectivity (ICA100 edge 105) | (Cuneus;Superior_occipital)<=>(Insula;Anterior_cingulate) | (Visual)<=>(Salience;Default_mode) |
| 408) | rfMRI connectivity (ICA100 edge 106) | (Calcarine;Lingual;Cuneus)<=>(Inferior_occipital;Middle_occipital) | (Visual)<=>(Visual) |
| 409) | rfMRI connectivity (ICA100 edge 107) | (Rolandic_operculum;SupraMarginal;Insula)<=>(Inferior_occipital;Middle_occipital) | (Salience;Motor)<=>(Visual) |
| 410) | rfMRI connectivity (ICA100 edge 108) | (Lingual;Fusiform)<=>(Inferior_occipital;Middle_occipital) | (Visual)<=>(Visual) |
| 411) | rfMRI connectivity (ICA100 edge 109) | (Middle_occipital;Superior_occipital)<=>(Inferior_occipital;Middle_occipital) | (Attention;Visual)<=>(Visual) |
| 412) | rfMRI connectivity (ICA100 edge 110) | (Precuneus;Angular;Middle_cingulate)<=>(Inferior_occipital;Middle_occipital) | (Default_mode;Central_executive)<=>(Visual) |

| | | | |
|---|---|---|---|
| 413) | rfMRI connectivity (ICA100 edge 111) | (Postcentral;Precentral)<=>(Inferior_occipital;Middle_occipital) | (Motor)<=>(Visual) |
| 414) | rfMRI connectivity (ICA100 edge 112) | (Superior_frontal;Anterior_cingulate)<=>(Inferior_occipital;Middle_occipital) | (Default_mode;Limbic)<=>(Visual) |
| 415) | rfMRI connectivity (ICA100 edge 113) | (Calcarine;Lingual)<=>(Inferior_occipital;Middle_occipital) | (Visual)<=>(Visual) |
| 416) | rfMRI connectivity (ICA100 edge 114) | (Middle_temporal;Temporal_pole)<=>(Inferior_occipital;Middle_occipital) | (Default_mode)<=>(Visual) |
| 417) | rfMRI connectivity (ICA100 edge 115) | (Middle_occipital;Precuneus;Calcarine)<=>(Inferior_occipital;Middle_occipital) | (Default_mode;Central_executive)<=>(Visual) |
| 418) | rfMRI connectivity (ICA100 edge 116) | (Angular;Middle_temporal)<=>(Inferior_occipital;Middle_occipital) | (Default_mode;Central_executive)<=>(Visual) |
| 419) | rfMRI connectivity (ICA100 edge 117) | (Middle_frontal;Cerebellum)<=>(Inferior_occipital;Middle_occipital) | (Central_executive;Default_mode)<=>(Visual) |
| 420) | rfMRI connectivity (ICA100 edge 118) | (Superior_frontal)<=>(Inferior_occipital;Middle_occipital) | (Default_mode)<=>(Visual) |
| 421) | rfMRI connectivity (ICA100 edge 119) | (Cuneus;Superior_occipital)<=>(Inferior_occipital;Middle_occipital) | (Visual)<=>(Visual) |
| 422) | rfMRI connectivity (ICA100 edge 120) | (Insula;Anterior_cingulate)<=>(Inferior_occipital;Middle_occipital) | (Salience;Default_mode)<=>(Visual) |
| 423) | rfMRI connectivity (ICA100 edge 121) | (Calcarine;Lingual;Cuneus)<=>(Cerebellum) | (Visual)<=>(Subcortical-cerebellum) |
| 424) | rfMRI connectivity (ICA100 edge 122) | (Rolandic_operculum;SupraMarginal;Insula)<=>(Cerebellum) | (Salience;Motor)<=>(Subcortical-cerebellum) |
| 425) | rfMRI connectivity (ICA100 edge 123) | (Lingual;Fusiform)<=>(Cerebellum) | (Visual)<=>(Subcortical-cerebellum) |
| 426) | rfMRI connectivity (ICA100 edge 124) | (Middle_occipital;Superior_occipital)<=>(Cerebellum) | (Attention;Visual)<=>(Subcortical-cerebellum) |
| 427) | rfMRI connectivity (ICA100 edge 125) | (Precuneus;Angular;Middle_cingulate)<=>(Cerebellum) | (Default_mode;Central_executive)<=>(Subcortical-cerebellum) |
| 428) | rfMRI connectivity (ICA100 edge 126) | (Postcentral;Precentral)<=>(Cerebellum) | (Motor)<=>(Subcortical-cerebellum) |
| 429) | rfMRI connectivity (ICA100 edge 127) | (Superior_frontal;Anterior_cingulate)<=>(Cerebellum) | (Default_mode;Limbic)<=>(Subcortical-cerebellum) |
| 430) | rfMRI connectivity (ICA100 edge 128) | (Calcarine;Lingual)<=>(Cerebellum) | (Visual)<=>(Subcortical-cerebellum) |
| 431) | rfMRI connectivity (ICA100 edge 129) | (Middle_temporal;Temporal_pole)<=>(Cerebellum) | (Default_mode)<=>(Subcortical-cerebellum) |
| 432) | rfMRI connectivity (ICA100 edge 130) | (Middle_occipital;Precuneus;Calcarine)<=>(Cerebellum) | (Default_mode;Central_executive)<=>(Subcortical-cerebellum) |
| 433) | rfMRI connectivity (ICA100 edge 131) | (Angular;Middle_temporal)<=>(Cerebellum) | (Default_mode;Central_executive)<=>(Subcortical-cerebellum) |
| 434) | rfMRI connectivity (ICA100 edge 132) | (Middle_frontal;Cerebellum)<=>(Cerebellum) | (Central_executive;Default_mode)<=>(Subcortical-cerebellum) |
| 435) | rfMRI connectivity (ICA100 edge 133) | (Superior_frontal)<=>(Cerebellum) | (Default_mode)<=>(Subcortical-cerebellum) |
| 436) | rfMRI connectivity (ICA100 edge 134) | (Cuneus;Superior_occipital)<=>(Cerebellum) | (Visual)<=>(Subcortical-cerebellum) |
| 437) | rfMRI connectivity (ICA100 edge 135) | (Insula;Anterior_cingulate)<=>(Cerebellum) | (Salience;Default_mode)<=>(Subcortical-cerebellum) |
| 438) | rfMRI connectivity (ICA100 edge 136) | (Inferior_occipital;Middle_occipital)<=>(Cerebellum) | (Visual)<=>(Subcortical-cerebellum) |
| 439) | rfMRI connectivity (ICA100 edge 137) | (Calcarine;Lingual;Cuneus)<=>(Inferior_parietal;Postcentral) | (Visual)<=>(Attention;Central_executive;Salience) |

| | | | |
|---|---|---|---|
| 440) | rfMRI connectivity (ICA100 edge 138) | (Rolandic_operculum;SupraMarginal;Insula)<=>(Inferior_parietal;Postcentral) | (Salience;Motor)<=>(Attention;Central_executive;Salience) |
| 441) | rfMRI connectivity (ICA100 edge 139) | (Lingual;Fusiform)<=>(Inferior_parietal;Postcentral) | (Visual)<=>(Attention;Central_executive;Salience) |
| 442) | rfMRI connectivity (ICA100 edge 140) | (Middle_occipital;Superior_occipital)<=>(Inferior_parietal;Postcentral) | (Attention;Visual)<=>(Attention;Central_executive;Salience) |
| 443) | rfMRI connectivity (ICA100 edge 141) | (Precuneus;Angular;Middle_cingulate)<=>(Inferior_parietal;Postcentral) | (Default_mode;Central_executive)<=>(Attention;Central_executive;Salience) |
| 444) | rfMRI connectivity (ICA100 edge 142) | (Postcentral;Precentral)<=>(Inferior_parietal;Postcentral) | (Motor)<=>(Attention;Central_executive;Salience) |
| 445) | rfMRI connectivity (ICA100 edge 143) | (Superior_frontal;Anterior_cingulate)<=>(Inferior_parietal;Postcentral) | (Default_mode;Limbic)<=>(Attention;Central_executive;Salience) |
| 446) | rfMRI connectivity (ICA100 edge 144) | (Calcarine;Lingual)<=>(Inferior_parietal;Postcentral) | (Visual)<=>(Attention;Central_executive;Salience) |
| 447) | rfMRI connectivity (ICA100 edge 145) | (Middle_temporal;Temporal_pole)<=>(Inferior_parietal;Postcentral) | (Default_mode)<=>(Attention;Central_executive;Salience) |
| 448) | rfMRI connectivity (ICA100 edge 146) | (Middle_occipital;Precuneus;Calcarine)<=>(Inferior_parietal;Postcentral) | (Default_mode;Central_executive)<=>(Attention;Central_executive;Salience) |
| 449) | rfMRI connectivity (ICA100 edge 147) | (Angular;Middle_temporal)<=>(Inferior_parietal;Postcentral) | (Default_mode;Central_executive)<=>(Attention;Central_executive;Salience) |
| 450) | rfMRI connectivity (ICA100 edge 148) | (Middle_frontal;Cerebellum)<=>(Inferior_parietal;Postcentral) | (Central_executive;Default_mode)<=>(Attention;Central_executive;Salience) |
| 451) | rfMRI connectivity (ICA100 edge 149) | (Superior_frontal)<=>(Inferior_parietal;Postcentral) | (Default_mode)<=>(Attention;Central_executive;Salience) |
| 452) | rfMRI connectivity (ICA100 edge 150) | (Cuneus;Superior_occipital)<=>(Inferior_parietal;Postcentral) | (Visual)<=>(Attention;Central_executive;Salience) |
| 453) | rfMRI connectivity (ICA100 edge 151) | (Insula;Anterior_cingulate)<=>(Inferior_parietal;Postcentral) | (Salience;Default_mode)<=>(Attention;Central_executive;Salience) |
| 454) | rfMRI connectivity (ICA100 edge 152) | (Inferior_occipital;Middle_occipital)<=>(Inferior_parietal;Postcentral) | (Visual)<=>(Attention;Central_executive;Salience) |
| 455) | rfMRI connectivity (ICA100 edge 153) | (Cerebellum)<=>(Inferior_parietal;Postcentral) | (Subcortical-cerebellum)<=>(Attention;Central_executive;Salience) |
| 456) | rfMRI connectivity (ICA100 edge 154) | (Calcarine;Lingual;Cuneus)<=>(Precuneus;Cuneus) | (Visual)<=>(Default_mode;Central_executive) |
| 457) | rfMRI connectivity (ICA100 edge 155) | (Rolandic_operculum;SupraMarginal;Insula)<=>(Precuneus;Cuneus) | (Salience;Motor)<=>(Default_mode;Central_executive) |
| 458) | rfMRI connectivity (ICA100 edge 156) | (Lingual;Fusiform)<=>(Precuneus;Cuneus) | (Visual)<=>(Default_mode;Central_executive) |
| 459) | rfMRI connectivity (ICA100 edge 157) | (Middle_occipital;Superior_occipital)<=>(Precuneus;Cuneus) | (Attention;Visual)<=>(Default_mode;Central_executive) |
| 460) | rfMRI connectivity (ICA100 edge 158) | (Precuneus;Angular;Middle_cingulate)<=>(Precuneus;Cuneus) | (Default_mode;Central_executive)<=>(Default_mode;Central_executive) |
| 461) | rfMRI connectivity (ICA100 edge 159) | (Postcentral;Precentral)<=>(Precuneus;Cuneus) | (Motor)<=>(Default_mode;Central_executive) |
| 462) | rfMRI connectivity (ICA100 edge 160) | (Superior_frontal;Anterior_cingulate)<=>(Precuneus;Cuneus) | (Default_mode;Limbic)<=>(Default_mode;Central_executive) |
| 463) | rfMRI connectivity (ICA100 edge 161) | (Calcarine;Lingual)<=>(Precuneus;Cuneus) | (Visual)<=>(Default_mode;Central_executive) |
| 464) | rfMRI connectivity (ICA100 edge 162) | (Middle_temporal;Temporal_pole)<=>(Precuneus;Cuneus) | (Default_mode)<=>(Default_mode;Central_executive) |

| | | | |
|---|---|---|---|
| 465) | rfMRI connectivity (ICA100 edge 163) | (Middle_occipital;Precuneus;Calcarine)<=>(Precuneus;Cuneus) | (Default_mode;Central_executive)<=>(Default_mode;Central_executive) |
| 466) | rfMRI connectivity (ICA100 edge 164) | (Angular;Middle_temporal)<=>(Precuneus;Cuneus) | (Default_mode;Central_executive)<=>(Default_mode;Central_executive) |
| 467) | rfMRI connectivity (ICA100 edge 165) | (Middle_frontal;Cerebellum)<=>(Precuneus;Cuneus) | (Central_executive;Default_mode)<=>(Default_mode;Central_executive) |
| 468) | rfMRI connectivity (ICA100 edge 166) | (Superior_frontal)<=>(Precuneus;Cuneus) | (Default_mode)<=>(Default_mode;Central_executive) |
| 469) | rfMRI connectivity (ICA100 edge 167) | (Cuneus;Superior_occipital)<=>(Precuneus;Cuneus) | (Visual)<=>(Default_mode;Central_executive) |
| 470) | rfMRI connectivity (ICA100 edge 168) | (Insula;Anterior_cingulate)<=>(Precuneus;Cuneus) | (Salience;Default_mode)<=>(Default_mode;Central_executive) |
| 471) | rfMRI connectivity (ICA100 edge 169) | (Inferior_occipital;Middle_occipital)<=>(Precuneus;Cuneus) | (Visual)<=>(Default_mode;Central_executive) |
| 472) | rfMRI connectivity (ICA100 edge 170) | (Cerebellum)<=>(Precuneus;Cuneus) | (Subcortical-cerebellum)<=>(Default_mode;Central_executive) |
| 473) | rfMRI connectivity (ICA100 edge 171) | (Inferior_parietal;Postcentral)<=>(Precuneus;Cuneus) | (Attention;Central_executive;Salience)<=>(Default_mode;Central_executive) |
| 474) | rfMRI connectivity (ICA100 edge 172) | (Calcarine;Lingual;Cuneus)<=>(Postcentral;Precentral) | (Visual)<=>(Motor;Attention) |
| 475) | rfMRI connectivity (ICA100 edge 173) | (Rolandic_operculum;SupraMarginal;Insula)<=>(Postcentral;Precentral) | (Salience;Motor)<=>(Motor;Attention) |
| 476) | rfMRI connectivity (ICA100 edge 174) | (Lingual;Fusiform)<=>(Postcentral;Precentral) | (Visual)<=>(Motor;Attention) |
| 477) | rfMRI connectivity (ICA100 edge 175) | (Middle_occipital;Superior_occipital)<=>(Postcentral;Precentral) | (Attention;Visual)<=>(Motor;Attention) |
| 478) | rfMRI connectivity (ICA100 edge 176) | (Precuneus;Angular;Middle_cingulate)<=>(Postcentral;Precentral) | (Default_mode;Central_executive)<=>(Motor;Attention) |
| 479) | rfMRI connectivity (ICA100 edge 177) | (Postcentral;Precentral)<=>(Postcentral;Precentral) | (Motor)<=>(Motor;Attention) |
| 480) | rfMRI connectivity (ICA100 edge 178) | (Superior_frontal;Anterior_cingulate)<=>(Postcentral;Precentral) | (Default_mode;Limbic)<=>(Motor;Attention) |
| 481) | rfMRI connectivity (ICA100 edge 179) | (Calcarine;Lingual)<=>(Postcentral;Precentral) | (Visual)<=>(Motor;Attention) |
| 482) | rfMRI connectivity (ICA100 edge 180) | (Middle_temporal;Temporal_pole)<=>(Postcentral;Precentral) | (Default_mode)<=>(Motor;Attention) |
| 483) | rfMRI connectivity (ICA100 edge 181) | (Middle_occipital;Precuneus;Calcarine)<=>(Postcentral;Precentral) | (Default_mode;Central_executive)<=>(Motor;Attention) |
| 484) | rfMRI connectivity (ICA100 edge 182) | (Angular;Middle_temporal)<=>(Postcentral;Precentral) | (Default_mode;Central_executive)<=>(Motor;Attention) |
| 485) | rfMRI connectivity (ICA100 edge 183) | (Middle_frontal;Cerebellum)<=>(Postcentral;Precentral) | (Central_executive;Default_mode)<=>(Motor;Attention) |
| 486) | rfMRI connectivity (ICA100 edge 184) | (Superior_frontal)<=>(Postcentral;Precentral) | (Default_mode)<=>(Motor;Attention) |
| 487) | rfMRI connectivity (ICA100 edge 185) | (Cuneus;Superior_occipital)<=>(Postcentral;Precentral) | (Visual)<=>(Motor;Attention) |
| 488) | rfMRI connectivity (ICA100 edge 186) | (Insula;Anterior_cingulate)<=>(Postcentral;Precentral) | (Salience;Default_mode)<=>(Motor;Attention) |
| 489) | rfMRI connectivity (ICA100 edge 187) | (Inferior_occipital;Middle_occipital)<=>(Postcentral;Precentral) | (Visual)<=>(Motor;Attention) |
| 490) | rfMRI connectivity (ICA100 edge 188) | (Cerebellum)<=>(Postcentral;Precentral) | (Subcortical-cerebellum)<=>(Motor;Attention) |

| | | | |
|---|---|---|---|
| 491) | rfMRI connectivity (ICA100 edge 189) | (Inferior_parietal;Postcentral)<=>(Postcentral;Precentral) | (Attention;Central_executive;Salience)<=>(Motor;Attention) |
| 492) | rfMRI connectivity (ICA100 edge 190) | (Precuneus;Cuneus)<=>(Postcentral;Precentral) | (Default_mode;Central_executive)<=>(Motor;Attention) |
| 493) | rfMRI connectivity (ICA100 edge 191) | (Calcarine;Lingual;Cuneus)<=>(Superior_frontal) | (Visual)<=>(Default_mode;Central_executive) |
| 494) | rfMRI connectivity (ICA100 edge 192) | (Rolandic_operculum;SupraMarginal;Insula)<=>(Superior_frontal) | (Salience;Motor)<=>(Default_mode;Central_executive) |
| 495) | rfMRI connectivity (ICA100 edge 193) | (Lingual;Fusiform)<=>(Superior_frontal) | (Visual)<=>(Default_mode;Central_executive) |
| 496) | rfMRI connectivity (ICA100 edge 194) | (Middle_occipital;Superior_occipital)<=>(Superior_frontal) | (Attention;Visual)<=>(Default_mode;Central_executive) |
| 497) | rfMRI connectivity (ICA100 edge 195) | (Precuneus;Angular;Middle_cingulate)<=>(Superior_frontal) | (Default_mode;Central_executive)<=>(Default_mode;Central_executive) |
| 498) | rfMRI connectivity (ICA100 edge 196) | (Postcentral;Precentral)<=>(Superior_frontal) | (Motor)<=>(Default_mode;Central_executive) |
| 499) | rfMRI connectivity (ICA100 edge 197) | (Superior_frontal;Anterior_cingulate)<=>(Superior_frontal) | (Default_mode;Limbic)<=>(Default_mode;Central_executive) |
| 500) | rfMRI connectivity (ICA100 edge 198) | (Calcarine;Lingual)<=>(Superior_frontal) | (Visual)<=>(Default_mode;Central_executive) |
| 501) | rfMRI connectivity (ICA100 edge 199) | (Middle_temporal;Temporal_pole)<=>(Superior_frontal) | (Default_mode)<=>(Default_mode;Central_executive) |
| 502) | rfMRI connectivity (ICA100 edge 200) | (Middle_occipital;Precuneus;Calcarine)<=>(Superior_frontal) | (Default_mode;Central_executive)<=>(Default_mode;Central_executive) |
| 503) | rfMRI connectivity (ICA100 edge 201) | (Angular;Middle_temporal)<=>(Superior_frontal) | (Default_mode;Central_executive)<=>(Default_mode;Central_executive) |
| 504) | rfMRI connectivity (ICA100 edge 202) | (Middle_frontal;Cerebellum)<=>(Superior_frontal) | (Central_executive;Default_mode)<=>(Default_mode;Central_executive) |
| 505) | rfMRI connectivity (ICA100 edge 203) | (Superior_frontal)<=>(Superior_frontal) | (Default_mode)<=>(Default_mode;Central_executive) |
| 506) | rfMRI connectivity (ICA100 edge 204) | (Cuneus;Superior_occipital)<=>(Superior_frontal) | (Visual)<=>(Default_mode;Central_executive) |
| 507) | rfMRI connectivity (ICA100 edge 205) | (Insula;Anterior_cingulate)<=>(Superior_frontal) | (Salience;Default_mode)<=>(Default_mode;Central_executive) |
| 508) | rfMRI connectivity (ICA100 edge 206) | (Inferior_occipital;Middle_occipital)<=>(Superior_frontal) | (Visual)<=>(Default_mode;Central_executive) |
| 509) | rfMRI connectivity (ICA100 edge 207) | (Cerebellum)<=>(Superior_frontal) | (Subcortical-cerebellum)<=>(Default_mode;Central_executive) |
| 510) | rfMRI connectivity (ICA100 edge 208) | (Inferior_parietal;Postcentral)<=>(Superior_frontal) | (Attention;Central_executive;Salience)<=>(Default_mode;Central_executive) |
| 511) | rfMRI connectivity (ICA100 edge 209) | (Precuneus;Cuneus)<=>(Superior_frontal) | (Default_mode;Central_executive)<=>(Default_mode;Central_executive) |
| 512) | rfMRI connectivity (ICA100 edge 210) | (Postcentral;Precentral)<=>(Superior_frontal) | (Motor;Attention)<=>(Default_mode;Central_executive) |
| 513) | rfMRI connectivity (ICA100 edge 211) | (Calcarine;Lingual;Cuneus)<=>(Superior_temporal) | (Visual)<=>(Default_mode;Motor) |
| 514) | rfMRI connectivity (ICA100 edge 212) | (Rolandic_operculum;SupraMarginal;Insula)<=>(Superior_temporal) | (Salience;Motor)<=>(Default_mode;Motor) |
| 515) | rfMRI connectivity (ICA100 edge 213) | (Lingual;Fusiform)<=>(Superior_temporal) | (Visual)<=>(Default_mode;Motor) |

| | | | |
|---|---|---|---|
| 516) | rfMRI connectivity (ICA100 edge 214) | (Middle_occipital;Superior_occipital)<=>(Superior_temporal) | (Attention;Visual)<=>(Default_mode;Motor) |
| 517) | rfMRI connectivity (ICA100 edge 215) | (Precuneus;Angular;Middle_cingulate)<=>(Superior_temporal) | (Default_mode;Central_executive)<=>(Default_mode;Motor) |
| 518) | rfMRI connectivity (ICA100 edge 216) | (Postcentral;Precentral)<=>(Superior_temporal) | (Motor)<=>(Default_mode;Motor) |
| 519) | rfMRI connectivity (ICA100 edge 217) | (Superior_frontal;Anterior_cingulate)<=>(Superior_temporal) | (Default_mode;Limbic)<=>(Default_mode;Motor) |
| 520) | rfMRI connectivity (ICA100 edge 218) | (Calcarine;Lingual)<=>(Superior_temporal) | (Visual)<=>(Default_mode;Motor) |
| 521) | rfMRI connectivity (ICA100 edge 219) | (Middle_temporal;Temporal_pole)<=>(Superior_temporal) | (Default_mode)<=>(Default_mode;Motor) |
| 522) | rfMRI connectivity (ICA100 edge 220) | (Middle_occipital;Precuneus;Calcarine)<=>(Superior_temporal) | (Default_mode;Central_executive)<=>(Default_mode;Motor) |
| 523) | rfMRI connectivity (ICA100 edge 221) | (Angular;Middle_temporal)<=>(Superior_temporal) | (Default_mode;Central_executive)<=>(Default_mode;Motor) |
| 524) | rfMRI connectivity (ICA100 edge 222) | (Middle_frontal;Cerebellum)<=>(Superior_temporal) | (Central_executive;Default_mode)<=>(Default_mode;Motor) |
| 525) | rfMRI connectivity (ICA100 edge 223) | (Superior_frontal)<=>(Superior_temporal) | (Default_mode)<=>(Default_mode;Motor) |
| 526) | rfMRI connectivity (ICA100 edge 224) | (Cuneus;Superior_occipital)<=>(Superior_temporal) | (Visual)<=>(Default_mode;Motor) |
| 527) | rfMRI connectivity (ICA100 edge 225) | (Insula;Anterior_cingulate)<=>(Superior_temporal) | (Salience;Default_mode)<=>(Default_mode;Motor) |
| 528) | rfMRI connectivity (ICA100 edge 226) | (Inferior_occipital;Middle_occipital)<=>(Superior_temporal) | (Visual)<=>(Default_mode;Motor) |
| 529) | rfMRI connectivity (ICA100 edge 227) | (Cerebellum)<=>(Superior_temporal) | (Subcortical-cerebellum)<=>(Default_mode;Motor) |
| 530) | rfMRI connectivity (ICA100 edge 228) | (Inferior_parietal;Postcentral)<=>(Superior_temporal) | (Attention;Central_executive;Salience)<=>(Default_mode;Motor) |
| 531) | rfMRI connectivity (ICA100 edge 229) | (Precuneus;Cuneus)<=>(Superior_temporal) | (Default_mode;Central_executive)<=>(Default_mode;Motor) |
| 532) | rfMRI connectivity (ICA100 edge 230) | (Postcentral;Precentral)<=>(Superior_temporal) | (Motor;Attention)<=>(Default_mode;Motor) |
| 533) | rfMRI connectivity (ICA100 edge 231) | (Superior_frontal)<=>(Superior_temporal) | (Default_mode;Central_executive)<=>(Default_mode;Motor) |
| 534) | rfMRI connectivity (ICA100 edge 232) | (Calcarine;Lingual;Cuneus)<=>(Cerebellum) | (Visual)<=>(Subcortical-cerebellum) |
| 535) | rfMRI connectivity (ICA100 edge 233) | (Rolandic_operculum;SupraMarginal;Insula)<=>(Cerebellum) | (Salience;Motor)<=>(Subcortical-cerebellum) |
| 536) | rfMRI connectivity (ICA100 edge 234) | (Lingual;Fusiform)<=>(Cerebellum) | (Visual)<=>(Subcortical-cerebellum) |
| 537) | rfMRI connectivity (ICA100 edge 235) | (Middle_occipital;Superior_occipital)<=>(Cerebellum) | (Attention;Visual)<=>(Subcortical-cerebellum) |
| 538) | rfMRI connectivity (ICA100 edge 236) | (Precuneus;Angular;Middle_cingulate)<=>(Cerebellum) | (Default_mode;Central_executive)<=>(Subcortical-cerebellum) |
| 539) | rfMRI connectivity (ICA100 edge 237) | (Postcentral;Precentral)<=>(Cerebellum) | (Motor)<=>(Subcortical-cerebellum) |
| 540) | rfMRI connectivity (ICA100 edge 238) | (Superior_frontal;Anterior_cingulate)<=>(Cerebellum) | (Default_mode;Limbic)<=>(Subcortical-cerebellum) |
| 541) | rfMRI connectivity (ICA100 edge 239) | (Calcarine;Lingual)<=>(Cerebellum) | (Visual)<=>(Subcortical-cerebellum) |
| 542) | rfMRI connectivity (ICA100 edge 240) | (Middle_temporal;Temporal_pole)<=>(Cerebellum) | (Default_mode)<=>(Subcortical-cerebellum) |

| | | | |
|---|---|---|---|
| 543) | rfMRI connectivity (ICA100 edge 241) | (Middle_occipital;Precuneus;Calcarine)<=>(Cerebellum) | (Default_mode;Central_executive)<=>(Subcortical-cerebellum) |
| 544) | rfMRI connectivity (ICA100 edge 242) | (Angular;Middle_temporal)<=>(Cerebellum) | (Default_mode;Central_executive)<=>(Subcortical-cerebellum) |
| 545) | rfMRI connectivity (ICA100 edge 243) | (Middle_frontal;Cerebellum)<=>(Cerebellum) | (Central_executive;Default_mode)<=>(Subcortical-cerebellum) |
| 546) | rfMRI connectivity (ICA100 edge 244) | (Superior_frontal)<=>(Cerebellum) | (Default_mode)<=>(Subcortical-cerebellum) |
| 547) | rfMRI connectivity (ICA100 edge 245) | (Cuneus;Superior_occipital)<=>(Cerebellum) | (Visual)<=>(Subcortical-cerebellum) |
| 548) | rfMRI connectivity (ICA100 edge 246) | (Insula;Anterior_cingulate)<=>(Cerebellum) | (Salience;Default_mode)<=>(Subcortical-cerebellum) |
| 549) | rfMRI connectivity (ICA100 edge 247) | (Inferior_occipital;Middle_occipital)<=>(Cerebellum) | (Visual)<=>(Subcortical-cerebellum) |
| 550) | rfMRI connectivity (ICA100 edge 248) | (Cerebellum)<=>(Cerebellum) | (Subcortical-cerebellum)<=>(Subcortical-cerebellum) |
| 551) | rfMRI connectivity (ICA100 edge 249) | (Inferior_parietal;Postcentral)<=>(Cerebellum) | (Attention;Central_executive;Salience)<=>(Subcortical-cerebellum) |
| 552) | rfMRI connectivity (ICA100 edge 250) | (Precuneus;Cuneus)<=>(Cerebellum) | (Default_mode;Central_executive)<=>(Subcortical-cerebellum) |
| 553) | rfMRI connectivity (ICA100 edge 251) | (Postcentral;Precentral)<=>(Cerebellum) | (Motor;Attention)<=>(Subcortical-cerebellum) |
| 554) | rfMRI connectivity (ICA100 edge 252) | (Superior_frontal)<=>(Cerebellum) | (Default_mode;Central_executive)<=>(Subcortical-cerebellum) |
| 555) | rfMRI connectivity (ICA100 edge 253) | (Superior_temporal)<=>(Cerebellum) | (Default_mode;Motor)<=>(Subcortical-cerebellum) |
| 556) | rfMRI connectivity (ICA100 edge 254) | (Calcarine;Lingual;Cuneus)<=>(Inferior_parietal;Angular) | (Visual)<=>(Central_executive;Attention) |
| 557) | rfMRI connectivity (ICA100 edge 255) | (Rolandic_operculum;SupraMarginal;Insula)<=>(Inferior_parietal;Angular) | (Salience;Motor)<=>(Central_executive;Attention) |
| 558) | rfMRI connectivity (ICA100 edge 256) | (Lingual;Fusiform)<=>(Inferior_parietal;Angular) | (Visual)<=>(Central_executive;Attention) |
| 559) | rfMRI connectivity (ICA100 edge 257) | (Middle_occipital;Superior_occipital)<=>(Inferior_parietal;Angular) | (Attention;Visual)<=>(Central_executive;Attention) |
| 560) | rfMRI connectivity (ICA100 edge 258) | (Precuneus;Angular;Middle_cingulate)<=>(Inferior_parietal;Angular) | (Default_mode;Central_executive)<=>(Central_executive;Attention) |
| 561) | rfMRI connectivity (ICA100 edge 259) | (Postcentral;Precentral)<=>(Inferior_parietal;Angular) | (Motor)<=>(Central_executive;Attention) |
| 562) | rfMRI connectivity (ICA100 edge 260) | (Superior_frontal;Anterior_cingulate)<=>(Inferior_parietal;Angular) | (Default_mode;Limbic)<=>(Central_executive;Attention) |
| 563) | rfMRI connectivity (ICA100 edge 261) | (Calcarine;Lingual)<=>(Inferior_parietal;Angular) | (Visual)<=>(Central_executive;Attention) |
| 564) | rfMRI connectivity (ICA100 edge 262) | (Middle_temporal;Temporal_pole)<=>(Inferior_parietal;Angular) | (Default_mode)<=>(Central_executive;Attention) |
| 565) | rfMRI connectivity (ICA100 edge 263) | (Middle_occipital;Precuneus;Calcarine)<=>(Inferior_parietal;Angular) | (Default_mode;Central_executive)<=>(Central_executive;Attention) |
| 566) | rfMRI connectivity (ICA100 edge 264) | (Angular;Middle_temporal)<=>(Inferior_parietal;Angular) | (Default_mode;Central_executive)<=>(Central_executive;Attention) |

| | | | |
|---|---|---|---|
| 567) | rfMRI connectivity (ICA100 edge 265) | (Middle_frontal;Cerebellum)<=>(Inferior_parietal;Angular) | (Central_executive;Default_mode)<=>(Central_executive;Attention) |
| 568) | rfMRI connectivity (ICA100 edge 266) | (Superior_frontal)<=>(Inferior_parietal;Angular) | (Default_mode)<=>(Central_executive;Attention) |
| 569) | rfMRI connectivity (ICA100 edge 267) | (Cuneus;Superior_occipital)<=>(Inferior_parietal;Angular) | (Visual)<=>(Central_executive;Attention) |
| 570) | rfMRI connectivity (ICA100 edge 268) | (Insula;Anterior_cingulate)<=>(Inferior_parietal;Angular) | (Salience;Default_mode)<=>(Central_executive;Attention) |
| 571) | rfMRI connectivity (ICA100 edge 269) | (Inferior_occipital;Middle_occipital)<=>(Inferior_parietal;Angular) | (Visual)<=>(Central_executive;Attention) |
| 572) | rfMRI connectivity (ICA100 edge 270) | (Cerebellum)<=>(Inferior_parietal;Angular) | (Subcortical-cerebellum)<=>(Central_executive;Attention) |
| 573) | rfMRI connectivity (ICA100 edge 271) | (Inferior_parietal;Postcentral)<=>(Inferior_parietal;Angular) | (Attention;Central_executive;Salience)<=>(Central_executive;Attention) |
| 574) | rfMRI connectivity (ICA100 edge 272) | (Precuneus;Cuneus)<=>(Inferior_parietal;Angular) | (Default_mode;Central_executive)<=>(Central_executive;Attention) |
| 575) | rfMRI connectivity (ICA100 edge 273) | (Postcentral;Precentral)<=>(Inferior_parietal;Angular) | (Motor;Attention)<=>(Central_executive;Attention) |
| 576) | rfMRI connectivity (ICA100 edge 274) | (Superior_frontal)<=>(Inferior_parietal;Angular) | (Default_mode;Central_executive)<=>(Central_executive;Attention) |
| 577) | rfMRI connectivity (ICA100 edge 275) | (Superior_temporal)<=>(Inferior_parietal;Angular) | (Default_mode;Motor)<=>(Central_executive;Attention) |
| 578) | rfMRI connectivity (ICA100 edge 276) | (Cerebellum)<=>(Inferior_parietal;Angular) | (Subcortical-cerebellum)<=>(Central_executive;Attention) |
| 579) | rfMRI connectivity (ICA100 edge 277) | (Calcarine;Lingual;Cuneus)<=>(Inferior_frontal;Precentral) | (Visual)<=>(Central_executive) |
| 580) | rfMRI connectivity (ICA100 edge 278) | (Rolandic_operculum;SupraMarginal;Insula)<=>(Inferior_frontal;Precentral) | (Salience;Motor)<=>(Central_executive) |
| 581) | rfMRI connectivity (ICA100 edge 279) | (Lingual;Fusiform)<=>(Inferior_frontal;Precentral) | (Visual)<=>(Central_executive) |
| 582) | rfMRI connectivity (ICA100 edge 280) | (Middle_occipital;Superior_occipital)<=>(Inferior_frontal;Precentral) | (Attention;Visual)<=>(Central_executive) |
| 583) | rfMRI connectivity (ICA100 edge 281) | (Precuneus;Angular;Middle_cingulate)<=>(Inferior_frontal;Precentral) | (Default_mode;Central_executive)<=>(Central_executive) |
| 584) | rfMRI connectivity (ICA100 edge 282) | (Postcentral;Precentral)<=>(Inferior_frontal;Precentral) | (Motor)<=>(Central_executive) |
| 585) | rfMRI connectivity (ICA100 edge 283) | (Superior_frontal;Anterior_cingulate)<=>(Inferior_frontal;Precentral) | (Default_mode;Limbic)<=>(Central_executive) |
| 586) | rfMRI connectivity (ICA100 edge 284) | (Calcarine;Lingual)<=>(Inferior_frontal;Precentral) | (Visual)<=>(Central_executive) |
| 587) | rfMRI connectivity (ICA100 edge 285) | (Middle_temporal;Temporal_pole)<=>(Inferior_frontal;Precentral) | (Default_mode)<=>(Central_executive) |
| 588) | rfMRI connectivity (ICA100 edge 286) | (Middle_occipital;Precuneus;Calcarine)<=>(Inferior_frontal;Precentral) | (Default_mode;Central_executive)<=>(Central_executive) |
| 589) | rfMRI connectivity (ICA100 edge 287) | (Angular;Middle_temporal)<=>(Inferior_frontal;Precentral) | (Default_mode;Central_executive)<=>(Central_executive) |
| 590) | rfMRI connectivity (ICA100 edge 288) | (Middle_frontal;Cerebellum)<=>(Inferior_frontal;Precentral) | (Central_executive;Default_mode)<=>(Central_executive) |
| 591) | rfMRI connectivity (ICA100 edge 289) | (Superior_frontal)<=>(Inferior_frontal;Precentral) | (Default_mode)<=>(Central_executive) |
| 592) | rfMRI connectivity (ICA100 edge 290) | (Cuneus;Superior_occipital)<=>(Inferior_frontal;Precentral) | (Visual)<=>(Central_executive) |

| | | | |
|---|---|---|---|
| 593) | rfMRI connectivity (ICA100 edge 291) | (Insula;Anterior_cingulate)<=>(Inferior_frontal;Precentral) | (Salience;Default_mode)<=>(Central_executive) |
| 594) | rfMRI connectivity (ICA100 edge 292) | (Inferior_occipital;Middle_occipital)<=>(Inferior_frontal;Precentral) | (Visual)<=>(Central_executive) |
| 595) | rfMRI connectivity (ICA100 edge 293) | (Cerebellum)<=>(Inferior_frontal;Precentral) | (Subcortical-cerebellum)<=>(Central_executive) |
| 596) | rfMRI connectivity (ICA100 edge 294) | (Inferior_parietal;Postcentral)<=>(Inferior_frontal;Precentral) | (Attention;Central_executive;Salience)<=>(Central_executive) |
| 597) | rfMRI connectivity (ICA100 edge 295) | (Precuneus;Cuneus)<=>(Inferior_frontal;Precentral) | (Default_mode;Central_executive)<=>(Central_executive) |
| 598) | rfMRI connectivity (ICA100 edge 296) | (Postcentral;Precentral)<=>(Inferior_frontal;Precentral) | (Motor;Attention)<=>(Central_executive) |
| 599) | rfMRI connectivity (ICA100 edge 297) | (Superior_frontal)<=>(Inferior_frontal;Precentral) | (Default_mode;Central_executive)<=>(Central_executive) |
| 600) | rfMRI connectivity (ICA100 edge 298) | (Superior_temporal)<=>(Inferior_frontal;Precentral) | (Default_mode;Motor)<=>(Central_executive) |
| 601) | rfMRI connectivity (ICA100 edge 299) | (Cerebellum)<=>(Inferior_frontal;Precentral) | (Subcortical-cerebellum)<=>(Central_executive) |
| 602) | rfMRI connectivity (ICA100 edge 300) | (Inferior_parietal;Angular)<=>(Inferior_frontal;Precentral) | (Central_executive;Attention)<=>(Central_executive) |
| 603) | rfMRI connectivity (ICA100 edge 301) | (Calcarine;Lingual;Cuneus)<=>(Inferior_parietal;Inferior_frontal;SupraMarginal) | (Visual)<=>(Attention;Central_executive) |
| 604) | rfMRI connectivity (ICA100 edge 302) | (Rolandic_operculum;SupraMarginal;Insula)<=>(Inferior_parietal;Inferior_frontal;SupraMarginal) | (Salience;Motor)<=>(Attention;Central_executive) |
| 605) | rfMRI connectivity (ICA100 edge 303) | (Lingual;Fusiform)<=>(Inferior_parietal;Inferior_frontal;SupraMarginal) | (Visual)<=>(Attention;Central_executive) |
| 606) | rfMRI connectivity (ICA100 edge 304) | (Middle_occipital;Superior_occipital)<=>(Inferior_parietal;Inferior_frontal;SupraMarginal) | (Attention;Visual)<=>(Attention;Central_executive) |
| 607) | rfMRI connectivity (ICA100 edge 305) | (Precuneus;Angular;Middle_cingulate)<=>(Inferior_parietal;Inferior_frontal;SupraMarginal) | (Default_mode;Central_executive)<=>(Attention;Central_executive) |
| 608) | rfMRI connectivity (ICA100 edge 306) | (Postcentral;Precentral)<=>(Inferior_parietal;Inferior_frontal;SupraMarginal) | (Motor)<=>(Attention;Central_executive) |
| 609) | rfMRI connectivity (ICA100 edge 307) | (Superior_frontal;Anterior_cingulate)<=>(Inferior_parietal;Inferior_frontal;SupraMarginal) | (Default_mode;Limbic)<=>(Attention;Central_executive) |
| 610) | rfMRI connectivity (ICA100 edge 308) | (Calcarine;Lingual)<=>(Inferior_parietal;Inferior_frontal;SupraMarginal) | (Visual)<=>(Attention;Central_executive) |
| 611) | rfMRI connectivity (ICA100 edge 309) | (Middle_temporal;Temporal_pole)<=>(Inferior_parietal;Inferior_frontal;SupraMarginal) | (Default_mode)<=>(Attention;Central_executive) |
| 612) | rfMRI connectivity (ICA100 edge 310) | (Middle_occipital;Precuneus;Calcarine)<=>(Inferior_parietal;Inferior_frontal;SupraMarginal) | (Default_mode;Central_executive)<=>(Attention;Central_executive) |
| 613) | rfMRI connectivity (ICA100 edge 311) | (Angular;Middle_temporal)<=>(Inferior_parietal;Inferior_frontal;SupraMarginal) | (Default_mode;Central_executive)<=>(Attention;Central_executive) |
| 614) | rfMRI connectivity (ICA100 edge 312) | (Middle_frontal;Cerebellum)<=>(Inferior_parietal;Inferior_frontal;SupraMarginal) | (Central_executive;Default_mode)<=>(Attention;Central_executive) |
| 615) | rfMRI connectivity (ICA100 edge 313) | (Superior_frontal)<=>(Inferior_parietal;Inferior_frontal;SupraMarginal) | (Default_mode)<=>(Attention;Central_executive) |
| 616) | rfMRI connectivity (ICA100 edge 314) | (Cuneus;Superior_occipital)<=>(Inferior_parietal;Inferior_frontal;SupraMarginal) | (Visual)<=>(Attention;Central_executive) |

| | | | |
|---|---|---|---|
| 617) | rfMRI connectivity (ICA100 edge 315) | (Insula;Anterior_cingulate)<=>(Inferior_parietal;Inferior_frontal;SupraMarginal) | (Salience;Default_mode)<=>(Attention;Central_executive) |
| 618) | rfMRI connectivity (ICA100 edge 316) | (Inferior_occipital;Middle_occipital)<=>(Inferior_parietal;Inferior_frontal;SupraMarginal) | (Visual)<=>(Attention;Central_executive) |
| 619) | rfMRI connectivity (ICA100 edge 317) | (Cerebellum)<=>(Inferior_parietal;Inferior_frontal;SupraMarginal) | (Subcortical-cerebellum)<=>(Attention;Central_executive) |
| 620) | rfMRI connectivity (ICA100 edge 318) | (Inferior_parietal;Postcentral)<=>(Inferior_parietal;Inferior_frontal;SupraMarginal) | (Attention;Central_executive;Salience)<=>(Attention;Central_executive) |
| 621) | rfMRI connectivity (ICA100 edge 319) | (Precuneus;Cuneus)<=>(Inferior_parietal;Inferior_frontal;SupraMarginal) | (Default_mode;Central_executive)<=>(Attention;Central_executive) |
| 622) | rfMRI connectivity (ICA100 edge 320) | (Postcentral;Precentral)<=>(Inferior_parietal;Inferior_frontal;SupraMarginal) | (Motor;Attention)<=>(Attention;Central_executive) |
| 623) | rfMRI connectivity (ICA100 edge 321) | (Superior_frontal)<=>(Inferior_parietal;Inferior_frontal;SupraMarginal) | (Default_mode;Central_executive)<=>(Attention;Central_executive) |
| 624) | rfMRI connectivity (ICA100 edge 322) | (Superior_temporal)<=>(Inferior_parietal;Inferior_frontal;SupraMarginal) | (Default_mode;Motor)<=>(Attention;Central_executive) |
| 625) | rfMRI connectivity (ICA100 edge 323) | (Cerebellum)<=>(Inferior_parietal;Inferior_frontal;SupraMarginal) | (Subcortical-cerebellum)<=>(Attention;Central_executive) |
| 626) | rfMRI connectivity (ICA100 edge 324) | (Inferior_parietal;Angular)<=>(Inferior_parietal;Inferior_frontal;SupraMarginal) | (Central_executive;Attention)<=>(Attention;Central_executive) |
| 627) | rfMRI connectivity (ICA100 edge 325) | (Inferior_frontal;Precentral)<=>(Inferior_parietal;Inferior_frontal;SupraMarginal) | (Central_executive)<=>(Attention;Central_executive) |
| 628) | rfMRI connectivity (ICA100 edge 326) | (Calcarine;Lingual;Cuneus)<=>(Precentral;Superior_frontal;Supp_motor_area) | (Visual)<=>(Attention;Salience;Motor) |
| 629) | rfMRI connectivity (ICA100 edge 327) | (Rolandic_operculum;SupraMarginal;Insula)<=>(Precentral;Superior_frontal;Supp_motor_area) | (Salience;Motor)<=>(Attention;Salience;Motor) |
| 630) | rfMRI connectivity (ICA100 edge 328) | (Lingual;Fusiform)<=>(Precentral;Superior_frontal;Supp_motor_area) | (Visual)<=>(Attention;Salience;Motor) |
| 631) | rfMRI connectivity (ICA100 edge 329) | (Middle_occipital;Superior_occipital)<=>(Precentral;Superior_frontal;Supp_motor_area) | (Attention;Visual)<=>(Attention;Salience;Motor) |
| 632) | rfMRI connectivity (ICA100 edge 330) | (Precuneus;Angular;Middle_cingulate)<=>(Precentral;Superior_frontal;Supp_motor_area) | (Default_mode;Central_executive)<=>(Attention;Salience;Motor) |
| 633) | rfMRI connectivity (ICA100 edge 331) | (Postcentral;Precentral)<=>(Precentral;Superior_frontal;Supp_motor_area) | (Motor)<=>(Attention;Salience;Motor) |
| 634) | rfMRI connectivity (ICA100 edge 332) | (Superior_frontal;Anterior_cingulate)<=>(Precentral;Superior_frontal;Supp_motor_area) | (Default_mode;Limbic)<=>(Attention;Salience;Motor) |
| 635) | rfMRI connectivity (ICA100 edge 333) | (Calcarine;Lingual)<=>(Precentral;Superior_frontal;Supp_motor_area) | (Visual)<=>(Attention;Salience;Motor) |
| 636) | rfMRI connectivity (ICA100 edge 334) | (Middle_temporal;Temporal_pole)<=>(Precentral;Superior_frontal;Supp_motor_area) | (Default_mode)<=>(Attention;Salience;Motor) |
| 637) | rfMRI connectivity (ICA100 edge 335) | (Middle_occipital;Precuneus;Calcarine)<=>(Precentral;Superior_frontal;Supp_motor_area) | (Default_mode;Central_executive)<=>(Attention;Salience;Motor) |
| 638) | rfMRI connectivity (ICA100 edge 336) | (Angular;Middle_temporal)<=>(Precentral;Superior_frontal;Supp_motor_area) | (Default_mode;Central_executive)<=>(Attention;Salience;Motor) |

| | | | |
|---|---|---|---|
| 639) | rfMRI connectivity (ICA100 edge 337) | (Middle_frontal;Cerebellum)<=>(Precentral;Superior_frontal;Supp_motor_area) | (Central_executive;Default_mode)<=>(Attention;Salience;Motor) |
| 640) | rfMRI connectivity (ICA100 edge 338) | (Superior_frontal)<=>(Precentral;Superior_frontal;Supp_motor_area) | (Default_mode)<=>(Attention;Salience;Motor) |
| 641) | rfMRI connectivity (ICA100 edge 339) | (Cuneus;Superior_occipital)<=>(Precentral;Superior_frontal;Supp_motor_area) | (Visual)<=>(Attention;Salience;Motor) |
| 642) | rfMRI connectivity (ICA100 edge 340) | (Insula;Anterior_cingulate)<=>(Precentral;Superior_frontal;Supp_motor_area) | (Salience;Default_mode)<=>(Attention;Salience;Motor) |
| 643) | rfMRI connectivity (ICA100 edge 341) | (Inferior_occipital;Middle_occipital)<=>(Precentral;Superior_frontal;Supp_motor_area) | (Visual)<=>(Attention;Salience;Motor) |
| 644) | rfMRI connectivity (ICA100 edge 342) | (Cerebellum)<=>(Precentral;Superior_frontal;Supp_motor_area) | (Subcortical-cerebellum)<=>(Attention;Salience;Motor) |
| 645) | rfMRI connectivity (ICA100 edge 343) | (Inferior_parietal;Postcentral)<=>(Precentral;Superior_frontal;Supp_motor_area) | (Attention;Central_executive;Salience)<=>(Attention;Salience;Motor) |
| 646) | rfMRI connectivity (ICA100 edge 344) | (Precuneus;Cuneus)<=>(Precentral;Superior_frontal;Supp_motor_area) | (Default_mode;Central_executive)<=>(Attention;Salience;Motor) |
| 647) | rfMRI connectivity (ICA100 edge 345) | (Postcentral;Precentral)<=>(Precentral;Superior_frontal;Supp_motor_area) | (Motor;Attention)<=>(Attention;Salience;Motor) |
| 648) | rfMRI connectivity (ICA100 edge 346) | (Superior_frontal)<=>(Precentral;Superior_frontal;Supp_motor_area) | (Default_mode;Central_executive)<=>(Attention;Salience;Motor) |
| 649) | rfMRI connectivity (ICA100 edge 347) | (Superior_temporal)<=>(Precentral;Superior_frontal;Supp_motor_area) | (Default_mode;Motor)<=>(Attention;Salience;Motor) |
| 650) | rfMRI connectivity (ICA100 edge 348) | (Cerebellum)<=>(Precentral;Superior_frontal;Supp_motor_area) | (Subcortical-cerebellum)<=>(Attention;Salience;Motor) |
| 651) | rfMRI connectivity (ICA100 edge 349) | (Inferior_parietal;Angular)<=>(Precentral;Superior_frontal;Supp_motor_area) | (Central_executive;Attention)<=>(Attention;Salience;Motor) |
| 652) | rfMRI connectivity (ICA100 edge 350) | (Inferior_frontal;Precentral)<=>(Precentral;Superior_frontal;Supp_motor_area) | (Central_executive)<=>(Attention;Salience;Motor) |
| 653) | rfMRI connectivity (ICA100 edge 351) | (Inferior_parietal;Inferior_frontal;SupraMarginal)<=>(Precentral;Superior_frontal;Supp_motor_area) | (Attention;Central_executive)<=>(Attention;Salience;Motor) |
| 654) | rfMRI connectivity (ICA100 edge 352) | (Calcarine;Lingual;Cuneus)<=>(Supp_motor_area;Inferior_frontal) | (Visual)<=>(Salience;Default_mode) |
| 655) | rfMRI connectivity (ICA100 edge 353) | (Rolandic_operculum;SupraMarginal;Insula)<=>(Supp_motor_area;Inferior_frontal) | (Salience;Motor)<=>(Salience;Default_mode) |
| 656) | rfMRI connectivity (ICA100 edge 354) | (Lingual;Fusiform)<=>(Supp_motor_area;Inferior_frontal) | (Visual)<=>(Salience;Default_mode) |
| 657) | rfMRI connectivity (ICA100 edge 355) | (Middle_occipital;Superior_occipital)<=>(Supp_motor_area;Inferior_frontal) | (Attention;Visual)<=>(Salience;Default_mode) |
| 658) | rfMRI connectivity (ICA100 edge 356) | (Precuneus;Angular;Middle_cingulate)<=>(Supp_motor_area;Inferior_frontal) | (Default_mode;Central_executive)<=>(Salience;Default_mode) |
| 659) | rfMRI connectivity (ICA100 edge 357) | (Postcentral;Precentral)<=>(Supp_motor_area;Inferior_frontal) | (Motor)<=>(Salience;Default_mode) |
| 660) | rfMRI connectivity (ICA100 edge 358) | (Superior_frontal;Anterior_cingulate)<=>(Supp_motor_area;Inferior_frontal) | (Default_mode;Limbic)<=>(Salience;Default_mode) |
| 661) | rfMRI connectivity (ICA100 edge 359) | (Calcarine;Lingual)<=>(Supp_motor_area;Inferior_frontal) | (Visual)<=>(Salience;Default_mode) |
| 662) | rfMRI connectivity (ICA100 edge 360) | (Middle_temporal;Temporal_pole)<=>(Supp_motor_area;Inferior_frontal) | (Default_mode)<=>(Salience;Default_mode) |

| | | | |
|---|---|---|---|
| 663) | rfMRI connectivity (ICA100 edge 361) | (Middle_occipital;Precuneus;Calcarine)<=>(Supp_motor_area;Inferior_frontal) | (Default_mode;Central_executive)<=>(Salience;Default_mode) |
| 664) | rfMRI connectivity (ICA100 edge 362) | (Angular;Middle_temporal)<=>(Supp_motor_area;Inferior_frontal) | (Default_mode;Central_executive)<=>(Salience;Default_mode) |
| 665) | rfMRI connectivity (ICA100 edge 363) | (Middle_frontal;Cerebellum)<=>(Supp_motor_area;Inferior_frontal) | (Central_executive;Default_mode)<=>(Salience;Default_mode) |
| 666) | rfMRI connectivity (ICA100 edge 364) | (Superior_frontal)<=>(Supp_motor_area;Inferior_frontal) | (Default_mode)<=>(Salience;Default_mode) |
| 667) | rfMRI connectivity (ICA100 edge 365) | (Cuneus;Superior_occipital)<=>(Supp_motor_area;Inferior_frontal) | (Visual)<=>(Salience;Default_mode) |
| 668) | rfMRI connectivity (ICA100 edge 366) | (Insula;Anterior_cingulate)<=>(Supp_motor_area;Inferior_frontal) | (Salience;Default_mode)<=>(Salience;Default_mode) |
| 669) | rfMRI connectivity (ICA100 edge 367) | (Inferior_occipital;Middle_occipital)<=>(Supp_motor_area;Inferior_frontal) | (Visual)<=>(Salience;Default_mode) |
| 670) | rfMRI connectivity (ICA100 edge 368) | (Cerebellum)<=>(Supp_motor_area;Inferior_frontal) | (Subcortical-cerebellum)<=>(Salience;Default_mode) |
| 671) | rfMRI connectivity (ICA100 edge 369) | (Inferior_parietal;Postcentral)<=>(Supp_motor_area;Inferior_frontal) | (Attention;Central_executive;Salience)<=>(Salience;Default_mode) |
| 672) | rfMRI connectivity (ICA100 edge 370) | (Precuneus;Cuneus)<=>(Supp_motor_area;Inferior_frontal) | (Default_mode;Central_executive)<=>(Salience;Default_mode) |
| 673) | rfMRI connectivity (ICA100 edge 371) | (Postcentral;Precentral)<=>(Supp_motor_area;Inferior_frontal) | (Motor;Attention)<=>(Salience;Default_mode) |
| 674) | rfMRI connectivity (ICA100 edge 372) | (Superior_frontal)<=>(Supp_motor_area;Inferior_frontal) | (Default_mode;Central_executive)<=>(Salience;Default_mode) |
| 675) | rfMRI connectivity (ICA100 edge 373) | (Superior_temporal)<=>(Supp_motor_area;Inferior_frontal) | (Default_mode;Motor)<=>(Salience;Default_mode) |
| 676) | rfMRI connectivity (ICA100 edge 374) | (Cerebellum)<=>(Supp_motor_area;Inferior_frontal) | (Subcortical-cerebellum)<=>(Salience;Default_mode) |
| 677) | rfMRI connectivity (ICA100 edge 375) | (Inferior_parietal;Angular)<=>(Supp_motor_area;Inferior_frontal) | (Central_executive;Attention)<=>(Salience;Default_mode) |
| 678) | rfMRI connectivity (ICA100 edge 376) | (Inferior_frontal;Precentral)<=>(Supp_motor_area;Inferior_frontal) | (Central_executive)<=>(Salience;Default_mode) |
| 679) | rfMRI connectivity (ICA100 edge 377) | (Inferior_parietal;Inferior_frontal;SupraMarginal)<=>(Supp_motor_area;Inferior_frontal) | (Attention;Central_executive)<=>(Salience;Default_mode) |
| 680) | rfMRI connectivity (ICA100 edge 378) | (Precentral;Superior_frontal;Supp_motor_area)<=>(Supp_motor_area;Inferior_frontal) | (Attention;Salience;Motor)<=>(Salience;Default_mode) |
| 681) | rfMRI connectivity (ICA100 edge 379) | (Calcarine;Lingual;Cuneus)<=>(SupraMarginal;Inferior_parietal) | (Visual)<=>(Central_executive;Salience) |
| 682) | rfMRI connectivity (ICA100 edge 380) | (Rolandic_operculum;SupraMarginal;Insula)<=>(SupraMarginal;Inferior_parietal) | (Salience;Motor)<=>(Central_executive;Salience) |
| 683) | rfMRI connectivity (ICA100 edge 381) | (Lingual;Fusiform)<=>(SupraMarginal;Inferior_parietal) | (Visual)<=>(Central_executive;Salience) |
| 684) | rfMRI connectivity (ICA100 edge 382) | (Middle_occipital;Superior_occipital)<=>(SupraMarginal;Inferior_parietal) | (Attention;Visual)<=>(Central_executive;Salience) |
| 685) | rfMRI connectivity (ICA100 edge 383) | (Precuneus;Angular;Middle_cingulate)<=>(SupraMarginal;Inferior_parietal) | (Default_mode;Central_executive)<=>(Central_executive;Salience) |

| | | | |
|---|---|---|---|
| 686) | rfMRI connectivity (ICA100 edge 384) | (Postcentral;Precentral)<=>(SupraMarginal;Inferior_parietal) | (Motor)<=>(Central_executive;Salience) |
| 687) | rfMRI connectivity (ICA100 edge 385) | (Superior_frontal;Anterior_cingulate)<=>(SupraMarginal;Inferior_parietal) | (Default_mode;Limbic)<=>(Central_executive;Salience) |
| 688) | rfMRI connectivity (ICA100 edge 386) | (Calcarine;Lingual)<=>(SupraMarginal;Inferior_parietal) | (Visual)<=>(Central_executive;Salience) |
| 689) | rfMRI connectivity (ICA100 edge 387) | (Middle_temporal;Temporal_pole)<=>(SupraMarginal;Inferior_parietal) | (Default_mode)<=>(Central_executive;Salience) |
| 690) | rfMRI connectivity (ICA100 edge 388) | (Middle_occipital;Precuneus;Calcarine)<=>(SupraMarginal;Inferior_parietal) | (Default_mode;Central_executive)<=>(Central_executive;Salience) |
| 691) | rfMRI connectivity (ICA100 edge 389) | (Angular;Middle_temporal)<=>(SupraMarginal;Inferior_parietal) | (Default_mode;Central_executive)<=>(Central_executive;Salience) |
| 692) | rfMRI connectivity (ICA100 edge 390) | (Middle_frontal;Cerebellum)<=>(SupraMarginal;Inferior_parietal) | (Central_executive;Default_mode)<=>(Central_executive;Salience) |
| 693) | rfMRI connectivity (ICA100 edge 391) | (Superior_frontal)<=>(SupraMarginal;Inferior_parietal) | (Default_mode)<=>(Central_executive;Salience) |
| 694) | rfMRI connectivity (ICA100 edge 392) | (Cuneus;Superior_occipital)<=>(SupraMarginal;Inferior_parietal) | (Visual)<=>(Central_executive;Salience) |
| 695) | rfMRI connectivity (ICA100 edge 393) | (Insula;Anterior_cingulate)<=>(SupraMarginal;Inferior_parietal) | (Salience;Default_mode)<=>(Central_executive;Salience) |
| 696) | rfMRI connectivity (ICA100 edge 394) | (Inferior_occipital;Middle_occipital)<=>(SupraMarginal;Inferior_parietal) | (Visual)<=>(Central_executive;Salience) |
| 697) | rfMRI connectivity (ICA100 edge 395) | (Cerebellum)<=>(SupraMarginal;Inferior_parietal) | (Subcortical-cerebellum)<=>(Central_executive;Salience) |
| 698) | rfMRI connectivity (ICA100 edge 396) | (Inferior_parietal;Postcentral)<=>(SupraMarginal;Inferior_parietal) | (Attention;Central_executive;Salience)<=>(Central_executive;Salience) |
| 699) | rfMRI connectivity (ICA100 edge 397) | (Precuneus;Cuneus)<=>(SupraMarginal;Inferior_parietal) | (Default_mode;Central_executive)<=>(Central_executive;Salience) |
| 700) | rfMRI connectivity (ICA100 edge 398) | (Postcentral;Precentral)<=>(SupraMarginal;Inferior_parietal) | (Motor;Attention)<=>(Central_executive;Salience) |
| 701) | rfMRI connectivity (ICA100 edge 399) | (Superior_frontal)<=>(SupraMarginal;Inferior_parietal) | (Default_mode;Central_executive)<=>(Central_executive;Salience) |
| 702) | rfMRI connectivity (ICA100 edge 400) | (Superior_temporal)<=>(SupraMarginal;Inferior_parietal) | (Default_mode;Motor)<=>(Central_executive;Salience) |
| 703) | rfMRI connectivity (ICA100 edge 401) | (Cerebellum)<=>(SupraMarginal;Inferior_parietal) | (Subcortical-cerebellum)<=>(Central_executive;Salience) |
| 704) | rfMRI connectivity (ICA100 edge 402) | (Inferior_parietal;Angular)<=>(SupraMarginal;Inferior_parietal) | (Central_executive;Attention)<=>(Central_executive;Salience) |
| 705) | rfMRI connectivity (ICA100 edge 403) | (Inferior_frontal;Precentral)<=>(SupraMarginal;Inferior_parietal) | (Central_executive)<=>(Central_executive;Salience) |
| 706) | rfMRI connectivity (ICA100 edge 404) | (Inferior_parietal;Inferior_frontal;SupraMarginal)<=>(SupraMarginal;Inferior_parietal) | (Attention;Central_executive)<=>(Central_executive;Salience) |
| 707) | rfMRI connectivity (ICA100 edge 405) | (Precentral;Superior_frontal;Supp_motor_area)<=>(SupraMarginal;Inferior_parietal) | (Attention;Salience;Motor)<=>(Central_executive;Salience) |
| 708) | rfMRI connectivity (ICA100 edge 406) | (Supp_motor_area;Inferior_frontal)<=>(SupraMarginal;Inferior_parietal) | (Salience;Default_mode)<=>(Central_executive;Salience) |
| 709) | rfMRI connectivity (ICA100 edge 407) | (Calcarine;Lingual;Cuneus)<=>(Paracentral) | (Visual)<=>(Motor) |

| | | | |
|---|---|---|---|
| 710) | rfMRI connectivity (ICA100 edge 408) | (Rolandic_operculum;SupraMarginal;Insula)<=>(Paracentral) | (Salience;Motor)<=>(Motor) |
| 711) | rfMRI connectivity (ICA100 edge 409) | (Lingual;Fusiform)<=>(Paracentral) | (Visual)<=>(Motor) |
| 712) | rfMRI connectivity (ICA100 edge 410) | (Middle_occipital;Superior_occipital)<=>(Paracentral) | (Attention;Visual)<=>(Motor) |
| 713) | rfMRI connectivity (ICA100 edge 411) | (Precuneus;Angular;Middle_cingulate)<=>(Paracentral) | (Default_mode;Central_executive)<=>(Motor) |
| 714) | rfMRI connectivity (ICA100 edge 412) | (Postcentral;Precentral)<=>(Paracentral) | (Motor)<=>(Motor) |
| 715) | rfMRI connectivity (ICA100 edge 413) | (Superior_frontal;Anterior_cingulate)<=>(Paracentral) | (Default_mode;Limbic)<=>(Motor) |
| 716) | rfMRI connectivity (ICA100 edge 414) | (Calcarine;Lingual)<=>(Paracentral) | (Visual)<=>(Motor) |
| 717) | rfMRI connectivity (ICA100 edge 415) | (Middle_temporal;Temporal_pole)<=>(Paracentral) | (Default_mode)<=>(Motor) |
| 718) | rfMRI connectivity (ICA100 edge 416) | (Middle_occipital;Precuneus;Calcarine)<=>(Paracentral) | (Default_mode;Central_executive)<=>(Motor) |
| 719) | rfMRI connectivity (ICA100 edge 417) | (Angular;Middle_temporal)<=>(Paracentral) | (Default_mode;Central_executive)<=>(Motor) |
| 720) | rfMRI connectivity (ICA100 edge 418) | (Middle_frontal;Cerebellum)<=>(Paracentral) | (Central_executive;Default_mode)<=>(Motor) |
| 721) | rfMRI connectivity (ICA100 edge 419) | (Superior_frontal)<=>(Paracentral) | (Default_mode)<=>(Motor) |
| 722) | rfMRI connectivity (ICA100 edge 420) | (Cuneus;Superior_occipital)<=>(Paracentral) | (Visual)<=>(Motor) |
| 723) | rfMRI connectivity (ICA100 edge 421) | (Insula;Anterior_cingulate)<=>(Paracentral) | (Salience;Default_mode)<=>(Motor) |
| 724) | rfMRI connectivity (ICA100 edge 422) | (Inferior_occipital;Middle_occipital)<=>(Paracentral) | (Visual)<=>(Motor) |
| 725) | rfMRI connectivity (ICA100 edge 423) | (Cerebellum)<=>(Paracentral) | (Subcortical-cerebellum)<=>(Motor) |
| 726) | rfMRI connectivity (ICA100 edge 424) | (Inferior_parietal;Postcentral)<=>(Paracentral) | (Attention;Central_executive;Salience)<=>(Motor) |
| 727) | rfMRI connectivity (ICA100 edge 425) | (Precuneus;Cuneus)<=>(Paracentral) | (Default_mode;Central_executive)<=>(Motor) |
| 728) | rfMRI connectivity (ICA100 edge 426) | (Postcentral;Precentral)<=>(Paracentral) | (Motor;Attention)<=>(Motor) |
| 729) | rfMRI connectivity (ICA100 edge 427) | (Superior_frontal)<=>(Paracentral) | (Default_mode;Central_executive)<=>(Motor) |
| 730) | rfMRI connectivity (ICA100 edge 428) | (Superior_temporal)<=>(Paracentral) | (Default_mode;Motor)<=>(Motor) |
| 731) | rfMRI connectivity (ICA100 edge 429) | (Cerebellum)<=>(Paracentral) | (Subcortical-cerebellum)<=>(Motor) |
| 732) | rfMRI connectivity (ICA100 edge 430) | (Inferior_parietal;Angular)<=>(Paracentral) | (Central_executive;Attention)<=>(Motor) |
| 733) | rfMRI connectivity (ICA100 edge 431) | (Inferior_frontal;Precentral)<=>(Paracentral) | (Central_executive)<=>(Motor) |
| 734) | rfMRI connectivity (ICA100 edge 432) | (Inferior_parietal;Inferior_frontal;SupraMarginal)<=>(Paracentral) | (Attention;Central_executive)<=>(Motor) |
| 735) | rfMRI connectivity (ICA100 edge 433) | (Precentral;Superior_frontal;Supp_motor_area)<=>(Paracentral) | (Attention;Salience;Motor)<=>(Motor) |
| 736) | rfMRI connectivity (ICA100 edge 434) | (Supp_motor_area;Inferior_frontal)<=>(Paracentral) | (Salience;Default_mode)<=>(Motor) |
| 737) | rfMRI connectivity (ICA100 edge 435) | (SupraMarginal;Inferior_parietal)<=>(Paracentral) | (Central_executive;Salience)<=>(Motor) |
| 738) | rfMRI connectivity (ICA100 edge 436) | (Calcarine;Lingual;Cuneus)<=>(Middel_frontal) | (Visual)<=>(Central_executive) |

| | | | |
|---|---|---|---|
| 739) | rfMRI connectivity (ICA100 edge 437) | (Rolandic_operculum;SupraMarginal;Insula)<=>(Middel_frontal) | (Salience;Motor)<=>(Central_executive) |
| 740) | rfMRI connectivity (ICA100 edge 438) | (Lingual;Fusiform)<=>(Middel_frontal) | (Visual)<=>(Central_executive) |
| 741) | rfMRI connectivity (ICA100 edge 439) | (Middle_occipital;Superior_occipital)<=>(Middel_frontal) | (Attention;Visual)<=>(Central_executive) |
| 742) | rfMRI connectivity (ICA100 edge 440) | (Precuneus;Angular;Middle_cingulate)<=>(Middel_frontal) | (Default_mode;Central_executive)<=>(Central_executive) |
| 743) | rfMRI connectivity (ICA100 edge 441) | (Postcentral;Precentral)<=>(Middel_frontal) | (Motor)<=>(Central_executive) |
| 744) | rfMRI connectivity (ICA100 edge 442) | (Superior_frontal;Anterior_cingulate)<=>(Middel_frontal) | (Default_mode;Limbic)<=>(Central_executive) |
| 745) | rfMRI connectivity (ICA100 edge 443) | (Calcarine;Lingual)<=>(Middel_frontal) | (Visual)<=>(Central_executive) |
| 746) | rfMRI connectivity (ICA100 edge 444) | (Middle_temporal;Temporal_pole)<=>(Middel_frontal) | (Default_mode)<=>(Central_executive) |
| 747) | rfMRI connectivity (ICA100 edge 445) | (Middle_occipital;Precuneus;Calcarine)<=>(Middel_frontal) | (Default_mode;Central_executive)<=>(Central_executive) |
| 748) | rfMRI connectivity (ICA100 edge 446) | (Angular;Middle_temporal)<=>(Middel_frontal) | (Default_mode;Central_executive)<=>(Central_executive) |
| 749) | rfMRI connectivity (ICA100 edge 447) | (Middle_frontal;Cerebellum)<=>(Middel_frontal) | (Central_executive;Default_mode)<=>(Central_executive) |
| 750) | rfMRI connectivity (ICA100 edge 448) | (Superior_frontal)<=>(Middel_frontal) | (Default_mode)<=>(Central_executive) |
| 751) | rfMRI connectivity (ICA100 edge 449) | (Cuneus;Superior_occipital)<=>(Middel_frontal) | (Visual)<=>(Central_executive) |
| 752) | rfMRI connectivity (ICA100 edge 450) | (Insula;Anterior_cingulate)<=>(Middel_frontal) | (Salience;Default_mode)<=>(Central_executive) |
| 753) | rfMRI connectivity (ICA100 edge 451) | (Inferior_occipital;Middle_occipital)<=>(Middel_frontal) | (Visual)<=>(Central_executive) |
| 754) | rfMRI connectivity (ICA100 edge 452) | (Cerebellum)<=>(Middel_frontal) | (Subcortical-cerebellum)<=>(Central_executive) |
| 755) | rfMRI connectivity (ICA100 edge 453) | (Inferior_parietal;Postcentral)<=>(Middel_frontal) | (Attention;Central_executive;Salience)<=>(Central_executive) |
| 756) | rfMRI connectivity (ICA100 edge 454) | (Precuneus;Cuneus)<=>(Middel_frontal) | (Default_mode;Central_executive)<=>(Central_executive) |
| 757) | rfMRI connectivity (ICA100 edge 455) | (Postcentral;Precentral)<=>(Middel_frontal) | (Motor;Attention)<=>(Central_executive) |
| 758) | rfMRI connectivity (ICA100 edge 456) | (Superior_frontal)<=>(Middel_frontal) | (Default_mode;Central_executive)<=>(Central_executive) |
| 759) | rfMRI connectivity (ICA100 edge 457) | (Superior_temporal)<=>(Middel_frontal) | (Default_mode;Motor)<=>(Central_executive) |
| 760) | rfMRI connectivity (ICA100 edge 458) | (Cerebellum)<=>(Middel_frontal) | (Subcortical-cerebellum)<=>(Central_executive) |
| 761) | rfMRI connectivity (ICA100 edge 459) | (Inferior_parietal;Angular)<=>(Middel_frontal) | (Central_executive;Attention)<=>(Central_executive) |
| 762) | rfMRI connectivity (ICA100 edge 460) | (Inferior_frontal;Precentral)<=>(Middel_frontal) | (Central_executive)<=>(Central_executive) |
| 763) | rfMRI connectivity (ICA100 edge 461) | (Inferior_parietal;Inferior_frontal;SupraMarginal)<=>(Middel_frontal) | (Attention;Central_executive)<=>(Central_executive) |
| 764) | rfMRI connectivity (ICA100 edge 462) | (Precentral;Superior_frontal;Supp_motor_area)<=>(Middel_frontal) | (Attention;Salience;Motor)<=>(Central_executive) |
| 765) | rfMRI connectivity (ICA100 edge 463) | (Supp_motor_area;Inferior_frontal)<=>(Middel_frontal) | (Salience;Default_mode)<=>(Central_executive) |
| 766) | rfMRI connectivity (ICA100 edge 464) | (SupraMarginal;Inferior_parietal)<=>(Middel_frontal) | (Central_executive;Salience)<=>(Central_executive) |

| | | | |
|---|---|---|---|
| 767) | rfMRI connectivity (ICA100 edge 465) | (Paracentral)<=>(Middel_frontal) | (Motor)<=>(Central_executive) |
| 768) | rfMRI connectivity (ICA100 edge 466) | (Calcarine;Lingual;Cuneus)<=>(Postcentral;Precentral) | (Visual)<=>(Motor;Attention) |
| 769) | rfMRI connectivity (ICA100 edge 467) | (Rolandic_operculum;SupraMarginal;Insula)<=>(Postcentral;Precentral) | (Salience;Motor)<=>(Motor;Attention) |
| 770) | rfMRI connectivity (ICA100 edge 468) | (Lingual;Fusiform)<=>(Postcentral;Precentral) | (Visual)<=>(Motor;Attention) |
| 771) | rfMRI connectivity (ICA100 edge 469) | (Middle_occipital;Superior_occipital)<=>(Postcentral;Precentral) | (Attention;Visual)<=>(Motor;Attention) |
| 772) | rfMRI connectivity (ICA100 edge 470) | (Precuneus;Angular;Middle_cingulate)<=>(Postcentral;Precentral) | (Default_mode;Central_executive)<=>(Motor;Attention) |
| 773) | rfMRI connectivity (ICA100 edge 471) | (Postcentral;Precentral)<=>(Postcentral;Precentral) | (Motor)<=>(Motor;Attention) |
| 774) | rfMRI connectivity (ICA100 edge 472) | (Superior_frontal;Anterior_cingulate)<=>(Postcentral;Precentral) | (Default_mode;Limbic)<=>(Motor;Attention) |
| 775) | rfMRI connectivity (ICA100 edge 473) | (Calcarine;Lingual)<=>(Postcentral;Precentral) | (Visual)<=>(Motor;Attention) |
| 776) | rfMRI connectivity (ICA100 edge 474) | (Middle_temporal;Temporal_pole)<=>(Postcentral;Precentral) | (Default_mode)<=>(Motor;Attention) |
| 777) | rfMRI connectivity (ICA100 edge 475) | (Middle_occipital;Precuneus;Calcarine)<=>(Postcentral;Precentral) | (Default_mode;Central_executive)<=>(Motor;Attention) |
| 778) | rfMRI connectivity (ICA100 edge 476) | (Angular;Middle_temporal)<=>(Postcentral;Precentral) | (Default_mode;Central_executive)<=>(Motor;Attention) |
| 779) | rfMRI connectivity (ICA100 edge 477) | (Middle_frontal;Cerebellum)<=>(Postcentral;Precentral) | (Central_executive;Default_mode)<=>(Motor;Attention) |
| 780) | rfMRI connectivity (ICA100 edge 478) | (Superior_frontal)<=>(Postcentral;Precentral) | (Default_mode)<=>(Motor;Attention) |
| 781) | rfMRI connectivity (ICA100 edge 479) | (Cuneus;Superior_occipital)<=>(Postcentral;Precentral) | (Visual)<=>(Motor;Attention) |
| 782) | rfMRI connectivity (ICA100 edge 480) | (Insula;Anterior_cingulate)<=>(Postcentral;Precentral) | (Salience;Default_mode)<=>(Motor;Attention) |
| 783) | rfMRI connectivity (ICA100 edge 481) | (Inferior_occipital;Middle_occipital)<=>(Postcentral;Precentral) | (Visual)<=>(Motor;Attention) |
| 784) | rfMRI connectivity (ICA100 edge 482) | (Cerebellum)<=>(Postcentral;Precentral) | (Subcortical-cerebellum)<=>(Motor;Attention) |
| 785) | rfMRI connectivity (ICA100 edge 483) | (Inferior_parietal;Postcentral)<=>(Postcentral;Precentral) | (Attention;Central_executive;Salience)<=>(Motor;Attention) |
| 786) | rfMRI connectivity (ICA100 edge 484) | (Precuneus;Cuneus)<=>(Postcentral;Precentral) | (Default_mode;Central_executive)<=>(Motor;Attention) |
| 787) | rfMRI connectivity (ICA100 edge 485) | (Postcentral;Precentral)<=>(Postcentral;Precentral) | (Motor;Attention)<=>(Motor;Attention) |
| 788) | rfMRI connectivity (ICA100 edge 486) | (Superior_frontal)<=>(Postcentral;Precentral) | (Default_mode;Central_executive)<=>(Motor;Attention) |
| 789) | rfMRI connectivity (ICA100 edge 487) | (Superior_temporal)<=>(Postcentral;Precentral) | (Default_mode;Motor)<=>(Motor;Attention) |
| 790) | rfMRI connectivity (ICA100 edge 488) | (Cerebellum)<=>(Postcentral;Precentral) | (Subcortical-cerebellum)<=>(Motor;Attention) |
| 791) | rfMRI connectivity (ICA100 edge 489) | (Inferior_parietal;Angular)<=>(Postcentral;Precentral) | (Central_executive;Attention)<=>(Motor;Attention) |
| 792) | rfMRI connectivity (ICA100 edge 490) | (Inferior_frontal;Precentral)<=>(Postcentral;Precentral) | (Central_executive)<=>(Motor;Attention) |
| 793) | rfMRI connectivity (ICA100 edge 491) | (Inferior_parietal;Inferior_frontal;SupraMarginal)<=>(Postcentral;Precentral) | (Attention;Central_executive)<=>(Motor;Attention) |
| 794) | rfMRI connectivity (ICA100 edge 492) | (Precentral;Superior_frontal;Supp_motor_area)<=>(Postcentral;Precentral) | (Attention;Salience;Motor)<=>(Motor;Attention) |

| | | | |
|---|---|---|---|
| 795) | rfMRI connectivity (ICA100 edge 493) | (Supp_motor_area;Inferior_frontal)<=>(Postcentral;Precentral) | (Salience;Default_mode)<=>(Motor;Attention) |
| 796) | rfMRI connectivity (ICA100 edge 494) | (SupraMarginal;Inferior_parietal)<=>(Postcentral;Precentral) | (Central_executive;Salience)<=>(Motor;Attention) |
| 797) | rfMRI connectivity (ICA100 edge 495) | (Paracentral)<=>(Postcentral;Precentral) | (Motor)<=>(Motor;Attention) |
| 798) | rfMRI connectivity (ICA100 edge 496) | (Middel_frontal)<=>(Postcentral;Precentral) | (Central_executive)<=>(Motor;Attention) |
| 799) | rfMRI connectivity (ICA100 edge 497) | (Calcarine;Lingual;Cuneus)<=>(Inferior_frontal;Middle_temporal;Supp_motor_area) | (Visual)<=>(Default_mode;Salience) |
| 800) | rfMRI connectivity (ICA100 edge 498) | (Rolandic_operculum;SupraMarginal;Insula)<=>(Inferior_frontal;Middle_temporal;Supp_motor_area) | (Salience;Motor)<=>(Default_mode;Salience) |
| 801) | rfMRI connectivity (ICA100 edge 499) | (Lingual;Fusiform)<=>(Inferior_frontal;Middle_temporal;Supp_motor_area) | (Visual)<=>(Default_mode;Salience) |
| 802) | rfMRI connectivity (ICA100 edge 500) | (Middle_occipital;Superior_occipital)<=>(Inferior_frontal;Middle_temporal;Supp_motor_area) | (Attention;Visual)<=>(Default_mode;Salience) |
| 803) | rfMRI connectivity (ICA100 edge 501) | (Precuneus;Angular;Middle_cingulate)<=>(Inferior_frontal;Middle_temporal;Supp_motor_area) | (Default_mode;Central_executive)<=>(Default_mode;Salience) |
| 804) | rfMRI connectivity (ICA100 edge 502) | (Postcentral;Precentral)<=>(Inferior_frontal;Middle_temporal;Supp_motor_area) | (Motor)<=>(Default_mode;Salience) |
| 805) | rfMRI connectivity (ICA100 edge 503) | (Superior_frontal;Anterior_cingulate)<=>(Inferior_frontal;Middle_temporal;Supp_motor_area) | (Default_mode;Limbic)<=>(Default_mode;Salience) |
| 806) | rfMRI connectivity (ICA100 edge 504) | (Calcarine;Lingual)<=>(Inferior_frontal;Middle_temporal;Supp_motor_area) | (Visual)<=>(Default_mode;Salience) |
| 807) | rfMRI connectivity (ICA100 edge 505) | (Middle_temporal;Temporal_pole)<=>(Inferior_frontal;Middle_temporal;Supp_motor_area) | (Default_mode)<=>(Default_mode;Salience) |
| 808) | rfMRI connectivity (ICA100 edge 506) | (Middle_occipital;Precuneus;Calcarine)<=>(Inferior_frontal;Middle_temporal;Supp_motor_area) | (Default_mode;Central_executive)<=>(Default_mode;Salience) |
| 809) | rfMRI connectivity (ICA100 edge 507) | (Angular;Middle_temporal)<=>(Inferior_frontal;Middle_temporal;Supp_motor_area) | (Default_mode;Central_executive)<=>(Default_mode;Salience) |
| 810) | rfMRI connectivity (ICA100 edge 508) | (Middle_frontal;Cerebellum)<=>(Inferior_frontal;Middle_temporal;Supp_motor_area) | (Central_executive;Default_mode)<=>(Default_mode;Salience) |
| 811) | rfMRI connectivity (ICA100 edge 509) | (Superior_frontal)<=>(Inferior_frontal;Middle_temporal;Supp_motor_area) | (Default_mode)<=>(Default_mode;Salience) |
| 812) | rfMRI connectivity (ICA100 edge 510) | (Cuneus;Superior_occipital)<=>(Inferior_frontal;Middle_temporal;Supp_motor_area) | (Visual)<=>(Default_mode;Salience) |
| 813) | rfMRI connectivity (ICA100 edge 511) | (Insula;Anterior_cingulate)<=>(Inferior_frontal;Middle_temporal;Supp_motor_area) | (Salience;Default_mode)<=>(Default_mode;Salience) |
| 814) | rfMRI connectivity (ICA100 edge 512) | (Inferior_occipital;Middle_occipital)<=>(Inferior_frontal;Middle_temporal;Supp_motor_area) | (Visual)<=>(Default_mode;Salience) |
| 815) | rfMRI connectivity (ICA100 edge 513) | (Cerebellum)<=>(Inferior_frontal;Middle_temporal;Supp_motor_area) | (Subcortical-cerebellum)<=>(Default_mode;Salience) |
| 816) | rfMRI connectivity (ICA100 edge 514) | (Inferior_parietal;Postcentral)<=>(Inferior_frontal;Middle_temporal;Supp_motor_area) | (Attention;Central_executive;Salience)<=>(Default_mode;Salience) |

| | | | |
|---|---|---|---|
| 817) | rfMRI connectivity (ICA100 edge 515) | (Precuneus;Cuneus)<=>(Inferior_frontal;Middle_temporal;Supp_motor_area) | (Default_mode;Central_executive)<=>(Default_mode;Salience) |
| 818) | rfMRI connectivity (ICA100 edge 516) | (Postcentral;Precentral)<=>(Inferior_frontal;Middle_temporal;Supp_motor_area) | (Motor;Attention)<=>(Default_mode;Salience) |
| 819) | rfMRI connectivity (ICA100 edge 517) | (Superior_frontal)<=>(Inferior_frontal;Middle_temporal;Supp_motor_area) | (Default_mode;Central_executive)<=>(Default_mode;Salience) |
| 820) | rfMRI connectivity (ICA100 edge 518) | (Superior_temporal)<=>(Inferior_frontal;Middle_temporal;Supp_motor_area) | (Default_mode;Motor)<=>(Default_mode;Salience) |
| 821) | rfMRI connectivity (ICA100 edge 519) | (Cerebellum)<=>(Inferior_frontal;Middle_temporal;Supp_motor_area) | (Subcortical-cerebellum)<=>(Default_mode;Salience) |
| 822) | rfMRI connectivity (ICA100 edge 520) | (Inferior_parietal;Angular)<=>(Inferior_frontal;Middle_temporal;Supp_motor_area) | (Central_executive;Attention)<=>(Default_mode;Salience) |
| 823) | rfMRI connectivity (ICA100 edge 521) | (Inferior_frontal;Precentral)<=>(Inferior_frontal;Middle_temporal;Supp_motor_area) | (Central_executive)<=>(Default_mode;Salience) |
| 824) | rfMRI connectivity (ICA100 edge 522) | (Inferior_parietal;Inferior_frontal;SupraMarginal)<=>(Inferior_frontal;Middle_temporal;Supp_motor_area) | (Attention;Central_executive)<=>(Default_mode;Salience) |
| 825) | rfMRI connectivity (ICA100 edge 523) | (Precentral;Superior_frontal;Supp_motor_area)<=>(Inferior_frontal;Middle_temporal;Supp_motor_area) | (Attention;Salience;Motor)<=>(Default_mode;Salience) |
| 826) | rfMRI connectivity (ICA100 edge 524) | (Supp_motor_area;Inferior_frontal)<=>(Inferior_frontal;Middle_temporal;Supp_motor_area) | (Salience;Default_mode)<=>(Default_mode;Salience) |
| 827) | rfMRI connectivity (ICA100 edge 525) | (SupraMarginal;Inferior_parietal)<=>(Inferior_frontal;Middle_temporal;Supp_motor_area) | (Central_executive;Salience)<=>(Default_mode;Salience) |
| 828) | rfMRI connectivity (ICA100 edge 526) | (Paracentral)<=>(Inferior_frontal;Middle_temporal;Supp_motor_area) | (Motor)<=>(Default_mode;Salience) |
| 829) | rfMRI connectivity (ICA100 edge 527) | (Middel_frontal)<=>(Inferior_frontal;Middle_temporal;Supp_motor_area) | (Central_executive)<=>(Default_mode;Salience) |
| 830) | rfMRI connectivity (ICA100 edge 528) | (Postcentral;Precentral)<=>(Inferior_frontal;Middle_temporal;Supp_motor_area) | (Motor;Attention)<=>(Default_mode;Salience) |
| 831) | rfMRI connectivity (ICA100 edge 529) | (Calcarine;Lingual;Cuneus)<=>(Superior_parietal;Postcentral;Precuneus) | (Visual)<=>(Attention) |
| 832) | rfMRI connectivity (ICA100 edge 530) | (Rolandic_operculum;SupraMarginal;Insula)<=>(Superior_parietal;Postcentral;Precuneus) | (Salience;Motor)<=>(Attention) |
| 833) | rfMRI connectivity (ICA100 edge 531) | (Lingual;Fusiform)<=>(Superior_parietal;Postcentral;Precuneus) | (Visual)<=>(Attention) |
| 834) | rfMRI connectivity (ICA100 edge 532) | (Middle_occipital;Superior_occipital)<=>(Superior_parietal;Postcentral;Precuneus) | (Attention;Visual)<=>(Attention) |
| 835) | rfMRI connectivity (ICA100 edge 533) | (Precuneus;Angular;Middle_cingulate)<=>(Superior_parietal;Postcentral;Precuneus) | (Default_mode;Central_executive)<=>(Attention) |
| 836) | rfMRI connectivity (ICA100 edge 534) | (Postcentral;Precentral)<=>(Superior_parietal;Postcentral;Precuneus) | (Motor)<=>(Attention) |
| 837) | rfMRI connectivity (ICA100 edge 535) | (Superior_frontal;Anterior_cingulate)<=>(Superior_parietal;Postcentral;Precuneus) | (Default_mode;Limbic)<=>(Attention) |
| 838) | rfMRI connectivity (ICA100 edge 536) | (Calcarine;Lingual)<=>(Superior_parietal;Postcentral;Precuneus) | (Visual)<=>(Attention) |
| 839) | rfMRI connectivity (ICA100 edge 537) | (Middle_temporal;Temporal_pole)<=>(Superior_parietal;Postcentral;Precuneus) | (Default_mode)<=>(Attention) |

| | | | |
|---|---|---|---|
| 840) | rfMRI connectivity (ICA100 edge 538) | (Middle_occipital;Precuneus;Calcarine)<=>(Superior_parietal;Postcentral;Precuneus) | (Default_mode;Central_executive)<=>(Attention) |
| 841) | rfMRI connectivity (ICA100 edge 539) | (Angular;Middle_temporal)<=>(Superior_parietal;Postcentral;Precuneus) | (Default_mode;Central_executive)<=>(Attention) |
| 842) | rfMRI connectivity (ICA100 edge 540) | (Middle_frontal;Cerebellum)<=>(Superior_parietal;Postcentral;Precuneus) | (Central_executive;Default_mode)<=>(Attention) |
| 843) | rfMRI connectivity (ICA100 edge 541) | (Superior_frontal)<=>(Superior_parietal;Postcentral;Precuneus) | (Default_mode)<=>(Attention) |
| 844) | rfMRI connectivity (ICA100 edge 542) | (Cuneus;Superior_occipital)<=>(Superior_parietal;Postcentral;Precuneus) | (Visual)<=>(Attention) |
| 845) | rfMRI connectivity (ICA100 edge 543) | (Insula;Anterior_cingulate)<=>(Superior_parietal;Postcentral;Precuneus) | (Salience;Default_mode)<=>(Attention) |
| 846) | rfMRI connectivity (ICA100 edge 544) | (Inferior_occipital;Middle_occipital)<=>(Superior_parietal;Postcentral;Precuneus) | (Visual)<=>(Attention) |
| 847) | rfMRI connectivity (ICA100 edge 545) | (Cerebellum)<=>(Superior_parietal;Postcentral;Precuneus) | (Subcortical-cerebellum)<=>(Attention) |
| 848) | rfMRI connectivity (ICA100 edge 546) | (Inferior_parietal;Postcentral)<=>(Superior_parietal;Postcentral;Precuneus) | (Attention;Central_executive;Salience)<=>(Attention) |
| 849) | rfMRI connectivity (ICA100 edge 547) | (Precuneus;Cuneus)<=>(Superior_parietal;Postcentral;Precuneus) | (Default_mode;Central_executive)<=>(Attention) |
| 850) | rfMRI connectivity (ICA100 edge 548) | (Postcentral;Precentral)<=>(Superior_parietal;Postcentral;Precuneus) | (Motor;Attention)<=>(Attention) |
| 851) | rfMRI connectivity (ICA100 edge 549) | (Superior_frontal)<=>(Superior_parietal;Postcentral;Precuneus) | (Default_mode;Central_executive)<=>(Attention) |
| 852) | rfMRI connectivity (ICA100 edge 550) | (Superior_temporal)<=>(Superior_parietal;Postcentral;Precuneus) | (Default_mode;Motor)<=>(Attention) |
| 853) | rfMRI connectivity (ICA100 edge 551) | (Cerebellum)<=>(Superior_parietal;Postcentral;Precuneus) | (Subcortical-cerebellum)<=>(Attention) |
| 854) | rfMRI connectivity (ICA100 edge 552) | (Inferior_parietal;Angular)<=>(Superior_parietal;Postcentral;Precuneus) | (Central_executive;Attention)<=>(Attention) |
| 855) | rfMRI connectivity (ICA100 edge 553) | (Inferior_frontal;Precentral)<=>(Superior_parietal;Postcentral;Precuneus) | (Central_executive)<=>(Attention) |
| 856) | rfMRI connectivity (ICA100 edge 554) | (Inferior_parietal;Inferior_frontal;SupraMarginal)<=>(Superior_parietal;Postcentral;Precuneus) | (Attention;Central_executive)<=>(Attention) |
| 857) | rfMRI connectivity (ICA100 edge 555) | (Precentral;Superior_frontal;Supp_motor_area)<=>(Superior_parietal;Postcentral;Precuneus) | (Attention;Salience;Motor)<=>(Attention) |
| 858) | rfMRI connectivity (ICA100 edge 556) | (Supp_motor_area;Inferior_frontal)<=>(Superior_parietal;Postcentral;Precuneus) | (Salience;Default_mode)<=>(Attention) |
| 859) | rfMRI connectivity (ICA100 edge 557) | (SupraMarginal;Inferior_parietal)<=>(Superior_parietal;Postcentral;Precuneus) | (Central_executive;Salience)<=>(Attention) |
| 860) | rfMRI connectivity (ICA100 edge 558) | (Paracentral)<=>(Superior_parietal;Postcentral;Precuneus) | (Motor)<=>(Attention) |
| 861) | rfMRI connectivity (ICA100 edge 559) | (Middel_frontal)<=>(Superior_parietal;Postcentral;Precuneus) | (Central_executive)<=>(Attention) |
| 862) | rfMRI connectivity (ICA100 edge 560) | (Postcentral;Precentral)<=>(Superior_parietal;Postcentral;Precuneus) | (Motor;Attention)<=>(Attention) |
| 863) | rfMRI connectivity (ICA100 edge 561) | (Inferior_frontal;Middle_temporal;Supp_motor_area)<=>(Superior_parietal;Postcentral;Precuneus) | (Default_mode;Salience)<=>(Attention) |
| 864) | rfMRI connectivity (ICA100 edge 562) | (Calcarine;Lingual;Cuneus)<=>(Precentral;Postcentral) | (Visual)<=>(Motor) |
| 865) | rfMRI connectivity (ICA100 edge 563) | (Rolandic_operculum;SupraMarginal;Insula)<=>(Precentral;Postcentral) | (Salience;Motor)<=>(Motor) |
| 866) | rfMRI connectivity (ICA100 edge 564) | (Lingual;Fusiform)<=>(Precentral;Postcentral) | (Visual)<=>(Motor) |

| | | | |
|---|---|---|---|
| 867) | rfMRI connectivity (ICA100 edge 565) | (Middle_occipital;Superior_occipital)<=>(Precentral;Postcentral) | (Attention;Visual)<=>(Motor) |
| 868) | rfMRI connectivity (ICA100 edge 566) | (Precuneus;Angular;Middle_cingulate)<=>(Precentral;Postcentral) | (Default_mode;Central_executive)<=>(Motor) |
| 869) | rfMRI connectivity (ICA100 edge 567) | (Postcentral;Precentral)<=>(Precentral;Postcentral) | (Motor)<=>(Motor) |
| 870) | rfMRI connectivity (ICA100 edge 568) | (Superior_frontal;Anterior_cingulate)<=>(Precentral;Postcentral) | (Default_mode;Limbic)<=>(Motor) |
| 871) | rfMRI connectivity (ICA100 edge 569) | (Calcarine;Lingual)<=>(Precentral;Postcentral) | (Visual)<=>(Motor) |
| 872) | rfMRI connectivity (ICA100 edge 570) | (Middle_temporal;Temporal_pole)<=>(Precentral;Postcentral) | (Default_mode)<=>(Motor) |
| 873) | rfMRI connectivity (ICA100 edge 571) | (Middle_occipital;Precuneus;Calcarine)<=>(Precentral;Postcentral) | (Default_mode;Central_executive)<=>(Motor) |
| 874) | rfMRI connectivity (ICA100 edge 572) | (Angular;Middle_temporal)<=>(Precentral;Postcentral) | (Default_mode;Central_executive)<=>(Motor) |
| 875) | rfMRI connectivity (ICA100 edge 573) | (Middle_frontal;Cerebellum)<=>(Precentral;Postcentral) | (Central_executive;Default_mode)<=>(Motor) |
| 876) | rfMRI connectivity (ICA100 edge 574) | (Superior_frontal)<=>(Precentral;Postcentral) | (Default_mode)<=>(Motor) |
| 877) | rfMRI connectivity (ICA100 edge 575) | (Cuneus;Superior_occipital)<=>(Precentral;Postcentral) | (Visual)<=>(Motor) |
| 878) | rfMRI connectivity (ICA100 edge 576) | (Insula;Anterior_cingulate)<=>(Precentral;Postcentral) | (Salience;Default_mode)<=>(Motor) |
| 879) | rfMRI connectivity (ICA100 edge 577) | (Inferior_occipital;Middle_occipital)<=>(Precentral;Postcentral) | (Visual)<=>(Motor) |
| 880) | rfMRI connectivity (ICA100 edge 578) | (Cerebellum)<=>(Precentral;Postcentral) | (Subcortical-cerebellum)<=>(Motor) |
| 881) | rfMRI connectivity (ICA100 edge 579) | (Inferior_parietal;Postcentral)<=>(Precentral;Postcentral) | (Attention;Central_executive;Salience)<=>(Motor) |
| 882) | rfMRI connectivity (ICA100 edge 580) | (Precuneus;Cuneus)<=>(Precentral;Postcentral) | (Default_mode;Central_executive)<=>(Motor) |
| 883) | rfMRI connectivity (ICA100 edge 581) | (Postcentral;Precentral)<=>(Precentral;Postcentral) | (Motor;Attention)<=>(Motor) |
| 884) | rfMRI connectivity (ICA100 edge 582) | (Superior_frontal)<=>(Precentral;Postcentral) | (Default_mode;Central_executive)<=>(Motor) |
| 885) | rfMRI connectivity (ICA100 edge 583) | (Superior_temporal)<=>(Precentral;Postcentral) | (Default_mode;Motor)<=>(Motor) |
| 886) | rfMRI connectivity (ICA100 edge 584) | (Cerebellum)<=>(Precentral;Postcentral) | (Subcortical-cerebellum)<=>(Motor) |
| 887) | rfMRI connectivity (ICA100 edge 585) | (Inferior_parietal;Angular)<=>(Precentral;Postcentral) | (Central_executive;Attention)<=>(Motor) |
| 888) | rfMRI connectivity (ICA100 edge 586) | (Inferior_frontal;Precentral)<=>(Precentral;Postcentral) | (Central_executive)<=>(Motor) |
| 889) | rfMRI connectivity (ICA100 edge 587) | (Inferior_parietal;Inferior_frontal;SupraMarginal)<=>(Precentral;Postcentral) | (Attention;Central_executive)<=>(Motor) |
| 890) | rfMRI connectivity (ICA100 edge 588) | (Precentral;Superior_frontal;Supp_motor_area)<=>(Precentral;Postcentral) | (Attention;Salience;Motor)<=>(Motor) |
| 891) | rfMRI connectivity (ICA100 edge 589) | (Supp_motor_area;Inferior_frontal)<=>(Precentral;Postcentral) | (Salience;Default_mode)<=>(Motor) |
| 892) | rfMRI connectivity (ICA100 edge 590) | (SupraMarginal;Inferior_parietal)<=>(Precentral;Postcentral) | (Central_executive;Salience)<=>(Motor) |
| 893) | rfMRI connectivity (ICA100 edge 591) | (Paracentral)<=>(Precentral;Postcentral) | (Motor)<=>(Motor) |
| 894) | rfMRI connectivity (ICA100 edge 592) | (Middel_frontal)<=>(Precentral;Postcentral) | (Central_executive)<=>(Motor) |
| 895) | rfMRI connectivity (ICA100 edge 593) | (Postcentral;Precentral)<=>(Precentral;Postcentral) | (Motor;Attention)<=>(Motor) |

| | | | |
|---|---|---|---|
| 896) | rfMRI connectivity (ICA100 edge 594) | (Inferior_frontal;Middle_temporal;Supp_motor_area)<=>(Precentral;Postcentral) | (Default_mode;Salience)<=>(Motor) |
| 897) | rfMRI connectivity (ICA100 edge 595) | (Superior_parietal;Postcentral;Precuneus)<=>(Precentral;Postcentral) | (Attention)<=>(Motor) |
| 898) | rfMRI connectivity (ICA100 edge 596) | (Calcarine;Lingual;Cuneus)<=>(Precuneus) | (Visual)<=>(Default_mode;Central_executive) |
| 899) | rfMRI connectivity (ICA100 edge 597) | (Rolandic_operculum;SupraMarginal;Insula)<=>(Precuneus) | (Salience;Motor)<=>(Default_mode;Central_executive) |
| 900) | rfMRI connectivity (ICA100 edge 598) | (Lingual;Fusiform)<=>(Precuneus) | (Visual)<=>(Default_mode;Central_executive) |
| 901) | rfMRI connectivity (ICA100 edge 599) | (Middle_occipital;Superior_occipital)<=>(Precuneus) | (Attention;Visual)<=>(Default_mode;Central_executive) |
| 902) | rfMRI connectivity (ICA100 edge 600) | (Precuneus;Angular;Middle_cingulate)<=>(Precuneus) | (Default_mode;Central_executive)<=>(Default_mode;Central_executive) |
| 903) | rfMRI connectivity (ICA100 edge 601) | (Postcentral;Precentral)<=>(Precuneus) | (Motor)<=>(Default_mode;Central_executive) |
| 904) | rfMRI connectivity (ICA100 edge 602) | (Superior_frontal;Anterior_cingulate)<=>(Precuneus) | (Default_mode;Limbic)<=>(Default_mode;Central_executive) |
| 905) | rfMRI connectivity (ICA100 edge 603) | (Calcarine;Lingual)<=>(Precuneus) | (Visual)<=>(Default_mode;Central_executive) |
| 906) | rfMRI connectivity (ICA100 edge 604) | (Middle_temporal;Temporal_pole)<=>(Precuneus) | (Default_mode)<=>(Default_mode;Central_executive) |
| 907) | rfMRI connectivity (ICA100 edge 605) | (Middle_occipital;Precuneus;Calcarine)<=>(Precuneus) | (Default_mode;Central_executive)<=>(Default_mode;Central_executive) |
| 908) | rfMRI connectivity (ICA100 edge 606) | (Angular;Middle_temporal)<=>(Precuneus) | (Default_mode;Central_executive)<=>(Default_mode;Central_executive) |
| 909) | rfMRI connectivity (ICA100 edge 607) | (Middle_frontal;Cerebellum)<=>(Precuneus) | (Central_executive;Default_mode)<=>(Default_mode;Central_executive) |
| 910) | rfMRI connectivity (ICA100 edge 608) | (Superior_frontal)<=>(Precuneus) | (Default_mode)<=>(Default_mode;Central_executive) |
| 911) | rfMRI connectivity (ICA100 edge 609) | (Cuneus;Superior_occipital)<=>(Precuneus) | (Visual)<=>(Default_mode;Central_executive) |
| 912) | rfMRI connectivity (ICA100 edge 610) | (Insula;Anterior_cingulate)<=>(Precuneus) | (Salience;Default_mode)<=>(Default_mode;Central_executive) |
| 913) | rfMRI connectivity (ICA100 edge 611) | (Inferior_occipital;Middle_occipital)<=>(Precuneus) | (Visual)<=>(Default_mode;Central_executive) |
| 914) | rfMRI connectivity (ICA100 edge 612) | (Cerebellum)<=>(Precuneus) | (Subcortical-cerebellum)<=>(Default_mode;Central_executive) |
| 915) | rfMRI connectivity (ICA100 edge 613) | (Inferior_parietal;Postcentral)<=>(Precuneus) | (Attention;Central_executive;Salience)<=>(Default_mode;Central_executive) |
| 916) | rfMRI connectivity (ICA100 edge 614) | (Precuneus;Cuneus)<=>(Precuneus) | (Default_mode;Central_executive)<=>(Default_mode;Central_executive) |
| 917) | rfMRI connectivity (ICA100 edge 615) | (Postcentral;Precentral)<=>(Precuneus) | (Motor;Attention)<=>(Default_mode;Central_executive) |
| 918) | rfMRI connectivity (ICA100 edge 616) | (Superior_frontal)<=>(Precuneus) | (Default_mode;Central_executive)<=>(Default_mode;Central_executive) |
| 919) | rfMRI connectivity (ICA100 edge 617) | (Superior_temporal)<=>(Precuneus) | (Default_mode;Motor)<=>(Default_mode;Central_executive) |

| | | | |
|---|---|---|---|
| 920) | rfMRI connectivity (ICA100 edge 618) | (Cerebellum)<=>(Precuneus) | (Subcortical-cerebellum)<=>(Default_mode;Central_executive) |
| 921) | rfMRI connectivity (ICA100 edge 619) | (Inferior_parietal;Angular)<=>(Precuneus) | (Central_executive;Attention)<=>(Default_mode;Central_executive) |
| 922) | rfMRI connectivity (ICA100 edge 620) | (Inferior_frontal;Precentral)<=>(Precuneus) | (Central_executive)<=>(Default_mode;Central_executive) |
| 923) | rfMRI connectivity (ICA100 edge 621) | (Inferior_parietal;Inferior_frontal;SupraMarginal)<=>(Precuneus) | (Attention;Central_executive)<=>(Default_mode;Central_executive) |
| 924) | rfMRI connectivity (ICA100 edge 622) | (Precentral;Superior_frontal;Supp_motor_area)<=>(Precuneus) | (Attention;Salience;Motor)<=>(Default_mode;Central_executive) |
| 925) | rfMRI connectivity (ICA100 edge 623) | (Supp_motor_area;Inferior_frontal)<=>(Precuneus) | (Salience;Default_mode)<=>(Default_mode;Central_executive) |
| 926) | rfMRI connectivity (ICA100 edge 624) | (SupraMarginal;Inferior_parietal)<=>(Precuneus) | (Central_executive;Salience)<=>(Default_mode;Central_executive) |
| 927) | rfMRI connectivity (ICA100 edge 625) | (Paracentral)<=>(Precuneus) | (Motor)<=>(Default_mode;Central_executive) |
| 928) | rfMRI connectivity (ICA100 edge 626) | (Middel_frontal)<=>(Precuneus) | (Central_executive)<=>(Default_mode;Central_executive) |
| 929) | rfMRI connectivity (ICA100 edge 627) | (Postcentral;Precentral)<=>(Precuneus) | (Motor;Attention)<=>(Default_mode;Central_executive) |
| 930) | rfMRI connectivity (ICA100 edge 628) | (Inferior_frontal;Middle_temporal;Supp_motor_area)<=>(Precuneus) | (Default_mode;Salience)<=>(Default_mode;Central_executive) |
| 931) | rfMRI connectivity (ICA100 edge 629) | (Superior_parietal;Postcentral;Precuneus)<=>(Precuneus) | (Attention)<=>(Default_mode;Central_executive) |
| 932) | rfMRI connectivity (ICA100 edge 630) | (Precentral;Postcentral)<=>(Precuneus) | (Motor)<=>(Default_mode;Central_executive) |
| 933) | rfMRI connectivity (ICA100 edge 631) | (Calcarine;Lingual;Cuneus)<=>(Middle_frontal) | (Visual)<=>(Central_executive;Salience) |
| 934) | rfMRI connectivity (ICA100 edge 632) | (Rolandic_operculum;SupraMarginal;Insula)<=>(Middle_frontal) | (Salience;Motor)<=>(Central_executive;Salience) |
| 935) | rfMRI connectivity (ICA100 edge 633) | (Lingual;Fusiform)<=>(Middle_frontal) | (Visual)<=>(Central_executive;Salience) |
| 936) | rfMRI connectivity (ICA100 edge 634) | (Middle_occipital;Superior_occipital)<=>(Middle_frontal) | (Attention;Visual)<=>(Central_executive;Salience) |
| 937) | rfMRI connectivity (ICA100 edge 635) | (Precuneus;Angular;Middle_cingulate)<=>(Middle_frontal) | (Default_mode;Central_executive)<=>(Central_executive;Salience) |
| 938) | rfMRI connectivity (ICA100 edge 636) | (Postcentral;Precentral)<=>(Middle_frontal) | (Motor)<=>(Central_executive;Salience) |
| 939) | rfMRI connectivity (ICA100 edge 637) | (Superior_frontal;Anterior_cingulate)<=>(Middle_frontal) | (Default_mode;Limbic)<=>(Central_executive;Salience) |
| 940) | rfMRI connectivity (ICA100 edge 638) | (Calcarine;Lingual)<=>(Middle_frontal) | (Visual)<=>(Central_executive;Salience) |
| 941) | rfMRI connectivity (ICA100 edge 639) | (Middle_temporal;Temporal_pole)<=>(Middle_frontal) | (Default_mode)<=>(Central_executive;Salience) |
| 942) | rfMRI connectivity (ICA100 edge 640) | (Middle_occipital;Precuneus;Calcarine)<=>(Middle_frontal) | (Default_mode;Central_executive)<=>(Central_executive;Salience) |
| 943) | rfMRI connectivity (ICA100 edge 641) | (Angular;Middle_temporal)<=>(Middle_frontal) | (Default_mode;Central_executive)<=>(Central_executive;Salience) |

| | | | |
|---|---|---|---|
| 944) | rfMRI connectivity (ICA100 edge 642) | (Middle_frontal;Cerebellum)<=>(Middle_frontal) | (Central_executive;Default_mode)<=>(Central_executive;Salience) |
| 945) | rfMRI connectivity (ICA100 edge 643) | (Superior_frontal)<=>(Middle_frontal) | (Default_mode)<=>(Central_executive;Salience) |
| 946) | rfMRI connectivity (ICA100 edge 644) | (Cuneus;Superior_occipital)<=>(Middle_frontal) | (Visual)<=>(Central_executive;Salience) |
| 947) | rfMRI connectivity (ICA100 edge 645) | (Insula;Anterior_cingulate)<=>(Middle_frontal) | (Salience;Default_mode)<=>(Central_executive;Salience) |
| 948) | rfMRI connectivity (ICA100 edge 646) | (Inferior_occipital;Middle_occipital)<=>(Middle_frontal) | (Visual)<=>(Central_executive;Salience) |
| 949) | rfMRI connectivity (ICA100 edge 647) | (Cerebellum)<=>(Middle_frontal) | (Subcortical-cerebellum)<=>(Central_executive;Salience) |
| 950) | rfMRI connectivity (ICA100 edge 648) | (Inferior_parietal;Postcentral)<=>(Middle_frontal) | (Attention;Central_executive;Salience)<=>(Central_executive;Salience) |
| 951) | rfMRI connectivity (ICA100 edge 649) | (Precuneus;Cuneus)<=>(Middle_frontal) | (Default_mode;Central_executive)<=>(Central_executive;Salience) |
| 952) | rfMRI connectivity (ICA100 edge 650) | (Postcentral;Precentral)<=>(Middle_frontal) | (Motor;Attention)<=>(Central_executive;Salience) |
| 953) | rfMRI connectivity (ICA100 edge 651) | (Superior_frontal)<=>(Middle_frontal) | (Default_mode;Central_executive)<=>(Central_executive;Salience) |
| 954) | rfMRI connectivity (ICA100 edge 652) | (Superior_temporal)<=>(Middle_frontal) | (Default_mode;Motor)<=>(Central_executive;Salience) |
| 955) | rfMRI connectivity (ICA100 edge 653) | (Cerebellum)<=>(Middle_frontal) | (Subcortical-cerebellum)<=>(Central_executive;Salience) |
| 956) | rfMRI connectivity (ICA100 edge 654) | (Inferior_parietal;Angular)<=>(Middle_frontal) | (Central_executive;Attention)<=>(Central_executive;Salience) |
| 957) | rfMRI connectivity (ICA100 edge 655) | (Inferior_frontal;Precentral)<=>(Middle_frontal) | (Central_executive)<=>(Central_executive;Salience) |
| 958) | rfMRI connectivity (ICA100 edge 656) | (Inferior_parietal;Inferior_frontal;SupraMarginal)<=>(Middle_frontal) | (Attention;Central_executive)<=>(Central_executive;Salience) |
| 959) | rfMRI connectivity (ICA100 edge 657) | (Precentral;Superior_frontal;Supp_motor_area)<=>(Middle_frontal) | (Attention;Salience;Motor)<=>(Central_executive;Salience) |
| 960) | rfMRI connectivity (ICA100 edge 658) | (Supp_motor_area;Inferior_frontal)<=>(Middle_frontal) | (Salience;Default_mode)<=>(Central_executive;Salience) |
| 961) | rfMRI connectivity (ICA100 edge 659) | (SupraMarginal;Inferior_parietal)<=>(Middle_frontal) | (Central_executive;Salience)<=>(Central_executive;Salience) |
| 962) | rfMRI connectivity (ICA100 edge 660) | (Paracentral)<=>(Middle_frontal) | (Motor)<=>(Central_executive;Salience) |
| 963) | rfMRI connectivity (ICA100 edge 661) | (Middel_frontal)<=>(Middle_frontal) | (Central_executive)<=>(Central_executive;Salience) |
| 964) | rfMRI connectivity (ICA100 edge 662) | (Postcentral;Precentral)<=>(Middle_frontal) | (Motor;Attention)<=>(Central_executive;Salience) |
| 965) | rfMRI connectivity (ICA100 edge 663) | (Inferior_frontal;Middle_temporal;Supp_motor_area)<=>(Middle_frontal) | (Default_mode;Salience)<=>(Central_executive;Salience) |
| 966) | rfMRI connectivity (ICA100 edge 664) | (Superior_parietal;Postcentral;Precuneus)<=>(Middle_frontal) | (Attention)<=>(Central_executive;Salience) |
| 967) | rfMRI connectivity (ICA100 edge 665) | (Precentral;Postcentral)<=>(Middle_frontal) | (Motor)<=>(Central_executive;Salience) |
| 968) | rfMRI connectivity (ICA100 edge 666) | (Precuneus)<=>(Middle_frontal) | (Default_mode;Central_executive)<=>(Central_executive;Salience) |
| 969) | rfMRI connectivity (ICA100 edge 667) | (Calcarine;Lingual;Cuneus)<=>(Putamen;Caudate) | (Visual)<=>(Subcortical-cerebellum) |

| | | | |
|---|---|---|---|
| 970) | rfMRI connectivity (ICA100 edge 668) | (Rolandic_operculum;SupraMarginal;Insula)<=>(Putamen;Caudate) | (Salience;Motor)<=>(Subcortical-cerebellum) |
| 971) | rfMRI connectivity (ICA100 edge 669) | (Lingual;Fusiform)<=>(Putamen;Caudate) | (Visual)<=>(Subcortical-cerebellum) |
| 972) | rfMRI connectivity (ICA100 edge 670) | (Middle_occipital;Superior_occipital)<=>(Putamen;Caudate) | (Attention;Visual)<=>(Subcortical-cerebellum) |
| 973) | rfMRI connectivity (ICA100 edge 671) | (Precuneus;Angular;Middle_cingulate)<=>(Putamen;Caudate) | (Default_mode;Central_executive)<=>(Subcortical-cerebellum) |
| 974) | rfMRI connectivity (ICA100 edge 672) | (Postcentral;Precentral)<=>(Putamen;Caudate) | (Motor)<=>(Subcortical-cerebellum) |
| 975) | rfMRI connectivity (ICA100 edge 673) | (Superior_frontal;Anterior_cingulate)<=>(Putamen;Caudate) | (Default_mode;Limbic)<=>(Subcortical-cerebellum) |
| 976) | rfMRI connectivity (ICA100 edge 674) | (Calcarine;Lingual)<=>(Putamen;Caudate) | (Visual)<=>(Subcortical-cerebellum) |
| 977) | rfMRI connectivity (ICA100 edge 675) | (Middle_temporal;Temporal_pole)<=>(Putamen;Caudate) | (Default_mode)<=>(Subcortical-cerebellum) |
| 978) | rfMRI connectivity (ICA100 edge 676) | (Middle_occipital;Precuneus;Calcarine)<=>(Putamen;Caudate) | (Default_mode;Central_executive)<=>(Subcortical-cerebellum) |
| 979) | rfMRI connectivity (ICA100 edge 677) | (Angular;Middle_temporal)<=>(Putamen;Caudate) | (Default_mode;Central_executive)<=>(Subcortical-cerebellum) |
| 980) | rfMRI connectivity (ICA100 edge 678) | (Middle_frontal;Cerebellum)<=>(Putamen;Caudate) | (Central_executive;Default_mode)<=>(Subcortical-cerebellum) |
| 981) | rfMRI connectivity (ICA100 edge 679) | (Superior_frontal)<=>(Putamen;Caudate) | (Default_mode)<=>(Subcortical-cerebellum) |
| 982) | rfMRI connectivity (ICA100 edge 680) | (Cuneus;Superior_occipital)<=>(Putamen;Caudate) | (Visual)<=>(Subcortical-cerebellum) |
| 983) | rfMRI connectivity (ICA100 edge 681) | (Insula;Anterior_cingulate)<=>(Putamen;Caudate) | (Salience;Default_mode)<=>(Subcortical-cerebellum) |
| 984) | rfMRI connectivity (ICA100 edge 682) | (Inferior_occipital;Middle_occipital)<=>(Putamen;Caudate) | (Visual)<=>(Subcortical-cerebellum) |
| 985) | rfMRI connectivity (ICA100 edge 683) | (Cerebellum)<=>(Putamen;Caudate) | (Subcortical-cerebellum)<=>(Subcortical-cerebellum) |
| 986) | rfMRI connectivity (ICA100 edge 684) | (Inferior_parietal;Postcentral)<=>(Putamen;Caudate) | (Attention;Central_executive;Salience)<=>(Subcortical-cerebellum) |
| 987) | rfMRI connectivity (ICA100 edge 685) | (Precuneus;Cuneus)<=>(Putamen;Caudate) | (Default_mode;Central_executive)<=>(Subcortical-cerebellum) |
| 988) | rfMRI connectivity (ICA100 edge 686) | (Postcentral;Precentral)<=>(Putamen;Caudate) | (Motor;Attention)<=>(Subcortical-cerebellum) |
| 989) | rfMRI connectivity (ICA100 edge 687) | (Superior_frontal)<=>(Putamen;Caudate) | (Default_mode;Central_executive)<=>(Subcortical-cerebellum) |
| 990) | rfMRI connectivity (ICA100 edge 688) | (Superior_temporal)<=>(Putamen;Caudate) | (Default_mode;Motor)<=>(Subcortical-cerebellum) |
| 991) | rfMRI connectivity (ICA100 edge 689) | (Cerebellum)<=>(Putamen;Caudate) | (Subcortical-cerebellum)<=>(Subcortical-cerebellum) |
| 992) | rfMRI connectivity (ICA100 edge 690) | (Inferior_parietal;Angular)<=>(Putamen;Caudate) | (Central_executive;Attention)<=>(Subcortical-cerebellum) |
| 993) | rfMRI connectivity (ICA100 edge 691) | (Inferior_frontal;Precentral)<=>(Putamen;Caudate) | (Central_executive)<=>(Subcortical-cerebellum) |
| 994) | rfMRI connectivity (ICA100 edge 692) | (Inferior_parietal;Inferior_frontal;SupraMarginal)<=>(Putamen;Caudate) | (Attention;Central_executive)<=>(Subcortical-cerebellum) |

| | | | |
|---|---|---|---|
| 995) | rfMRI connectivity (ICA100 edge 693) | (Precentral;Superior_frontal;Supp_motor_area)<=>(Putamen;Caudate) | (Attention;Salience;Motor)<=>(Subcortical-cerebellum) |
| 996) | rfMRI connectivity (ICA100 edge 694) | (Supp_motor_area;Inferior_frontal)<=>(Putamen;Caudate) | (Salience;Default_mode)<=>(Subcortical-cerebellum) |
| 997) | rfMRI connectivity (ICA100 edge 695) | (SupraMarginal;Inferior_parietal)<=>(Putamen;Caudate) | (Central_executive;Salience)<=>(Subcortical-cerebellum) |
| 998) | rfMRI connectivity (ICA100 edge 696) | (Paracentral)<=>(Putamen;Caudate) | (Motor)<=>(Subcortical-cerebellum) |
| 999) | rfMRI connectivity (ICA100 edge 697) | (Middel_frontal)<=>(Putamen;Caudate) | (Central_executive)<=>(Subcortical-cerebellum) |
| 1000) | rfMRI connectivity (ICA100 edge 698) | (Postcentral;Precentral)<=>(Putamen;Caudate) | (Motor;Attention)<=>(Subcortical-cerebellum) |
| 1001) | rfMRI connectivity (ICA100 edge 699) | (Inferior_frontal;Middle_temporal;Supp_motor_area)<=>(Putamen;Caudate) | (Default_mode;Salience)<=>(Subcortical-cerebellum) |
| 1002) | rfMRI connectivity (ICA100 edge 700) | (Superior_parietal;Postcentral;Precuneus)<=>(Putamen;Caudate) | (Attention)<=>(Subcortical-cerebellum) |
| 1003) | rfMRI connectivity (ICA100 edge 701) | (Precentral;Postcentral)<=>(Putamen;Caudate) | (Motor)<=>(Subcortical-cerebellum) |
| 1004) | rfMRI connectivity (ICA100 edge 702) | (Precuneus)<=>(Putamen;Caudate) | (Default_mode;Central_executive)<=>(Subcortical-cerebellum) |
| 1005) | rfMRI connectivity (ICA100 edge 703) | (Middle_frontal)<=>(Putamen;Caudate) | (Central_executive;Salience)<=>(Subcortical-cerebellum) |
| 1006) | rfMRI connectivity (ICA100 edge 704) | (Calcarine;Lingual;Cuneus)<=>(Precuneus;Superior_parietal) | (Visual)<=>(Attention;Central_executive) |
| 1007) | rfMRI connectivity (ICA100 edge 705) | (Rolandic_operculum;SupraMarginal;Insula)<=>(Precuneus;Superior_parietal) | (Salience;Motor)<=>(Attention;Central_executive) |
| 1008) | rfMRI connectivity (ICA100 edge 706) | (Lingual;Fusiform)<=>(Precuneus;Superior_parietal) | (Visual)<=>(Attention;Central_executive) |
| 1009) | rfMRI connectivity (ICA100 edge 707) | (Middle_occipital;Superior_occipital)<=>(Precuneus;Superior_parietal) | (Attention;Visual)<=>(Attention;Central_executive) |
| 1010) | rfMRI connectivity (ICA100 edge 708) | (Precuneus;Angular;Middle_cingulate)<=>(Precuneus;Superior_parietal) | (Default_mode;Central_executive)<=>(Attention;Central_executive) |
| 1011) | rfMRI connectivity (ICA100 edge 709) | (Postcentral;Precentral)<=>(Precuneus;Superior_parietal) | (Motor)<=>(Attention;Central_executive) |
| 1012) | rfMRI connectivity (ICA100 edge 710) | (Superior_frontal;Anterior_cingulate)<=>(Precuneus;Superior_parietal) | (Default_mode;Limbic)<=>(Attention;Central_executive) |
| 1013) | rfMRI connectivity (ICA100 edge 711) | (Calcarine;Lingual)<=>(Precuneus;Superior_parietal) | (Visual)<=>(Attention;Central_executive) |
| 1014) | rfMRI connectivity (ICA100 edge 712) | (Middle_temporal;Temporal_pole)<=>(Precuneus;Superior_parietal) | (Default_mode)<=>(Attention;Central_executive) |
| 1015) | rfMRI connectivity (ICA100 edge 713) | (Middle_occipital;Precuneus;Calcarine)<=>(Precuneus;Superior_parietal) | (Default_mode;Central_executive)<=>(Attention;Central_executive) |
| 1016) | rfMRI connectivity (ICA100 edge 714) | (Angular;Middle_temporal)<=>(Precuneus;Superior_parietal) | (Default_mode;Central_executive)<=>(Attention;Central_executive) |
| 1017) | rfMRI connectivity (ICA100 edge 715) | (Middle_frontal;Cerebellum)<=>(Precuneus;Superior_parietal) | (Central_executive;Default_mode)<=>(Attention;Central_executive) |
| 1018) | rfMRI connectivity (ICA100 edge 716) | (Superior_frontal)<=>(Precuneus;Superior_parietal) | (Default_mode)<=>(Attention;Central_executive) |
| 1019) | rfMRI connectivity (ICA100 edge 717) | (Cuneus;Superior_occipital)<=>(Precuneus;Superior_parietal) | (Visual)<=>(Attention;Central_executive) |
| 1020) | rfMRI connectivity (ICA100 edge 718) | (Insula;Anterior_cingulate)<=>(Precuneus;Superior_parietal) | (Salience;Default_mode)<=>(Attention;Central_executive) |
| 1021) | rfMRI connectivity (ICA100 edge 719) | (Inferior_occipital;Middle_occipital)<=>(Precuneus;Superior_parietal) | (Visual)<=>(Attention;Central_executive) |

| | | | |
|---|---|---|---|
| 1022) | rfMRI connectivity (ICA100 edge 720) | (Cerebellum)<=>(Precuneus;Superior_parietal) | (Subcortical-cerebellum)<=>(Attention;Central_executive) |
| 1023) | rfMRI connectivity (ICA100 edge 721) | (Inferior_parietal;Postcentral)<=>(Precuneus;Superior_parietal) | (Attention;Central_executive;Salience)<=>(Attention;Central_executive) |
| 1024) | rfMRI connectivity (ICA100 edge 722) | (Precuneus;Cuneus)<=>(Precuneus;Superior_parietal) | (Default_mode;Central_executive)<=>(Attention;Central_executive) |
| 1025) | rfMRI connectivity (ICA100 edge 723) | (Postcentral;Precentral)<=>(Precuneus;Superior_parietal) | (Motor;Attention)<=>(Attention;Central_executive) |
| 1026) | rfMRI connectivity (ICA100 edge 724) | (Superior_frontal)<=>(Precuneus;Superior_parietal) | (Default_mode;Central_executive)<=>(Attention;Central_executive) |
| 1027) | rfMRI connectivity (ICA100 edge 725) | (Superior_temporal)<=>(Precuneus;Superior_parietal) | (Default_mode;Motor)<=>(Attention;Central_executive) |
| 1028) | rfMRI connectivity (ICA100 edge 726) | (Cerebellum)<=>(Precuneus;Superior_parietal) | (Subcortical-cerebellum)<=>(Attention;Central_executive) |
| 1029) | rfMRI connectivity (ICA100 edge 727) | (Inferior_parietal;Angular)<=>(Precuneus;Superior_parietal) | (Central_executive;Attention)<=>(Attention;Central_executive) |
| 1030) | rfMRI connectivity (ICA100 edge 728) | (Inferior_frontal;Precentral)<=>(Precuneus;Superior_parietal) | (Central_executive)<=>(Attention;Central_executive) |
| 1031) | rfMRI connectivity (ICA100 edge 729) | (Inferior_parietal;Inferior_frontal;SupraMarginal)<=>(Precuneus;Superior_parietal) | (Attention;Central_executive)<=>(Attention;Central_executive) |
| 1032) | rfMRI connectivity (ICA100 edge 730) | (Precentral;Superior_frontal;Supp_motor_area)<=>(Precuneus;Superior_parietal) | (Attention;Salience;Motor)<=>(Attention;Central_executive) |
| 1033) | rfMRI connectivity (ICA100 edge 731) | (Supp_motor_area;Inferior_frontal)<=>(Precuneus;Superior_parietal) | (Salience;Default_mode)<=>(Attention;Central_executive) |
| 1034) | rfMRI connectivity (ICA100 edge 732) | (SupraMarginal;Inferior_parietal)<=>(Precuneus;Superior_parietal) | (Central_executive;Salience)<=>(Attention;Central_executive) |
| 1035) | rfMRI connectivity (ICA100 edge 733) | (Paracentral)<=>(Precuneus;Superior_parietal) | (Motor)<=>(Attention;Central_executive) |
| 1036) | rfMRI connectivity (ICA100 edge 734) | (Middel_frontal)<=>(Precuneus;Superior_parietal) | (Central_executive)<=>(Attention;Central_executive) |
| 1037) | rfMRI connectivity (ICA100 edge 735) | (Postcentral;Precentral)<=>(Precuneus;Superior_parietal) | (Motor;Attention)<=>(Attention;Central_executive) |
| 1038) | rfMRI connectivity (ICA100 edge 736) | (Inferior_frontal;Middle_temporal;Supp_motor_area)<=>(Precuneus;Superior_parietal) | (Default_mode;Salience)<=>(Attention;Central_executive) |
| 1039) | rfMRI connectivity (ICA100 edge 737) | (Superior_parietal;Postcentral;Precuneus)<=>(Precuneus;Superior_parietal) | (Attention)<=>(Attention;Central_executive) |
| 1040) | rfMRI connectivity (ICA100 edge 738) | (Precentral;Postcentral)<=>(Precuneus;Superior_parietal) | (Motor)<=>(Attention;Central_executive) |
| 1041) | rfMRI connectivity (ICA100 edge 739) | (Precuneus)<=>(Precuneus;Superior_parietal) | (Default_mode;Central_executive)<=>(Attention;Central_executive) |
| 1042) | rfMRI connectivity (ICA100 edge 740) | (Middle_frontal)<=>(Precuneus;Superior_parietal) | (Central_executive;Salience)<=>(Attention;Central_executive) |
| 1043) | rfMRI connectivity (ICA100 edge 741) | (Putamen;Caudate)<=>(Precuneus;Superior_parietal) | (Subcortical-cerebellum)<=>(Attention;Central_executive) |
| 1044) | rfMRI connectivity (ICA100 edge 742) | (Calcarine;Lingual;Cuneus)<=>(Superior_frontal;Middle_frontal) | (Visual)<=>(Central_executive) |
| 1045) | rfMRI connectivity (ICA100 edge 743) | (Rolandic_operculum;SupraMarginal;Insula)<=>(Superior_frontal;Middle_frontal) | (Salience;Motor)<=>(Central_executive) |

| | | | |
|---|---|---|---|
| 1046) | rfMRI connectivity (ICA100 edge 744) | (Lingual;Fusiform)<=>(Superior_frontal; Middle_frontal) | (Visual)<=>(Central_executive ) |
| 1047) | rfMRI connectivity (ICA100 edge 745) | (Middle_occipital;Superior_occipital)<= >(Superior_frontal;Middle_frontal) | (Attention;Visual)<=>(Central_ executive) |
| 1048) | rfMRI connectivity (ICA100 edge 746) | (Precuneus;Angular;Middle_cingulate)< =>(Superior_frontal;Middle_frontal) | (Default_mode;Central_executi ve)<=>(Central_executive) |
| 1049) | rfMRI connectivity (ICA100 edge 747) | (Postcentral;Precentral)<=>(Superior_fro ntal;Middle_frontal) | (Motor)<=>(Central_executive) |
| 1050) | rfMRI connectivity (ICA100 edge 748) | (Superior_frontal;Anterior_cingulate)<= >(Superior_frontal;Middle_frontal) | (Default_mode;Limbic)<=>(Ce ntral_executive) |
| 1051) | rfMRI connectivity (ICA100 edge 749) | (Calcarine;Lingual)<=>(Superior_frontal ;Middle_frontal) | (Visual)<=>(Central_executive ) |
| 1052) | rfMRI connectivity (ICA100 edge 750) | (Middle_temporal;Temporal_pole)<=>(S uperior_frontal;Middle_frontal) | (Default_mode)<=>(Central_ex ecutive) |
| 1053) | rfMRI connectivity (ICA100 edge 751) | (Middle_occipital;Precuneus;Calcarine)< =>(Superior_frontal;Middle_frontal) | (Default_mode;Central_executi ve)<=>(Central_executive) |
| 1054) | rfMRI connectivity (ICA100 edge 752) | (Angular;Middle_temporal)<=>(Superior _frontal;Middle_frontal) | (Default_mode;Central_executi ve)<=>(Central_executive) |
| 1055) | rfMRI connectivity (ICA100 edge 753) | (Middle_frontal;Cerebellum)<=>(Superi or_frontal;Middle_frontal) | (Central_executive;Default_mo de)<=>(Central_executive) |
| 1056) | rfMRI connectivity (ICA100 edge 754) | (Superior_frontal)<=>(Superior_frontal; Middle_frontal) | (Default_mode)<=>(Central_ex ecutive) |
| 1057) | rfMRI connectivity (ICA100 edge 755) | (Cuneus;Superior_occipital)<=>(Superio r_frontal;Middle_frontal) | (Visual)<=>(Central_executive ) |
| 1058) | rfMRI connectivity (ICA100 edge 756) | (Insula;Anterior_cingulate)<=>(Superior _frontal;Middle_frontal) | (Salience;Default_mode)<=>(C entral_executive) |
| 1059) | rfMRI connectivity (ICA100 edge 757) | (Inferior_occipital;Middle_occipital)<=> (Superior_frontal;Middle_frontal) | (Visual)<=>(Central_executive ) |
| 1060) | rfMRI connectivity (ICA100 edge 758) | (Cerebellum)<=>(Superior_frontal;Midd le_frontal) | (Subcortical-cerebellum)<=>(Central_execu tive) |
| 1061) | rfMRI connectivity (ICA100 edge 759) | (Inferior_parietal;Postcentral)<=>(Superi or_frontal;Middle_frontal) | (Attention;Central_executive;S alience)<=>(Central_executive) |
| 1062) | rfMRI connectivity (ICA100 edge 760) | (Precuneus;Cuneus)<=>(Superior_fronta l;Middle_frontal) | (Default_mode;Central_executi ve)<=>(Central_executive) |
| 1063) | rfMRI connectivity (ICA100 edge 761) | (Postcentral;Precentral)<=>(Superior_fro ntal;Middle_frontal) | (Motor;Attention)<=>(Central_ executive) |
| 1064) | rfMRI connectivity (ICA100 edge 762) | (Superior_frontal)<=>(Superior_frontal; Middle_frontal) | (Default_mode;Central_executi ve)<=>(Central_executive) |
| 1065) | rfMRI connectivity (ICA100 edge 763) | (Superior_temporal)<=>(Superior_fronta l;Middle_frontal) | (Default_mode;Motor)<=>(Cen tral_executive) |
| 1066) | rfMRI connectivity (ICA100 edge 764) | (Cerebellum)<=>(Superior_frontal;Midd le_frontal) | (Subcortical-cerebellum)<=>(Central_execu tive) |
| 1067) | rfMRI connectivity (ICA100 edge 765) | (Inferior_parietal;Angular)<=>(Superior _frontal;Middle_frontal) | (Central_executive;Attention)< =>(Central_executive) |
| 1068) | rfMRI connectivity (ICA100 edge 766) | (Inferior_frontal;Precentral)<=>(Superio r_frontal;Middle_frontal) | (Central_executive)<=>(Centra l_executive) |
| 1069) | rfMRI connectivity (ICA100 edge 767) | (Inferior_parietal;Inferior_frontal;Supra Marginal)<=>(Superior_frontal;Middle_f rontal) | (Attention;Central_executive)< =>(Central_executive) |
| 1070) | rfMRI connectivity (ICA100 edge 768) | (Precentral;Superior_frontal;Supp_motor _area)<=>(Superior_frontal;Middle_fron tal) | (Attention;Salience;Motor)<=> (Central_executive) |
| 1071) | rfMRI connectivity (ICA100 edge 769) | (Supp_motor_area;Inferior_frontal)<=>( Superior_frontal;Middle_frontal) | (Salience;Default_mode)<=>(C entral_executive) |
| 1072) | rfMRI connectivity (ICA100 edge 770) | (SupraMarginal;Inferior_parietal)<=>(Su perior_frontal;Middle_frontal) | (Central_executive;Salience)<= >(Central_executive) |

| | | | |
|---|---|---|---|
| 1073) | rfMRI connectivity (ICA100 edge 771) | (Paracentral)<=>(Superior_frontal;Middle_frontal) | (Motor)<=>(Central_executive) |
| 1074) | rfMRI connectivity (ICA100 edge 772) | (Middel_frontal)<=>(Superior_frontal;Middle_frontal) | (Central_executive)<=>(Central_executive) |
| 1075) | rfMRI connectivity (ICA100 edge 773) | (Postcentral;Precentral)<=>(Superior_frontal;Middle_frontal) | (Motor;Attention)<=>(Central_executive) |
| 1076) | rfMRI connectivity (ICA100 edge 774) | (Inferior_frontal;Middle_temporal;Supp_motor_area)<=>(Superior_frontal;Middle_frontal) | (Default_mode;Salience)<=>(Central_executive) |
| 1077) | rfMRI connectivity (ICA100 edge 775) | (Superior_parietal;Postcentral;Precuneus)<=>(Superior_frontal;Middle_frontal) | (Attention)<=>(Central_executive) |
| 1078) | rfMRI connectivity (ICA100 edge 776) | (Precentral;Postcentral)<=>(Superior_frontal;Middle_frontal) | (Motor)<=>(Central_executive) |
| 1079) | rfMRI connectivity (ICA100 edge 777) | (Precuneus)<=>(Superior_frontal;Middle_frontal) | (Default_mode;Central_executive)<=>(Central_executive) |
| 1080) | rfMRI connectivity (ICA100 edge 778) | (Middle_frontal)<=>(Superior_frontal;Middle_frontal) | (Central_executive;Salience)<=>(Central_executive) |
| 1081) | rfMRI connectivity (ICA100 edge 779) | (Putamen;Caudate)<=>(Superior_frontal;Middle_frontal) | (Subcortical-cerebellum)<=>(Central_executive) |
| 1082) | rfMRI connectivity (ICA100 edge 780) | (Precuneus;Superior_parietal)<=>(Superior_frontal;Middle_frontal) | (Attention;Central_executive)<=>(Central_executive) |
| 1083) | rfMRI connectivity (ICA100 edge 781) | (Calcarine;Lingual;Cuneus)<=>(Inferior_temporal;Middle_temporal) | (Visual)<=>(Attention;Visual) |
| 1084) | rfMRI connectivity (ICA100 edge 782) | (Rolandic_operculum;SupraMarginal;Insula)<=>(Inferior_temporal;Middle_temporal) | (Salience;Motor)<=>(Attention;Visual) |
| 1085) | rfMRI connectivity (ICA100 edge 783) | (Lingual;Fusiform)<=>(Inferior_temporal;Middle_temporal) | (Visual)<=>(Attention;Visual) |
| 1086) | rfMRI connectivity (ICA100 edge 784) | (Middle_occipital;Superior_occipital)<=>(Inferior_temporal;Middle_temporal) | (Attention;Visual)<=>(Attention;Visual) |
| 1087) | rfMRI connectivity (ICA100 edge 785) | (Precuneus;Angular;Middle_cingulate)<=>(Inferior_temporal;Middle_temporal) | (Default_mode;Central_executive)<=>(Attention;Visual) |
| 1088) | rfMRI connectivity (ICA100 edge 786) | (Postcentral;Precentral)<=>(Inferior_temporal;Middle_temporal) | (Motor)<=>(Attention;Visual) |
| 1089) | rfMRI connectivity (ICA100 edge 787) | (Superior_frontal;Anterior_cingulate)<=>(Inferior_temporal;Middle_temporal) | (Default_mode;Limbic)<=>(Attention;Visual) |
| 1090) | rfMRI connectivity (ICA100 edge 788) | (Calcarine;Lingual)<=>(Inferior_temporal;Middle_temporal) | (Visual)<=>(Attention;Visual) |
| 1091) | rfMRI connectivity (ICA100 edge 789) | (Middle_temporal;Temporal_pole)<=>(Inferior_temporal;Middle_temporal) | (Default_mode)<=>(Attention;Visual) |
| 1092) | rfMRI connectivity (ICA100 edge 790) | (Middle_occipital;Precuneus;Calcarine)<=>(Inferior_temporal;Middle_temporal) | (Default_mode;Central_executive)<=>(Attention;Visual) |
| 1093) | rfMRI connectivity (ICA100 edge 791) | (Angular;Middle_temporal)<=>(Inferior_temporal;Middle_temporal) | (Default_mode;Central_executive)<=>(Attention;Visual) |
| 1094) | rfMRI connectivity (ICA100 edge 792) | (Middle_frontal;Cerebellum)<=>(Inferior_temporal;Middle_temporal) | (Central_executive;Default_mode)<=>(Attention;Visual) |
| 1095) | rfMRI connectivity (ICA100 edge 793) | (Superior_frontal)<=>(Inferior_temporal;Middle_temporal) | (Default_mode)<=>(Attention;Visual) |
| 1096) | rfMRI connectivity (ICA100 edge 794) | (Cuneus;Superior_occipital)<=>(Inferior_temporal;Middle_temporal) | (Visual)<=>(Attention;Visual) |
| 1097) | rfMRI connectivity (ICA100 edge 795) | (Insula;Anterior_cingulate)<=>(Inferior_temporal;Middle_temporal) | (Salience;Default_mode)<=>(Attention;Visual) |
| 1098) | rfMRI connectivity (ICA100 edge 796) | (Inferior_occipital;Middle_occipital)<=>(Inferior_temporal;Middle_temporal) | (Visual)<=>(Attention;Visual) |
| 1099) | rfMRI connectivity (ICA100 edge 797) | (Cerebellum)<=>(Inferior_temporal;Middle_temporal) | (Subcortical-cerebellum)<=>(Attention;Visual) |

| | | | |
|---|---|---|---|
| 1100) | rfMRI connectivity (ICA100 edge 798) | (Inferior_parietal;Postcentral)<=>(Inferior_temporal;Middle_temporal) | (Attention;Central_executive;Salience)<=>(Attention;Visual) |
| 1101) | rfMRI connectivity (ICA100 edge 799) | (Precuneus;Cuneus)<=>(Inferior_temporal;Middle_temporal) | (Default_mode;Central_executive)<=>(Attention;Visual) |
| 1102) | rfMRI connectivity (ICA100 edge 800) | (Postcentral;Precentral)<=>(Inferior_temporal;Middle_temporal) | (Motor;Attention)<=>(Attention;Visual) |
| 1103) | rfMRI connectivity (ICA100 edge 801) | (Superior_frontal)<=>(Inferior_temporal;Middle_temporal) | (Default_mode;Central_executive)<=>(Attention;Visual) |
| 1104) | rfMRI connectivity (ICA100 edge 802) | (Superior_temporal)<=>(Inferior_temporal;Middle_temporal) | (Default_mode;Motor)<=>(Attention;Visual) |
| 1105) | rfMRI connectivity (ICA100 edge 803) | (Cerebellum)<=>(Inferior_temporal;Middle_temporal) | (Subcortical-cerebellum)<=>(Attention;Visual) |
| 1106) | rfMRI connectivity (ICA100 edge 804) | (Inferior_parietal;Angular)<=>(Inferior_temporal;Middle_temporal) | (Central_executive;Attention)<=>(Attention;Visual) |
| 1107) | rfMRI connectivity (ICA100 edge 805) | (Inferior_frontal;Precentral)<=>(Inferior_temporal;Middle_temporal) | (Central_executive)<=>(Attention;Visual) |
| 1108) | rfMRI connectivity (ICA100 edge 806) | (Inferior_parietal;Inferior_frontal;SupraMarginal)<=>(Inferior_temporal;Middle_temporal) | (Attention;Central_executive)<=>(Attention;Visual) |
| 1109) | rfMRI connectivity (ICA100 edge 807) | (Precentral;Superior_frontal;Supp_motor_area)<=>(Inferior_temporal;Middle_temporal) | (Attention;Salience;Motor)<=>(Attention;Visual) |
| 1110) | rfMRI connectivity (ICA100 edge 808) | (Supp_motor_area;Inferior_frontal)<=>(Inferior_temporal;Middle_temporal) | (Salience;Default_mode)<=>(Attention;Visual) |
| 1111) | rfMRI connectivity (ICA100 edge 809) | (SupraMarginal;Inferior_parietal)<=>(Inferior_temporal;Middle_temporal) | (Central_executive;Salience)<=>(Attention;Visual) |
| 1112) | rfMRI connectivity (ICA100 edge 810) | (Paracentral)<=>(Inferior_temporal;Middle_temporal) | (Motor)<=>(Attention;Visual) |
| 1113) | rfMRI connectivity (ICA100 edge 811) | (Middel_frontal)<=>(Inferior_temporal;Middle_temporal) | (Central_executive)<=>(Attention;Visual) |
| 1114) | rfMRI connectivity (ICA100 edge 812) | (Postcentral;Precentral)<=>(Inferior_temporal;Middle_temporal) | (Motor;Attention)<=>(Attention;Visual) |
| 1115) | rfMRI connectivity (ICA100 edge 813) | (Inferior_frontal;Middle_temporal;Supp_motor_area)<=>(Inferior_temporal;Middle_temporal) | (Default_mode;Salience)<=>(Attention;Visual) |
| 1116) | rfMRI connectivity (ICA100 edge 814) | (Superior_parietal;Postcentral;Precuneus)<=>(Inferior_temporal;Middle_temporal) | (Attention)<=>(Attention;Visual) |
| 1117) | rfMRI connectivity (ICA100 edge 815) | (Precentral;Postcentral)<=>(Inferior_temporal;Middle_temporal) | (Motor)<=>(Attention;Visual) |
| 1118) | rfMRI connectivity (ICA100 edge 816) | (Precuneus)<=>(Inferior_temporal;Middle_temporal) | (Default_mode;Central_executive)<=>(Attention;Visual) |
| 1119) | rfMRI connectivity (ICA100 edge 817) | (Middle_frontal)<=>(Inferior_temporal;Middle_temporal) | (Central_executive;Salience)<=>(Attention;Visual) |
| 1120) | rfMRI connectivity (ICA100 edge 818) | (Putamen;Caudate)<=>(Inferior_temporal;Middle_temporal) | (Subcortical-cerebellum)<=>(Attention;Visual) |
| 1121) | rfMRI connectivity (ICA100 edge 819) | (Precuneus;Superior_parietal)<=>(Inferior_temporal;Middle_temporal) | (Attention;Central_executive)<=>(Attention;Visual) |
| 1122) | rfMRI connectivity (ICA100 edge 820) | (Superior_frontal;Middle_frontal)<=>(Inferior_temporal;Middle_temporal) | (Central_executive)<=>(Attention;Visual) |
| 1123) | rfMRI connectivity (ICA100 edge 821) | (Calcarine;Lingual;Cuneus)<=>(Inferior_temporal;Inferior_occipital) | (Visual)<=>(Attention;Visual) |
| 1124) | rfMRI connectivity (ICA100 edge 822) | (Rolandic_operculum;SupraMarginal;Insula)<=>(Inferior_temporal;Inferior_occipital) | (Salience;Motor)<=>(Attention;Visual) |
| 1125) | rfMRI connectivity (ICA100 edge 823) | (Lingual;Fusiform)<=>(Inferior_temporal;Inferior_occipital) | (Visual)<=>(Attention;Visual) |

| | | | |
|---|---|---|---|
| 1126) | rfMRI connectivity (ICA100 edge 824) | (Middle_occipital;Superior_occipital)<=>(Inferior_temporal;Inferior_occipital) | (Attention;Visual)<=>(Attention;Visual) |
| 1127) | rfMRI connectivity (ICA100 edge 825) | (Precuneus;Angular;Middle_cingulate)<=>(Inferior_temporal;Inferior_occipital) | (Default_mode;Central_executive)<=>(Attention;Visual) |
| 1128) | rfMRI connectivity (ICA100 edge 826) | (Postcentral;Precentral)<=>(Inferior_temporal;Inferior_occipital) | (Motor)<=>(Attention;Visual) |
| 1129) | rfMRI connectivity (ICA100 edge 827) | (Superior_frontal;Anterior_cingulate)<=>(Inferior_temporal;Inferior_occipital) | (Default_mode;Limbic)<=>(Attention;Visual) |
| 1130) | rfMRI connectivity (ICA100 edge 828) | (Calcarine;Lingual)<=>(Inferior_temporal;Inferior_occipital) | (Visual)<=>(Attention;Visual) |
| 1131) | rfMRI connectivity (ICA100 edge 829) | (Middle_temporal;Temporal_pole)<=>(Inferior_temporal;Inferior_occipital) | (Default_mode)<=>(Attention;Visual) |
| 1132) | rfMRI connectivity (ICA100 edge 830) | (Middle_occipital;Precuneus;Calcarine)<=>(Inferior_temporal;Inferior_occipital) | (Default_mode;Central_executive)<=>(Attention;Visual) |
| 1133) | rfMRI connectivity (ICA100 edge 831) | (Angular;Middle_temporal)<=>(Inferior_temporal;Inferior_occipital) | (Default_mode;Central_executive)<=>(Attention;Visual) |
| 1134) | rfMRI connectivity (ICA100 edge 832) | (Middle_frontal;Cerebellum)<=>(Inferior_temporal;Inferior_occipital) | (Central_executive;Default_mode)<=>(Attention;Visual) |
| 1135) | rfMRI connectivity (ICA100 edge 833) | (Superior_frontal)<=>(Inferior_temporal;Inferior_occipital) | (Default_mode)<=>(Attention;Visual) |
| 1136) | rfMRI connectivity (ICA100 edge 834) | (Cuneus;Superior_occipital)<=>(Inferior_temporal;Inferior_occipital) | (Visual)<=>(Attention;Visual) |
| 1137) | rfMRI connectivity (ICA100 edge 835) | (Insula;Anterior_cingulate)<=>(Inferior_temporal;Inferior_occipital) | (Salience;Default_mode)<=>(Attention;Visual) |
| 1138) | rfMRI connectivity (ICA100 edge 836) | (Inferior_occipital;Middle_occipital)<=>(Inferior_temporal;Inferior_occipital) | (Visual)<=>(Attention;Visual) |
| 1139) | rfMRI connectivity (ICA100 edge 837) | (Cerebellum)<=>(Inferior_temporal;Inferior_occipital) | (Subcortical-cerebellum)<=>(Attention;Visual) |
| 1140) | rfMRI connectivity (ICA100 edge 838) | (Inferior_parietal;Postcentral)<=>(Inferior_temporal;Inferior_occipital) | (Attention;Central_executive;Salience)<=>(Attention;Visual) |
| 1141) | rfMRI connectivity (ICA100 edge 839) | (Precuneus;Cuneus)<=>(Inferior_temporal;Inferior_occipital) | (Default_mode;Central_executive)<=>(Attention;Visual) |
| 1142) | rfMRI connectivity (ICA100 edge 840) | (Postcentral;Precentral)<=>(Inferior_temporal;Inferior_occipital) | (Motor;Attention)<=>(Attention;Visual) |
| 1143) | rfMRI connectivity (ICA100 edge 841) | (Superior_frontal)<=>(Inferior_temporal;Inferior_occipital) | (Default_mode;Central_executive)<=>(Attention;Visual) |
| 1144) | rfMRI connectivity (ICA100 edge 842) | (Superior_temporal)<=>(Inferior_temporal;Inferior_occipital) | (Default_mode;Motor)<=>(Attention;Visual) |
| 1145) | rfMRI connectivity (ICA100 edge 843) | (Cerebellum)<=>(Inferior_temporal;Inferior_occipital) | (Subcortical-cerebellum)<=>(Attention;Visual) |
| 1146) | rfMRI connectivity (ICA100 edge 844) | (Inferior_parietal;Angular)<=>(Inferior_temporal;Inferior_occipital) | (Central_executive;Attention)<=>(Attention;Visual) |
| 1147) | rfMRI connectivity (ICA100 edge 845) | (Inferior_frontal;Precentral)<=>(Inferior_temporal;Inferior_occipital) | (Central_executive)<=>(Attention;Visual) |
| 1148) | rfMRI connectivity (ICA100 edge 846) | (Inferior_parietal;Inferior_frontal;SupraMarginal)<=>(Inferior_temporal;Inferior_occipital) | (Attention;Central_executive)<=>(Attention;Visual) |
| 1149) | rfMRI connectivity (ICA100 edge 847) | (Precentral;Superior_frontal;Supp_motor_area)<=>(Inferior_temporal;Inferior_occipital) | (Attention;Salience;Motor)<=>(Attention;Visual) |
| 1150) | rfMRI connectivity (ICA100 edge 848) | (Supp_motor_area;Inferior_frontal)<=>(Inferior_temporal;Inferior_occipital) | (Salience;Default_mode)<=>(Attention;Visual) |
| 1151) | rfMRI connectivity (ICA100 edge 849) | (SupraMarginal;Inferior_parietal)<=>(Inferior_temporal;Inferior_occipital) | (Central_executive;Salience)<=>(Attention;Visual) |
| 1152) | rfMRI connectivity (ICA100 edge 850) | (Paracentral)<=>(Inferior_temporal;Inferior_occipital) | (Motor)<=>(Attention;Visual) |

| | | | |
|---|---|---|---|
| 1153) | rfMRI connectivity (ICA100 edge 851) | (Middel_frontal)<=>(Inferior_temporal;Inferior_occipital) | (Central_executive)<=>(Attention;Visual) |
| 1154) | rfMRI connectivity (ICA100 edge 852) | (Postcentral;Precentral)<=>(Inferior_temporal;Inferior_occipital) | (Motor;Attention)<=>(Attention;Visual) |
| 1155) | rfMRI connectivity (ICA100 edge 853) | (Inferior_frontal;Middle_temporal;Supp_motor_area)<=>(Inferior_temporal;Inferior_occipital) | (Default_mode;Salience)<=>(Attention;Visual) |
| 1156) | rfMRI connectivity (ICA100 edge 854) | (Superior_parietal;Postcentral;Precuneus)<=>(Inferior_temporal;Inferior_occipital) | (Attention)<=>(Attention;Visual) |
| 1157) | rfMRI connectivity (ICA100 edge 855) | (Precentral;Postcentral)<=>(Inferior_temporal;Inferior_occipital) | (Motor)<=>(Attention;Visual) |
| 1158) | rfMRI connectivity (ICA100 edge 856) | (Precuneus)<=>(Inferior_temporal;Inferior_occipital) | (Default_mode;Central_executive)<=>(Attention;Visual) |
| 1159) | rfMRI connectivity (ICA100 edge 857) | (Middle_frontal)<=>(Inferior_temporal;Inferior_occipital) | (Central_executive;Salience)<=>(Attention;Visual) |
| 1160) | rfMRI connectivity (ICA100 edge 858) | (Putamen;Caudate)<=>(Inferior_temporal;Inferior_occipital) | (Subcortical-cerebellum)<=>(Attention;Visual) |
| 1161) | rfMRI connectivity (ICA100 edge 859) | (Precuneus;Superior_parietal)<=>(Inferior_temporal;Inferior_occipital) | (Attention;Central_executive)<=>(Attention;Visual) |
| 1162) | rfMRI connectivity (ICA100 edge 860) | (Superior_frontal;Middle_frontal)<=>(Inferior_temporal;Inferior_occipital) | (Central_executive)<=>(Attention;Visual) |
| 1163) | rfMRI connectivity (ICA100 edge 861) | (Inferior_temporal;Middle_temporal)<=>(Inferior_temporal;Inferior_occipital) | (Attention;Visual)<=>(Attention;Visual) |
| 1164) | rfMRI connectivity (ICA100 edge 862) | (Calcarine;Lingual;Cuneus)<=>(Inferior_temporal;Fusiform;Temporal_pole) | (Visual)<=>(Limbic;Default_mode) |
| 1165) | rfMRI connectivity (ICA100 edge 863) | (Rolandic_operculum;SupraMarginal;Insula)<=>(Inferior_temporal;Fusiform;Temporal_pole) | (Salience;Motor)<=>(Limbic;Default_mode) |
| 1166) | rfMRI connectivity (ICA100 edge 864) | (Lingual;Fusiform)<=>(Inferior_temporal;Fusiform;Temporal_pole) | (Visual)<=>(Limbic;Default_mode) |
| 1167) | rfMRI connectivity (ICA100 edge 865) | (Middle_occipital;Superior_occipital)<=>(Inferior_temporal;Fusiform;Temporal_pole) | (Attention;Visual)<=>(Limbic;Default_mode) |
| 1168) | rfMRI connectivity (ICA100 edge 866) | (Precuneus;Angular;Middle_cingulate)<=>(Inferior_temporal;Fusiform;Temporal_pole) | (Default_mode;Central_executive)<=>(Limbic;Default_mode) |
| 1169) | rfMRI connectivity (ICA100 edge 867) | (Postcentral;Precentral)<=>(Inferior_temporal;Fusiform;Temporal_pole) | (Motor)<=>(Limbic;Default_mode) |
| 1170) | rfMRI connectivity (ICA100 edge 868) | (Superior_frontal;Anterior_cingulate)<=>(Inferior_temporal;Fusiform;Temporal_pole) | (Default_mode;Limbic)<=>(Limbic;Default_mode) |
| 1171) | rfMRI connectivity (ICA100 edge 869) | (Calcarine;Lingual)<=>(Inferior_temporal;Fusiform;Temporal_pole) | (Visual)<=>(Limbic;Default_mode) |
| 1172) | rfMRI connectivity (ICA100 edge 870) | (Middle_temporal;Temporal_pole)<=>(Inferior_temporal;Fusiform;Temporal_pole) | (Default_mode)<=>(Limbic;Default_mode) |
| 1173) | rfMRI connectivity (ICA100 edge 871) | (Middle_occipital;Precuneus;Calcarine)<=>(Inferior_temporal;Fusiform;Temporal_pole) | (Default_mode;Central_executive)<=>(Limbic;Default_mode) |
| 1174) | rfMRI connectivity (ICA100 edge 872) | (Angular;Middle_temporal)<=>(Inferior_temporal;Fusiform;Temporal_pole) | (Default_mode;Central_executive)<=>(Limbic;Default_mode) |
| 1175) | rfMRI connectivity (ICA100 edge 873) | (Middle_frontal;Cerebellum)<=>(Inferior_temporal;Fusiform;Temporal_pole) | (Central_executive;Default_mode)<=>(Limbic;Default_mode) |
| 1176) | rfMRI connectivity (ICA100 edge 874) | (Superior_frontal)<=>(Inferior_temporal;Fusiform;Temporal_pole) | (Default_mode)<=>(Limbic;Default_mode) |
| 1177) | rfMRI connectivity (ICA100 edge 875) | (Cuneus;Superior_occipital)<=>(Inferior_temporal;Fusiform;Temporal_pole) | (Visual)<=>(Limbic;Default_mode) |

| | | | |
|---|---|---|---|
| 1178) | rfMRI connectivity (ICA100 edge 876) | (Insula;Anterior_cingulate)<=>(Inferior_temporal;Fusiform;Temporal_pole) | (Salience;Default_mode)<=>(Limbic;Default_mode) |
| 1179) | rfMRI connectivity (ICA100 edge 877) | (Inferior_occipital;Middle_occipital)<=>(Inferior_temporal;Fusiform;Temporal_pole) | (Visual)<=>(Limbic;Default_mode) |
| 1180) | rfMRI connectivity (ICA100 edge 878) | (Cerebellum)<=>(Inferior_temporal;Fusiform;Temporal_pole) | (Subcortical-cerebellum)<=>(Limbic;Default_mode) |
| 1181) | rfMRI connectivity (ICA100 edge 879) | (Inferior_parietal;Postcentral)<=>(Inferior_temporal;Fusiform;Temporal_pole) | (Attention;Central_executive;Salience)<=>(Limbic;Default_mode) |
| 1182) | rfMRI connectivity (ICA100 edge 880) | (Precuneus;Cuneus)<=>(Inferior_temporal;Fusiform;Temporal_pole) | (Default_mode;Central_executive)<=>(Limbic;Default_mode) |
| 1183) | rfMRI connectivity (ICA100 edge 881) | (Postcentral;Precentral)<=>(Inferior_temporal;Fusiform;Temporal_pole) | (Motor;Attention)<=>(Limbic;Default_mode) |
| 1184) | rfMRI connectivity (ICA100 edge 882) | (Superior_frontal)<=>(Inferior_temporal;Fusiform;Temporal_pole) | (Default_mode;Central_executive)<=>(Limbic;Default_mode) |
| 1185) | rfMRI connectivity (ICA100 edge 883) | (Superior_temporal)<=>(Inferior_temporal;Fusiform;Temporal_pole) | (Default_mode;Motor)<=>(Limbic;Default_mode) |
| 1186) | rfMRI connectivity (ICA100 edge 884) | (Cerebellum)<=>(Inferior_temporal;Fusiform;Temporal_pole) | (Subcortical-cerebellum)<=>(Limbic;Default_mode) |
| 1187) | rfMRI connectivity (ICA100 edge 885) | (Inferior_parietal;Angular)<=>(Inferior_temporal;Fusiform;Temporal_pole) | (Central_executive;Attention)<=>(Limbic;Default_mode) |
| 1188) | rfMRI connectivity (ICA100 edge 886) | (Inferior_frontal;Precentral)<=>(Inferior_temporal;Fusiform;Temporal_pole) | (Central_executive)<=>(Limbic;Default_mode) |
| 1189) | rfMRI connectivity (ICA100 edge 887) | (Inferior_parietal;Inferior_frontal;SupraMarginal)<=>(Inferior_temporal;Fusiform;Temporal_pole) | (Attention;Central_executive)<=>(Limbic;Default_mode) |
| 1190) | rfMRI connectivity (ICA100 edge 888) | (Precentral;Superior_frontal;Supp_motor_area)<=>(Inferior_temporal;Fusiform;Temporal_pole) | (Attention;Salience;Motor)<=>(Limbic;Default_mode) |
| 1191) | rfMRI connectivity (ICA100 edge 889) | (Supp_motor_area;Inferior_frontal)<=>(Inferior_temporal;Fusiform;Temporal_pole) | (Salience;Default_mode)<=>(Limbic;Default_mode) |
| 1192) | rfMRI connectivity (ICA100 edge 890) | (SupraMarginal;Inferior_parietal)<=>(Inferior_temporal;Fusiform;Temporal_pole) | (Central_executive;Salience)<=>(Limbic;Default_mode) |
| 1193) | rfMRI connectivity (ICA100 edge 891) | (Paracentral)<=>(Inferior_temporal;Fusiform;Temporal_pole) | (Motor)<=>(Limbic;Default_mode) |
| 1194) | rfMRI connectivity (ICA100 edge 892) | (Middel_frontal)<=>(Inferior_temporal;Fusiform;Temporal_pole) | (Central_executive)<=>(Limbic;Default_mode) |
| 1195) | rfMRI connectivity (ICA100 edge 893) | (Postcentral;Precentral)<=>(Inferior_temporal;Fusiform;Temporal_pole) | (Motor;Attention)<=>(Limbic;Default_mode) |
| 1196) | rfMRI connectivity (ICA100 edge 894) | (Inferior_frontal;Middle_temporal;Supp_motor_area)<=>(Inferior_temporal;Fusiform;Temporal_pole) | (Default_mode;Salience)<=>(Limbic;Default_mode) |
| 1197) | rfMRI connectivity (ICA100 edge 895) | (Superior_parietal;Postcentral;Precuneus)<=>(Inferior_temporal;Fusiform;Temporal_pole) | (Attention)<=>(Limbic;Default_mode) |
| 1198) | rfMRI connectivity (ICA100 edge 896) | (Precentral;Postcentral)<=>(Inferior_temporal;Fusiform;Temporal_pole) | (Motor)<=>(Limbic;Default_mode) |
| 1199) | rfMRI connectivity (ICA100 edge 897) | (Precuneus)<=>(Inferior_temporal;Fusiform;Temporal_pole) | (Default_mode;Central_executive)<=>(Limbic;Default_mode) |
| 1200) | rfMRI connectivity (ICA100 edge 898) | (Middle_frontal)<=>(Inferior_temporal;Fusiform;Temporal_pole) | (Central_executive;Salience)<=>(Limbic;Default_mode) |
| 1201) | rfMRI connectivity (ICA100 edge 899) | (Putamen;Caudate)<=>(Inferior_temporal;Fusiform;Temporal_pole) | (Subcortical-cerebellum)<=>(Limbic;Default_mode) |

| | | | |
|---|---|---|---|
| 1202) | rfMRI connectivity (ICA100 edge 900) | (Precuneus;Superior_parietal)<=>(Inferior_temporal;Fusiform;Temporal_pole) | (Attention;Central_executive)<=>(Limbic;Default_mode) |
| 1203) | rfMRI connectivity (ICA100 edge 901) | (Superior_frontal;Middle_frontal)<=>(Inferior_temporal;Fusiform;Temporal_pole) | (Central_executive)<=>(Limbic;Default_mode) |
| 1204) | rfMRI connectivity (ICA100 edge 902) | (Inferior_temporal;Middle_temporal)<=>(Inferior_temporal;Fusiform;Temporal_pole) | (Attention;Visual)<=>(Limbic;Default_mode) |
| 1205) | rfMRI connectivity (ICA100 edge 903) | (Inferior_temporal;Inferior_occipital)<=>(Inferior_temporal;Fusiform;Temporal_pole) | (Attention;Visual)<=>(Limbic;Default_mode) |
| 1206) | rfMRI connectivity (ICA100 edge 904) | (Calcarine;Lingual;Cuneus)<=>(Inferior_frontal) | (Visual)<=>(Default_mode;Central_executive) |
| 1207) | rfMRI connectivity (ICA100 edge 905) | (Rolandic_operculum;SupraMarginal;Insula)<=>(Inferior_frontal) | (Salience;Motor)<=>(Default_mode;Central_executive) |
| 1208) | rfMRI connectivity (ICA100 edge 906) | (Lingual;Fusiform)<=>(Inferior_frontal) | (Visual)<=>(Default_mode;Central_executive) |
| 1209) | rfMRI connectivity (ICA100 edge 907) | (Middle_occipital;Superior_occipital)<=>(Inferior_frontal) | (Attention;Visual)<=>(Default_mode;Central_executive) |
| 1210) | rfMRI connectivity (ICA100 edge 908) | (Precuneus;Angular;Middle_cingulate)<=>(Inferior_frontal) | (Default_mode;Central_executive)<=>(Default_mode;Central_executive) |
| 1211) | rfMRI connectivity (ICA100 edge 909) | (Postcentral;Precentral)<=>(Inferior_frontal) | (Motor)<=>(Default_mode;Central_executive) |
| 1212) | rfMRI connectivity (ICA100 edge 910) | (Superior_frontal;Anterior_cingulate)<=>(Inferior_frontal) | (Default_mode;Limbic)<=>(Default_mode;Central_executive) |
| 1213) | rfMRI connectivity (ICA100 edge 911) | (Calcarine;Lingual)<=>(Inferior_frontal) | (Visual)<=>(Default_mode;Central_executive) |
| 1214) | rfMRI connectivity (ICA100 edge 912) | (Middle_temporal;Temporal_pole)<=>(Inferior_frontal) | (Default_mode)<=>(Default_mode;Central_executive) |
| 1215) | rfMRI connectivity (ICA100 edge 913) | (Middle_occipital;Precuneus;Calcarine)<=>(Inferior_frontal) | (Default_mode;Central_executive)<=>(Default_mode;Central_executive) |
| 1216) | rfMRI connectivity (ICA100 edge 914) | (Angular;Middle_temporal)<=>(Inferior_frontal) | (Default_mode;Central_executive)<=>(Default_mode;Central_executive) |
| 1217) | rfMRI connectivity (ICA100 edge 915) | (Middle_frontal;Cerebellum)<=>(Inferior_frontal) | (Central_executive;Default_mode)<=>(Default_mode;Central_executive) |
| 1218) | rfMRI connectivity (ICA100 edge 916) | (Superior_frontal)<=>(Inferior_frontal) | (Default_mode)<=>(Default_mode;Central_executive) |
| 1219) | rfMRI connectivity (ICA100 edge 917) | (Cuneus;Superior_occipital)<=>(Inferior_frontal) | (Visual)<=>(Default_mode;Central_executive) |
| 1220) | rfMRI connectivity (ICA100 edge 918) | (Insula;Anterior_cingulate)<=>(Inferior_frontal) | (Salience;Default_mode)<=>(Default_mode;Central_executive) |
| 1221) | rfMRI connectivity (ICA100 edge 919) | (Inferior_occipital;Middle_occipital)<=>(Inferior_frontal) | (Visual)<=>(Default_mode;Central_executive) |
| 1222) | rfMRI connectivity (ICA100 edge 920) | (Cerebellum)<=>(Inferior_frontal) | (Subcortical-cerebellum)<=>(Default_mode;Central_executive) |
| 1223) | rfMRI connectivity (ICA100 edge 921) | (Inferior_parietal;Postcentral)<=>(Inferior_frontal) | (Attention;Central_executive;Salience)<=>(Default_mode;Central_executive) |
| 1224) | rfMRI connectivity (ICA100 edge 922) | (Precuneus;Cuneus)<=>(Inferior_frontal) | (Default_mode;Central_executive)<=>(Default_mode;Central_executive) |
| 1225) | rfMRI connectivity (ICA100 edge 923) | (Postcentral;Precentral)<=>(Inferior_frontal) | (Motor;Attention)<=>(Default_mode;Central_executive) |

| | | | |
|---|---|---|---|
| 1226) | rfMRI connectivity (ICA100 edge 924) | (Superior_frontal)<=>(Inferior_frontal) | (Default_mode;Central_executive)<=>(Default_mode;Central_executive) |
| 1227) | rfMRI connectivity (ICA100 edge 925) | (Superior_temporal)<=>(Inferior_frontal) | (Default_mode;Motor)<=>(Default_mode;Central_executive) |
| 1228) | rfMRI connectivity (ICA100 edge 926) | (Cerebellum)<=>(Inferior_frontal) | (Subcortical-cerebellum)<=>(Default_mode;Central_executive) |
| 1229) | rfMRI connectivity (ICA100 edge 927) | (Inferior_parietal;Angular)<=>(Inferior_frontal) | (Central_executive;Attention)<=>(Default_mode;Central_executive) |
| 1230) | rfMRI connectivity (ICA100 edge 928) | (Inferior_frontal;Precentral)<=>(Inferior_frontal) | (Central_executive)<=>(Default_mode;Central_executive) |
| 1231) | rfMRI connectivity (ICA100 edge 929) | (Inferior_parietal;Inferior_frontal;SupraMarginal)<=>(Inferior_frontal) | (Attention;Central_executive)<=>(Default_mode;Central_executive) |
| 1232) | rfMRI connectivity (ICA100 edge 930) | (Precentral;Superior_frontal;Supp_motor_area)<=>(Inferior_frontal) | (Attention;Salience;Motor)<=>(Default_mode;Central_executive) |
| 1233) | rfMRI connectivity (ICA100 edge 931) | (Supp_motor_area;Inferior_frontal)<=>(Inferior_frontal) | (Salience;Default_mode)<=>(Default_mode;Central_executive) |
| 1234) | rfMRI connectivity (ICA100 edge 932) | (SupraMarginal;Inferior_parietal)<=>(Inferior_frontal) | (Central_executive;Salience)<=>(Default_mode;Central_executive) |
| 1235) | rfMRI connectivity (ICA100 edge 933) | (Paracentral)<=>(Inferior_frontal) | (Motor)<=>(Default_mode;Central_executive) |
| 1236) | rfMRI connectivity (ICA100 edge 934) | (Middel_frontal)<=>(Inferior_frontal) | (Central_executive)<=>(Default_mode;Central_executive) |
| 1237) | rfMRI connectivity (ICA100 edge 935) | (Postcentral;Precentral)<=>(Inferior_frontal) | (Motor;Attention)<=>(Default_mode;Central_executive) |
| 1238) | rfMRI connectivity (ICA100 edge 936) | (Inferior_frontal;Middle_temporal;Supp_motor_area)<=>(Inferior_frontal) | (Default_mode;Salience)<=>(Default_mode;Central_executive) |
| 1239) | rfMRI connectivity (ICA100 edge 937) | (Superior_parietal;Postcentral;Precuneus)<=>(Inferior_frontal) | (Attention)<=>(Default_mode;Central_executive) |
| 1240) | rfMRI connectivity (ICA100 edge 938) | (Precentral;Postcentral)<=>(Inferior_frontal) | (Motor)<=>(Default_mode;Central_executive) |
| 1241) | rfMRI connectivity (ICA100 edge 939) | (Precuneus)<=>(Inferior_frontal) | (Default_mode;Central_executive)<=>(Default_mode;Central_executive) |
| 1242) | rfMRI connectivity (ICA100 edge 940) | (Middle_frontal)<=>(Inferior_frontal) | (Central_executive;Salience)<=>(Default_mode;Central_executive) |
| 1243) | rfMRI connectivity (ICA100 edge 941) | (Putamen;Caudate)<=>(Inferior_frontal) | (Subcortical-cerebellum)<=>(Default_mode;Central_executive) |
| 1244) | rfMRI connectivity (ICA100 edge 942) | (Precuneus;Superior_parietal)<=>(Inferior_frontal) | (Attention;Central_executive)<=>(Default_mode;Central_executive) |
| 1245) | rfMRI connectivity (ICA100 edge 943) | (Superior_frontal;Middle_frontal)<=>(Inferior_frontal) | (Central_executive)<=>(Default_mode;Central_executive) |
| 1246) | rfMRI connectivity (ICA100 edge 944) | (Inferior_temporal;Middle_temporal)<=>(Inferior_frontal) | (Attention;Visual)<=>(Default_mode;Central_executive) |
| 1247) | rfMRI connectivity (ICA100 edge 945) | (Inferior_temporal;Inferior_occipital)<=>(Inferior_frontal) | (Attention;Visual)<=>(Default_mode;Central_executive) |
| 1248) | rfMRI connectivity (ICA100 edge 946) | (Inferior_temporal;Fusiform;Temporal_pole)<=>(Inferior_frontal) | (Limbic;Default_mode)<=>(Default_mode;Central_executive) |

| | | | |
|---|---|---|---|
| 1249) | rfMRI connectivity (ICA100 edge 947) | (Calcarine;Lingual;Cuneus)<=>(Superior_frontal;Middle_frontal) | (Visual)<=>(Salience;Default_mode) |
| 1250) | rfMRI connectivity (ICA100 edge 948) | (Rolandic_operculum;SupraMarginal;Insula)<=>(Superior_frontal;Middle_frontal) | (Salience;Motor)<=>(Salience;Default_mode) |
| 1251) | rfMRI connectivity (ICA100 edge 949) | (Lingual;Fusiform)<=>(Superior_frontal;Middle_frontal) | (Visual)<=>(Salience;Default_mode) |
| 1252) | rfMRI connectivity (ICA100 edge 950) | (Middle_occipital;Superior_occipital)<=>(Superior_frontal;Middle_frontal) | (Attention;Visual)<=>(Salience;Default_mode) |
| 1253) | rfMRI connectivity (ICA100 edge 951) | (Precuneus;Angular;Middle_cingulate)<=>(Superior_frontal;Middle_frontal) | (Default_mode;Central_executive)<=>(Salience;Default_mode) |
| 1254) | rfMRI connectivity (ICA100 edge 952) | (Postcentral;Precentral)<=>(Superior_frontal;Middle_frontal) | (Motor)<=>(Salience;Default_mode) |
| 1255) | rfMRI connectivity (ICA100 edge 953) | (Superior_frontal;Anterior_cingulate)<=>(Superior_frontal;Middle_frontal) | (Default_mode;Limbic)<=>(Salience;Default_mode) |
| 1256) | rfMRI connectivity (ICA100 edge 954) | (Calcarine;Lingual)<=>(Superior_frontal;Middle_frontal) | (Visual)<=>(Salience;Default_mode) |
| 1257) | rfMRI connectivity (ICA100 edge 955) | (Middle_temporal;Temporal_pole)<=>(Superior_frontal;Middle_frontal) | (Default_mode)<=>(Salience;Default_mode) |
| 1258) | rfMRI connectivity (ICA100 edge 956) | (Middle_occipital;Precuneus;Calcarine)<=>(Superior_frontal;Middle_frontal) | (Default_mode;Central_executive)<=>(Salience;Default_mode) |
| 1259) | rfMRI connectivity (ICA100 edge 957) | (Angular;Middle_temporal)<=>(Superior_frontal;Middle_frontal) | (Default_mode;Central_executive)<=>(Salience;Default_mode) |
| 1260) | rfMRI connectivity (ICA100 edge 958) | (Middle_frontal;Cerebellum)<=>(Superior_frontal;Middle_frontal) | (Central_executive;Default_mode)<=>(Salience;Default_mode) |
| 1261) | rfMRI connectivity (ICA100 edge 959) | (Superior_frontal)<=>(Superior_frontal;Middle_frontal) | (Default_mode)<=>(Salience;Default_mode) |
| 1262) | rfMRI connectivity (ICA100 edge 960) | (Cuneus;Superior_occipital)<=>(Superior_frontal;Middle_frontal) | (Visual)<=>(Salience;Default_mode) |
| 1263) | rfMRI connectivity (ICA100 edge 961) | (Insula;Anterior_cingulate)<=>(Superior_frontal;Middle_frontal) | (Salience;Default_mode)<=>(Salience;Default_mode) |
| 1264) | rfMRI connectivity (ICA100 edge 962) | (Inferior_occipital;Middle_occipital)<=>(Superior_frontal;Middle_frontal) | (Visual)<=>(Salience;Default_mode) |
| 1265) | rfMRI connectivity (ICA100 edge 963) | (Cerebellum)<=>(Superior_frontal;Middle_frontal) | (Subcortical-cerebellum)<=>(Salience;Default_mode) |
| 1266) | rfMRI connectivity (ICA100 edge 964) | (Inferior_parietal;Postcentral)<=>(Superior_frontal;Middle_frontal) | (Attention;Central_executive;Salience)<=>(Salience;Default_mode) |
| 1267) | rfMRI connectivity (ICA100 edge 965) | (Precuneus;Cuneus)<=>(Superior_frontal;Middle_frontal) | (Default_mode;Central_executive)<=>(Salience;Default_mode) |
| 1268) | rfMRI connectivity (ICA100 edge 966) | (Postcentral;Precentral)<=>(Superior_frontal;Middle_frontal) | (Motor;Attention)<=>(Salience;Default_mode) |
| 1269) | rfMRI connectivity (ICA100 edge 967) | (Superior_frontal)<=>(Superior_frontal;Middle_frontal) | (Default_mode;Central_executive)<=>(Salience;Default_mode) |
| 1270) | rfMRI connectivity (ICA100 edge 968) | (Superior_temporal)<=>(Superior_frontal;Middle_frontal) | (Default_mode;Motor)<=>(Salience;Default_mode) |
| 1271) | rfMRI connectivity (ICA100 edge 969) | (Cerebellum)<=>(Superior_frontal;Middle_frontal) | (Subcortical-cerebellum)<=>(Salience;Default_mode) |
| 1272) | rfMRI connectivity (ICA100 edge 970) | (Inferior_parietal;Angular)<=>(Superior_frontal;Middle_frontal) | (Central_executive;Attention)<=>(Salience;Default_mode) |

| | | | |
|---|---|---|---|
| 1273) | rfMRI connectivity (ICA100 edge 971) | (Inferior_frontal;Precentral)<=>(Superior_frontal;Middle_frontal) | (Central_executive)<=>(Salience;Default_mode) |
| 1274) | rfMRI connectivity (ICA100 edge 972) | (Inferior_parietal;Inferior_frontal;SupraMarginal)<=>(Superior_frontal;Middle_frontal) | (Attention;Central_executive)<=>(Salience;Default_mode) |
| 1275) | rfMRI connectivity (ICA100 edge 973) | (Precentral;Superior_frontal;Supp_motor_area)<=>(Superior_frontal;Middle_frontal) | (Attention;Salience;Motor)<=>(Salience;Default_mode) |
| 1276) | rfMRI connectivity (ICA100 edge 974) | (Supp_motor_area;Inferior_frontal)<=>(Superior_frontal;Middle_frontal) | (Salience;Default_mode)<=>(Salience;Default_mode) |
| 1277) | rfMRI connectivity (ICA100 edge 975) | (SupraMarginal;Inferior_parietal)<=>(Superior_frontal;Middle_frontal) | (Central_executive;Salience)<=>(Salience;Default_mode) |
| 1278) | rfMRI connectivity (ICA100 edge 976) | (Paracentral)<=>(Superior_frontal;Middle_frontal) | (Motor)<=>(Salience;Default_mode) |
| 1279) | rfMRI connectivity (ICA100 edge 977) | (Middel_frontal)<=>(Superior_frontal;Middle_frontal) | (Central_executive)<=>(Salience;Default_mode) |
| 1280) | rfMRI connectivity (ICA100 edge 978) | (Postcentral;Precentral)<=>(Superior_frontal;Middle_frontal) | (Motor;Attention)<=>(Salience;Default_mode) |
| 1281) | rfMRI connectivity (ICA100 edge 979) | (Inferior_frontal;Middle_temporal;Supp_motor_area)<=>(Superior_frontal;Middle_frontal) | (Default_mode;Salience)<=>(Salience;Default_mode) |
| 1282) | rfMRI connectivity (ICA100 edge 980) | (Superior_parietal;Postcentral;Precuneus)<=>(Superior_frontal;Middle_frontal) | (Attention)<=>(Salience;Default_mode) |
| 1283) | rfMRI connectivity (ICA100 edge 981) | (Precentral;Postcentral)<=>(Superior_frontal;Middle_frontal) | (Motor)<=>(Salience;Default_mode) |
| 1284) | rfMRI connectivity (ICA100 edge 982) | (Precuneus)<=>(Superior_frontal;Middle_frontal) | (Default_mode;Central_executive)<=>(Salience;Default_mode) |
| 1285) | rfMRI connectivity (ICA100 edge 983) | (Middle_frontal)<=>(Superior_frontal;Middle_frontal) | (Central_executive;Salience)<=>(Salience;Default_mode) |
| 1286) | rfMRI connectivity (ICA100 edge 984) | (Putamen;Caudate)<=>(Superior_frontal;Middle_frontal) | (Subcortical-cerebellum)<=>(Salience;Default_mode) |
| 1287) | rfMRI connectivity (ICA100 edge 985) | (Precuneus;Superior_parietal)<=>(Superior_frontal;Middle_frontal) | (Attention;Central_executive)<=>(Salience;Default_mode) |
| 1288) | rfMRI connectivity (ICA100 edge 986) | (Superior_frontal;Middle_frontal)<=>(Superior_frontal;Middle_frontal) | (Central_executive)<=>(Salience;Default_mode) |
| 1289) | rfMRI connectivity (ICA100 edge 987) | (Inferior_temporal;Middle_temporal)<=>(Superior_frontal;Middle_frontal) | (Attention;Visual)<=>(Salience;Default_mode) |
| 1290) | rfMRI connectivity (ICA100 edge 988) | (Inferior_temporal;Inferior_occipital)<=>(Superior_frontal;Middle_frontal) | (Attention;Visual)<=>(Salience;Default_mode) |
| 1291) | rfMRI connectivity (ICA100 edge 989) | (Inferior_temporal;Fusiform;Temporal_pole)<=>(Superior_frontal;Middle_frontal) | (Limbic;Default_mode)<=>(Salience;Default_mode) |
| 1292) | rfMRI connectivity (ICA100 edge 990) | (Inferior_frontal)<=>(Superior_frontal;Middle_frontal) | (Default_mode;Central_executive)<=>(Salience;Default_mode) |
| 1293) | rfMRI connectivity (ICA100 edge 991) | (Calcarine;Lingual;Cuneus)<=>(Inferior_temporal;Middle_temporal) | (Visual)<=>(Central_executive;Default_mode) |
| 1294) | rfMRI connectivity (ICA100 edge 992) | (Rolandic_operculum;SupraMarginal;Insula)<=>(Inferior_temporal;Middle_temporal) | (Salience;Motor)<=>(Central_executive;Default_mode) |
| 1295) | rfMRI connectivity (ICA100 edge 993) | (Lingual;Fusiform)<=>(Inferior_temporal;Middle_temporal) | (Visual)<=>(Central_executive;Default_mode) |
| 1296) | rfMRI connectivity (ICA100 edge 994) | (Middle_occipital;Superior_occipital)<=>(Inferior_temporal;Middle_temporal) | (Attention;Visual)<=>(Central_executive;Default_mode) |
| 1297) | rfMRI connectivity (ICA100 edge 995) | (Precuneus;Angular;Middle_cingulate)<=>(Inferior_temporal;Middle_temporal) | (Default_mode;Central_executive)<=>(Central_executive;Default_mode) |

| | | | |
|---|---|---|---|
| 1298) | rfMRI connectivity (ICA100 edge 996) | (Postcentral;Precentral)<=>(Inferior_temporal;Middle_temporal) | (Motor)<=>(Central_executive;Default_mode) |
| 1299) | rfMRI connectivity (ICA100 edge 997) | (Superior_frontal;Anterior_cingulate)<=>(Inferior_temporal;Middle_temporal) | (Default_mode;Limbic)<=>(Central_executive;Default_mode) |
| 1300) | rfMRI connectivity (ICA100 edge 998) | (Calcarine;Lingual)<=>(Inferior_temporal;Middle_temporal) | (Visual)<=>(Central_executive;Default_mode) |
| 1301) | rfMRI connectivity (ICA100 edge 999) | (Middle_temporal;Temporal_pole)<=>(Inferior_temporal;Middle_temporal) | (Default_mode)<=>(Central_executive;Default_mode) |
| 1302) | rfMRI connectivity (ICA100 edge 1000) | (Middle_occipital;Precuneus;Calcarine)<=>(Inferior_temporal;Middle_temporal) | (Default_mode;Central_executive)<=>(Central_executive;Default_mode) |
| 1303) | rfMRI connectivity (ICA100 edge 1001) | (Angular;Middle_temporal)<=>(Inferior_temporal;Middle_temporal) | (Default_mode;Central_executive)<=>(Central_executive;Default_mode) |
| 1304) | rfMRI connectivity (ICA100 edge 1002) | (Middle_frontal;Cerebellum)<=>(Inferior_temporal;Middle_temporal) | (Central_executive;Default_mode)<=>(Central_executive;Default_mode) |
| 1305) | rfMRI connectivity (ICA100 edge 1003) | (Superior_frontal)<=>(Inferior_temporal;Middle_temporal) | (Default_mode)<=>(Central_executive;Default_mode) |
| 1306) | rfMRI connectivity (ICA100 edge 1004) | (Cuneus;Superior_occipital)<=>(Inferior_temporal;Middle_temporal) | (Visual)<=>(Central_executive;Default_mode) |
| 1307) | rfMRI connectivity (ICA100 edge 1005) | (Insula;Anterior_cingulate)<=>(Inferior_temporal;Middle_temporal) | (Salience;Default_mode)<=>(Central_executive;Default_mode) |
| 1308) | rfMRI connectivity (ICA100 edge 1006) | (Inferior_occipital;Middle_occipital)<=>(Inferior_temporal;Middle_temporal) | (Visual)<=>(Central_executive;Default_mode) |
| 1309) | rfMRI connectivity (ICA100 edge 1007) | (Cerebellum)<=>(Inferior_temporal;Middle_temporal) | (Subcortical-cerebellum)<=>(Central_executive;Default_mode) |
| 1310) | rfMRI connectivity (ICA100 edge 1008) | (Inferior_parietal;Postcentral)<=>(Inferior_temporal;Middle_temporal) | (Attention;Central_executive;Salience)<=>(Central_executive;Default_mode) |
| 1311) | rfMRI connectivity (ICA100 edge 1009) | (Precuneus;Cuneus)<=>(Inferior_temporal;Middle_temporal) | (Default_mode;Central_executive)<=>(Central_executive;Default_mode) |
| 1312) | rfMRI connectivity (ICA100 edge 1010) | (Postcentral;Precentral)<=>(Inferior_temporal;Middle_temporal) | (Motor;Attention)<=>(Central_executive;Default_mode) |
| 1313) | rfMRI connectivity (ICA100 edge 1011) | (Superior_frontal)<=>(Inferior_temporal;Middle_temporal) | (Default_mode;Central_executive)<=>(Central_executive;Default_mode) |
| 1314) | rfMRI connectivity (ICA100 edge 1012) | (Superior_temporal)<=>(Inferior_temporal;Middle_temporal) | (Default_mode;Motor)<=>(Central_executive;Default_mode) |
| 1315) | rfMRI connectivity (ICA100 edge 1013) | (Cerebellum)<=>(Inferior_temporal;Middle_temporal) | (Subcortical-cerebellum)<=>(Central_executive;Default_mode) |
| 1316) | rfMRI connectivity (ICA100 edge 1014) | (Inferior_parietal;Angular)<=>(Inferior_temporal;Middle_temporal) | (Central_executive;Attention)<=>(Central_executive;Default_mode) |
| 1317) | rfMRI connectivity (ICA100 edge 1015) | (Inferior_frontal;Precentral)<=>(Inferior_temporal;Middle_temporal) | (Central_executive)<=>(Central_executive;Default_mode) |
| 1318) | rfMRI connectivity (ICA100 edge 1016) | (Inferior_parietal;Inferior_frontal;SupraMarginal)<=>(Inferior_temporal;Middle_temporal) | (Attention;Central_executive)<=>(Central_executive;Default_mode) |
| 1319) | rfMRI connectivity (ICA100 edge 1017) | (Precentral;Superior_frontal;Supp_motor_area)<=>(Inferior_temporal;Middle_temporal) | (Attention;Salience;Motor)<=>(Central_executive;Default_mode) |
| 1320) | rfMRI connectivity (ICA100 edge 1018) | (Supp_motor_area;Inferior_frontal)<=>(Inferior_temporal;Middle_temporal) | (Salience;Default_mode)<=>(Central_executive;Default_mode) |

| | | | |
|---|---|---|---|
| 1321) | rfMRI connectivity (ICA100 edge 1019) | (SupraMarginal;Inferior_parietal)<=>(Inferior_temporal;Middle_temporal) | (Central_executive;Salience)<=>(Central_executive;Default_mode) |
| 1322) | rfMRI connectivity (ICA100 edge 1020) | (Paracentral)<=>(Inferior_temporal;Middle_temporal) | (Motor)<=>(Central_executive;Default_mode) |
| 1323) | rfMRI connectivity (ICA100 edge 1021) | (Middel_frontal)<=>(Inferior_temporal;Middle_temporal) | (Central_executive)<=>(Central_executive;Default_mode) |
| 1324) | rfMRI connectivity (ICA100 edge 1022) | (Postcentral;Precentral)<=>(Inferior_temporal;Middle_temporal) | (Motor;Attention)<=>(Central_executive;Default_mode) |
| 1325) | rfMRI connectivity (ICA100 edge 1023) | (Inferior_frontal;Middle_temporal;Supp_motor_area)<=>(Inferior_temporal;Middle_temporal) | (Default_mode;Salience)<=>(Central_executive;Default_mode) |
| 1326) | rfMRI connectivity (ICA100 edge 1024) | (Superior_parietal;Postcentral;Precuneus)<=>(Inferior_temporal;Middle_temporal) | (Attention)<=>(Central_executive;Default_mode) |
| 1327) | rfMRI connectivity (ICA100 edge 1025) | (Precentral;Postcentral)<=>(Inferior_temporal;Middle_temporal) | (Motor)<=>(Central_executive;Default_mode) |
| 1328) | rfMRI connectivity (ICA100 edge 1026) | (Precuneus)<=>(Inferior_temporal;Middle_temporal) | (Default_mode;Central_executive)<=>(Central_executive;Default_mode) |
| 1329) | rfMRI connectivity (ICA100 edge 1027) | (Middle_frontal)<=>(Inferior_temporal;Middle_temporal) | (Central_executive;Salience)<=>(Central_executive;Default_mode) |
| 1330) | rfMRI connectivity (ICA100 edge 1028) | (Putamen;Caudate)<=>(Inferior_temporal;Middle_temporal) | (Subcortical-cerebellum)<=>(Central_executive;Default_mode) |
| 1331) | rfMRI connectivity (ICA100 edge 1029) | (Precuneus;Superior_parietal)<=>(Inferior_temporal;Middle_temporal) | (Attention;Central_executive)<=>(Central_executive;Default_mode) |
| 1332) | rfMRI connectivity (ICA100 edge 1030) | (Superior_frontal;Middle_frontal)<=>(Inferior_temporal;Middle_temporal) | (Central_executive)<=>(Central_executive;Default_mode) |
| 1333) | rfMRI connectivity (ICA100 edge 1031) | (Inferior_temporal;Middle_temporal)<=>(Inferior_temporal;Middle_temporal) | (Attention;Visual)<=>(Central_executive;Default_mode) |
| 1334) | rfMRI connectivity (ICA100 edge 1032) | (Inferior_temporal;Inferior_occipital)<=>(Inferior_temporal;Middle_temporal) | (Attention;Visual)<=>(Central_executive;Default_mode) |
| 1335) | rfMRI connectivity (ICA100 edge 1033) | (Inferior_temporal;Fusiform;Temporal_pole)<=>(Inferior_temporal;Middle_temporal) | (Limbic;Default_mode)<=>(Central_executive;Default_mode) |
| 1336) | rfMRI connectivity (ICA100 edge 1034) | (Inferior_frontal)<=>(Inferior_temporal;Middle_temporal) | (Default_mode;Central_executive)<=>(Central_executive;Default_mode) |
| 1337) | rfMRI connectivity (ICA100 edge 1035) | (Superior_frontal;Middle_frontal)<=>(Inferior_temporal;Middle_temporal) | (Salience;Default_mode)<=>(Central_executive;Default_mode) |
| 1338) | rfMRI connectivity (ICA100 edge 1036) | (Calcarine;Lingual;Cuneus)<=>(Superior_frontal;Middle_frontal) | (Visual)<=>(Central_executive;Salience;Default_mode) |
| 1339) | rfMRI connectivity (ICA100 edge 1037) | (Rolandic_operculum;SupraMarginal;Insula)<=>(Superior_frontal;Middle_frontal) | (Salience;Motor)<=>(Central_executive;Salience;Default_mode) |
| 1340) | rfMRI connectivity (ICA100 edge 1038) | (Lingual;Fusiform)<=>(Superior_frontal;Middle_frontal) | (Visual)<=>(Central_executive;Salience;Default_mode) |
| 1341) | rfMRI connectivity (ICA100 edge 1039) | (Middle_occipital;Superior_occipital)<=>(Superior_frontal;Middle_frontal) | (Attention;Visual)<=>(Central_executive;Salience;Default_mode) |
| 1342) | rfMRI connectivity (ICA100 edge 1040) | (Precuneus;Angular;Middle_cingulate)<=>(Superior_frontal;Middle_frontal) | (Default_mode;Central_executive)<=>(Central_executive;Salience;Default_mode) |
| 1343) | rfMRI connectivity (ICA100 edge 1041) | (Postcentral;Precentral)<=>(Superior_frontal;Middle_frontal) | (Motor)<=>(Central_executive;Salience;Default_mode) |

| | | | |
|---|---|---|---|
| 1344) | rfMRI connectivity (ICA100 edge 1042) | (Superior_frontal;Anterior_cingulate)<=>(Superior_frontal;Middle_frontal) | (Default_mode;Limbic)<=>(Central_executive;Salience;Default_mode) |
| 1345) | rfMRI connectivity (ICA100 edge 1043) | (Calcarine;Lingual)<=>(Superior_frontal;Middle_frontal) | (Visual)<=>(Central_executive;Salience;Default_mode) |
| 1346) | rfMRI connectivity (ICA100 edge 1044) | (Middle_temporal;Temporal_pole)<=>(Superior_frontal;Middle_frontal) | (Default_mode)<=>(Central_executive;Salience;Default_mode) |
| 1347) | rfMRI connectivity (ICA100 edge 1045) | (Middle_occipital;Precuneus;Calcarine)<=>(Superior_frontal;Middle_frontal) | (Default_mode;Central_executive)<=>(Central_executive;Salience;Default_mode) |
| 1348) | rfMRI connectivity (ICA100 edge 1046) | (Angular;Middle_temporal)<=>(Superior_frontal;Middle_frontal) | (Default_mode;Central_executive)<=>(Central_executive;Salience;Default_mode) |
| 1349) | rfMRI connectivity (ICA100 edge 1047) | (Middle_frontal;Cerebellum)<=>(Superior_frontal;Middle_frontal) | (Central_executive;Default_mode)<=>(Central_executive;Salience;Default_mode) |
| 1350) | rfMRI connectivity (ICA100 edge 1048) | (Superior_frontal)<=>(Superior_frontal;Middle_frontal) | (Default_mode)<=>(Central_executive;Salience;Default_mode) |
| 1351) | rfMRI connectivity (ICA100 edge 1049) | (Cuneus;Superior_occipital)<=>(Superior_frontal;Middle_frontal) | (Visual)<=>(Central_executive;Salience;Default_mode) |
| 1352) | rfMRI connectivity (ICA100 edge 1050) | (Insula;Anterior_cingulate)<=>(Superior_frontal;Middle_frontal) | (Salience;Default_mode)<=>(Central_executive;Salience;Default_mode) |
| 1353) | rfMRI connectivity (ICA100 edge 1051) | (Inferior_occipital;Middle_occipital)<=>(Superior_frontal;Middle_frontal) | (Visual)<=>(Central_executive;Salience;Default_mode) |
| 1354) | rfMRI connectivity (ICA100 edge 1052) | (Cerebellum)<=>(Superior_frontal;Middle_frontal) | (Subcortical-cerebellum)<=>(Central_executive;Salience;Default_mode) |
| 1355) | rfMRI connectivity (ICA100 edge 1053) | (Inferior_parietal;Postcentral)<=>(Superior_frontal;Middle_frontal) | (Attention;Central_executive;Salience)<=>(Central_executive;Salience;Default_mode) |
| 1356) | rfMRI connectivity (ICA100 edge 1054) | (Precuneus;Cuneus)<=>(Superior_frontal;Middle_frontal) | (Default_mode;Central_executive)<=>(Central_executive;Salience;Default_mode) |
| 1357) | rfMRI connectivity (ICA100 edge 1055) | (Postcentral;Precentral)<=>(Superior_frontal;Middle_frontal) | (Motor;Attention)<=>(Central_executive;Salience;Default_mode) |
| 1358) | rfMRI connectivity (ICA100 edge 1056) | (Superior_frontal)<=>(Superior_frontal;Middle_frontal) | (Default_mode;Central_executive)<=>(Central_executive;Salience;Default_mode) |
| 1359) | rfMRI connectivity (ICA100 edge 1057) | (Superior_temporal)<=>(Superior_frontal;Middle_frontal) | (Default_mode;Motor)<=>(Central_executive;Salience;Default_mode) |
| 1360) | rfMRI connectivity (ICA100 edge 1058) | (Cerebellum)<=>(Superior_frontal;Middle_frontal) | (Subcortical-cerebellum)<=>(Central_executive;Salience;Default_mode) |
| 1361) | rfMRI connectivity (ICA100 edge 1059) | (Inferior_parietal;Angular)<=>(Superior_frontal;Middle_frontal) | (Central_executive;Attention)<=>(Central_executive;Salience;Default_mode) |
| 1362) | rfMRI connectivity (ICA100 edge 1060) | (Inferior_frontal;Precentral)<=>(Superior_frontal;Middle_frontal) | (Central_executive)<=>(Central_executive;Salience;Default_mode) |
| 1363) | rfMRI connectivity (ICA100 edge 1061) | (Inferior_parietal;Inferior_frontal;SupraMarginal)<=>(Superior_frontal;Middle_frontal) | (Attention;Central_executive)<=>(Central_executive;Salience;Default_mode) |

| | | | |
|---|---|---|---|
| 1364) | rfMRI connectivity (ICA100 edge 1062) | (Precentral;Superior_frontal;Supp_motor_area)<=>(Superior_frontal;Middle_frontal) | (Attention;Salience;Motor)<=>(Central_executive;Salience;Default_mode) |
| 1365) | rfMRI connectivity (ICA100 edge 1063) | (Supp_motor_area;Inferior_frontal)<=>(Superior_frontal;Middle_frontal) | (Salience;Default_mode)<=>(Central_executive;Salience;Default_mode) |
| 1366) | rfMRI connectivity (ICA100 edge 1064) | (SupraMarginal;Inferior_parietal)<=>(Superior_frontal;Middle_frontal) | (Central_executive;Salience)<=>(Central_executive;Salience;Default_mode) |
| 1367) | rfMRI connectivity (ICA100 edge 1065) | (Paracentral)<=>(Superior_frontal;Middle_frontal) | (Motor)<=>(Central_executive;Salience;Default_mode) |
| 1368) | rfMRI connectivity (ICA100 edge 1066) | (Middel_frontal)<=>(Superior_frontal;Middle_frontal) | (Central_executive)<=>(Central_executive;Salience;Default_mode) |
| 1369) | rfMRI connectivity (ICA100 edge 1067) | (Postcentral;Precentral)<=>(Superior_frontal;Middle_frontal) | (Motor;Attention)<=>(Central_executive;Salience;Default_mode) |
| 1370) | rfMRI connectivity (ICA100 edge 1068) | (Inferior_frontal;Middle_temporal;Supp_motor_area)<=>(Superior_frontal;Middle_frontal) | (Default_mode;Salience)<=>(Central_executive;Salience;Default_mode) |
| 1371) | rfMRI connectivity (ICA100 edge 1069) | (Superior_parietal;Postcentral;Precuneus)<=>(Superior_frontal;Middle_frontal) | (Attention)<=>(Central_executive;Salience;Default_mode) |
| 1372) | rfMRI connectivity (ICA100 edge 1070) | (Precentral;Postcentral)<=>(Superior_frontal;Middle_frontal) | (Motor)<=>(Central_executive;Salience;Default_mode) |
| 1373) | rfMRI connectivity (ICA100 edge 1071) | (Precuneus)<=>(Superior_frontal;Middle_frontal) | (Default_mode;Central_executive)<=>(Central_executive;Salience;Default_mode) |
| 1374) | rfMRI connectivity (ICA100 edge 1072) | (Middle_frontal)<=>(Superior_frontal;Middle_frontal) | (Central_executive;Salience)<=>(Central_executive;Salience;Default_mode) |
| 1375) | rfMRI connectivity (ICA100 edge 1073) | (Putamen;Caudate)<=>(Superior_frontal;Middle_frontal) | (Subcortical-cerebellum)<=>(Central_executive;Salience;Default_mode) |
| 1376) | rfMRI connectivity (ICA100 edge 1074) | (Precuneus;Superior_parietal)<=>(Superior_frontal;Middle_frontal) | (Attention;Central_executive)<=>(Central_executive;Salience;Default_mode) |
| 1377) | rfMRI connectivity (ICA100 edge 1075) | (Superior_frontal;Middle_frontal)<=>(Superior_frontal;Middle_frontal) | (Central_executive)<=>(Central_executive;Salience;Default_mode) |
| 1378) | rfMRI connectivity (ICA100 edge 1076) | (Inferior_temporal;Middle_temporal)<=>(Superior_frontal;Middle_frontal) | (Attention;Visual)<=>(Central_executive;Salience;Default_mode) |
| 1379) | rfMRI connectivity (ICA100 edge 1077) | (Inferior_temporal;Inferior_occipital)<=>(Superior_frontal;Middle_frontal) | (Attention;Visual)<=>(Central_executive;Salience;Default_mode) |
| 1380) | rfMRI connectivity (ICA100 edge 1078) | (Inferior_temporal;Fusiform;Temporal_pole)<=>(Superior_frontal;Middle_frontal) | (Limbic;Default_mode)<=>(Central_executive;Salience;Default_mode) |
| 1381) | rfMRI connectivity (ICA100 edge 1079) | (Inferior_frontal)<=>(Superior_frontal;Middle_frontal) | (Default_mode;Central_executive)<=>(Central_executive;Salience;Default_mode) |
| 1382) | rfMRI connectivity (ICA100 edge 1080) | (Superior_frontal;Middle_frontal)<=>(Superior_frontal;Middle_frontal) | (Salience;Default_mode)<=>(Central_executive;Salience;Default_mode) |
| 1383) | rfMRI connectivity (ICA100 edge 1081) | (Inferior_temporal;Middle_temporal)<=>(Superior_frontal;Middle_frontal) | (Central_executive;Default_mode)<=>(Central_executive;Salience;Default_mode) |
| 1384) | rfMRI connectivity (ICA100 edge 1082) | (Calcarine;Lingual;Cuneus)<=>(Middle_temporal) | (Visual)<=>(Default_mode;Central_executive) |

| | | | |
|---|---|---|---|
| 1385) | rfMRI connectivity (ICA100 edge 1083) | (Rolandic_operculum;SupraMarginal;Insula)<=>(Middle_temporal) | (Salience;Motor)<=>(Default_mode;Central_executive) |
| 1386) | rfMRI connectivity (ICA100 edge 1084) | (Lingual;Fusiform)<=>(Middle_temporal) | (Visual)<=>(Default_mode;Central_executive) |
| 1387) | rfMRI connectivity (ICA100 edge 1085) | (Middle_occipital;Superior_occipital)<=>(Middle_temporal) | (Attention;Visual)<=>(Default_mode;Central_executive) |
| 1388) | rfMRI connectivity (ICA100 edge 1086) | (Precuneus;Angular;Middle_cingulate)<=>(Middle_temporal) | (Default_mode;Central_executive)<=>(Default_mode;Central_executive) |
| 1389) | rfMRI connectivity (ICA100 edge 1087) | (Postcentral;Precentral)<=>(Middle_temporal) | (Motor)<=>(Default_mode;Central_executive) |
| 1390) | rfMRI connectivity (ICA100 edge 1088) | (Superior_frontal;Anterior_cingulate)<=>(Middle_temporal) | (Default_mode;Limbic)<=>(Default_mode;Central_executive) |
| 1391) | rfMRI connectivity (ICA100 edge 1089) | (Calcarine;Lingual)<=>(Middle_temporal) | (Visual)<=>(Default_mode;Central_executive) |
| 1392) | rfMRI connectivity (ICA100 edge 1090) | (Middle_temporal;Temporal_pole)<=>(Middle_temporal) | (Default_mode)<=>(Default_mode;Central_executive) |
| 1393) | rfMRI connectivity (ICA100 edge 1091) | (Middle_occipital;Precuneus;Calcarine)<=>(Middle_temporal) | (Default_mode;Central_executive)<=>(Default_mode;Central_executive) |
| 1394) | rfMRI connectivity (ICA100 edge 1092) | (Angular;Middle_temporal)<=>(Middle_temporal) | (Default_mode;Central_executive)<=>(Default_mode;Central_executive) |
| 1395) | rfMRI connectivity (ICA100 edge 1093) | (Middle_frontal;Cerebellum)<=>(Middle_temporal) | (Central_executive;Default_mode)<=>(Default_mode;Central_executive) |
| 1396) | rfMRI connectivity (ICA100 edge 1094) | (Superior_frontal)<=>(Middle_temporal) | (Default_mode)<=>(Default_mode;Central_executive) |
| 1397) | rfMRI connectivity (ICA100 edge 1095) | (Cuneus;Superior_occipital)<=>(Middle_temporal) | (Visual)<=>(Default_mode;Central_executive) |
| 1398) | rfMRI connectivity (ICA100 edge 1096) | (Insula;Anterior_cingulate)<=>(Middle_temporal) | (Salience;Default_mode)<=>(Default_mode;Central_executive) |
| 1399) | rfMRI connectivity (ICA100 edge 1097) | (Inferior_occipital;Middle_occipital)<=>(Middle_temporal) | (Visual)<=>(Default_mode;Central_executive) |
| 1400) | rfMRI connectivity (ICA100 edge 1098) | (Cerebellum)<=>(Middle_temporal) | (Subcortical-cerebellum)<=>(Default_mode;Central_executive) |
| 1401) | rfMRI connectivity (ICA100 edge 1099) | (Inferior_parietal;Postcentral)<=>(Middle_temporal) | (Attention;Central_executive;Salience)<=>(Default_mode;Central_executive) |
| 1402) | rfMRI connectivity (ICA100 edge 1100) | (Precuneus;Cuneus)<=>(Middle_temporal) | (Default_mode;Central_executive)<=>(Default_mode;Central_executive) |
| 1403) | rfMRI connectivity (ICA100 edge 1101) | (Postcentral;Precentral)<=>(Middle_temporal) | (Motor;Attention)<=>(Default_mode;Central_executive) |
| 1404) | rfMRI connectivity (ICA100 edge 1102) | (Superior_frontal)<=>(Middle_temporal) | (Default_mode;Central_executive)<=>(Default_mode;Central_executive) |
| 1405) | rfMRI connectivity (ICA100 edge 1103) | (Superior_temporal)<=>(Middle_temporal) | (Default_mode;Motor)<=>(Default_mode;Central_executive) |
| 1406) | rfMRI connectivity (ICA100 edge 1104) | (Cerebellum)<=>(Middle_temporal) | (Subcortical-cerebellum)<=>(Default_mode;Central_executive) |
| 1407) | rfMRI connectivity (ICA100 edge 1105) | (Inferior_parietal;Angular)<=>(Middle_temporal) | (Central_executive;Attention)<=>(Default_mode;Central_executive) |
| 1408) | rfMRI connectivity (ICA100 edge 1106) | (Inferior_frontal;Precentral)<=>(Middle_temporal) | (Central_executive)<=>(Default_mode;Central_executive) |

| | | | |
|---|---|---|---|
| 1409) | rfMRI connectivity (ICA100 edge 1107) | (Inferior_parietal;Inferior_frontal;SupraMarginal)<=>(Middle_temporal) | (Attention;Central_executive)<=>(Default_mode;Central_executive) |
| 1410) | rfMRI connectivity (ICA100 edge 1108) | (Precentral;Superior_frontal;Supp_motor_area)<=>(Middle_temporal) | (Attention;Salience;Motor)<=>(Default_mode;Central_executive) |
| 1411) | rfMRI connectivity (ICA100 edge 1109) | (Supp_motor_area;Inferior_frontal)<=>(Middle_temporal) | (Salience;Default_mode)<=>(Default_mode;Central_executive) |
| 1412) | rfMRI connectivity (ICA100 edge 1110) | (SupraMarginal;Inferior_parietal)<=>(Middle_temporal) | (Central_executive;Salience)<=>(Default_mode;Central_executive) |
| 1413) | rfMRI connectivity (ICA100 edge 1111) | (Paracentral)<=>(Middle_temporal) | (Motor)<=>(Default_mode;Central_executive) |
| 1414) | rfMRI connectivity (ICA100 edge 1112) | (Middel_frontal)<=>(Middle_temporal) | (Central_executive)<=>(Default_mode;Central_executive) |
| 1415) | rfMRI connectivity (ICA100 edge 1113) | (Postcentral;Precentral)<=>(Middle_temporal) | (Motor;Attention)<=>(Default_mode;Central_executive) |
| 1416) | rfMRI connectivity (ICA100 edge 1114) | (Inferior_frontal;Middle_temporal;Supp_motor_area)<=>(Middle_temporal) | (Default_mode;Salience)<=>(Default_mode;Central_executive) |
| 1417) | rfMRI connectivity (ICA100 edge 1115) | (Superior_parietal;Postcentral;Precuneus)<=>(Middle_temporal) | (Attention)<=>(Default_mode;Central_executive) |
| 1418) | rfMRI connectivity (ICA100 edge 1116) | (Precentral;Postcentral)<=>(Middle_temporal) | (Motor)<=>(Default_mode;Central_executive) |
| 1419) | rfMRI connectivity (ICA100 edge 1117) | (Precuneus)<=>(Middle_temporal) | (Default_mode;Central_executive)<=>(Default_mode;Central_executive) |
| 1420) | rfMRI connectivity (ICA100 edge 1118) | (Middle_frontal)<=>(Middle_temporal) | (Central_executive;Salience)<=>(Default_mode;Central_executive) |
| 1421) | rfMRI connectivity (ICA100 edge 1119) | (Putamen;Caudate)<=>(Middle_temporal) | (Subcortical-cerebellum)<=>(Default_mode;Central_executive) |
| 1422) | rfMRI connectivity (ICA100 edge 1120) | (Precuneus;Superior_parietal)<=>(Middle_temporal) | (Attention;Central_executive)<=>(Default_mode;Central_executive) |
| 1423) | rfMRI connectivity (ICA100 edge 1121) | (Superior_frontal;Middle_frontal)<=>(Middle_temporal) | (Central_executive)<=>(Default_mode;Central_executive) |
| 1424) | rfMRI connectivity (ICA100 edge 1122) | (Inferior_temporal;Middle_temporal)<=>(Middle_temporal) | (Attention;Visual)<=>(Default_mode;Central_executive) |
| 1425) | rfMRI connectivity (ICA100 edge 1123) | (Inferior_temporal;Inferior_occipital)<=>(Middle_temporal) | (Attention;Visual)<=>(Default_mode;Central_executive) |
| 1426) | rfMRI connectivity (ICA100 edge 1124) | (Inferior_temporal;Fusiform;Temporal_pole)<=>(Middle_temporal) | (Limbic;Default_mode)<=>(Default_mode;Central_executive) |
| 1427) | rfMRI connectivity (ICA100 edge 1125) | (Inferior_frontal)<=>(Middle_temporal) | (Default_mode;Central_executive)<=>(Default_mode;Central_executive) |
| 1428) | rfMRI connectivity (ICA100 edge 1126) | (Superior_frontal;Middle_frontal)<=>(Middle_temporal) | (Salience;Default_mode)<=>(Default_mode;Central_executive) |
| 1429) | rfMRI connectivity (ICA100 edge 1127) | (Inferior_temporal;Middle_temporal)<=>(Middle_temporal) | (Central_executive;Default_mode)<=>(Default_mode;Central_executive) |
| 1430) | rfMRI connectivity (ICA100 edge 1128) | (Superior_frontal;Middle_frontal)<=>(Middle_temporal) | (Central_executive;Salience;Default_mode)<=>(Default_mode;Central_executive) |
| 1431) | rfMRI connectivity (ICA100 edge 1129) | (Calcarine;Lingual;Cuneus)<=>(Middle_temporal;Angular) | (Visual)<=>(Default_mode) |

| | | | |
|---|---|---|---|
| 1432) | rfMRI connectivity (ICA100 edge 1130) | (Rolandic_operculum;SupraMarginal;Insula)<=>(Middle_temporal;Angular) | (Salience;Motor)<=>(Default_mode) |
| 1433) | rfMRI connectivity (ICA100 edge 1131) | (Lingual;Fusiform)<=>(Middle_temporal;Angular) | (Visual)<=>(Default_mode) |
| 1434) | rfMRI connectivity (ICA100 edge 1132) | (Middle_occipital;Superior_occipital)<=>(Middle_temporal;Angular) | (Attention;Visual)<=>(Default_mode) |
| 1435) | rfMRI connectivity (ICA100 edge 1133) | (Precuneus;Angular;Middle_cingulate)<=>(Middle_temporal;Angular) | (Default_mode;Central_executive)<=>(Default_mode) |
| 1436) | rfMRI connectivity (ICA100 edge 1134) | (Postcentral;Precentral)<=>(Middle_temporal;Angular) | (Motor)<=>(Default_mode) |
| 1437) | rfMRI connectivity (ICA100 edge 1135) | (Superior_frontal;Anterior_cingulate)<=>(Middle_temporal;Angular) | (Default_mode;Limbic)<=>(Default_mode) |
| 1438) | rfMRI connectivity (ICA100 edge 1136) | (Calcarine;Lingual)<=>(Middle_temporal;Angular) | (Visual)<=>(Default_mode) |
| 1439) | rfMRI connectivity (ICA100 edge 1137) | (Middle_temporal;Temporal_pole)<=>(Middle_temporal;Angular) | (Default_mode)<=>(Default_mode) |
| 1440) | rfMRI connectivity (ICA100 edge 1138) | (Middle_occipital;Precuneus;Calcarine)<=>(Middle_temporal;Angular) | (Default_mode;Central_executive)<=>(Default_mode) |
| 1441) | rfMRI connectivity (ICA100 edge 1139) | (Angular;Middle_temporal)<=>(Middle_temporal;Angular) | (Default_mode;Central_executive)<=>(Default_mode) |
| 1442) | rfMRI connectivity (ICA100 edge 1140) | (Middle_frontal;Cerebellum)<=>(Middle_temporal;Angular) | (Central_executive;Default_mode)<=>(Default_mode) |
| 1443) | rfMRI connectivity (ICA100 edge 1141) | (Superior_frontal)<=>(Middle_temporal;Angular) | (Default_mode)<=>(Default_mode) |
| 1444) | rfMRI connectivity (ICA100 edge 1142) | (Cuneus;Superior_occipital)<=>(Middle_temporal;Angular) | (Visual)<=>(Default_mode) |
| 1445) | rfMRI connectivity (ICA100 edge 1143) | (Insula;Anterior_cingulate)<=>(Middle_temporal;Angular) | (Salience;Default_mode)<=>(Default_mode) |
| 1446) | rfMRI connectivity (ICA100 edge 1144) | (Inferior_occipital;Middle_occipital)<=>(Middle_temporal;Angular) | (Visual)<=>(Default_mode) |
| 1447) | rfMRI connectivity (ICA100 edge 1145) | (Cerebellum)<=>(Middle_temporal;Angular) | (Subcortical-cerebellum)<=>(Default_mode) |
| 1448) | rfMRI connectivity (ICA100 edge 1146) | (Inferior_parietal;Postcentral)<=>(Middle_temporal;Angular) | (Attention;Central_executive;Salience)<=>(Default_mode) |
| 1449) | rfMRI connectivity (ICA100 edge 1147) | (Precuneus;Cuneus)<=>(Middle_temporal;Angular) | (Default_mode;Central_executive)<=>(Default_mode) |
| 1450) | rfMRI connectivity (ICA100 edge 1148) | (Postcentral;Precentral)<=>(Middle_temporal;Angular) | (Motor;Attention)<=>(Default_mode) |
| 1451) | rfMRI connectivity (ICA100 edge 1149) | (Superior_frontal)<=>(Middle_temporal;Angular) | (Default_mode;Central_executive)<=>(Default_mode) |
| 1452) | rfMRI connectivity (ICA100 edge 1150) | (Superior_temporal)<=>(Middle_temporal;Angular) | (Default_mode;Motor)<=>(Default_mode) |
| 1453) | rfMRI connectivity (ICA100 edge 1151) | (Cerebellum)<=>(Middle_temporal;Angular) | (Subcortical-cerebellum)<=>(Default_mode) |
| 1454) | rfMRI connectivity (ICA100 edge 1152) | (Inferior_parietal;Angular)<=>(Middle_temporal;Angular) | (Central_executive;Attention)<=>(Default_mode) |
| 1455) | rfMRI connectivity (ICA100 edge 1153) | (Inferior_frontal;Precentral)<=>(Middle_temporal;Angular) | (Central_executive)<=>(Default_mode) |
| 1456) | rfMRI connectivity (ICA100 edge 1154) | (Inferior_parietal;Inferior_frontal;SupraMarginal)<=>(Middle_temporal;Angular) | (Attention;Central_executive)<=>(Default_mode) |
| 1457) | rfMRI connectivity (ICA100 edge 1155) | (Precentral;Superior_frontal;Supp_motor_area)<=>(Middle_temporal;Angular) | (Attention;Salience;Motor)<=>(Default_mode) |
| 1458) | rfMRI connectivity (ICA100 edge 1156) | (Supp_motor_area;Inferior_frontal)<=>(Middle_temporal;Angular) | (Salience;Default_mode)<=>(Default_mode) |
| 1459) | rfMRI connectivity (ICA100 edge 1157) | (SupraMarginal;Inferior_parietal)<=>(Middle_temporal;Angular) | (Central_executive;Salience)<=>(Default_mode) |

| | | | |
|---|---|---|---|
| 1460) | rfMRI connectivity (ICA100 edge 1158) | (Paracentral)<=>(Middle_temporal;Angular) | (Motor)<=>(Default_mode) |
| 1461) | rfMRI connectivity (ICA100 edge 1159) | (Middel_frontal)<=>(Middle_temporal;Angular) | (Central_executive)<=>(Default_mode) |
| 1462) | rfMRI connectivity (ICA100 edge 1160) | (Postcentral;Precentral)<=>(Middle_temporal;Angular) | (Motor;Attention)<=>(Default_mode) |
| 1463) | rfMRI connectivity (ICA100 edge 1161) | (Inferior_frontal;Middle_temporal;Supp_motor_area)<=>(Middle_temporal;Angular) | (Default_mode;Salience)<=>(Default_mode) |
| 1464) | rfMRI connectivity (ICA100 edge 1162) | (Superior_parietal;Postcentral;Precuneus)<=>(Middle_temporal;Angular) | (Attention)<=>(Default_mode) |
| 1465) | rfMRI connectivity (ICA100 edge 1163) | (Precentral;Postcentral)<=>(Middle_temporal;Angular) | (Motor)<=>(Default_mode) |
| 1466) | rfMRI connectivity (ICA100 edge 1164) | (Precuneus)<=>(Middle_temporal;Angular) | (Default_mode;Central_executive)<=>(Default_mode) |
| 1467) | rfMRI connectivity (ICA100 edge 1165) | (Middle_frontal)<=>(Middle_temporal;Angular) | (Central_executive;Salience)<=>(Default_mode) |
| 1468) | rfMRI connectivity (ICA100 edge 1166) | (Putamen;Caudate)<=>(Middle_temporal;Angular) | (Subcortical-cerebellum)<=>(Default_mode) |
| 1469) | rfMRI connectivity (ICA100 edge 1167) | (Precuneus;Superior_parietal)<=>(Middle_temporal;Angular) | (Attention;Central_executive)<=>(Default_mode) |
| 1470) | rfMRI connectivity (ICA100 edge 1168) | (Superior_frontal;Middle_frontal)<=>(Middle_temporal;Angular) | (Central_executive)<=>(Default_mode) |
| 1471) | rfMRI connectivity (ICA100 edge 1169) | (Inferior_temporal;Middle_temporal)<=>(Middle_temporal;Angular) | (Attention;Visual)<=>(Default_mode) |
| 1472) | rfMRI connectivity (ICA100 edge 1170) | (Inferior_temporal;Inferior_occipital)<=>(Middle_temporal;Angular) | (Attention;Visual)<=>(Default_mode) |
| 1473) | rfMRI connectivity (ICA100 edge 1171) | (Inferior_temporal;Fusiform;Temporal_pole)<=>(Middle_temporal;Angular) | (Limbic;Default_mode)<=>(Default_mode) |
| 1474) | rfMRI connectivity (ICA100 edge 1172) | (Inferior_frontal)<=>(Middle_temporal;Angular) | (Default_mode;Central_executive)<=>(Default_mode) |
| 1475) | rfMRI connectivity (ICA100 edge 1173) | (Superior_frontal;Middle_frontal)<=>(Middle_temporal;Angular) | (Salience;Default_mode)<=>(Default_mode) |
| 1476) | rfMRI connectivity (ICA100 edge 1174) | (Inferior_temporal;Middle_temporal)<=>(Middle_temporal;Angular) | (Central_executive;Default_mode)<=>(Default_mode) |
| 1477) | rfMRI connectivity (ICA100 edge 1175) | (Superior_frontal;Middle_frontal)<=>(Middle_temporal;Angular) | (Central_executive;Salience;Default_mode)<=>(Default_mode) |
| 1478) | rfMRI connectivity (ICA100 edge 1176) | (Middle_temporal)<=>(Middle_temporal;Angular) | (Default_mode;Central_executive)<=>(Default_mode) |
| 1479) | rfMRI connectivity (ICA100 edge 1177) | (Calcarine;Lingual;Cuneus)<=>(Orbital) | (Visual)<=>(Limbic) |
| 1480) | rfMRI connectivity (ICA100 edge 1178) | (Rolandic_operculum;SupraMarginal;Insula)<=>(Orbital) | (Salience;Motor)<=>(Limbic) |
| 1481) | rfMRI connectivity (ICA100 edge 1179) | (Lingual;Fusiform)<=>(Orbital) | (Visual)<=>(Limbic) |
| 1482) | rfMRI connectivity (ICA100 edge 1180) | (Middle_occipital;Superior_occipital)<=>(Orbital) | (Attention;Visual)<=>(Limbic) |
| 1483) | rfMRI connectivity (ICA100 edge 1181) | (Precuneus;Angular;Middle_cingulate)<=>(Orbital) | (Default_mode;Central_executive)<=>(Limbic) |
| 1484) | rfMRI connectivity (ICA100 edge 1182) | (Postcentral;Precentral)<=>(Orbital) | (Motor)<=>(Limbic) |
| 1485) | rfMRI connectivity (ICA100 edge 1183) | (Superior_frontal;Anterior_cingulate)<=>(Orbital) | (Default_mode;Limbic)<=>(Limbic) |
| 1486) | rfMRI connectivity (ICA100 edge 1184) | (Calcarine;Lingual)<=>(Orbital) | (Visual)<=>(Limbic) |
| 1487) | rfMRI connectivity (ICA100 edge 1185) | (Middle_temporal;Temporal_pole)<=>(Orbital) | (Default_mode)<=>(Limbic) |

| | | | |
|---|---|---|---|
| 1488) | rfMRI connectivity (ICA100 edge 1186) | (Middle_occipital;Precuneus;Calcarine)<=>(Orbital) | (Default_mode;Central_executive)<=>(Limbic) |
| 1489) | rfMRI connectivity (ICA100 edge 1187) | (Angular;Middle_temporal)<=>(Orbital) | (Default_mode;Central_executive)<=>(Limbic) |
| 1490) | rfMRI connectivity (ICA100 edge 1188) | (Middle_frontal;Cerebellum)<=>(Orbital) | (Central_executive;Default_mode)<=>(Limbic) |
| 1491) | rfMRI connectivity (ICA100 edge 1189) | (Superior_frontal)<=>(Orbital) | (Default_mode)<=>(Limbic) |
| 1492) | rfMRI connectivity (ICA100 edge 1190) | (Cuneus;Superior_occipital)<=>(Orbital) | (Visual)<=>(Limbic) |
| 1493) | rfMRI connectivity (ICA100 edge 1191) | (Insula;Anterior_cingulate)<=>(Orbital) | (Salience;Default_mode)<=>(Limbic) |
| 1494) | rfMRI connectivity (ICA100 edge 1192) | (Inferior_occipital;Middle_occipital)<=>(Orbital) | (Visual)<=>(Limbic) |
| 1495) | rfMRI connectivity (ICA100 edge 1193) | (Cerebellum)<=>(Orbital) | (Subcortical-cerebellum)<=>(Limbic) |
| 1496) | rfMRI connectivity (ICA100 edge 1194) | (Inferior_parietal;Postcentral)<=>(Orbital) | (Attention;Central_executive;Salience)<=>(Limbic) |
| 1497) | rfMRI connectivity (ICA100 edge 1195) | (Precuneus;Cuneus)<=>(Orbital) | (Default_mode;Central_executive)<=>(Limbic) |
| 1498) | rfMRI connectivity (ICA100 edge 1196) | (Postcentral;Precentral)<=>(Orbital) | (Motor;Attention)<=>(Limbic) |
| 1499) | rfMRI connectivity (ICA100 edge 1197) | (Superior_frontal)<=>(Orbital) | (Default_mode;Central_executive)<=>(Limbic) |
| 1500) | rfMRI connectivity (ICA100 edge 1198) | (Superior_temporal)<=>(Orbital) | (Default_mode;Motor)<=>(Limbic) |
| 1501) | rfMRI connectivity (ICA100 edge 1199) | (Cerebellum)<=>(Orbital) | (Subcortical-cerebellum)<=>(Limbic) |
| 1502) | rfMRI connectivity (ICA100 edge 1200) | (Inferior_parietal;Angular)<=>(Orbital) | (Central_executive;Attention)<=>(Limbic) |
| 1503) | rfMRI connectivity (ICA100 edge 1201) | (Inferior_frontal;Precentral)<=>(Orbital) | (Central_executive)<=>(Limbic) |
| 1504) | rfMRI connectivity (ICA100 edge 1202) | (Inferior_parietal;Inferior_frontal;SupraMarginal)<=>(Orbital) | (Attention;Central_executive)<=>(Limbic) |
| 1505) | rfMRI connectivity (ICA100 edge 1203) | (Precentral;Superior_frontal;Supp_motor_area)<=>(Orbital) | (Attention;Salience;Motor)<=>(Limbic) |
| 1506) | rfMRI connectivity (ICA100 edge 1204) | (Supp_motor_area;Inferior_frontal)<=>(Orbital) | (Salience;Default_mode)<=>(Limbic) |
| 1507) | rfMRI connectivity (ICA100 edge 1205) | (SupraMarginal;Inferior_parietal)<=>(Orbital) | (Central_executive;Salience)<=>(Limbic) |
| 1508) | rfMRI connectivity (ICA100 edge 1206) | (Paracentral)<=>(Orbital) | (Motor)<=>(Limbic) |
| 1509) | rfMRI connectivity (ICA100 edge 1207) | (Middel_frontal)<=>(Orbital) | (Central_executive)<=>(Limbic) |
| 1510) | rfMRI connectivity (ICA100 edge 1208) | (Postcentral;Precentral)<=>(Orbital) | (Motor;Attention)<=>(Limbic) |
| 1511) | rfMRI connectivity (ICA100 edge 1209) | (Inferior_frontal;Middle_temporal;Supp_motor_area)<=>(Orbital) | (Default_mode;Salience)<=>(Limbic) |
| 1512) | rfMRI connectivity (ICA100 edge 1210) | (Superior_parietal;Postcentral;Precuneus)<=>(Orbital) | (Attention)<=>(Limbic) |
| 1513) | rfMRI connectivity (ICA100 edge 1211) | (Precentral;Postcentral)<=>(Orbital) | (Motor)<=>(Limbic) |
| 1514) | rfMRI connectivity (ICA100 edge 1212) | (Precuneus)<=>(Orbital) | (Default_mode;Central_executive)<=>(Limbic) |
| 1515) | rfMRI connectivity (ICA100 edge 1213) | (Middle_frontal)<=>(Orbital) | (Central_executive;Salience)<=>(Limbic) |
| 1516) | rfMRI connectivity (ICA100 edge 1214) | (Putamen;Caudate)<=>(Orbital) | (Subcortical-cerebellum)<=>(Limbic) |

| | | | |
|---|---|---|---|
| 1517) | rfMRI connectivity (ICA100 edge 1215) | (Precuneus;Superior_parietal)<=>(Orbital) | (Attention;Central_executive)<=>(Limbic) |
| 1518) | rfMRI connectivity (ICA100 edge 1216) | (Superior_frontal;Middle_frontal)<=>(Orbital) | (Central_executive)<=>(Limbic) |
| 1519) | rfMRI connectivity (ICA100 edge 1217) | (Inferior_temporal;Middle_temporal)<=>(Orbital) | (Attention;Visual)<=>(Limbic) |
| 1520) | rfMRI connectivity (ICA100 edge 1218) | (Inferior_temporal;Inferior_occipital)<=>(Orbital) | (Attention;Visual)<=>(Limbic) |
| 1521) | rfMRI connectivity (ICA100 edge 1219) | (Inferior_temporal;Fusiform;Temporal_pole)<=>(Orbital) | (Limbic;Default_mode)<=>(Limbic) |
| 1522) | rfMRI connectivity (ICA100 edge 1220) | (Inferior_frontal)<=>(Orbital) | (Default_mode;Central_executive)<=>(Limbic) |
| 1523) | rfMRI connectivity (ICA100 edge 1221) | (Superior_frontal;Middle_frontal)<=>(Orbital) | (Salience;Default_mode)<=>(Limbic) |
| 1524) | rfMRI connectivity (ICA100 edge 1222) | (Inferior_temporal;Middle_temporal)<=>(Orbital) | (Central_executive;Default_mode)<=>(Limbic) |
| 1525) | rfMRI connectivity (ICA100 edge 1223) | (Superior_frontal;Middle_frontal)<=>(Orbital) | (Central_executive;Salience;Default_mode)<=>(Limbic) |
| 1526) | rfMRI connectivity (ICA100 edge 1224) | (Middle_temporal)<=>(Orbital) | (Default_mode;Central_executive)<=>(Limbic) |
| 1527) | rfMRI connectivity (ICA100 edge 1225) | (Middle_temporal;Angular)<=>(Orbital) | (Default_mode)<=>(Limbic) |
| 1528) | rfMRI connectivity (ICA100 edge 1226) | (Calcarine;Lingual;Cuneus)<=>(Cerebellum;Inferior_temporal) | (Visual)<=>(Subcortical-cerebellum) |
| 1529) | rfMRI connectivity (ICA100 edge 1227) | (Rolandic_operculum;SupraMarginal;Insula)<=>(Cerebellum;Inferior_temporal) | (Salience;Motor)<=>(Subcortical-cerebellum) |
| 1530) | rfMRI connectivity (ICA100 edge 1228) | (Lingual;Fusiform)<=>(Cerebellum;Inferior_temporal) | (Visual)<=>(Subcortical-cerebellum) |
| 1531) | rfMRI connectivity (ICA100 edge 1229) | (Middle_occipital;Superior_occipital)<=>(Cerebellum;Inferior_temporal) | (Attention;Visual)<=>(Subcortical-cerebellum) |
| 1532) | rfMRI connectivity (ICA100 edge 1230) | (Precuneus;Angular;Middle_cingulate)<=>(Cerebellum;Inferior_temporal) | (Default_mode;Central_executive)<=>(Subcortical-cerebellum) |
| 1533) | rfMRI connectivity (ICA100 edge 1231) | (Postcentral;Precentral)<=>(Cerebellum;Inferior_temporal) | (Motor)<=>(Subcortical-cerebellum) |
| 1534) | rfMRI connectivity (ICA100 edge 1232) | (Superior_frontal;Anterior_cingulate)<=>(Cerebellum;Inferior_temporal) | (Default_mode;Limbic)<=>(Subcortical-cerebellum) |
| 1535) | rfMRI connectivity (ICA100 edge 1233) | (Calcarine;Lingual)<=>(Cerebellum;Inferior_temporal) | (Visual)<=>(Subcortical-cerebellum) |
| 1536) | rfMRI connectivity (ICA100 edge 1234) | (Middle_temporal;Temporal_pole)<=>(Cerebellum;Inferior_temporal) | (Default_mode)<=>(Subcortical-cerebellum) |
| 1537) | rfMRI connectivity (ICA100 edge 1235) | (Middle_occipital;Precuneus;Calcarine)<=>(Cerebellum;Inferior_temporal) | (Default_mode;Central_executive)<=>(Subcortical-cerebellum) |
| 1538) | rfMRI connectivity (ICA100 edge 1236) | (Angular;Middle_temporal)<=>(Cerebellum;Inferior_temporal) | (Default_mode;Central_executive)<=>(Subcortical-cerebellum) |
| 1539) | rfMRI connectivity (ICA100 edge 1237) | (Middle_frontal;Cerebellum)<=>(Cerebellum;Inferior_temporal) | (Central_executive;Default_mode)<=>(Subcortical-cerebellum) |
| 1540) | rfMRI connectivity (ICA100 edge 1238) | (Superior_frontal)<=>(Cerebellum;Inferior_temporal) | (Default_mode)<=>(Subcortical-cerebellum) |
| 1541) | rfMRI connectivity (ICA100 edge 1239) | (Cuneus;Superior_occipital)<=>(Cerebellum;Inferior_temporal) | (Visual)<=>(Subcortical-cerebellum) |
| 1542) | rfMRI connectivity (ICA100 edge 1240) | (Insula;Anterior_cingulate)<=>(Cerebellum;Inferior_temporal) | (Salience;Default_mode)<=>(Subcortical-cerebellum) |
| 1543) | rfMRI connectivity (ICA100 edge 1241) | (Inferior_occipital;Middle_occipital)<=>(Cerebellum;Inferior_temporal) | (Visual)<=>(Subcortical-cerebellum) |

| | | | |
|---|---|---|---|
| 1544) | rfMRI connectivity (ICA100 edge 1242) | (Cerebellum)<=>(Cerebellum;Inferior_temporal) | (Subcortical-cerebellum)<=>(Subcortical-cerebellum) |
| 1545) | rfMRI connectivity (ICA100 edge 1243) | (Inferior_parietal;Postcentral)<=>(Cerebellum;Inferior_temporal) | (Attention;Central_executive;Salience)<=>(Subcortical-cerebellum) |
| 1546) | rfMRI connectivity (ICA100 edge 1244) | (Precuneus;Cuneus)<=>(Cerebellum;Inferior_temporal) | (Default_mode;Central_executive)<=>(Subcortical-cerebellum) |
| 1547) | rfMRI connectivity (ICA100 edge 1245) | (Postcentral;Precentral)<=>(Cerebellum;Inferior_temporal) | (Motor;Attention)<=>(Subcortical-cerebellum) |
| 1548) | rfMRI connectivity (ICA100 edge 1246) | (Superior_frontal)<=>(Cerebellum;Inferior_temporal) | (Default_mode;Central_executive)<=>(Subcortical-cerebellum) |
| 1549) | rfMRI connectivity (ICA100 edge 1247) | (Superior_temporal)<=>(Cerebellum;Inferior_temporal) | (Default_mode;Motor)<=>(Subcortical-cerebellum) |
| 1550) | rfMRI connectivity (ICA100 edge 1248) | (Cerebellum)<=>(Cerebellum;Inferior_temporal) | (Subcortical-cerebellum)<=>(Subcortical-cerebellum) |
| 1551) | rfMRI connectivity (ICA100 edge 1249) | (Inferior_parietal;Angular)<=>(Cerebellum;Inferior_temporal) | (Central_executive;Attention)<=>(Subcortical-cerebellum) |
| 1552) | rfMRI connectivity (ICA100 edge 1250) | (Inferior_frontal;Precentral)<=>(Cerebellum;Inferior_temporal) | (Central_executive)<=>(Subcortical-cerebellum) |
| 1553) | rfMRI connectivity (ICA100 edge 1251) | (Inferior_parietal;Inferior_frontal;SupraMarginal)<=>(Cerebellum;Inferior_temporal) | (Attention;Central_executive)<=>(Subcortical-cerebellum) |
| 1554) | rfMRI connectivity (ICA100 edge 1252) | (Precentral;Superior_frontal;Supp_motor_area)<=>(Cerebellum;Inferior_temporal) | (Attention;Salience;Motor)<=>(Subcortical-cerebellum) |
| 1555) | rfMRI connectivity (ICA100 edge 1253) | (Supp_motor_area;Inferior_frontal)<=>(Cerebellum;Inferior_temporal) | (Salience;Default_mode)<=>(Subcortical-cerebellum) |
| 1556) | rfMRI connectivity (ICA100 edge 1254) | (SupraMarginal;Inferior_parietal)<=>(Cerebellum;Inferior_temporal) | (Central_executive;Salience)<=>(Subcortical-cerebellum) |
| 1557) | rfMRI connectivity (ICA100 edge 1255) | (Paracentral)<=>(Cerebellum;Inferior_temporal) | (Motor)<=>(Subcortical-cerebellum) |
| 1558) | rfMRI connectivity (ICA100 edge 1256) | (Middel_frontal)<=>(Cerebellum;Inferior_temporal) | (Central_executive)<=>(Subcortical-cerebellum) |
| 1559) | rfMRI connectivity (ICA100 edge 1257) | (Postcentral;Precentral)<=>(Cerebellum;Inferior_temporal) | (Motor;Attention)<=>(Subcortical-cerebellum) |
| 1560) | rfMRI connectivity (ICA100 edge 1258) | (Inferior_frontal;Middle_temporal;Supp_motor_area)<=>(Cerebellum;Inferior_temporal) | (Default_mode;Salience)<=>(Subcortical-cerebellum) |
| 1561) | rfMRI connectivity (ICA100 edge 1259) | (Superior_parietal;Postcentral;Precuneus)<=>(Cerebellum;Inferior_temporal) | (Attention)<=>(Subcortical-cerebellum) |
| 1562) | rfMRI connectivity (ICA100 edge 1260) | (Precentral;Postcentral)<=>(Cerebellum;Inferior_temporal) | (Motor)<=>(Subcortical-cerebellum) |
| 1563) | rfMRI connectivity (ICA100 edge 1261) | (Precuneus)<=>(Cerebellum;Inferior_temporal) | (Default_mode;Central_executive)<=>(Subcortical-cerebellum) |
| 1564) | rfMRI connectivity (ICA100 edge 1262) | (Middle_frontal)<=>(Cerebellum;Inferior_temporal) | (Central_executive;Salience)<=>(Subcortical-cerebellum) |
| 1565) | rfMRI connectivity (ICA100 edge 1263) | (Putamen;Caudate)<=>(Cerebellum;Inferior_temporal) | (Subcortical-cerebellum)<=>(Subcortical-cerebellum) |
| 1566) | rfMRI connectivity (ICA100 edge 1264) | (Precuneus;Superior_parietal)<=>(Cerebellum;Inferior_temporal) | (Attention;Central_executive)<=>(Subcortical-cerebellum) |
| 1567) | rfMRI connectivity (ICA100 edge 1265) | (Superior_frontal;Middle_frontal)<=>(Cerebellum;Inferior_temporal) | (Central_executive)<=>(Subcortical-cerebellum) |

| | | | |
|---|---|---|---|
| 1568) | rfMRI connectivity (ICA100 edge 1266) | (Inferior_temporal;Middle_temporal)<=>(Cerebellum;Inferior_temporal) | (Attention;Visual)<=>(Subcortical-cerebellum) |
| 1569) | rfMRI connectivity (ICA100 edge 1267) | (Inferior_temporal;Inferior_occipital)<=>(Cerebellum;Inferior_temporal) | (Attention;Visual)<=>(Subcortical-cerebellum) |
| 1570) | rfMRI connectivity (ICA100 edge 1268) | (Inferior_temporal;Fusiform;Temporal_pole)<=>(Cerebellum;Inferior_temporal) | (Limbic;Default_mode)<=>(Subcortical-cerebellum) |
| 1571) | rfMRI connectivity (ICA100 edge 1269) | (Inferior_frontal)<=>(Cerebellum;Inferior_temporal) | (Default_mode;Central_executive)<=>(Subcortical-cerebellum) |
| 1572) | rfMRI connectivity (ICA100 edge 1270) | (Superior_frontal;Middle_frontal)<=>(Cerebellum;Inferior_temporal) | (Salience;Default_mode)<=>(Subcortical-cerebellum) |
| 1573) | rfMRI connectivity (ICA100 edge 1271) | (Inferior_temporal;Middle_temporal)<=>(Cerebellum;Inferior_temporal) | (Central_executive;Default_mode)<=>(Subcortical-cerebellum) |
| 1574) | rfMRI connectivity (ICA100 edge 1272) | (Superior_frontal;Middle_frontal)<=>(Cerebellum;Inferior_temporal) | (Central_executive;Salience;Default_mode)<=>(Subcortical-cerebellum) |
| 1575) | rfMRI connectivity (ICA100 edge 1273) | (Middle_temporal)<=>(Cerebellum;Inferior_temporal) | (Default_mode;Central_executive)<=>(Subcortical-cerebellum) |
| 1576) | rfMRI connectivity (ICA100 edge 1274) | (Middle_temporal;Angular)<=>(Cerebellum;Inferior_temporal) | (Default_mode)<=>(Subcortical-cerebellum) |
| 1577) | rfMRI connectivity (ICA100 edge 1275) | (Orbital)<=>(Cerebellum;Inferior_temporal) | (Limbic)<=>(Subcortical-cerebellum) |
| 1578) | rfMRI connectivity (ICA100 edge 1276) | (Calcarine;Lingual;Cuneus)<=>(Cerebellum;Inferior_temporal) | (Visual)<=>(Subcortical-cerebellum) |
| 1579) | rfMRI connectivity (ICA100 edge 1277) | (Rolandic_operculum;SupraMarginal;Insula)<=>(Cerebellum;Inferior_temporal) | (Salience;Motor)<=>(Subcortical-cerebellum) |
| 1580) | rfMRI connectivity (ICA100 edge 1278) | (Lingual;Fusiform)<=>(Cerebellum;Inferior_temporal) | (Visual)<=>(Subcortical-cerebellum) |
| 1581) | rfMRI connectivity (ICA100 edge 1279) | (Middle_occipital;Superior_occipital)<=>(Cerebellum;Inferior_temporal) | (Attention;Visual)<=>(Subcortical-cerebellum) |
| 1582) | rfMRI connectivity (ICA100 edge 1280) | (Precuneus;Angular;Middle_cingulate)<=>(Cerebellum;Inferior_temporal) | (Default_mode;Central_executive)<=>(Subcortical-cerebellum) |
| 1583) | rfMRI connectivity (ICA100 edge 1281) | (Postcentral;Precentral)<=>(Cerebellum;Inferior_temporal) | (Motor)<=>(Subcortical-cerebellum) |
| 1584) | rfMRI connectivity (ICA100 edge 1282) | (Superior_frontal;Anterior_cingulate)<=>(Cerebellum;Inferior_temporal) | (Default_mode;Limbic)<=>(Subcortical-cerebellum) |
| 1585) | rfMRI connectivity (ICA100 edge 1283) | (Calcarine;Lingual)<=>(Cerebellum;Inferior_temporal) | (Visual)<=>(Subcortical-cerebellum) |
| 1586) | rfMRI connectivity (ICA100 edge 1284) | (Middle_temporal;Temporal_pole)<=>(Cerebellum;Inferior_temporal) | (Default_mode)<=>(Subcortical-cerebellum) |
| 1587) | rfMRI connectivity (ICA100 edge 1285) | (Middle_occipital;Precuneus;Calcarine)<=>(Cerebellum;Inferior_temporal) | (Default_mode;Central_executive)<=>(Subcortical-cerebellum) |
| 1588) | rfMRI connectivity (ICA100 edge 1286) | (Angular;Middle_temporal)<=>(Cerebellum;Inferior_temporal) | (Default_mode;Central_executive)<=>(Subcortical-cerebellum) |
| 1589) | rfMRI connectivity (ICA100 edge 1287) | (Middle_frontal;Cerebellum)<=>(Cerebellum;Inferior_temporal) | (Central_executive;Default_mode)<=>(Subcortical-cerebellum) |
| 1590) | rfMRI connectivity (ICA100 edge 1288) | (Superior_frontal)<=>(Cerebellum;Inferior_temporal) | (Default_mode)<=>(Subcortical-cerebellum) |
| 1591) | rfMRI connectivity (ICA100 edge 1289) | (Cuneus;Superior_occipital)<=>(Cerebellum;Inferior_temporal) | (Visual)<=>(Subcortical-cerebellum) |
| 1592) | rfMRI connectivity (ICA100 edge 1290) | (Insula;Anterior_cingulate)<=>(Cerebellum;Inferior_temporal) | (Salience;Default_mode)<=>(Subcortical-cerebellum) |

| | | | |
|---|---|---|---|
| 1593) | rfMRI connectivity (ICA100 edge 1291) | (Inferior_occipital;Middle_occipital)<=>(Cerebellum;Inferior_temporal) | (Visual)<=>(Subcortical-cerebellum) |
| 1594) | rfMRI connectivity (ICA100 edge 1292) | (Cerebellum)<=>(Cerebellum;Inferior_temporal) | (Subcortical-cerebellum)<=>(Subcortical-cerebellum) |
| 1595) | rfMRI connectivity (ICA100 edge 1293) | (Inferior_parietal;Postcentral)<=>(Cerebellum;Inferior_temporal) | (Attention;Central_executive;Salience)<=>(Subcortical-cerebellum) |
| 1596) | rfMRI connectivity (ICA100 edge 1294) | (Precuneus;Cuneus)<=>(Cerebellum;Inferior_temporal) | (Default_mode;Central_executive)<=>(Subcortical-cerebellum) |
| 1597) | rfMRI connectivity (ICA100 edge 1295) | (Postcentral;Precentral)<=>(Cerebellum;Inferior_temporal) | (Motor;Attention)<=>(Subcortical-cerebellum) |
| 1598) | rfMRI connectivity (ICA100 edge 1296) | (Superior_frontal)<=>(Cerebellum;Inferior_temporal) | (Default_mode;Central_executive)<=>(Subcortical-cerebellum) |
| 1599) | rfMRI connectivity (ICA100 edge 1297) | (Superior_temporal)<=>(Cerebellum;Inferior_temporal) | (Default_mode;Motor)<=>(Subcortical-cerebellum) |
| 1600) | rfMRI connectivity (ICA100 edge 1298) | (Cerebellum)<=>(Cerebellum;Inferior_temporal) | (Subcortical-cerebellum)<=>(Subcortical-cerebellum) |
| 1601) | rfMRI connectivity (ICA100 edge 1299) | (Inferior_parietal;Angular)<=>(Cerebellum;Inferior_temporal) | (Central_executive;Attention)<=>(Subcortical-cerebellum) |
| 1602) | rfMRI connectivity (ICA100 edge 1300) | (Inferior_frontal;Precentral)<=>(Cerebellum;Inferior_temporal) | (Central_executive)<=>(Subcortical-cerebellum) |
| 1603) | rfMRI connectivity (ICA100 edge 1301) | (Inferior_parietal;Inferior_frontal;SupraMarginal)<=>(Cerebellum;Inferior_temporal) | (Attention;Central_executive)<=>(Subcortical-cerebellum) |
| 1604) | rfMRI connectivity (ICA100 edge 1302) | (Precentral;Superior_frontal;Supp_motor_area)<=>(Cerebellum;Inferior_temporal) | (Attention;Salience;Motor)<=>(Subcortical-cerebellum) |
| 1605) | rfMRI connectivity (ICA100 edge 1303) | (Supp_motor_area;Inferior_frontal)<=>(Cerebellum;Inferior_temporal) | (Salience;Default_mode)<=>(Subcortical-cerebellum) |
| 1606) | rfMRI connectivity (ICA100 edge 1304) | (SupraMarginal;Inferior_parietal)<=>(Cerebellum;Inferior_temporal) | (Central_executive;Salience)<=>(Subcortical-cerebellum) |
| 1607) | rfMRI connectivity (ICA100 edge 1305) | (Paracentral)<=>(Cerebellum;Inferior_temporal) | (Motor)<=>(Subcortical-cerebellum) |
| 1608) | rfMRI connectivity (ICA100 edge 1306) | (Middel_frontal)<=>(Cerebellum;Inferior_temporal) | (Central_executive)<=>(Subcortical-cerebellum) |
| 1609) | rfMRI connectivity (ICA100 edge 1307) | (Postcentral;Precentral)<=>(Cerebellum;Inferior_temporal) | (Motor;Attention)<=>(Subcortical-cerebellum) |
| 1610) | rfMRI connectivity (ICA100 edge 1308) | (Inferior_frontal;Middle_temporal;Supp_motor_area)<=>(Cerebellum;Inferior_temporal) | (Default_mode;Salience)<=>(Subcortical-cerebellum) |
| 1611) | rfMRI connectivity (ICA100 edge 1309) | (Superior_parietal;Postcentral;Precuneus)<=>(Cerebellum;Inferior_temporal) | (Attention)<=>(Subcortical-cerebellum) |
| 1612) | rfMRI connectivity (ICA100 edge 1310) | (Precentral;Postcentral)<=>(Cerebellum;Inferior_temporal) | (Motor)<=>(Subcortical-cerebellum) |
| 1613) | rfMRI connectivity (ICA100 edge 1311) | (Precuneus)<=>(Cerebellum;Inferior_temporal) | (Default_mode;Central_executive)<=>(Subcortical-cerebellum) |
| 1614) | rfMRI connectivity (ICA100 edge 1312) | (Middle_frontal)<=>(Cerebellum;Inferior_temporal) | (Central_executive;Salience)<=>(Subcortical-cerebellum) |
| 1615) | rfMRI connectivity (ICA100 edge 1313) | (Putamen;Caudate)<=>(Cerebellum;Inferior_temporal) | (Subcortical-cerebellum)<=>(Subcortical-cerebellum) |
| 1616) | rfMRI connectivity (ICA100 edge 1314) | (Precuneus;Superior_parietal)<=>(Cerebellum;Inferior_temporal) | (Attention;Central_executive)<=>(Subcortical-cerebellum) |

| | | | |
|---|---|---|---|
| 1617) | rfMRI connectivity (ICA100 edge 1315) | (Superior_frontal;Middle_frontal)<=>(Cerebellum;Inferior_temporal) | (Central_executive)<=>(Subcortical-cerebellum) |
| 1618) | rfMRI connectivity (ICA100 edge 1316) | (Inferior_temporal;Middle_temporal)<=>(Cerebellum;Inferior_temporal) | (Attention;Visual)<=>(Subcortical-cerebellum) |
| 1619) | rfMRI connectivity (ICA100 edge 1317) | (Inferior_temporal;Inferior_occipital)<=>(Cerebellum;Inferior_temporal) | (Attention;Visual)<=>(Subcortical-cerebellum) |
| 1620) | rfMRI connectivity (ICA100 edge 1318) | (Inferior_temporal;Fusiform;Temporal_pole)<=>(Cerebellum;Inferior_temporal) | (Limbic;Default_mode)<=>(Subcortical-cerebellum) |
| 1621) | rfMRI connectivity (ICA100 edge 1319) | (Inferior_frontal)<=>(Cerebellum;Inferior_temporal) | (Default_mode;Central_executive)<=>(Subcortical-cerebellum) |
| 1622) | rfMRI connectivity (ICA100 edge 1320) | (Superior_frontal;Middle_frontal)<=>(Cerebellum;Inferior_temporal) | (Salience;Default_mode)<=>(Subcortical-cerebellum) |
| 1623) | rfMRI connectivity (ICA100 edge 1321) | (Inferior_temporal;Middle_temporal)<=>(Cerebellum;Inferior_temporal) | (Central_executive;Default_mode)<=>(Subcortical-cerebellum) |
| 1624) | rfMRI connectivity (ICA100 edge 1322) | (Superior_frontal;Middle_frontal)<=>(Cerebellum;Inferior_temporal) | (Central_executive;Salience;Default_mode)<=>(Subcortical-cerebellum) |
| 1625) | rfMRI connectivity (ICA100 edge 1323) | (Middle_temporal)<=>(Cerebellum;Inferior_temporal) | (Default_mode;Central_executive)<=>(Subcortical-cerebellum) |
| 1626) | rfMRI connectivity (ICA100 edge 1324) | (Middle_temporal;Angular)<=>(Cerebellum;Inferior_temporal) | (Default_mode)<=>(Subcortical-cerebellum) |
| 1627) | rfMRI connectivity (ICA100 edge 1325) | (Orbital)<=>(Cerebellum;Inferior_temporal) | (Limbic)<=>(Subcortical-cerebellum) |
| 1628) | rfMRI connectivity (ICA100 edge 1326) | (Cerebellum;Inferior_temporal)<=>(Cerebellum;Inferior_temporal) | (Subcortical-cerebellum)<=>(Subcortical-cerebellum) |
| 1629) | rfMRI connectivity (ICA100 edge 1327) | (Calcarine;Lingual;Cuneus)<=>(Superior_frontal) | (Visual)<=>(Limbic) |
| 1630) | rfMRI connectivity (ICA100 edge 1328) | (Rolandic_operculum;SupraMarginal;Insula)<=>(Superior_frontal) | (Salience;Motor)<=>(Limbic) |
| 1631) | rfMRI connectivity (ICA100 edge 1329) | (Lingual;Fusiform)<=>(Superior_frontal) | (Visual)<=>(Limbic) |
| 1632) | rfMRI connectivity (ICA100 edge 1330) | (Middle_occipital;Superior_occipital)<=>(Superior_frontal) | (Attention;Visual)<=>(Limbic) |
| 1633) | rfMRI connectivity (ICA100 edge 1331) | (Precuneus;Angular;Middle_cingulate)<=>(Superior_frontal) | (Default_mode;Central_executive)<=>(Limbic) |
| 1634) | rfMRI connectivity (ICA100 edge 1332) | (Postcentral;Precentral)<=>(Superior_frontal) | (Motor)<=>(Limbic) |
| 1635) | rfMRI connectivity (ICA100 edge 1333) | (Superior_frontal;Anterior_cingulate)<=>(Superior_frontal) | (Default_mode;Limbic)<=>(Limbic) |
| 1636) | rfMRI connectivity (ICA100 edge 1334) | (Calcarine;Lingual)<=>(Superior_frontal) | (Visual)<=>(Limbic) |
| 1637) | rfMRI connectivity (ICA100 edge 1335) | (Middle_temporal;Temporal_pole)<=>(Superior_frontal) | (Default_mode)<=>(Limbic) |
| 1638) | rfMRI connectivity (ICA100 edge 1336) | (Middle_occipital;Precuneus;Calcarine)<=>(Superior_frontal) | (Default_mode;Central_executive)<=>(Limbic) |
| 1639) | rfMRI connectivity (ICA100 edge 1337) | (Angular;Middle_temporal)<=>(Superior_frontal) | (Default_mode;Central_executive)<=>(Limbic) |
| 1640) | rfMRI connectivity (ICA100 edge 1338) | (Middle_frontal;Cerebellum)<=>(Superior_frontal) | (Central_executive;Default_mode)<=>(Limbic) |
| 1641) | rfMRI connectivity (ICA100 edge 1339) | (Superior_frontal)<=>(Superior_frontal) | (Default_mode)<=>(Limbic) |
| 1642) | rfMRI connectivity (ICA100 edge 1340) | (Cuneus;Superior_occipital)<=>(Superior_frontal) | (Visual)<=>(Limbic) |
| 1643) | rfMRI connectivity (ICA100 edge 1341) | (Insula;Anterior_cingulate)<=>(Superior_frontal) | (Salience;Default_mode)<=>(Limbic) |

| | | | |
|---|---|---|---|
| 1644) | rfMRI connectivity (ICA100 edge 1342) | (Inferior_occipital;Middle_occipital)<=>(Superior_frontal) | (Visual)<=>(Limbic) |
| 1645) | rfMRI connectivity (ICA100 edge 1343) | (Cerebellum)<=>(Superior_frontal) | (Subcortical-cerebellum)<=>(Limbic) |
| 1646) | rfMRI connectivity (ICA100 edge 1344) | (Inferior_parietal;Postcentral)<=>(Superior_frontal) | (Attention;Central_executive;Salience)<=>(Limbic) |
| 1647) | rfMRI connectivity (ICA100 edge 1345) | (Precuneus;Cuneus)<=>(Superior_frontal) | (Default_mode;Central_executive)<=>(Limbic) |
| 1648) | rfMRI connectivity (ICA100 edge 1346) | (Postcentral;Precentral)<=>(Superior_frontal) | (Motor;Attention)<=>(Limbic) |
| 1649) | rfMRI connectivity (ICA100 edge 1347) | (Superior_frontal)<=>(Superior_frontal) | (Default_mode;Central_executive)<=>(Limbic) |
| 1650) | rfMRI connectivity (ICA100 edge 1348) | (Superior_temporal)<=>(Superior_frontal) | (Default_mode;Motor)<=>(Limbic) |
| 1651) | rfMRI connectivity (ICA100 edge 1349) | (Cerebellum)<=>(Superior_frontal) | (Subcortical-cerebellum)<=>(Limbic) |
| 1652) | rfMRI connectivity (ICA100 edge 1350) | (Inferior_parietal;Angular)<=>(Superior_frontal) | (Central_executive;Attention)<=>(Limbic) |
| 1653) | rfMRI connectivity (ICA100 edge 1351) | (Inferior_frontal;Precentral)<=>(Superior_frontal) | (Central_executive)<=>(Limbic) |
| 1654) | rfMRI connectivity (ICA100 edge 1352) | (Inferior_parietal;Inferior_frontal;SupraMarginal)<=>(Superior_frontal) | (Attention;Central_executive)<=>(Limbic) |
| 1655) | rfMRI connectivity (ICA100 edge 1353) | (Precentral;Superior_frontal;Supp_motor_area)<=>(Superior_frontal) | (Attention;Salience;Motor)<=>(Limbic) |
| 1656) | rfMRI connectivity (ICA100 edge 1354) | (Supp_motor_area;Inferior_frontal)<=>(Superior_frontal) | (Salience;Default_mode)<=>(Limbic) |
| 1657) | rfMRI connectivity (ICA100 edge 1355) | (SupraMarginal;Inferior_parietal)<=>(Superior_frontal) | (Central_executive;Salience)<=>(Limbic) |
| 1658) | rfMRI connectivity (ICA100 edge 1356) | (Paracentral)<=>(Superior_frontal) | (Motor)<=>(Limbic) |
| 1659) | rfMRI connectivity (ICA100 edge 1357) | (Middel_frontal)<=>(Superior_frontal) | (Central_executive)<=>(Limbic) |
| 1660) | rfMRI connectivity (ICA100 edge 1358) | (Postcentral;Precentral)<=>(Superior_frontal) | (Motor;Attention)<=>(Limbic) |
| 1661) | rfMRI connectivity (ICA100 edge 1359) | (Inferior_frontal;Middle_temporal;Supp_motor_area)<=>(Superior_frontal) | (Default_mode;Salience)<=>(Limbic) |
| 1662) | rfMRI connectivity (ICA100 edge 1360) | (Superior_parietal;Postcentral;Precuneus)<=>(Superior_frontal) | (Attention)<=>(Limbic) |
| 1663) | rfMRI connectivity (ICA100 edge 1361) | (Precentral;Postcentral)<=>(Superior_frontal) | (Motor)<=>(Limbic) |
| 1664) | rfMRI connectivity (ICA100 edge 1362) | (Precuneus)<=>(Superior_frontal) | (Default_mode;Central_executive)<=>(Limbic) |
| 1665) | rfMRI connectivity (ICA100 edge 1363) | (Middle_frontal)<=>(Superior_frontal) | (Central_executive;Salience)<=>(Limbic) |
| 1666) | rfMRI connectivity (ICA100 edge 1364) | (Putamen;Caudate)<=>(Superior_frontal) | (Subcortical-cerebellum)<=>(Limbic) |
| 1667) | rfMRI connectivity (ICA100 edge 1365) | (Precuneus;Superior_parietal)<=>(Superior_frontal) | (Attention;Central_executive)<=>(Limbic) |
| 1668) | rfMRI connectivity (ICA100 edge 1366) | (Superior_frontal;Middle_frontal)<=>(Superior_frontal) | (Central_executive)<=>(Limbic) |
| 1669) | rfMRI connectivity (ICA100 edge 1367) | (Inferior_temporal;Middle_temporal)<=>(Superior_frontal) | (Attention;Visual)<=>(Limbic) |
| 1670) | rfMRI connectivity (ICA100 edge 1368) | (Inferior_temporal;Inferior_occipital)<=>(Superior_frontal) | (Attention;Visual)<=>(Limbic) |
| 1671) | rfMRI connectivity (ICA100 edge 1369) | (Inferior_temporal;Fusiform;Temporal_pole)<=>(Superior_frontal) | (Limbic;Default_mode)<=>(Limbic) |
| 1672) | rfMRI connectivity (ICA100 edge 1370) | (Inferior_frontal)<=>(Superior_frontal) | (Default_mode;Central_executive)<=>(Limbic) |

| | | | |
|---|---|---|---|
| 1673) | rfMRI connectivity (ICA100 edge 1371) | (Superior_frontal;Middle_frontal)<=>(Superior_frontal) | (Salience;Default_mode)<=>(Limbic) |
| 1674) | rfMRI connectivity (ICA100 edge 1372) | (Inferior_temporal;Middle_temporal)<=>(Superior_frontal) | (Central_executive;Default_mode)<=>(Limbic) |
| 1675) | rfMRI connectivity (ICA100 edge 1373) | (Superior_frontal;Middle_frontal)<=>(Superior_frontal) | (Central_executive;Salience;Default_mode)<=>(Limbic) |
| 1676) | rfMRI connectivity (ICA100 edge 1374) | (Middle_temporal)<=>(Superior_frontal) | (Default_mode;Central_executive)<=>(Limbic) |
| 1677) | rfMRI connectivity (ICA100 edge 1375) | (Middle_temporal;Angular)<=>(Superior_frontal) | (Default_mode)<=>(Limbic) |
| 1678) | rfMRI connectivity (ICA100 edge 1376) | (Orbital)<=>(Superior_frontal) | (Limbic)<=>(Limbic) |
| 1679) | rfMRI connectivity (ICA100 edge 1377) | (Cerebellum;Inferior_temporal)<=>(Superior_frontal) | (Subcortical-cerebellum)<=>(Limbic) |
| 1680) | rfMRI connectivity (ICA100 edge 1378) | (Cerebellum;Inferior_temporal)<=>(Superior_frontal) | (Subcortical-cerebellum)<=>(Limbic) |
| 1681) | rfMRI connectivity (ICA100 edge 1379) | (Calcarine;Lingual;Cuneus)<=>(Orbital;Inferior_temporal) | (Visual)<=>(Limbic) |
| 1682) | rfMRI connectivity (ICA100 edge 1380) | (Rolandic_operculum;SupraMarginal;Insula)<=>(Orbital;Inferior_temporal) | (Salience;Motor)<=>(Limbic) |
| 1683) | rfMRI connectivity (ICA100 edge 1381) | (Lingual;Fusiform)<=>(Orbital;Inferior_temporal) | (Visual)<=>(Limbic) |
| 1684) | rfMRI connectivity (ICA100 edge 1382) | (Middle_occipital;Superior_occipital)<=>(Orbital;Inferior_temporal) | (Attention;Visual)<=>(Limbic) |
| 1685) | rfMRI connectivity (ICA100 edge 1383) | (Precuneus;Angular;Middle_cingulate)<=>(Orbital;Inferior_temporal) | (Default_mode;Central_executive)<=>(Limbic) |
| 1686) | rfMRI connectivity (ICA100 edge 1384) | (Postcentral;Precentral)<=>(Orbital;Inferior_temporal) | (Motor)<=>(Limbic) |
| 1687) | rfMRI connectivity (ICA100 edge 1385) | (Superior_frontal;Anterior_cingulate)<=>(Orbital;Inferior_temporal) | (Default_mode;Limbic)<=>(Limbic) |
| 1688) | rfMRI connectivity (ICA100 edge 1386) | (Calcarine;Lingual)<=>(Orbital;Inferior_temporal) | (Visual)<=>(Limbic) |
| 1689) | rfMRI connectivity (ICA100 edge 1387) | (Middle_temporal;Temporal_pole)<=>(Orbital;Inferior_temporal) | (Default_mode)<=>(Limbic) |
| 1690) | rfMRI connectivity (ICA100 edge 1388) | (Middle_occipital;Precuneus;Calcarine)<=>(Orbital;Inferior_temporal) | (Default_mode;Central_executive)<=>(Limbic) |
| 1691) | rfMRI connectivity (ICA100 edge 1389) | (Angular;Middle_temporal)<=>(Orbital;Inferior_temporal) | (Default_mode;Central_executive)<=>(Limbic) |
| 1692) | rfMRI connectivity (ICA100 edge 1390) | (Middle_frontal;Cerebellum)<=>(Orbital;Inferior_temporal) | (Central_executive;Default_mode)<=>(Limbic) |
| 1693) | rfMRI connectivity (ICA100 edge 1391) | (Superior_frontal)<=>(Orbital;Inferior_temporal) | (Default_mode)<=>(Limbic) |
| 1694) | rfMRI connectivity (ICA100 edge 1392) | (Cuneus;Superior_occipital)<=>(Orbital;Inferior_temporal) | (Visual)<=>(Limbic) |
| 1695) | rfMRI connectivity (ICA100 edge 1393) | (Insula;Anterior_cingulate)<=>(Orbital;Inferior_temporal) | (Salience;Default_mode)<=>(Limbic) |
| 1696) | rfMRI connectivity (ICA100 edge 1394) | (Inferior_occipital;Middle_occipital)<=>(Orbital;Inferior_temporal) | (Visual)<=>(Limbic) |
| 1697) | rfMRI connectivity (ICA100 edge 1395) | (Cerebellum)<=>(Orbital;Inferior_temporal) | (Subcortical-cerebellum)<=>(Limbic) |
| 1698) | rfMRI connectivity (ICA100 edge 1396) | (Inferior_parietal;Postcentral)<=>(Orbital;Inferior_temporal) | (Attention;Central_executive;Salience)<=>(Limbic) |
| 1699) | rfMRI connectivity (ICA100 edge 1397) | (Precuneus;Cuneus)<=>(Orbital;Inferior_temporal) | (Default_mode;Central_executive)<=>(Limbic) |
| 1700) | rfMRI connectivity (ICA100 edge 1398) | (Postcentral;Precentral)<=>(Orbital;Inferior_temporal) | (Motor;Attention)<=>(Limbic) |
| 1701) | rfMRI connectivity (ICA100 edge 1399) | (Superior_frontal)<=>(Orbital;Inferior_temporal) | (Default_mode;Central_executive)<=>(Limbic) |

| | | | |
|---|---|---|---|
| 1702) | rfMRI connectivity (ICA100 edge 1400) | (Superior_temporal)<=>(Orbital;Inferior_temporal) | (Default_mode;Motor)<=>(Limbic) |
| 1703) | rfMRI connectivity (ICA100 edge 1401) | (Cerebellum)<=>(Orbital;Inferior_temporal) | (Subcortical-cerebellum)<=>(Limbic) |
| 1704) | rfMRI connectivity (ICA100 edge 1402) | (Inferior_parietal;Angular)<=>(Orbital;Inferior_temporal) | (Central_executive;Attention)<=>(Limbic) |
| 1705) | rfMRI connectivity (ICA100 edge 1403) | (Inferior_frontal;Precentral)<=>(Orbital;Inferior_temporal) | (Central_executive)<=>(Limbic) |
| 1706) | rfMRI connectivity (ICA100 edge 1404) | (Inferior_parietal;Inferior_frontal;SupraMarginal)<=>(Orbital;Inferior_temporal) | (Attention;Central_executive)<=>(Limbic) |
| 1707) | rfMRI connectivity (ICA100 edge 1405) | (Precentral;Superior_frontal;Supp_motor_area)<=>(Orbital;Inferior_temporal) | (Attention;Salience;Motor)<=>(Limbic) |
| 1708) | rfMRI connectivity (ICA100 edge 1406) | (Supp_motor_area;Inferior_frontal)<=>(Orbital;Inferior_temporal) | (Salience;Default_mode)<=>(Limbic) |
| 1709) | rfMRI connectivity (ICA100 edge 1407) | (SupraMarginal;Inferior_parietal)<=>(Orbital;Inferior_temporal) | (Central_executive;Salience)<=>(Limbic) |
| 1710) | rfMRI connectivity (ICA100 edge 1408) | (Paracentral)<=>(Orbital;Inferior_temporal) | (Motor)<=>(Limbic) |
| 1711) | rfMRI connectivity (ICA100 edge 1409) | (Middel_frontal)<=>(Orbital;Inferior_temporal) | (Central_executive)<=>(Limbic) |
| 1712) | rfMRI connectivity (ICA100 edge 1410) | (Postcentral;Precentral)<=>(Orbital;Inferior_temporal) | (Motor;Attention)<=>(Limbic) |
| 1713) | rfMRI connectivity (ICA100 edge 1411) | (Inferior_frontal;Middle_temporal;Supp_motor_area)<=>(Orbital;Inferior_temporal) | (Default_mode;Salience)<=>(Limbic) |
| 1714) | rfMRI connectivity (ICA100 edge 1412) | (Superior_parietal;Postcentral;Precuneus)<=>(Orbital;Inferior_temporal) | (Attention)<=>(Limbic) |
| 1715) | rfMRI connectivity (ICA100 edge 1413) | (Precentral;Postcentral)<=>(Orbital;Inferior_temporal) | (Motor)<=>(Limbic) |
| 1716) | rfMRI connectivity (ICA100 edge 1414) | (Precuneus)<=>(Orbital;Inferior_temporal) | (Default_mode;Central_executive)<=>(Limbic) |
| 1717) | rfMRI connectivity (ICA100 edge 1415) | (Middle_frontal)<=>(Orbital;Inferior_temporal) | (Central_executive;Salience)<=>(Limbic) |
| 1718) | rfMRI connectivity (ICA100 edge 1416) | (Putamen;Caudate)<=>(Orbital;Inferior_temporal) | (Subcortical-cerebellum)<=>(Limbic) |
| 1719) | rfMRI connectivity (ICA100 edge 1417) | (Precuneus;Superior_parietal)<=>(Orbital;Inferior_temporal) | (Attention;Central_executive)<=>(Limbic) |
| 1720) | rfMRI connectivity (ICA100 edge 1418) | (Superior_frontal;Middle_frontal)<=>(Orbital;Inferior_temporal) | (Central_executive)<=>(Limbic) |
| 1721) | rfMRI connectivity (ICA100 edge 1419) | (Inferior_temporal;Middle_temporal)<=>(Orbital;Inferior_temporal) | (Attention;Visual)<=>(Limbic) |
| 1722) | rfMRI connectivity (ICA100 edge 1420) | (Inferior_temporal;Inferior_occipital)<=>(Orbital;Inferior_temporal) | (Attention;Visual)<=>(Limbic) |
| 1723) | rfMRI connectivity (ICA100 edge 1421) | (Inferior_temporal;Fusiform;Temporal_pole)<=>(Orbital;Inferior_temporal) | (Limbic;Default_mode)<=>(Limbic) |
| 1724) | rfMRI connectivity (ICA100 edge 1422) | (Inferior_frontal)<=>(Orbital;Inferior_temporal) | (Default_mode;Central_executive)<=>(Limbic) |
| 1725) | rfMRI connectivity (ICA100 edge 1423) | (Superior_frontal;Middle_frontal)<=>(Orbital;Inferior_temporal) | (Salience;Default_mode)<=>(Limbic) |
| 1726) | rfMRI connectivity (ICA100 edge 1424) | (Inferior_temporal;Middle_temporal)<=>(Orbital;Inferior_temporal) | (Central_executive;Default_mode)<=>(Limbic) |
| 1727) | rfMRI connectivity (ICA100 edge 1425) | (Superior_frontal;Middle_frontal)<=>(Orbital;Inferior_temporal) | (Central_executive;Salience;Default_mode)<=>(Limbic) |
| 1728) | rfMRI connectivity (ICA100 edge 1426) | (Middle_temporal)<=>(Orbital;Inferior_temporal) | (Default_mode;Central_executive)<=>(Limbic) |
| 1729) | rfMRI connectivity (ICA100 edge 1427) | (Middle_temporal;Angular)<=>(Orbital;Inferior_temporal) | (Default_mode)<=>(Limbic) |
| 1730) | rfMRI connectivity (ICA100 edge 1428) | (Orbital)<=>(Orbital;Inferior_temporal) | (Limbic)<=>(Limbic) |

| | | | |
|---|---|---|---|
| 1731) | rfMRI connectivity (ICA100 edge 1429) | (Cerebellum;Inferior_temporal)<=>(Orbital;Inferior_temporal) | (Subcortical-cerebellum)<=>(Limbic) |
| 1732) | rfMRI connectivity (ICA100 edge 1430) | (Cerebellum;Inferior_temporal)<=>(Orbital;Inferior_temporal) | (Subcortical-cerebellum)<=>(Limbic) |
| 1733) | rfMRI connectivity (ICA100 edge 1431) | (Superior_frontal)<=>(Orbital;Inferior_temporal) | (Limbic)<=>(Limbic) |
| 1734) | rfMRI connectivity (ICA100 edge 1432) | (Calcarine;Lingual;Cuneus)<=>(Superior_frontal) | (Visual)<=>(Limbic;Default_mode) |
| 1735) | rfMRI connectivity (ICA100 edge 1433) | (Rolandic_operculum;SupraMarginal;Insula)<=>(Superior_frontal) | (Salience;Motor)<=>(Limbic;Default_mode) |
| 1736) | rfMRI connectivity (ICA100 edge 1434) | (Lingual;Fusiform)<=>(Superior_frontal) | (Visual)<=>(Limbic;Default_mode) |
| 1737) | rfMRI connectivity (ICA100 edge 1435) | (Middle_occipital;Superior_occipital)<=>(Superior_frontal) | (Attention;Visual)<=>(Limbic;Default_mode) |
| 1738) | rfMRI connectivity (ICA100 edge 1436) | (Precuneus;Angular;Middle_cingulate)<=>(Superior_frontal) | (Default_mode;Central_executive)<=>(Limbic;Default_mode) |
| 1739) | rfMRI connectivity (ICA100 edge 1437) | (Postcentral;Precentral)<=>(Superior_frontal) | (Motor)<=>(Limbic;Default_mode) |
| 1740) | rfMRI connectivity (ICA100 edge 1438) | (Superior_frontal;Anterior_cingulate)<=>(Superior_frontal) | (Default_mode;Limbic)<=>(Limbic;Default_mode) |
| 1741) | rfMRI connectivity (ICA100 edge 1439) | (Calcarine;Lingual)<=>(Superior_frontal) | (Visual)<=>(Limbic;Default_mode) |
| 1742) | rfMRI connectivity (ICA100 edge 1440) | (Middle_temporal;Temporal_pole)<=>(Superior_frontal) | (Default_mode)<=>(Limbic;Default_mode) |
| 1743) | rfMRI connectivity (ICA100 edge 1441) | (Middle_occipital;Precuneus;Calcarine)<=>(Superior_frontal) | (Default_mode;Central_executive)<=>(Limbic;Default_mode) |
| 1744) | rfMRI connectivity (ICA100 edge 1442) | (Angular;Middle_temporal)<=>(Superior_frontal) | (Default_mode;Central_executive)<=>(Limbic;Default_mode) |
| 1745) | rfMRI connectivity (ICA100 edge 1443) | (Middle_frontal;Cerebellum)<=>(Superior_frontal) | (Central_executive;Default_mode)<=>(Limbic;Default_mode) |
| 1746) | rfMRI connectivity (ICA100 edge 1444) | (Superior_frontal)<=>(Superior_frontal) | (Default_mode)<=>(Limbic;Default_mode) |
| 1747) | rfMRI connectivity (ICA100 edge 1445) | (Cuneus;Superior_occipital)<=>(Superior_frontal) | (Visual)<=>(Limbic;Default_mode) |
| 1748) | rfMRI connectivity (ICA100 edge 1446) | (Insula;Anterior_cingulate)<=>(Superior_frontal) | (Salience;Default_mode)<=>(Limbic;Default_mode) |
| 1749) | rfMRI connectivity (ICA100 edge 1447) | (Inferior_occipital;Middle_occipital)<=>(Superior_frontal) | (Visual)<=>(Limbic;Default_mode) |
| 1750) | rfMRI connectivity (ICA100 edge 1448) | (Cerebellum)<=>(Superior_frontal) | (Subcortical-cerebellum)<=>(Limbic;Default_mode) |
| 1751) | rfMRI connectivity (ICA100 edge 1449) | (Inferior_parietal;Postcentral)<=>(Superior_frontal) | (Attention;Central_executive;Salience)<=>(Limbic;Default_mode) |
| 1752) | rfMRI connectivity (ICA100 edge 1450) | (Precuneus;Cuneus)<=>(Superior_frontal) | (Default_mode;Central_executive)<=>(Limbic;Default_mode) |
| 1753) | rfMRI connectivity (ICA100 edge 1451) | (Postcentral;Precentral)<=>(Superior_frontal) | (Motor;Attention)<=>(Limbic;Default_mode) |
| 1754) | rfMRI connectivity (ICA100 edge 1452) | (Superior_frontal)<=>(Superior_frontal) | (Default_mode;Central_executive)<=>(Limbic;Default_mode) |
| 1755) | rfMRI connectivity (ICA100 edge 1453) | (Superior_temporal)<=>(Superior_frontal) | (Default_mode;Motor)<=>(Limbic;Default_mode) |
| 1756) | rfMRI connectivity (ICA100 edge 1454) | (Cerebellum)<=>(Superior_frontal) | (Subcortical-cerebellum)<=>(Limbic;Default_mode) |
| 1757) | rfMRI connectivity (ICA100 edge 1455) | (Inferior_parietal;Angular)<=>(Superior_frontal) | (Central_executive;Attention)<=>(Limbic;Default_mode) |
| 1758) | rfMRI connectivity (ICA100 edge 1456) | (Inferior_frontal;Precentral)<=>(Superior_frontal) | (Central_executive)<=>(Limbic;Default_mode) |

| | | | |
|---|---|---|---|
| 1759) | rfMRI connectivity (ICA100 edge 1457) | (Inferior_parietal;Inferior_frontal;SupraMarginal)<=>(Superior_frontal) | (Attention;Central_executive)<=>(Limbic;Default_mode) |
| 1760) | rfMRI connectivity (ICA100 edge 1458) | (Precentral;Superior_frontal;Supp_motor_area)<=>(Superior_frontal) | (Attention;Salience;Motor)<=>(Limbic;Default_mode) |
| 1761) | rfMRI connectivity (ICA100 edge 1459) | (Supp_motor_area;Inferior_frontal)<=>(Superior_frontal) | (Salience;Default_mode)<=>(Limbic;Default_mode) |
| 1762) | rfMRI connectivity (ICA100 edge 1460) | (SupraMarginal;Inferior_parietal)<=>(Superior_frontal) | (Central_executive;Salience)<=>(Limbic;Default_mode) |
| 1763) | rfMRI connectivity (ICA100 edge 1461) | (Paracentral)<=>(Superior_frontal) | (Motor)<=>(Limbic;Default_mode) |
| 1764) | rfMRI connectivity (ICA100 edge 1462) | (Middel_frontal)<=>(Superior_frontal) | (Central_executive)<=>(Limbic;Default_mode) |
| 1765) | rfMRI connectivity (ICA100 edge 1463) | (Postcentral;Precentral)<=>(Superior_frontal) | (Motor;Attention)<=>(Limbic;Default_mode) |
| 1766) | rfMRI connectivity (ICA100 edge 1464) | (Inferior_frontal;Middle_temporal;Supp_motor_area)<=>(Superior_frontal) | (Default_mode;Salience)<=>(Limbic;Default_mode) |
| 1767) | rfMRI connectivity (ICA100 edge 1465) | (Superior_parietal;Postcentral;Precuneus)<=>(Superior_frontal) | (Attention)<=>(Limbic;Default_mode) |
| 1768) | rfMRI connectivity (ICA100 edge 1466) | (Precentral;Postcentral)<=>(Superior_frontal) | (Motor)<=>(Limbic;Default_mode) |
| 1769) | rfMRI connectivity (ICA100 edge 1467) | (Precuneus)<=>(Superior_frontal) | (Default_mode;Central_executive)<=>(Limbic;Default_mode) |
| 1770) | rfMRI connectivity (ICA100 edge 1468) | (Middle_frontal)<=>(Superior_frontal) | (Central_executive;Salience)<=>(Limbic;Default_mode) |
| 1771) | rfMRI connectivity (ICA100 edge 1469) | (Putamen;Caudate)<=>(Superior_frontal) | (Subcortical-cerebellum)<=>(Limbic;Default_mode) |
| 1772) | rfMRI connectivity (ICA100 edge 1470) | (Precuneus;Superior_parietal)<=>(Superior_frontal) | (Attention;Central_executive)<=>(Limbic;Default_mode) |
| 1773) | rfMRI connectivity (ICA100 edge 1471) | (Superior_frontal;Middle_frontal)<=>(Superior_frontal) | (Central_executive)<=>(Limbic;Default_mode) |
| 1774) | rfMRI connectivity (ICA100 edge 1472) | (Inferior_temporal;Middle_temporal)<=>(Superior_frontal) | (Attention;Visual)<=>(Limbic;Default_mode) |
| 1775) | rfMRI connectivity (ICA100 edge 1473) | (Inferior_temporal;Inferior_occipital)<=>(Superior_frontal) | (Attention;Visual)<=>(Limbic;Default_mode) |
| 1776) | rfMRI connectivity (ICA100 edge 1474) | (Inferior_temporal;Fusiform;Temporal_pole)<=>(Superior_frontal) | (Limbic;Default_mode)<=>(Limbic;Default_mode) |
| 1777) | rfMRI connectivity (ICA100 edge 1475) | (Inferior_frontal)<=>(Superior_frontal) | (Default_mode;Central_executive)<=>(Limbic;Default_mode) |
| 1778) | rfMRI connectivity (ICA100 edge 1476) | (Superior_frontal;Middle_frontal)<=>(Superior_frontal) | (Salience;Default_mode)<=>(Limbic;Default_mode) |
| 1779) | rfMRI connectivity (ICA100 edge 1477) | (Inferior_temporal;Middle_temporal)<=>(Superior_frontal) | (Central_executive;Default_mode)<=>(Limbic;Default_mode) |
| 1780) | rfMRI connectivity (ICA100 edge 1478) | (Superior_frontal;Middle_frontal)<=>(Superior_frontal) | (Central_executive;Salience;Default_mode)<=>(Limbic;Default_mode) |
| 1781) | rfMRI connectivity (ICA100 edge 1479) | (Middle_temporal)<=>(Superior_frontal) | (Default_mode;Central_executive)<=>(Limbic;Default_mode) |
| 1782) | rfMRI connectivity (ICA100 edge 1480) | (Middle_temporal;Angular)<=>(Superior_frontal) | (Default_mode)<=>(Limbic;Default_mode) |
| 1783) | rfMRI connectivity (ICA100 edge 1481) | (Orbital)<=>(Superior_frontal) | (Limbic)<=>(Limbic;Default_mode) |
| 1784) | rfMRI connectivity (ICA100 edge 1482) | (Cerebellum;Inferior_temporal)<=>(Superior_frontal) | (Subcortical-cerebellum)<=>(Limbic;Default_mode) |
| 1785) | rfMRI connectivity (ICA100 edge 1483) | (Cerebellum;Inferior_temporal)<=>(Superior_frontal) | (Subcortical-cerebellum)<=>(Limbic;Default_mode) |

| | | | |
|---|---|---|---|
| 1786) | rfMRI connectivity (ICA100 edge 1484) | (Superior_frontal)<=>(Superior_frontal) | (Limbic)<=>(Limbic;Default_mode) |
| 1787) | rfMRI connectivity (ICA100 edge 1485) | (Orbital;Inferior_temporal)<=>(Superior_frontal) | (Limbic)<=>(Limbic;Default_mode) |
| 1788) | rfMRI connectivity ICA-features 1 | NA | Motor;Subcortical-cerebellum |
| 1789) | rfMRI connectivity ICA-features 2 | NA | Central_executive;Salience;Default_mode |
| 1790) | rfMRI connectivity ICA-features 3 | NA | Central_executive;Salience;Default_mode;Attention |
| 1791) | rfMRI connectivity ICA-features 4 | NA | Central_executive;Salience;Default_mode;Attention |
| 1792) | rfMRI connectivity ICA-features 5 | NA | Visual;Attention |
| 1793) | rfMRI connectivity ICA-features 6 | NA | Central_executive;Salience;Default_mode |

Edge IDs correspond to pairwise node connections in the UK Biobank resting-state functional connectivity matrices. Abbreviations: IDP, imaging-derived phenotype; tfMRI, task-based functional magnetic resonance imaging; BOLD, Blood oxygenation level dependent; rsfMRI, resting-state functional magnetic resonance imaging; ICA, independent component analysis.

## Appendix 3: Brain imaging confounds in UK Biobank (n = 613)

| | |
|---|---|
| 1) | Age_Site_1 |
| 2) | Age_Site_2 |
| 3) | Age_Site_3 |
| 4) | Sex_1_Site_1 |
| 5) | Sex_1_Site_2 |
| 6) | Sex_1_Site_3 |
| 7) | AgeSex_Site_1 |
| 8) | AgeSex_Site_2 |
| 9) | AgeSex_Site_3 |
| 10) | HeadSize_Site_1 |
| 11) | HeadSize_Site_2 |
| 12) | HeadSize_Site_3 |
| 13) | Site_1_vs_2 |
| 14) | Site_1_vs_3 |
| 15) | Batch_1_Site_1 |
| 16) | Batch_2_Site_1 |
| 17) | Batch_3_Site_1 |
| 18) | Batch_4_Site_1 |
| 19) | Batch_5_Site_1 |
| 20) | Batch_6_Site_1 |
| 21) | Batch_1_Site_2 |
| 22) | Batch_2_Site_2 |
| 23) | Batch_3_Site_2 |

| | |
|---|---|
| 24) | Batch_4_Site_2 |
| 25) | Batch_1_Site_3 |
| 26) | Batch_2_Site_3 |
| 27) | Batch_3_Site_3 |
| 28) | CMRR_1_Site_1 |
| 29) | CMRR_2_Site_1 |
| 30) | CMRR_3_Site_1 |
| 31) | CMRR_4_Site_1 |
| 32) | CMRR_5_Site_1 |
| 33) | CMRR_6_Site_1 |
| 34) | CMRR_7_Site_1 |
| 35) | CMRR_1_Site_2 |
| 36) | Protocol_1_Site_1 |
| 37) | Protocol_2_Site_1 |
| 38) | Protocol_3_Site_1 |
| 39) | Protocol_4_Site_1 |
| 40) | Protocol_5_Site_1 |
| 41) | Protocol_1_Site_3 |
| 42) | Service_Pack_1_Site_1 |
| 43) | ScanEvents_1_Site_1 |
| 44) | ScanEvents_2_Site_1 |
| 45) | ScanEvents_3_Site_1 |
| 46) | ScanEvents_4_Site_1 |
| 47) | ScanEvents_5_Site_1 |
| 48) | ScanEvents_6_Site_1 |
| 49) | ScanEvents_7_Site_1 |
| 50) | ScanEvents_8_Site_1 |
| 51) | ScanEvents_9_Site_1 |
| 52) | ScanEvents_10_Site_1 |
| 53) | ScanEvents_11_Site_1 |
| 54) | ScanEvents_12_Site_1 |
| 55) | ScanEvents_13_Site_1 |
| 56) | ScanEvents_14_Site_1 |
| 57) | ScanEvents_1_Site_2 |
| 58) | ScanEvents_2_Site_2 |
| 59) | ScanEvents_3_Site_2 |
| 60) | ScanEvents_4_Site_2 |
| 61) | ScanEvents_5_Site_2 |
| 62) | ScanEvents_6_Site_2 |
| 63) | ScanEvents_7_Site_2 |
| 64) | ScanEvents_1_Site_3 |
| 65) | ScanEvents_2_Site_3 |

| | |
|---|---|
| 66) | ScanEvents_3_Site_3 |
| 67) | ScanEvents_4_Site_3 |
| 68) | ScanEvents_5_Site_3 |
| 69) | Flipped_SWI_1_Site_1 |
| 70) | Flipped_SWI_1_Site_2 |
| 71) | Flipped_SWI_1_Site_3 |
| 72) | T1_and_T2_for_FreeSurfer_1_Site_1 |
| 73) | T1_and_T2_for_FreeSurfer_1_Site_2 |
| 74) | T1_and_T2_for_FreeSurfer_1_Site_3 |
| 75) | New_Eddy_1_Site_1 |
| 76) | New_Eddy_1_Site_2 |
| 77) | New_Eddy_1_Site_3 |
| 78) | SCALING_T1_1_Site_1 |
| 79) | SCALING_T2_FLAIR_1_Site_1 |
| 80) | SCALING_T2_FLAIR_2_Site_1 |
| 81) | SCALING_SWI_1_Site_1 |
| 82) | SCALING_SWI_1_Site_2 |
| 83) | SCALING_dMRI_1_Site_1 |
| 84) | SCALING_dMRI_1_Site_2 |
| 85) | SCALING_rfMRI_1_Site_1 |
| 86) | SCALING_tfMRI_1_Site_1 |
| 87) | TE_rfMRI_Site_1 |
| 88) | TE_tfMRI_Site_1 |
| 89) | TE_rfMRI_Site_2 |
| 90) | TE_tfMRI_Site_2 |
| 91) | TE_rfMRI_Site_3 |
| 92) | TE_tfMRI_Site_3 |
| 93) | StructHeadMotion_Site_1 |
| 94) | StructHeadMotion_Site_2 |
| 95) | StructHeadMotion_Site_3 |
| 96) | S_dirty_mean_Site_1 |
| 97) | S_dirty_median_Site_1 |
| 98) | S_dirty_p90_Site_1 |
| 99) | D_dirty_mean_Site_1 |
| 100) | D_dirty_median_Site_1 |
| 101) | D_dirty_p90_Site_1 |
| 102) | SD_dirty_mean_Site_1 |
| 103) | SD_dirty_median_Site_1 |
| 104) | SD_dirty_p90_Site_1 |
| 105) | S_clean_mean_Site_1 |
| 106) | S_clean_median_Site_1 |
| 107) | S_clean_p90_Site_1 |

| | |
|---|---|
| 108) | D_clean_mean_Site_1 |
| 109) | D_clean_median_Site_1 |
| 110) | D_clean_p90_Site_1 |
| 111) | SD_clean_mean_Site_1 |
| 112) | SD_clean_median_Site_1 |
| 113) | SD_clean_p90_Site_1 |
| 114) | S_dirty_mean_Site_2 |
| 115) | S_dirty_median_Site_2 |
| 116) | S_dirty_p90_Site_2 |
| 117) | D_dirty_mean_Site_2 |
| 118) | D_dirty_median_Site_2 |
| 119) | D_dirty_p90_Site_2 |
| 120) | SD_dirty_mean_Site_2 |
| 121) | SD_dirty_median_Site_2 |
| 122) | SD_dirty_p90_Site_2 |
| 123) | S_clean_mean_Site_2 |
| 124) | S_clean_median_Site_2 |
| 125) | S_clean_p90_Site_2 |
| 126) | D_clean_mean_Site_2 |
| 127) | D_clean_median_Site_2 |
| 128) | D_clean_p90_Site_2 |
| 129) | SD_clean_mean_Site_2 |
| 130) | SD_clean_median_Site_2 |
| 131) | SD_clean_p90_Site_2 |
| 132) | S_dirty_mean_Site_3 |
| 133) | S_dirty_median_Site_3 |
| 134) | S_dirty_p90_Site_3 |
| 135) | D_dirty_mean_Site_3 |
| 136) | D_dirty_median_Site_3 |
| 137) | D_dirty_p90_Site_3 |
| 138) | SD_dirty_mean_Site_3 |
| 139) | SD_dirty_median_Site_3 |
| 140) | SD_dirty_p90_Site_3 |
| 141) | S_clean_mean_Site_3 |
| 142) | S_clean_median_Site_3 |
| 143) | S_clean_p90_Site_3 |
| 144) | D_clean_mean_Site_3 |
| 145) | D_clean_median_Site_3 |
| 146) | D_clean_p90_Site_3 |
| 147) | SD_clean_mean_Site_3 |
| 148) | SD_clean_median_Site_3 |
| 149) | SD_clean_p90_Site_3 |

| | |
|---|---|
| 150) | HeadMotion_mean_rfMRI_abs_Site_1 |
| 151) | HeadMotion_median_rfMRI_abs_Site_1 |
| 152) | HeadMotion_p90_rfMRI_abs_Site_1 |
| 153) | HeadMotion_mean_rfMRI_rel_Site_1 |
| 154) | HeadMotion_median_rfMRI_rel_Site_1 |
| 155) | HeadMotion_p90_rfMRI_rel_Site_1 |
| 156) | HeadMotion_mean_tfMRI_abs_Site_1 |
| 157) | HeadMotion_median_tfMRI_abs_Site_1 |
| 158) | HeadMotion_p90_tfMRI_abs_Site_1 |
| 159) | HeadMotion_mean_tfMRI_rel_Site_1 |
| 160) | HeadMotion_median_tfMRI_rel_Site_1 |
| 161) | HeadMotion_p90_tfMRI_rel_Site_1 |
| 162) | HeadMotion_mean_dMRI_abs_Site_1 |
| 163) | HeadMotion_median_dMRI_abs_Site_1 |
| 164) | HeadMotion_p90_dMRI_abs_Site_1 |
| 165) | HeadMotion_mean_dMRI_rel_Site_1 |
| 166) | HeadMotion_median_dMRI_rel_Site_1 |
| 167) | HeadMotion_p90_dMRI_rel_Site_1 |
| 168) | HeadMotion_p90_dMRI_outliers_Site_1 |
| 169) | HeadMotion_mean_rfMRI_abs_Site_2 |
| 170) | HeadMotion_median_rfMRI_abs_Site_2 |
| 171) | HeadMotion_p90_rfMRI_abs_Site_2 |
| 172) | HeadMotion_mean_rfMRI_rel_Site_2 |
| 173) | HeadMotion_median_rfMRI_rel_Site_2 |
| 174) | HeadMotion_p90_rfMRI_rel_Site_2 |
| 175) | HeadMotion_mean_tfMRI_abs_Site_2 |
| 176) | HeadMotion_median_tfMRI_abs_Site_2 |
| 177) | HeadMotion_p90_tfMRI_abs_Site_2 |
| 178) | HeadMotion_mean_tfMRI_rel_Site_2 |
| 179) | HeadMotion_median_tfMRI_rel_Site_2 |
| 180) | HeadMotion_p90_tfMRI_rel_Site_2 |
| 181) | HeadMotion_mean_dMRI_abs_Site_2 |
| 182) | HeadMotion_median_dMRI_abs_Site_2 |
| 183) | HeadMotion_p90_dMRI_abs_Site_2 |
| 184) | HeadMotion_mean_dMRI_rel_Site_2 |
| 185) | HeadMotion_median_dMRI_rel_Site_2 |
| 186) | HeadMotion_p90_dMRI_rel_Site_2 |
| 187) | HeadMotion_p90_dMRI_outliers_Site_2 |
| 188) | HeadMotion_mean_rfMRI_abs_Site_3 |
| 189) | HeadMotion_median_rfMRI_abs_Site_3 |
| 190) | HeadMotion_p90_rfMRI_abs_Site_3 |
| 191) | HeadMotion_mean_rfMRI_rel_Site_3 |

| | |
|---|---|
| 192) | HeadMotion_median_rfMRI_rel_Site_3 |
| 193) | HeadMotion_p90_rfMRI_rel_Site_3 |
| 194) | HeadMotion_mean_tfMRI_abs_Site_3 |
| 195) | HeadMotion_median_tfMRI_abs_Site_3 |
| 196) | HeadMotion_p90_tfMRI_abs_Site_3 |
| 197) | HeadMotion_mean_tfMRI_rel_Site_3 |
| 198) | HeadMotion_median_tfMRI_rel_Site_3 |
| 199) | HeadMotion_p90_tfMRI_rel_Site_3 |
| 200) | HeadMotion_mean_dMRI_abs_Site_3 |
| 201) | HeadMotion_median_dMRI_abs_Site_3 |
| 202) | HeadMotion_p90_dMRI_abs_Site_3 |
| 203) | HeadMotion_mean_dMRI_rel_Site_3 |
| 204) | HeadMotion_median_dMRI_rel_Site_3 |
| 205) | HeadMotion_p90_dMRI_rel_Site_3 |
| 206) | HeadMotion_p90_dMRI_outliers_Site_3 |
| 207) | HeadMotionST_mean_inplane_time_Site_1 |
| 208) | HeadMotionST_median_inplane_time_Site_1 |
| 209) | HeadMotionST_p90_inplane_time_Site_1 |
| 210) | HeadMotionST_mean_Z_time_Site_1 |
| 211) | HeadMotionST_median_Z_time_Site_1 |
| 212) | HeadMotionST_p90_Z_time_Site_1 |
| 213) | HeadMotionST_median_inplane_space_Site_1 |
| 214) | HeadMotionST_p90_inplane_space_Site_1 |
| 215) | HeadMotionST_median_Z_space_Site_1 |
| 216) | HeadMotionST_p90_Z_space_Site_1 |
| 217) | HeadMotionST_mean_inplane_time_Site_2 |
| 218) | HeadMotionST_median_inplane_time_Site_2 |
| 219) | HeadMotionST_p90_inplane_time_Site_2 |
| 220) | HeadMotionST_mean_Z_time_Site_2 |
| 221) | HeadMotionST_median_Z_time_Site_2 |
| 222) | HeadMotionST_p90_Z_time_Site_2 |
| 223) | HeadMotionST_median_inplane_space_Site_2 |
| 224) | HeadMotionST_p90_inplane_space_Site_2 |
| 225) | HeadMotionST_median_Z_space_Site_2 |
| 226) | HeadMotionST_p90_Z_space_Site_2 |
| 227) | HeadMotionST_mean_inplane_time_Site_3 |
| 228) | HeadMotionST_median_inplane_time_Site_3 |
| 229) | HeadMotionST_p90_inplane_time_Site_3 |
| 230) | HeadMotionST_mean_Z_time_Site_3 |
| 231) | HeadMotionST_median_Z_time_Site_3 |
| 232) | HeadMotionST_p90_Z_time_Site_3 |
| 233) | HeadMotionST_median_inplane_space_Site_3 |

| | |
|---|---|
| 234) | HeadMotionST_p90_inplane_space_Site_3 |
| 235) | HeadMotionST_median_Z_space_Site_3 |
| 236) | HeadMotionST_p90_Z_space_Site_3 |
| 237) | TablePos_COG_X_Site_1 |
| 238) | TablePos_COG_Y_Site_1 |
| 239) | TablePos_COG_Z_Site_1 |
| 240) | TablePos_Table_Site_1 |
| 241) | TablePos_COG_X_Site_2 |
| 242) | TablePos_COG_Y_Site_2 |
| 243) | TablePos_COG_Z_Site_2 |
| 244) | TablePos_Table_Site_2 |
| 245) | TablePos_COG_X_Site_3 |
| 246) | TablePos_COG_Y_Site_3 |
| 247) | TablePos_COG_Z_Site_3 |
| 248) | TablePos_Table_Site_3 |
| 249) | Eddy_QC_X_Site_1 |
| 250) | Eddy_QC_Y_Site_1 |
| 251) | Eddy_QC_Z_Site_1 |
| 252) | YTranslation_Site_1 |
| 253) | Eddy_QC_X_Site_2 |
| 254) | Eddy_QC_Y_Site_2 |
| 255) | Eddy_QC_Z_Site_2 |
| 256) | YTranslation_Site_2 |
| 257) | Eddy_QC_X_Site_3 |
| 258) | Eddy_QC_Y_Site_3 |
| 259) | Eddy_QC_Z_Site_3 |
| 260) | YTranslation_Site_3 |
| 261) | Age_Site_1_squared |
| 262) | Age_Site_2_squared |
| 263) | Age_Site_3_squared |
| 264) | Age_Site_1_inormal |
| 265) | Age_Site_2_inormal |
| 266) | Age_Site_3_inormal |
| 267) | Age_Site_1_squared_inormal |
| 268) | Age_Site_2_squared_inormal |
| 269) | Age_Site_3_squared_inormal |
| 270) | AgeSex_Site_1_squared |
| 271) | AgeSex_Site_2_squared |
| 272) | AgeSex_Site_3_squared |
| 273) | AgeSex_Site_1_inormal |
| 274) | AgeSex_Site_2_inormal |
| 275) | AgeSex_Site_3_inormal |

| | |
|---|---|
| 276) | AgeSex_Site_1_squared_inormal |
| 277) | AgeSex_Site_2_squared_inormal |
| 278) | AgeSex_Site_3_squared_inormal |
| 279) | HeadSize_Site_1_squared |
| 280) | HeadSize_Site_3_squared |
| 281) | HeadSize_Site_1_inormal |
| 282) | HeadSize_Site_3_inormal |
| 283) | HeadSize_Site_3_squared_inormal |
| 284) | StructHeadMotion_Site_1_squared |
| 285) | StructHeadMotion_Site_2_squared |
| 286) | StructHeadMotion_Site_3_squared |
| 287) | StructHeadMotion_Site_1_inormal |
| 288) | StructHeadMotion_Site_2_inormal |
| 289) | StructHeadMotion_Site_3_inormal |
| 290) | StructHeadMotion_Site_1_squared_inormal |
| 291) | S_dirty_p90_Site_1_squared |
| 292) | D_dirty_median_Site_1_squared |
| 293) | SD_dirty_mean_Site_1_squared |
| 294) | SD_dirty_p90_Site_1_squared |
| 295) | S_clean_mean_Site_1_squared |
| 296) | S_clean_median_Site_1_squared |
| 297) | S_clean_p90_Site_1_squared |
| 298) | D_clean_mean_Site_1_squared |
| 299) | D_clean_median_Site_1_squared |
| 300) | D_clean_p90_Site_1_squared |
| 301) | SD_clean_mean_Site_1_squared |
| 302) | SD_clean_median_Site_1_squared |
| 303) | SD_clean_p90_Site_1_squared |
| 304) | S_dirty_p90_Site_2_squared |
| 305) | SD_dirty_p90_Site_2_squared |
| 306) | S_clean_mean_Site_2_squared |
| 307) | S_clean_median_Site_2_squared |
| 308) | S_clean_p90_Site_2_squared |
| 309) | D_clean_mean_Site_2_squared |
| 310) | D_clean_median_Site_2_squared |
| 311) | SD_clean_mean_Site_2_squared |
| 312) | SD_clean_median_Site_2_squared |
| 313) | SD_clean_p90_Site_2_squared |
| 314) | S_dirty_p90_Site_3_squared |
| 315) | SD_dirty_p90_Site_3_squared |
| 316) | S_clean_mean_Site_3_squared |
| 317) | S_clean_median_Site_3_squared |

| | |
|---|---|
| 318) | S_clean_p90_Site_3_squared |
| 319) | D_clean_mean_Site_3_squared |
| 320) | D_clean_median_Site_3_squared |
| 321) | SD_clean_mean_Site_3_squared |
| 322) | SD_clean_median_Site_3_squared |
| 323) | SD_clean_p90_Site_3_squared |
| 324) | S_dirty_p90_Site_1_inormal |
| 325) | S_clean_mean_Site_1_inormal |
| 326) | S_clean_median_Site_1_inormal |
| 327) | S_clean_p90_Site_1_inormal |
| 328) | D_clean_mean_Site_1_inormal |
| 329) | D_clean_median_Site_1_inormal |
| 330) | D_clean_p90_Site_1_inormal |
| 331) | SD_clean_mean_Site_1_inormal |
| 332) | SD_clean_median_Site_1_inormal |
| 333) | SD_clean_p90_Site_1_inormal |
| 334) | S_dirty_p90_Site_2_inormal |
| 335) | S_clean_mean_Site_2_inormal |
| 336) | S_clean_median_Site_2_inormal |
| 337) | S_clean_p90_Site_2_inormal |
| 338) | D_clean_mean_Site_2_inormal |
| 339) | D_clean_median_Site_2_inormal |
| 340) | D_clean_p90_Site_2_inormal |
| 341) | SD_clean_mean_Site_2_inormal |
| 342) | SD_clean_median_Site_2_inormal |
| 343) | SD_clean_p90_Site_2_inormal |
| 344) | S_dirty_p90_Site_3_inormal |
| 345) | S_clean_mean_Site_3_inormal |
| 346) | S_clean_median_Site_3_inormal |
| 347) | S_clean_p90_Site_3_inormal |
| 348) | D_clean_mean_Site_3_inormal |
| 349) | D_clean_median_Site_3_inormal |
| 350) | D_clean_p90_Site_3_inormal |
| 351) | SD_clean_mean_Site_3_inormal |
| 352) | SD_clean_median_Site_3_inormal |
| 353) | SD_clean_p90_Site_3_inormal |
| 354) | S_clean_mean_Site_1_squared_inormal |
| 355) | S_clean_median_Site_1_squared_inormal |
| 356) | S_clean_p90_Site_1_squared_inormal |
| 357) | D_clean_mean_Site_1_squared_inormal |
| 358) | D_clean_median_Site_1_squared_inormal |
| 359) | SD_clean_mean_Site_1_squared_inormal |

| | |
|---|---|
| 360) | SD_clean_median_Site_1_squared_inormal |
| 361) | SD_clean_p90_Site_1_squared_inormal |
| 362) | S_dirty_p90_Site_2_squared_inormal |
| 363) | S_clean_mean_Site_2_squared_inormal |
| 364) | S_clean_p90_Site_2_squared_inormal |
| 365) | D_clean_mean_Site_2_squared_inormal |
| 366) | D_clean_median_Site_2_squared_inormal |
| 367) | SD_clean_mean_Site_2_squared_inormal |
| 368) | SD_clean_median_Site_2_squared_inormal |
| 369) | SD_clean_p90_Site_2_squared_inormal |
| 370) | S_clean_mean_Site_3_squared_inormal |
| 371) | S_clean_median_Site_3_squared_inormal |
| 372) | S_clean_p90_Site_3_squared_inormal |
| 373) | D_clean_mean_Site_3_squared_inormal |
| 374) | D_clean_median_Site_3_squared_inormal |
| 375) | SD_clean_mean_Site_3_squared_inormal |
| 376) | SD_clean_median_Site_3_squared_inormal |
| 377) | SD_clean_p90_Site_3_squared_inormal |
| 378) | TablePos_COG_Z_Site_1_squared |
| 379) | TablePos_Table_Site_1_squared |
| 380) | TablePos_COG_Z_Site_2_squared |
| 381) | TablePos_COG_Z_Site_3_squared |
| 382) | TablePos_COG_Z_Site_1_inormal |
| 383) | TablePos_COG_Z_Site_2_inormal |
| 384) | TablePos_COG_Z_Site_3_inormal |
| 385) | TablePos_COG_Z_Site_1_squared_inormal |
| 386) | TablePos_COG_Z_Site_2_squared_inormal |
| 387) | TablePos_COG_Z_Site_3_squared_inormal |
| 388) | Eddy_QC_Y_Site_1_squared |
| 389) | Eddy_QC_Y_Site_2_squared |
| 390) | Eddy_QC_Y_Site_3_squared |
| 391) | Eddy_QC_Y_Site_1_inormal |
| 392) | Eddy_QC_Y_Site_2_inormal |
| 393) | Eddy_QC_Y_Site_3_inormal |
| 394) | Eddy_QC_Y_Site_1_squared_inormal |
| 395) | Age_Site_1__x__TablePos_Table_Site_1 |
| 396) | Age_Site_2__x__HeadMotion_p90_tfMRI_abs_Site_2 |
| 397) | Sex_1_Site_1__x__TablePos_COG_Z_Site_1 |
| 398) | Sex_1_Site_1__x__TablePos_Table_Site_1 |
| 399) | Sex_1_Site_2__x__TablePos_COG_Z_Site_2 |
| 400) | Sex_1_Site_3__x__TablePos_COG_Z_Site_3 |
| 401) | HeadSize_Site_1__x__TablePos_COG_Z_Site_1 |

| | |
|---|---|
| 402) | HeadSize_Site_1__x__TablePos_Table_Site_1 |
| 403) | HeadSize_Site_3__x__TablePos_COG_Z_Site_3 |
| 404) | HeadSize_Site_3__x__HeadSize_Site_3_squared |
| 405) | Batch_1_Site_1__x__SCALING_tfMRI_1_Site_1 |
| 406) | Batch_2_Site_1__x__SCALING_tfMRI_1_Site_1 |
| 407) | Batch_3_Site_1__x__SCALING_tfMRI_1_Site_1 |
| 408) | Batch_1_Site_2__x__SCALING_SWI_1_Site_2 |
| 409) | Batch_2_Site_2__x__SCALING_SWI_1_Site_2 |
| 410) | Batch_3_Site_2__x__SCALING_SWI_1_Site_2 |
| 411) | Batch_4_Site_2__x__SCALING_SWI_1_Site_2 |
| 412) | Batch_4_Site_2__x__D_clean_p90_Site_2_inormal |
| 413) | Batch_1_Site_3__x__Batch_2_Site_3 |
| 414) | Batch_1_Site_3__x__Batch_3_Site_3 |
| 415) | Batch_1_Site_3__x__ScanEvents_1_Site_3 |
| 416) | Batch_1_Site_3__x__ScanEvents_2_Site_3 |
| 417) | Batch_1_Site_3__x__ScanEvents_3_Site_3 |
| 418) | Batch_1_Site_3__x__ScanEvents_4_Site_3 |
| 419) | Batch_1_Site_3__x__ScanEvents_5_Site_3 |
| 420) | Batch_1_Site_3__x__TE_rfMRI_Site_3 |
| 421) | Batch_1_Site_3__x__Eddy_QC_Y_Site_3 |
| 422) | Batch_2_Site_3__x__Batch_3_Site_3 |
| 423) | Batch_2_Site_3__x__ScanEvents_1_Site_3 |
| 424) | Batch_2_Site_3__x__ScanEvents_2_Site_3 |
| 425) | Batch_2_Site_3__x__ScanEvents_3_Site_3 |
| 426) | Batch_2_Site_3__x__ScanEvents_4_Site_3 |
| 427) | Batch_2_Site_3__x__ScanEvents_5_Site_3 |
| 428) | Batch_2_Site_3__x__TE_rfMRI_Site_3 |
| 429) | Batch_3_Site_3__x__ScanEvents_1_Site_3 |
| 430) | Batch_3_Site_3__x__ScanEvents_2_Site_3 |
| 431) | Batch_3_Site_3__x__ScanEvents_3_Site_3 |
| 432) | Batch_3_Site_3__x__ScanEvents_4_Site_3 |
| 433) | Batch_3_Site_3__x__ScanEvents_5_Site_3 |
| 434) | Batch_3_Site_3__x__TE_rfMRI_Site_3 |
| 435) | CMRR_1_Site_1__x__SCALING_tfMRI_1_Site_1 |
| 436) | CMRR_1_Site_2__x__SCALING_SWI_1_Site_2 |
| 437) | Protocol_4_Site_1__x__Eddy_QC_Y_Site_1 |
| 438) | Service_Pack_1_Site_1__x__Eddy_QC_Y_Site_1 |
| 439) | ScanEvents_1_Site_2__x__SCALING_SWI_1_Site_2 |
| 440) | ScanEvents_2_Site_2__x__SCALING_SWI_1_Site_2 |
| 441) | ScanEvents_3_Site_2__x__SCALING_SWI_1_Site_2 |
| 442) | ScanEvents_5_Site_2__x__SCALING_SWI_1_Site_2 |
| 443) | ScanEvents_7_Site_2__x__SCALING_SWI_1_Site_2 |

| | |
|---|---|
| 444) | ScanEvents_7_Site_2__x__D_clean_median_Site_2_inormal |
| 445) | ScanEvents_7_Site_2__x__D_clean_p90_Site_2_inormal |
| 446) | ScanEvents_1_Site_3__x__Eddy_QC_Y_Site_3 |
| 447) | ScanEvents_2_Site_3__x__New_Eddy_1_Site_3 |
| 448) | ScanEvents_2_Site_3__x__Eddy_QC_Y_Site_3 |
| 449) | New_Eddy_1_Site_1__x__Eddy_QC_Y_Site_1 |
| 450) | SCALING_T2_FLAIR_1_Site_1__x__Eddy_QC_Y_Site_1 |
| 451) | SCALING_SWI_1_Site_1__x__Eddy_QC_Y_Site_1 |
| 452) | SCALING_dMRI_1_Site_1__x__Eddy_QC_Y_Site_1 |
| 453) | SCALING_rfMRI_1_Site_1__x__SCALING_tfMRI_1_Site_1 |
| 454) | S_clean_mean_Site_2__x__D_clean_median_Site_2 |
| 455) | S_clean_p90_Site_2__x__D_clean_median_Site_2 |
| 456) | D_clean_mean_Site_2__x__D_clean_median_Site_2 |
| 457) | D_clean_median_Site_2__x__SD_clean_mean_Site_2 |
| 458) | D_clean_median_Site_2__x__SD_clean_p90_Site_2 |
| 459) | S_clean_mean_Site_3__x__D_clean_mean_Site_3 |
| 460) | S_clean_p90_Site_3__x__D_clean_median_Site_3 |
| 461) | D_clean_median_Site_3__x__SD_clean_p90_Site_3 |
| 462) | D_clean_median_Site_3__x__D_clean_p90_Site_3_inormal |
| 463) | HeadMotion_p90_tfMRI_abs_Site_2__x__HeadMotionST_p90_inplane_time_Site_2 |
| 464) | HeadMotion_p90_tfMRI_abs_Site_2__x__S_clean_median_Site_2_squared |
| 465) | HeadMotion_p90_tfMRI_abs_Site_2__x__S_clean_median_Site_2_inormal |
| 466) | HeadMotion_p90_tfMRI_abs_Site_2__x__S_dirty_p90_Site_2_squared_inormal |
| 467) | HeadMotion_p90_tfMRI_abs_Site_2__x__SD_clean_median_Site_2_squared_inormal |
| 468) | HeadMotion_p90_tfMRI_abs_Site_2__x__TablePos_COG_Z_Site_2_squared_inormal |
| 469) | HeadMotion_mean_dMRI_abs_Site_3__x__Eddy_QC_Y_Site_3 |
| 470) | HeadMotion_median_dMRI_abs_Site_3__x__Eddy_QC_Y_Site_3 |
| 471) | TablePos_COG_Z_Site_1__x__Eddy_QC_Y_Site_1 |
| 472) | TablePos_Table_Site_1__x__Eddy_QC_Y_Site_1 |
| 473) | Eddy_QC_Y_Site_3__x__Eddy_QC_Y_Site_3_squared |
| 474) | HeadSize_Site_3_squared__x__TablePos_COG_Z_Site_3_squared |
| 475) | HeadSize_Site_3_inormal__x__TablePos_COG_Z_Site_3_inormal |
| 476) | S_dirty_p90_Site_2_squared__x__D_clean_median_Site_2_inormal |
| 477) | S_dirty_p90_Site_2_squared__x__D_clean_p90_Site_2_inormal |
| 478) | SD_dirty_p90_Site_2_squared__x__D_clean_p90_Site_2_inormal |
| 479) | D_clean_median_Site_2_inormal__x__D_clean_p90_Site_2_inormal |
| 480) | ACQT_Site_1__01 |
| 481) | ACQT_Site_1__02 |
| 482) | ACQT_Site_1__03 |
| 483) | ACQT_Site_1__04 |
| 484) | ACQT_Site_1__05 |
| 485) | ACQT_Site_1__06 |

| | |
|---|---|
| 486) | ACQT_Site_1__07 |
| 487) | ACQT_Site_1__08 |
| 488) | ACQT_Site_1__09 |
| 489) | ACQT_Site_1__10 |
| 490) | ACQT_Site_1__11 |
| 491) | ACQT_Site_1__12 |
| 492) | ACQT_Site_1__13 |
| 493) | ACQT_Site_1__14 |
| 494) | ACQT_Site_1__15 |
| 495) | ACQT_Site_1__16 |
| 496) | ACQT_Site_1__17 |
| 497) | ACQT_Site_1__18 |
| 498) | ACQT_Site_1__19 |
| 499) | ACQT_Site_2__01 |
| 500) | ACQT_Site_2__02 |
| 501) | ACQT_Site_2__03 |
| 502) | ACQT_Site_2__04 |
| 503) | ACQT_Site_2__05 |
| 504) | ACQT_Site_2__06 |
| 505) | ACQT_Site_2__07 |
| 506) | ACQT_Site_2__08 |
| 507) | ACQT_Site_2__09 |
| 508) | ACQT_Site_2__10 |
| 509) | ACQT_Site_2__11 |
| 510) | ACQT_Site_2__12 |
| 511) | ACQT_Site_2__13 |
| 512) | ACQT_Site_2__14 |
| 513) | ACQT_Site_2__15 |
| 514) | ACQT_Site_2__16 |
| 515) | ACQT_Site_2__17 |
| 516) | ACQT_Site_2__18 |
| 517) | ACQT_Site_2__19 |
| 518) | ACQT_Site_2__20 |
| 519) | ACQT_Site_3__01 |
| 520) | ACQT_Site_3__02 |
| 521) | ACQT_Site_3__03 |
| 522) | ACQT_Site_3__04 |
| 523) | ACQT_Site_3__05 |
| 524) | ACQT_Site_3__06 |
| 525) | ACQT_Site_3__07 |
| 526) | ACQT_Site_3__08 |
| 527) | ACQT_Site_3__09 |

| | |
|---|---|
| 528) | ACQT_Site_3__10 |
| 529) | ACQT_Site_3__11 |
| 530) | ACQT_Site_3__12 |
| 531) | ACQT_Site_3__13 |
| 532) | ACQT_Site_3__14 |
| 533) | ACQT_Site_3__15 |
| 534) | ACQT_Site_3__16 |
| 535) | ACQT_Site_3__17 |
| 536) | ACQT_Site_3__18 |
| 537) | ACQT_Site_3__19 |
| 538) | ACQT_Site_3__20 |
| 539) | ACQT_Site_3__21 |
| 540) | DATE_Site_1__01 |
| 541) | DATE_Site_1__02 |
| 542) | DATE_Site_1__03 |
| 543) | DATE_Site_1__04 |
| 544) | DATE_Site_1__05 |
| 545) | DATE_Site_1__06 |
| 546) | DATE_Site_1__07 |
| 547) | DATE_Site_1__08 |
| 548) | DATE_Site_1__09 |
| 549) | DATE_Site_1__10 |
| 550) | DATE_Site_1__11 |
| 551) | DATE_Site_1__12 |
| 552) | DATE_Site_1__13 |
| 553) | DATE_Site_1__14 |
| 554) | DATE_Site_1__15 |
| 555) | DATE_Site_1__16 |
| 556) | DATE_Site_1__17 |
| 557) | DATE_Site_1__18 |
| 558) | DATE_Site_1__19 |
| 559) | DATE_Site_1__20 |
| 560) | DATE_Site_1__21 |
| 561) | DATE_Site_1__22 |
| 562) | DATE_Site_1__23 |
| 563) | DATE_Site_1__24 |
| 564) | DATE_Site_1__25 |
| 565) | DATE_Site_1__26 |
| 566) | DATE_Site_1__27 |
| 567) | DATE_Site_1__28 |
| 568) | DATE_Site_1__29 |
| 569) | DATE_Site_1__30 |

| | |
|---|---|
| 570) | DATE_Site_1__31 |
| 571) | DATE_Site_1__32 |
| 572) | DATE_Site_1__33 |
| 573) | DATE_Site_1__34 |
| 574) | DATE_Site_1__35 |
| 575) | DATE_Site_1__36 |
| 576) | DATE_Site_1__37 |
| 577) | DATE_Site_1__38 |
| 578) | DATE_Site_1__39 |
| 579) | DATE_Site_2__01 |
| 580) | DATE_Site_2__02 |
| 581) | DATE_Site_2__03 |
| 582) | DATE_Site_2__04 |
| 583) | DATE_Site_2__05 |
| 584) | DATE_Site_2__06 |
| 585) | DATE_Site_2__07 |
| 586) | DATE_Site_2__08 |
| 587) | DATE_Site_2__09 |
| 588) | DATE_Site_2__10 |
| 589) | DATE_Site_2__11 |
| 590) | DATE_Site_2__12 |
| 591) | DATE_Site_2__13 |
| 592) | DATE_Site_2__14 |
| 593) | DATE_Site_2__15 |
| 594) | DATE_Site_2__16 |
| 595) | DATE_Site_2__17 |
| 596) | DATE_Site_2__18 |
| 597) | DATE_Site_2__19 |
| 598) | DATE_Site_2__20 |
| 599) | DATE_Site_2__21 |
| 600) | DATE_Site_3__01 |
| 601) | DATE_Site_3__02 |
| 602) | DATE_Site_3__03 |
| 603) | DATE_Site_3__04 |
| 604) | DATE_Site_3__05 |
| 605) | DATE_Site_3__06 |
| 606) | DATE_Site_3__07 |
| 607) | DATE_Site_3__08 |
| 608) | DATE_Site_3__09 |
| 609) | DATE_Site_3__10 |
| 610) | DATE_Site_3__11 |
| 611) | DATE_Site_3__12 |

| | |
|---|---|
| 612) | DATE_Site_3__13 |
| 613) | DATE_Site_3__14 |

Abbreviations: SWI, Susceptibility-Weighted Imaging; CMRR, Center for Magnetic Resonance Research (multiband EPI sequence); rfMRI, resting-state functional MRI; tfMRI, task functional MRI; dMRI, diffusion MRI; TE, Echo Time; QC, Quality Control; COG, Centre of Gravity (head/brain position); ACQT, Acquisition-time bin; DATE, Calendar-date bin; Eddy, FSL's eddy correction for dMRI; FreeSurfer, Structural MRI segmentation software; T1, T1-weighted MRI; T2 FLAIR, T2-weighted Fluid-Attenuated Inversion Recovery; SCALING, Global intensity scaling factor; HeadMotionST, Head-Motion Short-Term features; p90, 90th percentile; abs / rel, absolute / relative displacement; inormal, inverse-normal transformed; TablePos, Scanner table/bed position; YTranslation, Translation along scanner Y axis; StructHeadMotion, Head motion during structural scan; HeadSize, T1→MNI volumetric head-size scaling factor; Service_Pack, Scanner software service-pack version; Protocol, Acquisition protocol variant; Batch, Acquisition batch (within site); Site, Imaging centre indicator; Flipped_SWI, Flag for historical SWI reconstruction issue; New_Eddy, Flag for updated eddy configuration; S / D / SD, Global signal summary metrics: S = structural, D = diffusion, SD = susceptibility-derived.

## Appendix 4: GWAS data on cannabis use disorder used from Million Veteran Program

| **Population** | **Cohort** | **Status** | ***n*** | **Totals** | **Effective** |
|---|---|---|---|---|---|
| **European** | PGC+deCODE | Case | 14,522 | 313,463 | 55,397 |
| | | Control | 298,941 | | |
| | MVP | Case | 22,260 | 445,847 | 84,594 |
| | | Control | 423,587 | | |
| | iPSYCH2 | Case | 4,733 | 100,390 | 18,039 |
| | | Control | 95,657 | | |
| | MGB | Case | 456 | 24,544 | 1,790 |
| | | Control | 24,088 | | |
| | Yale–Penn 3 | Case | 310 | 1,781 | 1,024 |
| | | Control | 1,471 | | |
| | Total | Case | 42,281 | 886,025 | 161,053 |
| | | Control | 843,744 | | |

Abbreviations: PGC, Psychiatric Genomics Consortium; deCODE, deCODE Genetics (Iceland); MVP, Million Veteran Program; iPSYCH2, Integrative Psychiatric Research, phase 2 (Denmark); MGB, Mass General Brigham Biobank; Yale–Penn 3, Yale–Pennsylvania cohort, wave 3.

## Appendix 5a: ICD-9 codes used in the definition of Million Veteran Program (MVP) cases

| ICD Code | ICD Code Description | Code Type |
|---|---|---|
| 304.3 | Marijuana dependence unspecified | ICD-9 |
| 304.3 | Cannabis dependence unspecified | ICD-9 |
| 304.309 | Other cannabis dependence unspecified | ICD-9 |
| 304.31 | Cannabis dependence, continuous use | ICD-9 |
| 304.31 | Marijuana dependence continuous | ICD-9 |
| 304.319 | Other cannabis dependence continuous | ICD-9 |
| 304.32 | Cannabis dependence, episodic use | ICD-9 |
| 304.32 | Marijuana dependence episodic | ICD-9 |
| 304.329 | Other cannabis dependence episodic | ICD-9 |

| | | |
|---|---|---|
| 304.33 | Cannabis dependence, in remission | ICD-9 |
| 304.33 | Marijuana dependence in remission | ICD-9 |
| 304.339 | Other cannabis dependence in remission | ICD-9 |
| 304.39 | Other cannabis depend, nec | ICD-9 |
| 305.2 | Cannabis abuse unspecified | ICD-9 |
| 305.2 | Marijuana abuse unspecified | ICD-9 |
| 305.209 | Other cannabis abuse unspecified | ICD-9 |
| 305.21 | Cannabis abuse, continuous use | ICD-9 |
| 305.21 | Marijuana abuse continuous | ICD-9 |
| 305.219 | Other cannabis abuse continuous | ICD-9 |
| 305.22 | Cannabis abuse, episodic use | ICD-9 |
| 305.22 | Marijuana abuse episodic | ICD-9 |
| 305.229 | Other cannabis abuse episodic | ICD-9 |
| 305.23 | Cannabis abuse, in remission | ICD-9 |
| 305.23 | Marijuana abuse in remission | ICD-9 |
| 305.239 | Other cannabis abuse in remission | ICD-9 |
| 305.29 | Other cannabis use, nec | ICD-9 |

Abbreviations: ICD, International Classification of Diseases.

## Appendix 5b: ICD-10 codes used in the definition of Million Veteran Program (MVP) cases

| ICD Code | ICD Code Description | Code Type |
|---|---|---|
| F12.10 | Cannabis abuse, uncomplicated | ICD-10 |
| F12.11 | Cannabis abuse, in remission | ICD-10 |
| F12.120 | Cannabis abuse with intoxication, uncomplicated | ICD-10 |
| F12.121 | Cannabis abuse with intoxication delirium | ICD-10 |
| F12.122 | Cannabis abuse with intoxication with perceptual disturbance | ICD-10 |
| F12.129 | Cannabis abuse with intoxication, unspecified | ICD-10 |
| F12.150 | Cannabis abuse with psychotic disorder with delusions | ICD-10 |
| F12.151 | Cannabis abuse with psychotic disorder with hallucinations | ICD-10 |
| F12.159 | Cannabis abuse with psychotic disorder, unspecified | ICD-10 |
| F12.180 | Cannabis abuse with cannabis-induced anxiety disorder | ICD-10 |
| F12.188 | Cannabis abuse with other cannabis-induced disorder | ICD-10 |
| F12.19 | Cannabis abuse with unspecified cannabis-induced disorder | ICD-10 |
| F12.20 | Cannabis dependence, uncomplicated | ICD-10 |
| F12.21 | Cannabis dependence, in remission | ICD-10 |
| F12.220 | Cannabis dependence with intoxication, uncomplicated | ICD-10 |
| F12.221 | Cannabis dependence with intoxication delirium | ICD-10 |
| F12.222 | Cannabis dependence with intoxication with perceptual disturbance | ICD-10 |
| F12.229 | Cannabis dependence with intoxication, unspecified | ICD-10 |
| F12.23 | Cannabis dependence with withdrawal | ICD-10 |
| F12.250 | Cannabis dependence with psychotic disorder with delusions | ICD-10 |
| F12.251 | Cannabis dependence with psychotic disorder with hallucinations | ICD-10 |
| F12.259 | Cannabis dependence with psychotic disorder, unspecified | ICD-10 |
| F12.280 | Cannabis dependence with cannabis-induced anxiety disorder | ICD-10 |
| F12.288 | Cannabis dependence with other cannabis-induced disorder | ICD-10 |
| F12.29 | Cannabis dependence with unspecified cannabis-induced disorder | ICD-10 |
| F12.90 | Cannabis use, unspecified, uncomplicated | ICD-10 |

| | | |
|---|---|---|
| F12.920 | Cannabis use, unspecified with intoxication, uncomplicated | ICD-10 |
| F12.921 | Cannabis use, unspecified with intoxication delirium | ICD-10 |
| F12.922 | Cannabis use, unspecified with intoxication with perceptual disturbance | ICD-10 |
| F12.929 | Cannabis use, unspecified with intoxication, unspecified | ICD-10 |
| F12.93 | Cannabis use, unspecified with withdrawal | ICD-10 |
| F12.950 | Cannabis use, unspecified with psychotic disorder with delusions | ICD-10 |
| F12.951 | Cannabis use, unspecified with psychotic disorder with hallucinations | ICD-10 |
| F12.959 | Cannabis use, unspecified with psychotic disorder, unspecified | ICD-10 |
| F12.980 | Cannabis use, unspecified with anxiety disorder | ICD-10 |
| F12.988 | Cannabis use, unspecified with other cannabis-induced disorder | ICD-10 |
| F12.99 | Cannabis use, unspecified with unspecified cannabis-induced disorder | ICD-10 |

Abbreviations: ICD, International Classification of Diseases.

## Appendix 6: Demographic characteristics (missing vs non missing cannabis data)

| **Variables (at time of imaging)** | **Missing cannabis data (n = 18,056)** | **Non missing cannabis data (n = 15,896)** | **Statistics** | |
|---|---|---|---|---|
| | **Mean (SD) or % (n)** | | ***t* or $\chi^{2*}$** | ***p-value*** |
| Age at 1st scan (years) | 64.02 (7.78) | 63.69 (7.56) | 3.34 | 1.69E-03 |
| Sex (male % (n)) | 48.90% (8,829) | 45.89% (7,295) | 112.89* | 6.66E−27 |
| Townsend deprivation index | -1.85 (2.74) | -2.01 (2.65) | 4.10 | 4.12E-05 |
| Employment status (current; % (n)) | 38.89% (7,022) | 38.79% (6,166) | 0.07* | 4.80E−01 |
| College degree (% (n)) | 47.10% (8,504) | 50.71% (8,065) | 29.35* | 6.22E−08 |
| BMI (kg/m2) | 26.63 (4.20) | 26.33 (4.33) | 6.30 | 3.01E-10 |
| Diastolic BP (mmHg) | 78.96 (10.61) | 78.66 (10.65) | 3.39 | 6.90E-04 |
| Systolic BP (mmHg) | 141.42 (19.96) | 140.31 (19.79) | 6.54 | 6.54E-11 |
| Alcohol use (current; % (n)) | 92.91% (16,775) | 94.09% (14,955) | 5.05* | 2.45E−02 |
| Smoking (current; % (n)) | 3.58% (647) | 3.16% (506) | 3.28 | 7.04E−02 |
| Nerves, anxiety, tension, or depression status (% (n)) | 8.94% (1,614) | 8.72% (1,383) | 0.31 | 5.79E−01 |

Abbreviations: SD, standard deviation; BMI, body mass index; BP, blood pressure.

## Appendix 7: Associations between cannabis use and brain structure (Model 1: core covariates)

| **Brain measure** | **Beta** | **LCI** | **UCI** | **P-value** |
|---|---|---|---|---|
| **L3 Genu of corpus callosum** | 0.16 | 0.10 | 0.22 | 9.62E-07 |
| **FA Genu of corpus callosum** | −0.16 | −0.23 | −0.09 | 2.14E-06 |
| **L2 Genu of corpus callosum** | 0.15 | 0.09 | 0.22 | 5.90E-06 |
| **MD Genu of corpus callosum** | 0.13 | 0.07 | 0.20 | 2.45E-05 |
| **L3 Anterior corona radiata (Left)** | 0.13 | 0.07 | 0.19 | 3.23E-05 |
| **L3 Body of corpus callosum** | 0.14 | 0.07 | 0.21 | 4.48E-05 |
| **L3 Anterior corona radiata (Right)** | 0.13 | 0.06 | 0.19 | 7.74E-05 |
| **FA Body of corpus callosum** | −0.13 | −0.20 | −0.06 | 1.80E-04 |
| **L2 Body of corpus callosum** | 0.12 | 0.06 | 0.19 | 3.12E-04 |
| **ICVF Genu of corpus callosum** | −0.12 | −0.19 | −0.05 | 5.37E-04 |

Estimates represent beta coefficients from multiple linear regression models surviving FDR correction and adjusted for: age, sex, Townsend deprivation index, employment status, educational qualifications, body mass index, systolic and diastolic blood pressure, assessment centre, and brain imaging confounds including assessment centre, intracranial volume, head motion, table position, and scanner acquisition parameters (site, scanner software, protocol, scan ramp, head coil). Abbreviations: LCI, lower confidence interval; UCI, upper confidence interval; FA, fractional anisotropy; MD, mean diffusivity; L2 and L3, radial diffusivities; ICVF intracellular volume fraction.

## Appendix 8: Associations between cannabis use and brain structure (Model 2: core covariates + alcohol + smoking)

| Brain measure | Beta | LCI | UCI | P-value |
|---|---|---|---|---|
| **L3 Genu of corpus callosum** | 0.16 | 0.09 | 0.22 | 1.19E-06 |
| **FA Genu of corpus callosum** | −0.16 | −0.23 | −0.09 | 1.92E-06 |
| **L2 Genu of corpus callosum** | 0.15 | 0.09 | 0.22 | 5.31E-06 |
| **MD Genu of corpus callosum** | 0.13 | 0.07 | 0.19 | 3.25E-05 |
| **L3 Anterior corona radiata (Left)** | 0.13 | 0.07 | 0.19 | 3.89E-05 |
| **L3 Body of corpus callosum** | 0.14 | 0.07 | 0.21 | 5.21E-05 |
| **L3 Anterior corona radiata (Right)** | 0.13 | 0.06 | 0.19 | 7.39E-05 |
| **FA Body of corpus callosum** | −0.13 | −0.20 | −0.06 | 1.93E-04 |
| **L2 Body of corpus callosum** | 0.12 | 0.06 | 0.19 | 3.24E-04 |
| **ICVF Genu of corpus callosum** | −0.13 | −0.20 | −0.06 | 4.25E-04 |

Estimates represent beta coefficients from multiple linear regression models surviving FDR correction and adjusted for: age, sex, Townsend deprivation index, employment status, educational qualifications, alcohol drinking status, smoking status, body mass index, systolic and diastolic blood pressure, assessment centre, and brain imaging confounds including assessment centre, intracranial volume, head motion, table position, and scanner acquisition parameters (site, scanner software, protocol, scan ramp, head coil). Abbreviations: LCI, lower confidence interval; UCI, upper confidence interval; FA, fractional anisotropy; MD, mean diffusivity; L2 and L3, radial diffusivities; ICVF intracellular volume fraction.

## Appendix 9: Associations between cannabis use and brain function (Model 1: core covariates)

| Functional measures | ICA | Edge ID | Estimate | LCI | UCI | P-value |
|---|---|---|---|---|---|---|
| rsfMRI | 25 | 21 | 0.15 | 0.08 | 0.22 | 4.61E-05 |
| rsfMRI | 25 | 178 | −0.14 | −0.21 | −0.07 | 1.23E-04 |
| rsfMRI | 25 | 606 | −0.13 | −0.20 | −0.06 | 4.85E-04 |

Estimates represent beta coefficients from multiple linear regression models surviving FDR correction and adjusted for: age, sex, Townsend deprivation index, employment status, educational qualifications, body mass index, systolic and diastolic blood pressure, assessment centre, and brain imaging confounds including assessment centre, intracranial volume, head motion, table position, and scanner acquisition parameters (site, scanner software, protocol, scan ramp, head coil). Edge IDs correspond to pairwise node connections in the UK Biobank resting-state functional connectivity matrices. Abbreviations: ICA, independent component analysis; LCI, lower confidence interval; UCI, upper confidence interval; rsfMRI, resting-state functional magnetic resonance imaging.

## Appendix 10: Associations between cannabis use and brain function (Model 2: core covariates + alcohol + smoking)

| Functional measures | ICA | Edge ID | Estimate | LCI | UCI | P-value |
|---|---|---|---|---|---|---|
| **rsfMRI** | 25 | 21 | 0.15 | 0.07 | 0.22 | 7.92E-05 |
| **rsfMRI** | 25 | 178 | −0.14 | −0.21 | −0.07 | 1.52E-04 |
| **rsfMRI** | 25 | 606 | −0.13 | −0.20 | −0.06 | 5.07E-04 |

Estimates represent beta coefficients from multiple linear regression models surviving FDR correction and adjusted for: age, sex, Townsend deprivation index, employment status, educational qualifications, alcohol drinking status, smoking status, body mass index, systolic and diastolic blood pressure, assessment centre, and brain imaging confounds including assessment centre, intracranial volume, head motion, table position, and scanner acquisition parameters (site, scanner software, protocol, scan ramp, head coil). Edge IDs correspond to pairwise node connections in the UK Biobank resting-state functional connectivity matrices. Abbreviations: ICA, independent component analysis; LCI, lower confidence interval; UCI, upper confidence interval; rsfMRI, resting-state functional magnetic resonance imaging.

## Appendix 11: Associations between cannabis use and cognitive function (Model 1-5)

| Cognitive Test | Model | Estimate | LCI | UCI | P-value |
|---|---|---|---|---|---|
| Numeric Memory | Model 1 | 0.09 | 0.07 | 0.10 | 7.61E-23 |
| | Model 2 | 0.07 | 0.06 | 0.09 | 9.91E-16 |
| | Model 3 | 0.15 | 0.05 | 0.24 | 1.71E-03 |
| | Model 4 | 0.14 | 0.05 | 0.23 | 2.47E-03 |
| | Model 5 | 0.08 | 0.06 | 0.10 | 5.20E-14 |
| Fluid Intelligence | Model 1 | 0.11 | 0.09 | 0.12 | 4.82E-40 |
| | Model 2 | 0.12 | 0.10 | 0.13 | 1.04E-42 |
| | Model 3 | 0.26 | 0.18 | 0.35 | 9.28E-10 |
| | Model 4 | 0.26 | 0.17 | 0.34 | 3.34E-09 |
| | Model 5 | 0.13 | 0.11 | 0.14 | 1.21E-42 |

Estimates were generated from mixed effects models adjusted for age at baseline, sex, household income, Townsend deprivation index, educational qualifications, job type, alcohol drinking frequency, smoking status, body mass index, systolic and diastolic blood pressure, assessment centre, time between baseline and first cognitive assessment and time between cognitive assessment. The reference group are non-users. Model 1 included core demographic and health covariates; Model 2 added smoking and alcohol use; Model 3 further included psychological traits (risk-taking, standardised neuroticism, loneliness); Model 4 added subclinical mental-health symptoms (PHQ-9, GAD-2); and Model 5 additionally incorporated clinically diagnosed depression and anxiety (ICD-10). Abbreviations: LCI, lower confidence interval; UCI, upper confidence interval.